Thèse

En vue de l'obtention du

Doctorat

Délivré par : *l'Université de Guyane*

Présentée et soutenue publiquement le *7/12/2018* **par :**

CAMILLE PIPONIOT

Quel futur pour les forêts de production en Amazonie ?

Du bilan Carbone de l'exploitation forestière à la recherche de compromis entre services écosystémiques (bois d'œuvre, biodiversité et carbone)

JURY

AVNER BAR-HEN	Professeur d'Université	Rapporteur
RAPHAËL PELISSIER	Directeur de Recherche	Rapporteur
ERIC MARCON	Chercheur	Membre du Jury
FRANÇOISE BUREL	Directrice de Recherche	Membre du Jury
BRUNO HERAULT	Chercheur	Directeur de thèse
PLINIO SIST	Chercheur	Co-directeur de thèse

École doctorale et spécialité :
Diversités, santé et développement en Amazonie

Unité de Recherche :
UMR Écologie des Forêts de Guyane

Directeurs de thèse :
Bruno HERAULT et *Plinio SIST*

Rapporteurs :
Avner BAR-HEN et *Raphaël PELISSIER*

Table des matières

Avant-propos

Je voudrais d'abord remercier mes deux directeurs de thèse, Bruno Hérault et Plinio Sist, de m'avoir donné l'opportunité de faire cette thèse. Merci à eux de m'avoir fait confiance, de m'avoir accompagnée et transmis leur expérience, et permis de m'accomplir pendant ces trois ans.

Merci aux membres du jury, Avner Bar-Hen et Raphaël Pélissier, Eric Marcon et Françoise Burel, pour avoir accepté de dédier du temps à cette thèse.

Merci aussi à Ervan, Lucas, Marcus, Marielos, Allie, Jack et à toute l'équipe de TmFO pour avoir pris le temps et contribué à améliorer ce travail avec leurs conseils.

Merci à toutes les personnes qui m'ont accueillie pendant les nombreuses aventures qui ont ponctué ces trois ans, et qui m'ont fait découvrir et aimer leur coin sur Terre.

Merci enfin à la team EcoFoG et l'UR Forêts et Sociétés d'avoir été des collègues de rêve, qui m'ont fait piquer tant de fous rires aux pauses café, et qui ont su apprivoiser l'ours qui sommeillait en moi dans les derniers moments de rédaction ! J'espère avoir l'occasion de dire à chacun et de vive voix combien ces moments ont été précieux.

Cette thèse a été financée par le Cirad et par le programme «Investissements d'Avenir»de l'Agence Nationale de la Recherche, à travers le LabEx CEBA (ANR-10-LABEX-0025).

Résumé

La moitié des forêts tropicales du monde est désignée comme des forêts de production par les services forestiers nationaux[1]. Pour la seule Amazonie brésilienne (400 millions d'hectares), l'exploitation sélective affecte chaque année entre un et deux millions d'ha[2]. Si l'effet de la déforestation sur les émissions de carbone et les pertes de biodiversité en région tropicale ont fait l'objet de nombreuses études, les impacts à long terme de l'exploitation commerciale de bois sur ces forêts restent à ce jour très peu étudiés. Or, les enjeux sont grandissants pour ces forêts de production[3]. Non seulement elles doivent alimenter le commerce du bois tropical, mais leur rôle dans le stockage de carbone et dans la préservation de la biodiversité est de plus en plus reconnu. La thèse développée ici s'organise en trois temps. Premièrement, un modèle de bilan carbone de l'exploitation forestière est développé, et les différences régionales de dynamique de récupération du carbone post-exploitation sont modélisées. Deuxièmement, un modèle de récupération du volume de bois d'œuvre a été développé et calibré à l'échelle amazonienne. Ces résultats ont permis de montrer la lenteur de la récupération du volume de bois en Amazonie, et la non-durabilité des pratiques actuelles d'exploitation. Ces modèles (carbone et bois d'œuvre) ont été élaborés dans un cadre bayésien, avec l'appui et les données du *Tropical managed Forest Observatory* (TmFO : www.tmfo.org), réseau rassemblant 9 institutions de recherche et plus de 200 parcelles de suivi de la dynamique forestière après exploitation en Amazonie. Enfin, une analyse comparative de scénarios prospectifs a été effectuée, où les compromis possibles entre services écosystémiques (bois d'œuvre, carbone et biodiversité) ont été explorés par des techniques d'optimisation multicritère.

[1] J. Blaser et al. (2011). *Status of Tropical Forest Management 2011*. Rapp. tech., p. 418.

[2] G. P. Asner et al. (2005). « Selective Logging in the Brazilian Amazon ». In : *Science* 310.5747, p. 480–482.

[3] D. P. Edwards et al. (2014b). « Maintaining ecosystem function and services in logged tropical forests ». In : *Trends in Ecology & Evolution* 29.9, p. 511–520.

Abstract

Half of the world's tropical forests are designated by national forest services as production forests[4]. In the Brazilian Amazon alone (400 million ha), selective exploitation affects between one and two million ha every year[5]. While there has been numerous studies on the impact of deforestation on carbon emissions and biodiversity loss in the tropics, the long-term impacts of selective logging are still poorly studied. However, the importance of these production forests is increasing[6]. Not only must they meet the growing tropical timber demand, but their role in carbon storage and the biodiversity conservation is increasingly recognized. The studies developed in this thesis are threefold. First, a carbon balance model of logging is developed, and regional differences in post-logging carbon recovery dynamics are modeled. Secondly, a timber volume recovery model has been developed and calibrated at the Amazonian scale. These results point out the slow recovery of timber volume in the Amazon, and thus the unsustainability of current logging practices. These models (carbon and timber) were developed in a Bayesian framework, with support and data from the Tropical managed Forest Observatory (TmFO : www.tmfo.org), a network of 9 research institutions and more than 200 forest plots where post-logging forest dynamics have been monitored for > 30 years in the Amazon. Finally, a comparative analysis of prospective scenarios was carried out, where potential tradeoffs between ecosystem services (timber, carbon and biodiversity) were explored using multi-criteria optimization analysis.

[4] Blaser et al. (2011). Cf. note 1.

[5] Asner et al. (2005). Cf. note 2.

[6] Edwards et al. (2014b). Cf. note 3.

Lexique

- **Biomasse** masse contenue dans les êtres vivants ; la biomasse aérienne des arbres correspond à leur masse sans les parties souterraines (racines).
- **Biosphère** l'ensemble des organismes vivants.
- **Canopée** partie supérieure du couvert végétal forestier, correspondant à la cime des grands arbres.
- **DHP** diamètre d'un arbre à hauteur de poitrine, mesurée à 1,30 m de hauteur (DBH pour Diameter at Breast Height en anglais).
- **Diversité fonctionnelle** diversité des traits fonctionnels au sein d'un ensemble d'individus.
- **Domaine forestier permanent** (*permanent forest estate* en anglais) zones de couverture forestière qui ne peuvent légalement être converties pour d'autres usages.
- **Exploitation sélective** méthode d'exploitation du bois en forêt naturelle, majoritaire sous les tropiques, qui consiste à extraire uniquement quelques arbres de la forêt (les plus gros, d'espèces commerciales) et laisser le reste de la forêt se régénérer jusqu'au prochain cycle d'exploitation.
- **Exploitation à Faible Impact** (RIL pour *Reduced Impact Logging* en anglais) ensemble de techniques visant à réduire les dégâts causés par l'exploitation sélective et incluant (entre autres) : la planification des pistes d'exploitation, l'abattage directionnel des arbres, le débardage des arbres au câble, la suppression des lianes sur les arbres exploités.
- **Forêt dégradée** Forêt ayant subi une diminution significative de sa valeur environnementale (stocks de carbone, diversité, etc.) suite à des perturbations d'origine humaine, et ayant perdu la capacité à retrouver son état initial.
- **Forêt secondaire** Forêt issue de la régénération sur une zone ayant été déforestée.
- **Mitigation** atténuation des effets (négatifs) d'un phénomène ; dans le cas des changements climatiques, le stockage du carbone dans la biomasse vivante est une forme de mitigation.
- **Trait fonctionnel** caractéristique mesurable d'un être vivant ayant un impact sur sa reproduction, sa survie ou son rôle dans le fonctionnement de l'écosystème.

Chapitre 1

Introduction générale

1.1 L'Homme et l'Amazonie

1.1.1 Particularités et valeur environnementale des forêts amazoniennes

Le plus grand bassin tropical au monde

L'Amazonie est le plus grand massif tropical au monde, couvrant à lui seul 6 millions de km^2, soit plus de 50% des forêts tropicales humides au monde[1]. Situé en Amérique du Sud dont elle représente 30% de la surface totale (Figure 1.1), l'Amazonie est aussi une entité géopolitique complexe, à cheval entre 9 pays : le Brésil (59% de la surface totale), le Pérou (12%), la Bolivie (9%), la Colombie (7%), le Venezuela (5%), le Guyana (3%), l'Équateur (2%), le Suriname (2%) et la Guyane française (1%).

Le biome amazonien est caractérisé par un couvert végétal dense de type forêt tropicale humide. La pluviométrie y est de 1500 à 5000 mm par an selon les régions, et la durée de la saison sèche (moins de 100 mm par mois) ne dépasse pas 5 mois par an[2]. Les sols sont majoritairement pauvres en nutriments car lessivés par les forts niveaux de précipitation[3]. La végétation qui s'y développe est une forêt dense dont la canopée se trouve à 30 m de hauteur[4].

Les forêts tropicales humides sont parmi les écosystèmes les plus riches en carbone[5]. Le carbone des forêts tropicales est principalement contenu dans la biomasse aérienne des arbres et oscille entre 100-300 tonnes par hectare[6]. Par son étendue et par ses niveaux élevés de biomasse, l'Amazonie est donc l'un des principaux réservoirs de carbone terrestre. Le carbone total stocké dans les forêts amazoniennes est estimé à 86 milliards de tonnes ($\pm$ 20%)[7], soit environ 20% de tout le carbone contenu dans la biosphère[8]. De plus, les suivis de forêts naturelles en Amazonie montrent une nette accumulation de carbone[9], bien que la représentativité de ces données soit contestée[10] et que l'on observe un ralentissement de ce stockage de carbone[11]. Il n'est reste pas

[1] H. Eva et al. (2005). *A proposal for defining the geographical boundaries of Amazonia*. June, p. 1–40 ; FAO (2011). *The State of Forests in the Amazon Basin, Congo Basin and Southeast Asia*, p. 81.

[2] O. L. Phillips et al. (2008). « The changing Amazon forest. » In : *Philosophical transactions of the Royal Society of London. Series B, Biological sciences* 363.1498, p. 1819–1827.

[3] C. A. Quesada et al. (2011). « Soils of Amazonia with particular reference to the RAINFOR sites ». In : *Biogeosciences* 8.6, p. 1415–1440.

[4] M. Simard et al. (2011). « Mapping forest canopy height globally with spaceborne lidar ». In : *Journal of Geophysical Research : Biogeosciences* 116.4, p. 1–12. arXiv : `arXiv:1011.1669v3`.

[5] V. Avitabile et al. (2016). « An integrated pan-tropical biomass map using multiple reference datasets ». In : *Global change biology* 22.4.

[6] M. J. P. Sullivan et al. (2017). « Diversity and carbon storage across the tropical forest biome ». In : *Scientific Reports* 7.1, p. 39102.

[7] S. S. Saatchi et al. (2007). « Distribution of aboveground live biomass in the Amazon basin ». In : *Global Change Biology* 13.4, p. 816–837.

[8] J. T. Houghton et al. (2001). *Climate change 2001 : The scientific basis. Contribution of Working Group I to the Third Assessment Report of the Intergovernmental Panel on Climate Change*.

[9] T. R. Baker et al. (2004). « Increasing biomass in Amazonian forest plots ». In : *Philosophical Transactions of the Royal Society B : Biological Sciences* 359.1443, p. 353–365.

[10] C. N. H. McMichael et al. (2017). « Ancient human disturbances may be skewing our understanding of Amazonian forests ». In : *Proceedings of the National Academy of Sciences* 114.3, p. 522–527.

[11] R. J. W. Brienen et al. (2015). « Long-term decline of the Amazon carbon sink. » In : *Nature* 519.7543, p. 344–348.

moins que dans un contexte de changements climatiques où les émissions et le stockage de carbone sont au centre des discussions politiques[12], l'Amazonie revêt un rôle particulièrement important dans l'atténuation de ces changements.

Les forêts amazoniennes ont aussi une place importante dans d'autres cycles biogéochimiques régionaux, et notamment le cycle de l'eau. En effet, la végétation des forêts amazoniennes évapore en moyenne 1370 mm par an[13], ce qui lui confère un rôle de relai des précipitations à l'échelle du continent sud-américain à travers des cycles successifs de précipitation-transpiration[14]. Ainsi, les forêts amazoniennes jouent un rôle tampon dans les sécheresses qui affectent le sud-ouest de l'Amazonie et les régions adjacentes du continent sud-américain[15]. Ce rôle pourrait être encore accentué dans le futur, avec une prévision d'augmentation de la saisonnalité des précipitations particulièrement marquée dans les parties les plus occidentales de l'Amazonie[16].

Diversités amazoniennes

L'Amazonie n'est pas une unité homogène, mais est en fait constituée d'une grande diversité d'écosystèmes. Le biome amazonien est constitué d'au moins cinq entités géomorphologiques distinctes : (i) le bassin amazonien, *i.e.* les bassins versants des fleuve Amazone et Tapajós, (ii) la zone de transition andine à l'ouest, (iii) le planalto au sud-est, plus vallonné et avec une végétation proche des savanes du cerrado brésilien, (iv) la région de Gurupi à l'est, en transition avec la caatinga du nord-est brésilien dominée par des forêts de palmiers, et (v) le plateau des Guyanes au nord, aux sols plus anciens et plus pauvres en nutriments[17] (Figure 1.1). La formation de ces entités géomorphologiques, en particulier lors du soulèvement de la cordillère des Andes, a modifié profondément la région, et en particulier le régime de précipitations et la formation de sols plus fertiles grâce à l'apport de sédiments andins[18]. Ces modifications ont créé une diversification régionale des conditions environnementales qui explique la diversité d'écosystèmes aujourd'hui présents en Amazonie.

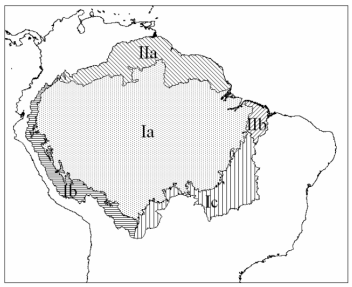

FIGURE 1.1 – Délimitation de cinq grandes entités géomorphologiques du biome amazonien d'après Eva *et al.* 2005[a]. Ia Bassin amazonien. Ib région andine. Ic Planalto. IIa Plateau des Guyanes. IIb Gurupi.

Outre les forêts tropicales humides de terre ferme qui couvrent la majorité du biome, d'autres formes de végétations peuvent être observées en Amazonie : les forêts de várzea saisonnièrement inondées ; les mangroves ; les savannes ; des forêts de sable blanc ; les *tepuis*, montagnes tabulaires du plateau des Guyane ; les *inselbergs*, collines granitiques présents au nord de l'Amazonie. Ces écosystèmes particuliers se distinguent des forêts de terre ferme par un fort endémisme, où des spéciations locales ont pu avoir lieu[19]. Le réseau de rivières, particulièrement dense, modèle aussi la diversité amazonienne. Ainsi, il a été montré que la diversité des oiseaux[20], des grands vertébrés[21] et insectes[22] est fortement structurée par la distribution des grands fleuves en Amazonie et

[12] D. J. GRIGGS et M. NOGUER (2002). « Climate change 2001 : the scientific basis. Contribution of working group I to the third assessment report of the intergovernmental panel on climate change ». In : *Weather* 57.8, p. 267–269.

[13] J. B. FISHER et al. (2009). « The land-atmosphere water flux in the tropics ». In : *Global Change Biology* 15.11, p. 2694–2714. arXiv : `arXiv : 1011.1669v3`.

[14] A. STAAL et al. (2018). « Forest-rainfall cascades buffer against drought across the Amazon ». In : *Nature Climate Change* 8.June, p. 1.

[15] STAAL et al. (2018). Cf. note 14 ; M RODELL et al. (2018). « Emerging trends in global freshwater availability ». In : *Nature*.

[16] A. KITOH et al. (2011). « Climate change projections over South America in the late 21st century with the 20 and 60 km mesh Meteorological Research Institute atmospheric general circulation model (MRI-AGCM) ». In : *Journal of Geophysical Research Atmospheres* 116.6, p. 1–21.

[17] EVA et al. (2005). *A proposal for defining the geographical boundaries of Amazonia*, cf. note 1, p. 1.

[18] C HOORN et al. (2010). « Amazonia Through Time : Andean Uplift, Climate Change, Landscape Evolution, and Biodiversity ». In : *Science* 330.6006, p. 927–931.

[a] EVA et al. (2005). *A proposal for defining the geographical boundaries of Amazonia*, cf. note 1, p. 1.

[19] G. T. PRANCE (1996). « Islands in Amazonia ». In : *Philosophical Transactions of the Royal Society : Biological Sciences* 351.1341, p. 823–833.

par la géomorphologie du paysage.

Cette diversité de conditions environnementales et d'habitats a permis l'apparition d'un grand nombre d'espèces[23]. Par rapport aux autres grands bassins tropicaux, l'Amazonie se distingue par une richesse d'espèce particulièrement élevée, à la fois floristique[24] et faunistique[25], et par les forts niveaux d'endémismes[26]. L'Amazonie contient environ 10-15% des espèces connues sur Terre[27] : au moins 40 000 espèces de plantes, 427 de mammifères, 1294 d'oiseaux, 378 de reptiles, 427 d'amphibiens, et environ 3000 de poissons ont été décrites en Amazonie[28]. L'Amazonie a été la principale source d'espèces pour le reste de l'Amérique tropicale, par des mécanismes de migration vers les autres biomes[29]. En plus de son rôle dans le fonctionnement et le maintien des forêts, la diversité a une valeur culturelle et économique[30] : par exemple, les pharmacopées traditionnelles et modernes dépendent de molécules issues de la grande diversité des organismes amazoniens[31].

1.1.2 Effets d'une anthropisation croissante

Occupations humaines de l'Amazonie

L'histoire récente de l'Amazonie a été marquée par l'occupation humaine, qui remonte à environ 10 000 ans. Contrairement à ce qui a été longtemps imaginé en Europe, l'Amazonie n'était pas couverte de forêts primaires inhabitées lors de l'arrivée des Européens, mais on estime qu'une population d'environ six à dix millions de personnes occupait la quasi totalité du paysage amazonien[32]. Ces populations pratiquaient pour la plupart une agriculture intensive, particulièrement sur les rives des grands fleuves[33], avec de nombreux foyers de domestication de plantes cultivables (manioc, patate douce, cacao, noix du Brésil, açaí, etc). Les marques de cette occupation du sol sont encore visibles sur la végétation amazonienne actuelle. Notons en particulier la grande diversité d'espèces utiles à proximité d'anciens villages amérindiens, et la présence sur au moins 0,2% de l'Amazonie de terres noires d'origine anthropique (*terra preta do índio* en portugais) particulièrement riches en matière organique[34]. L'arrivée des Européens au XVI^{e} siècle a décimé près de 95% des habitants de l'Amazonie, principalement par l'apport de maladies (variole, grippe, rougeole) apparues en Europe et jusqu'alors inconnues sur le continent sud-américain, puis par des massacres et asservissements de populations[35]. Les villages les plus proches des camps européens ont alors été rapidement abandonnés : la végétation qui y a repoussé pendant 500 ans est aujourd'hui souvent considérée comme de la forêt «primaire».

L'occupation de l'Amazonie reste alors relativement faible jusqu'au XIX^{e} siècle, se concentrant principalement dans les zones périphériques de l'Amazonie[36]. Le boom de l'exploitation du latex de l'hévéa (*Hevea brasiliensis*) pour la production de caoutchouc

[20] U. Oliveira et al. (2017). « Biogeography of Amazon birds : Rivers limit species composition, but not areas of endemism ». In : *Scientific Reports* 7.1, p. 1–11.

[21] C. Richard-Hansen et al. (2015). « Landscape patterns influence communities of medium-to large-bodied vertebrates in undisturbed terra firme forests of French Guiana ». In : *Journal of Tropical Ecology* 31.5, p. 423–436.

[22] L. S. Brasil et al. (2018). « Spatial, biogeographic and environmental predictors of diversity in Amazonian Zygoptera ». In : *Insect Conservation and Diversity* 11.2, p. 174–184.

[23] Hoorn et al. (2010). Cf. note 18.

[24] J. W. F. Slik et al. (2015). « An estimate of the number of tropical tree species ». In : *Proceedings of the National Academy of Sciences* 112.24, p. 7472–7477 ; Sullivan et al. (2017). « Diversity and carbon storage across the tropical forest biome », cf. note 6, p. 1.

[25] C. N. Jenkins et al. (2013). « Global patterns of terrestrial vertebrate diversity and conservation ». In : *Proceedings of the National Academy of Sciences* 110.28, E2602–E2610. arXiv : `arXiv:1408.1149`.

[26] J. M. C. Da Silva et al. (2005). « The fate of the Amazonian areas of endemism ». In : *Conservation Biology* 19.3, p. 689–694. arXiv : `j.1523-1739.2005.00705.x [10.1111]`.

[27] R. Dirzo et P. H. Raven (2003). « Global state of biodiversity and loss ». In : *Annual Review of Environment and Resources* 28.1, p. 137–167.

[28] Da Silva et al. (2005). Cf. note 26.

[29] A. Antonelli et al. (2018). « Amazonia is the primary source of Neotropical biodiversity ». In : *Proceedings of the National Academy of Sciences* 115.23, p. 6034–6039.

[30] F. S. Chapin III et al. (2000). « Consequences of changing biodiversity ». In : *Nature* 405.6783, p. 234–242. arXiv : `arXiv:1011.1669v3`.

[31] W. H. Lewis et M. P. Elvin-Lewis (1995). « Medicinal Plants as Sources of New Therapeutics ». In : *Annals of the Missouri Botanical Garden* 82.1, p. 16 ; R. R. Alves et I. M. Rosa (2007). « Biodiversity, traditional medicine and public health : where do they meet ? » In : *Journal of Ethnobiology and Ethnomedicine* 3.1, p. 14.

[32] C. R. Clement et al. (2015). « The domestication of Amazonia before European conquest ». In : *Proceedings of the Royal Society B : Biological Sciences* 282.1812, p. 20150813. arXiv : `9605103 [cs]`.

au XIX[e] siècle attire une première vague de colons, multipliant la population de l'Amazonie par quatre en un demi-siècle et provoquant la croissance fulgurante de métropoles telles que Manaus en plein cœur de la forêt et Belém dans l'estuaire de l'Amazone[37]. L'exploitation de l'hévéa ne nécessite cependant pas d'abattre les arbres, et elle n'est donc pas associée à une perte du couvert forestier en dehors des zones d'habitation et de culture. Ce boom économique ne dure cependant qu'une cinquantaine d'années, et bien que suivi par d'autres activités extrativistes, celles-ci n'atteignent pas la même ampleur économique[38].

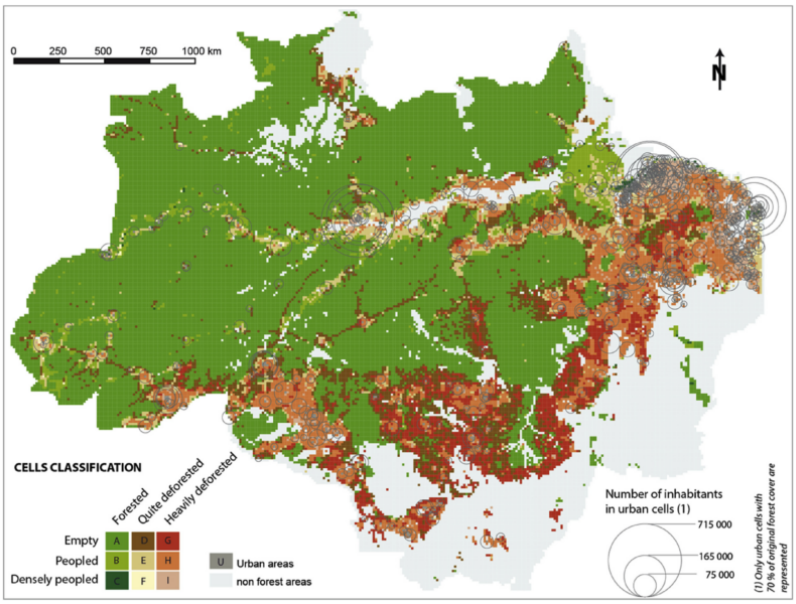

FIGURE 1.2 – Densité de peuplement et état de déforestation de l'Amazonie brésilienne en 2010. In Tritsch et Le Tourneau, 2016.

Dans les années 1940 et jusqu'aux années 1970, le gouvernement brésilien lance une suite de programmes visant l'occupation et le développement de l'agriculture en Amazonie. Cette politique prend un nouveau tournant à partir des années 1970 avec la construction de la route transamazonienne (1972) qui traverse l'Amazonie d'est en ouest, permettant l'accès à des zones jusqu'alors isolées[39]. La construction plus récente de nombreuses autres routes en Amazonie a encore accéléré cette tendance[40]. La déforestation se concentre alors sur l'ensemble de ces zones nouvellement accessibles dans le sud et sudest de l'Amazonie brésilienne (Figure 1.2), dans ce qui a été appelé l'«arc de déforestation », sur des fronts pionniers qui avancent graduellement depuis 50 ans. Dix-huit millions d'habitants vivent aujourd'hui en Amazonie, dont 13 dans les grands centres urbains[41]. Le reste de la population se trouve en majorité dans des zones rurales à moins de 30 km d'une route, où les densités humaines restent souvent relativement faibles (1 à 5 habitant par km^2)[42] (Figure 1.2).

[33] M. J. HECKENBERGER et al. (2007). « The legacy of cultural landscapes in the Brazilian Amazon : Implications for biodiversity ». In : *Philosophical Transactions of the Royal Society B : Biological Sciences* 362.1478, p. 197–208.

[34] CLEMENT et al. (2015). « The domestication of Amazonia before European conquest », cf. note 32, p. 3 ; M. W. PALACE et al. (2017). « Ancient Amazonian populations left lasting impacts on forest structure ». In : *Ecosphere* 8.12.

[35] D. CLEARY (2001). « Towards an Environmental History of the Amazon : From Prehistory to the Nineteenth Century ». In : *Latin American Research Review* 36.2, p. 64–96.

[36] Ibid.

[37] B. L. BARHAM et O. T. COOMES (1994). « Reinterpreting the Amazon rubber boom : Investment, the State, and Dutch disease ». In : *Latin American Research Review* 29.2, p. 73–109.

[38] CLEARY (2001). Cf. note 35.

[39] P. M. FEARNSIDE (2005). « Deforestation in Brazilian Amazonia : History, Rates, and Consequences ». In : *Conservation Biology* 19.3, p. 680–688.

[40] W. F. LAURANCE et al. (2009). « Impacts of roads and linear clearings on tropical forests ». In : *Trends in Ecology and Evolution* 24.12, p. 659–669. arXiv : `arXiv:1011.1669v3`.

[41] I. TRITSCH et F.-M. LE TOURNEAU (2016). « Population densities and deforestation in the Brazilian Amazon : New insights on the current human settlement patterns ». In : *Applied Geography* 76, p. 163–172.

[42] J. GODAR et al. (2012). « Who is responsible for deforestation in the Amazon ? A spatially explicit analysis along the Transamazon Highway in Brazil ». In : *Forest Ecology and Management* 267, p. 58–73.

Impacts des activités humaines récentes sur les forêts amazoniennes

Cette partie traite en particulier des activités humaines récentes (depuis les années 1970) qui ont suivi la construction de la Transamazonienne.

Déforestation et fragmentation Les modifications récentes affectant les forêts amazoniennes concernent principalement la conversion de forêts naturelles en zones agricoles. L'une des principales limites rencontrée est la perte rapide de la fertilité des sols, environ 2-3 ans après la défriche[43] : 80% des terres défrichées sont donc utilisées comme pâturage pour un élevage bovin très extensif[44]. Cet élevage requiert de grands terrains et génère peu d'emploi, ce qui a créé des conflits fonciers et favorisé un phénomène d'accumulation des parcelles par de grands propriétaires pratiquant principalement l'élevage et plus récemment la culture du soja[45]. Bien que la politique de développement lancée par le gouvernement brésilien visait initialement l'installation d'une agriculture familiale dans un but de réduction de pauvreté dans les régions au nord du pays, les zones déforestées sont aujourd'hui dominées par de grands propriétaires terriens (> 100 ha) et environ trois quarts de la déforestation est conduite par ces derniers[46]. La déforestation en Amazonie a ainsi crû entre 1970-2000 jusqu'à approcher les 30 000 km^2 par an en 1995 puis à nouveau en 2004 pour l'Amazonie brésilienne. L'aire totale déforestée atteint aujourd'hui les 64 Mha (17% de la surface des forêts amazoniennes)[47], soit une surface égale à l'intégralité du territoire français. Le rythme de perte des forêts amazonienne a alerté l'opinion publique internationale et l'Etat brésilien a en 2004 décidé de prendre des mesures drastiques pour réduire les émissions de carbone du pays, dont plus de 60% étaient générées par la déforestation[48]. De nombreux programmes publics ont été mis en place, notamment en Amazonie brésilienne, pour lutter contre la déforestation illégale : augmentation de la transparence par le développement d'outils de détection de la déforestation par satellite[49], renforcement de l'application des lois par l'intervention des forces militaires et la conditionnalité des prêts bancaires, augmentation de l'aire des zones protégées[50]. De plus, la pression de l'opinion publique a permis l'apparition d'initiatives privées de certification zero-déforestation dans la filière du soja. Ces mesures, ainsi que la chute des cours du soja en 2006, ont permis une diminution drastique de 70% du taux de déforestation à partir de 2005[51]. Les taux de déforestation avoisinent maintenant les 7 000 km^2 par an en Amazonie brésilienne, mais des études récentes montrent une augmentation de la déforestation de petites surfaces (< 1 ha) et un déplacement des fronts de déforestation vers la Bolivie et le Pérou (Figure 1.3)[52].

En plus de la perte nette de surface forestière, cette déforesta-

[43] P. Sanchez (1994). « Alternatives to slash and burn : a pragmatic approach for mitigating tropical deforestation ». In : *Agricultural Technology : Policy Issues for the International Community*. P. 45.

[44] J. B. Veiga et al. (2002). « Cattle ranching in the amazon rainforest ». In : *Proceedings of the Australian Society of Animal Production* 24.Br 010, p. 253–256.

[45] C. S. Simmons (2004). « The Political Economy of Land Conflict in the Eastern Brazilian Amazon ». In : *Annals of the Association of American Geographers* 94.January 2002, p. 183–206.

[46] Godar et al. (2012). Cf. note 42.

[47] INPE (2016). *Deforestation estimates in the Brazilian Amazon*.

[48] P Moutinho et al. (2005). *Tropical Deforestation and Climate Change*, p. 131.

[49] INPE (2018). *Programa DETER - Detecção de Desmatamento em Tempo Real*.

[50] D. Nepstad et al. (2014). « Slowing Amazon deforestation through public policy and interventions in beef and soy supply chains. » In : *Science* 344.6188, p. 1118–23.

[51] Ibid.

[52] M. Kalamandeen et al. (2018). « Pervasive Rise of Small-scale Deforestation in Amazonia ». In : *Scientific Reports* 8.1, p. 1–10.

tion intensive a conduit à la fragmentation des forêts naturelles restantes en des îlots de forêts dans un paysage anthropisé. Cette fragmentation est particulièrement importante dans les premiers fronts de déforestation au sud de l'Amazonie brésilienne, où les fragments de forêts font en moyenne moins de 10 ha[53]. La fragmentation a plusieurs conséquences sur les forêts (i) elle diminue la taille de l'habitat et sa perméabilité à la dispersion, ce qui peut entraîner la disparition de certaines espèces animales et végétales et donc une diminution de la diversité[54] ; (ii) la mortalité des arbres (surtout les plus grands) est plus élevée à proximité de la bordure des fragments, ce qui modifie la structure de la forêt et diminue sa biomasse[55].

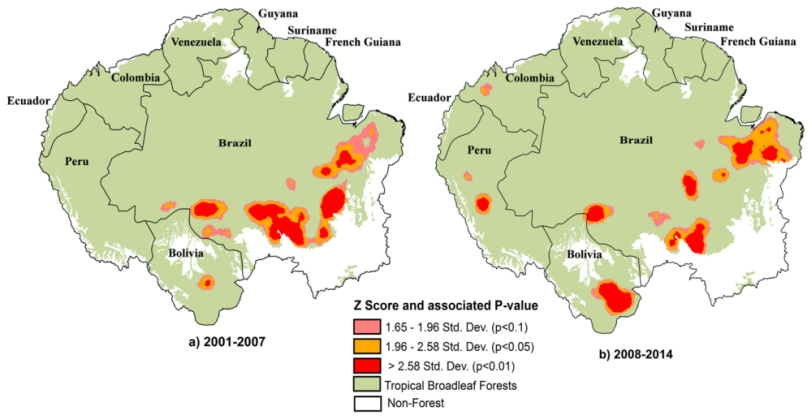

FIGURE 1.3 – Déplacement des fronts de déforestation de 2001 à 2014. In Kalamandeen et al, 2018[a].

(Sur)exploitation des ressources L'histoire récente de l'Amazonie a été marquée par plusieurs activités d'exploitation des ressources forestières, l'exemple le plus marquant étant l'extraction de l'hévéa qui a provoqué un boom économique majeur au XIX^{e} siècle[56]. Bien que le caoutchouc amazonien ait perdu son importance économique, d'autres produits non-ligneux jouent aujourd'hui un rôle socio-économique majeur, tels que la noix du Brésil (le premier producteur mondial est aujourd'hui la Bolivie avec la moitié de la production mondiale[57]) ; l'açaí (*Euterpe oleracea*[58]), ou encore l'huile de carapa (*Carapa guianensis*)[59]. Cependant la principale ressource exploitée en forêt amazonienne reste le bois : cette activité participe à environ 2% du produit intérieur brut des pays de la région et emploient un million de personnes[60].

L'exploitation sélective du bois affecte environ 2 millions d'hectares par an en Amazonie brésilienne[61] (Figure 1.4), soit une surface comparable à celle annuellement déforestée. L'exploitation sélective consiste en l'abattage et l'extraction de quelques grands arbres dans une parcelle, en général des espèces ayant une grande valeur commerciale. L'exploitation en Amazonie a longtemps été ultra-sélective, se concentrant sur quelques rares espèces nobles : acajou (*Swietenia macrophylla*), *ipê* au Brésil (*Handroantus spp.*) ou *morado* en Bolivie (*Machaerium spp.*). Cette sur-exploitation

[53] I. M. ROSA et al. (2017). « Spatial and temporal dimensions of landscape fragmentation across the Brazilian Amazon ». In : *Regional Environmental Change* 17.6, p. 1687–1699.

[54] N. M. HADDAD et al. (2015). « Habitat fragmentation and its lasting impact on Earth's ecosystems ». In : *Science Advances* 1.2, e1500052–e1500052.

[55] W. F. LAURANCE (2000). « Conservation : Rainforest fragmentation kills big trees ». In : *Nature* 404.6780, p. 836–836.

[a] M. KALAMANDEEN et al. (2018). « Pervasive Rise of Small-scale Deforestation in Amazonia ». In : *Scientific Reports* 8.1, p. 1–10.

[56] CLEARY (2001). « Towards an Environmental History of the Amazon : From Prehistory to the Nineteenth Century », cf. note 35, p. 4.

[57] M. PAZ SOLDÁN (2003). *The Impact of Certification on the Sustainable Use of Brazil Nut (Bertholletia excelsa) in Bolivia*. Rapp. tech.

[58] S WEINSTEIN et S MOEGENBURG (2004). « Açaí Palm Management in the Amazon Estuary : Course for Conservation or Passage to Plantations ? » In : *Conservation & Society* 2.2, p. 315–346.

[59] M. LONDRES et al. (2017). « Population Structure and Fruit Production of Carapa guianensis (Andiroba) in Amazonian Floodplain Forests ». In : *Tropical Conservation Science* 10, p. 194008291771883.

[60] FAO (2011). *The State of Forests in the Amazon Basin, Congo Basin and Southeast Asia*, cf. note 1, p. 1.

[61] ASNER et al. (2005). Cf. note 2.

de certaines espèces a conduit à leur raréfaction dans les zones proches des grands axes routiers[62].

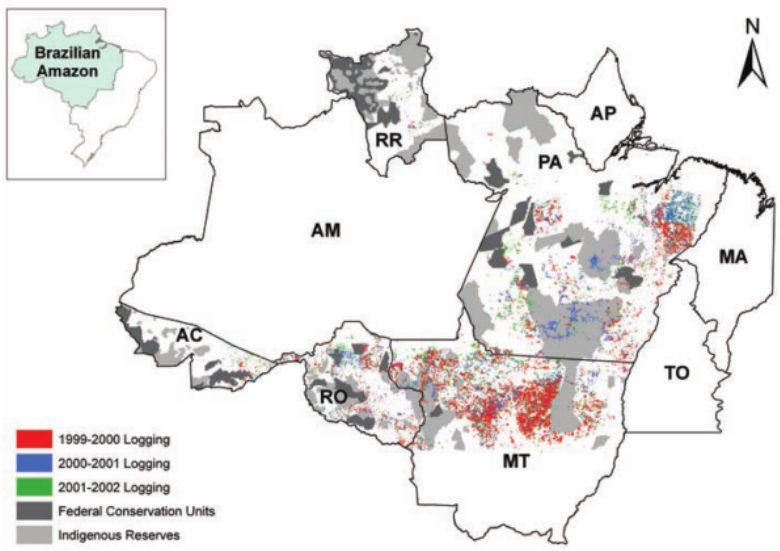

FIGURE 1.4 – Détection de l'exploitation sélective en Amazonie brésilienne entre 1999 et 2002. In Asner *et al.*, 2005[a].

Puisqu'elle ne vise que quelques arbres cette exploitation n'aboutit donc pas nécessairement à une déforestation totale. Souvent, pourtant, l'exploitation n'est qu'une première étape de la conversion des forêts en pâturage : les arbres commerciaux étaient exploités et vendus avant la déforestation totale de la parcelle. Dans les cas où l'exploitation n'est pas suivie de déforestation, la canopée se referme rapidement après la fin des opérations, et après 2-4 ans seules les pistes d'exploitation sont visibles sur des images satellites[63]. Pourtant, l'exploitation et les dégâts collatéraux (ouverture de pistes, abattage, extraction des grumes) modifient durablement les forêts exploitées, et les effets peuvent être visibles plusieurs décennies après la coupe : réduction et de la hauteur de la canopée[64], modification de la composition floristique[65]. De plus, l'ouverture de piste dans les massifs forestiers permet l'accès aux forêts pour d'autres activités telles que la chasse[66]. Ces activités réduisent la diversité des gros mammifères et oiseaux, diminuant alors la dispersion des graines et *in fine* la composition, la structure et la biomasse des forêts[67].

Les effets secondaires - feux et changements climatiques
Les changements climatiques anthropiques récents ont modifié le régime des précipitations en Amazonie, avec comme principale conséquence l'augmentation de la fréquence des épisodes de sécheresse. Il est prévu que cette tendance s'accentue au cours du XXI^{e} siècle : augmentation de la variabilité des précipitations et d'évènements climatiques extrêmes sur l'ensemble de l'Amazonie[68]. Ces sécheresses entraînent une surmortalité des arbres, et particulièrement des plus gros[69], modifiant ainsi la structure et la biomasse des forêts affectées[70]. Les sécheresses des années 2005,

[62] V. A. RICHARDSON et C. A. PERES (2016). « Temporal decay in timber species composition and value in amazonian logging concessions ». In : *PLoS ONE* 11.7, p. 1–22.

[a] G. P. ASNER et al. (2005). « Selective Logging in the Brazilian Amazon ». In : *Science* 310.5747, p. 480–482.

[63] G. P. ASNER et al. (2004). « Spatial and temporal dynamics of forest canopy gaps following selective logging in the eastern Amazon ». In : *Global Change Biology* 10.5, p. 765–783.

[64] E. RUTISHAUSER et al. (2016). « Tree Height Reduction After Selective Logging in a Tropical Forest ». In : *Biotropica* 48.3, p. 285–289.

[65] A. L. DE AVILA et al. (2015). « Medium-term dynamics of tree species composition in response to silvicultural intervention intensities in a tropical rain forest ». In : *Biological Conservation* 191, p. 577–586.

[66] LAURANCE et al. (2009). « Impacts of roads and linear clearings on tropical forests », cf. note 40, p. 4.

[67] C. A. PERES et al. (2016). « Dispersal limitation induces long-term biomass collapse in overhunted Amazonian forests ». In : *Proceedings of the National Academy of Sciences* 113.4, p. 892–897. arXiv : `arXiv:1408.1149`.

[68] P. B. DUFFY et al. (2015). « Projections of future meteorological drought and wet periods in the Amazon ». In : *Proceedings of the National Academy of Sciences* 112.43, p. 13172–13177.

[69] A. C. BENNETT et al. (2015). « Larger trees suffer most during drought in forests worldwide ». In : *Nature Plants* 1.10, p. 15139.

[70] M. LONGO et al. (2018). « Ecosystem heterogeneity and diversity mitigate Amazon forest resilience to frequent extreme droughts ». In : *New Phytologist*.

2010 et 2015/2016 ont été particulièrement fortes et ont globalement diminué la biomasse vivante des forêts amazoniennes[71].

L'effet conjoint de la fragmentation et des sécheresses a eu comme conséquence d'augmenter la fréquence des feux de forêt[72]. En effet, les forêts fragmentées ou ayant subi un épisode de sécheresse sont plus riches en bois mort, et ont une canopée plus ouverte donc une augmentation de la température au sol et un air plus sec sous la canopée. Ces conditions sont favorables à des départs de feux[73] qui ont été de plus en plus fréquents en Amazonie[74], surtout dans les forêts les plus dégradées (Figure 1.5).

L'Histoire récente de l'humanité a donc vu des modifications profondes des forêts amazoniennes, par la déforestation et l'exploitation des ressources, mais aussi à plus large échelle à travers les changements climatiques. De plus, les boucles de rétroaction sont nombreuses[75] et, sans modification proactive des dynamiques en cours, peuvent conduire à la transformation progressive des forêts amazoniennes en des paysages hautement dégradés[76] :

- la déforestation augmente la fragmentation du milieu et modifie les cycles du carbone et de l'eau, augmentant ainsi les changements climatiques[77] ;
- la fragmentation, l'exploitation (surtout intensive) et les changements climatiques augmentent le risque de feux ;
- les zones dégradées par l'exploitation et/ou des feux ont plus de chances d'être déforestées[78].

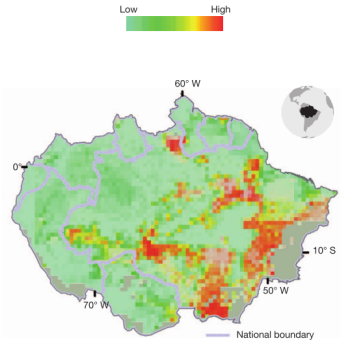

FIGURE 1.5 – Risques de feux en Amazonie. In Davidson *et al.*, 2012[a]. Les zones les plus propices aux départs de feux sont les fronts pionniers où les forêts sont intensément dégradées par les activités humaines.

1.1.3 Le rôle de la gestion forestière

À partir de la deuxième moitié du XX[e] siècle la prise de conscience des enjeux environnementaux liés aux forêts amazoniennes ont conduit les autorités publiques à réglementer leur usage.

Un réseau dense d'aires protégées

Le principal outil de conservation des forêts en Amazonie est le status légal de protection. Les aires protégées couvrent aujourd'hui plus de la moitié de la surface totale de l'Amazonie[79]. Ce status d'aire protégée regroupe en fait une grande diversité de cadres légaux et de niveaux de protection. Trois grands types de protection peuvent être différenciés :

- les aires de protection intégrale, dont l'accès est plus ou moins restreint et où aucun produit (ligneux ou non-ligneux) ne peut être exploité,
- les aires de gestion durable des ressources naturelles,
- les terres indigènes dont l'usage est réservé aux populations indigènes traditionnelles.

Par les restrictions d'usages qui y sont associées, les aires protégées comme les terres indigènes ont effectivement permis un ralentissement de la déforestation[80].

[71] O. L. PHILLIPS et al. (2009). « Drought Sensitivity of the Amazon Rainforest ». In : *Science* 323.5919, p. 1344–1347 ; S. L. LEWIS et al. (2011). « The 2010 Amazon drought. » In : *Science (New York, N.Y.)* 331.Ci, p. 554. arXiv : `science.1200807 [10.1126]` ; J. C. JIMÉNEZ-MUÑOZ et al. (2016). « Record-breaking warming and extreme drought in the Amazon rainforest during the course of El Niño 2015–2016 ». In : *Scientific Reports* 6.1, p. 33130.

[72] P. M. BRANDO et al. (2014). « Abrupt increases in Amazonian tree mortality due to drought-fire interactions ». In : *Proceedings of the National Academy of Sciences* 111.17, p. 6347–6352 ; A. A. ALENCAR et al. (2015). « Landscape fragmentation, severe drought, and the new Amazon forest fire regime ». In : *Ecological Applications* 25.6, p. 1493–1505. arXiv : `arXiv:1011.1669v3`.

[73] W. M. JOLLY et al. (2015). « Climate-induced variations in global wildfire danger from 1979 to 2013 ». In : *Nature Communications* 6.May, p. 1–11.

[74] L. E. O. C. ARAGÃO et al. (2018). « 21st Century drought-related fires counteract the decline of Amazon deforestation carbon emissions ». In : *Nature Communications* 9.1, p. 536.

[a] E. a. DAVIDSON et al. (2012). « The Amazon basin in transition ». In : *Nature* 481.7381, p. 321–328.

[75] DAVIDSON et al. (2012). Cf. note *a*.

[76] C. A. NOBRE et al. (2016). « Land-use and climate change risks in the Amazon and the need of a novel sustainable development paradigm ». In : *Proceedings of the National Academy of Sciences*, p. 1–10.

Les aires protégées ont cependant certaines limites. D'abord, la taille du territoire amazonien rend difficile leur surveillance et leur contrôle pour les autorités chargées de leur gestion. Les aires protégées ne sont donc pas des barrières absolues contre la déforestation et la dégradation des forêts : de l'exploitation et de la déforestation illégales peuvent être détectées dans des aires protégées[81]. Les aires protégées peuvent aussi générer des fuites, dans ce cas la déforestation ne serait pas évitée, mais déplacée vers des zones adjacentes[82]. De plus, les aires protégées sont souvent confinées aux zones les moins accessibles[83]. Lors de l'apparition d'un conflit d'utilisation (projets miniers, de barrage, etc.), le statut de protection s'est souvent révélé vulnérable face aux pressions économiques[84]. Un exemple marquant est le cas en Equateur du parc du Yasuni, l'une des zones où la biodiversité est la plus riche au monde[85]. D'importantes réserves de pétrole ont été découvertes dans la zone de cœur du parc. Après des négociations pour obtenir une compensation pour le coût d'opportunité de la protection du parc, le gouvernement équatorien a finalement décidé d'exploiter les réserves de pétrole[86].

Gestion des forêts de production

Au cours de la deuxième moitié du XX^{e} siècle, la prise de conscience de la limite finie des ressources exploitées dans les forêts naturelles d'Amazonie provoque un changement de paradigme dans leur utilisation. On passe alors d'une vision extractiviste où les ressources exploitées (caoutchouc, balata, bois précieux) semblent inépuisables à la volonté d'une gestion durable[87]. Les Etats ont défini des domaines forestiers permanents dédiés à la production, qui couvrent aujourd'hui 20% de l'Amazonie et sont principalement gérés pour la production de bois[88]. La gestion durable des forêts de production (*Sustainable forest management* en anglais) telle que définie par l'organisation internationale des bois tropicaux[89,90] doit :

- maintenir la valeur environnementale de ces forêts
- assurer leur productivité future
- éviter des effets indésirables sur l'environnement physique et social.

En Amazonie, les forêts de production ont divers types de gouvernance :

- des forêts publiques sont gérées par les services forestiers nationaux, qui accordent des concessions forestières à des entreprises privées contre une taxe sur la production,
- des forêts privées peuvent appartenir à des individus ou à des entreprises,
- des forêts communautaires sont gérées par des communautés locales, qui régissent les droits d'accès et d'usage de la forêt : ces droits peuvent être informels ou légalement établis[91].

[77] Y. Malhi et al. (2008). « Climate change, deforestation, and the fate of the Amazon. » In : *Science (New York, N.Y.)* 319.5860, p. 169–72.

[78] G. P. Asner et al. (2006). « Condition and fate of logged forests in the Brazilian Amazon. » In : *Proceedings of the National Academy of Sciences of the United States of America* 103.34, p. 12947–50.

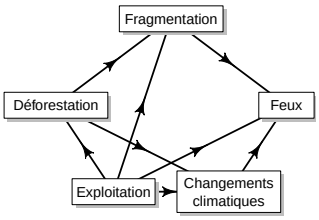

Figure 1.6 – Schéma des boucles de rétroaction potentielles dans les dynamiques d'anthropisation des forêts amazoniennes.

[79] W. Walker et al. (2014). « Forest carbon in Amazonia : the unrecognized contribution of indigenous territories and protected natural areas ». In : *Carbon Management* 3004.February 2015, p. 1–7.

[80] C. P. Barber et al. (2014). « Roads, deforestation, and the mitigating effect of protected areas in the Amazon ». In : *Biological Conservation* 177.November, p. 203–209.

[81] A. Pfaff et al. (2015). « Protected area types, strategies and impacts in Brazil's Amazon : Public protected area strategies do not yield a consistent ranking of protected area types by impact ». In : *Philosophical Transactions of the Royal Society B : Biological Sciences* 370.1681 ; J. J. Miranda et al. (2016). « Effects of Protected Areas on Forest Cover Change and Local Communities : Evidence from the Peruvian Amazon ». In : *World Development* 78, p. 288–307.

[82] Barber et al. (2014). Cf. note 80.

[83] L. N. Joppa et al. (2008). « On the protection of "protected areas". » In : *Proceedings of the National Academy of Sciences* 105.18, p. 6673–8.

[84] J. Ferreira et al. (2014). « Brazil's environmental leadership at risk ». In : *Science* 346.6210, p. 706–707.

[85] M. S. Bass et al. (2010). « Global conservation significance of Ecuador's Yasuní National Park ». In : *PLoS ONE* 5.1.

[86]L. G. Fierro (2016). « Oil or 'life' : the dilemma inherent in the yasuní-ITT initiative ». In : *Extractive Industries and Society* 3.4, p. 939–946.

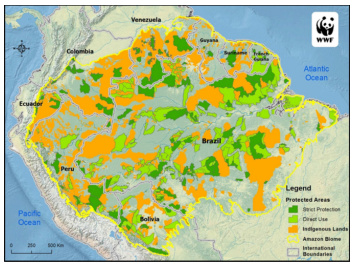

Figure 1.7 – Status de protection des forêts amazoniennes. Source : WWF

[87]K. G. MacDicken et al. (2015). « Global progress toward sustainable forest management ». In : *Forest Ecology and Management* 352, p. 47–56.

[88]FAO (2011). *The State of Forests in the Amazon Basin, Congo Basin and Southeast Asia*, cf. note 1, p. 1.

[89]International Tropical Timber Organization ou ITTO

[90]ITTO (1992). *Criteria for the measurement of sustainable forest management.*

[91]J. B. Alcorn (2014). « Lessons Learned From Community Forestry and Their Relevance for REDD+. USAID-supported Forest Carbon, Markets and Communities (FCMC) Program. » In : January.

[92]Blaser et al. (2011). *Status of Tropical Forest Management 2011*, cf. note 1, p. vi.

[93]T. S. Fredericksen et al. (2003). « Sustainable forestry in Bolivia - Beyond planning logging ». In : *Journal of Forestry* 101.2, p. 37–40.

[94]B. Soares-Filho et al. (2014). « Cracking Brazil ' s Forest Code ». In : *Science* 344.April, p. 363–364.

[95]M. Finer et al. (2014). « Logging Concessions Enable Illegal Logging Crisis in the Peruvian Amazon ». In : *Scientific reports* 4.4719, p. 1–6 ; P. H. S. Brancalion et al. (2018). « Fake legal logging in the Brazilian Amazon ». In : *Science Advances* 4.8, eaat1192.

[96]B. Pokorny et J. Johnson (2008). « Community forestry in the Amazon : The unsolved challenge of forests and the poor ». In : *Natural Resource Perspectives* 112.February, p. 1–4 ; M. G. Piketty et al. (2015). « Annual cash income from community forest management in the Brazilian Amazon : Challenges for the future ». In : *Forests* 6.11, p. 4228–4244.

Dès les années 1990, des codes forestiers ont été élaborés dans plusieurs pays d'Amazonie pour assurer une exploitation durable des ressources en bois[92]. Ces codes forestiers définissent notamment la durée minimum d'un cycle d'exploitation, c'est-à-dire le temps entre deux coupes (en général autour de 30 ans) ; le diamètre minimum d'exploitabilité des arbres (en général autour de 50 cm DHP) ; et l'intensité maximum d'exploitation (en général entre 20 et 30 m^3 de bois extrait par hectare). De plus, l'exploitation du bois est soumise au Brésil et en Bolivie à la validation d'un plan de gestion élaboré par le propriétaire et comprenant[93] :

- la délimitation de l'aire exploitée et la division en unités annuelles,
- au Brésil, la délimitation d'aires protégées au sein de l'exploitation (*reserva legal*)[94],
- un inventaire pré-exploitation de tous les arbres commerciaux,
- en Bolivie, des inventaires de suivi de la dynamique post-exploitation des zones exploitées.

Plusieurs critiques sont faites au système actuel de gestion des forêts de production. De nombreuses études montrent que 20-60% de l'exploitation forestière se fait de manière illégale en Amazonie : les plans de gestion sont rarement suivis[95], et le contrôle de la bonne application du code forestier reste difficile à vérifier et appliquer au vu de l'étendue des territoires. Enfin, il favorise l'exploitation par des entreprises ou des particuliers ayant les moyens financiers et l'accès à l'information facilitant l'obtention de permis d'exploiter. À l'inverse les communautés locales et petits producteurs rencontrent de nombreuses difficultés pour appliquer les réglementations en vigueur, questionnant ainsi la valeur sociale d'un tel système[96].

Sous l'influence de l'opinion publique de plus en plus sensible aux questions de déforestation et d'exploitation illégale[97], des initiatives privées de certification ont vu le jour dès 1992, pour assurer un plus grand contrôle de l'origine du bois et une amélioration des pratiques d'exploitation[98]. Aujourd'hui, deux grands organismes non-gouvernementaux certifient l'exploitation du bois : le *Forest Stewardship Council* (FSC) et le *Programme for the Endorsement of Forest Certification* (PEFC). Cinq-mille ha de forêts naturelles sont certifiées en Amazonie, soit 5% de l'aire totale des forêts de production[99]. La part de forêts certifiée est particulièrement importante en Bolivie : 2 millions d'hectares sont certifiés, soit 22% des forêts naturelles de production, et dont 60% de la production est destinée à l'export[100]. Dans les autres pays d'Amazonie, la certification a eu un succès plus mitigé (Brésil, Pérou) voire quasi-inexistant. La principale raison reste le coût élevé de la certification, qui la rend peu compétitive par rapport au bois issu de l'exploitation illégale[101].

Les initiatives publiques et privées pour lutter contre l'ex-

TABLE 1.1 – Caractéristiques de la gestion des forêts amazoniennes par pays. Source : FAO, 2011 et Blaser et al., 2011.

Pays	Bolivie	Brésil	Colombie	Equateur	Guyana	Guyane Fr.	Pérou	Suriname	Venezuela
Surface forestière (Mha)	52	354	41	10	17	8	73	14	32
Forêts protégées (Mha)	12	110	8	3	1	4	16	2	11
Forêts de production (Mha)	25	150	5	2	5	2	19	5	9
Forêts publiques (%)	51	51	22	15	80	100	62	85	96
Forêts privées (%)	36	19	67	2	20	-	18	15	4
Forêts communautaires (%)	13	30	11	83	-	-	20	-	-
Production de bois d'œuvre (Mm^3an^{-1})	0.91	28.2	0.81	1.18	0.37	0.08	1.30	0.38	0.18
Production de bois de sciage (Mm^3an^{-1})	0.46	8.56	0.38	0.42	0.07	0.03	0.67	0.11	0.28
Bois de sciage exporté (%)	23	8	4	28	45	18	43	12	0
Durée minimum d'une rotation (ans)	20	35	-	-	60	65	20	-	30
Intensité d'exploitation maximum légale (m^3ha^{-1})	-	30	-	-	20	-	25	25	-

ploitation illégale permettant un meilleur contrôle des modalités de l'exploitation. Elles n'assurent pas pour autant la durabilité des ressources exploitées. En effet, plusieurs études montrent que l'exploitation, même légale, n'est souvent pas durable au sens défini par l'ITTO, et en particulier que la quantité de bois exploitable diminue fortement après un ou deux cycles d'exploitation[102]. Parmi les pistes proposées pour améliorer le renouvellement des ressources en bois on trouve[103] :

- la réduction des dégâts liés à l'exploitation[104] : planification des pistes, abattage directionnel des arbres exploités[105],
- des traitements post-exploitation pour diminuer la compétition sur les futurs arbres exploitables : élimination des lianes[106], éclaircissement des plus gros individus d'espèces non-commerciales[107],
- des traitements post-exploitation pour augmenter la régénération des espèces commerciales : enrichissement des trouées d'exploitation avec des plantules d'espèces commerciales[108].

En dehors de certaines techniques d'exploitation à faible impact qui sont aujourd'hui exigées pour obtenir la certification FSC[109], l'application de traitements sylviculturaux post-exploitation reste quasi-inexistant sous les tropiques, principalement cantonné à des discussions académiques[110].

[97] GREENPEACE BRASIL (2014). *The Amazon 's silent crisis*. Rapp. tech., p. 4.

[98] E. RAMETSTEINER et M. SIMULA (2003). « Forest certification - An instrument to promote sustainable forest management ? » In : *Journal of Environmental Management* 67.1, p. 87–98.

[99] FAO (2011). *The State of Forests in the Amazon Basin, Congo Basin and Southeast Asia*, cf. note 1, p. 1.

[100] J. EBELING et M. YASUÉ (2009). « The effectiveness of market-based conservation in the tropics : Forest certification in Ecuador and Bolivia ». In : *Journal of Environmental Management* 90.2, p. 1145–1153.

[101] C. L. MCDERMOTT et al. (2015). « Forest certification and legality initiatives in the Brazilian Amazon : Lessons for effective and equitable forest governance ». In : *Forest Policy and Economics* 50, p. 134–142.

[102] P. SIST et F. N. FERREIRA (2007). « Sustainability of reduced-impact logging in the Eastern Amazon ». In : *Forest Ecology and Management* 243.2-3, p. 199–209 ; F. E. PUTZ et al. (2012). « Sustaining conservation values in selectively logged tropical forests : the attained and the attainable ». In : *Conservation Letters* 5.4, p. 296–303 ; B. L. ZIMMERMAN et C. F. KORMOS (2012). « Prospects for Sustainable Logging in Tropical Forests ». In : *BioScience* 62.5, p. 479–487.

1.2 La notion de résilience

L'un des fondements de la gestion durable des forêts est la notion de résilience. En effet, l'exploitation des ressources ne peut être maintenue dans le temps que si les ressources exploitées se régénèrent après leur exploitation. Sans cette capacité, une exploitation prolongée aboutirait au déclin des ressources et à la dégradation, voire la disparition, des écosystèmes ainsi modifiés. Cette persistance des écosystèmes et de leurs caractéristiques face aux perturbations est appelée résilience par analogie avec la physique des matériaux, et a été longtemps étudiée en écologie[111].

1.2.1 Des forêts perturbées

Définition de la perturbation

Pour comprendre la résilience, il faut se pencher sur ce que constitue une perturbation en écologie[112]. Une perturbation est un événement discret modifiant l'état d'un système, le plus souvent traduit par une surmortalité des individus d'une communauté, permettant ensuite à d'autres individus de prendre leur place[113]. Une perturbation provoque donc le passage abrupt d'un système dans un état transitoire. Lorsque la perturbation s'arrête, le système peut alors retourner à son état initial, ou basculer vers un nouvel état. Lorsqu'un système est soumis à des perturbations de manière récurrente, on parle alors du régime de perturbations. Les perturbations peuvent être caractérisées par leur durée, leur intensité, leur étendue spatiale et, lorsqu'il y a plusieurs évènements de perturbation, leur fréquence[114].

Bien que l'intensité et la durée de la perturbation modifient la dynamique de la forêt[115], il est rare d'avoir une caractérisation aussi fine de la perturbation dans les forêts tropicales, car souvent l'historique de la forêt avant et pendant la perturbation manque. Parce que l'exploitation est une perturbation contrôlée et qui a une grande importance économique, des forêts ont été expérimentalement exploitées et suivies dans plusieurs régions d'Amazonie, et ce, depuis plusieurs décennies. Les données utilisées dans cette thèse regroupent 15 sites expérimentaux où des forêts ont été suivies avant, pendant et après l'exploitation[116], et les résultats issus de cette étude pourront ainsi permettre de mieux comprendre la réponse des forêts amazoniennes aux perturbations.

Dans le cadre de cette thèse, le système étudié est la parcelle forestière. Ce système subit une unique perturbation : l'exploitation sélective, parfois accompagnée d'autres traitements sylviculturaux (exploitation des petites tiges pour du bois de feu, éclaircissement de gros arbres non-commerciaux, suppression des lianes). La perturbation a été caractérisée en fonction de l'évolution du stock de carbone aérien de la parcelle. La durée de la perturbation est définie comme l'intervalle de temps (de 1 à 4 ans) pendant lequel

[103] F. E. Putz et al. (2014). « A More Realistic Portrayal of Tropical Forestry : Response to Kormos and Zimmerman ». In : *Conservation Letters* 7.2, p. 145–146.

[104] Ces techniques sont regroupées sous le terme d'exploitation à faible impact, ou *Reduced-Impact Logging* en anglais.

[105] F. E. Putz et al. (2008). « Reduced-impact logging : Challenges and opportunities ». In : *Forest Ecology and Management* 256.7, p. 1427–1433.

[106] S. Estrada-Villegas et S. A. Schnitzer (2018). « A comprehensive synthesis of liana removal experiments in tropical forests ». In : *Biotropica*.

[107] M. Peña-Claros et al. (2008). « Regeneration of commercial tree species following silvicultural treatments in a moist tropical forest ». In : *Forest Ecology and Management* 255.3-4, p. 1283–1293.

[108] K. Keefe et al. (2009). « Enrichment planting as a silvicultural option in the eastern Amazon : Case study of Fazenda Cauaxi ». In : *Forest Ecology and Management* 258.9, p. 1950–1959.

[109] FSC (2014). *FSC Monitoring & Evaluation Report*. Rapp. tech.

[110] F. E. Putz et C. Romero (2014). « Futures of tropical forests (sensu lato) ». In : *Biotropica* 46.4, p. 495–505.

[111] C. S. Holling (1973). « Resilience and Stability of Ecological Systems ». In : *Annual Review of Ecology and Systematics* 4.1, p. 1–23.

[112] En anglais on distingue *disturbance*, le phénomène perturbateur, de *perturbation*, l'effet de ce phénomène sur le système étudié. Ici, la perturbation est comprise au sens de *disturbance*

[113] W. P. Sousa (1984). « The Role of Disturbance in Natural Communities ». In : *Annual Review of Ecology and Systematics* 15.1, p. 353–391 ; E. J. RYKIEL (1985). « Towards a definition of ecological disturbance ». In : *Austral Ecology* 10.3, p. 361–365.

[114] C. R. Drever et al. (2006). « Can forest management based on natural disturbances maintain ecological resilience ? » In : *Canadian Journal of Forest Research* 36.9, p. 2285–2299.

[115] J. F. Johnstone et al. (2016). « Changing disturbance regimes, ecological memory, and forest resilience ». In : *Frontiers in Ecology and the Environment* 14.7, p. 369–378. arXiv : `arXiv:1011.1669v3`.

[116] P. Sist et al. (2015). « The Tropical managed Forests Observatory : A research network addressing the future of tropical logged forests ». In : *Applied Vegetation Science* 18, p. 171–174.

le stock de carbone décroît après l'exploitation. La durée de cette surmortalité est due aux dégâts d'exploitation (arbres abîmés lors des opérations) et, lorsqu'il y en a eu, aux traitements sylviculturaux. L'intensité de l'exploitation est caractérisée par la perte de carbone entre le début et la fin de la perturbation, proportionnellement au stock initial (cf. exemple en Figure 1.8). L'intérêt de cette définition de la perturbation est qu'elle est suffisamment générique pour pouvoir décrire d'autres types de perturbations affectant les forêts tropicales selon un gradient allant de 0% à 100% de biomasse perdue (déforestation).

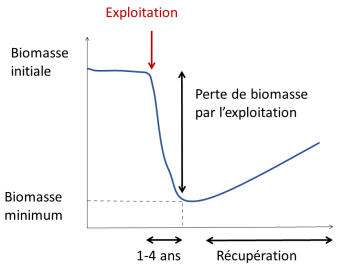

FIGURE 1.8 – Effet de l'exploitation sur la biomasse aérienne d'une parcelle forestière.

Perturbations et forêts amazoniennes

Les perturbations naturelles structurent les forêts amazoniennes En forêt amazonienne, les perturbations naturelles sont principalement créées par des chablis, *i.e.* le déracinement et la chute d'arbres de canopée créant des ouvertures dans la forêt. Ces ouvertures modifient l'environnement lumineux local. Lorsque la trouée est suffisamment grande, les nouvelles conditions ainsi créées favorisent l'apparition d'individus d'espèces dites pionnières à croissance rapide incapables de se développer dans des environnements de sous-canopée pauvres en lumière. Par la diversité de conditions qu'elles créent, les perturbations structurent les forêts, créant une hétérogénéité à la fois temporelle et spatiale. Selon l'hypothèse des perturbations intermédiaires, la diversité d'espèces est maximale pour un niveau de perturbation intermédiaire permettant à la fois la présence d'espèces favorisées par de hauts niveaux de perturbation, et d'espèces favorisées par de faibles niveaux de perturbation[117]. Le niveau de perturbation structure donc la diversité et la composition à l'échelle locale, mais aussi régionale[118].

[117] F. BONGERS et al. (2009). « The intermediate disturbance hypothesis applies to tropical forests, but disturbance contributes little to tree diversity ». In : *Ecology Letters* 12.8, p. 798–805.

[118] S. GUITET et al. (2018). « Disturbance Regimes Drive the Diversity of Regional Floristic Pools Across Guianan Rainforest Landscapes ». In : *Scientific Reports* 8.1, p. 1–12.

[119] cf. section 1.1.2

Augmentation du régime de perturbations anthropiques Les forêts amazoniennes sont soumises à des perturbations d'origine humaine : exploitation sélective, évènements climatiques extrêmes et feux[119]. Comme les perturbations naturelles, ce sont des évènements transitoires de surmortalité qui modifient significativement les caractéristiques des forêts affectées. Pourtant, ce nouveau régime de perturbations diffère du régime naturel principalement par la fréquence et l'intensité des perturbations qui est devenue plus élevée, et est prévue de continuer à augmenter dans le futur[120]. En effet, les évènements climatiques extrêmes vont devenir plus fréquents[121], augmentant aussi la fréquence des feux.

[120] Y. MALHI et al. (2015). « The linkages between photosynthesis , productivity , growth and biomass in lowland Amazonian forests ». In : *Global Change Biology* 21, p. 2283–2295.

[121] DUFFY et al. (2015). « Projections of future meteorological drought and wet periods in the Amazon », cf. note 68, p. 7.

1.2.2 Comment se maintiennent les écosystèmes malgré les perturbations ?

Historique de la notion de succession en écologie

La stabilité des écosystèmes a d'abord été expliquée comme le résultat d'un processus de succession amenant à un équilibre stable, ou climax, caractérisé par la composition des communautés d'organismes et déterminé par les conditions climatiques[122]. Cette notion de succession déterministe a connu un vif succès et a modelé l'écologie du XX^{e} siècle, mais a aussi été le sujet de nombreuses critiques. Une autre vision est développée à l'époque, plus individualiste, qui réfute la vision d'un écosystème comme une entité cohérente et prédictible et laisse plus de part au hasard[123]. Ces deux visions restent cependant très théoriques et manquent de cas d'études concrets, l'écologie étant à l'époque une science jeune. Avec l'accumulation de données, une vision plus inductive se développe, décrivant l'état d'équilibre des écosystèmes en fonction de caractéristiques telles que sa biomasse ou la diversité des organismes (et non plus l'identité des organismes eux-mêmes). Cette nouvelle vision se range dans la lignée clementsienne, car elle admet toujours un état d'équilibre vers lequel tend l'écosystème, et cet état correspond au niveau maximum de complexité (biomasse, diversité) que peut atteindre l'écosystème dans les limites de l'environnement physique local[124].

La principale limite de ces théories est qu'elles négligent à la fois les modifications temporelles de l'environnement et l'importance des perturbations. Or comme vu ci-dessus, les perturbations naturelles jouent un rôle central dans la structuration des écosystèmes. En effet, la fréquence des perturbations naturelles est en général bien supérieure au temps de succession[125] : les écosystèmes sont donc plutôt des mosaïques d'états post-perturbation que des entités homogènes et stables[126]. Aujourd'hui le paradigme dominant n'est plus celui d'un équilibre stable mais dynamique, définit par des cycles de perturbations - récupération[127].

Approche développée dans cette étude

L'approche de la phase de récupération post-exploitation développée dans cette étude s'inspire en grande partie de la littérature sur les successions écologiques. Le système étudié (l'ensemble des arbres d'une parcelle forestière) est décrit selon certaines caractéristiques écosystémiques : un stock (par exemple de carbone) et par des flux entrants et sortants. Au cours de la phase de récupération, le système converge vers un état d'équilibre caractérisé par des quantités constantes : les flux sont constants, et la résultante des flux (les gains moins les pertes) est nulle : les stocks sont donc aussi constants. L'état d'équilibre dépend des caractéristiques de l'environnement local (climat, sol) : il pourrait donc varier dans le temps (par exemple avec les changements

[122] F. E. Clements (1916). *Plant succession : an analysis of the development of vegetation*. Carnegie Institution of Washington.

[123] H. A. Gleason (1917). « The Structure and Development of the Plant Association ». In : *Bulletin of theTorrey Botanical Society* 44.10, p. 463–481.

[124] E. P. Odum (1969). « The Strategy of Ecosystem Development ». In : *Science* 164, p. 262–270.

[125] P. M. Attiwill (1994). « The disturbance of forest ecosystems : the ecological basis for conservative management ». In : *Forest Ecology and Management* 63.2-3, p. 247–300.

[126] Sousa (1984). « The Role of Disturbance in Natural Communities », cf. note 113, p. 12.

[127] Holling (1973). « Resilience and Stability of Ecological Systems », cf. note 111, p. 12.

prévus du régime de précipitation). Cependant dans l'ensemble des études présentées ici l'état d'équilibre a été décrit comme constant sur la période de mesure (de 10 à 30 ans selon les sites, Table 2.1). L'état d'équilibre ainsi décrit n'est cependant jamais atteint. L'état du système s'approche de cet état stationnaire tant qu'il n'y a pas de perturbation, et s'en éloigne dès que survient une perturbation (Figure 1.9).

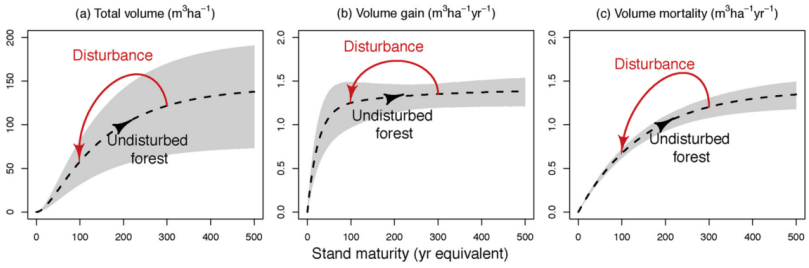

FIGURE 1.9 – Stock de volume (a) et des changements annuels : flux entrant (b) et sortant (c), tels que modélisés dans cette thèse à partir des données de Paracou (cf. Chapitre 6). Tant qu'il n'y a pas de perturbation, la maturité de la forêt augmente et la forêt tend vers un état d'équilibre asymptotique (i.e. l'équilibre n'est jamais atteint : il s'agit du comportement limite du système) ; quand survient une perturbation (flèche rouge) le système revient à un état antérieur.

Dans ce cadre d'analyse, défini de manière plus approfondie à partir du chapitre 6, l'état du système peut alors être caractérisé par sa maturité. La maturité est ici définie de la sorte : la maturité est nulle lorsque le stock est nul, et en absence de toute perturbation la maturité augmente avec le temps. Une perturbation (dans notre cas, l'exploitation sélective) est alors décrite comme un évènement ponctuel qui diminue de manière abrupte la maturité du système. Dès lors que la perturbation est finie, la maturité du système augmente de nouveau, progressivement. Les quantités étudiées (stocks et flux) peuvent alors être décrites en fonction de la maturité du système (Figure 1.9), selon les caractéristiques du système étudié.

L'hypothèse qui est faite est que dans des conditions environnementales données, le système étudié a une réponse cohérente quel que soit le type de perturbation. Cette vision simplifiée a l'avantage de faire ressortir les constantes dans le comportement des systèmes étudiés, offrant ainsi de la robustesse aux résultats obtenus d'un site à l'autre. Nous verrons par la suite l'importance que cela peut avoir pour passer de l'échelle de la parcelle (le système étudié) à celle de l'Amazonie.

1.2.3 Caractériser la réponse aux perturbations

Résistance et résilience

La réponse d'un système à une perturbation peut être décrite par deux propriétés fondamentales : sa résistance et sa résilience à la perturbation[128]. La résistance caractérise l'intensité du changement des propriétés du système après la perturbation. La résilience est la capacité du système à retrouver ses propriétés initiales. Cette

[128] D. HODGSON et al. (2015). « What do you mean, 'resilient'? » In : *Trends in Ecology and Evolution* 30.9, p. 503–506.

capacité est souvent caractérisée par la vitesse de retour à l'état pré-perturbation (Figure 1.10).

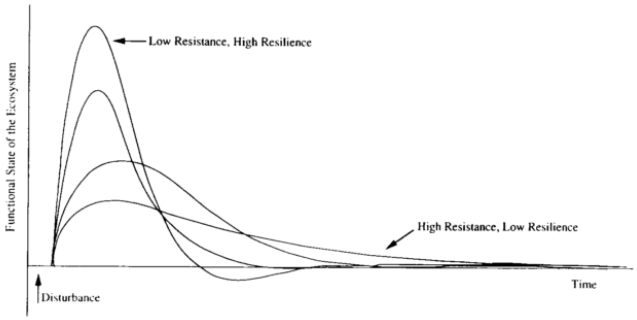

FIGURE 1.10 – Illustration des notions de résilience et résistance. In Attiwill, 1994[a].

[a] P. M. ATTIWILL (1994). « The disturbance of forest ecosystems : the ecological basis for conservative management ». In : *Forest Ecology and Management* 63.2-3, p. 247–300.

Mesures de la résilience

La résilience d'un système à une perturbation est étudiée à travers des indicateurs qui peuvent être quantitatifs ou qualitatifs. Ces indicateurs sont modifiés par la perturbation, et la dynamique de leur retour à une valeur pré-perturbation permet de caractériser la résilience du système. Ces indicateurs peuvent être définis à l'échelle de la communauté, par exemple en nombre d'individus, composition et diversité[129], ou à l'échelle de l'écosystème, par exemple en termes de stocks (exemple : biomasse[130]), de flux (exemple : productivité primaire[131]), ou autres (exemple : couvert forestier[132]). La résistance et résilience d'un système sont très dépendantes des propriétés mesurées, et toutes les caractéristiques d'un système n'ont pas la même dynamique de réponse à une perturbation, par exemple la récupération du carbone peut être plus rapide que la récupération du volume de bois exploité[133].

Dans l'étude présentée ici, la résilience de l'écosystème correspond à la vitesse à laquelle les stocks et flux (par exemple de carbone) tendent vers leur état d'équilibre asymptotique après l'exploitation.

Diversité et mémoire écologique

La résilience d'un écosystème à une perturbation dépend des caractéristiques de l'écosystème avant la perturbation. Cet état est la résultante de l'histoire de l'écosystème, et en particulier du régime historique des perturbations qui sélectionne progressivement des individus dont les traits sont adaptés aux perturbations[134]. Ce phénomène de mémoire écologique explique la stabilité temporelle des écosystèmes malgré les perturbations récurrentes qu'ils subissent. En Amazonie, des variations du régime de perturbations se reflètent sur la composition floristique des forêts[135]. Certaines espèces dites pionnières jouent un rôle clé dans la récupération de la forêt suite aux chablis. Une espèce pionnière type a une croissance rapide, un cycle de vie court et de petites graines faciles à disperser et qui peuvent rester longtemps en dormance. La

[129] DE AVILA et al. (2015). « Medium-term dynamics of tree species composition in response to silvicultural intervention intensities in a tropical rain forest », cf. note 65, p. 7.

[130] B. SAKSCHEWSKI et al. (2016). « Resilience of Amazon forests emerges from plant trait diversity ». In : *Nature Climate Change* 1.August, p. 1032–1036.

[131] T. RIUTTA et al. (2018). « Logging disturbance shifts net primary productivity and its allocation in Bornean tropical forests ». In : *Global Change Biology* 24.7, p. 2913–2928. arXiv : 0608246v3 [arXiv:physics].

[132] M. HIROTA et al. (2011). « Global Resilience of Tropical Forest and Savanna to Critical Transitions ». In : *Science* 334.6053, p. 232–235. arXiv : 20.

[133] A. ROOPSIND et al. (2018). « Trade-offs between carbon stocks and timber recovery in tropical forests are mediated by logging intensity ». In : *Global Change Biology* November 2017, p. 2862–2874.

[134] JOHNSTONE et al. (2016). « Changing disturbance regimes, ecological memory, and forest resilience », cf. note 115, p. 12.

[135] GUITET et al. (2018). « Disturbance Regimes Drive the Diversity of Regional Floristic Pools Across Guianan Rainforest Landscapes », cf. note 118, p. 13 ; R. NEGRÓN-JUÁREZ et al. (2018). « Vulnerability of Amazon forests to storm-driven tree mortality ». In : *Environmental Research Letters* 13, p. 054021.

dormance est levée avec l'augmentation de la lumière arrivant au sol lors d'une trouée. L'individu croît alors rapidement, ce qui permet de refermer le couvert forestier après 1-2 ans. La présence de ces espèces «sparadrap »est donc un élément clé de la résilience des forêts amazoniennes.

La résilience dépend du maintien de certaines fonctions clé du fonctionnement de l'écosystème après la perturbation. La diversité des individus, notamment leur diversité fonctionnelle, permet de réduire le risque de perdre totalement certaines fonctions indispensables au maintien de l'écosystème. Cet effet est d'autant plus fort que plusieurs espèces assurent le même rôle dans l'écosystème (on parle alors de redondance fonctionnelle[136]), et que leur réponse à la perturbation varient entre elles[137]. Dans ce cas le risque de perdre une espèce essentielle au fonctionnement de l'écosystème devient très faible. Il a ainsi été montré qu'à l'échelle de l'Amazonie la diversité fonctionnelle joue un rôle essentiel dans la résilience des forêts face aux changements climatiques[138].

[136] B. Walker (1992). « Biodiversity and Ecological Redundancy ». In : *Conservation Biology* 6.1, p. 18–23 ; S. Naeem (1998). « Species Redundancy and Ecosystem Reliability ». In : *Concservation Biology* 12.1, p. 39–45.

[137] T. Elmqvist et al. (2014). « Response diversity, ecosystem change and resilience ». In : *Frontiers in Ecology and the Environment* 1.9, p. 488–494.

[138] Sakschewski et al. (2016). Cf. note 130.

1.3 Quel futur pour les forêts de production en Amazonie ?

1.3.1 La foresterie tropicale en transition

La foresterie tropicale a connu plusieurs changements de paradigmes dominants qui ont affecté le mode de gestion des forêts tropicales.

Depuis les années 1990, la prise de conscience du besoin de gérer les ressources forestières en Amazonie afin d'éviter leur épuisement rapide a amené le concept de gestion durable des forêts. L'approche alors dominante est que la conservation des forêts tropicales sera d'autant plus efficace que ces forêts génèrent des revenus, grâce à la gestion durable de leurs ressources (bois et produits forestiers non-ligneux)[139]. Pourtant les normes de gestion établies sur ce principe[140] n'ont pas enrayé le déclin rapide des ressources en bois précieux[141], et l'exploitation sélective n'est souvent pas viable économiquement dès le deuxième cycle d'exploitation[142]. De plus en Amazonie la plupart de l'exploitation est illégale[143] et se fait donc sans souci de durabilité, ce qui aggrave encore le déclin rapide des ressources. Pour s'affranchir du risque de surexploitation des ressources, d'autres outils ont été développés, comme les payements pour services environnementaux qui rétribuent les usagers de la forêt en échange du maintien de sa valeur environnementale (par exemple le carbone stocké)[144]. Ces outils suivent la même logique que la gestion par l'exploitation durable : maintenir la forêt en lui conférant une valeur économique. Pourtant, d'un point de vue économique, l'exploitation du bois ou d'autres produits non-ligneux, même associée à des payements pour services environnementaux, peut difficilement

[139] B. Pokorny et P. Pacheco (2014). « Money from and for forests : A critical reflection on the feasibility of market approaches for the conservation of Amazonian forests ». In : *Journal of Rural Studies* 36, p. 441–452.

[140] cf. Table 1.1

[141] Richardson et Peres (2016). « Temporal decay in timber species composition and value in amazonian logging concessions », cf. note 62, p. 7.

[142] Sist et Ferreira (2007). « Sustainability of reduced-impact logging in the Eastern Amazon », cf. note 102, p. 11.

[143] Finer et al. (2014). « Logging Concessions Enable Illegal Logging Crisis in the Peruvian Amazon », cf. note 95, p. 10 ; Brancalion et al. (2018). « Fake legal logging in the Brazilian Amazon », cf. note 95, p. 10.

[144] S Wunder (2006). « Are direct payments for environmental services spelling doom for sustainable forest management in the tropics ? » In : *Ecology and Society* 11.2, p. 23–36.

compenser les coûts d'opportunité de ne pas transformer les forêts en terres agricoles[145]. La vision de l'exploitation sélective comme stratégie de conservation connaît donc de vives critiques[146]. La conservation des forêts tropicales n'émergera donc probablement pas uniquement d'incitations économiques, mais dépendra de décisions politiques volontaristes. Dans un contexte où la demande de bois est prévue de presque doubler dans les 50 ans à venir[147], la redéfinition d'une stratégie pour la gestion des forêts de production devient cruciale en Amazonie.

L'une des premières limites dans les forêts de production amazoniennes est le déclin rapide des ressources en bois après un ou deux cycles d'exploitation, même dans le cas de l'exploitation à faible impact[148]. L'une des interrogations du secteur forestier aujourd'hui est donc de savoir sous quelles conditions l'exploitation peut être durable, voire si cette durabilité est seulement possible et économiquement viable. D'autres débats, par exemple sur l'impact de l'exploitation sur les stocks de carbone[149], la diversité[150] ou le cycle de l'eau[151], sont autant de nouveaux éléments à prendre en compte dans la définition de nouvelles règles d'exploitation.

Un autre débat central, qui a été nommé *land sparing vs. land sharing* en anglais, peut se résumer à la question suivante : vaut-il mieux utiliser l'intégralité des forêts disponibles pour produire du bois avec de faibles intensités qui auront donc un impact local réduit, ou faut-il exploiter seulement une fraction des forêts avec des intensités plus élevées et laisser le reste intact[152] ? La première option a souvent été favorisée[153], sous l'hypothèse que ce type de perturbation serait suffisamment faible pour maintenir les forêts dans un état proche des forêts naturelles, et que l'augmentation de l'intensité risquerait de mettre en péril la provision des services écosystémiques[154]. Pourtant, de nombreux chercheurs soulignent la valeur irremplaçable des forêts naturelles, et le risque de perte d'espèces et d'homogénéisation des forêts sous ce type de scénario[155]. Viennent s'ajouter les coûts économiques[156] et environnementaux[157] de la construction d'infrastructure sur l'ensemble du paysage.

Les services forestiers des pays du bassin amazonien sont donc demandeurs d'informations leur permettant d'adapter leur gestion des forêts de production. Pour mieux comprendre l'effet de l'exploitation sur la dynamique des forêts, plusieurs informations ont été récoltées par les services forestiers de plusieurs pays du bassin amazonien. Dans les concessions brésiliennes, les exploitants ont l'obligation d'installer des parcelles de suivi de la dynamique forestière après exploitation (1 ha pour 250 ha exploités)[158] ; il en va de même pour les exploitants boliviens qui ont l'obligation légale d'installer 1 ha de parcelles pour chaque 1000 ha exploités[159]. Indépendamment de ces législations, des parcelles expérimentales ont été mises en place par des instituts de recherche pour répondre à ces mêmes questions. Il existe donc aujourd'hui une

[145] Pokorny et Pacheco (2014). « Money from and for forests : A critical reflection on the feasibility of market approaches for the conservation of Amazonian forests », cf. note 139, p. 17.

[146] Zimmerman et Kormos (2012). « Prospects for Sustainable Logging in Tropical Forests », cf. note 102, p. 11.

[147] J. Blaser et H. Gregersen (2013). « Forests in the next 300 years ». In : *Unasylva* 64.240, p. 61–73.

[148] Sist et Ferreira (2007). « Sustainability of reduced-impact logging in the Eastern Amazon », cf. note 102, p. 11.

[149] M. Huang et G. P. Asner (2010). « Long-term carbon loss and recovery following selective logging in Amazon forests ». In : *Global Biogeochemical Cycles* 24.November 2009, p. 1–15.

[150] Z. Burivalova et al. (2014). « Thresholds of Logging Intensity to Maintain Tropical Forest Biodiversity ». In : *Current Biology* 24.16, p. 1893–1898.

[151] A. R. Nik et D. Harding (1992). « Effects of Selective Logging Methods on Water Yield and Streamflow Parameters in Peninsular Malaysia ». In : *Journal of Tropical Forest Science* 5.2, p. 130–154.

[152] D. P. Edwards et al. (2014a). « Land-sharing versus land-sparing logging : reconciling timber extraction with biodiversity conservation ». In : *Global Change Biology* 20.1, p. 183–191.

[153] T. S. Fredericksen (1998). « Limitations of low-intensity selection and selective logging for sustainable tropical forestry ». In : *The Commonwealth Forestry Review* 77.4, p. 262–266.

[154] Burivalova et al. (2014). Cf. note 150 ; Miranda et al. (2016). « Effects of Protected Areas on Forest Cover Change and Local Communities : Evidence from the Peruvian Amazon », cf. note 81, p. 9 ; Roopsind et al. (2018). « Trade-offs between carbon stocks and timber recovery in tropical forests are mediated by logging intensity », cf. note 133, p. 16.

[155] L. Gibson et al. (2011). « Primary forests are irreplaceable for sustaining tropical biodiversity ». In : *Nature* 478.7369, p. 378–381. arXiv : `arXiv : 1011 . 1669v3` ; Edwards et al. (2014a). Cf. note 152.

[156] B. Pokorny et M. Steinbrenner (2005). « Collaborative monitoring of production and costs of timber harvest operations in the Brazilian Amazon ». In : *Ecology and Society* 10.1.

[157] Laurance et al. (2009). « Impacts of roads and linear clearings on tropical forests », cf. note 40, p. 4.

[158] M. R. Balieiro et al. (2010). *As Concessões de Florestas Públicas na Amazônia Brasileira*, p. 204.

grande quantité de données sur les forêts exploitées en Amazonie, certes pas toujours facilement accessibles ni utilisables[160], mais qui pourrait néanmoins permettre de prendre des décisions plus éclairées pour la gestion forestière.

[159] Fredericksen et al. (2003). « Sustainable forestry in Bolivia - Beyond planning logging », cf. note 93, p. 10.

[160] Ibid.

1.3.2 Les services écosystémiques comme outil de décision

La mise en place de la gestion forestière répond à un enjeu fondamental qui est celui de préserver les écosystèmes forestiers dont dépendent les sociétés humaines. La quantification de l'ensemble des biens et services que les sociétés humaines retirent des écosystèmes, regroupés sous le terme de «services écosystémiques», a connu un intérêt grandissant au cours des dernières décennies et a fait l'objet en 2005 d'un travail associant plus de 1360 chercheurs, le Millennium Ecosystem Assessment, pour évaluer l'impact global des activités humaines sur les services écosystémiques[161]. On distingue quatre types de services écosystémiques (Figure 1.11) :

- les services d'approvisionnement,
- les services de régulation,
- les services culturels,
- les services de support permettant l'approvisionnement des autres services.

[161] Millenium Ecosystem Assessment (2005). *Ecosystems and Human well-being*. Rapp. tech., p. 63.

La notion de service écosystémique a provoqué un changement marquant dans le paradigme de conservation, proposant une vision plus anthropocentrée : les écosystèmes ne sont plus conservés uniquement pour leur valeur intrinsèque, mais pour ce qu'ils peuvent offrir aux sociétés humaines. Elle a permis une reconnaissance formalisée de l'ensemble des biens retirés du fonctionnement des écosystèmes, et ainsi de rationaliser la gestion des écosystèmes en les regroupant sous un même concept[162]. Pour maintenir l'ensemble des services rendus par les écosystèmes, la gestion forestière ne peut se focaliser sur un unique objectif (par exemple, la production de bois ou la conservation d'une espèce) mais doit permettre de prendre en compte la multiplicité des services rendus par les forêts (valeur culturelle et esthétique, production de produits non-ligneux, régulation du climat, etc.). Le cadre conceptuel des services écosystémiques permet de concilier cet ensemble d'objectifs, et pose donc les bases pour le développement d'écosystèmes remplissant de nombreux objectifs auprès de divers usagers[163]. Cela est d'autant plus important dans les cas où certains services écosystémiques sont antagonistes. Un cas classique est le compromis entre un service d'approvisionnement (production de biens agricoles, d'énergie, de bois) et un service de support (renouvellement des populations, biodiversité, structure du sol). Négliger le deuxième type de service mettrait alors en péril l'approvisionnement du premier. Par exemple, l'extraction de noix du Brésil dans les forêts amazoniennes (*Bertholletia excelsa*)

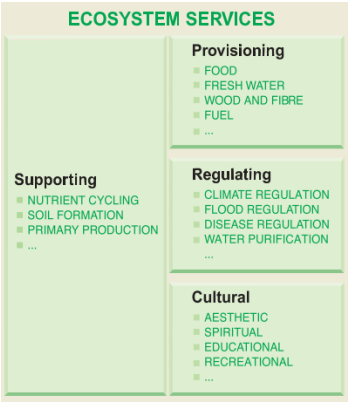

Figure 1.11 – Schéma conceptuel des services écosystémiques. In Millenium Ecosystem Assessment, 2005[a].

[a] Ibid.

[162] C. Kremen et R. S. Ostfeld (2005). « A call to ecologists : Measuring, analyzing, and managing ecosystem services ». In : *Frontiers in Ecology and the Environment* 3.10, p. 540–548.

[163] F. Van der Plas et al. (2018). « Continental mapping of forest ecosystem functions reveals a high but unrealised potential for forest multifunctionality ». In : *Ecology Letters* 21.1. Sous la dir. de D. Storch, p. 31–42.

provoquerait le déclin des populations adultes[164]. Il est donc nécessaire pour les gestionnaires forestiers de faire des choix informés afin d'optimiser les compromis entre services écosystémiques[165].

Dans cette thèse, l'impact de l'exploitation est quantifié selon trois services écosystémiques qui sont au centre des débats actuels : le service d'approvisionnement en bois d'œuvre, le service de stockage de carbone (régulation du climat) et le service de biodiversité comme service à la fois culturel et de support au fonctionnement des forêts tropicales.

1.3.3 Une approche régionale

Aujourd'hui, de nombreuses études ont permis de mieux comprendre l'effet de l'exploitation sur les services écosystémiques. Les conclusions de ces études sont souvent cohérentes : l'exploitation sélective telle que pratiquée aujourd'hui ne permet pas de récupérer le volume de bois, mais par contre les stocks de carbone sont rapidement récupérés[166], surtout lorsque les techniques d'exploitation à faible impact ont été appliquées[167]. L'exploitation modifie la composition des forêts : vers des espèces plus généralistes pour les animaux[168] et des essences à croissance rapide pour les plantes[169]. La persistance de ces effets après l'exploitation a cependant été peu étudiée. L'effet sur la diversité est plus difficile à interpréter[170], d'autant plus qu'il existe un grand nombre d'estimateurs de biodiversité[171] et que les mesures de biodiversité sont très sensibles à la surface échantillonnée et à la qualité de l'identification[172], deux facteurs limitants dans les forêts amazoniennes denses et riches en espèces.

Cependant, peu d'études ont été faites à l'échelle régionale pour comprendre les différences dans les dynamiques de réponse à l'exploitation. Surtout, il n'existe pas d'étude cherchant à concilier plusieurs services écosystémiques dans les forêts de production à l'échelle du bassin amazonien. La thèse développée ici cherche donc à répondre à ces questions centrales pour la gestion future des forêts de production en Amazonie :

1. Comment l'exploitation modifie l'approvisionnement des services écosystémiques (carbone, volume de bois), et comment ces services se reconstituent après l'exploitation (Figure 1.12) ?
2. Ces dynamiques sont-elles structurées à l'échelle amazonienne ? Quels facteurs permettent d'expliquer les éventuelles différences observées ?
3. Existe-t-il des compromis entre les services de stockage du carbone, d'approvisionnement de bois et de diversité à l'échelle régionale ? Comment les futurs choix de gestion pourraient-ils modifier l'approvisionnement de ces services ?

Pour répondre à ces questions ont été développés des modèles de permettant d'estimer les émissions de carbone et la récupération

[164] C. a. Peres et I. R. Lake (2003). « Extent of Nontimber Resource Extraction in Tropical Forests : Accessibility to Game Vertebrates by Hunters in the Amazon Basin ». In : *Conservation Biology* 17.2, p. 521–535.

[165] J. P. Rodríguez et al. (2006). « Trade-offs across space, time, and ecosystem services ». In : *Ecology and Society* 11.1.

[166] Putz et al. (2012). « Sustaining conservation values in selectively logged tropical forests : the attained and the attainable », cf. note 102, p. 11 ; E. Rutishauser et al. (2015). « Rapid tree carbon stock recovery in managed Amazonian forests ». In : *Current Biology* 25.18, R787–R788.

[167] T. a. P. West et al. (2014). « Forest biomass recovery after conventional and reduced-impact logging in Amazonian Brazil ». In : *Forest Ecology and Management* 314, p. 59–63.

[168] Burivalova et al. (2014). « Thresholds of Logging Intensity to Maintain Tropical Forest Biodiversity », cf. note 150, p. 18.

[169] De Avila et al. (2015). « Medium-term dynamics of tree species composition in response to silvicultural intervention intensities in a tropical rain forest », cf. note 65, p. 7 ; C. C. Jakovac et al. (2016). « Land use as a filter for species composition in Amazonian secondary forests ». In : *Journal of Vegetation Science* 27.6, p. 1104–1116.

[170] Gibson et al. (2011). « Primary forests are irreplaceable for sustaining tropical biodiversity », cf. note 155, p. 18 ; G. Carreño-Rocabado et al. (2012). « Effects of disturbance intensity on species and functional diversity in a tropical forest ». In : *Journal of Ecology* 100.6, p. 1453–1463.

[171] S. H. Hurlbert (1971). « The Nonconcept of Species Diversity : A Critique and Alternative Parameters ». In : *Ecology* 52.4, p. 577–586.

[172] O. Arrhenius (1921). « Species and Area ». In : *The Journal of Ecology* 9.1, p. 95.

du volume de bois à l'échelle d'une parcelle exploitée (Chapitres 3 et 6). Les dynamiques de récupération du carbone et de volume de bois après l'exploitation ont été étudiées à l'échelle régionale, et leurs prédictions spatialisées (Chapitres 4 et 7). En combinant ces prédictions avec des cartes de richesse de vertébrés, l'approvisionnement des trois services écosystémiques (carbone, bois, diversité) a été optimisé spatialement, sous contrainte d'une production de bois d'œvre répondant à la demande locale.

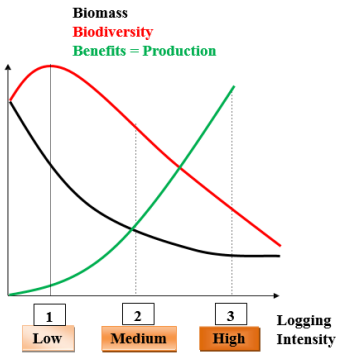

FIGURE 1.12 – Effet attendu de l'intensité d'exploitation sur les services écosystémiques dans les forêts de production, d'après Sist, 2014.

Chapitre 2

Données et outils méthodologiques

2.1 L'environnement physique et biologique

La structure et la dynamique des forêts amazoniennes sont principalement liées au régime de perturbations, lui-même dépendant des conditions abiotiques dans lesquelles se développent les forêts.

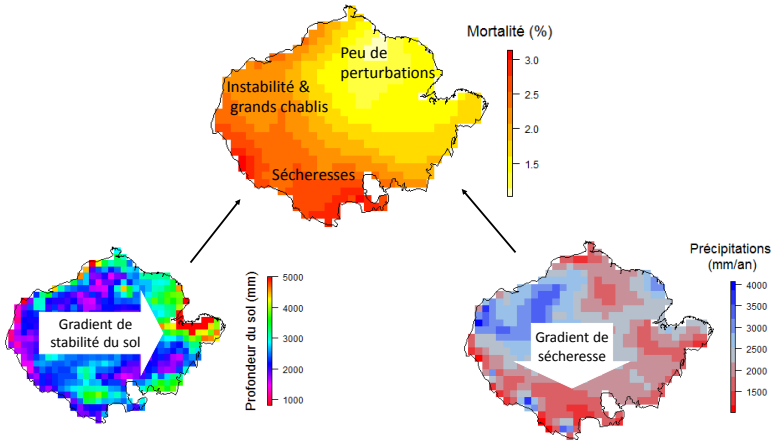

Figure 2.1 – Explication du taux de mortalité annuelle (% des tiges, d'après Johnson et al. 2016) par deux gradients environnementaux : un gradient de sécheresse nord-sud, ici représenté par les précipitations annuelles (www.worldclim.org) et un gradient de stabilité du sol ouest-est, ici représenté par la profondeur du sol (www.soilgrids.org).

Il existe en Amazonie deux grands gradients particulièrement structurants pour la végétation (Figure 2.1) : un gradient de stabilité et de fertilité du sol est-ouest, avec des sols récents et fertiles mais superficiels du côté andin (ouest), et à l'est des sols anciens et profonds mais particulièrement appauvris par le lessivage des nutriments[1]. Le deuxième gradient est un gradient de sécheresse nord-sud[2] : les précipitations sont plus importantes au nord, et la durée de la saison sèche est plus courte.

Les variations du niveau de perturbation s'expliquent donc principalement par la stabilité des sols[3], et par la fréquence des tempêtes dans les régions nord-est de l'Amazonie[4]. Les forêts y sont moins stables et soumises à des chablis plus fréquents et de plus grande ampleur[5]. Les taux de renouvellement sont particulièrement élevés (Figure 2.1), ce qui favorise les espèces à

[1] C. a. Quesada et al. (2012). « Basin-wide variations in Amazon forest structure and function are mediated by both soils and climate ». In : *Biogeosciences* 9.6, p. 2203–2246.

[2] Malhi et al. (2015). « The linkages between photosynthesis , productivity , growth and biomass in lowland Amazonian forests », cf. note 120, p. 13.

[3] Quesada et al. (2012). Cf. note 1.

[4] Negrón-Juárez et al. (2018). « Vulnerability of Amazon forests to storm-driven tree mortality », cf. note 135, p. 16.

[5] F. D. Espírito-Santo et al. (2014). « Size and frequency of natural forest disturbances and the Amazon forest carbon balance ». In : *Nature Communications* 5, p. 3434 ; Negrón-Juárez et al. (2018). « Vulnerability of Amazon forests to storm-driven tree mortality », cf. note 135, p. 16.

croissance rapide et à cycle de vie court, avec peu d'investissement dans des structures pérennes. A l'inverse, les forêts du nord-est de l'Amazonie et du plateau des Guyanes poussent sur des sols pauvres mais particulièrement stables car profonds et peu denses ; de plus, ces forêts sont peu soumises à des stress hydriques, car le régime de précipitation est faiblement saisonnier[6]. Cet environnement favorise des peuplements denses et à croissance lente, surtout limités par la compétition pour la lumière et par l'apport de nutriments stockés principalement dans la biomasse[7].

Ces différences de dynamique expliquent la distribution de la biomasse[8], avec des forêts plus riches en biomasse au nord-est de l'Amazonie où le taux de mortalité est le plus faible (Figure 2.2). La distribution des traits fonctionnels suit un gradient similaire : au nord-est les traits fonctionnels moyens reflètent un fort investissement dans les structures (grande densité du bois : Figure 2.3a), permettant de croître plus haut, mais lentement. À l'inverse, la fable masse des graines à l'ouest de l'Amazonie reflète une stratégie opportuniste, adaptée aux environnements très perturbés : ces graines sont facilement dispersées, mais ont peu de réserves, elles dépendent donc de l'apparition de trouées et de l'apport lumineux immédiat pour que les plantules puissent se développer.

[6] Malhi et al. (2015). « The linkages between photosynthesis , productivity , growth and biomass in lowland Amazonian forests », cf. note 120, p. 13.

[7] O. Grau et al. (2017). « Nutrient-cycling mechanisms other than the direct absorption from soil may control forest structure and dynamics in poor Amazonian soils ». In : *Scientific Reports* 7.March, p. 45017.

[8] M. O. Johnson et al. (2016). « Variation in stem mortality rates determines patterns of above-ground biomass in Amazonian forests : implications for dynamic global vegetation models ». In : *Global Change Biology* 22.12, p. 3996–4013.

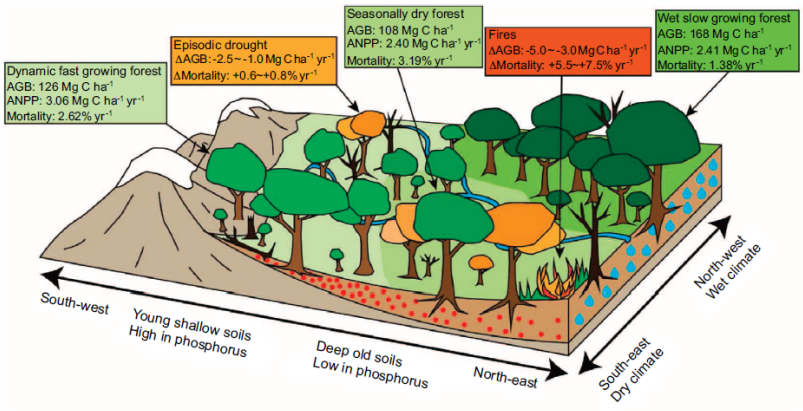

Figure 2.2 – Lien entre les gradients édaphiques et climatiques, le régime de perturbation et le carbone (stock et flux) des forêts amazoniennes. In Dolman et al. 2018[a].

[a] A Dolman et T Janssen (2018). « The enigma of the Amazonian carbon balance The enigma of the Amazonian carbon balance ». In : p. 6–9.

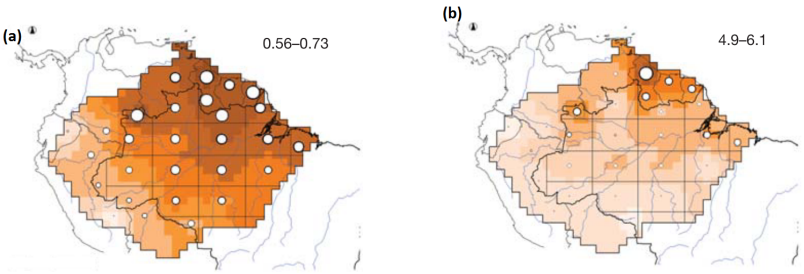

Figure 2.3 – Distribution de deux traits fonctionnels dans les forêts amazoniennes. In ter Steege et al. 2006[a]. (a) Densité moyenne du bois. (b) Masse moyenne des graines (échelle logarithmique).

[a] H. Ter Steege et al. (2006). « Continental-scale patterns of canopy tree composition and function across Amazonia. » In : *Nature* 443.24, p. 444–447.

Les gradients décrits ci-dessus affectent la dynamique des forêts naturelles ; de même, il est attendu qu'une fois exploitées la réponse des forêts à la perturbation soit influencée par ces différences. Les forêts soumises à de fortes perturbations naturelles

pourraient avoir une récupération plus rapide que les forêts peu perturbées du plateau des Guyanes, car le pool d'espèces déjà présent est plus adapté à ces conditions environnementales.

2.2 Les inventaires forestiers

Les inventaires forestiers ont été utilisés depuis plusieurs siècles en foresterie pour caractériser les peuplements d'arbres[9]. Des parcelles, dont la taille est en général de l'ordre de l'hectare, sont délimitées, et l'ensemble des arbres au-dessus d'une certaine taille pré-définie (par exemple 10 cm DHP) sont recensés, cartographiés, et leurs caractéristiques mesurées : diamètre, hauteur, identification de l'espèce. Ces données peuvent ensuite être utilisées pour estimer d'autres variables à partir d'équations allométriques, telles que la biomasse de chaque individu[10]. Pour décrire les dynamiques du peuplement, les parcelles peuvent être mesurées régulièrement, on parle alors de parcelle permanente. Dans cette étude, deux ensembles de parcelles situés dans des forêts de terre ferme ont été utilisées : un réseau de parcelles permanentes (TmFO) et un ensemble de parcelles mesurées une seule fois (RadamBrasil).

[9] H. Pretzsch (2010). *Forest Dynamics, Growth and Yield*. arXiv : arXiv:1011.1669v3.

[10] J. Chave et al. (2014). « Improved allometric models to estimate the aboveground biomass of tropical trees ». In : *Global Change Biology* 20.10, p. 3177–3190.

2.2.1 Le réseau TmFO

Ce travail a été mené au sein du Tropical managed Forest Observatory (TmFO)[11]. Ce réseau pan-tropical, formé en 2012, regroupe 17 institutions ayant installé des dispositifs de suivi de parcelles permanentes exploitées. Le but est de comprendre la réponse des forêts tropicales à des perturbations anthropiques telles que l'exploitation[12].

En Amazonie, ce réseau regroupe 166 parcelles permanentes (845 ha) réparties dans 15 sites couvrant une grande partie de l'Amazonie (Figure 2.4a). L'ensemble de ces sites a été exploité, avec au moins un inventaire pré-exploitation (caractérisation de l'état initial) et deux inventaires post-exploitation (suivi des dynamiques post-exploitation). Les modalités d'exploitation et de suivi des parcelles sont synthétisées dans la Table 2.1. Certains sites ont été exploités expérimentalement, et dans ce cas l'intensité d'exploitation est contrôlée et dans certains cas plusieurs traitements ont pu être testés (différentes intensités d'exploitation ; traitements post-exploitation : éclaircissement, élimination des lianes). D'autres sites ont été installés sur des zones exploitées par des entreprises privées[13]. Dans ce cas les effets de l'exploitation sont souvent plus variables.

[11] www.tmfo.org

[12] Sist et al. (2015). « The Tropical managed Forests Observatory : A research network addressing the future of tropical logged forests », cf. note 116, p. 12.

[13] La certification FSC demande la mise en place de parcelles de suivi post-exploitation ; c'est aussi stipulé dans le code forestier bolivien.

2.2.2 RadamBrasil

Le deuxième ensemble de parcelles utilisé dans cette étude sont issues du projet RadamBrasil[14]. Ce projet, initié par le gouvernement brésilien dans les années 1970, avait pour but d'inventorier

[14] M. d. M. e. E. Brasil (1973). *Projeto Radambrasil. Levantamento de recursos naturais*, 34 vols.

Table 2.1 – Caractéristiques des sites TmFO.

Site	Traitement	Nombre de parcelles	Taille des parcelles	Période de mesure	Année d'exploitation
Braga-Supay	Exploitation sélective	7	1 ha	1993-2008	1994
Chico-Bocão	Exploitation sélective	7	1 ha	2001-2011	2002
Cumaru	Exploitation sélective	7	1 ha	2002-2011	2005
Ecosilva	Exploitation sélective	18	1 ha	2002-2012	2003
INPA	Contrôle	2	22 ha	2002-2012	
	Exploitation sélective	2	22 ha	2002-2012	
	Traitements sylv.	4	22 ha	2002-2012	2003
Iracema	Exploitation sélective	30	1 ha	2002-2015	2003
Itacoatiara	Exploitation sélective	40	1 ha	1996-2014	1997
Jari	Contrôle	4	1 ha	1984-2011	
	Exploitation sélective	12	1 ha	1984-2011	
	Traitements sylv.	24	1 ha	1984-2011	1985
La Chonta	Contrôle	3	27 ha	2000-2011	2001
	Exploitation sélective	3	27 ha	2000-2011	2001
	Traitements sylv.	6	27 ha	2000-2011	2001
Peteco	Exploitation sélective	40	0.25 ha	1996-2014	1997
Paracou	Contrôle	3	6.25 ha	1984-2015	1986
	Exploitation sélective	3	6.25 ha	1984-2015	1986
	Traitements sylv.	3	6.25 ha	1984-2015	1986
	Traitements sylv. et bois de feu	3	6.25 ha	1984-2015	1986
Paragominas	Contrôle	1	25.4 ha	1993-2014	
	Exploitation sélective	2	25.4 ha	1993-2014	1994
Tabocal	Contrôle	10	1 ha	1999-2011	
Tortue	Contrôle	1	6 ha	2002-2016	
	Exploitation sélective	2	4.5 ha	2002-2016	
Tapajos	Contrôle	12	6.25 ha	1984-2015	
	Exploitation sélective	12	6.25 ha	1984-2015	
	Traitements sylv.	36	6.25 ha	1984-2015	

les ressources naturelles (biotiques et abiotiques) des forêts amazoniennes. Les données sont aujourd'hui disponibles en libre-accès sur le site de l'institut brésilien de géographie et statistiques (IBGE)[15]. Les données de 2660 parcelles d'un hectare (mesurées une seule fois) ont été utilisées dans cette étude (Figure 2.4b), comprenant : les coordonnées de la parcelle, le diamètre de tous les arbres au-dessus de 32 cm DHP, leur hauteur commerciale et leur identification à l'espèce (99.7% des individus mesurés ont été identifiés).

[15] IBGE (2017). *Produção da Extração Vegetal e da Silvicultura - PEVS*.

2.3 Quantités modélisées - approche écosystémique

Au cours de cette étude ont été étudiés trois services écosystémiques majeurs rendus par les forêts naturelles amazoniennes :

- la production de bois d'œuvre comme service d'approvision-

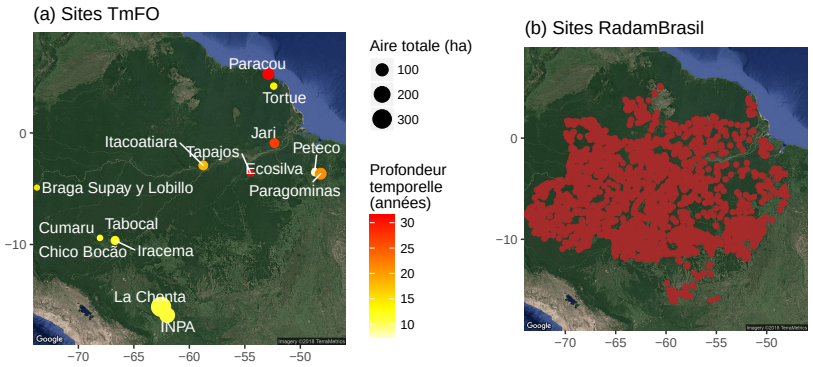

FIGURE 2.4 – Localisation des sites d'inventaires (a) du réseau TmFO : parcelles permanentes exploitées ; (b) du projet RadamBrasil : un unique inventaires, forêts naturelles.

nement ;
- le stockage de carbone comme service de régulation par mitigation des changements climatiques ;
- la biodiversité comme service de support aux autres services écosystémiques[16].

L'objectif final de ce travail est de comprendre les compromis qui existent entre ces services écosystémiques dans les forêts de production en Amazonie, et les implications que cela amène pour l'optimisation de la gestion future de ces forêts.

À l'échelle individuelle, le stock de carbone aérien a été estimé pour tous les individus >20 cm DHP[17] avec une équation allométrique pan-tropicale, à partir du diamètre et de la densité moyenne du bois de l'espèce[18] [19]. Le volume de grume de chaque individu >50 cm DHP[20] a été calculé avec une équation reliant DHP et volume de la grume développée à partir des données des inventaires RadamBrasil (pour plus de détails voir les méthodes dans le chapitre 7).

Le choix a été fait d'étudier les dynamiques de reconstitution post-exploitation agrégées à l'échelle de la parcelle, sans expliciter le rôle des individus. Le but est ainsi de caractériser la réponse globale de l'écosystème, non pas comme une somme d'individus, mais comme un ensemble cohérent, et d'en faire ressortir les propriétés émergentes[21]. Les quantités étudiées sont : (i) les stocks (de carbone, de bois d'œuvre) et (ii) les flux, c'est-à-dire les changements annuels des stocks. Dans l'étude du carbone, deux compartiments ont été différenciés :

- le stock des survivants, *i.e.* les arbres présents avant l'exploitation et y ayant survécu ;
- le stock des recrutés, *i.e.* tous les arbres ayant atteint le diamètre minimum de recensement.

Trois types de flux ont été mesurés :

- le recrutement, *i.e.* l'augmentation du stock lié aux individus ayant atteint le diamètre minimum de recensement[22] ;
- la croissance, *i.e.* l'augmentation du stock lié à la croissance

[16] P. A. HARRISON et al. (2014). « Linkages between biodiversity attributes and ecosystem services : A systematic review ». In : *Ecosystem Services* 9, p. 191–203.

[17] Cette taille minimum correspond au maximum de tous les seuils de DHP dans les sites TmFO : ainsi tous les sites ont pu être utilisés dans l'étude.

[18] M. RÉJOU-MÉCHAIN et al. (2017). « BIOMASS : An R Package for estimating above-ground biomass and its uncertainty in tropical forests ». In : *Methods in Ecology and Evolution* February.

[19] cf. annexe

[20] Cette taille a été choisie car elle correspond au diamètre minimum d'exploitabilité dans la plupart des pays amazoniens

[21] cf. section 1.2.2

[22] Le flux de recrutement des survivants est par définition nul.

des individus déjà recensés à l'inventaire précédent ;
- la mortalité, *i.e.* la diminution du stock lié à la mortalité d'individus recensés à l'inventaire précédent.

L'une des difficultés pour décrire la trajectoire d'un système à partir de changements annuels est la forte variabilité inter-annuelle de ces changements, qui peut masquer leurs modifications sur des échelles de temps plus longues (Figure 2.5). De plus, modéliser explicitement l'intégrale des flux permet de décrire (et donc de réfléchir à) la trajectoire du système sur l'ensemble de la période d'observation. Le choix a donc été fait de modéliser les flux cumulatifs, *i. e.* la somme cumulée des flux sur la période d'étude, au lieu des flux annuels.

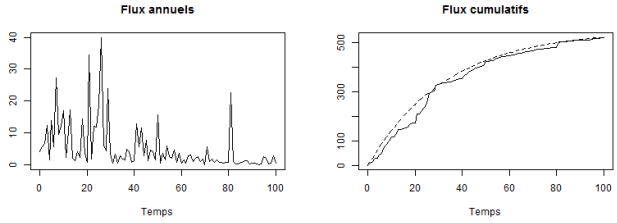

FIGURE 2.5 – Illustration du gain de prédictibilité de la trajectoire entre : (a) les flux annuels, (b) les flux cumulatifs.

2.4 Changement d'échelle (bottom up)

Démarche générale

Les données d'inventaires permettent d'avoir des estimations locales des quantités et flux modélisés et de leur variabilité. L'intérêt, ensuite, est d'en déduire des patterns régionaux qui permettront de faire des prédictions à l'échelle amazonienne. La démarche générale suivie dans cette étude pour faire ce changement d'échelle est la suivante :

1. un modèle est développé pour décrire l'évolution temporelle des flux et de stocks ($Y_{t,s}$) en fonction du temps depuis la perturbation t sur une parcelle s ;
2. dans le modèle sont identifiés des paramètres clé θ_s qui sont représentatifs du phénomène modélisé et devraient varier géographiquement ;
3. les paramètres θ_s sont écrits comme fonction d'un vecteur de paramètres non-spatialisés θ_{Am}, valables à l'échelle de l'Amazonie, et de N covariables spatialement explicites $(Vi)_{i\in[1:N]}$: ces variables peuvent être abiotiques (sol, climat) ou biotiques (stock de carbone, taux de mortalité), et des cartes de ces variables doivent être disponibles à l'échelle amazonienne ;
4. les valeurs de ces covariables en chaque site ($(Vi_s)_{i\in[1:N]}$) sont extraites des cartes globales ;
5. le vecteur de paramètres non-spatialisés θ_{Am} est estimé avec l'ensemble des données : les données agrégées de stocks et flux

issues des inventaires $(Y_{t,s})$, et les covariables $(Vi_s)_{i\in[1:N]}$ extraites des cartes ;

6. des prédictions peuvent alors être faites pour l'ensemble de l'Amazonie, et l'incertitude associée quantifiée.

Ces étapes sont illustrées dans la Figure 2.6.

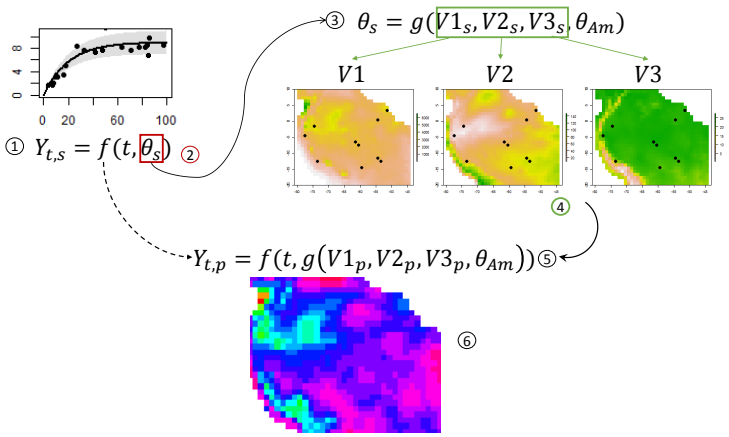

FIGURE 2.6 – Schéma des étapes de changement d'échelle, de la parcelle à l'Amazonie. (1) écriture du modèle de la variable $Y_{t,s}$ en fonction du temps t et de paramètres θ_s dépendant du site s. (2) Identification des paramètres clé. (3) Ecriture des paramètres en fonctions de covariables ($V1$, $V2$, $V3$) spatialement explicites. (4) Extraction de la valeur des variables. (5) Estimation des nouveaux paramètres non-spatialisés θ_{Am}, valables pour toute l'Amazonie. (6) Prédictions $Y_{t,p}$ pour chaque pixel p en Amazonie.

Sources des variables utilisées

Les covariables climatiques (précipitations annuelles, saisonnalité des précipitations) ont été extraites de la base de données WorldClim[23] à une résolution de 30 arc-secondes. La densité du sol a été extraite de la Harmonized World Soil Database (HWSD) développée par la FAO[24]. Des variables décrivant les caractéristiques attendues pour un peuplement mature ont été obtenues à partir de prédictions du modèle individu-centré FORMIND[25] (voir le chapitre 7 pour plus de détails). Certaines variables ont été obtenues par extrapolation de mesures faites localement sur des parcelles Radam Brasil ou du réseau Rainfor[26].

2.5 Les outils statistiques

Les modèles ont été inférés dans un cadre bayésien hiérarchique. Dans ce cadre d'inférence, basé sur le théorème de Bayes[27] les paramètres ne sont pas considérés des valeurs fixes dont on cherche à estimer la "vraie" valeur, mais comme des variables aléatoires. On estime le postérior, c'est-à-dire la distribution des valeurs prises par le paramètre, en mettant à jour une information *a priori*, ou prior, avec des données observées. Les liens des paramètres entre eux sont explicitement pris en compte.

Ce cadre d'inférence présente plusieurs avantages pour des études en écologie, et plus particulièrement pour l'inférence des modèles développés dans cette étude. D'abord la définition du prior permet la prise en compte d'informations qui ne sont pas strictement contenues dans les données. Cela permet, par exemple,

[23] S. E. FICK et R. J. HIJMANS (2017). « WorldClim 2 : new 1-km spatial resolution climate surfaces for global land areas ». In : *International Journal of Climatology* 37.12, p. 4302–4315.

[24] F. NACHTERGAELE et al. (2008). *Harmonized world soil database*. Rapp. tech., p. 43.

[25] E. RÖDIG et al. (2017). « Spatial heterogeneity of biomass and forest structure of the Amazon rain forest : Linking remote sensing, forest modelling and field inventory ». In : *Global Ecology and Biogeography* 26.11, p. 1292–1302.

[26] JOHNSON et al. (2016). « Variation in stem mortality rates determines patterns of above-ground biomass in Amazonian forests : implications for dynamic global vegetation models », cf. note 8, p. 24.

[27] T BAYES (1763). « An Essay Towards Solving a Problem in the Doctrines of Chances ». In : *Philosophical Transactions* 53.1764, p. 370–418.

d'intégrer des contraintes physiques sur des paramètres en restreignant l'intervalle des valeurs prises par le prior ; ou encore d'expliciter une connaissance issue de l'expertise et indépendante des données. De plus, les paramètres des modèles sont souvent des entités complexes qui dépendent d'autres phénomènes, ce qui peut être explicité dans la structure hiérarchique. L'estimation dans un cadre bayésien permet de prendre en compte simplement la structure de covariance entre les paramètres du modèle, sans avoir à faire des hypothèses sur les lois sous-jacentes. Enfin, la propagation des incertitudes se fait facilement entre les différents niveaux d'un modèle : il suffit d'échantillonner les postériors et de calculer les résultats obtenus. En répétant l'opération un nombre suffisant de fois (suffisant pour stabiliser la variance des résultats) on obtient l'incertitude sur les résultats finaux du modèle.

Les modèles ont été développés dans l'environnement de programmation R[28] avec inférés avec un algorithme de Monte Carlo hamiltonien grâce au logiciel Stan[29]. Les algorithmes de chaînes de Markov par Monte Carlo génèrent des chaînes de valeurs de paramètres grâce à des processus sans mémoire (chaîne de Markov) et des règles de transition d'un pas de la chaîne à l'autre. Lorsque la chaîne se stabilise (on dit qu'elle converge), les valeurs ainsi échantillonnées doivent être représentatives du postérior des paramètres. Ces algorithmes se sont développés grâce à l'avènement d'ordinateurs puissants avec de grandes capacités de calcul, et permettent une grande flexibilité dans l'écriture des modèles, car ils ne nécessitent pas de résolution analytique.

L'algorithme de Monte Carlo hamiltonien (ou Monte Carlo hybride) est un type particulier de chaîne de Markov par Monte Carlo permettant de limiter l'autocorrélation dans les chaînes de postériors et ainsi d'accélérer la convergence[30], même pour des modèles avec de nombreux paramètres, ce qui est le cas dans cette étude. Ce qui permet de limiter l'autocorrélation dans la chaîne de paramètres est la capacité d'échantillonner la quasi-intégralité de l'espace des paramètres, et non simplement la fraction de l'espace des paramètres à proximité des dernières valeurs de la chaîne. Le fonctionnement de l'algorithme de proposition d'un nouveau vecteur de paramètres peut être décrit par analogie avec un système mécanique, par exemple une bille sur une surface dont la hauteur serait la vraisemblance du postérior. La bille ne subit pas de frottement : la somme de l'énergie potentielle, liée à la hauteur de la bille, et de son énergie cinétique, liée à sa vitesse, est conservée dans le temps. La position initiale du système est le dernier vecteur de paramètres de la chaîne de Markov. L'algorithme de HMC simule alors une trajectoire du système à partir d'une impulsion initiale aléatoire, et s'arrête pour une longueur de la trajectoire prédéterminée. La position du système à la fin de la trajectoire donne la nouvelle proposition d'un vecteur de paramètres.

[28] R Core Team (2017). *R : A Language and Environment for Statistical Computing.*

[29] B. Carpenter et al. (2017). « Stan : A Probabilistic Programming Language ». In : *Journal of Statistical Software* 76.1.

[30] C. C. Monnahan et al. (2017). « Faster estimation of Bayesian models in ecology using Hamiltonian Monte Carlo ». In : *Methods in Ecology and Evolution* 8.3, p. 339–348.

2.6 Outils d'optimisation spatiale

Pour trouver des compromis à l'échelle du bassin amazonien, des méthodes d'optimisation sous contrainte ont été utilisées. Pour ce faire, l'Amazonie a été divisée en pixels de 1° de longitude par 1° de latitude. Chaque pixel peut être exploité ou pas, et lorsqu'il est exploité les durées de rotations peuvent être de 15, 30 ou 65 ans et l'intensité d'exploitation de 10, 20 ou 30 $m^3 ha^{-1}$, des valeurs qui restent cohérentes par rapport à ce qui est pratiqué actuellement en Amazonie. Pour chaque pixel et chacune des modalités d'exploitation (intensité, temps de rotation) les coûts en termes (i) d'émissions de carbone, (ii) de biodiversité et (iii) de perte de volume de bois à la fin de la première rotation ont été estimés à partir des modèles développés dans cette thèse[31]. Dans le cas où le pixel n'est pas exploité, les coûts sont nuls. Des coefficients ont été attribués à chacun de ces coûts pour obtenir un coût total par pixel en fonction des modalités d'exploitation. L'optimisation spatiale permet d'attribuer à chaque pixel un usage (intensité et temps de rotation, ou pas d'exploitation) afin de minimiser le coût total sous contrainte d'un certain niveau de production de bois, et d'autres contraintes complémentaires selon les scénarios décrits. L'algorithme utilise la programmation linéaire en nombres entiers (*integer linear programming* en anglais), une méthode d'optimisation qui s'est révélée particulièrement efficace dans les problèmes d'optimisation sous contrainte[32].

[31] Pour la biodiversité, les cartes de richesse de vertébrés ont été utilisées(Jenkins et al. [2013]. « Global patterns of terrestrial vertebrate diversity and conservation », cf. note 25, p. 3). La perte d'espèces causée par l'exploitation a été estimée avec un modèle développé par Burivalova et al., 2014(Burivalova et al. [2014]. « Thresholds of Logging Intensity to Maintain Tropical Forest Biodiversity », cf. note 150, p. 18).

[32] H. L. Beyer et al. (2016). « Solving conservation planning problems with integer linear programming ». In : *Ecological Modelling* 328, p. 14–22.

Chapitre 3

Comment quantifier le bilan carbone des forêts exploitées ?

Ce premier chapitre vise à établir une méthodologie complète pour permettre de déterminer le bilan carbone de l'exploitation forestière. La méthodologie présentée a été développée en Guyane française, où la qualité des données, à la fois pour la calibration et l'utilisation du modèle, sont exceptionnelles en Amazonie.

Des modèles de bilan carbone de l'exploitation avaient déjà été développés[1] mais présentaient plusieurs inconvénients :

- pas de prise en compte de l'ensemble des sources d'incertitudes,
- pas de temporalité des émissions de carbone (décomposition progressive de la biomasse[2]),
- pas de récupération du carbone après la coupe (repousse de la forêt), ou avec des modèles pas ou peu spatialement-explicites[3].

Le modèle présenté ici permet de pallier à ces manques. Il a été développé à l'échelle de la parcelle, et dans un cadre bayésien : les paramètres sont donc tous considérés comme des variables aléatoires. Ce cadre d'analyse a permis (i) d'intégrer l'information *a priori* sur certains paramètres ; (ii) de faire un minimum d'hypothèses quant à la distribution des paramètres ; (iii) de propager simplement l'incertitude liée aux différents sous-modèles et aux données. Les valeurs prises par les paramètres ont été soit extraites de la littérature (avec leur distribution dans les cas où elle était disponible), soit calibrées avec les données disponibles en Guyane française et en Amazonie. Une analyse de sensibilité a permis de révéler la part de l'incertitude des résultats attribuable à chaque sous-modèle.

La temporalité des émissions et de la récupération post-exploitation du carbone ont aussi été prises en compte. La biomasse perdue par exploitation a été divisée en quatre sous-compartiments, et se décompose selon une loi exponentielle, avec une vitesse de décomposition différente par compartiment. Deux

[1] T. R. H. Pearson et al. (2014). « Carbon emissions from tropical forest degradation caused by logging ». In : *Environmental Research Letters* 034017.9, p. 11.

[2] B. Hérault et al. (2010). « Modeling decay rates of dead wood in a neotropical forest. » In : *Oecologia* 164.1, p. 243–51 ; C. T. Numazawa et al. (2017). « Logging residues and CO 2 of Brazilian Amazon timber : Two case studies of forest harvesting ». In : *Resources, Conservation and Recycling* 122, p. 280–285.

[3] Huang et Asner (2010). « Long-term carbon loss and recovery following selective logging in Amazon forests », cf. note 149, p. 18 ; R. a. Houghton et al. (2012). « Carbon emissions from land use and land-cover change ». In : *Biogeosciences* 9.12, p. 5125–5142.

modèles permettent de prendre en compte la récupération de la biomasse :

- un modèle de repousse de forêt secondaire (sur les pistes d'exploitation abandonnées) qui a été calibré avec les données d'Arbocel en Guyane française, un site défriché puis inventorié pendant 40 ans. Un nouveau modèle de régénération des forêts secondaires calibré avec des données plus complètes du site d'Arbocel a été ajouté en annexe à la fin de l'ouvrage ; l'article a été soumis à la revue *Ecological Applications* ;
- un modèle de récupération de la biomasse post-exploitation, précédemment développé à partir des données du réseau TmFO en Amazonie[4]. Ce dernier modèle sera approfondi dans le chapitre 4.

Le modèle a ensuite été appliqué au cas de l'exploitation en Guyane française. Pour ce faire, des données fournies par l'Office National des Forêts ont été utilisées, stipulant pour chaque unité d'exploitation depuis 1974 : (i) les coordonnées (longitude, latitude) ; (ii) l'année d'exploitation ; (iii) la surface exploitée ; (iv) l'intensité d'exploitation (en m^3 de bois extrait par ha). Cela a permis de quantifier le bilan carbone de l'exploitation en Guyane française, ainsi que les incertitudes associées. Une perspective serait d'appliquer ce modèle à l'ensemble de l'Amazonie, mais la difficulté d'accès et de traitement des données des services forestiers, ainsi que la prévalence de l'exploitation illégale dans la plupart des autres pays amazoniens[5], rendent la tâche plus ardue.

Ce chapitre a fait l'objet d'une publication en 2016 dans la revue *Carbon Balance and Management*, de l'éditeur Springer[6]. Une nouvelle version du modèle est développée au sein du projet GFClim, intégrant le modèle de récupération du carbone post-exploitation développé dans le chapitre 4, le nouveau modèle de régénération des forêts secondaires [7], et de nouvelles données, notamment pour l'amélioration du sous-modèle des dégâts d'exploitation, principale source d'incertitude du modèle. Un package R basé sur ce modèle de bilan carbone est en cours de développement. Le but est de faire du modèle un outil fonctionnel et flexible pour les gestionnaires forestiers, en Guyane française et dans d'autres pays tropicaux.

[4] Rutishauser et al. (2015). « Rapid tree carbon stock recovery in managed Amazonian forests », cf. note 166, p. 20.

[5] S. Lawson et al. (2010). « Illegal Logging and Related Trade. Indicators of the Global Response ». In : *Review of European Community and International Environmental Law* 14.July, p. 132 + xix.

[6] C. Piponiot et al. (2016a). « A methodological framework to assess the carbon balance of tropical managed forests ». In : *Carbon Balance and Management* 11.1, p. 15.

[7] cf. annexe : article «Slow rate of secondary forest carbon accumulation in the Guianas compared with the rest of the Neotropics»soumis à la revue *Ecological applications*

Piponiot *et al. Carbon Balance Manage (2016) 11:15*
DOI 10.1186/s13021-016-0056-7

Carbon Balance and Management

RESEARCH Open Access

A methodological framework to assess the carbon balance of tropical managed forests

Camille Piponiot[1,9], Antoine Cabon[2], Laurent Descroix[3], Aurélie Dourdain[4], Lucas Mazzei[5], Benjamin Ouliac[6], Ervan Rutishauser[7], Plinio Sist[8] and Bruno Hérault[4*]

Abstract

Background: Managed forests are a major component of tropical landscapes. Production forests as designated by national forest services cover up to 400 million ha, i.e. half of the forested area in the humid tropics. Forest management thus plays a major role in the global carbon budget, but with a lack of unified method to estimate carbon fluxes from tropical managed forests. In this study we propose a new time- and spatially-explicit methodology to estimate the above-ground carbon budget of selective logging at regional scale.

Results: The yearly balance of a logging unit, i.e. the elementary management unit of a forest estate, is modelled by aggregating three sub-models encompassing (i) emissions from extracted wood, (ii) emissions from logging damage and deforested areas and (iii) carbon storage from post-logging recovery. Models are parametrised and uncertainties are propagated through a MCMC algorithm. As a case study, we used 38 years of National Forest Inventories in French Guiana, northeastern Amazonia, to estimate the above-ground carbon balance (i.e. the net carbon exchange with the atmosphere) of selectively logged forests. Over this period, the net carbon balance of selective logging in the French Guianan Permanent Forest Estate is estimated to be comprised between 0.12 and 1.33 Tg C, with a median value of 0.64 Tg C. Uncertainties over the model could be diminished by improving the accuracy of both logging damage and large woody necromass decay submodels.

Conclusions: We propose an innovating carbon accounting framework relying upon basic logging statistics. This flexible tool allows carbon budget of tropical managed forests to be estimated in a wide range of tropical regions.

Keywords: Carbon cycle, Selective logging, Error propagation, Amazonia, Production forests

Background

There is a growing interest of the international community in tropical forests and their key role in the global carbon cycle. In particular, tropical managed forests, i.e. tropical forests managed for timber production, are important in the context of climate change mitigation as they might either act as carbon source or sink, depending on their management type and cutting cycle length [1]. With half of tropical humid forests, i.e. more than 400 million ha, designated by National Forest Services (NFS) as production forests [2], forest management will play a decisive role in future global carbon cycle. However, while there is extensive scientific literature on undisturbed tropical forests, our knowledge on carbon balance (i.e. the net carbon exchange with the atmosphere) in managed forests remains to be improved. With international programs like REDD+ (Reducing Emissions from Deforestation and Degradation) aiming at mitigating carbon emissions, notably through improved forest management, it is essential to have a clear understanding of the carbon balance of tropical managed forests in order to develop unified accounting methods for carbon emissions.

The second "D" of REDD+, forest degradation, refers to the reduction of carbon stocks in areas that have retained sufficient canopy cover to be still considered as forests [3]. In tropical forests, selective logging is generally

*Correspondence: bruno.herault@cirad.fr
[4] Cirad, UMR EcoFoG (AgroParisTech, CNRS, Inra, Université de la Guyane, Université des Antilles), Campus agronomique, 97310 Kourou, French Guiana
Full list of author information is available at the end of the article

considered an important factor of forest degradation. Selective logging consists in harvesting only a few trees and leaving the rest of the forest to natural regeneration until the next logging event. Selective logging practices result in long-lasting carbon emissions to the atmosphere [4]. In the sole Brazilian Amazon, forestry-related carbon emissions are estimated to be equivalent to 60–123 % of deforestation emissions [5]. Emissions come from (i) the extracted wood, (ii) logging damage, i.e. trees killed (purposely or incidentally) during logging operations and (iii) skid trails, logging roads and decks used for log yarding. Logging operations (e.g. tree felling, log yarding or skidding) induce incidental damage to surrounding trees, proportional to logging intensity in conventional [6] or reduced impact logging [7]. Injured or smashed trees generally die soon after logging operation [8, 9], and, along with log residuals such as crowns or stumps, are left over in the forest. The quite slow decay of these woody debris and harvested logs is a long-term source of carbon to the atmosphere.

However selective logging does not induce carbon emissions only. Logging gaps and incidental mortality release local competition for key resources, such as light [10], and enhance carbon accumulation in remnant trees [11]. Some local studies suggest that carbon emissions peak soon after logging (5–10 years), while tree growth and recruitment counterbalance tree mortality after a decade, resulting in positive carbon accumulation in logged forests until an equilibrium is reached [12]. If not further disturbed, forests recover most of their initial carbon stock at the end of the cutting cycle, depending on logging intensity and damage [13, 14]. While skid trails and logging decks generally close rapidly after logging, logging roads may be reopened and persist for decades in the landscape [15].

Most studies on the carbon balance of selectively logged forests have estimated pre- and post-logging carbon stocks with remote sensing methods [16], allowing large-scale estimation of logging extent and quantification of canopy damage [14, 17, 18]. However optical remote sensing methods require further field calibration to avoid estimation biases [17, 19]. Accurate estimation of carbon loss and recovery based on evolution of canopy openness is questionable, as ground damage remain poorly assessed with remote sensing and canopy rapidly closes with crown expansion of survivors. [20]. Another problem lies in estimating carbon recovery rates when canopy gaps rapidly close with crown expansion of survivors and growth of recruits [21]. LiDAR and RADAR are a promising tools to overcome those limitations but remain expensive to be applied over large areas [22]. The International Panel on Climate Change [23] recommends basic methods based on activity data, e.g. the annual volume of extracted roundwood (in $m^3 \cdot year^{-1}$) or the annual logged area (in $ha \cdot year^{-1}$). So far, only a few studies have estimated the carbon balance of tropical logged forests from activity data. Griscom et al. [24] estimated carbon emissions at concession level with detailed maps of skidtrails, logged trees, damage and logging decks. But such maps are generally not available at regional level impeding the wide-use of this approach. Pearson et al. [25] developed emissions factors for the main logging compartments to be multiplied to extracted volumes, as a surrogate for carbon emissions from selective logging. For sake of simplicity, most studies have estimated committed emissions, i.e. all the carbon lost by logging is assumed to return instantaneously to the atmosphere. This choice is highly questionable as carbon emissions are spread over decades [4]. Some studies have indeed adopted a more dynamic approach, considering carbon emissions through time in managed forests [26]. However to date there is no method assessing all carbon fluxes (carbon accumulation as well as all emissions) from tropical managed forests through time.

In this study we developed a methodological framework to estimate the above-ground carbon fluxes from selective logging. Carbon fluxes are assessed first at the logging unit scale, i.e. the elementary management unit of the forest estate, and then integrated in space and time to estimate the regional carbon balance over time. The annual carbon net change of a given logging unit is estimated by aggregating carbon fluxes of three sub-models: (1) emissions from extracted wood, (2) emissions from woody debris (logging residues, damage, road and logging deck openings) left in the forest, and (3) sequestration from forest regrowth. Some submodels come from the literature while others were specifically developed and parameterised in a Bayesian framework for this study. Uncertainty over the global model are propagated through a Markov Chain Monte Carlo algorithm.

Our case study is French Guiana, a French territory located in the Guiana shield (northeastern Amazonia) with a total area of 84,000 km^2. Above 95 % of its area (8Mha) is occupied by tropical rainforest: timber extraction by selective logging is the 3rd economic sector. Selective logging occurs exclusively in the Permanent Forest Estate (2.4 Mha) (Fig. 1), an area managed by the French National Forest Service (NFS). We used 38-year NFS statistics on 1155 logging units (Fig. 2) to estimate the carbon balance of managed forests at countrywide scale.

Methods

The model framework

Methods overview We created a model to assess annual above-ground carbon fluxes at the logging unit scale,

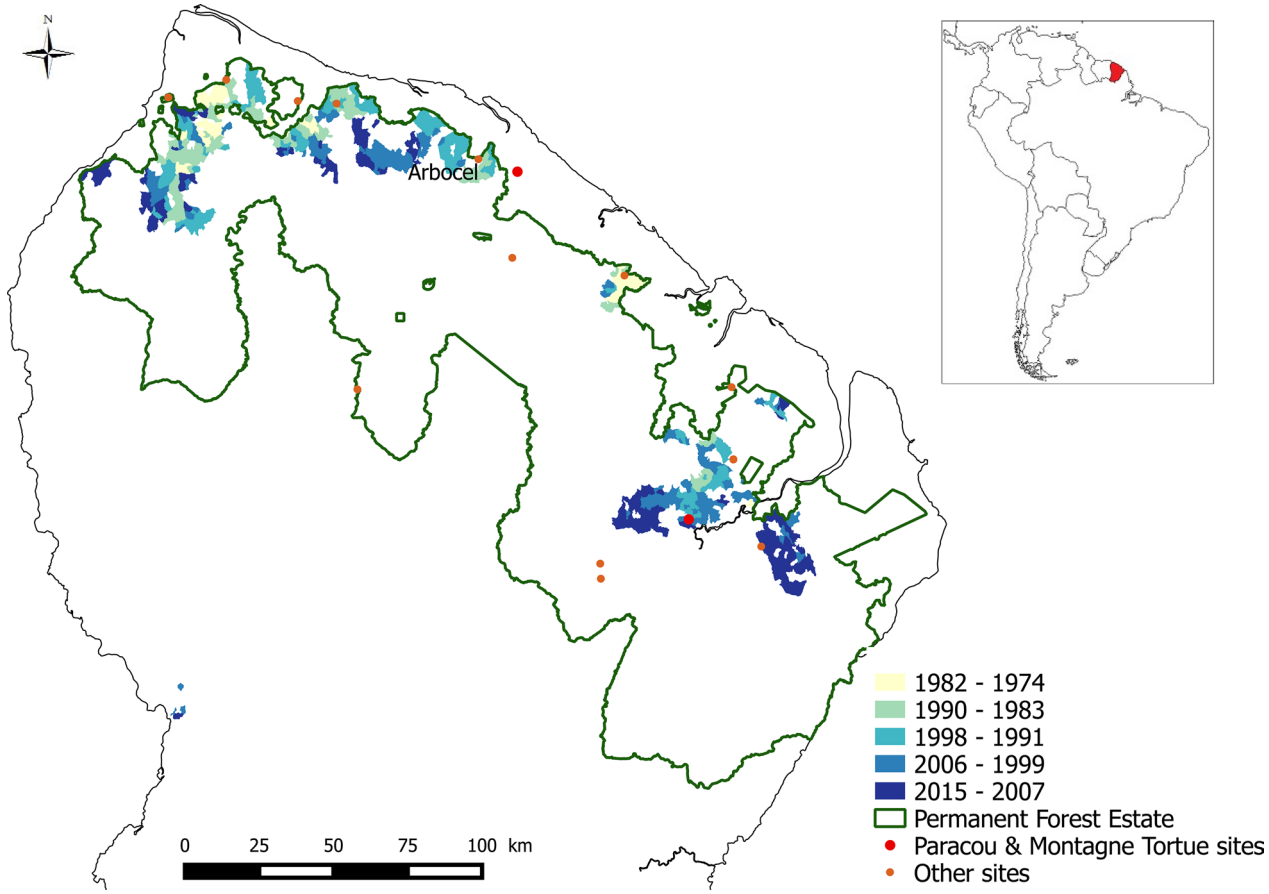

Fig. 1 Map of the Permanent Forest Estate in French Guiana. Logging units are *coloured* according to the year of logging: from *white and light blue* for most anciently logged plots to *dark blue* for most recently logged plots. *Dots* are experimental sites from the Guyafor network: *red dots* have both logged and control plots (Paracou and Tortue sites); *smaller orange dots* have only control plots. The borders of the Permanent Forest Estate are the *bold green lines*

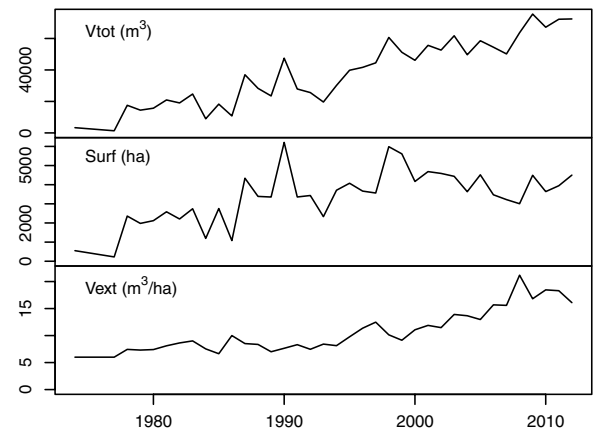

Fig. 2 National Forest Service statistics on selective logging in the French Guiana Permanent Forest Estate between 1974–2012. *Top graph* annual extracted volumes of roundwood *Vtot* (m^3) ; *middle graph* annual logged areas *Surf* (ha); *bottom graph* annual logging intensities *Vext* ($m^3 \cdot ha^{-1}$)

from the logging year up to the last year of NFS statistics, and then integrated these results over time and space. Conventionally, fluxes from carbon emissions are positive and fluxes from carbon accumulation are negative.

We modeled separately (1) emissions from extracted wood decay (Sawmill); (2) emissions from woody debris decay (Dead wood), divided into (2.a) logging damage and (2.b) deforestation on logging roads, main skid trails and logging decks; (3) sequestration from forest regrowth (3.a) in logging gaps and (3.b) on abandoned skid trails (Live biomass) (Fig. 3). For each submodel we first assessed the evolution of post-logging carbon stocks (in $MgC \cdot ha^{-1}$) in each logging unit. Annual carbon fluxes at time t (in $MgC \cdot year^{-1}$) are obtained by calculating the difference between stocks at time t and $t-1$, and multiplied by the logged area (in ha). Model parameters are considered as uncertain quantities, and the error is propagated with Monte Carlo methods. Doing so, we were

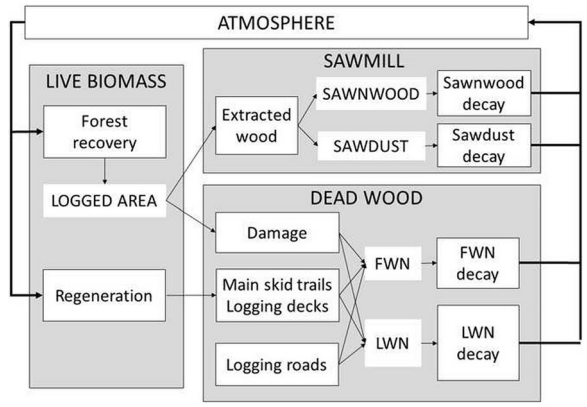

Fig. 3 Overall scheme of the carbon balance and submodels articulation. *Thick arrows* are carbon fluxes. *Grey boxes* are the three carbon compartments: Sawmill, Dead Wood and Live Biomass. Submodels are in surrounded white boxes. FWN and LWN are fine and large woody necromass respectively

able to track the annual carbon budget in each logging unit, and to conduct simultaneously a sensitivity analysis to identify the main sources of uncertainties in the global model.

Calibration data In some cases, submodels come from the literature. In other cases, and especially when there was no existing model, submodels were developed and parametrised with data from Amazonian permanent forest plots. We used data from control plots to assess pre-logging forest structure variables and logged plots to assess post-logging dynamics. Two networks of permanent forest plots were used in this study: (i) Guyafor in French Guiana (regional scale) (Fig. 1); (ii) TmFO, a network of logged plots spread across Amazonia (continental scale) [27]. From Guyafor, we used data from 11 sites, all containing control plots and two of them (Montagne Tortue, Paracou) also containing logged plots. From the TmFO network, we used data from four Amazonian sites (Jari, Tapajos, Tortue, Paracou) that have logged plots where extracted volumes have been measured. To calibrate the model of forest regeneration on logging decks and main skid trails, we used data from a 25-ha plot in French Guiana, Arbocel (see Fig. 1): the plot was clearcut in 1976 and then left to natural regeneration [28]. Some submodels and/or calibration data are specific to the context of selective logging in French Guiana: adapting this framework to other areas, countries or for upscaling purposes may require new data or new submodels to be regenerated. However, the general structure and the articulation of the different submodels is generic enough to be applied elsewhere.

Input data To run the model, we need basic NFS statistics available for every logging unit p: (i) the logged surface $Surf_p$ (ha), corresponding in French Guiana to on average 50 % of the total area, (ii) the total extracted volume $Vtot_p$ (m^3), (iii) the year of logging $t0_p$ and (iv) the initial above-ground carbon stock ACS_p ($MgC{\cdot}ha^{-1}$).

For our study, statistics on selective logging in the Permanent Forest Estate over the 1974–2012 time period were provided by the French NFS. According to NFS expertise, between 1974 and 1994 logging intensities are assumed to be equal to 6 $m^3{\cdot}ha^{-1}$ in the western forests, and equal to 10 $m^3{\cdot}ha^{-1}$ in the rest of the Permanent Forest Estate. After 1994, logging statistics are highly reliable and logging intensities $Vext_p$ are calculated as follows:

$$Vext_p = \frac{Vtot_p}{Surf_p} \quad (1)$$

Initial above-ground carbon stocks were extracted from the recently developed carbon map of French Guiana [29].

Sawmill

The carbon Ext_p ($MgC{\cdot}ha^{-1}$) of logs extracted from the logging unit p is defined as :

$$Ext_p = Vext_p \times dext \times 0.5 \quad (2)$$

where $Vext_p$ is the logging intensity ($m^3{\cdot}ha^{-1}$), the biomass is assumed to be 50 % carbon [30] and $dext = 0.736$ is the mean wood density of timber species in French Guiana. $dext$ has been estimated as the mean wood density of *Dicorynia guianensis* ($d = 0.76$), *Qualea rosea* ($d = 0.725$) and *Sextonia rubra* ($d = 0.65$) [31], weighted by their relative contribution to annual timber extraction [32].

The carbon stored in extracted wood (Ext_p) is then transformed into sawnwood with an efficiency of $f_{SW} = 0.33$ [33], the remaining 67 % consisting of sawdust. Sawnwood and sawdust then decompose with different decay rates. Sawdust is considered to decompose entirely within the first year after logging [34]. The quantity of sawdust $DecSD_p$ ($MgC{\cdot}ha^{-1}$) in the logging unit p at the year of logging $t0_p$ is:

$$DecSD_p = (1 - f_{SW}) \times Ext_p \quad (3)$$

Sawnwood decay is approximated with an exponential decay. The carbon in sawnwood $DecSW_{p,t}$ ($MgC{\cdot}ha^{-1}$) from logging unit p at time t is :

$$DecSW_{p,t} = f_{SW} \times Ext_p \times exp\Big(- \lambda_{SW} \times (t - t0_p)\Big) \quad (4)$$

with Ext_p the carbon in extracted wood, $t0_p$ the year of logging and λ_{SW} the decay rate of sawnwood in the tropics estimated as

$$\lambda_{SW} = \frac{ln(2)}{t_{0.5}} \quad (5)$$

with

$$t_{0.5} \sim N_{t0}(30, 15^2) \quad (6)$$

where $N_{t0}(30, 15^2)$ is the normal distribution truncated at zero with mean equal to 30 and standard deviation equal to 15, according to IPCC guidelines [30]. So far, no life cycle analysis has yet been done for woody products in the tropics and adapting the framework developed in Europe and North America in tropical countries remains challenging [35].

Dead wood

Both logging damage and deforestation on roads, main skid trails and logging decks are sources of dead wood that is left in the forest.

Logging damage

The logging damage Dam_p (MgC·ha^{-1}) within the logging unit p consists in above-ground carbon in trees harvested or killed (purposely or incidentally) during logging operations (tree felling and log yarding or skidding) minus carbon of extracted logs (Ext_p). Logging damage were assessed with data from 4 TmFO sites in the Eastern Amazon, where we have logging intensities $Vext_p$ and logging damage Dam_p (Fig. 4). Logging gaps and secondary skid trails are accounted for as logging damage, whereas main skid trails and logging roads are located outside of calibration plots and are considered as deforestation.

The relationship between $Vext_p$ and Dam_p was modelled as follows:

$$Dam_p \sim lnN(\theta_0 + \theta_1 \times Vext_p; \sigma^2_{dam}) \quad (7)$$

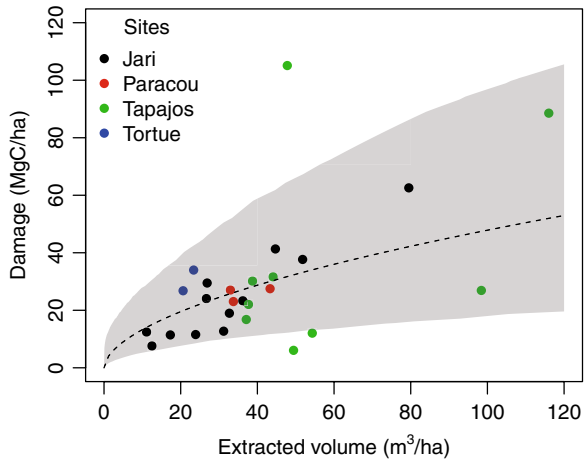

Fig. 4 Modelling logging damage (MgC·ha^{-1}) from extracted wood (m^3·ha^{-1}). The *dashed line* is the prediction with maximum likelihood, the shaded area is the 95 % credibility interval on the prediction. Data are taken from four Amazonian sites: Jari (*black*), Paracou (*red*), Tortue (*green*), Tapajos (*blue*)

where $lnN(\mu, \sigma^2_{dam})$ is the lognormal distribution of mean μ and standard deviation σ_{dam}. We chose the lognormal distribution to have errors proportional to the extracted volume, i.e. damage is less predictable for higher logging intensities.

The parameters $(\theta_0, \theta_1, \sigma_{dam})$ were estimated with a Bayesian inference, using a Markov Chain Monte Carlo method to obtain the posterior joint distribution. Uninformative priors were chosen. Each observation (one plot) was given a weight equal to the area of the plot.

Deforestation

Some basic infrastructure (logging roads, main skid trails, logging decks) is generally set up to store boles and get them out of the forest. As it has to be easily reached from every part of a logging unit p, the total area cleared for infrastructure is assumed to be proportional to the total logged area $Surf_p$. The length of logging roads may depend on the topography but, in the French Guiana Permanent Forest Estate, the topography is quite homogeneous.

Logging roads According to NFS expertise (personal communication):

$$\delta_p \sim U(0.12; 0.25) \quad (8)$$

where δ_p is the entire width of clearing for logging roads in logging unit p (expressed in hectometers hm). Based on the study of Guitet et al. [36], we fit the length of logging roads η_p (hm·ha^{-1}) as:

$$\eta_p \sim exp(17.95) \quad (9)$$

The carbon removed for road clearing $Road_p$ (MgC·ha^{-1}) and left to decay in the logging unit p is :

$$Road_p = ACS_p \times \delta_p \times \eta_p \quad (10)$$

where ACS_p is the initial above-ground carbon stock (MgC·ha^{-1}).

Main skid trails Main skid trails are built to allow the skidders to get in the logging units. According to Guitet et al. [36]:

$$SurfST_p \sim U(0.04; 0.10) \quad (11)$$

where $SurfST_p$ is the area (ha) of main skid trails per hectare logged. As large trees are generally avoided by skidders during yarding, we assumed that only trees with *DBH* (Diameter at Breast Height) $\leq$50 cm were killed. For a logging unit p, the above-ground carbon removed on skid trails $STrail_p$ (Mg·ha^{-1}) is:

$$STrail_p = ACS_p \times SurfST_p \times f_{50} \quad (12)$$

where ACS_p is the initial above-ground carbon stock of the logging unit p (Mg·ha^{-1}) and f_{50} is the proportion

of ACS_p in trees DBH <50 cm. f_{50} was estimated with data from the control plots of the 11 Guyafor sites. For one site j, the proportion $f_{50,j}$ was calculated as follows:

$$f_{50,j} = \frac{\sum_{DBH_k \leq 50} ACS_{j,k}}{\sum_k ACS_{j,k}} \quad (13)$$

where $\sum_{DBH \leq 50} ACS_{j,k}$ is the above-ground carbon of all trees with $DBH \leq 50$ cm and $\sum_k ACS_{j,k}$ is the total above-ground carbon of the site. We report the obtained distribution in Table 1.

Logging decks Logging decks are cleared to store harvested boles. Based on detailed mapping of 11 logging decks in logging units HKO95 (283 ha) and HKO96 (466 ha) and with the information that one logging deck is set up for every 70 ha (NFS expertise, personal communication), we used:

$$\frac{LDeck_p}{ACS_p} \sim lnN(-6.12, 0.58^2) \quad (14)$$

with ACS_p the above ground carbon stock of the logging unit p, and $LDeck_p$ (MgC·ha^{-1}) is the carbon removed in logging decks.

Dead wood decay

Assuming that all woody debris are left out for decay in situ, dead wood was divided into two pools with different decay rates: (i) fine woody necromass (FWN), i.e. leaves, twigs, and branches with diameter <10 cm, and (ii) large woody necromass (LWN), i.e. logs and branches with diameter ≥10 cm.

Fraction of Large Woody Necromass We used Chambers et al. [37] model to estimate the fraction of large woody necromass LWN_i at tree scale (i).

For a tree i : If $DBH_i < 100$ cm:

Table 1 Parameters of the carbon balance model

Submodel	Parameter	Distribution	Justification	Data source
Extracted wood	*dext*	0.736	3 main commercial species	[31, 32][a]
	f_{SW}	0.33	No uncertainty reported	[33][b]
Sawnwood decay	λ_{SW}	$N_{t0}(30, 15^2)$	Positive normal distribution	[30][c]
Damage	θ_0	$N(1.28, 0.48^2)$	Normal approximation of the posterior	TmFO sites[b]
	θ_1	$N(0.56, 0.14^2)$	Normal approximation of the posterior	TmFO sites[b]
	σ_{dam}	$N(0.37, 0.04^2)$	Normal approximation of the posterior	TmFO sites[b]
Logging roads	δ	$U(0.12, 0.25)$	Personal communication	NFS expertise[a]
	η	$exp(17.95)$	Decreasing monotonic distribution	[36][a]
Main skid trails	*SurfST*	$U(0.04, 0.10)$	Only range of values is reported	[36][a]
	f_{50}	*Beta*(15.10, 15.32)	Proportion	Guyafor[a]
Logging decks	*LDeck*	$ACS \times lnN(-6.12, 0.58)$	Positive distribution	Original data[a]
LWN decay	*fLWN*	*Beta*(1115, 169)	Proportion	Guyafor[a]
	λ_1	$N(0.069, 0.028^2)$	Normal approximation of the posterior	Guyafor[a]
	λ_2	$N(0.198, 0.074^2)$	Normal approximation of the posterior	Guyafor[a]
	π_1	$N(0.512, 0.032^2)$	Normal approximation of the posterior	Guyafor[a]
	σ_{LWN}	$N(0.015, 0.0035^2)$	Normal approximation of the posterior	Guyafor[a]
FWN decay	λ_{FWN}	$N(0.19, 0.026^2)$	Reported distribution	[37][c]
Forest recovery	α	$N(1.100, 0.03^2)$	Reported distribution	[13][c]
Regeneration	μ_0	$N(-4.505, 0.124^2)$	Maximum likelihood estimate	Arbocel[a]
	μ_1	$N(1.085, 0.038^2)$	Maximum likelihood estimate	Arbocel[a]
	φ	490.7	Maximum likelihood estimate	Arbocel[a]

Parameters are grouped by submodel in which they appear. *FWN* fine woody necromass decay; *LWN* large woody necromass. *ACS* initial above-ground carbon stock (MgC·ha^{-1}). Parameters are: *dext* mean density of extracted roundwood in French Guiana; f_{SW} efficiency of wood transformation in sawmills; λ_{SW} decay rate of sawnwood; $(\theta_0, \theta_1, \sigma_{dam})$ parameters of the relationship between extracted wood and logging damage; (η, δ) length (hm·ha^{-1}) and width (hm) of logging roads; *SurfST* main skid trails area (ha); f_{50} proportion of above-ground carbon in trees DBH <50 cm; *LDeck* carbon loss in logging decks; f_{LWN} fraction of necromass carbon in large woody necromass; $(\lambda_1, \lambda_2, \pi_1, \sigma_{LWN})$ parameters of large woody necromass decay; α parameter of the recovery model; μ_0, μ_1 and φ: parameters of the regeneration beta model

[a] Valid in French Guiana

[b] Valid in Amazonia

[c] Valid in the tropics

$$LWN_i = 0.774 + 0.0018 \times DBH_i \quad (15)$$

else $LWN_i = 0.95$.

This fraction of large woody necromass has been estimated for all individuals in control plots of the 11 Guyafor sites. For one site j, the fraction of large woody necromass is:

$$fLWN_j = \frac{\sum_i (LWN_{i,j} \times ACS_{i,j})}{\sum_i ACS_{i,j}} \quad (16)$$

We report the obtained distribution of $fLWN_j$ in Table 1.

At $t = t0_p$ ($t0_p$: year of logging) in the logging unit p:

$$FWN_{p,t0_p} = (1 - f_{LWN}) \times (Dam_p + Road_p + STrail_p + LDeck_p) \quad (17)$$

$$LWN_{p,t0_p} = f_{LWN} \times (Dam_p + Road_p + STrail_p + Ldeck_p) \quad (18)$$

where $FWN_{p,t0_p}$ and $LWN_{p,t0_p}$ (MgC·ha^{-1}) are the carbon in fine and large woody necromass, respectively, left on the logging unit p at $t0_p$.

Decay of Fine Woody Necromass Fine woody necromass decay in logging unit p at time t is estimated by the following model [38]:

$$DecFWN_{p,t} = FWN_{p,t0_p} \times exp\Big(- \lambda_{FWN} \times (t - t0)\Big) \quad (19)$$

where $DecFWN_{p,t}$ (MgC·ha^{-1}) is the fine woody necromass left in the logging unit p at time t and λ_{FWN} is the decay rate of fine woody necromass (Table 1).

Decay of Large Woody Necromass There was no published model for decay of large woody necromass at the logging unit level and derived individual tree large woody necromass (LWN) decay from [4]:

$$LWN_{i,t} = LWN_{i,t0} \times exp\Big(- \frac{\gamma_1}{WD_i^{\gamma_2} \times (circ_i)^{\gamma_3}} \times (t - t0)\Big) \quad (20)$$

where $LWN_{i,t}$ is the large woody necromass of the individual i at time t, WD_i the wood density of the individual i and $circ_i$ the circumference at breast height of the individual i, and $(\gamma_k)_{1,2,3}$ are parameters of the model [4]. For all 11 Guyafor sites, the model was applied to all individuals i of the control plots. Individual trajectories are then aggregated to have the large woody necromass left at time t on the site j:

$$LWN_{j,t} = \sum_i LWN_{i,j,t} \quad (21)$$

where $LWN_{j,t}$ is the large woody necromass left at time t on the site j; $LWN_{i,j,t}$ is the large woody necromass at time t of the individual i from the site j.

A new model was developed at the logging unit level: to better fit the data, a double-decay model was chosen instead of a one-parameter decay model, because it drastically reduced the bias in our predictions. The double-decay model works as if there were two pools of large woody necromass (i.e. sap- and heart-wood) with two different decay rates.

$$\frac{DecLWN_{p,t}}{LWN_{p,t0}} = \pi_1 \times exp\Big(- \lambda_1 \times (t - t0_p)\Big) + (1 - \pi_1) \times exp\Big(- \lambda_2 \times (t - t0_p)\Big) + \varepsilon_{LWN,p} \quad (22)$$

with

$$\pi_1 > 0.5$$

and

$$\varepsilon_{LWN,p} \sim N(0; \sigma_{LWN})$$

where $\frac{DecLWN_{p,t}}{LWN_{p,t0_p}}$ is the fraction of the initial large woody necromass left on logging unit p at time t ; λ_1 and λ_2 are the two decay rates and π_1 the fraction of large woody necromass decomposing with the rate λ_1; $\varepsilon_{LWN,p}$ is the additive error for the logging unit p, taken in $N(0; \sigma^2_{LWN})$, the centred normal distribution of standard deviation σ_{LWN}.

Parameters $(\lambda_1; \lambda_2; \pi_1; \sigma_{LWN})$ were estimated as follows: (i) 100 sets of parameters $(\gamma_k)_{1,2,3}$ of the individual decay model were taken in their distribution; (ii) for each set of individual parameters $(\gamma_k)_{1,2,3}$, the trajectories of large woody necromass $LWN_{j,t}$ for each site j in the 11 Guyafor sites was estimated; (iii) parameters $(\lambda_1; \lambda_2; \pi_1; \sigma_{LWN})$ were then estimated using a Bayesian inference with a Markov Chain Monte Carlo method. Uninformative priors were chosen. One set of parameters $(\lambda_1; \lambda_2; \pi_1; \sigma_{LWN})$ was stored for every set of individual parameters $(\gamma_k)_{1,2,3}$. 100 sets of parameters $(\lambda_1; \lambda_2; \pi_1; \sigma_{LWN})$ were then stored to be used in the full model (the normal approximations of the posterior distributions are in Table 1).

Live biomass

Carbon recovery in logged areas

The assumption of a linear carbon recovery was made, i.e. the rate at which a logged area stores above-ground

carbon after logging is constant and becomes null at recovery time, when the above-ground carbon has reached its original level. This assumption is arguable but is consistent with available data on post-logging dynamics in the region [13]. Under this assumption, the recovery time (RT) can be estimated with the sole percentage of above-ground carbon loss caused by logging:

$$RT_p = \left(\frac{100 \times (Ext_p + Dam_p)}{ACS_p}\right)^{\alpha} \quad (23)$$

with

$$\alpha \sim \mathcal{N}(1.100, 0.013^2) \quad (24)$$

with RT_p (yr) the recovery time of the logging unit p, $Ext_p + Dam_p$ (MgC·ha^{-1}) the above-ground carbon loss per ha logged in the logging unit p and ACS_p the initial above-ground carbon stock (MgC·ha^{-1}).

The above-ground carbon recovered $Recov_{p,t}$ (MgC·ha^{-1}) at time t in the logged area of the logging unit p is then :

$$Recov_{p,t} = \min\left(Ext_p + Dam_p; (t - t0_p) \times \frac{Ext_p + Dam_p}{RT_p}\right) \quad (25)$$

When $t - t0_p \leq RT_p$ (i.e. before recovery time), the logged area stores carbon with a rate $\frac{Ext_p + Dam_p}{RT_p}$. When $t - t0_p > RT_p$, the logged area has recovered all the above-ground carbon lost $Ext_p + Dam_p$ and the carbon storage stops.

Regeneration on abandoned main skid trails and logging decks

The fate of the carbon dynamics on abandonned skid trails and logging decks was modelled taking advantage of four 1.65-ha plots clearcut 38 years ago (Fig. 5), and regularly measured since [28]. Carbon stocks regeneration on skid trails with compacted soils may be expected to be slower than on large clear-cuts but no data on skid trails reforestation have been produced in French Guiana. The following model was inferred:

$$Rege_{p,t} = ACS_p \times Y_{p,t} \quad (26)$$

with

$$Y_{p,t} \sim Beta\left(\mu_0 + \mu_1 \times log(t - t0_p + 1); \varphi\right) \quad (27)$$

where $Rege_{p,t}$ (MgC·ha^{-1}) is the above-ground carbon gain from forest regeneration on plot p at time t, ACS_p (MgC·ha^{-1}) is the initial above-ground carbon stock of the plot p (i.e. before the clear cut), $Y_{p,t}$ is the proportion of the initial above-ground carbon stock recovered on the plot p at time t. $Y_{p,t}$ follows a beta distribution of mean $\mu_0 + \mu_1 \times log(t - t0_p + 1)$ and of precision φ (parameters (μ_0, μ_1, φ) estimated distributions are in Table 1). The beta distribution is defined on [0, 1] and takes two shape parameters.

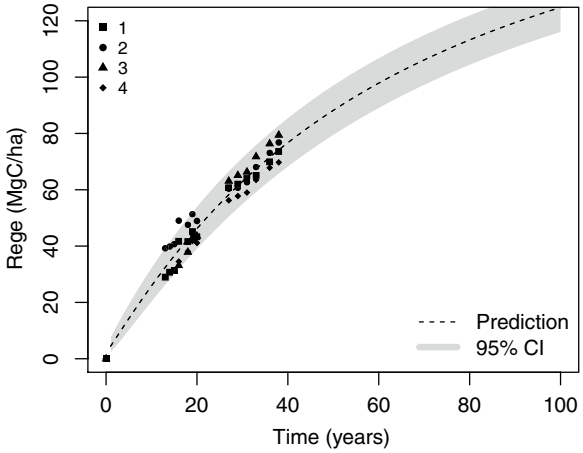

Fig. 5 Beta model of carbon regeneration (*Rege*, MgC·ha^{-1}) on four clearcut plots. The *dashed line* is the prediction with maximum likelihood, the shaded area is the 95 % credibility interval on the prediction. Data are taken from four 1.65-ha plots in Arbocel site (French Guiana), clearcut 38 year ago and let to natural regeneration

Accounting for uncertainties

Uncertainty propagation

The model was built and parametrised with MCMC algorithms in order to track uncertainties. Uncertainty propagation was done with the following steps: (i) every parameter is randomly taken in its distribution; (ii) the model is applied over all logging units of the region with these parameters values; (iii) results are integrated in space and time and stored. These three steps are repeated 5000 times and summary statistics are then calculated.

Sensitivity analysis

To assess the uncertainty induced by each submodel, we carried out a sensitivity analysis where the parameters of each submodel are set to their maximum likelihood values one after the other, making the submodel deterministic while the rest of the model remains stochastic. The results for each deterministic submodel are then compared to the total model: the "shrinkage" of their summary statistics reflects the uncertainty linked to the parameters of a specific submodel, more than the model and modelling choices themselves.

Results and discussion

Methodological aspects

In this study we developed a new methodology to assess the above-ground carbon balance of tropical managed

forests. The model is based on a book-keeping approach: it aggregates post-logging carbon fluxes of every logging unit over a given area and period of time to obtain the regional carbon balance. The main advantage of our methodology compared to other published methods estimating emissions from selectively logged concessions [24, 25] lies in the fact that both post-logging carbon sequestration and necromass respiration are explicit functions of time. This framework is flexible enough to be adapted to new situations and areas, but potential users should keep in mind that applying this model to other areas will require in-depth analysis on the suitability of the parameters value, variables distribution and submodels choices. The framework can also be adapted to integrate new information on post-logging forest dynamics or to take into account new logging technique, e.g. new techniques of reduced impact logging (RIL) likely to decrease the quantity of damage for the same logging intensity [39] but used in less than 5 % of selectively logged areas so far [1]. Part of logging damage may also be used for new purposes, e.g. burned in energy plants as wood fuel [40]. The model can be adapted and re-parametrised very quickly to take into account such changes.

We aknowledge that French Guiana is a special case in the tropics in regards to data quality and availability. It is therefore easier to develop a methodology there than in other countries where both input and calibration data are scarse. Submodels were either taken from the literature or specifically developed for this study with data at regional and continental scales. For each submodel, parameters are considered as uncertain quantities making good use of the Bayesian inference framework. Depending on spatial extent of the data used to calibrate the corresponding submodel, parameters distribution have different geographic validity (Table 1). Submodels from the literature and our submodel of logging damage (*Dam*) are considered to be valid over Amazonia. The estimated distribution of corresponding parameters could therefore be used for assessing the carbon balance of any Amazonian region. The other models developed in this study [deforestation on roads, main skid trails and decks, large woody necromass (LWN) decay and forest regeneration] were calibrated with data from a regional plot network, Guyafor or with NFS data and should be used with caution elsewhere. In order to study the carbon balance of other regions, data from permanent plots in the region of interest should be used to validate, and if necessary recalibrate submodels.

The method is simple and only requires two sets of input data : logged areas in space and time and the intensities at which these forest areas were logged. These data can come either from official logging statistics or from remote sensing methods. In many countries, logging operations occur almost exclusively inside logging concessions for which management plans do exist. For instance, in the Congo Basin, 45 Mha of forest are managed under the concession system [41]. In these cases, the logging statistics needed can be taken directly from management plans. In other countries where management plans do not exist or are not fully applied [42], remote sensing tools can be useful to map logged areas. For instance, Asner et al. [5] tracked logged areas in five States of the Brazilian Amazon during three consecutive years using Landsat imagery and CLAS methodology. Logging intensities are more difficult to obtain with remote sensing methods: a way to overcome this problem is to use region-wide statistics on commercialized wood that are generally quite robust because wood boles from either legal or illegal logging eventually need authorizations to be transported and commercialized. The simplest way to estimate logging intensities is then to use an average logging intensity, or to use local expertise to locally refine this average value. Bayesian approaches are quite appropriate to mix *a priori* knowledge with quantitative datasets. For both logged areas and and logging intensities, a close attention should be paid to uncertainties and their propagation into the complete model.

Carbon balance at the logging unit scale

To fully understand the theoretical behaviour of our model we focused on two logging units both logged in 1996: one with a low logging intensity (1.1 $m^3 \cdot ha^{-1}$) and one with a high logging intensity (33 $m^3 \cdot ha^{-1}$). For those two logging units, we estimated carbon fluxes ($MgC \cdot ha^{-1} \cdot year^{-1}$) during an 65-year period, which corresponds to the official cutting cycle in French Guiana (Fig. 6).

Annual fluxes

At low logging intensity, the two main sources of carbon are both logging damage and deforestation (on roads and main skid trails). At higher logging intensities, emissions from deforestation become negligible compared to emissions from damage, consistent with previous remote-sensing results in the Brazilian Amazon [43]. According to our model, carbon fluxes reach a steady state before the end of the 65-year period for both logging units (Fig. 6).

The different trends of the net carbon change are mostly explained by the interplay of two components: emissions from logging damage and accumulation from recovery in logging gaps. On one hand, higher logging intensities obviously cause more logging damage, resulting in higher carbon emissions from damage decay. On the other hand, the annual carbon flux from recovery in logging gaps is less dependent on logging damage (Fig. 6): a logging unit that has undergone high logging intensities will thus take longer to recover.

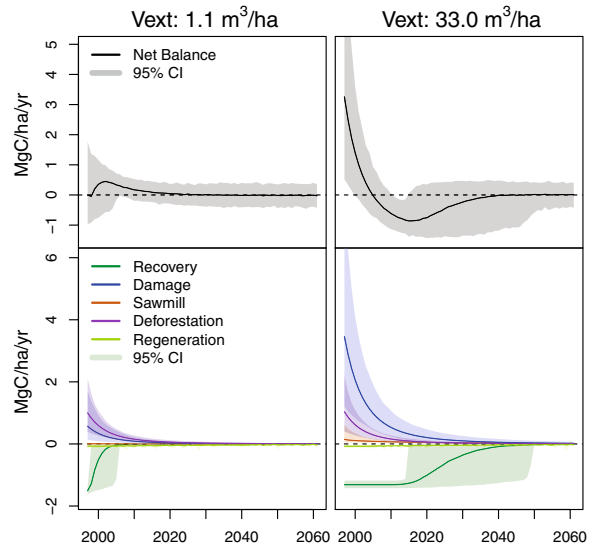

Fig. 6 Annual above-ground carbon fluxes from logging on a 65-year period in two logging units logged in 1994 with different logging intensities. The first logging unit underwent a low-intensity logging (*left*) with a mean extracted volume V_{ext} = 1.1 $m^3 \cdot ha^{-1}$ whereas the second logging unit underwent a high-intensity logging (*right*) with a mean extracted volume V_{ext} = 33.0 $m^3 \cdot ha^{-1}$. For each plot, the net carbon flux (*top*) is the result of four components: emissions from logging damage (*blue*), emissions from road, deforestation on main skid trail and logging deck (*purple*), emissions from extracted timber (*red*), accumulation from post-logging recovery on the plot (*forest green*) and accumulation from regeneration on main skid trails and logging decks (*light green*). The *shaded areas* correspond to the 95 % credibility intervals

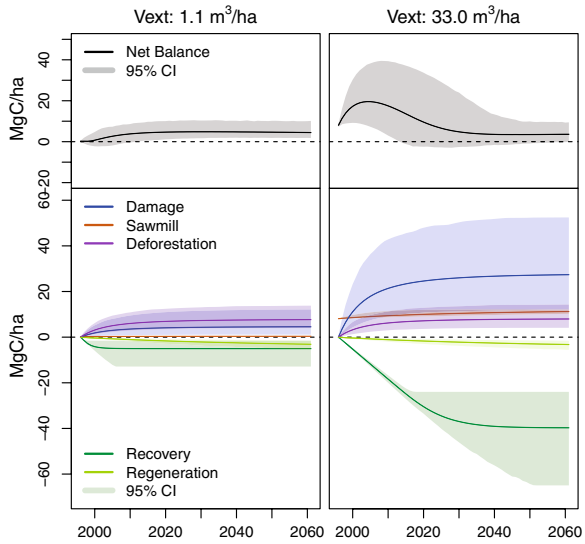

Fig. 7 Above-ground carbon balance from logging on a 65-year period in two logging units logged in 1994 with different logging intensities. The carbon balance at time *t* is the integral of annual carbon fluxes, i.e. the sum of annual carbon fluxes from the year of logging (1996) to *t*. The first logging unit underwent a low-intensity logging (*left*) with a mean extracted volume V_{ext}=1.1 $m^3 \cdot ha^{-1}$ whereas the second logging unit underwent a high-intensity logging (*right*) with a mean extracted volume V_{ext} = 33.0 $m^3 \cdot ha^{-1}$. For each plot, the net carbon balance (*top*) is the result of fourcomponents: emissions from logging damage (*blue*), emissions from road, deforestation on main skid trail and logging deck (*purple*), emissions from extracted timber (*red*), accumulation from post-logging recovery on the plot (*forest green*) and accumulation from regeneration on main skid trails and logging decks (*light green*). The *shaded areas* correspond to the 95 % credibility intervals

Even under high logging intensity (33 $m^3 \cdot ha^{-1}$), the time to null carbon fluxes does not exceed 50 year. Previous results from satellite data have shown that in the Brazilian Amazon, where logging intensities usually range between 20 and 30 $m^3 \cdot ha^{-1}$, carbon emissions last for 2–3 decades [14]. This last study also showed that carbon forest recovery may last for up to a century, twice as much as our highest prediction (Fig. 6). This difference in recovery times may arise from the model of forest recovery chosen in our study. We chose the model proposed in Rutishauser et al. [13], that assumes a constant recovery rate. With lack of insight in long-term dynamics of recovering forests, we made the conservative assumption that the carbon accumulation stops when initial carbon stock is recovered. However it is possible that recovering forests behave differently when the carbon stock approaches its initial value. The carbon storage could have a logistic behaviour, decelerating when approaching the initial carbon stock, or could oscillate around an equilibrium value (i.e. the initial carbon stock) and stabilize only after a longer time period [44].

Under the assumptions of our model, the carbon fluxes of a logged forest return to their equilibrium state before the end of the cutting cycle. At second harvest cycle, the carbon stocks will likely be close to their initial value, except on logging roads and skid trails. This does not mean that the forest will have returned to its original state as selective logging is known to have long-lasting effects on forest structure, timber volume and biodiversity [45].

Cumulative fluxes

To assess the carbon balance of our two logging units, we estimated the cumulative carbon fluxes (Fig. 7). The cumulative carbon flux at time *t* is the sum of annual carbon fluxes between the logging year and *t*.

The carbon balance of the first logging unit (with low logging intensity) is not different from zero in the first years because the recovery rate is quite similar to emissions from dead wood decay and deforestation. At the

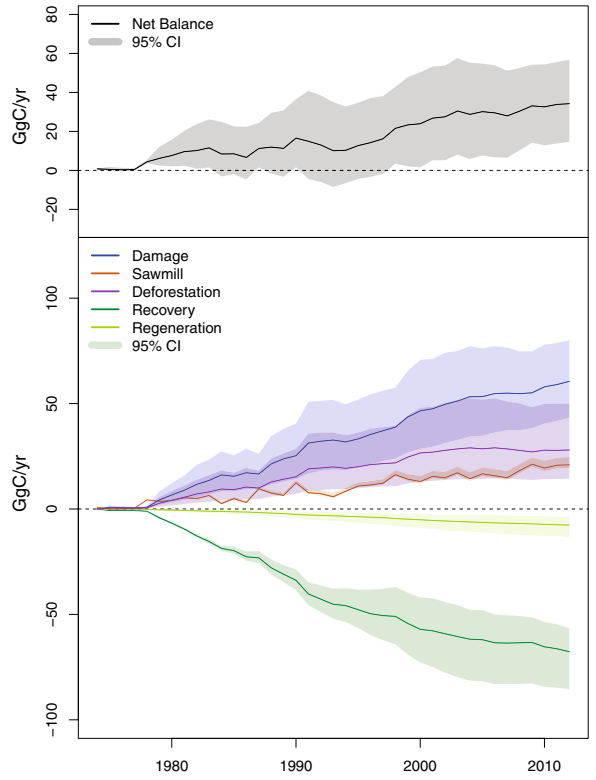

Fig. 8 Annual above-ground carbon fluxes from logging in the Permanent Forest Estate between 1974–2012. The net carbon flux (*top*) is the result of four components: emissions from logging damage (*blue*), emissions from road, deforestation on main skid trail and logging deck (*purple*), emissions from extracted timber (*red*), accumulation from post-logging recovery on the plot (*forest green*) and accumulation from regeneration on main skid trails and logging decks (*light green*). The *shaded areas* correspond to the 95 % credibility intervals

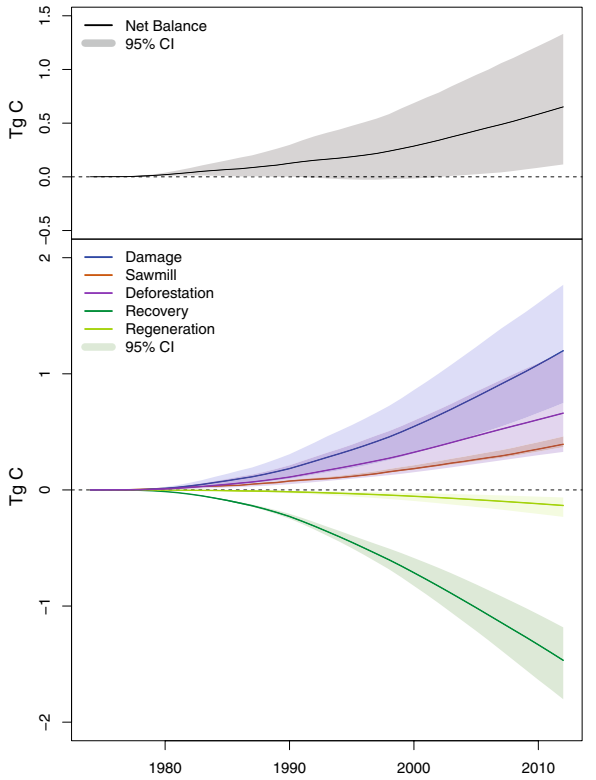

Fig. 9 Above-ground carbon balance of the French Guiana Permanent Forest Estate between 1974–2012. The carbon balance at time *t* is the integral of annual carbon fluxes, i.e. the sum of annual carbon fluxes from the first year (1974) to *t*. The net carbon balance (*top*) is the result of four components: emissions from logging damage (*blue*), emissions from road, deforestation on main skid trail and logging deck (*purple*), emissions from extracted timber (*red*), accumulation from post-logging recovery on the plot *(forest green*) and accumulation from regeneration on main skid trails and logging decks (*light green*). The *shaded areas* correspond to the 95 % credibility intervals

end of the cutting cycle, the carbon balance of the logging unit is about equal to the carbon emissions from deforestation (on roads and skid trails). The second logging unit (with high logging intensity) has high emissions from damage decay in the first 8 years after logging, that exceed carbon accumulation from forest recovery: the carbon balance of the logging unit increases. Between 8 and 40 years after logging, carbon accumulation from forest recovery exceeds carbon emissions: the carbon balance decreases. After 40 years, the carbon balance of the logging unit stabilizes at a value about equal to the emissions from deforestation.

In the first years after logging, the net carbon balance is mostly driven by the logging damage, directly related to logging intensity. High logging intensities cause more damage, and thus induce higher emissions from dead wood decay. At the end of the cutting cycle, both logging units have the same carbon balance, corresponding to the carbon emissions from deforestation on logging roads and main skid trails. Indeed, there is little regeneration in main skid trails, and no regeneration in deforested roads whereas carbon recovery in logging gaps compensates the carbon emissions from extracted wood and logging damage. In terms of forest management, the carbon balance of a logging unit at the end of a cutting cycle thus depends mostly on the total surface of logging roads and skid trails. To mitigate carbon emissions, logging should be planned to avoid road and skid trail opening. This can be done by intensifying timber extraction per logged area and thus lowering the amount of infrastructure needed to get the logs out of the area.

Carbon balance at the regional scale

After assessing carbon fluxes for each logged logging unit, results were aggregated over space to assess the carbon fluxes over the whole Permanent Forest Estate, and

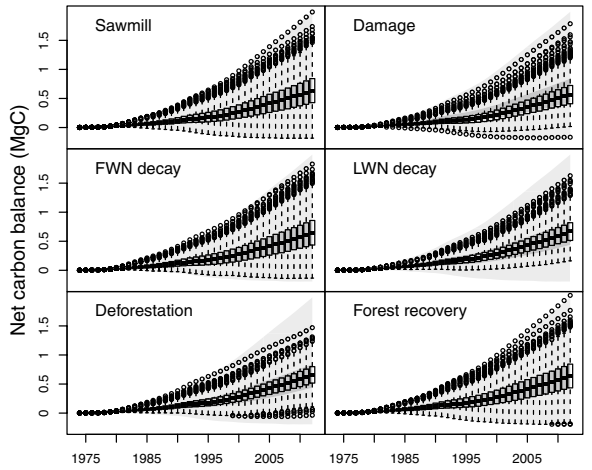

Fig. 10 Estimating the uncertainty due to each submodel into the net carbon balance. The box plots represent the distribution of the net carbon balance when parameters of each submodel are set to their maximum likelihood value. The shaded area is the range of the net carbon balance for the total model, i.e. when all parameters are taken in their statistical distribution

over time to assess the carbon balance between 1974 and 2012 (Figs. 8, 9).

Annual fluxes

As for the logging unit level, the largest carbon emissions arise from the decay of logging damage (Fig. 8): this is consistent with results from field data on other Amazonian countries [25]. Carbon accumulation is mainly explained by forest recovery in the logged area, forest regeneration on main skid trails and logging decks being negligible.

Net carbon fluxes are positive: the Permanent Forest Estate in French Guiana behaves like a carbon source during the 1974–2012 period. However zero is included in the 95 % credibility interval until 2000: the positiveness of carbon fluxes is not significant between 1974 and 2000. In the mid 1990' there is a sudden increase in net carbon fluxes, and after 2000 the lower bound of the 95 % credibility interval is positive: between 2000 and 2012, logging in the Permanent Forest Estate significantly emitted carbon to the atmosphere. This change in the trend of net carbon flux corresponds to increased logging intensities in the mid 1990s (Fig. 2).

The carbon balance at the regional scale

Selective logging countrywide has induced significant carbon emissions since 2000 (Fig. 8), resulting in a positive net carbon balance in 2012 (Fig. 9). The net above-ground carbon balance in 2012 is estimated to be comprised between 0.12 and 1.33 Tg C, with a median value of 0.64 Tg C. With 1.36 Pg C stored in above-ground carbon [29], selective logging has emitted between 0.01 and 0.10 % of the French Guiana forest stock over the 1974–2012 period. Such ratio may look quite low when compared to the above-ground carbon stock of all the total forested area, but we have to keep in mind that the units logged over the 1974–2012 in the Permanent Forest Estate cover 0.12 Mha, i.e. 5 % of the total forested area in French Guiana (Fig. 1). Moreover, logging intensities in French Guiana are low (12.7 $m^3 \cdot ha^{-1} \cdot year^{-1}$, Fig. 2) compared to the Brazilian Amazon where logging intensities average 23.2 $m^3 \cdot ha^{-1} \cdot year^{-1}$ [5]. Applying our model to the rest of Amazonian managed forests should thus raise higher carbon emissions.

Possible model improvements

Deforestation, damage and LWN decay are key submodels

The sensitivity analysis reveals three main sources of uncertainty in our model: deforestation, large woody necromass decay and logging damage (Fig. 10). Despite relatively low values of logging areas that are annually deforested, the key role of the deforestation submodel in generating the net carbon balance uncertainties (Fig. 10) may look quite surprising. Because the carbon loss on permanently-deforested logging roads will never be recovered, carbon emissions accumulate over time, and their uncertainties as well. At the end of the 40-year period, the cumulative uncertainties then become non-negligible. The quantity of damage intervenes in two carbon fluxes: emissions from logging damage decay and carbon recovery (Fig. 3). If the objective is to estimate one of these two fluxes, efforts should be made to improve the prediction of logging damage. Until now the only explanatory variable of our logging damage model is the logging intensity *Vext* ($m^3 \cdot ha^{-1}$). A great proportion of the variability remains unexplained, and other factors may help improve the prediction of logging damage. For instance, including further information such as the logging techniques applied (conventional or reduced-impact logging), the local topography, or the forest structure would certainly have improved damage predictions. Nevertheless, the main objective is to estimate the net carbon balance, improving the estimation of logging damage should not be a priority. Indeed, recovery dynamics are very fast, lasting for a few decades at the most (Fig. 6). At the regional scale, emissions from damage decay are almost instantaneously mitigated by recovery mechanisms (Figs. 8, 9), so the variability of logging damage has little influence on the overall variability of the carbon balance (Fig. 10). On the contrary, the variability of large woody necromass decay explains a great part of the overall uncertainty of the total carbon balance (Fig. 10). In this submodel, uncertainties come from the individual-based

model [4] and from the error propagation during the passage to the logging unit scale. To reduce uncertainties over the large woody necromass decay model, direct field measurements should be made to estimate the decay rate directly at the logging unit scale.

Below-ground carbon

This study remains restricted to aboveground carbon, the main carbon pool in tropical forests [46], but belowground carbon (roots, soil) could also be impacted by selective logging and result in carbon emissions. Some studies suggest that soil carbon stocks may decrease after selective logging [47], but carbon sequestration in roots and in the woody debris that are not respired and that return to soil could also be expected [48]. In this study we do not consider below-ground carbon fluxes due to lack of robust information. Gathering more information and adding below-ground carbon dynamics into the model would further improve the model.

Conclusions

We here provide a comprehensive methodology to estimate above-ground carbon fluxes in managed tropical forests at both local and regional scales, easily replicable in other tropical regions. This is a further contribution towards more accurate assessment of the carbon budget of tropical managed forests. The framework is also flexible and easy to adapt to new models: in particular, new logging techniques or new management practices (*e.g. fuel wood*) could be added to the model. This can be useful when investigating the carbon balance of upcoming opportunities and of future management choices for tropical production forests.

Authors' contributions

Study conception and design: CP, AC, BH. Acquisition of data: LD, AD, BO, LM, ER, PS. Analysis and interpretation of data: CP, AC, LD, AD, BO, BH. Drafting of manuscript: CP, BH. Critical revision: CP, AC, LD, AD, BO, LM, ER, PS, BH. All authors read and approved the final manuscript.

Author details

[1] Université de la Guyane, UMR EcoFoG (AgroParisTech, CNRS, Inra, Université des Antilles, Cirad), Campus agronomique, 97310 Kourou, French Guiana. [2] Centre Tecnològic Forestal de Catalunya, Crta. de Sant Llorenç de Morunys, Km.2, 25280 Solsona, Spain. [3] ONF-Guyane, Réserve de Montabo, 97307 Cayenne, French Guiana. [4] Cirad, UMR EcoFoG (AgroParisTech, CNRS, Inra, Université de la Guyane, Université des Antilles), Campus agronomique, 97310 Kourou, French Guiana. [5] EMBRAPA Amazônia Oriental, Trav. Dr. Enéas Pinheiro, Belém, Brazil. [6] Guyane Energie Climat, 16 rue Victor Schoelcher, 97300 Cayenne, French Guiana. [7] CarboForExpert, 1248 Hermance, Switzerland. [8] Cirad UR Forêts et Sociétés, 34398 Montpellier, France. [9] CNRS, UMR EcoFoG (AgroParisTech, Inra, Université de la Guyane, Université des Antilles, Cirad), Campus Agronomique, 97310 Kourou, French Guiana.

Acknowledgements

We are grateful to CIRAD and the Observatoire du Carbone project (French Guiana Region and European structural fundings) for financial support. This study was partially funded by an Investissement d'Avenir Grant of the ANR (CEBA: ANR-10-LABEX-0025).

Competing interests

The authors declare that they have no competing interests.

Received: 15 March 2016 Accepted: 5 July 2016
Published online: 29 July 2016

References

1. Putz FE, Zuidema PA, Pinard MA, Boot RG, Sayer JA, Sheil D, et al. Improved tropical forest management for carbon retention. PLoS Biol. 2008;6(7):1368–9.
2. Blaser J, Sarre A, Poore D, Johnson S. Status of tropical forest management 2011, vol 38. ITTO; 2011. p. 27–31.
3. Mertz O, Müller D, Sikor T, Hett C, Heinimann A, Castella JC, et al. The forgotten D: challenges of addressing forest degradation in complex mosaic landscapes under REDD+. Geografisk Tidsskrift-Danish J Geogr. 2012;112:63–76.
4. Hérault B, Beauchêne J, Muller F, Wagner F, Baraloto C, Blanc L, et al. Modeling decay rates of dead wood in a neotropical forest. Oecologia. 2010;164(1):243–51.
5. Asner GP, Knapp DE, Broadbent EN, Oliveira PJC, Keller M, Silva JN. Selective logging in the Brazilian Amazon. Science. 2005;310(5747):480–2.
6. Picard N, Gourlet-Fleury S, Forni É. Estimating damage from selective logging and implications for tropical forest management. Can J For Res. 2012;42(3):605–13.
7. Sist P, Ferreira FN. Sustainability of reduced-impact logging in the Eastern Amazon. For Ecol Manag. 2007;243(2–3):199–209.
8. Sist P, Mazzei L, Blanc L, Rutishauser E. Large trees as key elements of carbon storage and dynamics after selective logging in the Eastern Amazon. For Ecol Manag. 2014;318:103–9.
9. Shenkin A, Bolker B, Peña-Claros M, Licona JC, Putz FE. Fates of trees damaged by logging in Amazonian Bolivia. For Ecol Manag. 2016;2015(357):50–9.
10. Rutishauser E, Hérault B, Petronelli P, Sist P. Tree height reduction after selective logging in a tropical forest. Biotropica. 2016;48(3):285–9.
11. Hérault B, Ouallet J, Blanc L, Wagner F, Baraloto C. Growth responses of neotropical trees to logging gaps. J Appl Ecol. 2010;47(4):821–31.
12. Blanc L, Echard M, Herault B, Bonal D, Marcon E, Chave J, et al. Dynamics of aboveground carbon stocks in a selectively logged tropical forest. Ecol Appl. 2009;19(6):1397–404.
13. Rutishauser E, Hérault B, Baraloto C, Blanc L, Descroix L, Sotta ED, et al. Rapid tree carbon stock recovery in managed Amazonian forests. Curr Biol. 2015;25(18):R787–8.
14. Huang M, Asner GP. Long-term carbon loss and recovery following selective logging in Amazon forests. Glob Biogeochem Cycles. 2010;24(3):1–15.
15. Kleinschroth F, Gourlet-Fleury S, Sist P, Mortier F, Healey JR. Legacy of logging roads in the Congo Basin: how persistent are the scars in forest cover? Ecosphere. 2015;6(4):1–17.
16. Goetz SJ, Baccini A, Laporte NT, Johns T, Walker W, Kellndorfer J, et al. Mapping and monitoring carbon stocks with satellite observations: a comparison of methods. Carbon Balance Manag. 2009;4:2.
17. Asner GP, Keller M, Pereira R, Zweede JC. Remote sensing of selective logging in Amazonia. Remote Sens Environ. 2002;80(3):483–96.
18. Asner GP, Powell GVN, Mascaro J, Knapp DE, Clark JK, Jacobson J, et al. High-resolution forest carbon stocks and emissions in the Amazon. Proc Natl Acad Sci. 2010;107(38):16738–42.
19. Réjou-Méchain M, Muller-Landau HC, Detto M, Thomas SC, Le Toan T, Saatchi SS, et al. Local spatial structure of forest biomass and its consequences for remote sensing of carbon stocks. Biogeosci Discuss. 2014;11(4):5711–42.
20. Peres CA, Barlow J, Laurance WF. Detecting anthropogenic disturbance in tropical forests. Trends Ecol Evol. 2006;21(5):227–9.
21. Pereira R, Zweede J, Asner GP, Keller M. Forest canopy damage and recovery in reduced-impact and conventional selective logging in eastern Para, Brazil. For Ecol Manag. 2002;168:77–89.
22. Meyer V, Saatchi SS, Chave J, Dalling JW, Bohlman S, Ga Fricker, et al. Detecting tropical forest biomass dynamics from repeated airborne lidar measurements. Biogeosciences. 2013;10(8):5421–38.

23. IPCC. 2006 IPCC guidelines for national greenhouse gas inventories, chapter 4. 2006, p. 4.14.
24. Griscom B, Ellis P, Putz FE. Carbon emissions performance of commercial logging in East Kalimantan, Indonesia. Glob Change Biol. 2014;20(3):923–37.
25. Pearson TRH, Brown S, Casarim FM. Carbon emissions from tropical forest degradation caused by logging. Environ Res Lett. 2014;9(3):034017.
26. Khun V, Sasaki N. Cumulative carbon fluxes due to selective logging in Southeast Asia. Low Carbon Econ. 2014;5:180–91.
27. Sist P, Rutishauser E, Peña-Claros M, Shenkin A, Hérault B, Blanc L, et al. The tropical managed forests observatory: a research network addressing the future of tropical logged forests. Appl Veg Sci. 2014;18:171–4.
28. Toriola D, Chareyre P, Buttler A. Distribution of primary forest plant species in a 19-year old secondary forest in French Guiana. J Trop Ecol. 1998;14(3):323–40.
29. Guitet S, Hérault B, Molto Q, Brunaux O, Couteron P. Spatial structure of above-ground biomass limits accuracy of carbon mapping in rainforest but large scale forest inventories can help to overcome. PLoS One. 2015;10:e0138456.
30. Penman J, Gytarsky M, Hiraishi T, Krug T. Good practice guidance for land use, land-use change and forestry. Intergovernmental Panel on Climate Change (IPCC), chapter 3, Appendix 3.A.1.3. UNEP; 2003. p. 268–70.
31. Ollivier M, Baraloto C, Marcon E. A trait database for Guianan rain forest trees permits intra- and inter-specific contrasts. Ann For Sci. 2007;64(7):781–6.
32. Fargeon H, Aubry-kientz M, Brunaux O, Descroix L, Guitet S, Rossi V, et al. Vulnerability of commercial tree species to water stress in logged forests of the Guiana shield. Forests. 2016;7(105):1–21.
33. Keller M, Asner GP, Silva JNM, Palace M. Sustainability of selective logging of upland forests in the Brazilian Amazon: carbon budgets and remote sensing as tools for evaluation of logging effects. In: Working forests in the tropics: conservation through sustainable management? New York: Columbia University Press; 2004. p. 41–63.
34. Asner GP, Keller M, Lentini M, Merry F, Souza CJ. Selective logging and its relation to deforestation. Geophys Monogr Ser. 2009;186:25–42.
35. Eshun JF, Potting J, Leemans R. LCA of the timber sector in Ghana: preliminary life cycle impact assessment (LCIA). Int J Life Cycle Assess. 2011;16(7):625–38.
36. Guitet S, Pithon S, Brunaux O, Jubelin G, Gond V. Impacts of logging on the canopy and the consequences for forest management in French Guiana. For Ecol Manag. 2012;277:124–31.
37. Chambers JQ, Higuchi N, Teixeira LM, dos Santos J, Laurance SG, Trumbore SE. Response of tree biomass and wood litter to disturbance in a Central Amazon forest. Oecologia. 2004;141(4):596–611.
38. Chambers JQ, Higuchi N, Schimel JP, Ferreira LV, Melack JM. Decomposition and carbon cycling of dead trees in tropical forests of the central Amazon. Oecologia. 2000;122:380–8.
39. Putz FE, Sist P, Fredericksen T, Dykstra D. Reduced-impact logging: challenges and opportunities. For Ecol Manag. 2008;256(7):1427–33.
40. Berndes G, Hoogwijk M, van den Broek R. The contribution of biomass in the future global energy supply: a review of 17 studies. Biomass Bioenerg. 2003;25(1):1–28.
41. Karsenty A, Vermuelen C. Toward "Concessions 2.0": articulating inclusive and exclusive management in production forests in Central Africa. Int For Rev. 2016;18:1.
42. Monteiro A, Cardoso D, Conrado D, Veríssimo A, Souza C. Forest management transparency report—State of Pará (2012–2013). Imazon; 2013. http://imazon.org.br/publicacoes/forest-management-transparency-reportstate-of-para-2011-to-2012/?lang=en.
43. Asner GP, Keller M, Silva J. Spatial and temporal dynamics of forest canopy gaps following selective logging in the eastern Amazon. Glob Change Biol. 2004;10(5):765–83.
44. Holling CS. Resilience and stability of ecological systems. Annu Rev Ecol Syst. 1973;4(1):1–23.
45. Putz FE, Pa Zuidema, Synnott T, Peña-Claros M, Ma Pinard, Sheil D, et al. Sustaining conservation values in selectively logged tropical forests: the attained and the attainable. Conserv Lett. 2012;5(4):296–303.
46. Pan Y, Birdsey RA, Phillips OL, Jackson RB. The structure, distribution, and biomass of the World's forests. Annu Rev Ecol Evol Syst. 2013;44:593–622.
47. Chiti T, Perugini L, Vespertino D, Valentini R. Effect of selective logging on soil organic carbon dynamics in tropical forests in central and western Africa. Plant Soil. 2015;399:283–94.
48. Chambers JQ, Schimel JP, Nobre CA. Respiration from coarse wood litter in central Amazon forests. Biogeochemistry. 2001;52:115–31.

Chapitre 4

Dynamiques de carbone post-exploitation en Amazonie

Les forêts naturelles amazoniennes présentent de grandes différences dans leur dynamique[1]. L'étude présentée dans ce chapitre vise à comprendre comment ces différences régionales se reflètent sur la dynamique du carbone post-exploitation, afin de mieux caractériser la reconstitution des stocks de carbone une fois la forêt exploitée.

L'exploitation sélective affecte une surface supérieure à 2 Mha chaque année sur l'ensemble des forêts amazoniennes. Les surfaces de forêt aujourd'hui en récupération représentent donc un potentiel de stockage de carbone énorme. Les variations de récupération du stock de carbone peuvent donc être particulièrement importantes dans les bilans carbone régionaux, ainsi que dans des politiques de mitigation des changements climatiques. Pourtant, il n'existait pas de modèle spatialement explicite de la récupération de carbone post-exploitation à l'échelle de l'Amazonie. Les études précédentes n'avaient soit pas trouvé de lien entre le taux de récupération et la localisation[2], soit ce lien tenait uniquement au niveau de précipitation : > 1500 mm ou < 1500 mm[3].

L'objectif de ce chapitre est double : il s'agit à la fois de comprendre la réponse des forêts amazoniennes à la perturbation (dans notre cas l'exploitation) afin ensuite de quantifier la récupération du carbone post-exploitation et d'affiner ainsi le bilan carbone de l'exploitation.

Pour pouvoir mieux comprendre la réponse à la perturbation deux pools d'arbres ont été séparés :

- les arbres dits «survivants», qui étaient présents avant l'exploitation et y ont survécu,
- les arbres dits «recrutés», qui passent au dessus de 20 cm DHP après l'exploitation.

Pour chacun des groupes les flux de carbone liés au recrutement, à la croissance et à la mortalité ont été séparés et un

[1] cf. Section 2.1.

[2] Rutishauser et al. (2015). « Rapid tree carbon stock recovery in managed Amazonian forests », cf. note 166, p. 20.

[3] Huang et Asner (2010). « Long-term carbon loss and recovery following selective logging in Amazon forests », cf. note 149, p. 18.

modèle calibré à partir des données des parcelles de TmFIO (voir Section 2.2.1). Outre la compréhension plus fine des mécanismes en œvre, cette approche par les processus permet de modéliser plus finement les flux de carbone post-exploitation [4]. Étudier la dynamique de ces deux groupes séparément permet de tester s'il existe des différences régionales dans la dynamique des grands arbres (ici les survivants) et la dynamique de régénération. En effet, on peut s'attendre à voir une récupération du carbone post-exploitation qui dépende principalement du recrutement dans l'ouest amazonien composé de forêts plus jeunes, et des survivants dans le nord-est moins dynamique.

[4] cf. annexe en fin de chapitre

L'importance de l'environnement (précipitation, saisonnalité des précipitations et densité du sol), de la biomasse pré-exploitation et de l'intensité de la perturbation pour expliquer les variations des dynamiques post-exploitation a été quantifiée. Les résultats obtenus montrent qu'en Amazonie ces variations sont expliquées principalement par l'intensité de la perturbation et par le régime de précipitations. Ces résultats ont permis d'établir une première carte du potentiel de récupération du carbone des forêts exploitées d'Amazonie. Ils mettent aussi l'accent sur les effets que pourraient avoir les changements climatiques et du régime de perturbation sur le cycle du carbone des forêts amazoniennes.

Ces résultats ont été publiés en 2016 dans la revue *eLife*[5]. Les prédictions ont été intégrées ensuite dans le modèle de bilan carbone, et dans le package R en développement [6]. Les résultats ont aussi fait l'objet d'un communiqué de presse du Cirad [7], d'une interview dans un podcast[8] et d'un article de vulgarisation dans *Frontiers in Ecology and the Environment* [9].

[5] C. Piponiot et al. (2016b). « Carbon recovery dynamics following disturbance by selective logging in Amazonian forests ». In : *eLife* 5.C.

[6] cf. Chapitre 3 et Chapitre 8

[7] `www.cirad.fr/en/news/all-news-items/press-releases/2016/amazonia-mapping-carbon-storage-after-logging`

[8] `elifesciences.org/podcast`, episode 36

[9] cf. annexe en fin d'ouvrage

eLIFE elifesciences.org

RESEARCH ARTICLE

Carbon recovery dynamics following disturbance by selective logging in Amazonian forests

Camille Piponiot[1,2,3,4]*, Plinio Sist[4], Lucas Mazzei[5], Marielos Peña-Claros[6], Francis E Putz[7], Ervan Rutishauser[8], Alexander Shenkin[9], Nataly Ascarrunz[10], Celso P de Azevedo[11], Christopher Baraloto[12], Mabiane França[11], Marcelino Guedes[13], Eurídice N Honorio Coronado[14], Marcus VN d'Oliveira[15], Ademir R Ruschel[5], Kátia E da Silva[11], Eleneide Doff Sotta[13], Cintia R de Souza[11], Edson Vidal[16], Thales AP West[7], Bruno Hérault[2]*

[1]Université de Guyane, UMR EcoFoG (Agroparistech, CNRS, Inra, Université des Antilles, Cirad), Kourou, French Guiana; [2]Cirad, UMR EcoFoG (Agroparistech, CNRS, Inra, Université des Antilles, Université de Guyane), Kourou, French Guiana; [3]CNRS, UMR EcoFoG (Agroparistech, Inra, Université des Antilles, Université de Guyane, Cirad), Kourou, French Guiana; [4]Cirad, UR Forests and Societies, Montpellier, France; [5]Embrapa Amazônia Oriental, Belém, Brazil; [6]Forest Ecology and Forest Management Group, Wageningen University, Wageningen, Netherlands; [7]Department of Biology, University of Florida, Gainesville, United States; [8]CarbonForExpert, Hermance, Switzerland; [9]Environmental Change Institute, University of Oxford, Oxford, United Kingdom; [10]Instituto Boliviano de Investigación Forestal, Santa Cruz, Bolivia; [11]Embrapa Amazônia Ocidental, Belém, Brazil; [12]Department of Biological Sciences, International Center for Tropical Botany, Florida International University, Miami, United States; [13]Embrapa Amapa, Macapa, Brazil; [14]Instituto de Investigaciones de la Amazonia Peruana, Iquitos, Peru; [15]Embrapa Acre, Rio Branco, Brazil; [16]Departamento de Ciências Florestais, University of São Paulo, Piracicaba, Brazil

***For correspondence:** camille.piponiot@gmail.com (CP); bruno.herault@cirad.fr (BH)

Competing interests: The authors declare that no competing interests exist.

Funding: See page 13

Received: 10 September 2016
Accepted: 08 December 2016
Published: 20 December 2016

Reviewing editor: Susan Trumbore, Max-Planck-Institute for Biogeochemistry, Germany

Abstract When 2 Mha of Amazonian forests are disturbed by selective logging each year, more than 90 Tg of carbon (C) is emitted to the atmosphere. Emissions are then counterbalanced by forest regrowth. With an original modelling approach, calibrated on a network of 133 permanent forest plots (175 ha total) across Amazonia, we link regional differences in climate, soil and initial biomass with survivors' and recruits' C fluxes to provide Amazon-wide predictions of post-logging C recovery. We show that net aboveground C recovery over 10 years is higher in the Guiana Shield and in the west (21 $\pm$3 Mg C ha^{-1}) than in the south (12 $\pm$3 Mg C ha^{-1}) where environmental stress is high (low rainfall, high seasonality). We highlight the key role of survivors in the forest regrowth and elaborate a comprehensive map of post-disturbance C recovery potential in Amazonia.
DOI: 10.7554/eLife.21394.001

Introduction

With on-going climate change, attention is increasingly drawn to the impacts of human activities on carbon (C) cycles (***Griggs and Noguer, 2002***), and in particular to the 2.1 $\pm$ 1.1 Pg C yr^{-1} of C loss caused by various forms and intensities of anthropogenic disturbances in tropical forests

eLife digest The Amazon rainforest in South America is the largest tropical forest in the world. Along with being home to a huge variety of plants and wildlife, rainforests also play an important role in storing an element called carbon, which is a core component of all life on Earth. Certain forms of carbon, such as the gas carbon dioxide, contribute to climate change so researchers want to understand what factors affect how much carbon is stored in rainforests. Trees and other plants absorb carbon dioxide from the atmosphere and then incorporate the carbon into carbohydrates and other biological molecules. The Amazon rainforest alone holds around 30% of the total carbon stored in land-based ecosystems.

Humans selectively harvest certain species of tree that produce wood with commercial value from the Amazon rainforest. This "selective logging" results in the loss of stored carbon from the rainforest, but the loss can be compensated for in the medium to long term if the forest is left to regrow. New trees and trees that survived the logging grow to fill the gaps left by the felled trees. However, it is not clear how differences in the forest (for example, forest maturity), environmental factors (such as climate or soil) and the degree of the disturbance caused by the logging affect the ability of the forest ecosystem to recover the lost carbon.

Piponiot et al. used computer modeling to analyze data from over a hundred different forest plots across the Amazon rainforest. The models show that the forest's ability to recover carbon after selective logging greatly differs between regions. For example, the overall amount of carbon recovered in the first ten years is predicted to be higher in a region in the north known as the Guiana Shield than in the south of the Amazonian basin where the climate is less favorable.

The findings of Piponiot et al. highlight the key role the trees that survive selective logging play in carbon recovery. The next step would be to couple this model to historical maps of logging to estimate how the areas of the rainforest that are managed by selective logging shape the overall carbon balance of the Amazon rainforest.

DOI: 10.7554/eLife.21394.002

(*Grace et al., 2014*). Among those disturbances, selective logging, i.e. the selective harvest of a few merchantable tree species, is particularly widespread: in the Brazilian Amazon alone, about 2 Mha yr^{-1} were logged in 1999–2002 (*Asner et al., 2005*). The extent of selective logging in the Brasilian Amazon was equivalent to annual deforestation in the same period, and resulted in C emissions of 90 Tg C yr^{-1} (*Huang and Asner, 2010*) which increased anthropogenic C emissions by almost 25% over deforestation alone (*Asner et al., 2005*). In contrast to deforested areas that are used for agriculture and grazing, most selectively logged forests remain as forested areas (*Asner et al., 2006*) and may recover C stocks (*West et al., 2014*). Previously logged Amazonian forests may thus accumulate large amounts of C (*Pan et al., 2011*), but this C uptake is difficult to accurately estimate, because while detecting selective logging from space is increasingly feasible (*Frolking et al., 2009*) (even if very few of the IPCC models effectively account for logging), directly quantifying forest recovery remains challenging (*Asner et al., 2009*; *Houghton et al., 2012*; *Goetz et al., 2015*). Studies based on field measurements (e.g. *Sist and Ferreira, 2007*; *Blanc et al., 2009*; *West et al., 2014*; *Vidal et al., 2016*), sometimes coupled with modeling approaches (e.g. *Gourlet-Fleury et al., 2005*; *Valle et al., 2007*) or airborne light detection and ranging (LiDAR) measurements (e.g. *Andersen et al., 2014*) have assessed post-logging dynamics at particular sites. Nonetheless, to our knowledge no spatially-explicit investigation of post-logging C dynamics at the Amazon biome scale is available.

C losses from selective logging are determined by harvest intensity (i.e. number of trees felled or volume of wood extracted) plus the care with which harvest operations are conducted, which affects the amount of collateral damage. After logging, C losses continue for several years due to elevated mortality rates of trees injured during harvesting operations (*Shenkin et al., 2015*). Logged forests may recover their aboveground carbon stocks (ACS) via enhanced growth of survivors and recruited trees (*Blanc et al., 2009*). Full recovery of pre-disturbance ACS in logged stands reportedly requires up to 125 years, depending primarily on disturbance intensity (*Rutishauser et al., 2015*). The underlying recovery processes (i.e. tree mortality, growth and recruitment) are likely to vary with the clear

geographical patterns in forest structure and dynamics across the Amazon Basin and Guiana Shield. In particular, northeast-southwest gradients have been reported for ACS (**Malhi and Wright, 2004**), net primary productivity (**Aragão et al., 2009**), wood density (**Baker et al., 2004**), and floristic composition (**ter Steege et al., 2006**). Such gradients coincide with climate and edaphic conditions that range from nearly a seasonal nutrient-limited in the northeast to seasonally dry and nutrient-rich in the southwest (**Quesada et al., 2012**). These regional differences in biotic and abiotic conditions largely constrain demographic processes that ultimately shape forest C balances.

Here we partition the contributions to post-disturbance ACS gain (from growth and recruitment of trees $\geq$20 cm DBH) and ACS loss (from mortality) of survivors and recruited trees to detect the main drivers and patterns of ACS recovery in forests disturbed by selective logging across Amazonia sensu lato (that includes the Amazon Basin and the Guiana Shield). Based on long-term (8–30 year) inventory data from 13 experimentally-disturbed sites (**Sist et al., 2015**) across Amazonia (**Figure 1—figure supplement 1**), 133 permanent forest plots (175 ha in total) that cover a large gradient of disturbance intensities (ACS losses ranging from 1% to 71%) were used to model the trajectory of those

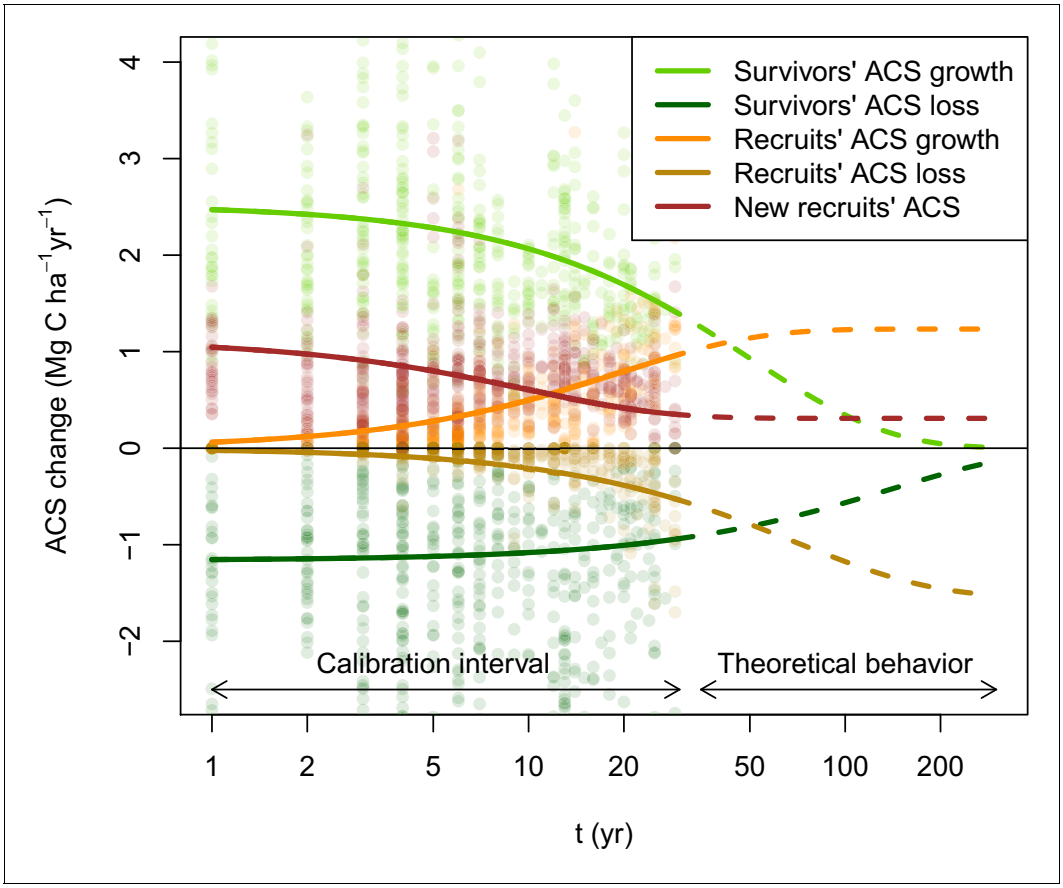

Figure 1. Post-disturbance annual ACS changes of survivors and recruits in 133 Amazonian selectively logged plots. Data is available between the year of minimum ACS ($t = 0$) and t =30 years. ACS changes are: recruits' ACS growth (orange), recruits' ACS loss (gold), new recruits' ACS (red), survivors' ACS growth (light green) and survivors' ACS loss (dark green). Thick solid lines are the maximum-likelihood predictions (for an average plot, when all covariates are null), and dashed lines are the model theoretical behaviour. New recruits' ACS, recruits' ACS growth, and recruits' ACS loss converge over time to constant values. A dynamic equilibrium is then reached: ACS gain from recruitment and recruits' growth compensate ACS loss from recruits' mortality. Survivors' ACS growth and loss. decline over time and tend to zero when all initial survivors have died.

DOI: 10.7554/eLife.21394.003

The following figure supplement is available for figure 1:

Figure supplement 1. Experimental sites location, each site being composed of permanent forest plots varying in logging intensities, census length (colour) and total area (size).

DOI: 10.7554/eLife.21394.004

post-disturbance ACS changes (***Figure 1***) in a comprehensive Bayesian framework. We quantify the effect of pre-disturbance ecosystem characteristics [the site's average pre-logging ACS ($acs0$) and the relative difference between each plot and $acs0$ as a proxy of forest maturity ($dacs$)], disturbance intensity [percentage of pre-logging ACS lost ($loss$)], and interactions with the environment [annual precipitation ($prec$), seasonality of precipitation ($seas$), and soil bulk density (bd)] (***Figure 2***) on the rates at which post-disturbance ACS changes converge to a theoretical steady state (as in ***Figure 1***, see Materials and methods for more details). With global maps of ACS (***Avitabile et al., 2016***), climatic conditions (***Hijmans et al., 2005***) and soil bulk density (***Nachtergaele et al., 2008***), we upscale our results to Amazonia (sensu lato) and elaborate predictive maps of potential ACS changes over 10 years under the hypothesis of a 40% ACS loss, which is a common disturbance intensity after conventional logging in Amazonia (***Blanc et al., 2009***; ***Martin et al., 2015***; ***West et al., 2014***). Summing these ACS changes over time gives the net post-disturbance rate of ACS accumulation. Disentangling ACS recovery into demographic processes and cohorts is essential to reveal mechanisms underlying ACS responses to disturbance and to make more robust predictions of ACS recovery compared to an all-in-one approach (see Appendix).

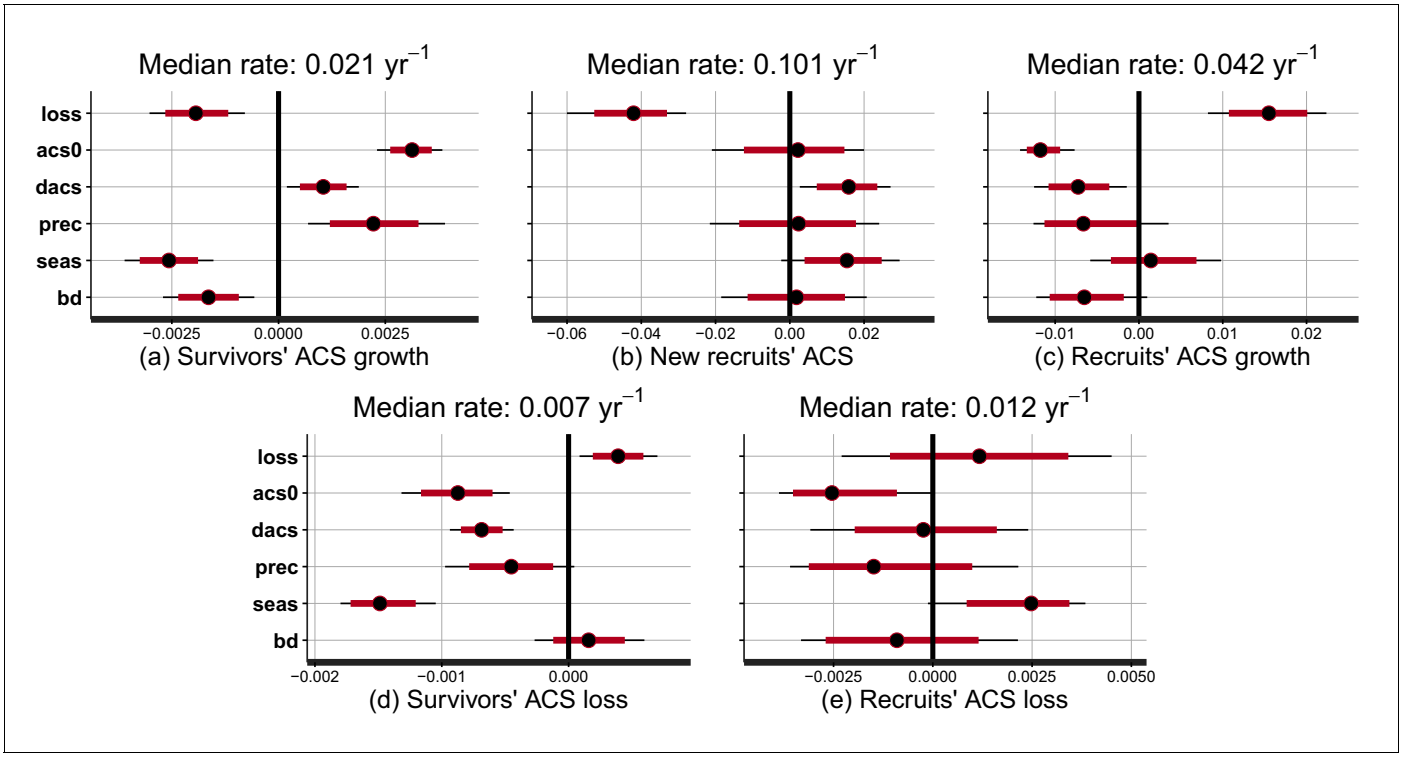

Figure 2. Effect of covariates on the rate at which post-disturbance ACS changes converge to a theoretical steady state (in yr^{-1}). Covariates are : disturbance intensity ($loss$) , i.e. the proportion of initial ACS loss; mean site's ACS ($acs0$), and relative forest maturity, i.e. pre-logging plot ACS as a % of $acs0$ ($dacs$); annual precipitation ($prec$); seasonality of precipitation ($seas$), soil bulk density (bd). Covariates are centred and standardized. Red and black levels are 80% and 95% credible intervals, respectively. The median rate is the prediction of the convergence rate for an average plot (when all covariates are set to zero). Negative covariate values indicate slowing and positive values indicate accelerating rates. (**a**) Survivors' ACS growth. (**b**) New recruits' ACS. (**c**) Recruits' ACS growth. (**d**) Survivors' ACS loss. (**e**) Recruits' ACS loss.

DOI: 10.7554/eLife.21394.005

The following source data and figure supplement are available for figure 2:

Source data 1. Parameters posterior distribution.

DOI: 10.7554/eLife.21394.006

Figure supplement 1. Fitted vs observed values of cumulative ACS changes (Mg C ha^{-1}).

DOI: 10.7554/eLife.21394.007

Results

Local variations of ACS changes

At a given site, variations of post-logging ACS changes are explained with the disturbance intensity (*loss*) and the relative forest maturity (*dacs*). At high disturbance intensity (positive *loss*) as well as in relatively immature forests (negative *dacs*), ACS gain from recruits is high: recruitment decreases slowly (***Figure 2b*** and ***Figure 3b***) and recruits' growth increases rapidly (***Figure 2c*** and ***Figure 3c***). In the same conditions of high disturbance intensity, survivors' ACS growth is lower in the first years following logging than for low disturbance intensities, but declines slowly (***Figure 2a*** and ***Figure 3a***). Disturbance intensity and relative forest maturity have a weak effect on ACS loss from both survivors and recruits (***Figures 2d,e*** and ***3d,e***). Overall, net ACS change stays high longer at high disturbance intensity (***Figure 3f***).

Regional variations of ACS changes

Variations of post-logging ACS changes between sites are explained with the mean ACS of each site (*acs*0), climatic conditions [annual precipitation (*prec*), seasonality of precipitation (*seas*)] and the soil bulk density (*bd*). Contribution of survivors' growth to ACS recovery declined slowly in sites with low *acs*0 and high water stress (low precipitation, high seasonality and high bulk density) (***Figure 2a***). Survivors' ACS loss showed the opposite pattern (***Figure 2d***) except in apparent response to high seasonality of precipitation (*seas*) that slowed the post-disturbance rates of decline of both ACS growth and loss. Despite slower recruits' ACS growth in sites with high pre-logging ACS (*acs*0), no other regional covariate had significant effects on recruits' ACS changes (***Figure 2b,c and e***).

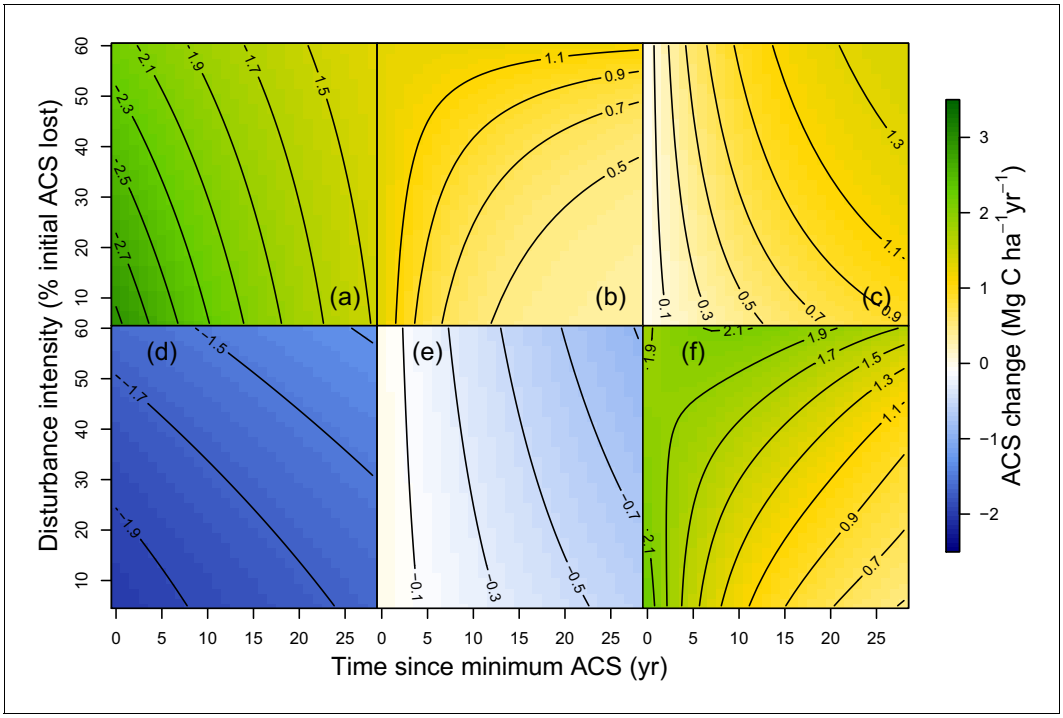

Figure 3. Predicted effect of disturbance intensity on ACS changes along time in an Amazonian-average plot. (**a**) Survivors' ACS growth. (**b**) New recruits' ACS. (**c**) Recruits' ACS growth. (**d**) Survivors' ACS loss. (**e**) Recruits' ACS loss. (**f**) Net ACS change. The net ACS change is the sum of all five ACS changes. ACS changes were calculated with all parameters set to their maximum-likelihood value and covariates (except standardized disturbance intensity *loss*) set to 0. Time since minimum ACS varies from 0 to 30 year (i.e. the calibration interval) and disturbance intensity ranges between 5% and 60% of initial ACS loss.

DOI: 10.7554/eLife.21394.008

Prediction maps

While no significant environmental effects were detected for recruits' ACS changes (***Figures 2*** and ***4***), the survivors showed a highly structured regional gradient: (i) ACS gain from survivors' ACS growth is high in the west and in the Guiana Shield, but low in the south (***Figure 4a***), whereas (ii) survivors' ACS loss is low in the south and in the Guiana Shield but high in the west (***Figure 4d***). To illustrate how these regional differences will be critical for future ACS across Amazonia, we developed a map of net ACS recovery over the first 10 years after a 40% ACS loss by integrating the sum of ACS change predictions through time (***Figure 5***). Across the region, net ACS recovery over the first ten years after a 40% ACS loss is predicted to be 17 $\pm$ 7 Mg C ha^{-1}, with higher values in the west and in the Guiana Shield (***Figure 5a***). The uncertainty in predictions was low to medium (coefficient of variation under 40%) in 82% of the mapped area, and high (coefficient of variation above 50%) in 5% of the mapped area (***Figure 5b***).

Four areas (***Figure 5a***) were selected to represent four contrasted cases of net ACS recovery in time (***Figure 6***): two areas, northwestern Amazonia and the Guiana Shield, with high ACS accumulation (21 $\pm$ 3 Mg C ha^{-1} over 10 year), one intermediate area, central Amazonia (15 $\pm$ 1 Mg C ha^{-1}

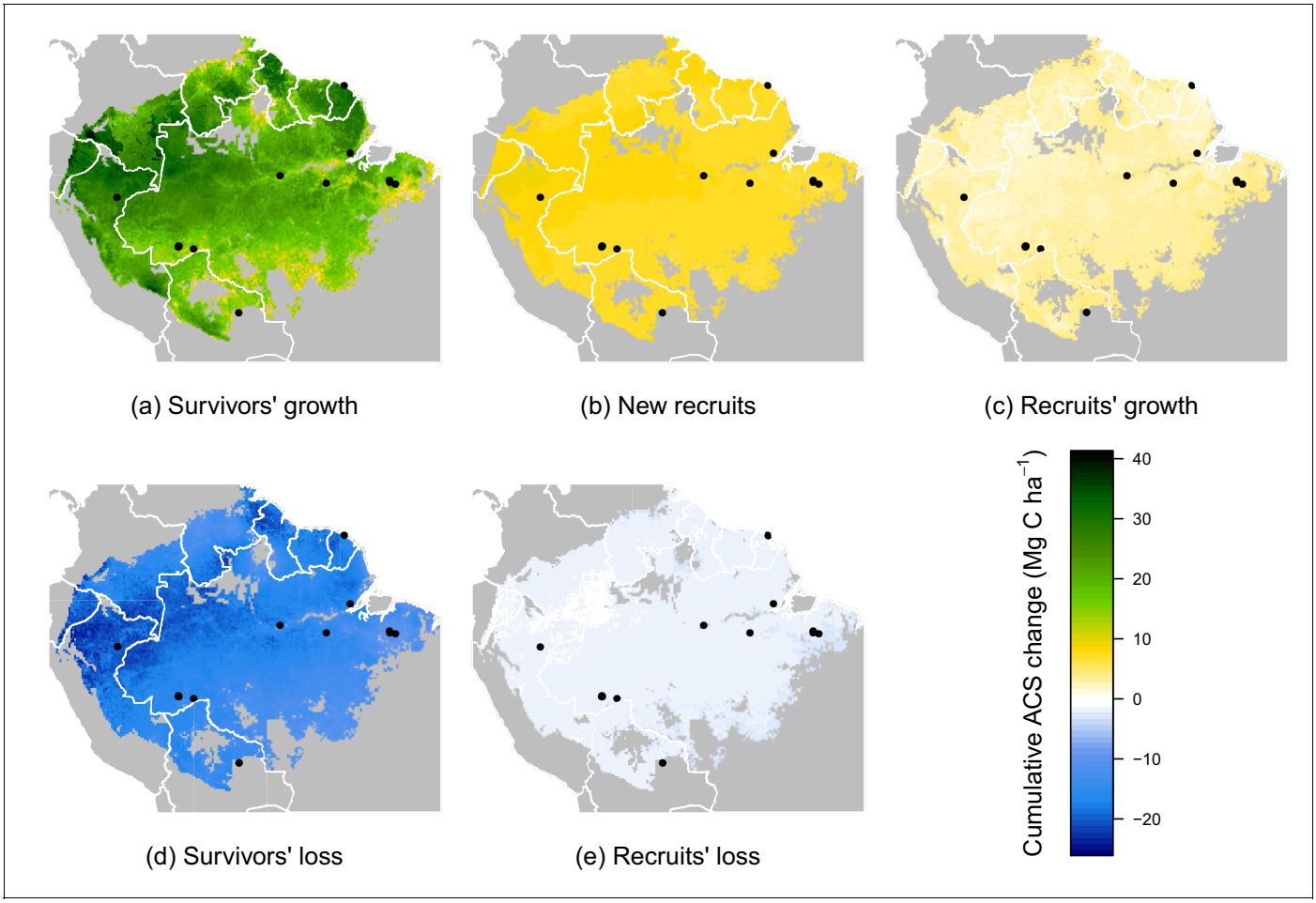

Figure 4. Predicted cumulative ACS changes (Mg C ha^{-1}) over the first 10 year after losing 40% of ACS. Extrapolation was based on global rasters: topsoil bulk density from the Harmonized global soil database (***Nachtergaele et al., 2008***), Worldclim precipitation data (***Hijmans et al., 2005***) and biomass stocks from Avitabile et al. map (***Avitabile et al., 2016***). Cumulative ACS changes are obtained by integrating annual ACS changes through time. We here show the median of each pixel. Top graphs are ACS gain and bottom graphs are ACS loss. (**a**) ACS gain from survivors' growth. (**b**) ACS gain from new recruits. (**c**) ACS gain from recruits' growth. (**d**) ACS loss from survivors' mortality. (**e**) ACS loss from recruits' mortality. Black dots are the location of our experimental sites. Survivors' ACS changes (**a** and **d**) show strong regional variations unlike to recruits' ACS changes (**b**,**c** and **e**).
DOI: 10.7554/eLife.21394.009

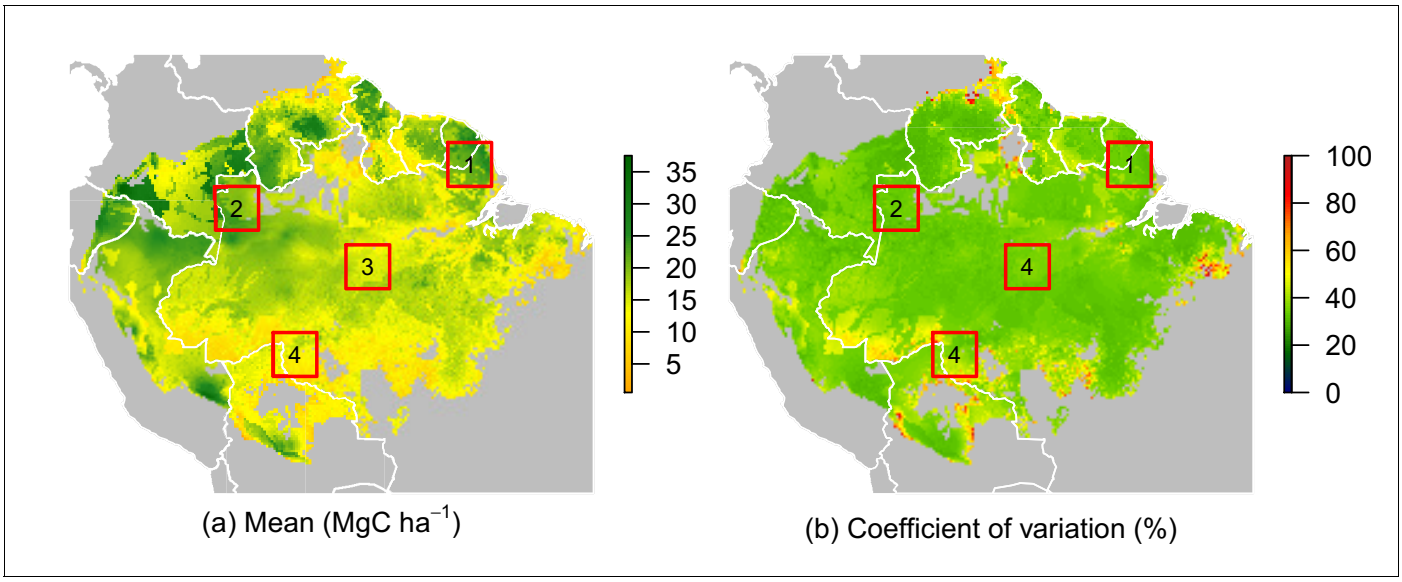

Figure 5. Predicted net ACS recovery over the first 10 year after losing 40% of pre-logging ACS. (**a**) median predictions. (**b**) coefficient of variation (per pixel). Four areas were arbitrarily chosen to illustrate four different geographical behaviours: (1) the Guiana Shield and (2) northwestern Amazonia are two areas with high ACS recovery; the Guiana Shield has higher initial ACS and slower ACS dynamics whereas northwestern Amazonia has lower initial ACS and faster ACS dynamics. (3) central Amazonia has intermediate ACS recovery. (4) southern Amazonia has low ACS recovery.
DOI: 10.7554/eLife.21394.010

over 10 year) and one area with low ACS accumulation, southern Amazonia (12 $\pm$ 3 Mg C ha^{-1} over 10 year). Survivors' contribution to the sum of ACS gains (recruitment and growth) over the first 10 years after disturbance was 71 $\pm$ 4% in the Guiana Shield, 71 $\pm$ 2% in the west; 63 $\pm$ 4% in central Amazonia and 55 $\pm$ 6% in the south. Predicted net ACS recovery (***Figure 5***) and survivors' ACS growth (***Figure 4a***) are highly correlated: $\rho = 0.90$ (Pearson's correlation coefficient).

Discussion

Contrasting post-disturbance ACS dynamics were detected among the western Amazon, Guiana Shield, and southern Amazon (***Figure 4***). (i) In the western Amazon, environmental stress is reduced due to fertile soils and abundant, mostly non-seasonal precipitation, but forests are prone to frequent and sometimes large-scale wind-induced disturbances (***Espírito-Santo et al., 2014***). Such conditions of low stress and high disturbance tend to favor fast-growing species with rapid life cycles (***He et al., 2013***), which results in fast ACS gain and loss from survivors even after the logging disturbance (***Figures 4a,d*** and ***6***). (ii) Forests of the Guiana Shield are generally dense and grow on nutrient-poor soils (***Quesada et al., 2012***), where wood productivity is highly constrained by competition for key nutrients, especially phosphorus and nitrogen (***Santiago, 2015***; ***Mercado et al., 2011***). The short duration pulse of nutrients released from readily decomposed stems, twigs and leaves of trees damaged and killed by logging may thus explain the substantial but limited-duration increase in growth of survivors on these nutrient-poor soils (***Figure 6***). Yet post-disturbance ACS loss from survivors' mortality decreases slowly in the Guiana Shield (***Figure 6***). This is consistent with the low mortality rates and the high tree longevity reported in old-growth forests of this region (***Phillips et al., 2004***). (iii) In the southern Amazon, high seasonal water stress is the main constraint on ACS recovery (***Wagner et al., 2016***). Stress-tolerant trees are generally poor competitors (***He et al., 2013***) and this may explain the slow ACS changes of survivors in this region (***Figures 4a,d*** and ***6***). Finally, Central Amazonia is a transition zone for the main environmental and biotic gradients found in Amazonia: (1) a competition gradient between dense and nutrient-poor northeastern forests and nutrient-rich western forests; (2) an environmental gradient between northern wet forests and southern drier forests (***Quesada et al., 2012***).

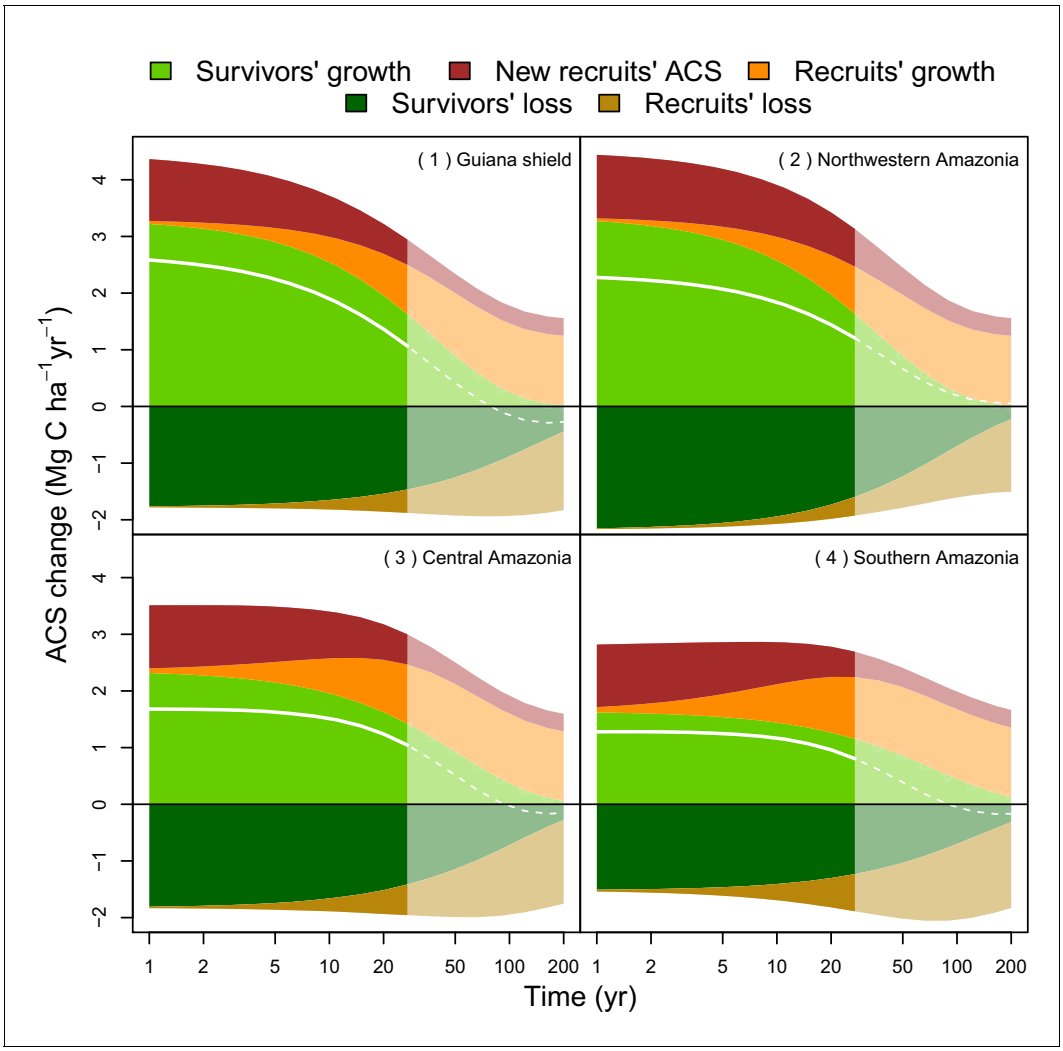

Figure 6. Predicted contribution of annual ACS changes in ACS recovery in four regions of Amazonia (***Figure 5***). The white line is the net annual ACS recovery, i.e. the sum of all annual ACS changes. Survivors' (green) and recruits' (orange) contribution are positive for ACS gains (survivors' ACS growth, new recruits' ACS and recruits' ACS growth) and negative for survivors' and recruits' ACS loss. Areas with higher levels of transparency and dotted lines are out of the calibration period (0–30 year). In the Guiana Shield and in nothwestern Amazonia, high levels of net ACS recovery are explained by large ACS gain from survivors' growth. Extrapolation was based on global rasters: topsoil bulk density from the Harmonized global soil database (***Nachtergaele et al., 2008***), precipitation data from Worldclim (***Hijmans et al., 2005***) and biomass stocks from Avitabile et al. (***Avitabile et al., 2016***) map.

DOI: 10.7554/eLife.21394.011

Across Amazonia, survivors contribute most to post-disturbance ACS recovery. In regions where survivors' ACS gain is high (west and northeast), net ACS recovery is also high: annual ACS recovery is between 1 and 3 Mg C ha^{-1} yr^{-1} in the first 10 year after logging (***Figure 6***), lower than in Amazonian secondary forests (3–5 Mg C ha^{-1} yr^{-1} in the first 20 year after abandonment of land use [***Poorter et al., 2016***]). Recruits, for their part, have very low geographical variations in post-logging ACS changes: 10 years after the disturbance they are predicted to store similar amounts of ACS almost everywhere in Amazonia. Nevertheless, small trees with DBH <20 cm have not been accounted for in our study and may play an important role in post-logging ACS changes. The 10–20 cm DBH size class contains as much as 14% of total ACS and may be highly dynamic in some Amazonian forests (***Vieira et al., 2004***). Because of the slow tree growth rates in Amazonia (***Vieira et al., 2005***; ***Herault et al., 2010***), many trees will not reach the 20 cm DBH threshold 10 years after logging: the effects of the 10–20 cm DBH stratum on post-logging ACS changes are likely to be missed

in sites with less than 10 years of measurements (e.g. Peteco, Ecosilva, Iracema, Cumaru) and should be studied, together with the natural regeneration, in the future.

At the stand level, high disturbance intensities reduce survivors' ACS: survivors' ACS growth is consequently lower (***Figure 3a***), resulting in lower net ACS change during the first 10 years of the recovery period (***Figure 3f***). High disturbance intensities as well as relatively low forest maturity alleviate competition, and this is probably why ACS contributions from recruits remain high for longer (***Figure 2b***) in such enhanced growth conditions (***Herault et al., 2010***). In the first years after logging, net ACS recovery depends little on disturbance intensity (***Figure 3f***), but recovery is predicted to last longer in heavily logged forests. In immature forests, intense self-thinning (***Swaine et al., 1987***) may explain fast ACS losses from survivors' mortality (***Figure 2d***).

In the tropics, reduced-impact logging techniques (RIL; [***Putz et al., 2008***]) are promoted to reduce collateral damage to residual stands and biodiversity. Our results reveal that lower disturbance intensities, as a direct consequence of the employment of RIL techniques, could increase survivors' ACS growth and slow down their ACS loss. Given that government specified minimum cutting cycles are short, e.g. 35 year in the Brazilian Amazon (***Blaser et al., 2011***), and that many commercial species are slow-growing and dense-wooded (***Dauber et al., 2005***; ***Wright et al., 2010***), available timber stocks for the next cutting cycle will be comprised mostly of survivors. Attention should be taken to high harvest intensities and/or substantial incidental damage due to poor harvesting practices that diminish stocks of survivors, even if they promote recruitment. Most trees that recruit are fast-growing pioneers that are favored by disturbance but are vulnerable to water stress (***Bonal et al., 2016***) and competition (***Valladares and Niinemets, 2008***), and because their height is lower than in mature forests (***Rutishauser et al., 2016***), they might have reduced carbon sequestration potential. With ongoing climate change and increased frequencies and intensities of droughts in Amazonia (***Malhi et al., 2008***), betting on recruits to store C in forests disturbed by selective logging might thus be a risky gamble.

In this study, we focus on one type of disturbance: selective logging. Because of its economic value and implications for forest management, selective logging is a long-studied human disturbance in tropical forests, and the data gathered by the TmFO network are unique in terms of experiment duration and spatial extent. We nevertheless believe that our study gives clues on the regional differences in Amazonian forests response to large ACS losses induced by other disturbances (e.g. droughts, fire) that are expected to increase in frequency with ongoing global changes (***Bonal et al., 2016***).

Materials and methods

Site description

Our study includes data from thirteen long-term (8–30 year) experimental forest sites located in the Amazon Basin and the Guiana Shield (***Figure 1—figure supplement 1***). Sites meet the following criteria: (i) located in tropical forests with mean annual precipitation above 1000 mm; (ii) a total censused area above 1 ha; (iii) at least one pre-logging census and (iv) at least two post-logging censuses. For each site, we extracted annual precipitation and seasonality of precipitation data from WorldClim (RRID:SCR_010244) (***Hijmans et al., 2005***), topsoil bulk density data from the Harmonized World Soil database (***Nachtergaele et al., 2008***), and the synthetic climatic index from Chave et al. (***Chave et al., 2014***), using in all cases the highest resolution data available (30 arc-seconds). For one of our sites (La Chonta, see ***Figure 1—figure supplement 1***), field measurements of precipitation (mean = 1580 mm yr^{-1}) differed substantially from WorldClim data (1032 mm yr^{-1}): in this particular case we used the measured value and adjusted the synthetic climatic index (E) in the allometric equation (***Chave et al., 2014***) accordingly.

ACS computation

In all plots, diameter at breast height (DBH) of trees >20 cm DBH were measured, and trees were identified to the lowest taxonomic level: to the species level (75%) when possible, or to the genus level (15%); 10% of trees were not identified. To get the wood density, we applied the following standardized protocol to all sites: (i) trees identified to the species level were assigned the corresponding wood specific gravity value from the Global Wood Density Database (GWDD,

doi:10.5061/dryad.234/1) (**Zanne et al., 2009**); (ii) trees identified to the genus level were assigned a genus-average wood density; (iii) trees with no botanical identification or that were not in the GWDD were assigned the site-average wood density. The aboveground biomass (AGB) was estimated with the allometric equations from Chave et al. (**Chave et al., 2014**). Biomass was assumed to be 50% carbon (**Penman et al., 2003**). The ACS of every tree i was then computed as follows:

$$\hat{ACS}_i = exp\Big(-1.803 - 0.976 \times E + 0.976 \times ln(WD_i) + \\ +2.673 \times ln(DBH_i) - 0.0299 \times ln(DBH_i^2)\Big) \times 0.5 \quad (1)$$

where WD_i and DBH_i are the specific wood density and diameter at breast height of the tree i and E is the synthetic climatic index (**Chave et al., 2014**).

The recovery period

After logging, plot ACS decreases rapidly until it reaches its minimum value ($acsmin$) a few years later. This transition point determines the beginning $t_{min} = t_0$ of the recovery period. $acsmin$ was estimated as the minimum ACS in the 4 years following logging activities. Because our focus is on post-logging ACS recovery, we did not include in our analysis plots where the minimum ACS value was not reached within the 4 years after logging, either because the logging activity did not affect the plot or because there were other sources of disturbance long after logging (fire, road opening, silvicultural treatments).

ACS changes computation

For each plot j and census k, with t_k the time since the beginning of the recovery period t_0, we define 5 ACS changes : new recruits' ACS ($Rr_{j,k}$) is the ACS of all trees <20 cm DBH at t_{k-1} and ≥20 cm DBH at t_k; recruits' ACS growth ($Rg_{j,k}$) is the ACS increment of living recruits between t_{k-1} and t_k ; recruits' ACS loss ($Rl_{j,k}$) is the C in recruits that die between t_{k-1} and t_k; survivors' ACS growth ($Sg_{j,k}$) is the ACS increment of living survivors between t_{k-1} and t_k; survivors' ACS loss ($Sl_{j,k}$) is the ACS of survivors that die between t_{k-1} and t_k. ACS gains (Sg, Rr, Rg) are positive and ACS losses (Sl, Rl) are negative. Instantaneous ACS changes are subject to stochastic variation over time: because we are less interested in year-to-year variations than in long-term ACS trajectories, we modelled cumulative ACS changes instead of annual ACS changes. Cumulative ACS changes (Mg C ha^{-1}) were defined as follows:

$$cChange_{j,k} = \sum_{m=0}^{k} Change_{j,m} \quad (2)$$

where j is the plot, t_k the time since t_0 (yr) and $Change$ is the annual ACS change (Mg C ha^{-1} yr^{-1}), either recruits' ACS (Rr), recruits' ACS growth (Rg), recruits' ACS loss (Rl), survivors' ACS growth (Sg), or survivors' ACS loss (Sl).

Covariates

To model ACS changes, we chose six covariates : (1) $loss$ disturbance intensity, i.e. percentage of initial ACS loss; (2) $acs0$ mean ACS of the site; (3) $dacs$ relative ACS of the plot, as a % of $acs0$; (4) $prec$ annual precipitation; (5) $seas$ precipitation seasonality; (6) bd topsoil bulk density. To give equivalent weight to all covariates, we centred and standardized them in order to have a mean of zero and a standard deviation of one over all observations. The uncertainty associated with ACS covariates ($loss$, $acs0$, $dacs$) is less than 10% (**Chave et al., 2014**). Climatic covariates (annual precipitation $prec$ and precipitation seasonality $seas$) were extracted from Worldclim rasters (RRID:SCR_010244). Error in Worldclim precipitation data was estimated to be <10 mm in Amazonia (**Hijmans et al., 2005**). There is no information on the uncertainty on topsoil bulk density but we expect it to be higher than the uncertainty on other covariates, due to measurement (**De Vos et al., 2005**) and interpolation methods (**Hendriks et al., 2016**).

Survivors' model

Survivors' cumulative ACS changes are null at $t = 0$ (by definition). When all survivors are dead, their ACS changes stop: annual ACS changes become null and cumulative ACS changes reach a constant/finite limit. We decided to model survivors' cumulative ACS growth cSg and ACS loss cSl as:

$$cS_{i,j,k} \sim \mathcal{N}\left(\alpha_j^S \times \left(1 - exp(-\beta_j^S \times t_k)\right), (\sigma_E^S)^2\right) \quad (3)$$

where j is the plot, t_k is the time since t_0,S is either Sg or Sl.α_j^S is the finite limit of the cumulative ACS change and β_j^S the rate at which the cumulative ACS change converges to this limit. By choosing an exponential kernel, we assume that survivors' ACS change at t_k is proportional to survivors' ACS change at $t_k - 1$.

Because α_j^S values are expected to vary among plots, they are modelled with the following distribution:

$$\alpha_j^S \sim \mathcal{N}\left(\alpha_0^S, (\sigma_\alpha^S)^2\right) \quad (4)$$

Parameter β_j^S is the rate at which survivors' ACS change (from growth or mortality) on plot j converges to a finite limit after the disturbance: it reflects the response rapidity of survivors' ACS changes to disturbance. Because we are interested in predicting variations in β_j^S (S is either Sg or Sl), we expressed β_j^S as a function of covariates:

$$\beta_j^S = \beta_0^S + \sum_{l=1}^{6} (\lambda_l^S \times V_{j,l}) \quad (5)$$

where $\sum_{l=1}^{6} (\lambda_l^S \times V_{j,l})$, is the effect of covariates ($V_{j,l}$) on the post-logging rate β_j. Covariates are centred and standardized and are (1) $loss$: disturbance intensity, i.e. percentage of initial ACS loss; (2) $acs0$: mean ACS of the site; (3) $dacs$ relative ACS of the plot, as a % of $acs0$; (4) $prec$ annual precipitation; (5) $seas$ precipitation seasonality; (6) bd topsoil bulk density.

When all survivors in plot j are dead, all the C gained by their growth ($cSg_{j,\infty} = \alpha_j^{Sg}$) plus their initial ACS ($acsmin_j$) will have been lost ($cSl_{j,\infty} = \alpha_j^{Sl}$). We thus added the following constraint to each plot j:

$$\alpha_j^{Sl} + \alpha_j^{Sg} + acsmin_j = 0 \quad (6)$$

with $\alpha_j^{Sg}, \alpha_j^{Sl}$ the finite limits of survivors' cumulative ACS growth and ACS loss respectively, and $acsmin_j$ the ACS of the plot j at $t_{min} = t_0$.

Recruits' model

When survivors are all dead, recruits will constitute the new forest. We made the assumption that the ACS of this new forest will reach a dynamic equilibrium: recruits' annual ACS changes are expected to converge to constant values (that are however prone to small inter-annual variations), with ACS gains compensating ACS losses. Because there are no recruits yet at t_0, recruits' annual ACS growth (Rg) and ACS loss (Rl) are zero, and progressively increase to reach their asymptotic values. Recruits' annual ACS growth and ACS loss can be thus modelled with the function:

$$f(t; \alpha, \beta) = \alpha \times \left(1 - exp(-\beta \times t)\right) \quad (7)$$

where t is the time since the beginning of the recovery period. In the same logic as survivors' cumulative ACS change, α is the asymptotic value of recruits' annual ACS change (Mg C ha^{-1} yr^{-1}), and β is the rate at which this asymptotic value is reached.

Contrary to recruits' annual ACS growth and ACS loss, the ACS of new recruits (Rr) is high at t_0 because of the competition drop induced by logging, but then progressively decreases to reach its asymptotic value. We modelled it with the following function:

$$f(t;\alpha,\beta,\eta) = \alpha \times \left(1 + \eta \times exp(-\beta \times t)\right) \quad (8)$$

where t is the time since logging. The parameter η was added to allow annual recruited ACS to be higher than α at t_0.

As stated before, we chose to model cumulative ACS changes instead of annual ACS changes. The general model for recruits' cumulative ACS changes is deduced by integrating annual ACS changes from t_0 to t_k:

$$cR_{i,j,k} \sim \mathcal{N}\left(\alpha_i^R \times \left(t_k + \eta \times \frac{1 - exp(-\beta_j^R \times t_k)}{\beta_j^R}\right), (\sigma_E^R)^2\right) \quad (9)$$

where i is the site, j is the plot, t_k is the time since t_0 is either Rr, Rg or Rl. When R is Rg or Rl, $\eta = -1$; when R is Rr, $\eta > 0$.

Once the forest reaches a new dynamic equilibrium, recruits' annual ACS changes should depend mostly on each site's characteristics: we expect there to be more inter-site than intra-site variation in recruits' asymptotic ACS changes α^R. This is why we use one value α_i^R per site i, and model it as follows:

$$\alpha_i^R \sim \mathcal{N}\left(\alpha_0^R; (\sigma_\alpha^R)^2\right) \quad (10)$$

When the dynamic equilibrium is reached, annual ACS gain (growth and recruitment) compensates annual ACS loss (mortality). We thus added the following constraint for every site i:

$$\alpha_i^{Rr} + \alpha_i^{Rg} + \alpha_i^{Rl} = 0 \quad (11)$$

With the same logic as for survivors, we are interested in predicting variation in β^R. Given that we use one value α_i^R per site i (i.e. all plots in one site i have the same value for α_i^R), we chose to take into account the inter-plot variability as follows:

$$\beta_j^R \sim \mathcal{N}\left(\beta_0^R + \sum_{l=1}^{6} (\lambda_l^R \times V_{j,l}), (\sigma_\beta^R)^2\right) \quad (12)$$

Inference

Bayesian hierarchical models were inferred through MCMC methods using an adaptive form of the Hamiltonian Monte Carlo sampling (***Carpenter et al., 2015***). Each observation was given a weight proportional to the size of the plot. Codes were developed using the R language (RRID:SCR_001905) (***R Developement Core Team, 2015***) and the Rstan package (***Carpenter et al., 2015***). A detailed list of priors is provided in ***Table 1***.

Prediction maps

Maps were obtained with the following steps: (i) spatially-explicit covariates are extracted at the resolution of 30 arc-second from: the pan-tropical carbon map of Avitabile et al. for pre-disturbance aboveground carbon stocks (***Avitabile et al., 2016***); WorldClim (RRID:SCR_010244) (***Hijmans et al., 2005***) for annual precipitation and seasonality of precipitation, and the Harmonized World Soil database (***Nachtergaele et al., 2008***) for topsoil bulk density; (ii) disturbance intensity is set to 40% of pre-logging ACS loss, which is a common value for disturbance intensity after conventional logging in Amazonia (***West et al., 2014***; ***Blanc et al., 2009***; ***Martin et al., 2015***) , and the relative forest maturity $dacs$ is set to zero; (iii) parameters are drawn from their previously calibrated distribution; (iv) to simulate random effects, all five parameters (α) are taken from their distribution $\mathcal{N}(\alpha_0, \sigma_\alpha^2)$; (v) for every pixel, we estimate the five cumulative ACS changes (cSg, cSl, cRr,cRg,cRl) 10 years after the 40% ACS loss, given the parameters value and the pixel covariates values extracted from global rasters. Steps (iii) to (v) are repeated 200 times and summary statistics are calculated for every pixel. Because a significant part of our sites have experiment duration lower than 10 years (***Figure 1—figure supplement 1***), we are less confident in Amazonian-wide predictions after that 10 year period. Maps were elaborated under the R statistical software (RRID:SCR_001905) (***R Developement Core Team, 2015***).

Table 1. List of priors used to infer ACS changes in a Bayesian framework. Models are : (Sg) survivors' ACS growth, (Sl) survivors' ACS loss, (Rr) new recruits' ACS, (Rg) recruits' ACS growth, (Rl) recruits' ACS loss. λ_{loss} is the parameter relative to the covariate $loss$ (logging intensity).

Model	Parameter	Prior	Justification
Sg	α_j^{Sg}	$\mathcal{U}[25, 250]$	On average 100 survivors/ha storing 0.25 to 2.5 MgC each
Sg	β_j^{Sg}	$\mathcal{U}[0.015, 0.04]$	$75<t_{0.95}^{Sg\,*}<200$ yr
Sl	β_j^{Sl}	$\mathcal{U}[0.006, \beta^{Sg}]$	$t_{0.95}^{Sg}<t_{0.95}^{Sl\,*}<500$ yr
Rr	α_i^{Rr}	$\mathcal{U}[0.1, 1]$	Range of observed values in TmFO control plots
Rr	β_j^{Rr}	$\mathcal{U}[0.006, 0.6]$	$5<t_{0.95}^{Rr\,*}<500$ yr
Rr	η	$\mathcal{U}[0, 3]$	$Rr(t=0)<3\times Rr(t=\infty)$
Rg	α_i^{Rg}	$\mathcal{U}[0.5, 3]$	Range of observed values in Amazonia (***Johnson et al., 2016***)
Rg	β_j^{Rg}	$\mathcal{U}[0.006, 0.15]$	$20<t_{0.95}^{Rg\,*}<500$ yr
Rl	β_j^{Rl}	$\mathcal{U}[0.003, 0.06]$	$50<t_{0.95}^{Rl\,*}<1000$ yr
All models M†	λ_{loss}^{M}	$\mathcal{U}[-\beta^{M}, \beta^{M}]$	Avoid multicollinearity problems
All models M†	$(\lambda_l^{M})_{l\neq loss}$	$\mathcal{U}[-\frac{\beta^{M}}{4}, \frac{\beta^{M}}{4}]$	Avoid multicollinearity problems

*$t_{0.95} = \frac{ln(20)}{\beta}$ is the time when the ACS change has reached 95% of its asymptotic value.

†M is one of the five models: either Sg, Sl, Rr, Rg, Rl.

DOI: 10.7554/eLife.21394.012

Acknowledgements

We are in debt with all technicians and colleagues who helped setting up the plots and collecting data over years. Without their precious work, this study would have not been possible and they may be warmly thanked here. We are grateful to CIRAD, the GFclim project (FEDER 2014–2020, Project GY0006894) and the Sao Paulo Research Foundation (FAPESP: 2013/16262–4 and 2013/50718–5) for financial support. This study was partially funded by an Investissement d'Avenir grant of the ANR (CEBA: ANR-10-LABEX-0025) and carried out in the framework of the Tropical managed Forests Observatory (TmFO), supported by the Sentinel Landscape program of CGIAR (Consultative Group on International Agricultural Research) - Forest Tree and Agroforestry Research Program.

Additional information

Funding

Funder	Grant reference number	Author
Agence Nationale de la Recherche	ANR-10-LABEX-0025	Camille Piponiot Bruno Hérault
Fundação de Amparo à Pesquisa do Estado de São Paulo	FAPESP: 2013/16262-4 and 2013/50718-5	Edson Vidal
European Regional Development Fund	FEDER 2014-2020, GY0006894	Camille Piponiot Bruno Hérault

The funders had no role in study design, data collection and interpretation, or the decision to submit the work for publication.

Author contributions

CP, ER, Conception and design, Analysis and interpretation of data, Drafting or revising the article; PS, BH, Conception and design, Acquisition of data, Analysis and interpretation of data, Drafting or revising the article; LM, CPdA, MF, MVNd'O, CRdS, Acquisition of data, Analysis and interpretation of data, Drafting or revising the article; MP-C, Conception and design, Acquisition of data, Drafting

or revising the article; FEP, AS, CB, Analysis and interpretation of data, Drafting or revising the article; NA, MG, ENHC, ARR, KEdS, EDS, EV, TAPW, Acquisition of data, Drafting or revising the article

Author ORCIDs
Camille Piponiot, http://orcid.org/0000-0002-3473-1982
Eurídice N Honorio Coronado, http://orcid.org/0000-0003-2314-590X
Bruno Hérault, http://orcid.org/0000-0002-6950-7286

Additional files

Major datasets

The following dataset was generated:

Author(s)	Year	Dataset title	Dataset URL	Database, license, and accessibility information
Piponiot C, Sist P, Mazzei L, Peña-Claros M, Putz F, Rutishauser E, Shenkin A, Ascarrunz N, de Azevedo C, Baraloto C, França M, Guedes M, Honorio Coronado E, d'Oliveira MVN, Ruschel AR, da Silva KE, Doff Sotta E, de Souza CR, Vidal E, West TAP, Hérault B	2016	Data from: Post-disturbance carbon recovery in Amazonian forests	http://dx.doi.org/10.5061/dryad.rc279	Available at Dryad Digital Repository under a CC0 Public Domain Dedication

References

Andersen H-E, Reutebuch SE, McGaughey RJ, d'Oliveira MVN, Keller M. 2014. Monitoring selective logging in western Amazonia with repeat lidar flights. *Remote Sensing of Environment* **151**:157–165. doi: 10.1016/j.rse.2013.08.049

Aragão LEOC, Malhi Y, Metcalfe DB, Silva-Espejo JE, Jiménez E, Navarrete D, Almeida S, Costa ACL, Salinas N, Phillips OL, Anderson LO, Alvarez E, Baker TR, Goncalvez PH, Huamán-Ovalle J, Mamani-Solórzano M, Meir P, Monteagudo A, Patiño S, Peñuela MC, et al. 2009. Above- and below-ground net primary productivity across ten Amazonian forests on contrasting soils. *Biogeosciences* **6**:2759–2778. doi: 10.5194/bg-6-2759-2009

Asner GP, Broadbent EN, Oliveira PJ, Keller M, Knapp DE, Silva JN. 2006. Condition and fate of logged forests in the brazilian Amazon. *PNAS* **103**:12947–12950. doi: 10.1073/pnas.0604093103, PMID: 16901980

Asner GP, Knapp DE, Broadbent EN, Oliveira PJ, Keller M, Silva JN. 2005. Selective logging in the brazilian Amazon. *Science* **310**:480–482. doi: 10.1126/science.1118051, PMID: 16239474

Asner GP, Rudel TK, Aide TM, Defries R, Emerson R. 2009. A contemporary assessment of change in humid tropical forests. *Conservation Biology* **23**:1386–1395. doi: 10.1111/j.1523-1739.2009.01333.x, PMID: 20078639

Avitabile V, Herold M, Heuvelink GB, Lewis SL, Phillips OL, Asner GP, Armston J, Ashton PS, Banin L, Bayol N, Berry NJ, Boeckx P, de Jong BH, DeVries B, Girardin CA, Kearsley E, Lindsell JA, Lopez-Gonzalez G, Lucas R, Malhi Y, et al. 2016. An integrated pan-tropical biomass map using multiple reference datasets. *Global Change Biology* **22**:1406–1420. doi: 10.1111/gcb.13139, PMID: 26499288

Baker TR, Phillips OL, Malhi Y, Almeida S, Arroyo L, Di Fiore A, Erwin T, Killeen TJ, Laurance SG, Laurance WF, Lewis SL, Lloyd J, Monteagudo A, Neill DA, Patino S, Pitman NCA, M. Silva JN, Vasquez Martinez R. 2004. Variation in wood density determines spatial patterns inAmazonian forest biomass. *Global Change Biology* **10**:545–562. doi: 10.1111/j.1365-2486.2004.00751.x

Blanc L, Echard M, Herault B, Bonal D, Marcon E, Chave J, Baraloto C. 2009. Dynamics of aboveground carbon stocks in a selectively logged tropical forest. *Ecological Applications* **19**:1397–1404. doi: 10.1890/08-1572.1, PMID: 19769089

Blaser J, Sarre A, Poore D, Johnson S. 2011. *Status of Tropical Forest Management*.

Bonal D, Burban B, Stahl C, Wagner F, Hérault B. 2016. The response of tropical rainforests to drought-lessons from recent research and future prospects. *Annals of Forest Science* **73**:27–44. doi: 10.1007/s13595-015-0522-5, PMID: 27069374

Carpenter B, Gelman A, Hoffman M, Lee D, Goodrich B, Betancourt M, Brubaker MA, Li P, Riddell A. 2015. Stan : A probabilistic programming language. *Journal of Statistical Software*.

Chave J, Réjou-Méchain M, Búrquez A, Chidumayo E, Colgan MS, Delitti WB, Duque A, Eid T, Fearnside PM, Goodman RC, Henry M, Martínez-Yrízar A, Mugasha WA, Muller-Landau HC, Mencuccini M, Nelson BW, Ngomanda A, Nogueira EM, Ortiz-Malavassi E, Pélissier R, et al. 2014. Improved allometric models to estimate the aboveground biomass of tropical trees. *Global Change Biology* **20**:3177–3190. doi: 10.1111/gcb.12629, PMID: 24817483

Dauber E, Fredericksen TS, Peña M. 2005. Sustainability of timber harvesting in bolivian tropical forests. *Forest Ecology and Management* **214**:294–304. doi: 10.1016/j.foreco.2005.04.019

De Vos B, Van Meirvenne M, Quataert P, Deckers J, Muys B. 2005. Predictive quality of pedotransfer functions for estimating bulk density of forest soils. *Soil Science Society of America Journal* **69**:500. doi: 10.2136/sssaj2005.0500

Espírito-Santo FD, Gloor M, Keller M, Malhi Y, Saatchi S, Nelson B, Junior RC, Pereira C, Lloyd J, Frolking S, Palace M, Shimabukuro YE, Duarte V, Mendoza AM, López-González G, Baker TR, Feldpausch TR, Brienen RJ, Asner GP, Boyd DS, et al. 2014. Size and frequency of natural forest disturbances and the Amazon forest carbon balance. *Nature Communications* **5**:3434. doi: 10.1038/ncomms4434, PMID: 24643258

Frolking S, Palace MW, Clark DB, Chambers JQ, Shugart HH, Hurtt GC. 2009. Forest disturbance and recovery: A general review in the context of spaceborne remote sensing of impacts on aboveground biomass and canopy structure. *Journal of Geophysical Research: Biogeosciences* **114**:n/a. doi: 10.1029/2008JG000911

Goetz SJ, Hansen M, Houghton RA, Walker W, Laporte N, Busch J. 2015. Measurement and monitoring needs, capabilities and potential for addressing reduced emissions from deforestation and forest degradation under REDD+. *Environmental Research Letters* **10**:123001. doi: 10.1088/1748-9326/10/12/123001

Gourlet-Fleury S, Cornu G, Jésel S, Dessard H, Jourget J-G, Blanc L, Picard N. 2005. Using models to predict recovery and assess tree species vulnerability in logged tropical forests: A case study from French Guiana. *Forest Ecology and Management* **209**:69–85. doi: 10.1016/j.foreco.2005.01.010

Grace J, Mitchard E, Gloor E. 2014. Perturbations in the carbon budget of the tropics. *Global Change Biology* **20**:3238–3255. doi: 10.1111/gcb.12600, PMID: 24902948

Griggs DJ, Noguer M. 2002. Climate change 2001: The scientific basis. contribution of working group I to the third assessment report of the intergovernmental panel on climate change. *Weather* **57**:267–269. doi: 10.1256/004316502320517344

He Q, Bertness MD, Altieri AH. 2013. Global shifts towards positive species interactions with increasing environmental stress. *Ecology Letters* **16**:695–706. doi: 10.1111/ele.12080, PMID: 23363430

Hendriks CMJ, Stoorvogel JJ, Claessens L. 2016. Exploring the challenges with soil data in regional land use analysis. *Agricultural Systems* **144**:9–21. doi: 10.1016/j.agsy.2016.01.007

Hijmans RJ, Cameron SE, Parra JL, Jones PG, Jarvis A. 2005. Very high resolution interpolated climate surfaces for global land areas. *International Journal of Climatology* **25**:1965–1978. doi: 10.1002/joc.1276

Houghton RA, House JI, Pongratz J, van der Werf GR, DeFries RS, Hansen MC, Le Quéré C, Ramankutty N. 2012. Carbon emissions from land use and land-cover change. *Biogeosciences* **9**:5125–5142. doi: 10.5194/bg-9-5125-2012

Huang M, Asner GP. 2010. Long-term carbon loss and recovery following selective logging in Amazon forests. *Global Biogeochemical Cycles* **24**:n/a. doi: 10.1029/2009GB003727

Herault B, Ouallet J, Blanc L, Wagner F, Baraloto C. 2010. Growth responses of neotropical trees to logging gaps. *Journal of Applied Ecology* **47**:821–831. doi: 10.1111/j.1365-2664.2010.01826.x

Johnson MO, Galbraith D, Gloor E, De Deurwaerder H, Guimberteau M, Rammig A, Thonicke K, Verbeeck H, von Randow C, Monteagudo A, Phillips OL, Brienen RJW, Feldpausch TR, Lopez Gonzalez G, Fauset S, Quesada C, Christoffersen B, Ciais P, Gilvan S, Kruijt B, et al. 2016. Variation in stem mortality rates determines patterns of aboveground biomaass inAmazonian forests: implications for dynamic global vegetation models. *Global Change Biology* **44**:1–18. doi: 10.1111/gcb.13315

Malhi Y, Roberts JT, Betts RA, Killeen TJ, Li W, Nobre CA. 2008. Climate change, deforestation, and the fate of the Amazon. *Science* **319**:169–172. doi: 10.1126/science.1146961, PMID: 18048654

Malhi Y, Wright J. 2004. Spatial patterns and recent trends in the climate of tropical rainforest regions. *Philosophical Transactions of the Royal Society B: Biological Sciences* **359**:311–329. doi: 10.1098/rstb.2003.1433, PMID: 15212087

Martin PA, Newton AC, Pfeifer M, Khoo M, Bullock JM. 2015. Impacts of tropical selective logging on carbon storage and tree species richness: A meta-analysis. *Forest Ecology and Management* **356**:224–233. doi: 10.1016/j.foreco.2015.07.010

Mercado LM, Patino S, Domingues TF, Fyllas NM, Weedon GP, Sitch S, Quesada CA, Phillips OL, Aragao LEOC, Malhi Y, Dolman AJ, Restrepo-Coupe N, Saleska SR, Baker TR, Almeida S, Higuchi N, Lloyd J. 2011. Variations in Amazon forest productivity correlated with foliar nutrients and modelled rates of photosynthetic carbon supply. *Philosophical Transactions of the Royal Society B: Biological Sciences* **366**:3316–3329. doi: 10.1098/rstb.2011.0045

Nachtergaele F, Velthuizen HV, Verelst L. 2008. Harmonized world soil database. *Technical Report*.

Pan Y, Birdsey RA, Fang J, Houghton R, Kauppi PE, Kurz WA, Phillips OL, Shvidenko A, Lewis SL, Canadell JG, Ciais P, Jackson RB, Pacala SW, McGuire AD, Piao S, Rautiainen A, Sitch S, Hayes D. 2011. A large and persistent carbon sink in the world's forests. *Science* **333**:988–993. doi: 10.1126/science.1201609, PMID: 21764754

Penman J, Gytarsky M, Hiraishi T, Krug T. 2003. *Good Practice Guidance for Land Use, Land-Use Change and Forestry*. The Intergovernmental Panel on Climate Change.

Phillips OL, Baker TR, Arroyo L, Higuchi N, Killeen TJ, Laurance WF, Lewis SL, Lloyd J, Malhi Y, Monteagudo A, Neill DA, Vargas PN, Silva JN, Terborgh J, Martínez RV, Alexiades M, Almeida S, Brown S, Chave J, Comiskey JA, et al. 2004. Pattern and process in Amazon tree turnover, 1976-2001. *Philosophical Transactions of the Royal Society B: Biological Sciences* **359**:381–407. doi: 10.1098/rstb.2003.1438, PMID: 15212092

Piponiot C, Sist P, Mazzei L, Peña-Claros M, Putz F, Rutishauser E, Shenkin A, Ascarrunz N, de Azevedo CP, Baraloto C, França M, Guedes M, Honorio Coronado E, d'Oliveira MVN, Ruschel AR, da Silva KE, Doff Sotta E, de Souza CR, Vidal E, West TAP, et al. 2016. Data from: Post-disturbance carbon recovery in Amazonian forests. *Dryad Digital Repository*. doi: http://dx.doi.org/10.5061/dryad.rc279

Poorter L, Bongers F, Aide TM, Almeyda Zambrano AM, Balvanera P, Becknell JM, Boukili V, Brancalion PH, Broadbent EN, Chazdon RL, Craven D, de Almeida-Cortez JS, Cabral GA, de Jong BH, Denslow JS, Dent DH, DeWalt SJ, Dupuy JM, Durán SM, Espírito-Santo MM, et al. 2016. Biomass resilience of neotropical secondary forests. *Nature* **530**:211–214. doi: 10.1038/nature16512, PMID: 26840632

Putz FE, Sist P, Fredericksen T, Dykstra D. 2008. Reduced-impact logging: Challenges and opportunities. *Forest Ecology and Management* **256**:1427–1433. doi: 10.1016/j.foreco.2008.03.036

Quesada CA, Phillips OL, Schwarz M, Czimczik CI, Baker TR, Patiño S, Fyllas NM, Hodnett MG, Herrera R, Almeida S, Alvarez Dávila E, Arneth A, Arroyo L, Chao KJ, Dezzeo N, Erwin T, di Fiore A, Higuchi N, Honorio Coronado E, Jimenez EM, et al. 2012. Basin-wide variations in Amazon forest structure and function are mediated by both soils and climate. *Biogeosciences* **9**:2203–2246. doi: 10.5194/bg-9-2203-2012

R Developement Core Team. 2015. *R: A Language and Environment for Statistical Computing*. Vienna, Austria: R Foundation for Statistical Computing. p. 409

Rutishauser E, Hérault B, Baraloto C, Blanc L, Descroix L, Sotta ED, Ferreira J, Kanashiro M, Mazzei L, d'Oliveira MV, de Oliveira LC, Peña-Claros M, Putz FE, Ruschel AR, Rodney K, Roopsind A, Shenkin A, da Silva KE, de Souza CR, Toledo M, et al. 2015. Rapid tree carbon stock recovery in managed Amazonian forests. *Current Biology* **25**:R787–R788. doi: 10.1016/j.cub.2015.07.034, PMID: 26394096

Rutishauser E, Hérault B, Petronelli P, Sist P. 2016. Tree height reduction after selective logging in a tropical forest. *Biotropica* **48**:285–289. doi: 10.1111/btp.12326

Santiago LS. 2015. Nutrient limitation of eco-physiological processes in tropical trees. *Trees* **29**:1291–1300. doi: 10.1007/s00468-015-1260-x

Shenkin A, Bolker B, Peña-Claros M, Licona JC, Putz FE. 2015. Fates of trees damaged by logging in amazonian Bolivia. *Forest Ecology and Management* **357**:50–59. doi: 10.1016/j.foreco.2015.08.009

Sist P, Ferreira FN. 2007. Sustainability of reduced-impact logging in the Eastern Amazon. *Forest Ecology and Management* **243**:199–209. doi: 10.1016/j.foreco.2007.02.014

Sist P, Rutishauser E, Peña-Claros M, Shenkin A, Hérault B, Blanc L, Baraloto C, Baya F, Benedet F, da Silva KE, Descroix L, Ferreira JN, Gourlet-Fleury S, Guedes MC, Bin Harun I, Jalonen R, Kanashiro M, Krisnawati H, Kshatriya M, Lincoln P, et al. 2015. The tropical managed forests observatory: a research network addressing the future of tropical logged forests. *Applied Vegetation Science* **18**:171–174. doi: 10.1111/avsc.12125

Swaine MD, Lieberman D, Putz FE. 1987. The dynamics of tree populations in tropical forest: a review. *Journal of Tropical Ecology* **3**:359–366. doi: 10.1017/S0266467400002339

ter Steege H, Pitman NC, Phillips OL, Chave J, Sabatier D, Duque A, Molino JF, Prévost MF, Spichiger R, Castellanos H, von Hildebrand P, Vásquez R, Steege HT. 2006. Continental-scale patterns of canopy tree composition and function across Amazonia. *Nature* **443**:444–447. doi: 10.1038/nature05134, PMID: 17006512

Valladares F, Niinemets Ülo. 2008. Shade tolerance, a Key Plant Feature of Complex Nature and Consequences. *Annual Review of Ecology, Evolution, and Systematics* **39**:237–257. doi: 10.1146/annurev.ecolsys.39.110707.173506

Valle D, Phillips P, Vidal E, Schulze M, Grogan J, Sales M, van Gardingen P. 2007. Adaptation of a spatially explicit individual tree-based growth and yield model and long-term comparison between reduced-impact and conventional logging in eastern Amazonia, Brazil. *Forest Ecology and Management* **243**:187–198. doi: 10.1016/j.foreco.2007.02.023

Vidal E, West TAP, Putz FE. 2016. Recovery of biomass and merchantable timber volumes twenty years after conventional and reduced-impact logging in amazonian Brazil. *Forest Ecology and Management* **376**:1–8. doi: 10.1016/j.foreco.2016.06.003

Vieira S, de Camargo PB, Selhorst D, da Silva R, Hutyra L, Chambers JQ, Brown IF, Higuchi N, dos Santos J, Wofsy SC, Trumbore SE, Martinelli LA. 2004. Forest structure and carbon dynamics in amazonian tropical rain forests. *Oecologia* **140**:468–479. doi: 10.1007/s00442-004-1598-z, PMID: 15221436

Vieira S, Trumbore S, Camargo PB, Selhorst D, Chambers JQ, Higuchi N, Martinelli LA. 2005. Slow growth rates of amazonian trees: Consequences for carbon cycling. *PNAS* **102**:18502–18507. doi: 10.1073/pnas.0505966102

Wagner FH, Hérault B, Bonal D, Stahl C, Anderson LO, Baker TR, Becker GS, Beeckman H, Boanerges Souza D, Botosso PC, Bowman DMJS, Bräuning A, Brede B, Brown FI, Camarero JJ, Camargo PB, Cardoso FCG, Carvalho FA, Castro W, Chagas RK, et al. 2016. Climate seasonality limits leaf carbon assimilation and wood productivity in tropical forests. *Biogeosciences* **13**:2537–2562. doi: 10.5194/bg-13-2537-2016

West TAP, Vidal E, Putz FE. 2014. Forest biomass recovery after conventional and reduced-impact logging in Amazonian Brazil. *Forest Ecology and Management* **314**:59–63. doi: 10.1016/j.foreco.2013.11.022

Wright SJ, Kitajima K, Kraft NJ, Reich PB, Wright IJ, Bunker DE, Condit R, Dalling JW, Davies SJ, Díaz S, Engelbrecht BM, Harms KE, Hubbell SP, Marks CO, Ruiz-Jaen MC, Salvador CM, Zanne AE. 2010. Functional traits and the growth-mortality trade-off in tropical trees. *Ecology* **91**:3664–3674. doi: 10.1890/09-2335.1, PMID: 21302837

Zanne AE, Lopez-Gonzalez G, Coomes DAA, Ilic J, Jansen S, Lewis S, Miller RBB, Swenson NGG, Wiemann MCC, Chave J. 2009. Global wood density database. *Technical Report* **235**. doi: 10.5061/dryad.234/1

Appendix

The importance of a process-based approach

We here study C recovery dynamics with a demographic process-based approach, i.e. by segregating ACS changes into cohorts (survivors and recruits) and demographic processes (growth, recruitment, mortality), as opposed to an all-in-one model in which only the ecosystem net ACS change is modelled, without examination of demographic processes.

To compare the goodness of fit of the two approaches (all-in-one and process-based), we calibrated an all-in-one model with our data and compared the accuracy of its predictions with the process-based predictions reported in this study. The all-in-one model was written as follows:

$$C_{j,k} \sim \mathcal{N}\left((acs0_j - acsmin_j) \times (1 - exp(-\beta_j^C \times t_k)), (\sigma_E^C)^2\right) \quad (13)$$

where $C_{j,k}$ (MgC ha^{-1}) is the total C accumulation t_k years after the disturbance in plot j is the ACS lost by logging and β_j^C is the rate at which the plot ACS returns to its pre-logging ACS. We took into account the effect of covariates and dependencies for β_j^C :

$$\beta_j^C \sim N\left(\beta_0^C + \sum_{l=1}^{6}(\lambda_l^C \times V_{j,l}); (\sigma_\beta^C)^2\right) \quad (14)$$

The process-based model made better predictions (RMSE = 0.24) than the all-in-one model (RMSE = 0.31). In some sites, for example Paracou (black diamonds in ***Appendix—figure 1***), there is a clear bias in the all-in-one model predictions: C accumulation is overestimated at the beginning of the recovery period and underestimated towards the end. This bias may be due to the non-adequacy of the negative exponential curve in the classic all-in-one model (***Appendix—figure 2a***) to the C recovery observed in experimental plots (***Rutishauser et al., 2015***). The process-based model does not predict a constant instantaneous C accumulation rate (***Appendix—figure 2b***), and is thus more accurate.

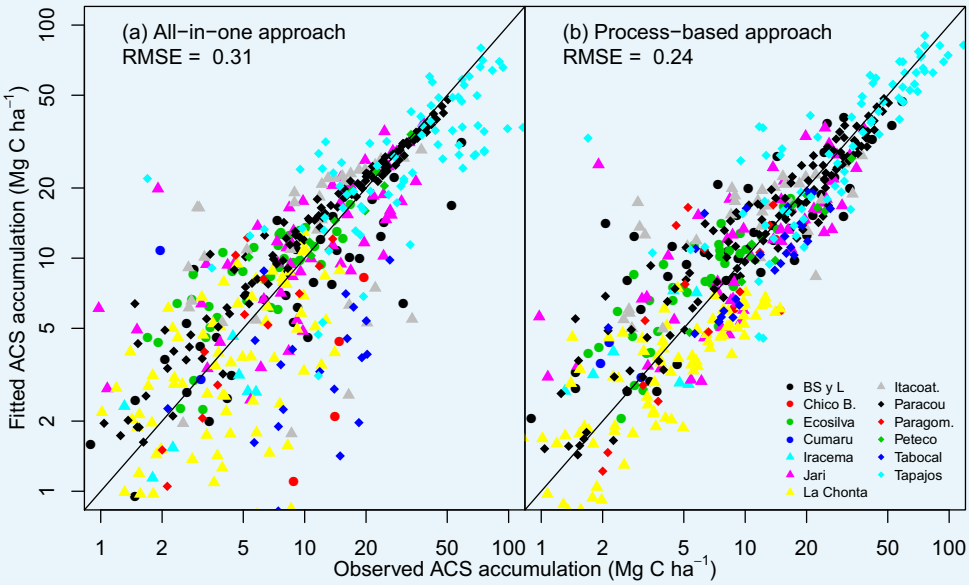

Appendix 1—figure 1. Observed vs fitted values of net ACS accumulation (MgC ha^{-1}). (**a**) Fitted values from the all-in-one model. (**b**) Fitted values from the process-based model (right). Net ACS accumulation is the sum of cumulative ACS changes (gain and loss). Each combination of a colour and shape is specific to a site. The closer the dots are to the x=y line, the better the prediction.

DOI: 10.7554/eLife.21394.013

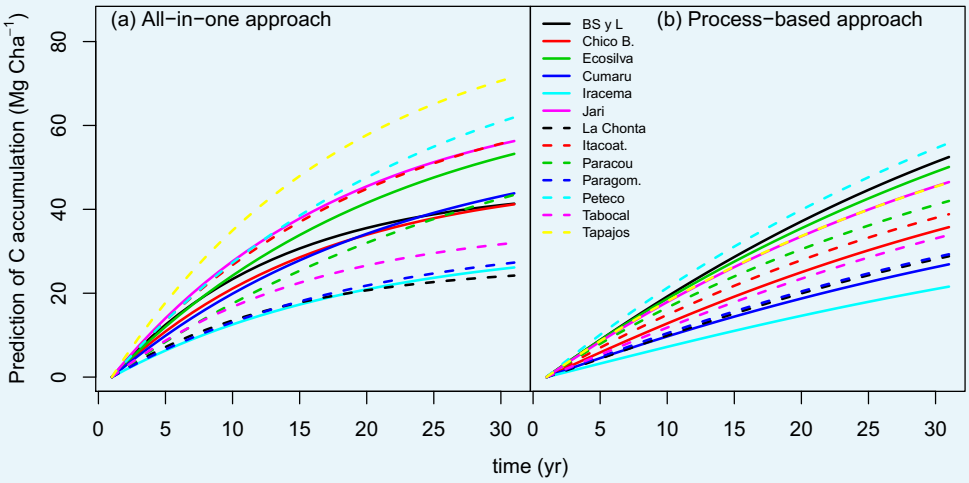

Appendix 1—figure 2. Predicted trajectories of net ACS accumulation (MgC ha^{-1}) per site with (**a**) the all-in-one model and (**b**) the process-based model.

DOI: 10.7554/eLife.21394.014

Chapitre 5

Structuration locale des dynamiques post-exploitation

Ce chapitre a pour objectif d'approfondir la structuration locale des dynamiques de carbone post-exploitation à partir du modèle présenté dans le chapitre précédent, en étudiant leur lien avec (i) les caractéristiques du peuplement local (structure et composition fonctionnelle) et (ii) les conditions environnementales locales (topographie et conditions climatiques annuelles).

Les données utilisées viennent de la station expérimentale de Paracou en Guyane française, où douze parcelles de 6.25 ha ont été suivies depuis 1984, dont 9 ont été exploitées à différentes intensités en 1986. Des inventaires ont été menés tous les 1 à 2 ans et tous les arbres >10 cm DHP ont été mesurés et identifiés par un botaniste. De plus une cartographie détaillée des sols et de la topographie de Paracou sont disponibles, ainsi que des données climatiques récoltées dans une station météo sur le site. Enfin, une grande base de données de 4 709 mesures (683 espèces) de 10 traits fonctionnels a été développée en Guyane au cours du projet BRIDGE[1], ce qui a permis d'avoir une estimation précise de la composition fonctionnelle des parcelles.

[1] C. Baraloto et al. (2010). « Functional trait variation and sampling strategies in species-rich plant communities ». In : *Functional Ecology* 24.1, p. 208–216.

Le modèle développé au chapitre précédent a été appliqué aux données de Paracou, et les variations des dynamiques post-exploitation ont été reliées aux variables endogènes et exogènes présentées ci-dessus. Cette étude a permis notamment de montrer l'importance de la composition fonctionnelle sur la récupération du carbone après la perturbation. Les parcelles dont la composition fonctionnelle est proche de forêts très perturbées (traits caractéristiques d'espèces pionnières à croissance rapide : faible densité du bois, petites graines) récupèrent moins rapidement. Ces résultats montrent l'importance de la prise en compte de la composition, et surtout des caractéristiques fonctionnelles, dans la régénération des forêts tropicales. Les implications pour le futur des forêts tropicales sont aussi cruciales : avec l'augmentation de la fréquence des perturbations [2] la composition des forêts pourrait

[2] cf. section 1.2.1

être de plus en plus dominée par des espèces pionnières, ce qui pourrait diminuerait d'autant leur récupération post-perturbation.

Ce chapitre a été publié dans la revue *Forest Ecosystems* en 2018.

Forest Ecosystems

RESEARCH Open Access

Key drivers of ecosystem recovery after disturbance in a neotropical forest

Long-term lessons from the Paracou experiment, French Guiana

Bruno Hérault[1,2*] and Camille Piponiot[3]

Abstract

Background: Natural disturbance is a fundamental component of the functioning of tropical rainforests let to natural dynamics, with tree mortality the driving force of forest renewal. With ongoing global (i.e. land-use and climate) changes, tropical forests are currently facing deep and rapid modifications in disturbance regimes that may hamper their recovering capacity so that developing robust predictive model able to predict ecosystem resilience and recovery becomes of primary importance for decision-making: (i) Do regenerating forests recover faster than mature forests given the same level of disturbance? (ii) Is the local topography an important predictor of the post-disturbance forest trajectories? (iii) Is the community functional composition, assessed with community weighted-mean functional traits, a good predictor of carbon stock recovery? (iv) How important is the climate stress (seasonal drought and/or soil water saturation) in shaping the recovery trajectory?

Methods: Paracou is a large scale forest disturbance experiment set up in 1984 with nine 6.25 ha plots spanning on a large disturbance gradient where 15 to 60% of the initial forest ecosystem biomass were removed. More than 70,000 trees belonging to ca. 700 tree species have then been censused every 2 years up today. Using this unique dataset, we aim at deciphering the endogenous (forest structure and composition) and exogenous (local environment and climate stress) drivers of ecosystem recovery in time. To do so, we disentangle carbon recovery into demographic processes (recruitment, growth, mortality fluxes) and cohorts (recruited trees, survivors).

Results: Variations in the pre-disturbance forest structure or in local environment do not shape significantly the ecosystem recovery rates. Variations in the pre-disturbance forest composition and in the post-disturbance climate significantly change the forest recovery trajectory. Pioneer-rich forests have slower recovery rates than assemblages of late-successional species. Soil water saturation during the wet season strongly impedes ecosystem recovery but not seasonal drought. From a sensitivity analysis, we highlight the pre-disturbance forest composition and the post-disturbance climate conditions as the primary factors controlling the recovery trajectory.

Conclusions: Highly-disturbed forests and secondary forests because they are composed of a lot of pioneer species will be less able to cope with new disturbance. In the context of increasing tree mortality due to both (i) severe droughts imputable to climate change and (ii) human-induced perturbations, tropical forest management should focus on reducing disturbances by developing Reduced Impact Logging techniques.

Keywords: Ecosystem modeling, Tropical forests, Carbon fluxes, Ecological resilience, Climate change, Amazonia

*Correspondence: bruno.herault@cirad.fr
[1]Cirad, UMR EcoFoG (AgroParistech, CNRS, Inra, Université des Antilles, Université de la Guyane), Campus Agronomique, 97310 Kourou, French Guiana, France
[2]INPHB (Institut National Polytechnique Félix Houphouët Boigny), Yamoussoukro, Ivory Coast
Full list of author information is available at the end of the article

Background

In tropical forests, natural disturbances caused by the death of one or more trees are the dominant forms of forest regeneration as the creation of canopy openings continuously reshapes forest structure (Goulamoussène et al. 2017). The immediate increase in light intensity allows the sunlight to penetrate the understorey (Goulamoussène et al. 2016) and light-demanding trees (Denslow et al. 1998) to establish and grow, thus contributing to the maintenance of biodiversity that shapes forest functionning (Liang et al. 2016). Another effect of canopy gaps is the local modification of the forest nutrient balance due to the large amounts of dead leaves and wood that decompose and mineralize (Brokaw and Busing 2000) and that shapes in turn the small-scale spatial variations in forest carbon balance (Feeley et al. 2007; Guitet et al. 2015; Rutishauser et al. 2010). In this way, the natural disturbance regime is a fundamental component of the functioning of tropical forests (Sheil and Burslem 2003).

With ongoing global (i.e land-use and climate) changes, tropical forests are currently facing deep and rapid changes in disturbance regimes that may hamper their recovering capacity (Hérault and Gourlet-Fleury 2016; Brienen et al. 2015). Human-induced disturbances may encompass a wide range of perturbations from long-lasting ones such as land-cover changes for industrial agriculture, slash-and-burn agriculture or mining (Dezécache et al. 2017a,b) to more insiduous modifications such as selective logging that may not affect the forest cover but modify forest functioning (Rutishauser et al. 2015). An even more insiduous perturbation is climate change (Hérault and Gourlet-Fleury 2016). Global circulation models have shown high probabilities of significant precipitation decrease for tropical areas with a risk of transition from short-dry-season rainforest to long-dry- season savannah ecosystems (Davidson et al. 2012). For instance, after the intense 2005 drought in Amazonia, the forest suffered an additional mortality, leading to a huge loss of live biomass (Phillips et al. 2009) with similar mortality events observed in Panama (Condit 1995), in China (Tan et al. 2013) or in South-East Asia (Slik 2004).

To our opinion, the drivers of the post-disturbance system trajectory may first be defined based on their origin: endogeneous and exogeneous. (1) Endogenous drivers refer to the internal properties of the system that may influence its post-disturbance behavior. A significant example for ecological systems is the species composition that partially informs on the immediate potential of the system to recover after disturbance. In that respect, the species identity is far less important than the functional signature of the species assemblage (Kunstler et al. 2016): for example, an assemblage of light-demanding species will respond differently to disturbance from an assemblage of shade-tolerant understorey species (Herault et al. 2010). Structural characteristics of the pre-disturbance species community (stem density, average size, live biomass and so on) may also be of primary importance because they are core indicators of the silvigenetic stage of the forest (Pillet et al. 2017). (2) Exogenous drivers refer to external constraints or forces that limit the possible system trajectories. They can be grouped into two broad categories: drivers that vary in space and those that vary in time. The local environment, i.e. the physical characteristics of the abiotic environment, is here defined in space but not in time. On the contrary, external conditions such as climatic stress are here considered to vary in time but not in space.

This study draws upon the long-term disturbance experiment of Paracou, French Guiana, to develop a modeling approach in order to mechanistically link the endo- and exogenous ecosystem drivers to the ecosystem recovery trajectory after disturbance. More specifically, we ask the following questions: (i) Do regenerating forests recover faster than mature forests given the same level of disturbance? (ii) Is the local topography an important predictor of the forest recovery rates? (iii) Is the community functional composition, assessed with community weighted-mean functional traits, a good predictor of carbon stock recovery? (iv) How important is the climate stress (drought and/or soil water saturation) to shape the rate of carbon recovery? To do so, we partition the contributions to post-disturbance ACS (Aboveground Carbon Stock) gain (from growth and recruitment of trees sup 10 cm DBH) and ACS loss (from mortality) of survivors and recruited trees to detect the main drivers and patterns of ACS recovery after disturbance. We model the trajectory of those post-disturbance ACS changes (Piponiot et al. 2016b) in a comprehensive Bayesian framework. We then quantify the effect of (i) endogeneous (forest structure and composition) and (ii) exogeneous (local environment and climate stress) drivers on the rates at which post-disturbance ACS changes converge to a theoretical steady state. Summing these ACS changes over time gives the net post-disturbance rate of ACS accumulation, an indicator of the ecosystem recovery rate. Disentangling ACS recovery with a demographic process-based approach, i.e. by segregating ACS changes into cohorts (survivors and recruits) and demographic processes (growth, recruitment, mortality), as opposed to an all-in-one model in which only the ecosystem net ACS change is modeled without examination of demographic processes, has been shown to be essential to reveal mechanisms underlying ACS responses to disturbance and to make more robust predictions of ACS recovery (Piponiot et al. 2016b).

Methods

Study site

The study was conducted at the Paracou experimental site (5°18'N, 52°55'W), a lowland tropical rain forest near Sinnamary, French Guiana. The site receives nearly two-thirds of the annual 3041 mm of precipitation between mid-March and mid-June, and < 50 mm per month in September and October (Wagner et al. 2011). More than 700 woody species attaining 2 cm DBH (diameter at breast height) have been described at the site, with 150 - 210 species of trees > 10 cm DBH per hectare. The floristic composition is typical of Guianan rainforests with dominant families including Leguminoseae, Chrysobalanaceae, Lecythidaceae, Sapotaceae and Burseraceae (Guitet et al. 2014). In 1984, nine 6.25 ha plots, each one divided into 4 subplots of 1.56 ha each, were established for a complete inventory of all trees > 10 cm DBH. From October 1986 to May 1987, the plots underwent three disturbance treatments (details in Table 1 and in (Blanc et al. 2009)).

Input data

Aboveground Carbon Stock (ACS) computation In all plots, diameter at breast height (DBH) of trees > 10 cm DBH were measured every two years from 1982 to 2016 resulting in 18 forest censuses. Trees were identified to the lowest taxonomic level. To get wood density, we applied the following standardized protocol: (i) tree identified to the species level were assigned the corresponding wood specific gravity value from the Global Wood Density Database (GWDD) (Chave et al. 2009); (ii) trees identified to the genus level were assigned a genus-average wood density and (iii) trees with no botanical identification or that were not in the GWDD were assigned the subplot-average wood density. The aboveground biomass (AGB) was estimated taking all uncertainties into account using the BIOMASS package (Réjou-Méchain et al. 2017). Biomass was assumed to be 47% carbon.

Disturbance intensity After disturbance, the subplot's ACS decreases rapidly until it reaches its minimum value acs_{min} a few years later. This transition point determines the beginning of the recovery period. The difference between the averaged pre-disturbance ACS acs_{pre} and this post-logging minimum value acs_{min} reached at time $t = t_{min}$ defines the disturbance intensity $DIST$. In other words, the disturbance intensity is defined as the amount of aboveground carbon lost in the forest ecosystem during the first years during and after the disturbance.

Structure drivers The pre-disturbance forest structure was assessed with three variables: the stem density S_N (from 483 to 727 ind·ha^{-1}) and the basal area S_{BA} (from 27 to 36 m$^2 \cdot$ ha^{-1}) of subplot j at t_{pre}, the year preceding the disturbance experiment.

Environment drivers Three environmental drivers were selected from a preliminary exploratory analysis to represent independent source of variation in the local forest physical conditions: the proportion of bottom-lands E_{BOTTOM}, the average topographical slopes of the plot E_{SLOPE} and the standard deviation, i.e the heterogeneity, of the altitudinal distribution E_{HETE}.

Composition drivers The pre-disturbance forest composition was assessed in a functional trait space to avoid local taxonomic variations in tree assemblages that are of little importance for forest functioning. The four chosen orthogonal traits FT represent key dimensions of the tree functional strategy (Baraloto et al. 2010): wood density T_{WD}, seed mass T_{SEED}, specific leaf area T_{SLA} and maximum diameter T_{DBH95} estimated as the 95th percentile of the species DBH distribution in the Guyafor database. The community weighted means of these functional traits were calculated the year preceding the disturbance experiment.

Climate drivers We considered two main sources of climate stress: soil drought $C_{DROUGHT}$ and soil water saturation C_{WATER}. These variables were quantified using a water balance model, developed and calibrated in Paracou (Wagner et al. 2011), that was run using precipitation and evapotranspiration as inputs over the 1982-2016 time period. $C_{DROUGHT}$ was estimated as the number of days with REW, Relative Extractable Water, below 0.4 while the number of days with REW equal to 1, the soil is

Table 1 Disturbance treatments (T1, T2, T3) implemented on the Paracou plots in 1986-1987

	Timber logging	Fuelwood logging	Thinning	% ACS loss
T1	DBH $\geq$ 50 cm, mean of 10 trees·ha^{-1}	-	-	[12 – 33%]
T2	DBH $\geq$ 50 cm, mean of 10 trees·ha^{-1}	-	DBH $\geq$ 40cm, all non-valuable species, mean of 30 trees·ha^{-1}	[33 – 56%]
T3	DBH $\geq$ 50 cm, mean of 10 trees·ha^{-1}	40 cm $\leq$ DBH $\leq$ 50 cm, all non-valuable species, mean of 20 trees·ha^{-1}	DBH $\geq$ 40cm, all non-valuable species, mean of 15 trees·ha^{-1}	[35 – 66%]

The percentage of Aboveground Carbon Stock loss (% ACS loss) is defined as the difference between the pre-disturbance ACS and its minimum value reached during the 4 years after the disturbance treatments

full of water, defined C_{WATER}. These two covariates were computed between 2 consecutive censuses and then standardized at a yearly time-step.

Modeling strategy

We define two cohorts of trees. First, recruits are all the trees (> 10 cm DBH) that have been recruited since the perturbation. Trees that, for a given census, first went through the 10 cm DBH are called new recruits. Thereafter, they are called, for the following censuses, recruits and may grow or may eventually die between 2 censuses. Second, survivors are trees that were present in the forest before the disturbance and that survived the disturbance event.

For each subplot j and census k, with t_k the time since the beginning of the recovery period, we thus define 5 ACS changes : new recruits' ACS ($Rr_{j,k}$) is the ACS of all trees < 10 cm DBH at t_{k-1} and ≥ 10 cm DBH at t_k; recruits' ACS growth ($Rg_{j,k}$) is the ACS increment of living recruits between t_{k-1} and t_k ; recruits' ACS loss ($Rl_{j,k}$) is the *ACS* in recruits that die between t_{k-1} and t_k; survivors' ACS growth ($Sg_{j,k}$) is the ACS increment of living survivors between t_{k-1} and t_k; survivors' ACS loss ($Sl_{j,k}$) is the ACS of survivors that die between t_{k-1} and t_k. ACS changes are subject to large stochastic variation over time: because we are less interested in year-to-year variations than in long-term ACS trajectories, we modeled the cumulative ACS changes over time. Cumulative ACS changes (Mg C·ha^{-1}) were defined as follows:

$$cChange_{j,k} = \sum_{m=0}^{k} (Change_{j,m} \times (t_k - t_{k-1})) \quad (1)$$

where j is the subplot, k is the census number, t_k the time since t_0 (yr) and *Change* is the annual ACS change (Mg C·ha^{-1} · yr^{-1}), either recruits' ACS (*Rr*), recruits' ACS growth (*Rg*), recruits' ACS loss (*Rl*), survivors' ACS growth (*Sg*), or survivors' ACS loss (*Sl*).

Survivors Survivors' cumulative ACS changes are null at $t = 0$ and have a finite limit, attained once survivors have all died. We modeled survivors' cumulative ACS growth *cSg* as:

$$cSg_{j,p,k} \sim \mathcal{N}\left(\alpha_p^{Sg} \times \left(1 - exp\left(-\beta_{j,k}^{Sg} \times t_k\right)\right), \left(\sigma^{Sg}\right)^2\right) \quad (2)$$

where j is the subplot, p the plot it belongs to, t_k is the time since t_0. α_p^{Sg} is the finite limit of the cumulative ACS change, $\beta_{j,k}^{Sg}$ the rate at which the cumulative ACS change converges to this limit and $\left(\sigma^{Sg}\right)^2$ the variance of the model. By choosing an exponential kernel, we assume that survivors' ACS growth at t_k is proportional to survivors' ACS growth at t_{k-1}.

Because of our nested design with subplots j within plots p, we modeled the α_p^{Sg} values with a random plot effect of mean α_0^{Sg} and variance $\left(\sigma_\alpha^{Sg}\right)^2$:

$$\alpha_p^{Sg} \sim \mathcal{N}\left(\alpha_0^{Sg}, \left(\sigma_\alpha^{Sg}\right)^2\right) \quad (3)$$

Parameter $\beta_{j,k}^{Sg}$ is the rate at which survivors' ACS growth on plot j at time t_k converges to a finite limit after the disturbance: it reflects the response rapidity of survivors' ACS growth to disturbance. Because we are interested in predicting variations in $\beta_{j,k}^{Sg}$, we expressed the latter as a function of covariates:

$$\beta_{j,k}^{Sg} = \beta_0^{Sg} + \sum_{l=1}^{13} \left(\lambda_l^{Sg} \times V_{j,t_k,l}\right) \quad (4)$$

with β_0^{Sg} the model intercept, λ_l^{Sg} the vector of l parameters associated to the covariates $V_{j,k,l}$ for which we looked at their effects on the post-logging rate $\beta_{j,k}^{Sg}$ in subplot j at time t_k. The covariates are defined above and related to the disturbance intensity *DIST*, the structure of the forest before disturbance (S_N, S_{DG}, S_{BA}), the functional trait composition of the forest before disturbance (T_{SEED}, T_{SLA}, T_{WD}, T_{DBH95}), the local environment (E_{BOTTOM}, E_{SLOPE}, E_{HETE}) and the climate stress ($C_{DROUGHT}$, C_{WATER}). Note that values of the two later covariates changed with times. All covariates are centered and standardized before the inference. When all survivors in plot p are dead, all the C gained by their growth $\left(cSg_{j,p,\infty} = \alpha_p^{Sg}\right)$ plus their initial ACS ($acsmin_j$) will have been lost $\left(cSl_{j,\infty} = \alpha_j^{Sl}\right)$. We thus defined

$$\alpha_j^{Sl} = \alpha_p^{Sg} + acsmin_j \quad (5)$$

with $\alpha_p^{Sg}, \alpha_j^{Sl}$ the finite limits of survivors' cumulative ACS growth and ACS loss respectively, and $acsmin_j$ the ACS of the subplot j at $t_{min} = t_0$. Then the cumulative carbon loss is

$$cSl_{j,p,k} \sim \mathcal{N}\left(\alpha_j^{Sl} \times \left(1 - exp\left(-\beta_{j,t}^{Sl} \times t_k\right)\right), \left(\sigma^{Sl}\right)^2\right) \quad (6)$$

where j is the subplot, p the plot it belongs to, t_k is the time since t_0. α_j^{Sl} is the finite limit of the cumulative ACS change, $\beta_{j,k}^{Sl}$ the rate at which the cumulative ACS change converges to this limit and $\left(\sigma^{Sl}\right)^2$ the variance of the model. And with

$$\beta_{j,t}^{Sl} = \beta_0^{Sl} + \sum_{l=1}^{6} \left(\lambda_l^{Sl} \times V_{j,t,l}\right) \quad (7)$$

with β_0^{Sl} the model intercept, λ_l^{Sl} the vector of l parameters associated to the covariates $V_{j,k,l}$ for which we looked at their effects on the post-logging rate $\beta_{j,k}^{Sl}$ in subplot j at time t_k.

Recruits When survivors are all dead, newcomers or recruits will constitute the new forest. We made the assumption that the recruits' annual ACS changes will converge to constant values, with ACS gains compensating ACS losses. Because there are no recruits yet at t_0, recruits' annual ACS growth (*Rg*) and ACS loss (*Rl*) are zero, and progressively increase to reach their asymptotic values. Recruits' annual ACS growth and ACS loss can be modeled with the function:

$$f(t;\alpha,\beta) = \alpha \times (1 - exp(-\beta \times t)) \tag{8}$$

where t the time since the beginning of the recovery period. In the same logic as survivors' cumulative ACS changes, α is the asymptotic value of recruits' annual ACS change (Mg C·ha^{-1} · yr^{-1}), and β is the rate at which this asymptotic value is reached. Contrary to recruits' annual ACS growth and ACS loss, the ACS of new recruits (*Rr*, the ACS of tree reaching the 10 cm DBH threshold) is high at t_0 because of the competition drop induced by logging, but then progressively decreases to reach its asymptotic value. We modeled it with the following function:

$$f(t;\alpha,\beta) = \alpha \times (1 + exp(-\beta \times t)) \tag{9}$$

where t is the time since disturbance. As stated before, we chose to model cumulative ACS changes instead of annual ACS changes. The general model for recruits' cumulative ACS changes (ACS growth *Rg*, ACS loss *Rl* and ACS of new recruits *Rr*) is obtained by mathematical integrating from t_0 to t_k annual ACS changes:

$$cR_{j,p,k} \sim \mathcal{N}\left(\alpha_p^R \times \left(t_k + \eta \times \frac{1 - exp\left(-\beta_{j,k}^R \times t_k\right)}{\beta_{j,k}^R}\right), \left(\sigma^R\right)^2\right) \tag{10}$$

where j is the subplot, p the plot, t_k is the time since t_0, R is the annual ACS change, either *Rr*, *Rg* or *Rl* and $(\sigma^R)^2$ the variance of the model. When R is *Rg* or *Rl*, $\eta = -1$; when R is *Rr*, $\eta = 1$. Because of our nested design with subplots j within plots p, we modeled the α_p^R values with a random plot effect of mean α_0^R and variance $\left(\sigma_\alpha^R\right)^2$:

$$\alpha_p^R \sim \mathcal{N}\left(\alpha_0^R; \left(\sigma_\alpha^R\right)^2\right) \tag{11}$$

When the dynamic equilibrium is reached, annual ACS gain (growth and recruitment) compensates annual ACS loss (mortality). We thus added the following constraint for every plot p:

$$\alpha_p^{Rr} + \alpha_p^{Rg} + \alpha_p^{Rl} = 0 \tag{12}$$

Using the same logic as for survivors, we are interested in predicting variation in β^R as follows:

$$\beta_{j,k}^R \sim \mathcal{N}\left(\beta_0^R + \sum_{l=1}^{6}\left(\lambda_l^R \times V_{j,k,l}\right), \left(\sigma_\beta^R\right)^2\right) \tag{13}$$

with R being *Rg*, *Rl* or *Rr* depending on the process we were interested in, with β_0^R the model intercept, λ_l^R the vector of l parameters associated to the covariates $V_{j,k,l}$ for which we looked at their effects on the post-logging rate $\beta_{j,k}^R$ in subplot j at time t_k.

Model inference

Bayesian hierarchical models were inferred through MCMC methods using an adaptive form of the Hamiltonian Monte Carlo sampling (Carpenter et al. 2017). Codes were developed using the R language and the Rstan package (Carpenter et al. 2017). A detailed list of priors is provided in Table 2.

Identifying the key drivers of the post-disturbance system recovery

To assess the importance of the pre- (forest structure, environment and composition) and post- (climate stress) disturbance forest conditions, we simulated different scenarios modifying the covariate values but keeping an averaged (set to 0) disturbance intensity *DIST*. Note that all model covariates $V_{j,t,l}$ were standardized before modeling so that, for a given covariate, a -2, 0 or 2 value respectively refers to a very low, average or very high observed value.

Forest structure The effects of a regenerating (high stem density $S_N = 1$, low basal area $S_{BA} = -1$), intermediate (medium stem density $S_N = 0$, medium basal area $S_{BA} = 0$) and mature (low stem density $S_N = -1$, high basal area $S_{BA} = 1$) pre-disturbance forest structure on ecosystem recovery were compared.

Forest environment The effect of three contrasted forest environment were compared: predominance of bottom-lands (high proportion of bottom-lands $E_{BOTTOM} = 2$, medium slope values $E_{SLOPE} = 0$, medium altitudinal heterogeneity $E_{HETE} = 0$), predominance of slopes (medium proportion of bottom-lands $E_{BOTTOM} = 0$, high slope values $E_{SLOPE} = 2$, medium altitudinal heterogeneity $E_{HETE} = 0$) and hilly landscapes (medium proportion of bottom-lands $E_{BOTTOM} = 0$, medium slope values $E_{SLOPE} = 0$, high altitudinal heterogeneity $E_{HETE} = 2$).

Forest composition The effect of pre-logging forest community dominated by conservative tree species (high wood density $T_{WD} = 2$, high seed mass $T_{SEED} = 2$, low specific leaf area $T_{SLA} = -2$, high maximal stature

Table 2 List of priors used to infer ACS changes in a Bayesian framework

Model	Parameter	Prior	Justification
Sg	α_p^{Sg}	$\mathcal{U}(10, 200)$	Around 100 survivors/ha storing 0.1 to 2.0 MgC each
Sg	$\beta_{j,t}^{Sg}$	$\mathcal{U}(0, 0.25)$	$12 < t_{0.95}^{Sg\ *} < +\infty$
Sl	$\beta_{j,t}^{Sl}$	$\mathcal{U}(0, \beta_{j,t}^{Sg})$	$t_{0.95}^{Sg} < t_{0.95}^{Sl\ *} < +\infty$
Rr	α_p^{Rr}	$\mathcal{U}(0.1, 1)$	TmFO observed values (Piponiot et al. 2016b)
Rr	$\beta_{j,t}^{Rr}$	$\mathcal{U}(0, 0.75)$	$4 < t_{0.95}^{Rr\ *} < +\infty$
Rr	α_p^{Rg}	$\mathcal{U}(0.1, 3)$	Amazonian values (Johnson et al. 2016)
Rr	$\beta_{j,t}^{Rg}$	$\mathcal{U}(0, 0.5)$	$6 < t_{0.95}^{Rg\ *} < +\infty$
Rr	$\beta_{j,t}^{Rl}$	$\mathcal{U}(0, 0.5)$	$6 < t_{0.95}^{Rl\ *} < +\infty$
*All models M***	λ_l^M	$\mathcal{U}(-\beta_{j,t}^M, \beta_{j,t}^M)$	avoid multicollinearity problems

Models are : (*Sg*) survivors' ACS growth, (*Sl*) survivors' ACS loss, (*Rr*) new recruits' ACS, (*Rg*) recruits' ACS growth, (*Rl*) recruits' ACS loss
* $t_{0.95}$ is the time when the ACS change has reached 95% of its asymptotic value
** *M* is one of the five models, either *Sg*, *Sl*, *Rr*, *Rg* or *Rl*

$T_{DBH95} = 2$), by a disturbed community (low wood density $T_{WD} = -2$, low seed mass $T_{SEED} = -2$, high specific leaf area $T_{SLA} = 2$, low maximal stature $T_{DBH95} = -2$) and by a true pioneer community (very low wood density $T_{WD} = -4$, very low seed mass $T_{SEED} = -4$, very high specific leaf area $T_{SLA} = 4$, very low maximal stature $T_{DBH95} = -4$). The values of the last scenario may appear extreme but note that the model was calibrated with mature forest stands only so that covariate values have to be set out of the calibration range to get a true pioneer community.

Climate stress The effects of a wetter (nor or a few seasonal drought $C_{DROUGHT} = -2$, high soil water saturation during the wet season $C_{WET} = 2$), a drier (seasonal droughts $C_{DROUGHT} = 1$, medium soil water saturation during the wet season $C_{WET} = 0$) and a even drier (heavy seasonal droughts $C_{DROUGHT} = 2$, medium soil water saturation during the wet season $C_{WET} = 0$) climate on ecosystem recovery were compared.

Sensitivity analysis

To assess the sensitivity of the ecosystem recovery process to the pre- (forest structure, environment and composition) and post- (climate stress) disturbance forest conditions, we simulated the model for an average disturbance intensity $DIST = 0$ and, for each group of covariates $V_{j,t,l \neq DIST}$, varying the values within a group of covariate while setting the other covariates to 0. In a nutshell, for each group of covariates *Climate*, *Composition*, *Environment* and *Structure* (i) we independently sampled covariate values from $\mathcal{U}(-2; 2)$ while the covariates from the 3 other groups are set to 0, (ii) we ran the model using the sampled covariate values for a set of 100 parameter values drawn from the posterior chains, (iii) we estimated, after 30 years of simulation, the net carbon balance and (iv) we did the procedure 1000 times per group of covariates. Doing so, the variability of the net carbon balance after 30 years reflects the sensitivity of ecosystem recovery to the varying group of covariates.

Results

Given that all the covariates were standardized before modeling, the absolute values of their associated parameters give the weight of each variable in shaping the rates β at which the ACS changes reach their asymptotic state. Negative covariate values indicate slowing and positive values indicate accelerating rates. The values of the disturbance intensity *DIST* parameters always ranked among the highest absolute values, with negative values for *Survivors' ACS growth* and *Newrecruits' ACS* (Fig. 1a, c) and positive ones for the other three cumulative fluxes (Fig. 1b, d, e).

Pre-disturbance forest structure

The two variables chosen to describe the pre-disturbance forest structure, i.e. basal area S_{BA} and stem density S_N, have contrasted behaviors. Basically, associated parameters get their highest absolute values for the two growth models, both Survivors' and Recruits' (Fig. 1a and d), while being close to zero for the other three models (Fig. 1b, c, e). Contribution of Survivors' growth to ACS recovery is higher but declines quicker with high pre-disturbance S_{BA} values and low S_N values (Fig. 1a). Contribution of Recruits' growth to ACS recovery declines slowly with high S_N values (Fig. 1d). Mature forests (high S_{BA}, low S_N) thus recovers faster than regenerating ones (Fig. 2). The relative importance of the pre-disturbance forest structure on the variability of ACS recovery rates is low, with 30 to 50 MgC·ha^{-1} recovered after 30 years (Fig. 6).

Local environment

Three variables inform on the forest local environment, i.e. altitudinal heterogeneity E_{HETE}, proportion of

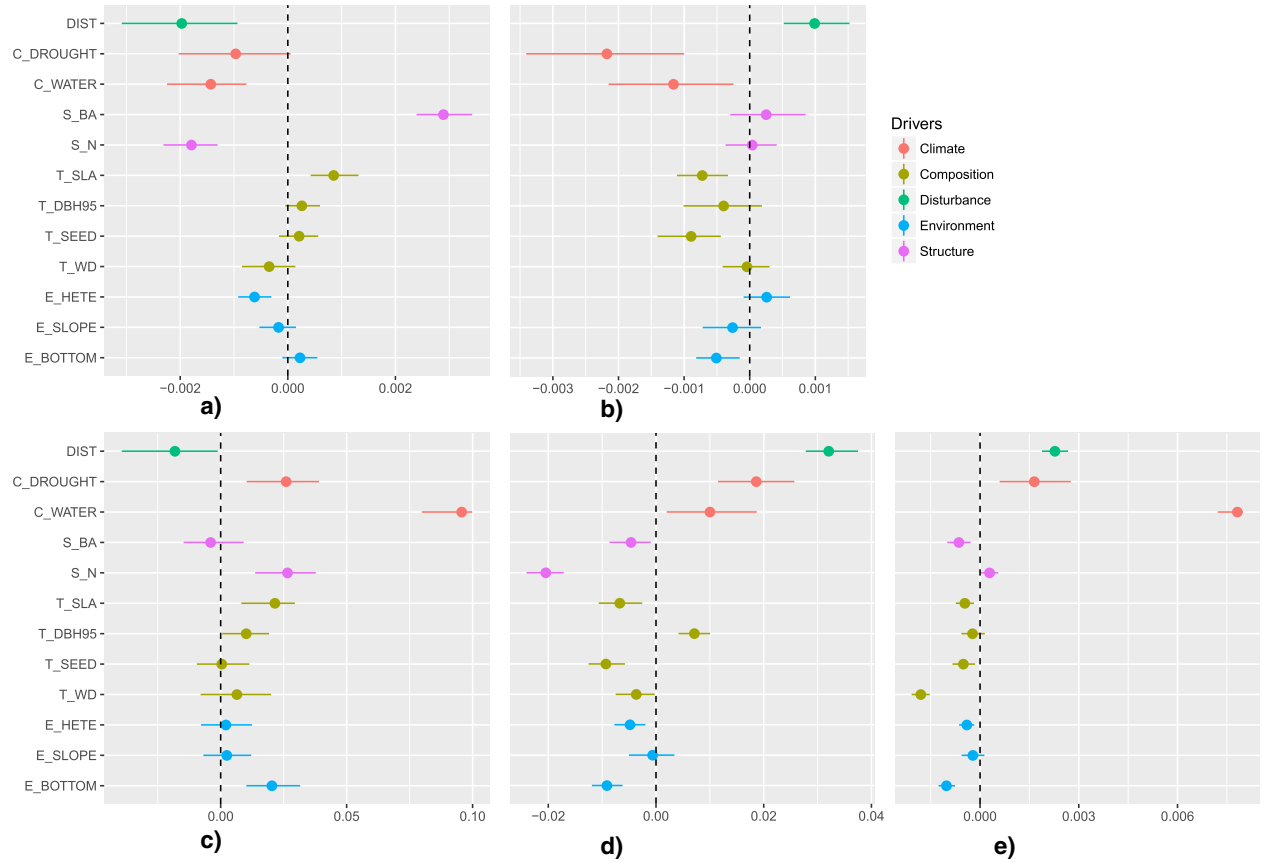

Fig. 1 Effect of covariates on the rate at which post-disturbance ACS changes converge to a theoretical steady state. Covariates are the disturbance intensity *DIST* (in green), the structure of the forest before disturbance (the number of individual trees S_N, the basal area S_{BA}, in pink), the functional trait composition of the forest before disturbance (seed mass T_{SEED}, specific leaf area T_{SLA}, wood density T_{WD}, maximum size T_{DBH95}, in maroon), the local environment (proportion of bottomlands E_{BOTTOM}, average slope E_{SLOPE}, altitudinal heterogeneity E_{HETE}, in blue) and the climate stress (drought intensity $C_{DROUGHT}$, days with water saturation C_{WATER}, in red). Covariates are centred and standardized. Posterior distribution (median and 0.95 credibility intervals) are reported. Negative covariate values indicate slowing and positive values indicate accelerating rates. **a** Survivors' ACS growth. **b** Survivors' ACS loss. **c** New recruits' ACS. **d** Recruits' ACS growth. **e** Recruits' ACS loss

bottomlands E_{BOTTOM} and the average slope E_{SLOPE}. The latter never significantly contributes to the β variability (Fig. 1). E_{BOTTOM} is important in defining recruits ACS fluxes, with positive parameter values for New recruits' ACS and negative ones for growth and loss (Fig. 1c, d, e). All fluxes together, recovery rates do not differ markedly with environmental conditions (Fig. 3) so that the importance of the local forest environment on the variability of ACS recovery rates is quite low, with 30 to 50 MgC·ha^{-1} recovered after 30 years (Fig. 6).

Pre-disturbance forest composition

Four orthogonal functional traits (i.e. specific leaf area T_{SLA}, maximum stature T_{DBH95}, seed mass T_{SLEED} and wood density T_{WD}) have been retained to summarize differences in pre-disturbance forest composition. All these traits have been found to influence post-disturbance ACS recovery rates (Fig. 1). For Survivors, the contribution of growth to ACS recovery is higher but declines quicker with high T_{SLA} and low T_{WD} (Fig. 1a) while losses declines slowly with high T_{SLA} and high T_{SEED} (Fig. 1b). For Recruits, the contribution of growth to ACS recovery is higher but declines quicker with high T_{DBH95} and low T_{SLA} and T_{SEED} (Fig. 1d) while losses declines slowly with low T_{WD} (Fig. 1e). Forests, for which the pre-disturbance composition is dominated by conservative ecological strategies (high wood density, seed mass, maximal stature and low specific leaf area) recovers faster than disturbed forests dominated pioneer species (very low wood density, very low seed mass, very high specific leaf area and very low maximal stature) (Fig. 4). The relative importance of the pre-disturbance forest composition on the variability of ACS recovery rates is high, with 0 to 100 MgC·ha^{-1} recovered after 30 years (Fig. 6).

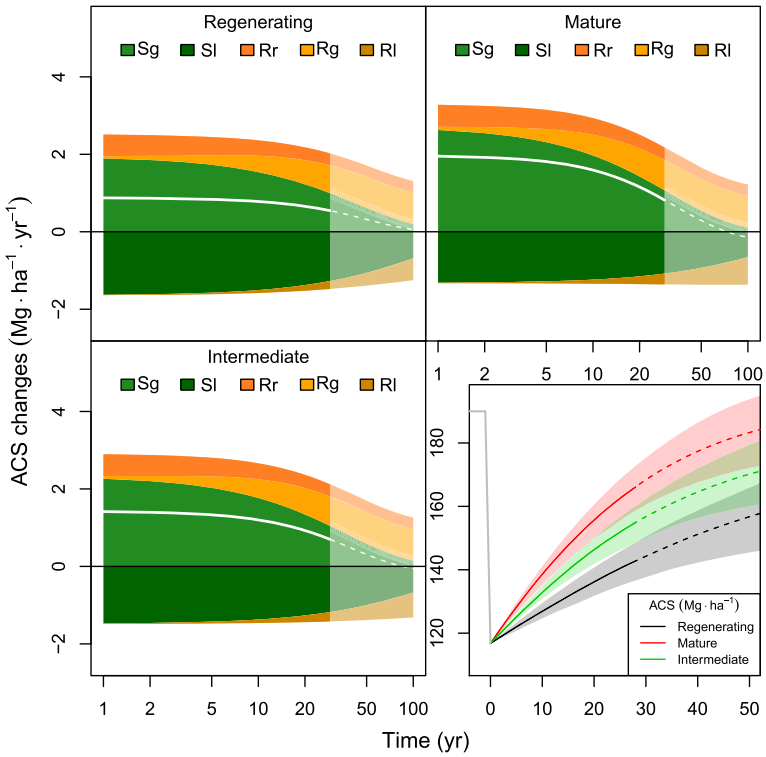

Fig. 2 Predicted contribution of annual ACS changes in three contrasted scenarios of pre-logging forest structure : Regenerating, Mature and Intermediate are defined with standardized covariates S_N and S_{BA} respectively set to $[1, -1, 0]$ and to $[-1, 1, 0]$. The white line is the net annual ACS recovery, i.e. the sum of all annual ACS changes: survivors' ACS growth *Sg* and loss *Sl*, new recruits' ACS *Rr* and recruits' ACS growth *Rg* and loss *Rl*. Dotted lines are out of the calibration period (0–30 year). Maximum-likelihood predictions for ACS stocks (bottom-right) are projected within their credibility intervals (areas with higher levels of transparency

Post-disturbance climate

Two variables related to climate stress occurring during the recovery process were tested. The intensity of the dry season $C_{DROUGHT}$ decelerates the decline of Survivors' ACS changes (Fig. 1a, b) while it accelerates the decline of all the recruits' ACS changes (Fig. 1c, d, e). High soil water saturation during the wet season has a similar effect but with very high β values for recruits' ACS loss (Fig. 1e). The forest recovers faster in the driest climate scenarios and this is mainly due to the important Survivors' ACS losses in the wettest scenarios (Fig. 5). The effect of climate stress on the variability of ACS recovery rates ranks 2nd among the 4 groups of covariates, with 10 to 80 MgC·ha^{-1}, depending on the post-disturbance climate conditions, recovered after 30 years (Fig. 6).

Discussion

In this study, we modeled the post-disturbance ACS fluxes in a neotropical forest and found that by testing a few variables that are related to the main endogenous (forest structure and composition) and exogeneous (local environment and climate stress) drivers of ecological community dynamics, we could successfully predict ecosystem trajectories in a wide range of pre- and post-disturbance conditions. Modeling separately the surviving and recruited cohorts was confirmed to be an important methodological choice (Piponiot et al. 2016b), given that the highlighted drivers did not overlap, whether for the growth (Fig. 1a and d) or the loss (Fig. 1b and e) processes. This suggests that our methodological approach, deciphering ecosystem fluxes by demographic processes, could be very useful to predict the long-term trajectories in highly diverse tropical forests for which precise demographic data may be lacking, but aggregative forest dynamic censuses are available from forest inventories. In this study, the disturbance intensity gradient was induced by combining logging to thinning operations (Table 1). Because of its economic value and implications for forest management, selective logging experiments were set up very early on, and the data gathered by these experiments are unique in terms of experiment duration and spatial extent. Despite the particular nature of logging operations (focus on large and commercially-valuable trees even though logging damage concerns all DBH classes), we believe that our study gives clues on the key drivers of ecosystem recovery after large ACS losses

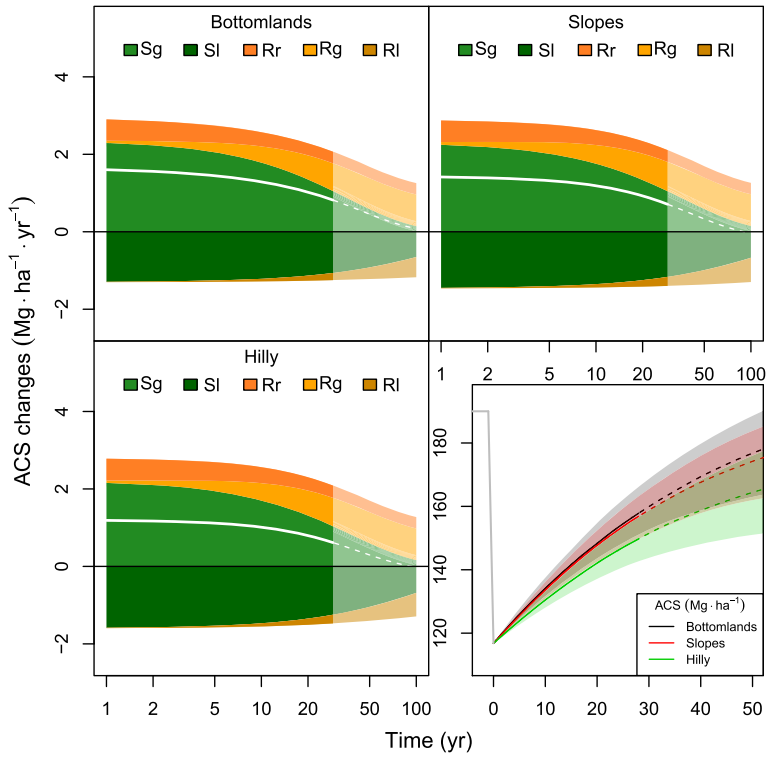

Fig. 3 Predicted contribution of annual ACS changes in three contrasted scenarios of forest environment : Bottomlands, Slopes and Hilly environment are defined with standardized covariates E_{BOTTOM}, E_{SLOPE} and E_{HETE} respectively set to [2, 0, 0], [0, 2, 0] and [0, 0, 2]. The white line is the net annual ACS recovery, i.e. the sum of all annual ACS changes: survivors' ACS growth *Sg* and loss *Sl*, new recruits' ACS *Rr* and recruits' ACS growth *Rg* and loss *Rl*. Dotted lines are out of the calibration period (0–30 year). Maximum-likelihood predictions for ACS stocks (bottom-right) are projected within their credibility intervals (areas with higher levels of transparency

induced by other disturbances (e.g. droughts, fire) that are expected to increase in intensity with ongoing global changes (Bonal et al. 2016).

On disturbance intensity

Disturbance intensity *DIST* remains, by far, the first predictor of the post-disturbance system trajectory (Fig. 1).

Survivors

High disturbance intensities obviously reduce the residual survivors' ACS so that ACS changes from survivors' growth is lower at the beginning but, because of the lower competition between survivors, they tend to live longer and reach the asymptotic state slowly (lower β, Fig. 1a). The positive β for Survivors' ACS loss, meaning that survivors tend to die faster after high levels of disturbance, may look surprising because this goes against the growth result. We believe that a high tree mortality, due to the low survival of damaged trees in highly disturbed systems, in the early post-disturbance years may have resulted in increased β values. However, those losses should rapidly decrease after a decade (Thorpe et al. 2008).

Recruits

High disturbance intensities alleviate competition, and this is probably why recruits' ACS growth is high just after disturbance in the enhanced growth conditions (Herault et al. 2010) and then quickly decrease (high βs, Fig. 1d and e). In these disturbed forests, intense self-thinning (Feldpausch et al. 2007) may explain the fast but limited-in-times ACS losses from survivors' mortality (Fig. 1e).

Endogeneous drivers

Pre-disturbance Forest structure All else being equal, mature forests (high S_{BA}, low S_N) recover faster than regenerating ones. And this is mainly due to the higher ACS incoming fluxes from Survivors' growth (Fig. 2). Regenerating forests are composed of short-living fast-growing small species. These species are poorly efficient at carbon accumulation because of their limited growth response to canopy openings and competition alleviation. Indeed, it has been shown in the Paracou forests that species with the highest inherent growth rate (in the absence of disturbance) have the lowest growth response when a disturbance occurs (Herault et al. 2010). On the contrary, large mature trees

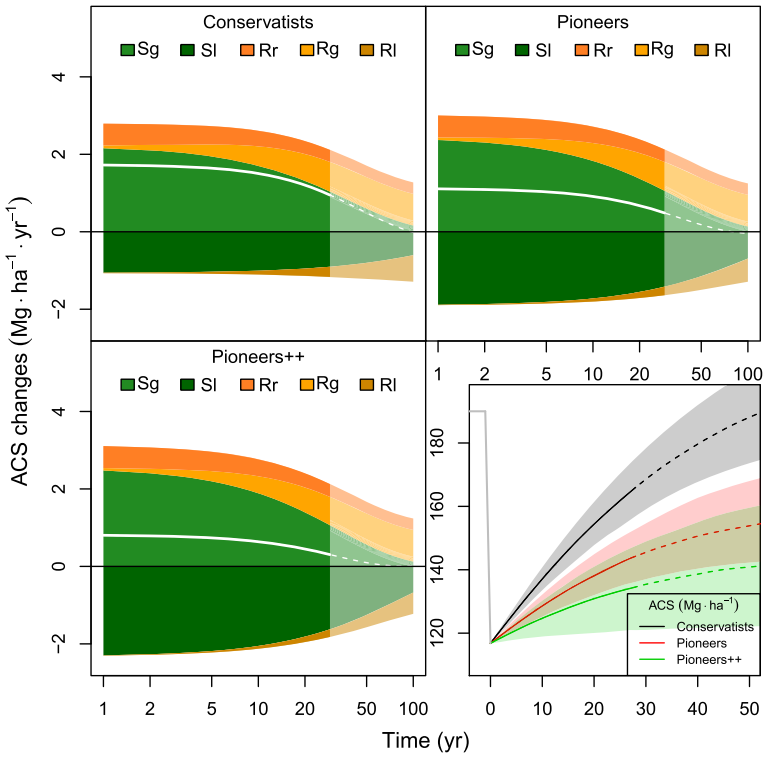

Fig. 4 Predicted contribution of annual ACS changes in three contrasted scenarios of pre-logging forest composition: Conservatists, Pioneers and Pioneers++ communities are defined with standardized covariates T_{WD}, T_{SEED}, T_{SLA} and T_{DBH95} respectively set to [2, −2, −4], [2, −2, −4], [−2, 2, 4] and [2, −2, −4]. Pioneers++ refer to a true pioneer community (very low wood density, very low seed mass, very high specific leaf area and very low maximal stature). The white line is the net annual ACS recovery, i.e. the sum of all annual ACS changes: survivors' ACS growth *Sg* and loss *Sl*, new recruits' ACS *Rr* and recruits' ACS growth *Rg* and loss *Rl*. Dotted lines are out of the calibration period (0–30 year). Maximum-likelihood predictions for ACS stocks (bottom-right) are projected within their credibility intervals (areas with higher levels of transparency

are, despite their low numbers in many forests, key elements of carbon storage (Lindenmayer et al. 2012) and dynamics (Sist et al. 2014). Previously disturbed, logged or secondary forests, for which forest structure is characterized by low S_{BA}, and high S_N, may thus be far less resilient to new disturbance than natural undisturbed forests. This also means that post-logging ACS recovery that is currently estimated from the first logging rotation (Rutishauser et al. 2015) may be overestimated for the following logging rotations (Rutishauser et al. 2016). Finally, despite these clear outcomes, the importance of the pre-disturbance forest structure on the variability of ACS recovery rates, as compared to the other covariates (forest composition, environment and climate), remains low (Fig. 6) in the sensitivity analysis. However, we should keep in mind that all the disturbed plots were established in a natural undisturbed forest area so that the model has been parameterized with low pre-disturbance forest structure variability. We thus suggest that, in landscapes with contrasted and tumultuous history, the role of the forest structure in shaping the post-disturbance system trajectory would be much higher.

Pre-disturbance Forest composition The importance of the pre-disturbance forest composition on the variability of the post-disturbance ACS recovery rates is unexpected, with 0 to 100 MgC·ha^{-1}, depending on the initial species assemblage, recovered after 30 years (Fig. 6). All the studied functional traits are implied in shaping one or more of the investigated ACS changes. When comparing two typical forest composition, i.e. an assemblage of conservative trees (high wood density, seed mass, maximal stature and low specific leaf area) and an assemblage of pioneer trees (exact opposite trait composition), the pioneer assemblage recovers much slower. This difference is mainly due to highly contrasted survivors' ACS changes. Both ACS growth and loss increase rapidly in surviving pioneers. This result is consistent with the acquisitive strategy of species with a high carbon budget (Sterck et al. 2011), that are well-known to have very fast turn-over rates (Aubry-Kientz et al. 2013; Hérault et al. 2011; Flores et al. 2014). Even if both survivors ACS growth and loss are boosted in pioneer assemblages, it is quite remarkable that the ACS balance in time is mainly under the control of survivors'

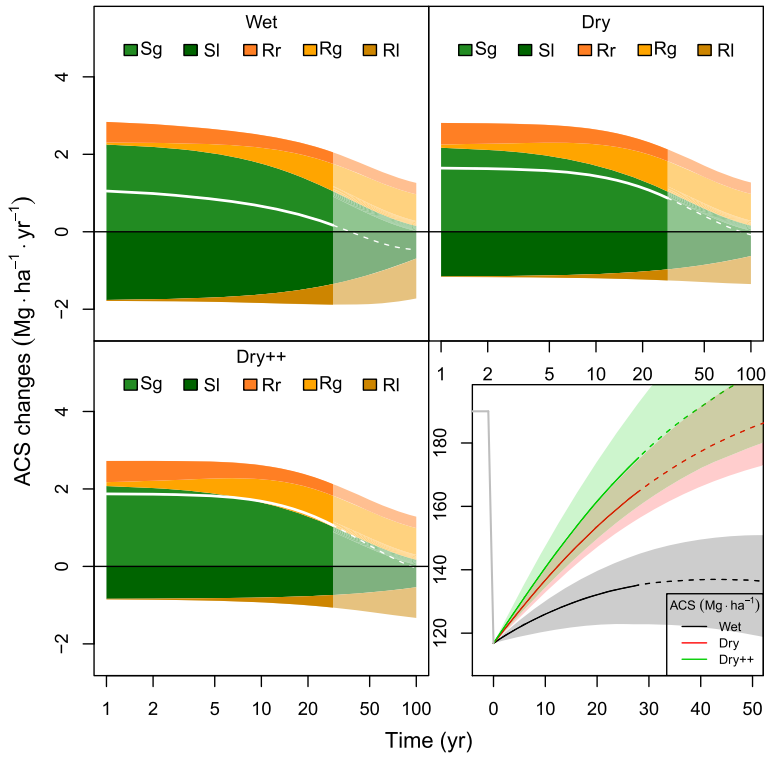

Fig. 5 Predicted contribution of annual ACS changes in three contrasted climate scenarios: Wet, Dry and Dry++ climates are defined with standardized covariates $C_{DROUGHT}$ and C_{WATER} respectively set to [-2,1,2] and [2,0,0]. Dry++ refer to an extremely-dry climate (very high seasonal drought in the dry season, medium soil water saturation in the rain season). The white line is the net annual ACS recovery, i.e. the sum of all annual ACS changes: survivors' ACS growth *Sg* and loss *Sl*, new recruits' ACS *Rr* and recruits' ACS growth *Rg* and loss *Rl*. Dotted lines are out of the calibration period (0–30 year). Maximum-likelihood predictions for ACS stocks (bottom-right) are projected within their credibility intervals (areas with higher levels of transparency

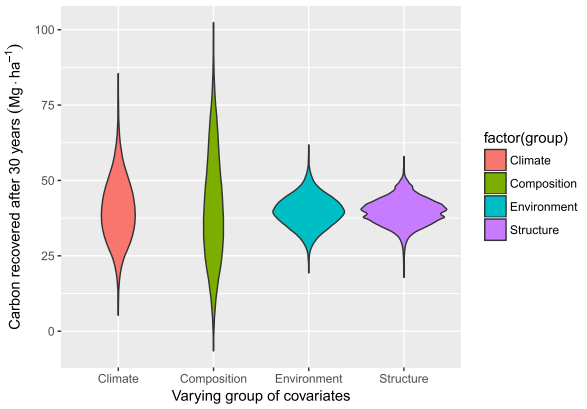

Fig. 6 Estimating the relative importance of the *Climate* stress, the pre-disturbance forest *Composition*, *Environment* and *Structure* in driving ecosystem recovery 30 years after disturbance. The violin plots represent the variability of the distribution of the net carbon balance when covariates within a given group are independently and randomly drawn from $\mathcal{U}(-2;2)$ while the covariates from other groups are set to 0 (the longest the boxplot the highest the sensitivity of ecosystem recovery to this given group of covariates)

ACS loss *Sl*. Survivors' ACS loss can cancel survivors' ACS growth in pioneer-dominated communities, resulting in a null ACS balance (zero is included in the simulations results, see Fig. 6). Why do those pre-disturbance pioneer communities have such high ACS losses in the post-disturbance times? Fast-growing pioneers are generally both poor competitors and poor stress-tolerant trees (He et al. 2013). A first possible explanation is thus that the stress induced by disturbance may be too high for these species that undergo, after disturbance, heavy losses. An alternative explanation is that the higher ACS growth mechanically induces, after a while, higher ACS losses. If pioneers grow faster as a result of growth-stimulating disturbance, they will pass through their natural life span faster, resulting in a transitory gain in carbon storage followed by a massive carbon release when these pioneers get older (Körner 2017). Introducing a time lag for the ACS loss models would be the only way to test the last hypothesis.

Exogeneous drivers

Local environment The forest local environment defined by the altitudinal heterogeneity, the proportion of

bottomlands and the average slope, have been found to be of low importance in shaping variability of ACS recovery rates (Fig. 3). This result is quite surprising, given that the local environment is very often referred to as a driver of ecological processes in tropical forests (Grau et al. 2017), from fine pairwise interactions between individual trees (Kraft et al. 2008) to regional variation in community assemblages (Fayad et al. 2016). For instance, in the Paracou forest, the proportion of bottomlands have been found to be of primary importance for forest dynamics: treefall rates are twice as high as on hilltops and tree recruitment and growth rates are higher, leading to a lower basal area and ACS (Ferry et al. 2010). Nearly three fourths of the Paracou taxa are locally distributed as a function of relative elevation, with seasonally inundated bottomlands and well-drained plateaus revealing contrasted species associations (Allié et al. 2015). Despite the relative importance of E_{BOTTOM} in defining recruits' ACS changes, with positive β parameter values for new recruits' ACS and negative ones for recruits' ACS growth and loss (Fig. 1), all in all ACS recovery rates differ very little from hilly or sloppy plots (Fig. 3). On the one hand, the low-stress conditions of bottomlands (no seasonal drought, less wind) should induce a faster ecosystem recovery. On the other hand, the lower final ACS (Ferry et al. 2010) may mechanically lead to lower absolute carbon storage during recovery. All together, the two processes could be canceling each other, explaining why absolute carbon recovery is similar between bottomlands and hilltops. We also should keep in mind that the disturbance experiment was made by logging. During logging operations, bottomlands are avoided and logging is preferentially conducted in easier-to-access hilltop areas, whatever their proportion in the plot. This may have artificially reduced the environmental difference between logged plots and, in turn, the ACS recovery trajectories.

Post-disturbance climate stress Two seasonal climate stresses were studied: soil water saturation in the wet season and drought intensity in the dry season. The importance of the post-disturbance climate stress on the variability of ACS recovery rates was very high with, depending on the climate scenarios, 10 to 80 $MgC{\cdot}ha^{-1}$ recovered after 30 years (Fig. 6). The 2 driest scenarios recover initial ACS very quickly, i.e. in less than 60 years while the wettest one would reach a new asymptotic values, far below the initial system ACS (Fig. 6). The main difference between the 3 scenarios lies in the absolute values of the Survivors' ACS loss, with very high values for the wet scenario. This result may look strange given that drought has often been identified as one of the main climate drivers of tropical forest dynamics (Bonal et al. 2016; Wagner et al. 2012, 2013, 2014, 2016), with large mortality events among tropical trees during El Nino years for instance (Phillips et al. 2009) that have not only immediate but also long-term and cumulative impacts on the carbon cycle (Doughty et al. 2015). Those large mortality events are associated with tree hydraulic traits, the most susceptible species being those having a low hydraulic safety margin (Anderegg et al. 2016). In this context, why do the most intense dry season generate the lowest carbon losses? In our training dataset, the natural variability of the total rainfall from 2700 to 3100 $mm{\cdot}yr^{-1}$ is quite low and, moreover, is far above the 1500 $mm{\cdot}yr^{-1}$, the evapotranspiration threshold. This means that our experimental forest, located in the Guiana Shield, is not water-limited at all (Stahl et al. 2013), just like the Northern part of the Amazonian basin (Wagner et al. 2017). One may also expect that, because of hydraulic failure, standing death is more frequent during the driest years but, when plotting the tree mode of death registered at Paracou for each dead tree against the drought estimator, no evidence was observed for a potential trend (Aubry-Kientz et al. 2015). Our results thus reinforce the idea that the dominant seasonal climate stress in the Paracou forest is not drought during dry season but water saturation during wet season. This confirms the hypothesis that waterlogged soils in space or in time are risky for trees (Ferry et al. 2010). Moreover, during the rainy season, strong rainfall events often come with strong winds that may reinforce ACS losses (Toledo et al. 2011) and we know, from the Paracou dataset, that the highest total precipitation leads to the highest proportion of tree-fall deaths (Aubry-Kientz et al. 2015). Global climate models converge to simulate, at least for the Amazonian region, a change in precipitation regime over the coming decades (Malhi et al. 2009). Seasonal droughts are expected to become longer and stronger in the future (Joetzjer et al. 2013). Our simulations would suggest that post-disturbance forest recovery would be faster with these new climate conditions. However, we should keep in mind that our simulations were based on a model calibrated with data from a natural, undisturbed forest (Fargeon et al. 2016). With increasing mortality rates due to increasing drought occurrence and severity, the new tree community may be richer in post-disturbance pioneer species. And we have already seen that these new assemblages will slowly recover (Fig. 4) so that recurrent climate-stress in time would not lead to faster recovery rates, but rather to pioneer-rich forest communities with slow recovery rates.

Conclusion

More than half of the tropical forest area are currently designated by National Forests Services as production forests (Blaser et al. 2011) and they consequently play a key role in the tropical forest carbon balance

(Piponiot et al. 2016a; Sist et al. 2015). In the Amazon, forest logging and degradation combined to climate change would render up to 80% of the forest area susceptible to major disturbance events in the coming decades (Asner et al. 2010). We have shown that the pre-disturbance forest composition and the post-disturbance climate conditions are of primary importance to predict the recovery potential of tropical forest ecosystems. From the Paracou long-term experiment, it becomes increasingly clear that highly-disturbed forests, because they contain a lot of pioneer species (Baraloto et al. 2012), will be less able to cope with (i) new disturbance such as logging and (ii) the drier conditions induced by climate change. In other words, already-disturbed forests are likely to be the most vulnerable systems in the current global change context. Forest managers should thus (i) encourage the development of Reduced-Impact Logging techniques in order to minimize disturbance intensity and (ii) pay a deep attention when drawing management plans to avoid logging pioneer-rich forest units. In the context of increasing disturbances on tropical forests, the lower capacity of disturbed forests to recover is not good news in our fight against climate change.

Acknowledgements
We are in debt with all technicians and colleagues who helped setting up the plots and collecting data over years. Without their precious work, this study would have not been possible and they may be warmly thanked here.

Funding
This study was funded by (i) the GFclim project (FEDER 2014–2020, Project GY0006894) and (ii) an Investissement d'avenir grant of the ANR (CEBA: ANR-10-LABEX-0025).

Availability of data and materials
Datasets supporting the conclusions of this article are available upon request to the scientific director of the Paracou Station (https://paracou.cirad.fr).

Authors' contributions
BH and CP drew the concept of the paper, developed the modeling mathematical framework and worked on the parametrization of the model. BH worked on the first draft and both authors improved and approved the final manuscript.

Authors' information
BH is an ecological modeler at Cirad (French research institute specialized in development-oriented research for the tropics). He was the scientific coordinator of the Paracou Research Station from 2012 to 2017. He is currently welcomed by Institut National Polytechnique Félix Houphouët-Boigny, Ivory Coast, to develop researches on forest restoration in West Africa. CP is a recent forest engineer from France. She is a PhD candidate at the Joint Research Unit 'Ecology of French Guianan Forests' - Université de Guyane. She is currently working on modeling the recovery of ecosystem services in disturbed amazonian forests under the Tropical Managed Forest Observatory (http://www.tmfo.org) framework.

Ethics approval and consent to participate
Not applicable.

Consent for publication
Not applicable.

Competing interests
The authors declare that they have no competing interests.

Author details
[1]Cirad, UMR EcoFoG (AgroParistech, CNRS, Inra, Université des Antilles, Université de la Guyane), Campus Agronomique, 97310 Kourou, French Guiana, France. [2]INPHB (Institut National Polytechnique Félix Houphouët Boigny), Yamoussoukro, Ivory Coast. [3]Université de la Guyane, UMR EcoFoG (AgroParistech, Cirad, CNRS, Inra, Université des Antilles), Campus Agronomique, 97310 Kourou, French Guiana, France.

Received: 9 July 2017 Accepted: 20 December 2017

References

Allié E, Pélissier R, Engel J, Petronelli P, Freycon V, Deblauwe V, Soucémarianadin L, Weigel J, Baraloto C (2015) Pervasive Local-Scale Tree-Soil Habitat Association in a Tropical Forest Community. Plos ONE 10(11):e0141488
Anderegg WRL, Klein T, Bartlett M, Sack L, Pellegrini AFA, Choat B, Jansen S (2016) Meta-analysis reveals that hydraulic traits explain cross-species patterns of drought-induced tree mortality across the globe. Proc Natl Acad Sci 113(18):201525678
Asner GP, Loarie SR, Heyder U (2010) Combined effects of climate and land-use change on the future of humid tropical forests. Conserv Lett 3(6):395–403
Aubry-Kientz M, Hérault B, Ayotte-Trépanier C, Baraloto C, Rossi V (2013) Toward trait-based mortality models for tropical forests. PloS one 8(5):e63678
Aubry-Kientz M, Rossi V, Wagner F, Hérault B (2015) Identifying climatic drivers of tropical forest dynamics. Biogeosciences 12(19):5583–5596
Baraloto C, Hérault B, Paine CET, Massot H, Blanc L, Bonal D, Molino J-F, Nicolini Ea, Sabatier D (2012) Contrasting taxonomic and functional responses of a tropical tree community to selective logging. J Appl Ecol 49(4):861–870
Baraloto C, Timothy Paine CE, Poorter L, Beauchene J, Bonal D, Domenach A-M, Hérault B, Patiño S, Roggy J-C, Chave J (2010) Decoupled leaf and stem economics in rain forest trees. Ecol Lett 13(11):1338–47
Blanc L, Echard M, Herault B, Bonal D, Marcon E, Chave J, Baraloto C (2009) Dynamics of aboveground carbon stocks in a selectively logged tropical forest. Ecol Appl 19(6):1397–1404
Blaser J, Sarre A, Poore D, Johnson S (2011) Status of Tropical Forest Management 2011. ITTO Technical Series No 38. International Tropical Timber Organization. Yokohama, Japan
Bonal D, Burban B, Stahl C, Wagner F, Hérault B (2016) The response of tropical rainforests to drought—lessons from recent research and future prospects. Ann For Sci 73(1):27–44
Brienen RJW, Phillips OL, Feldpausch TR, et al. (2015) Long-term decline of the Amazon carbon sink. Nature 519(7543):344–348
Brokaw N, Busing R (2000) Niche versus chance and tree diversity in forest gaps. Trends Ecol Evol 15(5):183–188
Carpenter B, Gelman A, Hoffman MD, Lee D, Goodrich B, Betancourt M, Brubaker M, Guo J, Li P, Riddell A (2017) Stan : A Probabilistic Programming Language. J Stat Softw 76(1). doi:10.18637/jss.v076.i01
Chave J, Coomes D, Jansen S, Lewis SL, Swenson NG, Zanne AE (2009) Towards a worldwide wood economics spectrum. Ecol Lett 12(4):351–366
Condit R (1995) Research in large, long-term tropical forest plots. Trends Ecol Evol 10(1):18–22
Davidson Ea, de Araújo AC, Artaxo P, Balch JK, Brown IF, C Bustamante MM, Coe MT, DeFries RS, Keller M, Longo M, Munger JW, Schroeder W, Soares-Filho BS, Souza CM, Wofsy SC (2012) The Amazon basin in transition. Nature 481(7381):321–8
Denslow JS, Ellison AM, Sanford RE (1998) Treefall gap size effects on above- and below-ground processes in a tropical wet forest. J Ecol 86(4):597–609
Dezécache C, Faure E, Gond V, Salles J-M, Vieilledent G, Hérault B (2017a) Gold-Rush in a forested El Dorado: Deforestation leakages and the need for regional cooperation. Environ Res Lett 034013:19
Dezécache C, Salles JM, Vieilledent G, Hérault B (2017b) Moving forward socio-economically focused models of deforestation. Glob Chang Biol 23(9):3484–3500
Doughty CE, Metcalfe DB, Girardin CAJ, Amézquita FF, Cabrera DG, Huasco WH, Silva-Espejo JE, Araujo-Murakami A, da Costa MC, Rocha W, Feldpausch TR, Mendoza ALM, da Costa ACL, Meir P, Phillips OL, Malhi Y (2015) Drought

impact on forest carbon dynamics and fluxes in Amazonia. Nature 519(7541):78–82
Fargeon H, Aubry-kientz M, Brunaux O, Descroix L, Guitet S, Rossi V, Hérault B (2016) Vulnerability of commercial tree species to water stress in logged forests of the Guiana shield. Forests 7(105):1–21
Fayad I, Baghdadi N, Guitet S, Bailly J-S, Hérault B, Gond V, El Hajj M, Tong Minh DH (2016) Aboveground biomass mapping in French Guiana by combining remote sensing, forest inventories and environmental data. Int J Appl Earth Obs Geoinformation 52(August):502–514
Feeley KJ, Joseph Wright S, Nur Supardi MN, Kassim AR, Davies SJ (2007) Decelerating growth in tropical forest trees. Ecol Lett 10(6):461–9
Feldpausch TR, Prates-Clark CdC, Fernandes EC, Riha SJ (2007) Secondary forest growth deviation from chronosequence predictions in central Amazonia. Glob Chang Biol 13(5):967–979
Ferry B, Bontemps J-d, Blanc L, Freycon V, Nancy E, Nancy F (2010) Higher treefall rates on slopes and waterlogged soils result in lower stand biomass and productivity in a tropical rain forest. J Ecol 98:106–116
Flores O, Hérault B, Delcamp M, Garnier E, Gourlet-Fleury S (2014) Functional traits help predict post-disturbance demography of tropical trees. PloS one 9(9):e105022
Goulamoussène Y, Bedeau C, Descroix L, Deblauwe V, Linguet L, Hérault B (2016) Weak Environmental Controls of Tropical Forest Canopy Height in the Guiana Shield. Remote Sens 8:747
Goulamoussène Y, Bedeau C, Descroix L, Linguet L, Hérault B (2017) Environmental control of natural gap size distribution in tropical forests. Biogeosciences 14(2):353–364
Grau O, Peñuelas J, Ferry B, Freycon V, Blanc L, Desprez M, Baraloto C, Chave J, Descroix L, Dourdain A, Guitet S, Janssens IA, Sardans J, Hérault B (2017) Nutrient-cycling mechanisms other than the direct absorption from soil may control forest structure and dynamics in poor Amazonian soils. Sci Rep 7(February):45017
Guitet S, Hérault B, Molto Q, Brunaux O, Couteron P (2015) Spatial Structure of Above-Ground Biomass Limits Accuracy of Carbon Mapping in Rainforest but Large Scale Forest Inventories Can Help to Overcome. PLoS ONE 10(9):e0138456
Guitet S, Sabatier D, Brunaux O, Hérault B, Aubry-Kientz M, Molino J-F, Baraloto C (2014) Estimating tropical tree diversity indices from forestry surveys: A method to integrate taxonomic uncertainty. For Ecol Manag 328:270–281
He Q, Bertness MD, Altieri AH (2013) Global shifts towards positive species interactions with increasing environmental stress. Ecol Lett 16(5):695–706
Hérault B, Bachelot B, Poorter L, Rossi V, Bongers F, Chave J, Paine CET, Wagner F, Baraloto C (2011) Functional traits shape ontogenetic growth trajectories of rain forest tree species. J Ecol 99(6):1431–1440
Hérault B, Gourlet-Fleury S (2016) Will Tropical Rainforests Survive Climate Change? In: Torquebiau E (ed). Climate Change and Agriculture Worldwide. Editions Q. Versailles. Springer, France. pp 183–196. doi:10.1007/978-94-017-7462-8_14
Herault B, Ouallet J, Blanc L, Wagner F, Baraloto C (2010) Growth responses of neotropical trees to logging gaps. J Appl Ecol 47(4):821–831
Joetzjer E, Douville H, Delire C, Ciais P (2013) Present-day and future Amazonian precipitation in global climate models: CMIP5 versus CMIP3. Clim Dyn 41(11-12):2921–2936
Johnson MO, Galbraith D, Gloor M, De Deurwaerder H, Guimberteau M, Rammig A, Thonicke K, Verbeeck H, von Randow C, Monteagudo A, Phillips OL, Brienen RJ, Feldpausch TR, Lopez Gonzalez G, Fauset S, Quesada CA, Christoffersen B, Ciais P, Sampaio G, Kruijt B, Meir P, Moorcroft P, Zhang K, Alvarez-Davila E, Alves de Oliveira A, Amaral I, Andrade A, Aragao LE, Araujo-Murakami A, Arets EJ, Arroyo L, Aymard GA, Baraloto C, Barroso J, Bonal D, Boot R, Camargo J, Chave J, Cogollo A, Cornejo Valverde F, Lola da Costa AC, Di Fiore A, Ferreira L, Higuchi N, Honorio EN, Killeen TJ, Laurance SG, Laurance WF, Licona J, Lovejoy T, Malhi Y, Marimon B, Marimon BH, Matos DC, Mendoza C, Neill DA, Pardo G, Peña-Claros M, Pitman NC, Poorter L, Prieto A, Ramirez-Angulo H, Roopsind A, Rudas A, Salomao RP, Silveira M, Stropp J, ter Steege H, Terborgh J, Thomas R, Toledo M, Torres-Lezama A, van der Heijden GM, Vasquez R, Guimã IC, Vilanova E, Vos VA, Baker TR (2016). Variation in stem mortality rates determines patterns of above-ground biomass in Amazonian forests: implications for dynamic global vegetation models. Glob Chang Biol 22(12):3996–4013
Körner C (2017) A matter of tree longevity. Science 355(6321):130–131
Kraft NJB, Valencia R, Ackerly DD (2008) Functional traits and niche-based tree community assembly in an Amazonian forest. Science 322(5901):580–2
Kunstler G, Falster D, Coomes DA, Hui F, Kooyman RM, Laughlin DC, Poorter L, Vanderwel M, Vieilledent G, Wright SJ, Aiba M, Baraloto C, Caspersen J, Cornelissen JHC, Gourlet-Fleury S, Hanewinkel M, Herault B, Kattge J, Kurokawa H, Onoda Y, Peñuelas J, Poorter H, Uriarte M, Richardson S, Ruiz-Benito P, Sun I-F, Ståhl G, Swenson NG, Thompson J, Westerlund B, Wirth C, Zavala MA, Zeng H, Zimmerman JK, Zimmermann NE, Westoby M (2016) Plant functional traits have globally consistent effects on competition. Nature 529(7585):204–207
Liang J, Crowther TW, Picard N, Wiser S, Zhou M, Alberti G, Schulze E-D, McGuire AD, Bozzato F, Pretzsch H, De-Miguel S, Paquette A, Herault B, Scherer-Lorenzen M, Barrett CB, Glick HB, Hengeveld GM, Nabuurs G-J, Pfautsch S, Viana H, Vibrans AC, Ammer C, Schall P, Verbyla D, Tchebakova N, Fischer M, Watson JV, Chen HYH, Lei X, Schelhaas M-J, Lu H, Gianelle D, Parfenova EI, Salas C, Lee E, Lee B, Kim HS, Bruelheide H, Coomes DA, Piotto D, Sunderland T, Schmid B, Gourlet-Fleury S, Sonke B, Tavani R, Zhu J, Brandl S, Vayreda J, Kitahara F, Searle EB, Neldner VJ, Ngugi MR, Baraloto C, Frizzera L, Ba azy R, Oleksyn J, Zawi a Niedwiecki T, Bouriaud O, Bussotti F, Finer L, Jaroszewicz B, Jucker T, Valladares F, Jagodzinski AM, Peri PL, Gonmadje C, Marthy W, OBrien T, Martin EH, Marshall AR, Rovero F, Bitariho R, Niklaus PA, Alvarez-Loayza P, Chamuya N, Valencia R, Mortier F, Wortel V, Engone-Obiang NL, Ferreira LV, Odeke DE, Vasquez RM, Lewis SL, Reich PB (2016) Positive biodiversity-productivity relationship predominant in global forests. Science 354(6309):aaf8957–aaf8957
Lindenmayer DB, Laurance WF, Franklin JF (2012) Ecology. Global decline in large old trees. Science 338(6112):1305–6
Malhi Y, Aragao LEOC, Galbraith D, Huntingford C, Fisher R, Zelazowski P, Sitch S, McSweeney C, Meir P (2009) Exploring the likelihood and mechanism of a climate-change-induced dieback of the Amazon rainforest. Proc Natl Acad Sci 106(49):20610–20615
Phillips OL, Aragão LEOC, Lewis SL, Fisher JB, Lloyd J, López-Gonzàlez G, Malhi Y, Monteagudo A, Peacock J, Quesada CA, van der Heijden G, Almeida S, Amaral I, Arroyo L, Aymard G, Baker TR, Bánki O, Blanc L, Bonal D, Brando P, Chave J, de Oliveira ACA, Cardozo ND, Czimczik CI, Feldpausch TR, Freitas MA, Gloor E, Higuchi N, Jiménez E, Lloyd G, Meir P, Mendoza C, Morel A, Neill DA, Nepstad D, Patiño S, Peñuela MC, Prieto A, Ramirez F, Schwarz M, Silva J, Silveira M, Thomas AS, Steege HT, Stropp J, Vàsquez R, Zelazowski P, Alvarez Dávila E, Andelman S, Andrade A, Chao K-j, Erwin T, Di Fiore A, Honorio CE, Keeling H, Killeen TJ, Laurance WF, Peña Cruz A, Pitman NCA, Núñez Vargas P, Ramirez-Angulo H, Rudas A, Salamào R, Silva N, Terborgh J, Torres-Lezama A (2009) Drought sensitivity of the Amazon rainforest. Sci (New York, NY) 323(5919):1344–1347
Pillet M, Joetzjer E, Belmin C, Chave J, Ciais P, Dourdain A, Evans M, Hérault B, Luyssaert S, Poulter B (2017) Disentangling competitive vs. climatic drivers of tropical forest mortality. J Ecol 38(1):42–49
Piponiot C, Cabon A, Descroix L, Dourdain A, Mazzei L, Ouliac B, Rutishauser E, Sist P, Hérault B (2016a) A methodological framework to assess the carbon balance of tropical managed forests. Carbon Balance Manag 11(1):15
Piponiot C, Sist P, Mazzei L, Peña-Claros M, Putz FE, Rutishauser E, Shenkin A, Ascarrunz N, de Azevedo CP, Baraloto C, França M, Guedes M, Honorio Coronado EN, D'Oliveira MV, Ruschel AR, da Silva KE, Doff Sotta E, de Souza CR, Vidal E, West TA, Hérault B (2016b) Carbon recovery dynamics following disturbance by selective logging in Amazonian forests. eLife 5:e21394
Réjou-Méchain M, Tanguy A, Piponiot C, Chave J, Hérault B (2017) biomass?: an r package for estimating above-ground biomass and its uncertainty in tropical forests. Methods Ecol Evol 8(9):1163–67. doi:10.1111/2041-210X.12753
Rutishauser E, Hérault B, Baraloto C, Blanc L, Descroix L, Sotta ED, Ferreira J, Kanashiro M, Mazzei L, D'Oliveira MV, de Oliveira LC, Peña-Claros M, Putz FE, Ruschel AR, Rodney K, Roopsind A, Shenkin A, da Silva KE, de Souza CR, Toledo M, Vidal E, West TA, Wortel V, Sist P (2015) Rapid tree carbon stock recovery in managed Amazonian forests. Curr Biol 25(18):R787—R788
Rutishauser E, Hérault B, Petronelli P, Sist P (2016) Tree Height Reduction After Selective Logging in a Tropical Forest. Biotropica 48(3):285–289
Rutishauser E, Wagner F, Herault B, Nicolini E-A, Blanc L (2010) Contrasting above-ground biomass balance in a Neotropical rain forest. J Veg Sci 21(4):672–82. doi:10.1111/j.1654-1103.2010.01175.x
Sheil D, Burslem D (2003) Disturbing hypotheses in tropical forests. Trends Ecol Evol 18(1):5–8
Sist P, Mazzei L, Blanc L, Rutishauser E (2014) Large trees as key elements of carbon storage and dynamics after selective logging in the Eastern Amazon. For Ecol Manag 318:103–109

Sist P, Rutishauser E, Peña-Claros M, Shenkin A, Hérault B, Blanc L, Baraloto C, Baya F, Benedet F, da Silva KE, Descroix L, Ferreira JN, Gourlet-Fleury S, Guedes MC, Bin Harun I, Jalonen R, Kanashiro M, Krisnawati H, Kshatriya M, Lincoln P, Mazzei L, Medjibé V, Nasi R, D'Oliveira MVN, de Oliveira LC, Picard N, Pietsch S, Pinard M, Priyadi H, Putz FE, Rodney K, Rossi V, Roopsind A, Ruschel AR, Shari NHZ, Rodrigues de Souza C, Susanty FH, Sotta ED, Toledo M, Vidal E, aP West T, Wortel V, Yamada T (2015) The Tropical managed Forests Observatory: a research network addressing the future of tropical logged forests. Appl Veg Sci 18:171–174

Slik JWF (2004) El Niño droughts and their effects on tree species composition and diversity in tropical rain forests. Oecologia 141(1):114–120

Stahl C, Hérault B, Rossi V, Burban B, Bréchet C, Bonal D (2013) Depth of soil water uptake by tropical rainforest trees during dry periods: does tree dimension matter? Oecologia 173(4):1191–201

Sterck F, Markesteijn L, Schieving F, Poorter L (2011) Functional traits determine trade-offs and niches in a tropical forest community. Proc Natl Acad Sci U S A 108(51):20627–32

Tan ZH, Cao M, Yu GR, Tang JW, Deng XB, Song QH, Tang Y, Zheng Z, Liu WJ, Feng ZL, Deng Y, Zhang JL, Liang N, Zhang YP (2013) High sensitivity of a tropical rainforest to water variability: Evidence from 10 years of inventory and eddy flux data. J Geophys Res Atmos 118(16):9393–9400

Thorpe HC, Thomas SC, Caspersen JP (2008) Tree mortality following partial harvests is determned by skidding proximity. Ecol Appl 18(7):1652–1663

Toledo M, Poorter L, Peña-Claros M, Alarcón A, Balcázar J, Leaño C, Licona JC, Llanque O, Vroomans V, Zuidema P, Bongers F (2011) Climate is a stronger driver of tree and forest growth rates than soil and disturbance. J Ecol 99(1):254–264

Wagner F, Herault B, Rossi V, Hilker T, Maeda E, Sanchez A, Lyapustin A, Galyao L, Wang Y, Aragao L (2017) Climate drivers of the Amazon forest greening. PloS ONE 12:e0180932

Wagner F, Hérault B, Stahl C, Bonal D, Rossi V (2011) Modeling water availability for trees in tropical forests. Agric For Meteorol 151(9):1202–1213

Wagner F, Rossi V, Aubry-Kientz M, Bonal D, Dalitz H, Gliniars R, Stahl C, Trabucco A, Hérault B (2014) Pan-tropical analysis of climate effects on seasonal tree growth. PloS ONE 9(3):e92337

Wagner F, Rossi V, Stahl C, Bonal D, Hérault B (2012) Water availability is the main climate driver of neotropical tree growth. PloS ONE 7(4):e34074

Wagner, F, Rossi V, Stahl C, Bonal D, Hérault B (2013) Asynchronism in leaf and wood production in tropical forests: a study combining satellite and ground-based measurements. Biogeosciences 10(11):7307–7321

Wagner FH, Hérault B, Bonal D, Stahl C, Anderson LO, Baker TR, Becker GS, Beeckman H, Boanerges Souza D, Botosso PC, Bowman DMJS, Bräuning A, Brede B, Brown FI, Camarero JJ, Camargo PB, Cardoso FCG, Carvalho FA, Castro W, Chagas RK, Chave J, Chidumayo EN, Clark DA, Costa FRC, Couralet C, da Silva Mauricio PH, Dalitz H, de Castro VR, de Freitas Milani JE, de Oliveira EC, de Souza Arruda L, Devineau J-L, Drew DM, Dünisch O, Durigan G, Elifuraha E, Fedele M, Ferreira Fedele L, Figueiredo Filho A, Finger CAG, Franco AC, Freitas Júnior JL, Galvão F, Gebrekirstos A, Gliniars R, Graça PMLdA, Griffiths AD, Grogan J, Guan K, Homeier J, Kanieski MR, Kho LK, Koenig J, Kohler SV, Krepkowski J, Lemos-Filho JP, Lieberman D, Lieberman ME, Lisi CS, Longhi Santos T, López Ayala JL, Maeda EE, Malhi Y, Maria VRB, Marques MCM, Marques R, Maza Chamba H, Mbwambo L, Melgaço KLL, Mendivelso HA, Murphy BP, O'Brien JJ, Oberbauer SF, Okada N, Pélissier R, Prior LD, Roig FA, Ross M, Rossatto DR, Rossi V, Rowland L, Rutishauser E, Santana H, Schulze M, Selhorst D, Silva WR, Silveira M, Spannl S, Swaine MD, Toledo JJ, Toledo MM, Toledo M, Toma T, Tomazello Filho M, Valdez Hernández JI, Verbesselt J, Vieira SA, Vincent G, Volkmer de Castilho C, Volland F, Worbes M, Zanon MLB, Aragão LEOC (2016) Climate seasonality limits leaf carbon assimilation and wood productivity in tropical forests. Biogeosciences 13(8):2537–2562

Chapitre 6

Une nouvelle approche pour quantifier la récupération du volume de bois

Le bois d'œuvre est la première ressource extraite des forêts amazoniennes : assurer l'approvisionnement à long terme de cette ressource est l'un des principaux objectifs de la gestion de ces forêts. Ce chapitre propose une nouvelle approche pour quantifier la reconstitution des stocks de bois d'œuvre après exploitations. Contrairement aux modèles individu-centrés et matriciels qui avaient été utilisés précédemment dans la littérature, ce modèle a l'avantage de pouvoir être calibré avec des données restreintes (mesure des plus gros arbres uniquement) ce qui est un grand avantage en forêt tropicale où les données sont rares et les inventaires forestiers ne prennent souvent en compte que les arbres de taille commerciale. Par exemple au Brésil seuls les arbres au dessus de 33 cm DHP ont été inventoriés dans le projet RadamBrasil ; et dans le nouvel inventaire forestier en cours, 50% de la surface inventoriée ne concerne que les arbres $>$ 40 cm DHP[1].

Le modèle présenté ici décrit l'évolution du volume en fonction d'une variable décrivant la maturité de la forêt : lorsque la forêt est perturbée (par exemple par l'exploitation), la maturité diminue brutalement ; puis lorsque la forêt repousse la maturité ainsi que le volume augmentent à nouveau. Ce modèle a été calibré à titre d'exemple avec les données de Paracou. L'étude a fait l'objet d'une publication dans la revue *Ecological modelling* en 2018.

[1] S. F. B. Brasil (2018). *Inventário Florestal Nacional.*

Ecological Modelling 384 (2018) 353–369

Contents lists available at ScienceDirect

Ecological Modelling

journal homepage: www.elsevier.com/locate/ecolmodel

Assessing timber volume recovery after disturbance in tropical forests – A new modelling framework

Camille Piponiot[a,b,c,*], Géraldine Derroire[b], Laurent Descroix[d], Lucas Mazzei[e], Ervan Rutishauser[f,g], Plinio Sist[h], Bruno Hérault[h,i,**]

[a] Université de Guyane, UMR EcoFoG (AgroParistech, Cirad, CNRS, Inra, Université des Antilles), Campus Agronomique, Kourou, French Guiana
[b] Cirad, UMR EcoFoG (AgroParistech, CNRS, Inra, Université des Antilles, Université de la Guyane), Campus Agronomique, Kourou, French Guiana
[c] CNRS, UMR EcoFoG (AgroParistech, Cirad, Inra, Université des Antilles, Université de la Guyane), Campus Agronomique, Kourou, French Guiana
[d] ONF-Guyane, Réserve de Montabo, 97307 Cayenne, French Guiana
[e] Embrapa Amazônia Oriental, Belém, Brazil
[f] CarboForExpert, Geneva, Switzerland
[g] Smithsonian Tropical Research Institute, Gamboa, Panama
[h] Cirad, Univ Montpellier, UR Forests and Societies, Montpellier, France
[i] INPHB (Institut National Polytechnique Félix Houphouet Boigny), Yamoussoukro, Cote d'Ivoire

ARTICLE INFO

Keywords:
Disturbance
Recovery
Tropical forest management
Sustainability
Ecosystem modelling

ABSTRACT

One third of contemporary tropical forests is designated by national forest services for timber production. Tropical forests are also increasingly affected by anthropogenic disturbances. However, there is still much uncertainty around the capacity of tropical forests to recover their timber volume after logging as well as other disturbances such as fires, large blow-downs and extreme droughts, and thus on the long-term sustainability of logging.

We developed an original Bayesian hierarchical model of Volume Dynamics with Differential Equations (VDDE) to infer the dynamic of timber volumes as the result of two ecosystem processes: volume gains from tree growth and volume losses from tree mortality. Both processes are expressed as explicit functions of the forest maturity, *i.e.* the overall successional stage of the forest that primarily depends on the frequency and severity of the disturbances that the forest has undergone. As a case study, the VDDE model was calibrated with data from Paracou, a long-term disturbance experiment in a neotropical forest where over 56 ha of permanent forest plots were logged with different intensities and censused for 31 years. With this model, we could predict timber recovery at Paracou at the end of a cutting cycle depending on the logging intensity, the rotation cycle length, and the proportion of commercial volume.

The VDDE modelling framework developed presents three main advantages: (i) it can be calibrated with large tree inventories which are widely available from national forest inventories or logging concession management plans and are easy to measure, both on the field and with remote sensing; (ii) it depends on only a few input parameters, which can be an advantage in tropical regions where data availability is scarce; (iii) the modelling framework is flexible enough to explicitly include the effect of other types of disturbances (both natural and anthropogenic: e.g. blow-downs, fires and climate change) on the forest maturity, and thus to predict future timber provision in the tropics in a context of global changes.

1. Introduction

Tropical forests are increasingly prone to anthropogenic disturbances: in 2017, only 20% of the remaining tropical forests were considered as undisturbed and structurally intact (Potapov et al., 2017), and this proportion is likely to decrease under future human pressure (Lewis et al., 2015). Disturbances, here defined as occasional events provoking sharp biomass losses (Rykiel, 1985), alter forest structure, notably average tree height (Tyukavina et al., 2016; Rutishauser et al., 2016), thus decreasing in turn carbon and timber stocks (Espírito-Santo et al., 2014). Human activities are increasing the frequency and severity of disturbances in tropical forests, both directly (e.g. through logging

* Corresponding author at: Université de la Guyane, UMR EcoFoG (AgroParistech, Cirad, CNRS, Inra, Université des Antilles), Campus Agronomique, 97310 Kourou, French Guiana.
** Corresponding author at: Cirad, UR Forests and Societies, Campus International de Baillarguet, 34398 Montpellier, Cedex 5, France.
E-mail addresses: camille.piponiot@gmail.com (C. Piponiot), bruno.herault@cirad.fr (B. Hérault).

https://doi.org/10.1016/j.ecolmodel.2018.05.023
Received 8 December 2017; Received in revised form 25 May 2018; Accepted 27 May 2018

and fires (Potapov et al., 2017)) and indirectly (e.g. through climate change and forest fragmentation (Laurance and Williamson, 2001)). In this context, assessing the effect of disturbances on the recovery of tropical forests is of paramount importance to better estimate future timber provision. The latter is predominantly done through selective logging that consists in harvesting a few high-value tree species and leaving the rest of the forest to natural recovery. Such forest management is widespread: it has been estimated that between 2005 and 2010, more than 50% of carbon emissions from tropical forest degradation were caused by selective logging (Pearson et al., 2017) and 425 Mha (c. 30% of the world wet tropical forests) are currently intended for timber production by National Forest Services (Blaser et al., 2011; Pan et al., 2013).

Though most of the forest cover is maintained after selective logging, typically 50–90% (Asner et al., 2002; Cannon et al., 1994; Laporte et al., 2007), opening the forest and felling trees has deep environmental consequences, such as an obvious reduction of timber stocks (Keller et al., 2004), but also large carbon emissions due to wood harvest and incidental mortality (Pearson et al., 2014), modification of tree species composition (de Avila et al., 2015) or fauna diversity (Burivalova et al., 2014). In the absence of subsequent disturbances (*e.g.* clear-cutting, fire, new logging events), the forest naturally regenerates and recovers at least part of its ecosystem values (e.g. carbon and timber stocks Piponiot et al., 2016a,b; Rutishauser et al., 2015; Blanc et al., 2009), before being selectively logged again. With logging rotation generally ranging between 20 and 30 years (Blaser et al., 2011), such cutting cycle duration may be sufficient to recover C stocks but not the volume of commercial species (Rutishauser et al., 2015; Roopsind et al., 2017) leading to unsustainable wood production on the long run.

There has been a strong debate over the past two decades on the role of selective logging in production forests as a tool for tropical forest conservation (Rice et al., 1997; Bawa and Seidler, 1998; Putz et al., 2001; Edwards et al., 2014). If logged forests are to be considered as a piece of an integrative conservation scheme, they should at least retain most of their environmental and economical values in time: this is the main challenge for modern tropical forest management. Sustainable forest management is indeed defined by the International Tropical Timber Organisation as "*the process of managing forest to achieve one or more clearly specified objectives of management […] without undue reduction of its inherent values and future productivity and without undue undesirable effects on the physical and social environment*" (ITTO, 1992). Due to the social and economical benefits it brings, sustainable timber harvest is even considered to be an efficient tool that gives additional value to forests that would else be cleared for agriculture (Edwards et al., 2014). One of the cornerstone of sustainability in forest management is the maintenance of high productivity (ITTO, 1992) to allow the recovery of timber stocks at the end of a cutting cycle. This is a critical point as in most selectively logged forests, this criterion is not achieved and many studies report a drop in total volume at the end of the first cutting cycle (Putz et al., 2012).

Previous studies simulating post-logging timber recovery have made large uses of individual-based models (Huth and Ditzer, 2001; Kammesheidt et al., 2001; Valle et al., 2007; Sebbenn et al., 2008) or transition matrix models (Macpherson et al., 2010; Gourlet-Fleury et al., 2005a,b). Such models perform well at locally predicting forest dynamics (Liang and Picard, 2013), but their high level of complexity and data requirements make the understanding of emergent patterns uneasy (Grimm, 2005). Furthermore, recruitment of small trees is a key process for long-term prediction in transition matrix models as well as in individual-based models (Liang and Picard, 2013; Berger et al., 2008; Fischer et al., 2016) and requires data from permanent sample plots with measurements of trees from relatively low size classes, typically above 10 cm of Diameter at Breast Height (DBH) or less (Gourlet-Fleury et al., 2005a,b; Phillips et al., 2004). Because small trees are particularly numerous in tropical forests, measuring them is costly (Picard et al., 2010; Kiyono et al., 2011): for example it takes approximately 10–15 times longer to measure all trees above 10 cm DBH than only trees above 50 cm DBH (Alder and Synnott, 1992). In this context, high-quality data coming from long-running permanent sample plots remain scarce in the tropics, hampering large-scale modelling of forest dynamics that would feed forest management plans with robust productivity predictions (Picard et al., 2010).

On the other side of the spectrum, coarse scale models such as Dynamic Global Vegetation Models (DGVM; e.g. LPJ-DGVM Sitch et al., 2003) allow efficient large-scale forest dynamics prediction with little input data, relying on a wide set of mechanistic assumptions. These models were initially developed to simulate ecosystem carbon fluxes, but can be used to predict volume dynamics when coupled with individual-based models (e.g. SEIB-DGVM Sato et al., 2007). Nevertheless DGVMs generally adopt a top-down approach, and are thus not fit to integrate field data such as inventory data, that are merely used for validation. As a consequence DGVMs can sometimes have conflicting results and poorly predict observed regional patterns of carbon dynamics (Johnson et al., 2016).

In this study, we propose an original model of Volume Dynamics with Differential Equations (VDDE) to assess total volume stocks and recovery based on forest inventory data. Instead of using detailed information (*i.e.* all trees) to model all demographic process (*i.e.* recruitment, growth and mortality) with great precision, we deliberately chose to favour model simplicity and rely upon broadly available data, *i.e.* the volume of all trees above 50 cm DBH (the official minimum cutting DBH in most tropical countries Blaser et al., 2011) hereinafter referred to as total volume. The VDDE model was developed and calibrated with data from the Paracou research station, a long-term large-scale disturbance experiment in Amazonia, where 56 ha of tropical forest have been monitored for 30 years after being disturbed (selective logging, poison girdling, fuelwood harvesting).

Anthropogenic or natural disturbances, such as logging or droughts, affect forests as a whole and induce a shift in forest functioning (Hérault and Piponiot, 2018). Even though the return frequency of these episodic succession-inducing events is not well known, this abrupt disturbance – slow recovery has long been described in tropical forests, as well as in temperate and boreal forests (Frolking et al., 2009; Liu et al., 2011; Chambers et al., 2013). Our assumption is that both the volume gain and the volume loss from mortality (hereinafter referred to as volume mortality) inherently depend on the overall successional stage of a forest (Rödig et al., 2018; Volkova et al., 2018), hereinafter referred to as forest maturity. While at our study site, a limited number of disturbances (selective logging, poison girdling and fuelwood harvesting) were experienced, tropical forests may undergo many other forms of anthropogenic and natural disturbances, such as droughts or fires that, similarly to logging, are associated with over-mortality that can drastically decrease trees > 50 cm DBH volume. Their effect on the forest volume dynamics can thus be modelled within the VDDE framework as a decrease in the forest maturity.

2. Methods

2.1. Study site

The study is based on data from Paracou research station (5°18′ N, 52°55′ W), a long-term large-scale disturbance experiment located in a lowland tropical forest in French Guiana (Gourlet-Fleury et al., 2004). The climate is affected by the north/south movements of the Inter-Tropical Convergence Zone and the site receives nearly two-thirds of its annual 3041 mm of precipitation between mid-March and mid-June, and less than 50 mm per month in September and October (Wagner et al., 2011). The forest composition is typical of the Guyana Shield rainforests (ter Steege et al., 2013), dominated by Chrysobalanaceae, Fabaceae and Lecythidaceae, and with approximately 180 species of trees ≥10 cm DBH per ha. 12 permanent forest plots (75 ha total) were

monitored for 31 year (from 1984 to 2015). 9 plots (56.25 ha total) of the 12 plots underwent different logging treatments from 1986 to 1988: (i) 3 plots were selectively logged in 1986, causing a median volume loss of 34.1 m^3 (95% credibility interval: 24.4–62.0 $m^3\,ha^{-1}$); (ii) 6 were selectively logged in 1986 and were then applied timber stand improvement from 1987 to 1988; treatment-induced over-mortality in those plots lasted until 1990, causing a median volume loss of 90.1 $m^3\,ha^{-1}$ (95% credibility interval: 52.4–138.3 $m^3\,ha^{-1}$).

2.2. Measurements and volume computation

In all plots all trees ≥10 cm DBH were identified, tagged and mapped, and had their DBH measured every year between 1984 and 1995 and every 2 years since then (1997–2015). The volume $V_{i,p,k}$ (m^3) of each tree i in plot p at census $k \geq 1$ was calculated using a locally calibrated equation (Guitet et al., 2016) currently used by the National Forest Service:

$$\forall\, i \in I_{p,k},\ V_{i,p,k} = -0.035829 + 8.7634 \times \mathrm{DBH}^2_{i,p,k} \tag{1}$$

where $I_{p,k}$ is the set of live trees ≥50 cm DBH in plot p at census k and $DBH_{i,p,k}$ is the diameter at breast height (in m) of the tree i at census k. The total volume ($m^3\,ha^{-1}$) of plot p, with a total area $Surf_p$ (ha), at census k is thus:

$$V_{p,k} = \sum_{i \in I_{p,k}} V_{i,p,k} \times (\mathrm{Surf}_p)^{-1} \tag{2}$$

Annual volume gain $\Delta Vg_{p,k}$ and annual volume mortality $\Delta Vm_{p,k}$ ($m^3\,ha^{-1}\,yr^{-1}$) were computed as:

$$\forall\, k \geq 2,\ \begin{cases} \Delta \mathrm{Vg}_{p,k} = \sum_{i \in I_{p,k}} (V_{i,p,k} - V_{i,p,k-1}) \times [\Delta t_k \times \mathrm{Surf}_p]^{-1} \\ \Delta \mathrm{Vm}_{p,k} = \sum_{i \in I_{p,k-1} \cap \overline{I_{p,k}}} (V_{i,p,k} - V_{i,p,k-1}) \times [\Delta t_k \times \mathrm{Surf}_p]^{-1} \end{cases} \tag{3}$$

where $I_{p,k}$ is the set of live trees ≥50 cm DBH in plot p at census k and $I_{p,k-1} \cap \overline{I_{p,k}}$ is the set of trees that died between censuses $k-1$ and k in plot p. If a given tree $i \in I_{p,k}$ was < 50 cm DBH at census $k-1$, then $V_{i,p,k-1} = 0$, and Δt_k is the time interval between censuses k and $k-1$.

The commercial volume, *i.e.* the volume of merchantable trees, was computed as the sum of all trees from species that were effectively logged in Paracou at the time of the experiment. The list of logged species in Paracou is provided in Table E2.

2.3. Conceptual framework

Forest maturity. In the newly developed VDDE model presented here, the dynamic of total volume is the result of two ecosystem processes: volume gains from tree growth and volume losses from tree mortality (Fig. 1). These processes are both expressed as functions of forest maturity. Forest maturity is a hidden variable of the VDDE model that gradually increases over time until a new disturbance, either natural (e.g. large blow-down) or human-induced (e.g. logging), occurs and abruptly decreases forest maturity (see Fig. 2). To capture the disturbance-recovery dynamic, we define the forest maturity as the time it would take for a given forest stand to grow from scratch and reach its current state in the absence of major disturbances. The forest maturity is thus expressed in a time-equivalent measure (for example in years). By definition, the maturity and total volume are null when no tree has reached 50 cm DBH (not observed in our data).

Let us consider the theoretical case where the forest recovers from scratch and is not subject to any disturbance. Let t be the maturity of the stand, in years: $V(t=0) = 0$ and $\forall t > 0$, $V(t) > 0$, with $V(t)$ the total volume of the stand at maturity t. The total volume change is modelled as:

$$\frac{\mathrm{dV}(t)}{\mathrm{dt}} = g(t) - m(t) \tag{4}$$

The volume gain from growth $g(t)$ is the stand annual volume productivity. By analogy with carbon sequestration in plants (Malhi, 2012), we consider this net volume productivity to be the difference of gross volume productivity $GVP(t)$ and the volume loss due to respiration $VR(t)$.

The gross volume productivity GVP increases with forest maturity until reaching a finite limit, the maximum gross productivity α_G:

$$\mathrm{GVP}(t) = \alpha_G \times (1 - e^{-\beta_G \times t}) \tag{5}$$

where β_G is the rate at which the asymptotic state is reached. Note that $GVP(t)$ increases with forest maturity and decelerates when approaching maximum gross productivity.

The respiration VR, *i.e.* the energy cost of maintenance, is proportional to the total volume:

$$\mathrm{VR}(t) = \theta \times V(t) \tag{6}$$

where θ is a constant. Note that $VR(t)$ is assumed to increase linearly with total volume.

The net volume productivity is given by the difference of $GVP(t)$ and $VR(t)$, resulting in a hump-shaped curve (Fig. 3), similar to previous results from forest carbon cycle (Chen et al., 2002; He et al., 2012; Volkova et al., 2018).

We expect the annual volume mortality to reach in time a finite limit α_M at a rate β_M. We thus have:

$$\forall\, t > 0,\ \begin{cases} g(t) = \mathrm{GVP}(t) - \mathrm{VR}(t) = \alpha_G \times (1 - e^{-\beta_G t}) - \theta \times V(t) \\ m(t) = \alpha_M \times (1 - e^{-\beta_M t}) \\ \frac{\mathrm{dV}(t)}{\mathrm{dt}} = g(t) - m(t) \end{cases} \tag{7}$$

We get the non-homogeneous differential equation of 1st order:

$$\begin{cases} \frac{\mathrm{dV}(t)}{\mathrm{dt}} = \alpha_G \times (1 - e^{-\beta_G t}) - \theta \times V(t) - \alpha_M \times (1 - e^{-\beta_M t}) \\ \text{with } V(0) = 0 \end{cases} \tag{8}$$

The solution of this equation is:

$$V(t) = \frac{\alpha_G}{\theta}\left(1 - \frac{\theta \times e^{-\beta_G t} - \beta_G \times e^{-\theta t}}{\theta - \beta_G}\right) - \frac{\alpha_M}{\theta}\left(1 - \frac{\theta \times e^{-\beta_M t} - \beta_M \times e^{-\theta t}}{\theta - \beta_M}\right) \tag{9}$$

To have $\forall t \geq 0$, $V(t) \geq 0$, we must have $\alpha_G \geq \alpha_M$ and $\beta_M \geq \beta_G \times \frac{\alpha_G}{\alpha_M}$.

We thus have the following equations:

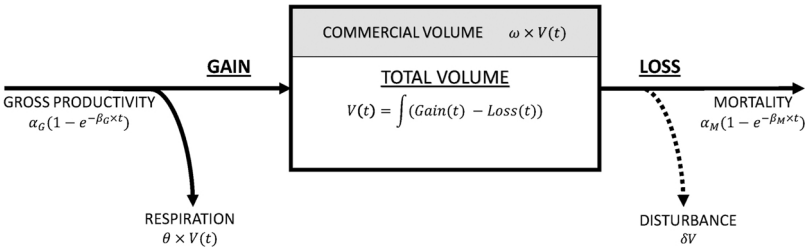

Fig. 1. Diagram of the main components of the VDDE model. The measured quantities are underlined. Solid arrows represent annual volume changes, the dashed arrow represents an *occasional* volume change, and the box represents the volume stock. Values of volume changes and stocks at a given forest maturity t are given by the equations, with the following parameters: α_G and α_M the gross volume productivity and mortality (resp.) of an infinitely mature stand and β_G, β_M the respective rate at which these values are reached; θ the volume respiration rate; ω the proportion of commercial volume; δV the volume loss caused by a given disturbance. Parameters posterior distributions are given in Table 1.

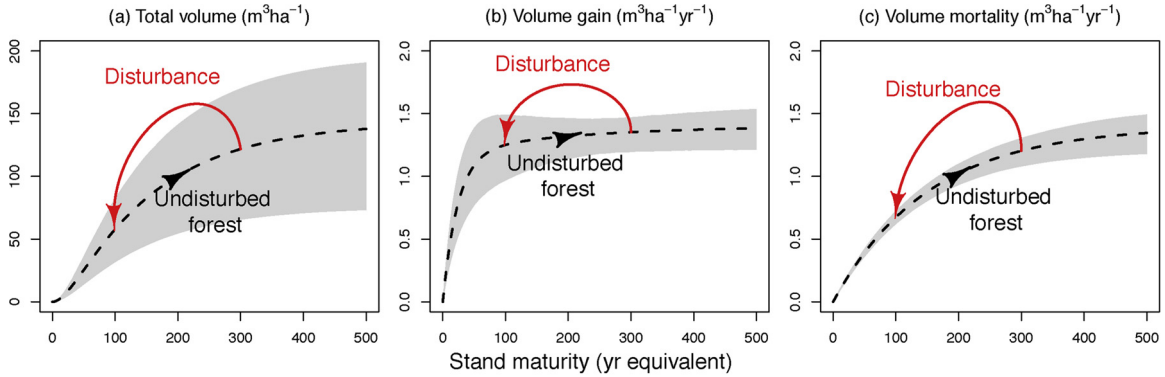

Fig. 2. Total volume and annual volume changes along a forest maturity axis. (a) Total volume; (b) annual volume gain; (c) annual volume mortality. Parameter values are from calibration with Paracou station data: the middle dashed lines are the maximum likelihood prediction, with the arrowheads representing the direction of changes in the absence of disturbances, and the shaded areas are the 95% credibility intervals on predictions. The red arrows represent the sudden decrease in forest maturity caused by a large disturbance. (For interpretation of the references to color in this figure legend, the reader is referred to the web version of this article.)

$$\begin{cases} g(t) = \frac{\alpha_G \times \beta_G}{\theta - \beta_G}(e^{-\beta_G t} - e^{-\theta t}) + \alpha_M \left(1 - \frac{\theta \times e^{-\beta_M t} - \beta_M \times e^{-\theta t}}{\theta - \beta_M}\right) \\ m(t) = \alpha_M \times (1 - e^{-\beta_M t}) \end{cases} \quad (10)$$

The volume potential of the forest stand (*i.e.* the volume at full capacity) is:

$$\text{vmax} = \lim_{t \to \infty}(V(t)) = \frac{\alpha_G - \alpha_M}{\theta} \quad (11)$$

All calculation details (equation solving, limits and constraints on parameters) are in Appendix D.

The effect of logging on commercial species. Only a proportion of the total volume is made of commercial species (*i.e.* species that have a merchantable value): we define $V_k^* = \omega_k \times V(t_k)$ the volume of commercial species at census k, where ω_k is the proportion of commercial species (as a % of total volume) and t_k the maturity. Selective logging targets commercial species. Depending on the logging techniques and the precision of timber harvesting, logging can cause a varying amount of damage to the residual stand.

Let δV be the total volume loss caused by logging. Part of this volume loss is the extracted volume (*Vext*), *i.e.* the volume of commercial trees that have been purposely felled; the rest is the incidental damage to non-commercial trees. The extracted volume is modelled as:

$$\text{Vext} = \omega_0^{1-\psi} \times \delta V \quad (12)$$

where ω_0 is the initial proportion of commercial species (prior to logging), $\psi \leq 1$ is the precision of tree harvesting (*i.e.* how well it targets commercial species): if $\psi = 1$, $\delta V = Vext$: all the volume loss is intentional and there is no incidental damage. If $\psi = 0$, $Vext = \omega_0 \times \delta V$: the volume loss caused by logging (harvested trees + incidental damage) is not directional and affects randomly commercial and non commercial trees, in the same proportion as their occurrence in the forest. If $\psi < 0$, $Vext < \omega_0 \times \delta V$: logging affects particularly non-commercial species, which can be the specific case of silvicultural treatments when the largest non-commercial trees are purposely killed to release competition.

Logging thus changes the proportion of commercial species: let ω_0 be the initial proportion of commercial species and ω_1 the post-logging proportion of commercial species. We have:

$$\omega_1 = \frac{V_0^* - \text{Vext}}{V_0 - \delta V} = \omega_0 \times \frac{1 - \omega_0^{-\psi} \times \frac{\delta V}{V_0}}{1 - \frac{\delta V}{V_0}} \quad (13)$$

with V_0^* the initial commercial volume, V_0 the initial total volume, δV the total volume loss caused by logging, *Vext* the extracted commercial volume and $\psi \leq 1$ the logging precision.

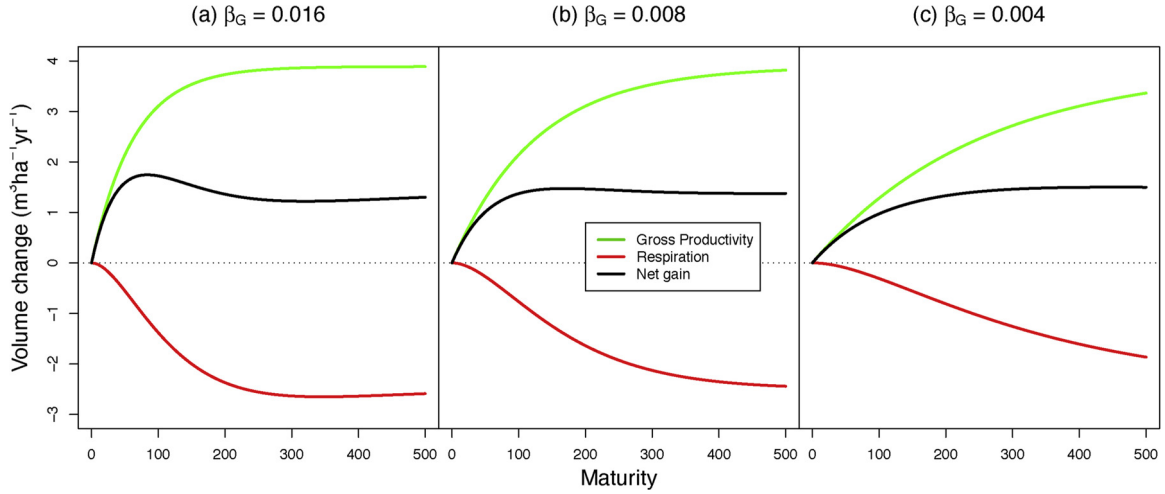

Fig. 3. Illustrative example of the hump-shaped net volume gain (black) when defined as the difference of gross volume productivity (green) and respiration (red). Parameters have been set to their maximum likelihood value in Paracou, except for the gross productivity rate β_G that decreases from (a) 0.016, (b) 0.008 to (c) 0.004 (the maximum likelihood value in Paracou is $\beta_G = 0.0063$). The hump can be more or less pronounced depending on parameter values, giving some flexibility to the relationship between the forest maturity and the net volume gain. (For interpretation of the references to color in this figure legend, the reader is referred to the web version of this article.)

Modelling recruitment. In the absence of further information, we make the conservative assumption that the growth and mortality of trees > 50 cm DBH do not differ between commercial and none commercial species. However, if the proportion of commercial volume ω differs between trees ≥50 cm DBH and trees < 50 cm DBH (as can happen when big commercial trees are selectively logged, decreasing the proportion of commercial volume in trees ≥50 cm DBH), the proportion of commercial volume can recover through the recruitment of trees from DBH < 50 cm to DBH > 50 cm. Let pR_j be the proportion of volume gain from the recruitment of trees < 50 cm DBH to ≥50 cm DBH (the remaining volume gain comes from the growth of trees already DBH ≥50 cm DBH) j years after logging. The proportion of commercial volume in recruited trees is not significantly different from the pre-logging proportion of commercial volume ω_0 (see Appendix A, Fig. A2). We thus have:

$$V(t_{j+1}) \times \omega_{j+1} = V(t_j) \times \omega_j + g(t_j)(\underbrace{\omega_0 \times \mathrm{pR}_j}_{\text{recruitment}} + \underbrace{\omega_j \times (1 - \mathrm{pR}_j)}_{\text{growth}}) - m(t_j) \times \omega_j \quad (14)$$

with pR_j the proportion of recruitment (over the total volume gain $g(t_j)$) j years after logging, and t_j the maturity of the plot j years after logging. We model the proportion of recruitment of trees < 50 cm DBH as a function of the total volume $V(t_j)$:

$$\mathrm{logit}(\mathrm{pR}_j) = \gamma_0 + \gamma_1 \times \ln(V(t_j)) \quad (15)$$

In this model, the proportion of recruitment is 1 when the total volume is null and decreases thereafter. Observations and predictions in Paracou are presented in Appendix A, Fig. A3.

2.4. Inference

Bayesian hierarchical models were inferred through MCMC methods using an adaptive form of the Hamiltonian Monte Carlo sampling (Carpenter et al., 2015). Codes were developed using the R language (R Development Core Team, 2008). We hereafter explicit the models that were inferred. Parameters priors distribution are reported in Table E1.

Covariance structure. In this study we have data from 12 plots, all from a single area of about 500 ha. We assume that all plots have similar disturbance history prior to logging and that they consequently have the same initial forest maturity t_0. For control plots p, we thus have $t_{p,a} = t_0$, with $t_{p,1}$ the maturity at first census. For disturbed plots, the forest maturity at the first census after the disturbance (1987 for logged plots without timber stand improvement, and 1990 for plots with timber stand improvement) is $t_{p,1} = t_0 - tloss_p$ where $tloss_p$ is the maturity loss caused by disturbance in plot p. To account for inter-plot variation, we add a random effect on $vmax_p$ assuming that plots have different productivity potentials:

$$\mathrm{vmax}_p \sim \mathcal{N}(\mu_{\mathrm{vmax}}, \sigma^2_{\mathrm{vmax}}) \quad (16)$$

where μ_{vmax} and σ_{vmax} are the hyperparameters (respectively the mean and standard deviation) of the distribution of $vmax_p$. All other parameters ($\alpha_M, \beta_G, \beta_M, \theta$) do not vary between plots. Parameter $\alpha_{G,p}$ for plot p is mathematically deduced from other parameter values:

$$\alpha_{G,p} = \theta \times \mathrm{vmax}_p + \alpha_M \quad (17)$$

Total volume. The total volume of plot p at census k was modelled as:

$$V_{p,k} \sim \ln \mathcal{N}(\mu v_{p,k}, \sigma^2_V) \quad (18)$$

with σ_V the volume's standard deviation and $\mu v_{p,k}$ the mean, which value was deduced from Eqs. (9) and (17):

$$\begin{aligned}\mu v_{p,k} = & \frac{\alpha_{G,p} - \alpha_M}{\theta} - \frac{\alpha_{G,p}}{\theta} \times \frac{\theta \times e^{-\beta_G t_{p,k}} - \beta_G \times e^{-\theta t_{p,k}}}{\theta - \beta_G} \\ & + \frac{\alpha_M}{\theta} \times \frac{\theta \times e^{-\beta_M t_{p,k}} - \beta_M \times e^{-\theta t_{p,k}}}{\theta - \beta_M} \\ \mu v_{p,k} = & \ \mathrm{vmax}_p - \left(\mathrm{vmax}_p + \frac{\alpha_M}{\theta}\right) \times \frac{\theta \times e^{-\beta_G t_{p,k}} - \beta_G \times e^{-\theta t_{p,k}}}{\theta - \beta_G} \\ & + \frac{\alpha_M}{\theta} \times \frac{\theta \times e^{-\beta_M t_{p,k}} - \beta_M \times e^{-\theta t_{p,k}}}{\theta - \beta_M}\end{aligned} \quad (19)$$

Disturbance intensity and extracted volume. The volume loss caused by disturbance δV (in $\mathrm{m^3\,ha^{-1}}$), analogous to a disturbance intensity, is the difference (in each disturbed plot) between the pre-disturbance volume (in 1986 in Paracou) and the volume at the first post-disturbance census. For selectively-logged plots, the first post-disturbance census is 1987; in plots that underwent silvicultural treatments, over-mortality from tree poisoning and girdling lasted for as long as 4 years, the first post-disturbance census was then set to 1990. The extracted volume *Vext* is the volume of harvested trees (in $\mathrm{m^3\,ha^{-1}}$).

All plots p in Paracou were subdivided in 4 subplots j, and for each subplot the logging efficiency $\omega\mathrm{ext}_{p,j} = \frac{\mathrm{Vext}_{p,j}}{\delta V_{p,j}}$ and the proportion of commercial volume $\omega_{0,p,j}$ were assessed. We then modelled the logging efficiency as:

$$\omega\mathrm{ext}_{p,j} \sim \mathscr{B}\mathrm{eta}(\alpha_{p,j}, \beta_{p,j}) \quad (20)$$

where $\alpha_{p,j} > 0$ and $\beta_{p,j} > 0$ are the shape parameters of the beta distribution. According to Eq. (12), we modelled the mean of the distribution as:

$$E(\omega\mathrm{ext}) = \omega_{0,p,j}^{(1-\psi_T)} = \frac{\alpha_{p,j}}{\alpha_{p,j} + \beta_{p,j}} \quad (21)$$

with ψ_T the precision of logging, defined in the conceptual framework, and T the logging treatment, either conventional logging or timber stand improvement. To have a variance that is null when $\omega_0 = 0$ and $\omega_0 = 1$ (where ωext is known with certainty, being resp. 0 and 1) and satisfy the conditions $\alpha_{p,j} > 0$ and $\beta_{p,j} > 0$, we modelled the variance of the beta distribution as:

$$\mathrm{Var}(\omega\mathrm{ext}) = E(\omega\mathrm{ext})^2 \times (1 - E(\omega\mathrm{ext})) \times \varepsilon_T \quad (22)$$

with $\varepsilon_T > 0$ an error parameter. The data and results are presented in Appendix A.

Cumulative volume changes. To avoid focusing on yearly fluctuations and improve our predictive strength, instead of annual volume changes we used, to infer the VDDE model, cumulative volume changes, *i.e.* the annual volume changes integrated over time (as suggested for example in Walters, 1999; Thompson et al., 2001). Cumulative volume growth (cVg) and mortality (cVm) are defined as:

$$\begin{cases} \mathrm{cVg}_{p,1} = \mathrm{cVm}_{p,1} = 0 \\ \forall\ k \geq 2, \begin{cases} \mathrm{cVg}_{p,k} = \sum_{j=2}^{k} \Delta\mathrm{Vg}_{p,j} \times (t_j - t_{j-1}) \\ \mathrm{cVm}_{p,k} = \sum_{j=2}^{k} \Delta\mathrm{Vm}_{p,j} \times (t_j - t_{j-1}) \end{cases} \end{cases} \quad (23)$$

with p the plot and k the census. We model cumulative volume changes as follows:

$$\begin{cases} \mathrm{cVg}_{p,k} \sim \ln \mathcal{N}(\mu g_{p,k}, \sigma^2_G) \\ \mathrm{cVm}_{p,k} \sim \ln \mathcal{N}(\mu m_k, \sigma^2_M) \end{cases} \quad (24)$$

with σ_G and σ_M the standard deviations and $\mu g_{p,k}$ and $\mu m_{p,k}$ the means at census k and in plot p of cumulative volume gain and mortality resp.:

Table 1
Parameters posterior descriptions. We give the median value, 95% credibility interval (CI) and the maximum likelihood value of the VDDE model parameters: t_0 initial forest maturity; *vmax* maximum volume potential, α_M maximum volume mortality; β_G convergence rate of volume growth, β_M convergence rate of volume mortality, θ relative metabolic volume loss, σ_V, σ_G, σ_M standard deviation of volume, cumulative volume gain and cumulative volume mortality resp.

Parameter	Name	95% CI	Max. likelihood value
t_0	Initial forest maturity	186–238	212
vmax	Maximum volume potential	109–261	126
α_M	Maximum volume mortality	1.10–1.44	1.22
β_G	Productivity convergence rate	(7.32–13.8) $\times 10^{-3}$	9.97×10^{-3}
β_M	Mortality convergence rate	(6.93–11.3) $\times 10^{-3}$	9.20×10^{-3}
θ	Relative metabolic volume loss	(6.82–16.54) $\times 10^{-3}$	1.04×10^{-2}
γ_0	Intercept of the recruitment model	1.87–2.74	2.29
γ_1	Slope of the recruitment model	(−0.516) – (−0.295)	−0.400
σ_V	Volume standard deviation	0.06–0.017	0.059
σ_G	Cum. volume gain standard deviation	0.196–0.243	0.227
σ_M	Cum. volume mortality standard deviation	0.464–0.521	0.512
σ_R	Proportion of recruitment standard deviation	0.560–0.673	0.611

$$\mu g_{p,k} = \int_{t_{p,1}}^{t_{p,k}} g(t)\mathrm{d}t = \frac{(\mathrm{vmax}_p \times \theta + \alpha_M) \times \beta_G}{\theta - \beta_G}\left(\frac{e^{-\beta_G t_{p,1}} - e^{-\beta_G t_{p,k}}}{\beta_G} - \frac{e^{-\theta t_{p,1}} - e^{-\theta t_{p,k}}}{\theta}\right) + \alpha_M\left((t_{p,k} - t_{p,1}) - \frac{\frac{\theta}{\beta_M} \times (e^{-\beta_M t_{p,1}} - e^{-\beta_M t_{p,k}}) - \frac{\beta_M}{\theta} \times (e^{-\theta t_{p,1}} - e^{-\theta t_{p,k}})}{\theta - \beta_M}\right) \quad (25)$$

and

$$\mu m_{p,k} = \int_{t_{p,1}}^{t_{p,k}} m(t)\mathrm{d}t = \alpha_M\left((t_{p,k} - t_{p,1}) - \frac{e^{-\beta_M t_{p,1}} - e^{-\beta_M t_{p,k}}}{\beta_M}\right) \quad (26)$$

where $t_{p,k}$ the forest maturity of plot p at census k.

Proportion of commercial volume in recruited trees. We infer the relationship between the total volume $V_{p,k}$ in plot p at census k and the proportion of commercial volume in recruited trees $pR_{p,k}$ according to Eq. (15):

$$\mathrm{logit}(\mathrm{pR}_{p,k}) \sim \mathcal{N}(\gamma_0 + \gamma_1 \times \ln(V_{p,k}),\ \sigma_R^2) \quad (27)$$

where γ_0 and $\gamma_1 > 0$ are resp. the intercept and slope of the relationship, and σ_R the standard deviation.

Validation. To evaluate the predictiveness of the VDDE model we use the first 15 years post-logging (approximately half of the censused period) to calibrate the model, and make predictions over the validation period (≥16 years post-logging). Predictions are then compared with the original data (Fig. 5).

2.5. Simulations

To illustrate some possible uses of the VDDE model, we simulated commercial volume recovery at our site under (i) current conditions and (ii) scenarios reflecting possible effects of future climate changes on disturbance regimes.

Current conditions. Commercial volume recovery at the end of a cutting cycle in Paracou conditions, depending on the logging intensity (extracted volume in $\mathrm{m^3\,ha^{-1}}$), on the cutting cycle length and on the initial proportion of commercial timber was assessed with the following steps: (a) a set of parameters is randomly picked from the parameter posterior distribution; (b) for every values of logging intensity *Vext* between 0 and $30\,\mathrm{m^3\,ha^{-1}}$, we calculate the volume loss $\delta V = \mathrm{Vext} \times \omega_0^{\psi-1}$ and the corresponding post-logging maturity t_1 estimated as: $V(t_1) = V(t_0) - \delta V$, with $V(t_0)$ the volume at the initial maturity t_0 and $V(t_1)$ the volume at the post-logging maturity, given the set of parameters from (a); (c) the post-logging proportion of commercial timber ω_1 is calculated with Eq. (13), with the initial proportion of commercial timber ω_0 being either 10%, 20%, 50% or 100% (in the latter case, $\omega_1 = \omega_0 = 1$), and the proportion ωf of commercial volume at the end of the cutting cycle is estimated with Eq. (14). (d) the commercial volume recovery is then estimated as:

$$\mathrm{Vrec} = V(t_1 + \mathrm{trot}) \times \omega_f - V(t_1) \times \omega_1 \quad (28)$$

with *trot* the cutting cycle length, between 5 and 100 yr. (e) steps (a–d) are repeated with 1000 sets of parameters and summary statistics are then calculated.

In the context of global changes. To illustrate the potential effect of anthropogenic impacts on future volume stocks, we tested how sensitive our results were to modifications in mortality (parameter α_M) and initial maturity (parameter t_0). The total volume was simulated under the hypothesis of a decrease in initial maturity (caused for example by increased frequency of disturbances), and an increase of volume mortality, following the steps: (a) a set of parameters is randomly picked from the posterior distribution; (b) new parameters are calculated: $\alpha'_M = (1 + \pi_M) \times \alpha_M$ (π_M between 0 and 1, corresponding to an increase in mortality between 0% and 100%) and $t'_0 = (1 - \pi_t) \times t_0$ (π_t between 0 and 1, corresponding to a decrease in initial maturity between 0 and 100%); (c) total volume predictions are made with those new sets of parameters; (d) steps (a–c) are repeated with 1000 sets of parameters and summary statistics are calculated.

3. Results and discussion

3.1. Accuracy of the model predictions

In this study, we developed an original model that combines stocks (here total volumes) and fluxes (here volume changes) estimation in one single integrative framework. Stocks are the integrated resultant of fluxes, and the estimation of one flux affects the estimation of the others. Parameters posterior, calibrated with Paracou data, are reported in Table 1. The goodness of prediction of the volume recovery is illustrated in Figs. 4 and B.4. With this rather simple model, we were able to predict the variability of trajectories in total volume recovery for the Paracou dataset (Fig. 4). When calibrating the VDDE model with only the first 15 years of post-logging data (i.e. approx. half of the censused

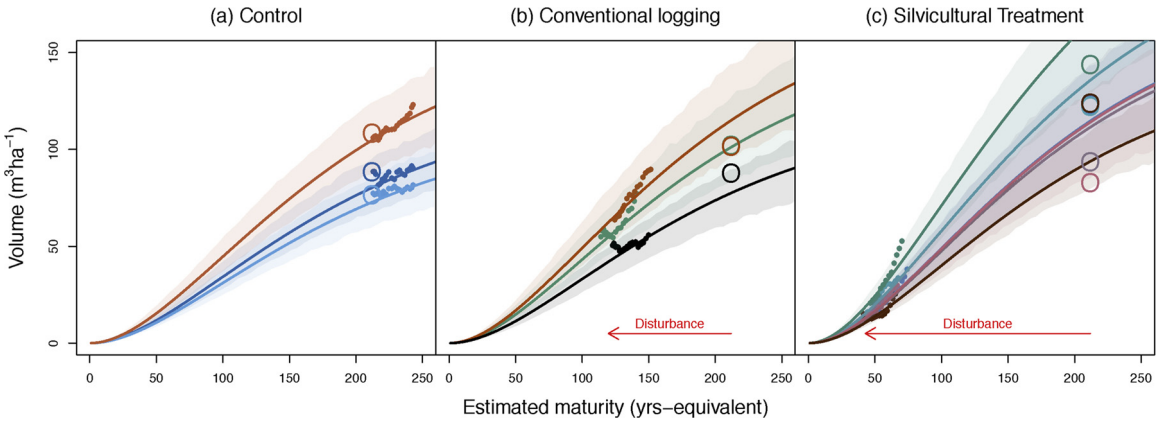

Fig. 4. Predicted and observed trajectories of total volumes in Paracou plots. (a) In control plots. (b) In moderately-disturbed plots (selective logging). (c) In intensively-disturbed plots (selective logging, fuelwood logging, poison girdling). Each plot is represented by a colour. Points represent observed total volumes (*y*-axis) plotted against their predicted maturity (*x*-axis, max-likelihood value), with the large empty dots being the initial total volume (before disturbance for disturbed plots). Lines are the predicted trajectories (max-likelihood value) with the shaded areas being the corresponding 95% credibility intervals. In panels (b) and (c), the arrow represents the effect of logging and additional treatments on the estimated forest maturity. (For interpretation of the references to color in this figure legend, the reader is referred to the web version of this article.)

period), predictions on the last 10–15 years of data (Fig. 5) were still satisfyingly accurate. The predicted pre-logging maturity value is 212 [186–238] yrs-equivalent (Table 1); this does not mean that the forest has 212 years but rather that it would take an estimated 212 years for the forest to reach its pre-logging state in the absence of disturbance. Logging provokes an estimated loss of maturity 90 [62-117] yrs-equivalent, and an additional 72 [64–80] yrs-equivalent after silvicultural treatments (Fig. 4).

3.2. Calibration data may come from diverse sources

One of the main advantages of the VDDE modelling framework is the basic requirement in terms of calibration data. Only measurements of trees above 50 cm are needed, which are rather easy to measure (typically 35 trees ≥50 cm DBH per ha in the tropics (Alder and Synnott, 1992), and 22 to 32 trees per ha in Paracou) and can thus be measured on wide areas covered by National Forest Inventories.

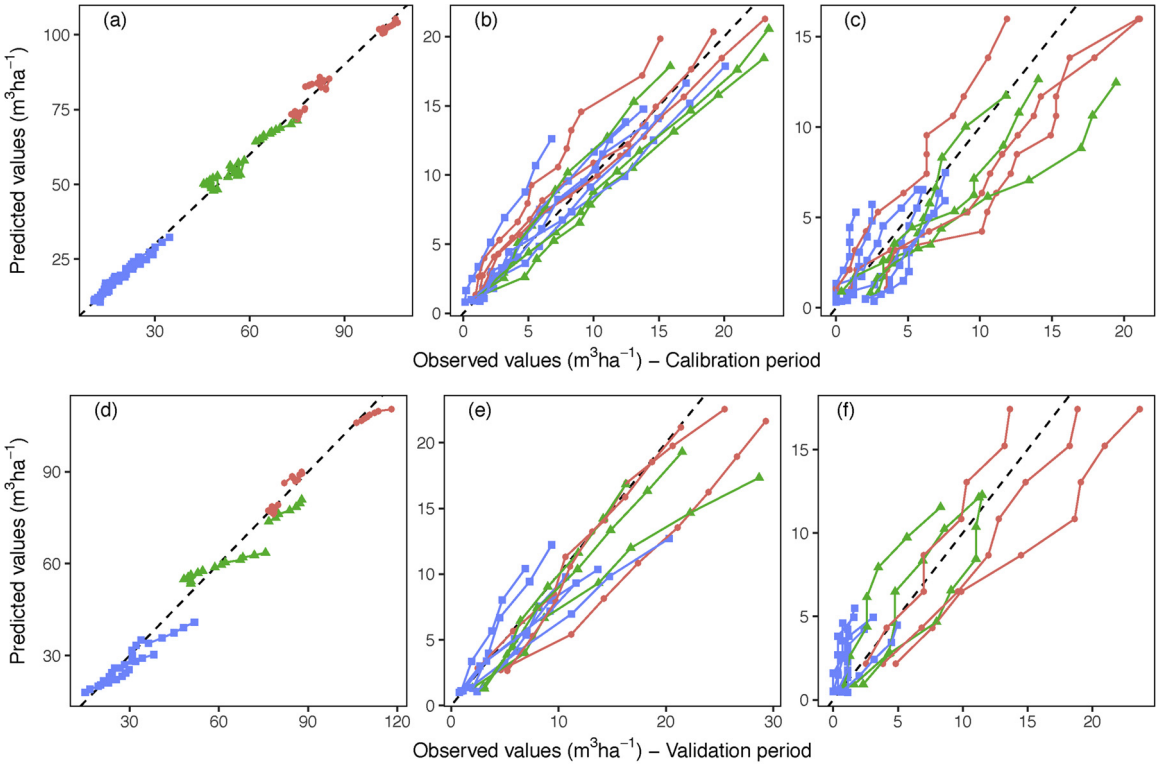

Fig. 5. Predictions vs. observations from the calibration and validation periods in Paracou. All upper panels (a–c) represent data from the calibration period (first 15 years of post-logging observations) and all lower panels (d–f) represent the data from the validation period (more than 15 years after logging); *x*-axes are observations and *y*-axes are maximum-likelihood predictions. Red dots are control plots, green triangles are logged plots, and blue squares are logged plots with silvicultural treatments (poison girdling and fuelwood harvest). (a, d) Total volume ($m^3\,ha^{-1}$). (b, e) Cumulative volume gain. (c, f) Cumulative volume mortality. (For interpretation of the references to color in this figure legend, the reader is referred to the web version of this article.)

Therefore, the VDDE model could be calibrated on a wide range of readily available data. The only restriction lies in the fact that the VDDE model requires at least 2 censuses to estimate total volume stocks and changes. Fortunately, many territories are currently implementing long-term monitoring of their forests under the REDD+ scheme (Maniatis and Mollicone, 2010) and these datasets could be fruitfully used to calibrate the VDDE model. Similarly, in the Brazilian Amazon, logging concessions in national forests are required to have Permanent Sample Plots (1 ha for every 250 ha of logged forests) (Balieiro et al., 2010) that could also be used to estimate the potential for volume recovery at concession level, or wider scale when aggregated. Static data can also be used to calibrate the VDDE model, by adding the measurements of total volume stocks to the overall likelihood of the model. This means that data such as static national inventories can also greatly help improve estimates of total volume and volume recovery. For example, the National Forest Inventory that is being carried out in Brazil aims at measuring all trees above 40 cm DBH in 4 0.2 ha plots in each 20 km × 20 km cell in the whole Brazilian Amazon (Brando et al., 2014). In National forest concessions, the Brazilian Forest Service carries out large inventories of all trees above 50 cm DBH to assess the available timber resource previous to logging (Balieiro et al., 2010).

We developed the VDDE modelling framework to estimate the total volume and commercial volume recovery after selective logging, but this framework could be extended to carbon stocks. Because it is generic enough in terms of ecosystem dynamics, this model could also be used to explore tropical forests resilience to other disturbance types, such as fire and/or drought (Holdsworth and Uhl, 1997; Brando et al., 2014), or even the forest recovery after clear-cutting (Poorter et al., 2016). Results could then be compared to explore the resilience of tropical forests to human and natural disturbances. The methodology may need some adaptations, as some specific problems may require a more complex model.

3.3. Model limitations

While the VDDE model relies upon sensible assumptions, their consequences on the model behaviour may be questioned. For instance, we assumed that the volume change of commercial species is similar to the total volume change during the recovery period. However, because the designation of timber species is generally based on their mechanical wood properties, the commercial species pool may be biased towards hard-wood species (Chave et al., 2009) with generally slow growth rates (Fargeon et al., 2016). However, not all commercial species do grow slowly, as shown by some fast-growing light-wood species (like Balsa (*Ochroma pyramidale*) (Condit et al., 1993)), with interesting mechanical properties (Bossu et al., 2016). The conservative hypothesis of equal relative volume changes is, to our point of view, sensible. It is however worth mentioning that harvesting only very slow growing species would have the effect of lowering the volume recovery, and thus the sustainable logging intensity.

Logging has been proven to lower the height (and thus the volume) of the stand (Rutishauser et al., 2016) resulting in a possible overestimation of timber volume recovery with current allometric equations calibrated in old-growth forests (Guitet et al., 2016). When data becomes available, some new volumetric equations should be calibrated in 2nd harvest forests to update volume estimates.

Assigning the same initial maturity value to all plots may also be questioned: indeed, tropical forests are shaped by very local treefall gap dynamics (Swaine et al., 1987), that could explain small inter-plot variations in forest maturity. From a practical standpoint however, it is difficult to disentangle the inter-plot variations in initial forest maturity from the inter-plot variations in potential volume (*vmax*) with limited time series. In the absence of further information, we thus made the hypothesis that local disturbances from treefall gaps were evened out across our relatively large-size plots (6.25 ha), and that all plots had the same disturbance history.

The model as presented here has been shown to be a useful predictor of post-logging volume recovery at a local scale. However one key challenge for forest management today, especially in the tropics where data is scarce, is to have an understanding of ecological processes at a wider scale, from the landscape to the regional scale (Makela et al., 2000). As stated before, one advantage of the VDDE modelling framework is to allow a variety of widely available calibration data, which makes robust regional estimates of volume recovery possible. To upscale predictions, a possible way is to add spatially-explicit covariates to the model parameters (for instance global maps of climatic (Fick and Hijmans, 2017) or soil variables (Hengl et al., 2014)) as proxies of model parameters.

3.4. Applying the VDDE model to assess logging sustainability

The commercial volume recovered at the end of the cutting cycle is presented in Fig. 6, depending on the cutting cycle length, logging intensity and proportion of commercial volume. The most influential variable on the volume recovery is the proportion of commercial species (increasing proportion of commercial species in panels from left to right on Fig. 6). Both the logging intensity (y-axis) and the length of the cutting cycle (*x*-axis) increases the volume recovery. When the initial proportion of commercial volume is 10% (left panel), the forest hardly recovers more than 5 $m^3\,ha^{-1}$, even after a cutting cycle of 100 years. On the contrary, if all species are commercial (100% of commercial volume), commercial volume recovery following a logging intensity of 20 $m^3\,ha^{-1}$ can be as high as 23 [19–39] $m^3\,ha^{-1}$ at the end of a 60 years cutting cycle.

To be considered sustainable, selective logging should at least allow the recovery of initial timber volumes at the end of each cutting cycle; otherwise, the depletion of timber stocks could undermine the conservation value of managed forests in the long term as the loss of economical value would make them more prone to conversion to other land uses with lower ecological benefits (Edwards et al., 2014). In French Guiana, 75% of timber production depends solely on 3 species: *Dicorynia guianenesis*, *Qualea rosea* and *Sextonia rubra* (French Guiana NFS statistics, unpublished data). In Paracou, the volume of those 3 species represents 20% of the total volume and is consistent with what can be seen over the Guyafor network, a network of permanent plots distributed over the French Guiana permanent forest estate (Piponiot et al., 2016a; Grau et al., 2017). The official cutting cycle length is 65 yr in French Guiana (which is particularly high for the tropics (Blaser et al., 2011)) and the logging intensity for the past 15 years has been 8–29 $m^3\,ha^{-1}$ (Piponiot et al., 2016a). Under such conditions, the results of our model show that only 0–4.1 $m^3\,ha^{-1}$ of commercial volume are recovered at the end of the cutting cycle (Fig. 6): selective logging cannot thus be considered sustainable under current conditions in French Guiana. Compared to other tropical countries, French Guiana's logging policies are especially strict (*e.g.* cutting cycles longer than the usual 30 years) (Blaser et al., 2011). If commercial timber stocks are far from being recovered in French Guiana, there is little chance that logging can be considered sustainable in other tropical countries. It is however worth mentioning that neighbouring countries like Suriname and Brazil harvest a larger variety of commercial tree species (Reis et al., 2010), which might allow higher commercial volume recovery (see Fig. 6). Nevertheless, most studies show that initial volume stocks

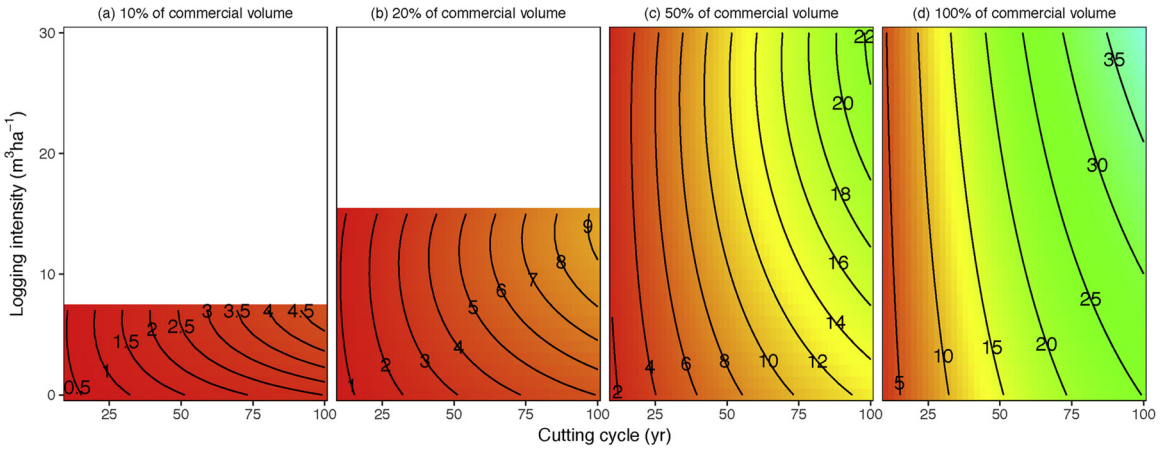

Fig. 6. Commercial volume recovered at the end of the cutting cycle ($m^3\,ha^{-1}$) as a function of cutting cycle length (in years), logging intensity ($m^3\,ha^{-1}$), and initial fraction of commercial species (%), in Paracou conditions. All other parameters are set to their maximum likelihood value. In each panel (a to d), the colors and level lines represent the commercial volume recovered at the end of the cutting cycle. The proportion of commercial species increases from left to right: (a) 10% of total volume is initially composed of commercial species, (b) 20% of total volume is initially composed of commercial species, (c) 50% of total volume is initially composed of commercial species, (d) 100% of total volume is initially composed of commercial species. In all panels, the *x*-axis represents the cutting cycle length; the *y*-axis represents the logging intensity, i.e. the volume of all trees killed during logging operations ($m^3\,ha^{-1}$). The corresponding 95% credibility interval can be found in Fig. C5.

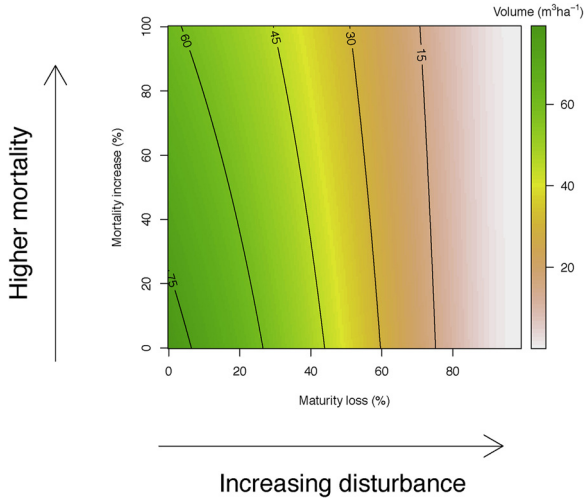

Fig. 7. Total volume ($m^3\,ha^{-1}$) in scenarios with an increase of volume mortality (in % of current mortality in Paracou, *y*-axis) and a decrease of the forest maturity (in % of current mean forest maturity in Paracou, *x*-axis). All other parameters are set to their maximum likelihood value. In each panel, the colors and level lines represent the total volume. The 95% credibility interval (upper and lower bounds) can be found in Fig. C6. (For interpretation of the references to color in this figure legend, the reader is referred to the web version of this article.)

are indeed not recovered in selectively logged forests across the tropics (Putz et al., 2012).

3.5. Applying the VDDE model to assess the effect of diversifying timber sources

For a proportion of commercial species of 100% (*i.e.* the total volume is commercial), the volume recovered at the end of the rotation cycle increases with the logging intensity (Fig. 6). Nevertheless, when the proportion of commercial volume decreases (panel b), increasing the logging intensity can decrease the commercial volume recovery. This is because when logging focuses on only a few commercial species, their proportion at the next logging cycle is inevitably lower (see 2.3) as compared to the other species. This means that even when the total volume is recovered at the end of the cutting cycle, the relative proportion of commercial species will be lower and thus at the next logging cycle the volume recovery will decrease. After a few logging cycles, the proportion of commercial species might be so low that their exploitation may become not economically sound. The smaller the initial pool of commercial species the stronger the depletion. This clearly highlights the benefits of diversifying the pool of harvested species not only at one cutting cycle, but also for changing this pool in time, so that different species are harvested across different cutting cycles. Indeed, the commercial volume recovery is low in the case of a restrictive pool of commercial species (*e.g.* less than $6\,m^3\,ha^{-1}$ after 65 yr in Paracou if only 20% of the total volume is commercial). At the 2nd harvest the available commercial volume will be too low, such that harvesting the same forest stands several times will inevitably mean changing the pool of harvested species at the 2nd harvest.

3.6. Applying the VDDE model to assess timber availability in human-modified forests under climate change

Tropical forests are not spared from ongoing global changes (Malhi et al., 2014): most tropical forests undergo increasing disturbance regimes such as fires, logging, or drought (Lewis et al., 2015). Today, the so-called intact forest landscape in the tropics has been reduced to 20% of the tropical forest area (Potapov et al., 2017), and this proportion is likely to continue decreasing. Future climate is predicted to be hotter and seasonally drier in most tropical landscapes (Stocker, 2014), provoking a decrease in biomass through the increase of tree mortality (Allen et al., 2010). In Amazonian forests, this continuous increase in tree mortality has already been described (Brienen et al., 2015). Within our modeling framework, an increased disturbance regime will

inevitably decrease the forest maturity (we simulated a 0–100% decrease of forest maturity), and a drier climate will inevitably increase the volume mortality (Fig. 7). For instance, biomass mortality has increased by approximately 30% in Amazonian Permanent sample plots between 1985 and 2010 (Brienen et al., 2015). For a similar increase in volume mortality, total volume stocks in Paracou are predicted to decrease from 80 (68–167) to 65 (86–153) $m^3\,ha^{-1}$, *i.e.* a 19% decrease (numbers between brackets are the 95% credibility interval). And if those forests also suffer from increasing disturbances and their forest maturity subsequently decreases, for example by 40%, then the total volume would be 47 (40–100) $m^3\,ha^{-1}$, *i.e.* a 41% decrease. The combined effect of an increase of mortality and of the disturbance regime could thus seriously lower available timber resource in tropical forests. This has to be taken into account for future scenarios of timber provision in increasingly human-modified forests.

4. Conclusion

In this study we present an original modelling approach of timber volume recovery in tropical forests. As a case study, we assess the volume recovery potential of a selectively logged forest in French Guiana. We show that under current conditions, selective logging is not sustainable insofar as the commercial volume, which is the main productive value of a logged forest, is not recovered at the end of a typical logging cycle. We also predict timber availability in the case of an increase mortality and a decrease of forest maturity, that will likely be triggered by future climate change and human disturbances such as fires, clearcuts and logging. The main advantages of the modelling framework presented here are threefold: (i) it can be calibrated with widely available data (*i.e.* the volume of trees ≥50 cm DBH), (ii) it can explicitly integrate the effect of disturbances and (iii) it is generic enough to be applied for instance to carbon stocks. To provide meaningful insights to forest managers and policy makers, this model should now be applied to a larger scale, integrating data from permanent forest plots as well as national forest inventories.

Availability of data and materials

Data and R codes will be made available on an online repository.

Competing interests

The authors declare no competing interest.

Funding

This study was partially funded by the GFclim project (FEDER 20142020, Project GY0006894), an Investissement dAvenir grant of the ANR (CEBA: ANR-10-LABEX-0025) and carried out in the framework of the Tropical managed Forests Observatory (TmFO), supported by the Sentinel Landscape program of CGIAR (Consultative Group on International Agricultural Research) – Forest Tree and Agroforestry Research Program.

Author's contributions

Acquisition of data: BH. Conception & design: CP, BH. Model Development: CP, BH. Data analysis & interpretation: CP, BH. Drafting the manuscript: CP. Manuscript revision: BH, ER, PS, LM, GD, LD, CP.

Acknowledgements

We are in debt with all technicians and colleagues who helped setting up the plots and collecting data over years. Without their precious work, this study would not have been possible and they may be warmly thanked here. We would also like to thank the 2 anonymous reviewers for their in-depth reading and valuable comments.

Appendix A. Proportion of commercial volume

Figs. A1–A3

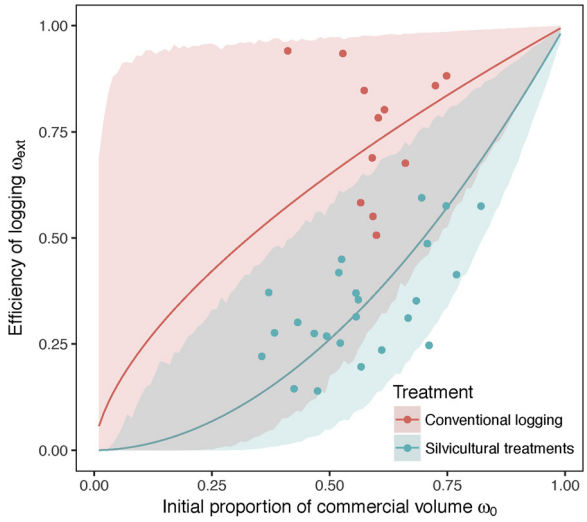

Fig. A1. Efficiency of selective logging ωext as a function of the proportion of commercial species ω_0. The efficiency of logging $\omega ext = \frac{Vext}{\delta V}$ was modelled as $\omega ext = {\omega_0}^{1-\psi}$, and the model was calibrated for subplots (4 subplots by plot, 1.5625 ha each) that underwent conventional logging (red dots) and intensive logging with timber stand improvement (green dots). The red and green lines are the maximum likelihood prediction of the model for conventional logging and silvicultural treatments resp., and the shaded areas are the 95% credibility intervals.

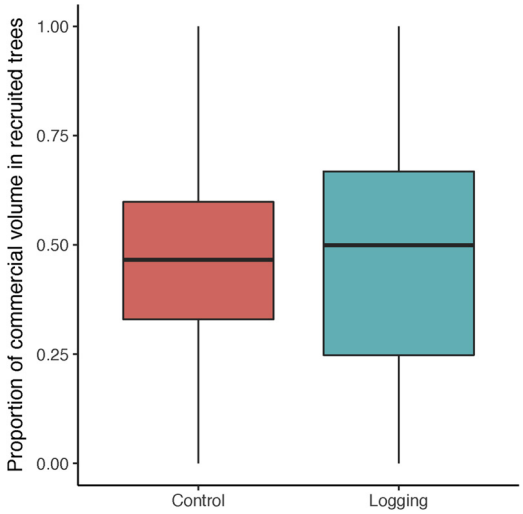

Fig. A2. Comparison of the proportion of commercial volume in recruited trees in control plots and conventionally logged plots in Paracou.

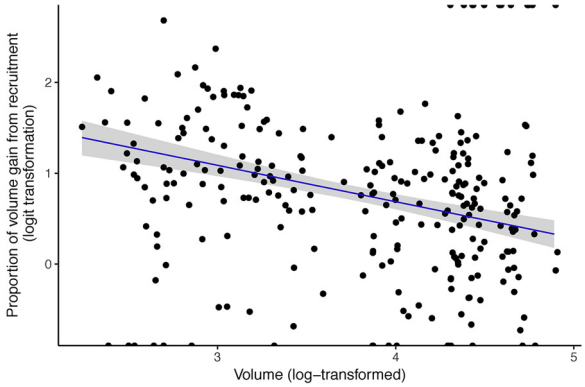

Fig. A3. Proportion of volume gain from recruitment (*pR*, on the *y*-axis, after a logit-transformation) as a function of the total volume (*x*-axis, after log-transformation). Dots are observations in Paracou, the blue line is the linear model prediction, and the shaded area is the associated 95% credibility interval. (For interpretation of the references to color in this figure legend, the reader is referred to the web version of this article.)

Appendix B. Goodness of fit

Fig. B4

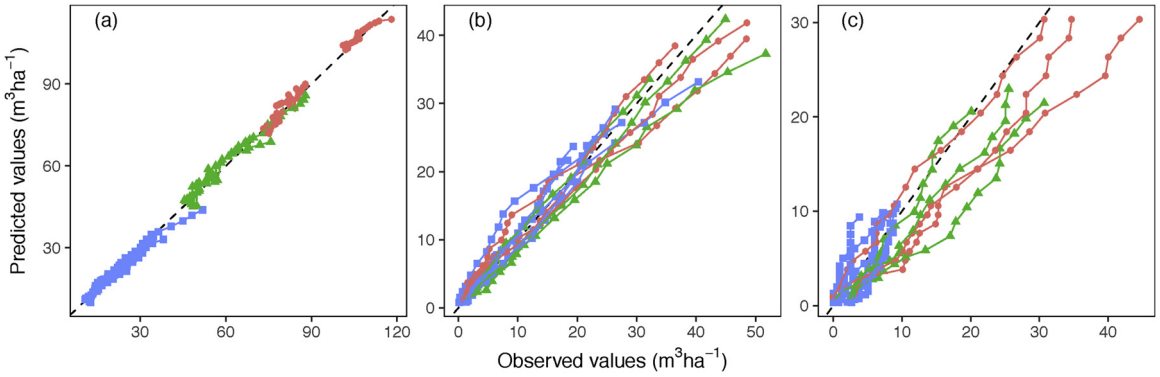

Fig. B4. Goodness of fit of the model predictions to Paracou data. Observed values of (a) total volume, (b) cumulative volume gain, (c) cumulative volume mortality are on the *x*-axis, while the predicted values are on the *y*-axis. Red dots are control plots, green triangles are logged plots and blue squares are logged plots with silvicultural treatments (poison gridling and fuelwood harvest). (For interpretation of the references to color in this figure legend, the reader is referred to the web version of this article.)

Appendix C. 95% credibility intervals of simulation predictions

Figs. C5 and C6

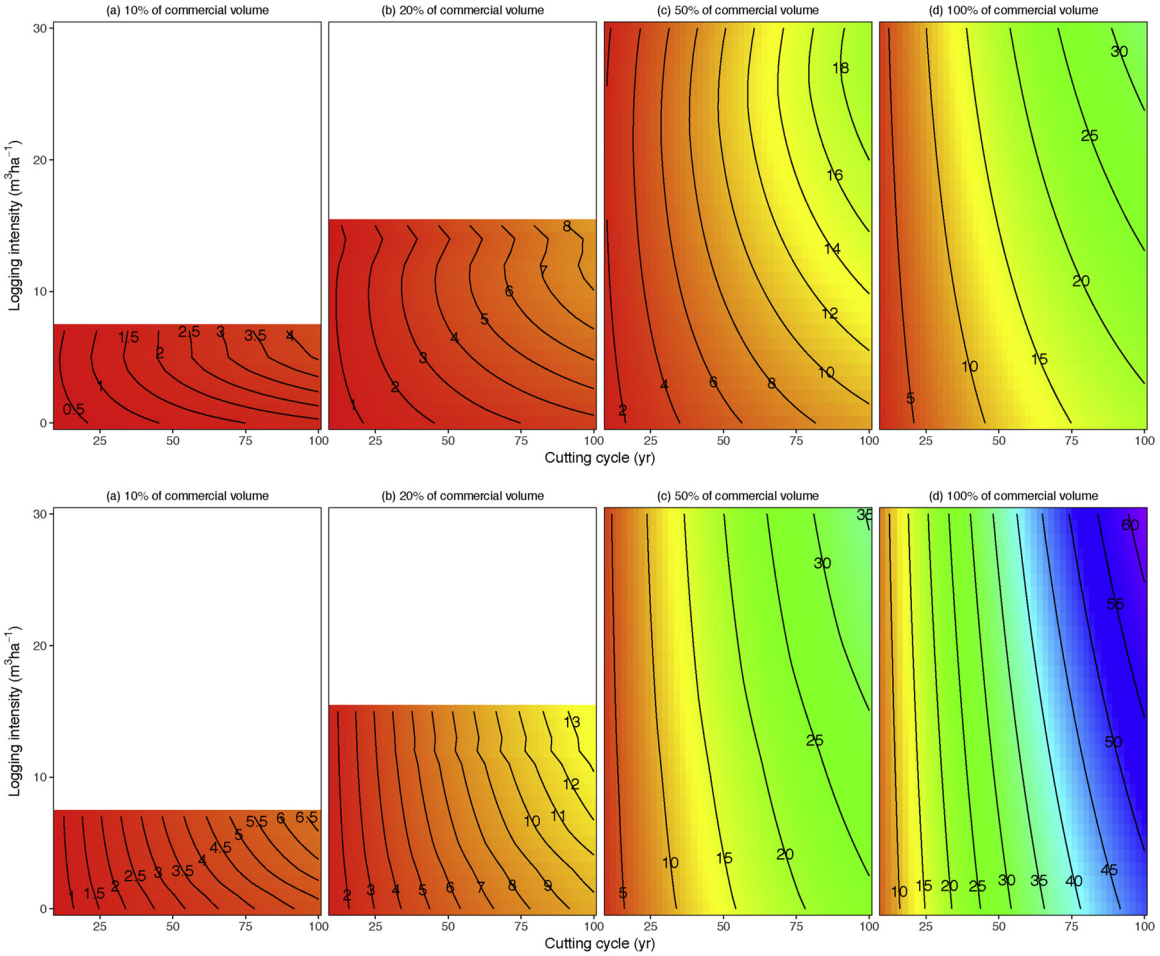

Fig. C5. 95% credibility interval of commercial volume recovered at the end of the cutting cycle ($m^3\,ha^1$) as a function of cutting cycle length (in years), logging intensity ($m^3\,ha^1$), and initial fraction of commercial species (%), in Paracou conditions. All other parameters are set to their maximum likelihood value. (a) Lower bound (2.5th percentile); (b) upper bound (97.5th percentile). In each panel, the colours and level lines represent the commercial volume recovered at the end of the cutting cycle. The proportion of commercial species increases from left to right: it is lowest in extreme-left panels (10% of total volume belongs to commercial species) and highest in extreme-right panels (100% of total volume). In all panels, the *x*-axis represents the cutting cycle length; the *y*-axis represents the logging intensity, i.e. the volume of all trees killed during logging operations ($m^3\,ha^1$). (For interpretation of the references to color in this figure legend, the reader is referred to the web version of this article.)

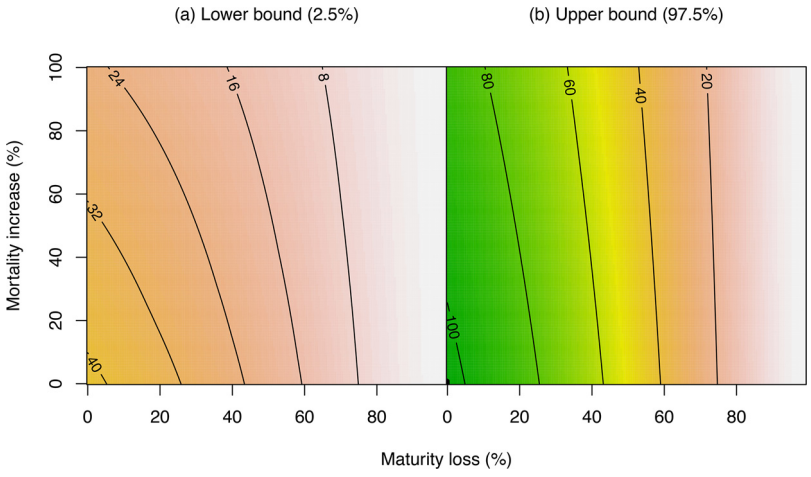

Fig. C6. 95% credibility interval of total volume ($m^3\,ha^1$) in scenarios with an increase of volume mortality (in % of current mortality in Paracou, *y*-axis) and a decrease of the forest maturity (in % of current mean forest maturity in Paracou, *x*-axis). All other parameters are set to their maximum likelihood value. (a) Lower bound (2.5th percentile); (b) upper bound (97.5th percentile). In each panel, the colors and level lines represent the total volume. (For interpretation of the references to color in this figure legend, the reader is referred to the web version of this article.)

Appendix D. Extensive equation material

D.1 Solving the differential equation (8)

According to Eq. (8) we have:

$$\frac{\mathrm{dV}(t)}{\mathrm{dt}} = \alpha_G(1 - e^{-\beta_G t}) - \theta V(t) - \alpha_M(1 - e^{-\beta_M t})$$

Let's solve the nonhomogeneous differential equation of 1st order:

$$\frac{\mathrm{dV}(t)}{\mathrm{dt}} + \theta V(t) = \alpha_G(1 - e^{-\beta_G t}) - \alpha_M(1 - e^{-\beta_M t}) \tag{D.1}$$

We define $u(t) = e^{\theta t}$.
We have:

$$\begin{aligned}(u(t) \times V(t))' &= u'(t) \times V(t) + u(t) \times V'(t)\\ &= \theta e^{\theta t} \times V(t) + e^{\theta t} \times \frac{\mathrm{dV}(t)}{\mathrm{dt}}\\ &= u(t)\left(\frac{\mathrm{dV}(t)}{\mathrm{dt}} + \theta V(t)\right)\\ (u(t) \times V(t))' &= u(t)(\alpha_G(1 - e^{-\beta_G t}) - \alpha_M(1 - e^{-\beta_M t}))\end{aligned} \tag{D.2}$$

Thus:

$$\begin{aligned}u(t) \times V(t) &= \int e^{\theta t}(\alpha_G(1 - e^{-\beta_G t}) - \alpha_M(1 - e^{-\beta_M t}))\mathrm{dt}\\ &= \alpha_G\left(\frac{e^{\theta t}}{\theta} - \frac{e^{(\theta-\beta_G)t}}{\theta-\beta_G}\right) - \alpha_M\left(\frac{e^{\theta t}}{\theta} - \frac{e^{(\theta-\beta_M)t}}{\theta-\beta_M}\right) + K\\ e^{\theta t} \times V(t) &= e^{\theta t}\left(\alpha_G\left(\frac{1}{\theta} - \frac{e^{-\beta_G t}}{\theta-\beta_G}\right) - \alpha_M\left(\frac{1}{\theta} - \frac{e^{-\beta_M t}}{\theta-\beta_M}\right) + K \times e^{-\theta t}\right)\end{aligned} \tag{D.3}$$

with K a constant, and $\beta_G \neq \theta \neq \beta_M$. Because $V(0) = 0$ (see Eq. (8)), we get:

$$\begin{cases} V(t) = \alpha_G\left(\frac{1}{\theta} - \frac{e^{-\beta_G t}}{\theta-\beta_G}\right) - \alpha_M\left(\frac{1}{\theta} - \frac{e^{-\beta_M t}}{\theta-\beta_M}\right) + K \times e^{-\theta t}\\ V(0) = 0 \end{cases} \tag{D.4}$$

And thus:

$$K = \alpha_G\left(\frac{1}{\theta - \beta_G} - \frac{1}{\theta}\right) - \alpha_M\left(\frac{1}{\theta - \beta_M} - \frac{1}{\theta}\right) \tag{D.5}$$

$$V(t) = \frac{\alpha_G}{\theta}\left(1 - \frac{\theta e^{-\beta_G t} - \beta_G e^{-\theta t}}{\theta - \beta_G}\right) - \frac{\alpha_M}{\theta}\left(1 - \frac{\theta e^{-\beta_M t} - \beta_M e^{-\theta t}}{\theta - \beta_M}\right) \tag{D.6}$$

$$\begin{cases} g(t) = \frac{\alpha_G\beta_G}{\theta-\beta_G}(e^{-\beta_G t} - e^{-\theta t}) + \alpha_M\left(1 - \frac{\theta e^{-\beta_M t} - \beta_M e^{-\theta t}}{\theta - \beta_M}\right)\\ m(t) = \alpha_M(1 - e^{-\beta_M t}) \end{cases} \tag{D.7}$$

D.2 Additional constraints on the model parameters

We have the natural constraint: $\forall t \geq 0$, $V(t) \geq 0$. We here develop the few steps that allowed us to translate this inequality into contraints on the model parameters. To do so we studied the function $V(t)$ limits when $t \to +\infty$ and when $t \to 0$.

Because $\theta > 0$, $\alpha_G > 0$ and $\alpha_M > 0$, we have:

$$\lim_{t\to+\infty}(e^{-\beta_G t}) = \lim_{t\to+\infty}(e^{-\beta_M t}) = \lim_{t\to+\infty}(e^{-\theta t}) = 0 \tag{D.8}$$

$$\begin{aligned}\Rightarrow \lim_{t\to\infty} V(t) &= \frac{\alpha_G}{\theta}(1 - 0) - \frac{\alpha_M}{\theta}(1 - 0)\\ \lim_{t\to\infty} V(t) &= \frac{\alpha_G - \alpha_M}{\theta}\end{aligned} \tag{D.9}$$

$$\lim_{t\to\infty} V(t) \geq 0 \Leftrightarrow \alpha_G \geq \alpha_M \tag{D.10}$$

When $t = 0$, there is no volume (by definition): $V(0) = 0$. Consequently, for the volume to take positive values near $t = 0$, we must have $\frac{\mathrm{dV}}{\mathrm{dt}} \geq 0$ near $t = 0$ (i.e. the volume can only increase, else it will take negative values, which is absurd).

$$\begin{aligned}\frac{dV}{dt} &= g(t) - m(t)\\ &= \alpha_G(1 - e^{-\beta_G t}) - \theta V(t) - \alpha_M(1 - e^{-\beta_M t})\\ &= \alpha_G(1 - e^{-\beta_G t}) - \alpha_M(1 - e^{-\beta_M t}) - \alpha_G\left(1 - \frac{\theta e^{-\beta_G t} - \beta_G e^{-\theta t}}{\theta - \beta_G}\right)\\ &+ \alpha_M\left(1 - \frac{\theta e^{-\beta_M t} - \beta_M e^{-\theta t}}{\theta - \beta_M}\right)\\ &= e^{-\beta_G t}\left(\frac{\alpha_G\beta_G}{\theta - \beta_G}\right) - e^{-\beta_M t}\left(\frac{\alpha_M\beta_M}{\theta - \beta_M}\right) - e^{-\theta t}\left(\frac{\alpha_G\beta_G}{\theta - \beta_G} - \frac{\alpha_M\beta_M}{\theta - \beta_M}\right)\end{aligned} \tag{D.11}$$

By using the Taylor series (of order 1) of the exponential function when $t \to 0$, we get:

$$\begin{aligned}\frac{dV}{dt} &\sim -t \times \beta_G\left(\frac{\alpha_G\beta_G}{\theta - \beta_G}\right) + t \times \beta_M\left(\frac{\alpha_M\beta_M}{\theta - \beta_M}\right) + t \times \theta\left(\frac{\alpha_G\beta_G}{\theta - \beta_G} - \frac{\alpha_M\beta_M}{\theta - \beta_M}\right)\\ \frac{dV}{dt} &\sim t \times (\alpha_G\beta_G - \alpha_M\beta_M)\end{aligned} \tag{D.12}$$

To have an increase in volume (and thus $V(t) \geq 0$) when $t \geq 0$ is close to 0, we must have:

$$\alpha_G \times \beta_G \geq \alpha_M \times \beta_M \tag{D.13}$$

Appendix E. Additional tables

Tables E1 and E2

Table E1
Parameters prior distribution.

Parameter	Prior distribution	Justification
t_0	$\mathscr{U}[100, 300]$	Expected maturity in Paracou
vmax	$\mathscr{U}[\max(V), 3\max(V)]$	*vmax* must be bigger than the max. observed volume, and can harldy be more than 3 times as much
α_M	$\mathscr{U}[0.5, 5]$	Range of observed values for biomass mortality in the Guiana Shield (Johnson et al., 2016) divided by 1.5 (2: carbon:biomass ratio × 0.75: mean wood density in Paracou)
β_G	$\mathscr{U}[0.005, 0.05]$	$60 < t_{95} < 600$[a] yr
β_M	$\mathscr{U}[0.001, \beta_G \times \frac{\alpha_G}{\alpha_M}]$	$t_{95} > 3000$[a] yr and slower than growth
θ	$\mathscr{U}[0.005, 0.05]$	Respiration < $max(vmax) \times 0.05 = 17\ m^3\ ha^{-1}\ yr^{-1}$
ω_0	$\mathcal{N}(0, 0.001)$	Uninformative prior
ω_1	$\mathcal{N}_{]-\infty,0]}(0, 0.001)$[b]	Negative: *pR* decreases when the volume increases
σ_V	$\mathcal{N}_{[0,2]}(0, 1)$	Positive variance
σ_G	$\mathcal{N}_{[0,2]}(0, 1)$	Positive variance
σ_M	$\mathcal{N}_{[0,2]}(0, 1)$	Positive variance
σ_R	$\mathcal{N}_{[0,+\infty[}(0, 1)$	Positive variance

[a] $t_{0.95}$ is the time when the volume change has reached 95% of its asymptotic value.
[b] $\mathcal{N}_{[a,b]}$ is the normal distribution truncated in [a,b].

Table E2
List of commercial species in Paracou.

Local name	Scientific name	Proportion of initial volume (%)	Proportion of logged volume (%)
Gonfolo	*Qualea rosea*	2.71	26.98
Wapa	*Eperua falcata*	7.96	12.74
Grignon franc	*Sextonia rubra*	1.92	12.53
Angélique	*Dicorynia guianensis*	2.31	9.19
Manil	*Moronobea coccinea*	1.00	4.47
Chawari	*Caryocar glabrum*	0.94	3.86
Wakapu	*Vouacapoua americana*	3.07	2.77
Asao	*Albizia pedicellaris*	0.50	2.38
Maho cigare	*Couratari multiflora*	1.01	1.93
Diagidia	*Tachigali melinonii*	0.79	1.78
Saint martin rouge	*Andira coriacea*	0.46	1.76
Balata pomme	*Chrysophyllum sanguinolentum*	1.17	1.64
Maho cochon	*Sterculia pruriens*	0.98	1.57
Goupi	*Goupia glabra*	1.17	1.40
Dodomisinga	*Parkia nitida*	0.65	1.36
Busi kanambuli	*Simaba sp.*	0.32	1.23
Yayamadou marcage	*Virola surinamensis*	0.31	1.13

(*continued on next page*)

Table E2 (*continued*)

Local name	Scientific name	Proportion of initial volume (%)	Proportion of logged volume (%)
Wakapu gitin	*Recordoxylon speciosum*	0.90	1.04
Parcouri	*Platonia insignis*	0.34	0.98
Alimiao	*Pseudopiptadenia suaveolens*	0.12	0.95
Cèdre	*Ocotea argyrophylla*	0.26	0.84
Balata franc	*Manilkara bidentata*	0.37	0.73
Acacia franc	*Enterolobium schomburgkii*	0.28	0.56
Maho coton	*Pachira dolichocalyx*	0.27	0.53
Inkasa	*Vataireopsis surinamensis*	0.05	0.48
Boco	*Bocoa prouacensis*	2.22	0.45
Kwata kaman	*Parkia pendula*	0.08	0.43
Kaiman udu	*Laetia procera*	0.13	0.41
Bois saint jean	*Protium opacum*	0.17	0.38
Encens	*Schefflera decaphylla*	0.98	0.38
Cèdre cannelle	*Licaria cannella*	0.08	0.34
Dokali	*Brosimum utile*	0.13	0.33
Lebi sali	*Trichilia schomburgkii*	0.18	0.30
Coeur dehors	*Diplotropis purpurea*	0.17	0.29
Kumanti udu	*Aspidosperma sp.*	0.22	0.26
Mapa	*Lacmellea aculeata*	0.24	0.25
Wana kwali	*Vochysia tomentosa*	0.06	0.19
Kwali	*Vochysia guianensis*	0.06	0.19
Saint martin jaune	*Hymenolobium flavum*	0.03	0.16
Simarouba	*Simarouba amara*	0.05	0.16
Gaan moni	*Trattinnickia rhoifolia*	0.13	0.15
Lakasi	*Caraipa racemosa*	0.04	0.13
Canari macaque	*Lecythis zabucajo*	0.17	0.13

Appendix F. Supplementary data

Supplementary data associated with this article can be found, in the online version, at https://doi.org/10.1016/j.ecolmodel.2018.05.023.

References

Alder, D., Synnott, T., 1992. Permanent Sample Plot Techniques for Mixed Tropical Forest. Oxford Forestry Institute. http://www.fao.org/sustainable-forest-management/toolbox/tools/tool-detail/en/c/340781/.

Allen, C.D., Macalady, A.K., Chenchouni, H., Bachelet, D., McDowell, N., Vennetier, M., Kitzberger, T., Rigling, A., Breshears, D.D., Hogg, E.T., Gonzalez, P., Fensham, R., Zhang, Z., Castro, J., Demidova, N., Lim, J.-H., Allard, G., Running, S.W., Semerci, A., Cobb, N., 2010. A global overview of drought and heat-induced tree mortality reveals emerging climate change risks for forests. For. Ecol. Manag. 259 (4), 660–684. http://dx.doi.org/10.1016/j.foreco.2009.09.001. arXiv:1011.1669v3.

Asner, G.P., Keller, M., Pereira, R., Zweede, J.C., 2002. Remote sensing of selective logging in Amazonia. Remote Sens. Environ. 80 (3), 483–496. http://dx.doi.org/10.1016/S0034-4257(01)00326-1.

Balieiro, M.R., Espada, A.L.V., Nogueira, O., Palmieri, R., Lentini, M., 2010. As Concessoes de Florestas Públicas na Amazônia Brasileira. http://www.fundovale.org/wp-content/uploads/2016/01/Concessoes-Florestais_ift_imaflora.pdf.

Bawa, K.S., Seidler, R., 1998. Natural forest management and conservation of biodiversity in tropical forests. Conserv. Biol. 12 (1), 46–55. http://dx.doi.org/10.1046/j.1523-1739.1998.96480.x.

Berger, U., Rivera-Monroy, V.H., Doyle, T.W., Dahdouh-Guebas, F., Duke, N.C., Fontalvo-Herazo, M.L., Hildenbrandt, H., Koedam, N., Mehlig, U., Piou, C., Twilley, R.R., 2008. Advances and limitations of individual-based models to analyze and predict dynamics of mangrove forests: a review. Aquat. Bot. 89 (2), 260–274. http://dx.doi.org/10.1016/j.aquabot.2007.12.015. http://linkinghub.elsevier.com/retrieve/pii/S0304377008000090.

Blanc, L., Echard, M., Herault, B., Bonal, D., Marcon, E., Chave, J., Baraloto, C., 2009. Dynamics of aboveground carbon stocks in a selectively logged tropical forest. Ecol. Appl. 19 (6), 1397–1404. http://dx.doi.org/10.1890/08-1572.1.

Blaser, J., Sarre, A., Poore, D., Johnson, S., 2011. Status of Tropical Forest Management 2011, Tech. rep. http://www.itto.int/news_releases/id=2663.

Bossu, J., Beauchêne, J., Estevez, Y., Duplais, C., Clair, B., 2016. New insights on wood dimensional stability influenced by secondary metabolites: the case of a fast-growing tropical species *Bagassa guianensis* Aubl. PLOS ONE 11 (3). http://dx.doi.org/10.1371/journal.pone.0150777.

Brando, P.M., Balch, J.K., Nepstad, D.C., Morton, D.C., Putz, F.E., Coe, M.T., Silverio, D., Macedo, M.N., Davidson, E.A., Nobrega, C.C., Alencar, A., Soares-Filho, B.S., 2014. Abrupt increases in Amazonian tree mortality due to drought-fire interactions. Proc. Natl. Acad. Sci. 111 (17), 6347–6352. http://dx.doi.org/10.1073/pnas.1305499111.

Brienen, R.J.W., Phillips, O.L., Feldpausch, T.R., Gloor, E., Baker, T.R., Lloyd, J., Lopez-Gonzalez, G., Monteagudo-Mendoza, A., Malhi, Y., Lewis, S.L., Vásquez Martinez, R., Alexiades, M., Álvarez Dávila, E., Alvarez-Loayza, P., Andrade, A., Arag ao, L.E.O.C., Araujo-Murakami, A., Arets, E.J.M.M., Arroyo, L., Aymard, G.A., Bánki, C.O.S., Baraloto, C., Barroso, J., Bonal, D., Boot, R.G.A., Camargo, J.L.C., Castilho, C.V., Chama, V., Chao, K.J., Chave, J., Comiskey, J.A., Cornejo Valverde, F., da Costa, L., de Oliveira, E.A., Di Fiore, A., Erwin, T.L., Fauset, S., Forsthofer, M., Galbraith, D.R., Grahame, E.S., Groot, N., Hérault, B., Higuchi, N., Honorio Coronado, E.N., Keeling, H., Killeen, T.J., Laurance, W.F., Laurance, S., Licona, J., Magnussen, W.E., Marimon, B.S., Marimon-Junior, B.H., Mendoza, C., Neill, D.A., Nogueira, E.M., Nú nez, P., Pallqui Camacho, N.C., Parada, A., Pardo-Molina, G., Peacock, J., Pe na-Claros, M., Pickavance, G.C.N., 2015. Long-term decline of the Amazon carbon sink. Nature 519 (7543), 344–348. http://dx.doi.org/10.1038/nature14283. http://www.scopus.com/inward/record.url?eid=2-s2.0-84925302004&partnerID=tZOtx3y1, http://www.scopus.com/inward/record.url?eid=2-s2.0-84925302004%7B&%7DpartnerID=tZOtx3y1.

Burivalova, Z., Sekercioglu, Ç.H., Koh, L.P., 2014. Thresholds of logging intensity to maintain tropical forest biodiversity. Curr. Biol. 24 (16), 1893–1898. http://dx.doi.org/10.1016/j.cub.2014.06.065. http://linkinghub.elsevier.com/retrieve/pii/S0960982214007829.

Cannon, C.H., Peart, D.R., Leighton, M., Kartawinata, K., Leighton, M., Peart David, R., 1994. The structure of lowland rainforest after selective logging in West Kalimantan, Indonesia. For. Ecol. Manag. 67 (1–3), 49–68. http://dx.doi.org/10.1016/0378-1127(94)90007-8. http://www.sciencedirect.com/science/article/pii/0378112794900078%5Cnhttp://ac.els-cdn.com/0378112794900078/1-s2.0-0378112794900078-main.pdf?_tid=5f25b186-940b-11e3-81e7-00000aacb35f&acdnat=1392226411%_924eea2edad54c40bba98edf7f52d5b1.

Carpenter, B., Gelman, A., Hoffman, M.D., Lee, D., Goodrich, B., Betancourt, M., Brubaker, M., Guo, J., Li, P., Riddell, A., 2015. Stan: a probabilistic programming language. J. Stat. Softw. 76 (1). http://dx.doi.org/10.18637/jss.v076.i01. http://www.jstatsoft.org/v76/i01/.

Chambers, J.Q.J., Negron-Juarez, R.I.R., Marra, D.M.D.D.M., Di Vittorio, A., Tews, J., Roberts, D., Ribeiro, G.H.P.M.G., Trumbore, S.E.S., Higuchi, N., 2013. The steady-state mosaic of disturbance and succession across an old-growth Central Amazon forest landscape. Proc. Natl. Acad. Sci. U. S. A. 110 (10), 3949–3954. http://dx.doi.org/10.1073/pnas.1202894110. http://www.pubmedcentral.nih.gov/articlerender.fcgi?artid=3593828&tool=pmcentrez&rendertype=abstract.

Chave, J., Coomes, D., Jansen, S., Lewis, S.L., Swenson, N.G., Zanne, A.E., 2009. Towards a worldwide wood economics spectrum. Ecol. Lett. 12 (4), 351–366. http://dx.doi.org/10.1111/j.1461-0248.2009.01285.x.

Chen, W., Chen, J.M., Price, D.T., Cihlar, J., 2002. Effects of stand age on net primary productivity of boreal black spruce forests in Ontario, Canada. Can. J. For. Res. 32 (5), 833–842. http://dx.doi.org/10.1139/x01-165.

Condit, R., Hubbell, S.P., Foster, R.B., 1993. Identifying fast-growing native trees from the neotropics using data from a large, permanent census plot. For. Ecol. Manage. 62

(1–4), 123–143. http://dx.doi.org/10.1016/0378-1127(93)90046-Pc.
de Avila, A.L., Ruschel, A.R., de Carvalho, J.O.P., Mazzei, L., Silva, J.N.M., Lopes, J.D.C., Araujo, M.M., Dormann, C.F., Bauhus, J., 2015. Medium-term dynamics of tree species composition in response to silvicultural intervention intensities in a tropical rain forest. Biol. Conserv. 191, 577–586. http://dx.doi.org/10.1016/j.biocon.2015.08.004.
R Development Core Team, 2008. Computational Many-Particle Physics. R Foundation for Statistical Computing 739, pp. 409. http://dx.doi.org/10.1007/978-3-540-74686-7. http://www.r-project.org/%5Cnhttp://www.r-project.org.
Edwards, D.P., Tobias, J.A., Sheil, D., Meijaard, E., Laurance, W.F., 2014. Maintaining ecosystem function and services in logged tropical forests. Trends Ecol. Evol. 29 (9), 511–520. http://dx.doi.org/10.1016/j.tree.2014.07.003.
Espírito-Santo, F.D., Gloor, M., Keller, M., Malhi, Y., Saatchi, S., Nelson, B., Junior, R.C.O., Pereira, C., Lloyd, J., Frolking, S., Palace, M., Shimabukuro, Y.E., Duarte, V., Mendoza, A.M., López-González, G., Baker, T.R., Feldpausch, T.R., Brienen, R.J., Asner, G.P., Boyd, D.S., Phillips, O.L., 2014. Size and frequency of natural forest disturbances and the Amazon forest carbon balance. Nat. Commun. 5, 3434. http://dx.doi.org/10.1038/ncomms4434. http://www.ncbi.nlm.nih.gov/pubmed/24643258.
Fargeon, H., Aubry-Kientz, M., Brunaux, O., Descroix, L., Gaspard, R., Guitet, S., Rossi, V., Hérault, B., 2016. Vulnerability of commercial tree species to water stress in logged forests of the Guiana shield. Forests 7 (12), 105. http://dx.doi.org/10.3390/f7050105. http://www.mdpi.com/1999-4907/7/5/105.
Fick, S.E., Hijmans, R.J., 2017. WorldClim 2: new 1-km spatial resolution climate surfaces for global land areas. Int. J. Climatol. 4315 (May), 4302–4315. http://dx.doi.org/10.1002/joc.5086.
Fischer, R., Bohn, F., Dantas de Paula, M., Dislich, C., Groeneveld, J., Gutiérrez, A.G., Kazmierczak, M., Knapp, N., Lehmann, S., Paulick, S., Pütz, S., Rödig, E., Taubert, F., Köhler, P., Huth, A., 2016. Lessons learned from applying a forest gap model to understand ecosystem and carbon dynamics of complex tropical forests. Ecol. Model. 326, 124–133. http://dx.doi.org/10.1016/j.ecolmodel.2015.11.018.
Frolking, S., Palace, M.W., Clark, D.B., Chambers, J.Q., Shugart, H.H., Hurtt, G.C., 2009. Forest disturbance and recovery: a general review in the context of spaceborne remote sensing of impacts on aboveground biomass and canopy structure. J. Geophys. Res.: Biogeosci. 114 (3). http://dx.doi.org/10.1029/2008JG000911. n/a-n/a.
Gourlet-Fleury, S., Guehl, J.-M., Laroussinie, O., 2004. Ecology and Management of a Neotropical Rainforest: Lessons Drawn from Paracou, a Long-Term Experimental Research Site in French Guiana. Elsevier. http://agritrop.cirad.fr/522004/.
Gourlet-Fleury, S., Blanc, L., Picard, N., Sist, P., Dick, J., Nasi, R., Swaine, M.D., Forni, E., 2005a. Grouping species for predicting mixed tropical forest dynamics: looking for a strategy. Ann. For. Sci. 62 (8), 785–796. http://dx.doi.org/10.1051/forest:2005084.
Gourlet-Fleury, S., Cornu, G., Jésel, S., Dessard, H., Jourget, J.-G., Blanc, L., Picard, N., 2005b. Using models to predict recovery and assess tree species vulnerability in logged tropical forests: a case study from French Guiana. For. Ecol. Manag. 209 (1-2), 69–85. http://dx.doi.org/10.1016/j.foreco.2005.01.010. http://linkinghub.elsevier.com/retrieve/pii/S0378112705000149.
Grau, O., Peñuelas, J., Ferry, B., Freycon, V., Blanc, L., Desprez, M., Baraloto, C., Chave, J., Descroix, L., Dourdain, A., Guitet, S., Janssens, I.A., Sardans, J., Hérault, B., 2017. Nutrient-cycling mechanisms other than the direct absorption from soil may control forest structure and dynamics in poor Amazonian soils. Sci. Rep. 7 (March), 45017. http://dx.doi.org/10.1038/srep45017.
Grimm, V., 2005. Pattern-oriented modeling of agent-based complex systems: lessons from ecology. Science 310 (5750), 987–991. http://dx.doi.org/10.1126/science.1116681. arXiv:1011.1669v3.
Guitet, S., Brunaux, O., Traissac, S., April 2016. Sylviculture pour la production de bois d'oeuvre des forêts du Nord de la Guyane. http://www.onf.fr/guyane/++oid++57df/@@display_media.html.
Hérault, B., Piponiot, C., 2018. Key drivers of ecosystem recovery after disturbance in a neotropical forest. For. Ecosyst. 5 (1), 2. http://dx.doi.org/10.1186/s40663-017-0126-7.
He, L., Chen, J.M., Pan, Y., Birdsey, R., Kattge, J., 2012. Relationships between net primary productivity and forest stand age in U.S. forests. Glob. Biogeochem. Cycles 26 (3), 1–19. http://dx.doi.org/10.1029/2010GB003942.
Hengl, T., de Jesus, J.M., MacMillan, R.A., Batjes, N.H., Heuvelink, G.B.M., Ribeiro, E., Samuel-Rosa, A., Kempen, B., Leenaars, J.G.B., Walsh, M.G., Gonzalez, M.R., 2014. SoilGrids1km – global soil information based on automated mapping. PLOS ONE 9 (8), e105992. http://dx.doi.org/10.1371/journal.pone.0105992.
Holdsworth, A.R., Uhl, C., 1997. Fire in Amazonian selectively logged rain forest and the potential for fire reduction. Ecol. Appl. 7 (2), 713. http://dx.doi.org/10.2307/2269533. http://www.jstor.org/stable/2269533?origin=crossref.
Huth, A., Ditzer, T., 2001. Long-term impacts of logging in a tropical rain forest – a simulation study. For. Ecol. Manag. 142 (1–3), 33–51. http://dx.doi.org/10.1016/S0378-1127(00)00338-8. http://linkinghub.elsevier.com/retrieve/pii/S0378112700003388.
ITTO, 1992. Criteria for the Measurement of Sustainable Forest Management. http://www.itto.int/resource04/.
Johnson, M.O., Galbraith, D., Gloor, M., De Deurwaerder, H., Guimberteau, M., Rammig, A., Thonicke, K., Verbeeck, H., von Randow, C., Monteagudo, A., Phillips, O.L., Brienen, R.J.W., Feldpausch, T.R., Lopez Gonzalez, G., Fauset, S., Quesada, C.A., Christoffersen, B., Ciais, P., Sampaio, G., Kruijt, B., Meir, P., Moorcroft, P., Zhang, K., Alvarez-Davila, E., Alves de Oliveira, A., Amaral, I., Andrade, A., Aragao, L.E.O.C., Araujo-Murakami, A., Arets, E.J.M.M., Arroyo, L., Aymard, G.A., Baraloto, C., Barroso, J., Bonal, D., Boot, R., Camargo, J., Chave, J., Cogollo, A., Cornejo Valverde, F., Lola da Costa, A.C., Di Fiore, A., Ferreira, L., Higuchi, N., Honorio, E.N., Killeen, T.J., Laurance, S.G., Laurance, W.F., Licona, J., Lovejoy, T., Malhi, Y., Marimon, B., Marimon, B.H., Matos, D.C.L., Mendoza, C., Neill, D.A., Pardo, G., Peña-Claros, M., Pitman, N.C.A., Poorter, L., Prieto, A., Ramirez-Angulo, H., Roopsind, A., Rudas, A., Salomao, R.P., Silveira, M., Stropp, J., ter Steege, H., Terborgh, J., Thomas, R., T, M., 2016. Variation in stem mortality rates determines patterns of above-ground biomass in Amazonian forests: implications for dynamic global vegetation models. Glob. Change Biol. 22 (12), 3996–4013. http://dx.doi.org/10.1111/gcb.13315.
Kammesheidt, L., Kohler, P., Huth, A., 2001. Sustainable timber harvesting in Venezuela: a modelling approach. J. Appl. Ecol. 38 (4), 756–770. http://dx.doi.org/10.1046/j.1365-2664.2001.00629.x.
Keller, M., Palace, M., Asner, G.P., Pereira, R., Silva, J.N.M., 2004. Coarse woody debris in undisturbed and logged forests in the eastern Brazilian Amazon. Glob. Change Biol. 10 (5), 784–795. http://dx.doi.org/10.1111/j. 1529-8817.2003.00770.x.
Kiyono, Y., Saito, S., Takahashi, T., Toriyama, J., Awaya, Y., Asai, H., Furuya, N., Ochiai, Y., Inoue, Y., Sato, T., Sophal, C., Sam, P., Tith, B., Ito, E., Siregar, C.A., Matsumoto, M., 2011. Practicalities of non-destructive methodologies in monitoring anthropogenic greenhouse gas emissions from tropical forests under the influence of human intervention. Jpn. Agric. Res. Q. 45 (2), 233–242. http://dx.doi.org/10.6090/jarq.45.233. http://joi.jlc.jst.go.jp/JST.JSTAGE/jarq/45.233?from=CrossRef.
Laporte, N.T., Stabach, J.A., Grosch, R., Lin, T.S., Goetz, S.J., 2007. Expansion of industrial logging in Central Africa. Science 316 (5830), 1451. http://dx.doi.org/10.1126/science.1141057.
Laurance, W.F., Williamson, G.B., 2001. Positive feedbacks among forest fragmentation, drought, and climate change in the Amazon. Conserv. Biol. 15 (6), 1529–1535. http://dx.doi.org/10.1046/j.1523-1739.2001.01093.x.
Lewis, S.L., Edwards, D.P., Galbraith, D., 2015. Increasing human dominance of tropical forests. Science 349 (6250), 827–832. http://dx.doi.org/10.1126/science.aaa9932.
Liang, J., Picard, N., 2013. Matrix model of forest dynamics: an overview and outlook. For. Sci. 59 (3), 359–378. http://dx.doi.org/10.5849/forsci.11-123. https://academic.oup.com/forestscience/article/59/3/359-378/4583685.
Liu, S., Bond-Lamberty, B., Hicke, J.A., Vargas, R., Zhao, S., Chen, J., Edburg, S.L., Hu, Y., Liu, J., McGuire, A.D., Xiao, J., Keane, R., Yuan, W., Tang, J., Luo, Y., Potter, C., Oeding, J., 2011. Simulating the impacts of disturbances on forest carbon cycling in North America: processes, data, models, and challenges. J. Geophys. Res. 116 (4), G00K08. http://dx.doi.org/10.1029/2010JG001585.
Macpherson, A.J., Schulze, M.D., Carter, D.R., Vidal, E., 2010. A model for comparing reduced impact logging with conventional logging for an Eastern Amazonian Forest. For. Ecol. Manag. 260 (11), 2002–2011. http://dx.doi.org/10.1016/j.foreco.2010.08.050. http://linkinghub.elsevier.com/retrieve/pii/S0378112710005219.
Makela, A., Landsberg, J., Ek, A.R., Burk, T.E., Ter-Mikaelian, M., Agren, G.I., Oliver, C.D., Puttonen, P., 2000. Process-based models for forest ecosystem management: current state of the art and challenges for practical implementation. Tree Physiol. 20 (5–6), 289–298. http://dx.doi.org/10.1093/treephys/20. 5-6.289.
Malhi, Y., Gardner, T.A., Goldsmith, G.R., Silman, M.R., Zelazowski, P., 2014. Tropical forests in the Anthropocene. Annu. Rev. Environ. Resour. 39 (1), 125–159. http://dx.doi.org/10.1146/annurev-environ-030713-155141.
Malhi, Y., January 2012. The Productivity, Metabolism and Carbon Cycle of Tropical Forest Vegetation. http://dx.doi.org/10.1111/j. 1365-2745.2011.01916.x.
Maniatis, D., Mollicone, D., 2010. Options for sampling and stratification for national forest inventories to implement REDD+ under the UNFCCC. Carbon Balance Manag. 5 (1), 9. http://dx.doi.org/10.1186/1750-0680-5-9.
Pan, Y., Birdsey, R.A., Phillips, O.L., Jackson, R.B., 2013. The structure, distribution, and biomass of the world's forests. Annu. Rev. Ecol. Evol. Syst. 44 (1), 593–622. http://dx.doi.org/10.1146/annurev-ecolsys-110512-135914.
Pearson, T.R.H., Brown, S., Casarim, F.M., 2014. Carbon emissions from tropical forest degradation caused by logging. Environ. Res. Lett. 034017 (9), 11. http://dx.doi.org/10.1088/1748-9326/9/3/034017.
Pearson, T.R.H., Brown, S., Murray, L., Sidman, G., 2017. Greenhouse gas emissions from tropical forest degradation: an underestimated source. Carbon Balance Manag. 12 (1), 3. http://dx.doi.org/10.1186/s13021-017-0072-2.
Phillips, P., de Azevedo, C., Degen, B., Thompson, I., Silva, J., van Gardingen, P., 2004. An individual-based spatially explicit simulation model for strategic forest management planning in the eastern Amazon. Ecol. Model. 173 (4), 335–354. http://dx.doi.org/10.1016/j.ecolmodel.2003.09.023. http://linkinghub.elsevier.com/retrieve/pii/S030438000300423X.
Picard, N., Magnussen, S., Banak, L.N., Namkosserena, S., Yalibanda, Y., 2010. Permanent sample plots for natural tropical forests: a rationale with special emphasis on Central Africa. Environ. Monit. Assess. 164, 279–295. http://dx.doi.org/10.1007/s10661-009-0892-y.
Piponiot, C., Cabon, A., Descroix, L., Dourdain, A., Mazzei, L., Ouliac, B., Rutishauser, E., Sist, P., Hérault, B., 2016a. A methodological framework to assess the carbon balance of tropical managed forests. Carbon Balance Manag. 11 (1), 15. http://dx.doi.org/10.1186/s13021-016-0056-7.
Piponiot, C., Sist, P., Mazzei, L., Peña-Claros, M., Putz, F.E., Rutishauser, E., Shenkin, A., Ascarrunz, N., de Azevedo, C.P., Baraloto, C., França, M., Guedes, M., Honorio Coronado, E.N., D'Oliveira, M.V., Ruschel, A.R., da Silva, K.E., Doff Sotta, E., de Souza, C.R., Vidal, E., West, T.A., Hérault, B., 2016b. Carbon recovery dynamics following disturbance by selective logging in Amazonian forests. eLife 5 (C). http://dx.doi.org/10.7554/eLife.21394.
Poorter, L., Bongers, F., Aide, T.M., Almeyda Zambrano, A.M., Balvanera, P., Becknell, J.M., Boukili, V., Brancalion, P.H.S., Broadbent, E.N., Chazdon, R.L., Craven, D., de Almeida-Cortez, J.S., Cabral, G.A.L., de Jong, B.H.J., Denslow, J.S., Dent, D.H., DeWalt, S.J., Dupuy, J.M., Durán, S.M., Espírito-Santo, M.M., Fandino, M.C., César, R.G., Hall, J.S., Hernandez-Stefanoni, J.L., Jakovac, C.C., Junqueira, A.B., Kennard, D., Letcher, S.G., Licona, J.-c., Lohbeck, M., Marín-Spiotta, E., Martínez-Ramos, M., Massoca, P., Meave, J.A., Mesquita, R., Mora, F., Muñoz, R., Muscarella, R., Nunes, Y.R.F., Ochoa-Gaona, S., de Oliveira, A.A., Orihuela-Belmonte, E., Peña-Claros, M., Pérez-García, E.A., Piotto, D., Powers, J.S., Rodríguez-Velázquez, J., Romero-Pérez,

I.E., Ruíz, J., Saldarriaga, J.G., Sanchez-Azofeifa, A., Schwartz, N.B., Steininger, M.K., Swenson, N.G., Toledo, M., Uriarte, M., van Breugel, M., van der Wal, H., Velo, M.D.M., 2016. Biomass resilience of neotropical secondary forests. Nature 530 (7589), 211–214. http://dx.doi.org/10.1038/nature16512.

Potapov, P., Hansen, M.C., Laestadius, L., Turubanova, S., Yaroshenko, A., Thies, C., Smith, W., Zhuravleva, I., Komarova, A., Minnemeyer, S., Esipova, E., 2017. The last frontiers of wilderness: tracking loss of intact forest landscapes from 2000 to 2013. Sci. Adv. 3 (1), e1600821. http://dx.doi.org/10.1126/sciadv.1600821.

Putz, F.E., Blate, G.M., Redford, K.H., Fimbel, R., Robinson, J., 2001. Tropical forest management and conservation of biodiversity: an overview. Conserv. Biol. 15 (1), 7–20. http://dx.doi.org/10.1046/j.1523-1739.2001.00018.x. http://www.jstor.org/stable/2641641.

Putz, F.E., Zuidema, P.A., Synnott, T., Peña-Claros, M., Pinard, M.A., Sheil, D., Vanclay, J.K., Sist, P., Gourlet-Fleury, S., Griscom, B., Palmer, J., Zagt, R., 2012. Sustaining conservation values in selectively logged tropical forests: the attained and the attainable. Conserv. Lett. 5 (4), 296–303. http://dx.doi.org/10.1111/j.1755-263X.2012.00242.x.

Rödig, E., Cuntz, M., Rammig, A., Fischer, R., Taubert, F., Huth, A., 2018. The importance of forest structure for carbon fluxes of the Amazon rainforest. Environ. Res. Lett. 13 (5), 054013. http://dx.doi.org/10.1088/1748-9326/aabc61. http://iopscience.iop.org/article/10.1088/1748-9326/aabc61, http://stacks.iop.org/1748-9326/13/i=5/a=054013?key=crossref.0c1e0cf4d5b39bc1cc775f788a94fc7c.

Reis, L.P., Ruschel, A.R., Coelho, A.A., da Luz, A.S., Martins-da Silva, R.C.V., 2010. Avaliaç ao do potencial madeireiro na Floresta Nacional do Tapajós após 28 anos da exploraç ao florestal. Pesqui. Florest. Bras. 30 (64), 265–281. http://dx.doi.org/10.4336/2010.pfb.30.64.265. http://www.cnpf.embrapa.br/pfb/index.php/pfb/article/view/144/138.

Rice, R.E., Gullison, R.E., Reid, J.W., 1997. Can sustainable management save tropical forests? Sci. Am. 276 (4), 44–49. http://dx.doi.org/10.1038/scientificamerican0497-44.

Roopsind, A., Wortel, V., Hanoeman, W., Putz, F.E., 2017. Quantifying uncertainty about forest recovery 32-years after selective logging in Suriname. For. Ecol. Manag. 391, 246–255. http://dx.doi.org/10.1016/j.foreco.2017.02.026. http://linkinghub.elsevier.com/retrieve/pii/S0378112717302256.

Rutishauser, E., Hérault, B., Baraloto, C., Blanc, L., Descroix, L., Sotta, E.D., Ferreira, J., Kanashiro, M., Mazzei, L., D'Oliveira, M.V., de Oliveira, L.C., Peña-Claros, M., Putz, F.E., Ruschel, A.R., Rodney, K., Roopsind, A., Shenkin, A., da Silva, K.E., de Souza, C.R., Toledo, M., Vidal, E., West, T.A., Wortel, V., Sist, P., 2015. Rapid tree carbon stock recovery in managed Amazonian forests. Curr. Biol. 25 (18), R787–R788. http://dx.doi.org/10.1016/j.cub.2015.07.034. http://linkinghub.elsevier.com/retrieve/pii/S0960982215008684.

Rutishauser, E., Hérault, B., Petronelli, P., Sist, P., 2016. Tree height reduction after selective logging in a tropical forest. Biotropica 48 (3), 285–289. http://dx.doi.org/10.1111/btp.12326.

Rykiel, E.J., 1985. Towards a definition of ecological disturbance. Austral Ecol. 10 (3), 361–365. http://dx.doi.org/10.1111/j. 1442-9993.1985.tb00897.x.

Sato, H., Itoh, A., Kohyama, T., 2007. SEIB-DGVM: a new dynamic global vegetation model using a spatially explicit individual-based approach. Ecol. Model. 200 (3–4), 279–307. http://dx.doi.org/10.1016/j.ecolmodel.2006.09.006.

Sebbenn, A.M., Degen, B., Azevedo, V.C.R., Silva, M.B., de Lacerda, A.E.B., Ciampi, A.Y., Kanashiro, M., Carneiro, F.D.S., Thompson, I., Loveless, M.D., 2008. Modelling the long-term impacts of selective logging on genetic diversity and demographic structure of four tropical tree species in the Amazon forest. For. Ecol. Manag. 254 (2), 335–349. http://dx.doi.org/10.1016/j.foreco.2007.08.009.

Sitch, S., Bondeau, A., Cramer, W., Venevsky, S., Analysis, E., 2003. Evaluation of ecosystem dynamics, plant geography and terrestrial carbon cycling in the LPJ dynamic global vegetation model. Glob. Change Biol. 161–185.

Stocker, T., 2014. Climate Change 2013 – The Physical Science Basis. Cambridge University Press, Cambridge. http://dx.doi.org/10.1017/CBO9781107415324. arXiv:1011.1669v3.

Swaine, M.D., Lieberman, D., Putz, F.E., 1987. The dynamics of tree populations in tropical forest: a review. J. Trop. Ecol. 3 (04), 359–366. http://dx.doi.org/10.1017/S0266467400002339.

ter Steege, H., Pitman, N.C.A., Sabatier, D., Baraloto, C., Salomao, R.P., Guevara, J.E., Phillips, O.L., Castilho, C.V., Magnusson, W.E., Molino, J.-F., Monteagudo, A., Nunez Vargas, P., Montero, J.C., Feldpausch, T.R., Coronado, E.N.H., Killeen, T.J., Mostacedo, B., Vasquez, R., Assis, R.L., Terborgh, J., Wittmann, F., Andrade, A., Laurance, W.F., Laurance, S.G.W., Marimon, B.S., Marimon, B.-H., Guimaraes Vieira, I.C., Amaral, I.L., Brienen, R., Castellanos, H., Cardenas Lopez, D., Duivenvoorden, J.F., Mogollon, H.F., Matos, F.D.D.A., Davila, N., Garcia-Villacorta, R., Stevenson Diaz, P.R., Costa, F., Emilio, T., Levis, C., Schietti, J., Souza, P., Alonso, A., Dallmeier, F., Montoya, A.J.D., Fernandez Piedade, M.T., Araujo-Murakami, A., Arroyo, L., Gribel, R., Fine, P.V.A., Peres, C.A., Toledo, M., Aymard, G.A., Baker, C.T.R., Ceron, C., Engel, J., Henkel, T.W., Maas, P., Petronelli, P., Stropp, J., Zartman, C.E., Daly, D., Neill, D., Silveira, M., Paredes, M.R., Chave, J., Lima Filho, D.D.A.P., 2013. Hyperdominance in the Amazonian Tree Flora. Science 342 (6156), 1243092. http://dx.doi.org/10.1126/science.1243092.

Thompson, J.N., Reichman, O.J., Morin, P.J., Polis, G.A., Power, M.E., Sterner, R.W., Couch, C.A., Gough, L., Holt, R., Hooper, D.U., Keesing, F., Lovell, C.R., Milne, B.T., Molles, M.C., Roberts, D.W., Strauss, S.Y., 2001. Frontiers of ecology. BioScience 51 (1), 15–24. http://dx.doi.org/10.1641/0006-3568(2001)051[0015:foe]2.0.co;2.

Tyukavina, A., Hansen, M.C., Potapov, P.V., Krylov, A.M., Goetz, S.J., 2016. Pan-tropical hinterland forests: mapping minimally disturbed forests. Glob. Ecol. Biogeogr. 25 (2), 151–163. http://dx.doi.org/10.1111/geb.12394.

Valle, D., Phillips, P., Vidal, E., Schulze, M., Grogan, J., Sales, M., van Gardingen, P., 2007. Adaptation of a spatially explicit individual tree-based growth and yield model and long-term comparison between reduced-impact and conventional logging in eastern Amazonia, Brazil. For. Ecol. Manag. 243 (2–3), 187–198. http://dx.doi.org/10.1016/j.foreco.2007.02.023. http://linkinghub.elsevier.com/retrieve/pii/S0378112707001417.

Volkova, L., Roxburgh, S.H., Weston, C.J., Benyon, R.G., Sullivan, A.L., Polglase, P.J., 2018. Importance of disturbance history on net primary productivity in the world's most productive forests and implications for the global carbon cycle. Glob. Change Biol. 0–2. http://dx.doi.org/10.1111/gcb.14309.

Wagner, F., Hérault, B., Stahl, C., Bonal, D., Rossi, V., 2011. Modeling water availability for trees in tropical forests. Agric. For. Meteorol. 151 (9), 1202–1213. http://dx.doi.org/10.1016/j.agrformet.2011.04.012. http://linkinghub.elsevier.com/retrieve/pii/S0168192311001419.

Walters, C., 1999. Ecospace: prediction of mesoscale spatial patterns in trophic relationships of exploited ecosystems, with emphasis on the impacts of marine protected areas. Ecosystems 2 (6), 539–554. http://dx.doi.org/10.1007/s100219900101.

Chapitre 7

La production de bois des forêts amazoniennes peut-elle être durable ?

Dans ce chapitre le modèle de récupération du bois d'œuvre présenté dans le chapitre 6 a été calibré avec l'ensemble des données TmFO pour pouvoir faire des prédictions à l'échelle de l'Amazonie.

Les principaux résultats de cette étude sont que la production de bois d'œuvre telle qu'elle est faite aujourd'hui en Amazonie n'est pas durable. En effet la vitesse de récupération du bois d'œuvre des forêts naturelles exploitées n'est pas suffisante pour retrouver la quantité exploitée à la fin d'un cycle d'exploitation de 30 ans, et cela est exacerbé lorsque seule une fraction de toutes les espèces potentiellement exploitables est réellement exploitée.

En rallongeant les cycles et en diminuant l'intensité d'exploitation, il est possible d'avoir une exploitation durable au sens où elle permet une récupération du stock à la fin d'un cycle. Mais une nouvelle question se pose alors : la surface des forêts de production en Amazonie est-elle suffisante pour fournir la demande actuelle de bois d'œuvre (autour de 30-35 Mm^3 par an[1]) avec une exploitation si extensive ? Les résultats présentés dans ce chapitre montrent qu'une telle exploitation ne permettrait pas de produire suffisamment de bois par rapport à la demande, alors qu'une exploitation plus intensive résulterait en une diminution rapide des volumes de bois dans les forêts de production. Il est donc temps de modifier les pratiques d'exploitation, et de préparer des modes de production alternatifs pour l'approvisionnement futur d'une demande en bois qui est prévue d'augmenter[2].

Les données utilisées sont disponibles sur le lien : `https://figshare.com/s/336dcbff400a812a56ea`, et les codes R associés sur `https://figshare.com/s/9873edea9c1e8fe98993`.

[1] M. Lentini et al. (2005). *Fatos Florestais da Amazônia 2005 (Amazonian Forest Facts)*, p. 142.

[2] J. Buongiorno et al. (2012). « Outlook to 2060 for World Forests and Forest Industries : A Technical Document Supporting the Forest Service 2010 RPA Assessment ». In : *U.S. Department of Agriculture Forest Service, Southern Research Station*, p. 88.

Can timber provision from Amazonian natural forests be sustainable ?

Camille Piponiot[1,2,3,4], Edna Rödig[5], Francis E Putz[6], Ervan Rutishauser[7,8], Plinio Sist[4], Nataly Ascarrunz[9], Lilian Blanc[4], Géraldine Derroire[2], Laurent Descroix[10], Marcelino Carneiro Guedes[11], Euridice Honorio Coronado[12], Andreas Huth[5], Milton Kanashiro[13], Juan Carlos Licona[9], Lucas Mazzei[13], Marcus Vinicio Neves d'Oliveira[14], Marielos Peña-Claros[15], Alexander Shenkin[16], Cintia Rodrigues de Souza[17], Edson Vidal[18], Thales West[6] & Bruno Hérault[4,19]

1. Université de Guyane, UMR EcoFoG (Agroparistech, CNRS, Inra, Université des Antilles, Cirad), Kourou, French Guiana.
2. Cirad, UMR EcoFoG (Agroparistech, CNRS, Inra, Université des Antilles, Université de Guyane), Kourou, French Guiana.
3. CNRS, UMR EcoFoG (Agroparistech, Inra, Université des Antilles, Université de Guyane, Cirad), Kourou, French Guiana.
4. Cirad, Univ Montpellier, UR Forests and Societies, Montpellier, France.
5. UFZ - Helmholtz Centre for Environmental Research, Permoserstr. 15, 04318, Leipzig, Germany
6. Department of Biology, University of Florida, Gainesville, United States.
7. CarboForExpert, Hermance, Switzerland.
8. Smithsonian Tropical Research Institute, Balboa, Ancón 03092, Panamá.
9. Instituto Boliviano de Investigación Forestal, Santa Cruz, Bolivia
10. ONF-Guyane, Réserve de Montabo, 97307 Cayenne, French Guiana.
11. Embrapa Amapá, Macapá, Brazil.
12. Instituto de Investigaciones de la Amazonía Peruana, Iquitos, Peru.
13. Embrapa Amazônia Oriental, Belém, Brazil
14. Embrapa Acre, Rio Branco, Brazil.
15. Forest Ecology and Forest Management Group, Wageningen University, Wageningen, Netherlands.
16. Environmental Change Institute, University of Oxford, Oxford, United Kingdom.
17. Embrapa Amazônia Ocidental, Manaus, Brazil.
18. Departamento de Ciências Florestais, University of São Paulo, Piracicaba, Brazil.
19. INP-HB (Institut National Polytechnique Félix Houphouët Boigny), Yamoussoukro, Côte d'Ivoire.

Around 30 Mm^3 of sawlogs are extracted annually by selective logging of natural forests in Amazonia, Earth's most extensive tropical forest. This study examines the sustainability of these harvests based on a Bayesian hierarchical model calibrated with data from 3,500 ha of forest inventory plots. Our results show that the average harvests of 20 m^3ha^{-1} will not recover by the end of a standard 30-year cutting cycle. Timber recovery within a cutting cycle is enhanced by commercial acceptance of more species and with adoption of longer cutting cycles

and lower logging intensities. Recovery rates are faster in Western Amazonia than on the Guiana Shield. Our simulations suggest that regardless of cutting cycle durations and logging intensities, selectively logged forests are unlikely to meet timber demands over the long term. There is thus an urgent need to develop an integrated forest resource management policy that combines active management of natural forests with restoration of degraded and secondary forests for timber production.

In Amazonia, 108 Mha of forest (20%) are currently exploited for timber production typically by selective harvest of a few merchantable trees per hectare followed by regrowth until the next logging event[3]. In addition to providing income and employment[4], selectively logged forests retain most of the carbon stocks and biodiversity of old-growth forests[5]. Implementing techniques of reduced-impact logging can further reduce logging damage and thus enhance the environmental value of logged forests[6]. Forest management of selectively logged forests is thus often seen as a tool for Amazonian forest conservation[7].

Logged forests must be carefully managed to avoid post-logging degradation (e.g. uncontrolled and illegal logging, fire or poaching), given that additional degradation greatly diminish the timber value of next harvests, as well as other environmental benefits like carbon storage and biodiversity[8]. Moreover, selectively-logged and subsequently degraded forests are more prone to be converted into more profitable land uses[9]. Numerous countries have enacted logging regulations that set maximum logging intensities (m^3ha^{-1}) and cutting cycles, *i.e.* minimum time intervals between harvests[10] to avoid depletion of timber stocks. Typically, the minimum cutting cycles over which timber stocks are assumed to recover to pre-harvesting levels are 25-35 years despite substantial evidence that without strong limits on logging intensities, these cycles are too short to sustain yields[11]. Shortfalls in timber are likely to be exacerbated further in Amazonia by ongoing climate changes[12], including increased frequency and severity of droughts and wildfire events due to drier and hotter conditions[13]. A consequence of these changes is increased tree mortality, especially of large trees (loggers' main target) that are particularly sensitive to intense droughts[14].

Here we investigate the potential for timber recovery across Amazonian production forests using VDDE, a volume dynamics with differential equations model[15]. The VDDE model was calibrated at the Amazon Basin scale in a Bayesian framework with data from 3500 ha of forest plots. Among those plots, 845 ha are from 15 sites monitored for as long as 30 years after being subjected to conventional logging (8% of plots), reduced-impact logging techniques (e.g. skid-trail planning and directional felling ; 33%), post-logging liberation thinning (37%), and control plots with no

[3] FAO (2011). *The State of Forests in the Amazon Basin, Congo Basin and Southeast Asia*, cf. note 1, p. 1.

[4] Blaser et al. (2011). *Status of Tropical Forest Management 2011*, cf. note 1, p. vi.

[5] Putz et al. (2012). « Sustaining conservation values in selectively logged tropical forests : the attained and the attainable », cf. note 102, p. 11.

[6] Putz et al. (2008). « Reduced-impact logging : Challenges and opportunities », cf. note 105, p. 12.

[7] Edwards et al. (2014b). « Maintaining ecosystem function and services in logged tropical forests », cf. note 3, p. vi.

[8] J. A. Foley et al. (2007). « Amazonia revealed : forest Degradation and Loss of Ecosystem Goods and Services in the Amazon Basin ». In : *Front Ecol Environ* 5.1, p. 25–32.

[9] Asner et al. (2006). « Condition and fate of logged forests in the Brazilian Amazon. », cf. note 78, p. 9.

[10] Blaser et al. (2011). *Status of Tropical Forest Management 2011*, cf. note 1, p. vi.

[11] Putz et al. (2012). « Sustaining conservation values in selectively logged tropical forests : the attained and the attainable », cf. note 102, p. 11 ; P. Shearman et al. (2012). « Are we approaching 'peak timber' in the tropics ? » In : *Biological Conservation* 151.1, p. 17–21.

[12] H. Fargeon et al. (2016). « Vulnerability of Commercial Tree Species to Water Stress in Logged Forests of the Guiana Shield ». In : *Forests* 7.12, p. 105.

[13] Malhi et al. (2008). « Climate change, deforestation, and the fate of the Amazon. », cf. note 77, p. 9.

[14] R. T. Corlett (2016). « The Impacts of Droughts in Tropical Forests ». In : *Trends in Plant Science* 21.7, p. 584–593.

[15] C. Piponiot et al. (2018). « Assessing timber volume recovery after disturbance in tropical forests – A new modelling framework ». In : *Ecological Modelling* 384.December 2017, p. 353–369.

logging (22%)[16]. The VDDE model focuses on the volume of live trees with diameter at breast height (DBH) $\geq$ 50 cm (the standard minimum cutting size in the Amazon Basin), hereinafter referred to simply as volume. Spatial variation in volume recovery was modelled through variation in (i) the pre-logging forest maturity, *i.e.* the time needed for the forest to reach its current state in the absence of disturbance[17] : forests under low-disturbance regime can thus reach higher maturity levels ; (ii) the volume potential, *i.e.* the maximum volume asymptotically reached by a mature forest ; and (iii) the maximum gross volume production, *i.e.* the annual gross volume increment from trees > 50 cm DBH (without volume losses from respiration and mortality) in a mature forest.

First, we explore the relationship between volume recovery rates and local abundance of commercial trees using the list of commercial species harvested at each experimental site during the first cutting cycle (Figure 7.1). The volume of those species represented 9-79% of the total pre-logging plot volumes. We simulated volume recovery at each site under five scenarios : (1) a standard-practice scenario, with a logging intensity of 20 m^3ha^{-1}, which is the average logging intensity in Amazonia[18], and with a standard 30-year cutting cycle ; (2) a low-intensity scenario (10 m^3ha^{-1}) with a 30-year cutting cycle ; (3) a high-intensity scenario (30 m^3ha^{-1}) with a 30-year cutting cycle ; (4) a short-cycle (15 years) scenario, with a logging intensity of 20 m^3ha^{-1} ; and, (5) a long-cycle (65 years) scenario, with a logging intensity of 20 m^3ha^{-1}.

We next explore potential timber recovery using an extended pool of all species that are harvested for commercial purposes anywhere in Amazonia (potential timber species ; see Section 7.7.1 in the Supplementary Material for a full list of species). Across an extensive forest plot network[19], potential timber volume ranged 50-100% of total volume (Figure 7.8). We then model potential timber recovery using the 5 scenarios described above to produce regional maps of potential timber recovery at the end of the first cutting cycle (Figure 7.2). Additionally, we evaluated whether Amazonian natural forests could support the commercial demand for sawlogs, assessed as the sawlog consumption from the Amazon region[20], by simulating the long-term trajectory of potential timber stocks for varying logging intensities and cutting cycles (Figure 7.3). To do this we assume that all forests within 25 km of maintained roads and tracks[21], and without a full protection status could be logged. To avoid having to make assumptions about highly unpredictable patterns of future deforestation and road building, our study is based on the current forest areas available for logging. Finally, we tested the effect of increased annual mortality rates and increased disturbances (*i.e.* discrete events like fires cause pulses of elevated mortality and therefore reduce stand maturity) on timber stocks and recovery (Figure 7.4), to assess the potential effects of climate

[16] Sist et al. (2015). « The Tropical managed Forests Observatory : A research network addressing the future of tropical logged forests », cf. note 116, p. 12.

[17] Piponiot et al. (2018). « Assessing timber volume recovery after disturbance in tropical forests – A new modelling framework », cf. note 15, p. 109.

[18] Asner et al. (2005). « Selective Logging in the Brazilian Amazon », cf. note *a*, p. 7.

[19] Brasil (1973). *Projeto Radambrasil. Levantamento de recursos naturais*, cf. note 14, p. 25.

[20] Lentini et al. (2005). *Fatos Florestais da Amazônia 2005 (Amazonian Forest Facts)*, cf. note 1, p. 107.

[21] Asner et al. (2006). « Condition and fate of logged forests in the Brazilian Amazon. », cf. note 78, p. 9.

change on timber provision from Amazonian production forests.

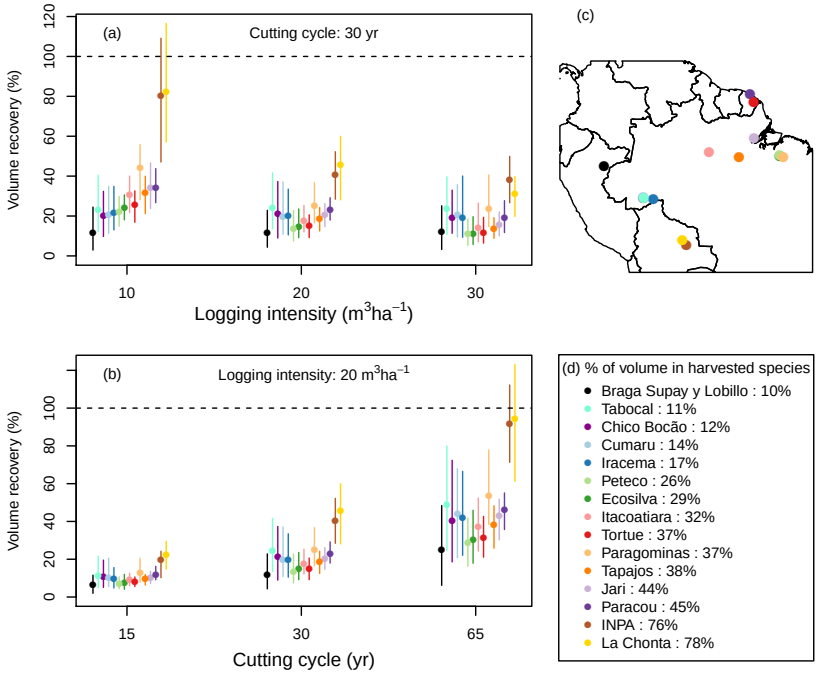

FIGURE 7.1 – Predicted volume recovery, defined as the percentage of the volume of trees > 50 cm DBH extracted that is recovered at a given site (colours) by the locally-defined pool of harvested commercial species, (a) under 3 logging intensities (10, 20 and 30 m^3ha^{-1}) at the end of a 30-year cutting cycle ; (b) with 3 cutting cycles (15, 30 and 65 years) with a logging intensity of 20 m^3ha^{-1}. Dots are median values and vertical bars are 95% credibility intervals. (c) Map (see Figure 7.6 for a more detailed map) of the 15 study sites ranked by increasing proportions of total volume found in the locally-defined pool of harvested commercial species (d), the greater the proportion the more likely the recovery.

7.1 What affects timber recovery ?

Recovery of harvested species volume by the end of the first cutting cycle varied threefold across the experimental sites (Figure 7.1a) and increased with the pre-logging proportion of the total volume shared by the local pool of harvested commercial species (Pearson's coefficient $\rho = 0.58$). At the sites with the largest abundance and diversity of locally harvested species (INPA and La Chonta with 70% of stems $\geq$ 50 cm DBH), timber volumes are predicted to recover faster. This finding highlights the importance of diversifying the local pool of species harvested to maintain timber stocks over time.

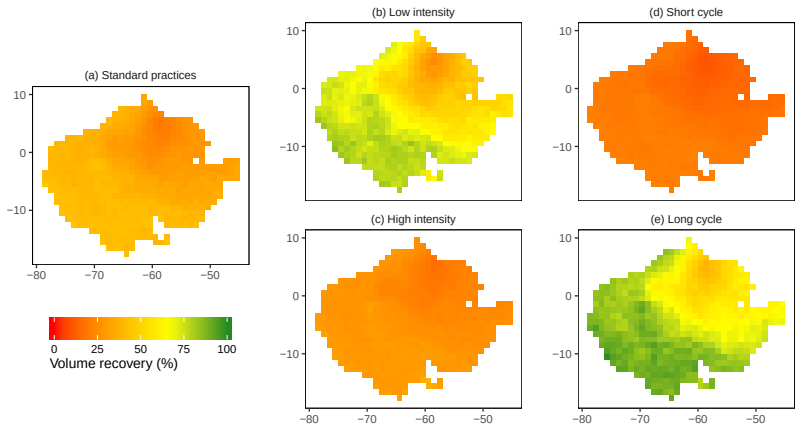

FIGURE 7.2 – Potential timber volume recovery in Amazonia after one selective harvest predicted under 5 scenarios : (a) standard practices : 20 m^3ha^{-1} of timber extracted and a cutting cycle length of 30 years ; (b) low logging intensity : 10 m^3ha^{-1}, 30 years ; (c) high logging intensity : 30 m^3ha^{-1}, 30 years ; (d) short cutting cycle : 15 years, 20 m^3ha^{-1} ; (e) long cutting cycle : 65 years, 20 m^3ha^{-1}. Colours range from red (no recovery) to green (full recovery). Median values are shown and the 95% credibility intervals can be found in the supplementary information (Figure 7.11, 7.12).

Regional variation in the rate of timber volume recovery of all potential timber species was consistent across logging intensities and cutting cycle lengths (Figure 7.2a-e). Median timber recovery was highest in Western Amazonia (0.26 [0.17,0.34] $m^3ha^{-1}yr^{-1}$ - numbers in [] represent the 95% credibility interval) and lowest on the Guiana Shield (0.20 [0.13, 0.27] $m^3ha^{-1}yr^{-1}$). These results resemble those from studies in old-growth forests that revealed higher rates of both wood production and stand turnover in western Amazonia than in the northeast[22] that correlate with lower community wood densities[23] and are potentially due to more frequent natural disturbances[24], or spatial differences in seasonality and soil properties[25]. For forest managed for timber, this result means that logging regulations need to reflect regional differences.

We stress that our model estimates are based on optimal scenarios of the recovery potential of Amazonian production forests insofar as our plots showed no signs of having suffered severe recent human disturbance prior to logging (e.g., fire, uncontrolled logging, or fragmentation) whereas this is not the case for an estimated one-third of Amazonian forests[26] ; such disturbances might reduce forest resilience to logging[27]. Furthermore, reduced-impact logging techniques were employed in most of our experimental sites[28], but these recommended logging practices are seldom implemented in the tropics[29]. Moreover, by not harvesting big defective trees and keeping them in the forest where they will produce seeds, future tree generations could be more prone to rot or misshapes. Finally, our scenarios do not account for post-logging degradation (e.g., fires and illegal logging[30]) or deforestation[31], which are fairly ubiquitous in the region[32].

7.2 Would timber wood diversification make selective logging sustainable ?

Lesser known Amazonian timber species compose a small share of the global tropical timber market, which remains heavily dominated by a few overexploited species[33]. Selective logging in Amazonia usually targets one or two high-value species such as mahogany (*Swietenia macrophylla*) and ipê (*Handroanthus* spp)[34] that typically represent <20% of the total volume in a particular site[35] and when overexploited their volume recovery within a typical 30-year cutting cycle is compromised[36]. Due to low recovery rates of prized timber species, what is available for second harvests is often species with low timber market values compared to the costs of extraction and transport[37]. Because low timber values of logged forests render them more prone to clearance, we echo the familiar recommendation to develop markets for lesser-known timber species[38]. Given the thousands of tropical species with potentially merchantable timber[39], it is unfortunate that the cur-

[22] Quesada et al. (2012). « Basin-wide variations in Amazon forest structure and function are mediated by both soils and climate », cf. note 1, p. 23 ; Johnson et al. (2016). « Variation in stem mortality rates determines patterns of above-ground biomass in Amazonian forests : implications for dynamic global vegetation models », cf. note 8, p. 24.

[23] Johnson et al. (2016). « Variation in stem mortality rates determines patterns of above-ground biomass in Amazonian forests : implications for dynamic global vegetation models », cf. note 8, p. 24.

[24] Espírito-Santo et al. (2014). « Size and frequency of natural forest disturbances and the Amazon forest carbon balance », cf. note 5, p. 23.

[25] Quesada et al. (2012). « Basin-wide variations in Amazon forest structure and function are mediated by both soils and climate », cf. note 1, p. 23.

[26] A. Tyukavina et al. (2017). « Types and rates of forest disturbance in Brazilian Legal Amazon, 2000–2013 ». In : *Science Advances* 3.4, e1601047.

[27] Y. Malhi et al. (2014). « Tropical Forests in the Anthropocene ». In : *Annual Review of Environment and Resources* 39.1, p. 125–159.

[28] Sist et al. (2015). « The Tropical managed Forests Observatory : A research network addressing the future of tropical logged forests », cf. note 116, p. 12.

[29] Putz et al. (2008). « Reduced-impact logging : Challenges and opportunities », cf. note 105, p. 12.

[30] Laurance et al. (2009). « Impacts of roads and linear clearings on tropical forests », cf. note 40, p. 4.

[31] Asner et al. (2006). « Condition and fate of logged forests in the Brazilian Amazon. », cf. note 78, p. 9.

[32] Asner et al. (2005). « Selective Logging in the Brazilian Amazon », cf. note *a*, p. 7 ; Malhi et al. (2014). Cf. note 27.

[33] M. Schulze et al. (2008). « How rare is too rare to harvest ?. Management challenges posed by timber species occurring at low densities in the Brazilian Amazon ». In : *Forest Ecology and Management* 256.7, p. 1443–1457 ; Richardson et Peres (2016). « Temporal decay in timber species composition and value in amazonian logging concessions », cf. note 62, p. 7.

[34] Schulze et al. (2008). Cf. note 33.

rent hyper-selectivity of selective logging in Amazonia continues to be due to consumer preferences[40]. Therefore, efforts should be done to change these preferences both in terms of species and size of logs, e.g. the potential use of branches (and not only trunks) could increase timber production without additional damage to the stand.

Even if volume recovery scenarios include all the 348 lesser-known timber species, our simulations indicated that with a logging intensity of 20 m^3ha^{-1} logged forests recover at most 70% of their pre-logging timber volumes (Figure 7.2) within a typical 30-yr cutting cycle. This result is consistent with a variety of studies reporting that standard 30-yr to 40-yr cutting cycles are insufficient for full recovery of timber stocks[41]. This means that even with a substantial increase in the number of merchantable species, timber stocks will continue to decline in Amazonian production forests if current logging practices (extraction of around 20 m^3ha^{-1} every 30 years) persist (Figure 7.3).

7.3 Slow recovery and rising pressure on natural forests

In only two scenarios, low logging intensity and long cutting cycle, Amazon-region wide timber production was sustained over time at approximately 30 Mm^3yr^{-1} (Figure 7.3b), close to the actual timber demand in the region. However, in all scenarios, median timber recovery from forest regrowth was < 30 Mm^3yr^{-1} for the first 200 years of simulation (Figure 7.3c). This overharvesting results in a reduction in Amazon-wide timber stocks in all scenarios (Figure 7.3a), meaning that natural forest regrowth will be insufficient to supply the commercial demand in the long-term. Moreover, the actual sawlog extraction could be higher than official numbers suggest : illegal logging is ubiquitous in the region and is estimated to produce a volume of wood equivalent to 20-60% of the legal timber markets[42], further decreasing the likelihood of a sustainable timber supply from Amazonian natural forests.

While the fate of Amazonian production forests remains uncertain, several studies call attention to the rising impacts of human activities on the functioning and provision of ecosystem services[43]. Deforestation, forest degradation, and climate change will continue to affect the resilience of Amazonian forests to future disturbances including their ability to recover timber stocks after logging[44]. Moreover, trends in deforestation can be substantially affected by political choices (e.g., road building[45], law enforcement, agricultural subsidies, access to credit[46], and corruption[47]), which were not considered in our conservative scenarios with no deforestation. Therefore, our results represent the maximum po-

[35] J. Grogan et al. (2008). « What loggers leave behind : Impacts on big-leaf mahogany (Swietenia macrophylla) commercial populations and potential for post-logging recovery in the Brazilian Amazon ». In : *Forest Ecology and Management* 255.2, p. 269–281 ; Richardson et Peres (2016). « Temporal decay in timber species composition and value in amazonian logging concessions », cf. note 62, p. 7.

[36] Schulze et al. (2008). Cf. note 33.

[37] Pokorny et Pacheco (2014). « Money from and for forests : A critical reflection on the feasibility of market approaches for the conservation of Amazonian forests », cf. note 139, p. 17.

[38] F. B. Yeom (1984). « Lesser-known tropical wood species : How bright is their future ? » In : *Unasylva (FAO)* 36.3.

[39] FSC (2016). *Lesser Known Timber Species*.

[40] Pokorny et Pacheco (2014). « Money from and for forests : A critical reflection on the feasibility of market approaches for the conservation of Amazonian forests », cf. note 139, p. 17.

[41] Schulze et al. (2008). Cf. note 33 ; Putz et al. (2012). « Sustaining conservation values in selectively logged tropical forests : the attained and the attainable », cf. note 102, p. 11.

[42] Lawson et al. (2010). « Illegal Logging and Related Trade. Indicators of the Global Response », cf. note 5, p. 34 ; Finer et al. (2014). « Logging Concessions Enable Illegal Logging Crisis in the Peruvian Amazon », cf. note 95, p. 10.

[43] Malhi et al. (2008). « Climate change, deforestation, and the fate of the Amazon. », cf. note 77, p. 9 ; G. P. Asner et al. (2010). « Combined effects of climate and land-use change on the future of humid tropical forests ». In : *Conservation Letters* 3.6, p. 395–403 ; M. Guimberteau et al. (2016). « Impacts of future deforestation and climate change on the hydrology of the Amazon basin : a multi-model analysis with a new set of land-cover change scenarios ». In : *Hydrology and Earth System Sciences Discussions* August, p. 1–34.

[44] Foley et al. (2007). « Amazonia revealed : forest Degradation and Loss of Ecosystem Goods and Services in the Amazon Basin », cf. note 8, p. 109 ; Malhi et al. (2014). Cf. note 27.

[45] Laurance et al. (2009). « Impacts of roads and linear clearings on tropical forests », cf. note 40, p. 4.

[46] Nepstad et al. (2014). « Slowing Amazon deforestation through public policy and interventions in beef and soy supply chains. », cf. note 50, p. 5.

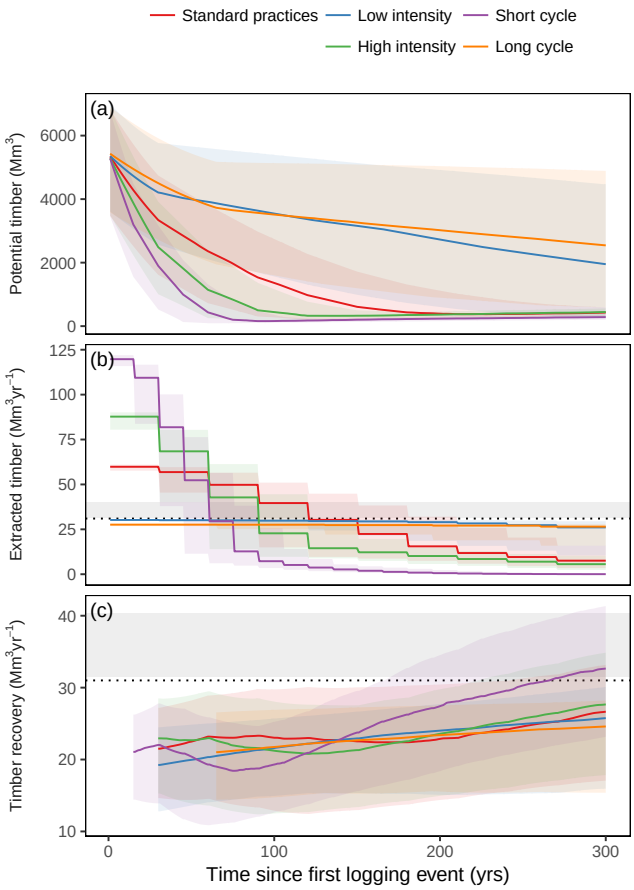

FIGURE 7.3 – Predicted volume trajectories (x-axis : time since first logging, in years) of (a) total potential timber, (b) potential timber extracted annually and (c) annual potential timber recovery over 300 years in Amazonian forests under 5 scenarios : standard logging rules (20 m^3ha^{-1}, 30 yrs, red), low intensity (10 m^3ha^{-1}, 30 yrs, blue), high intensity (30 m^3ha^{-1} 30 yrs, green), short cutting cycle (20 m^3ha^{-1}, 15 yrs, purple), long cutting cycle (20 m^3ha^{-1}, 65 yrs, orange). The area available for logging in every pixel of the map (Figure 7.2) was divided into as many annual units as the length of the cutting cycle (15, 30 or 65) so that one unit is logged each year and each unit is logged again at the end of the cutting cycle. Solid lines are the median predictions, and shaded areas are the 95% credibility intervals. The dotted lines (panels b and c) correspond to the demand for sawlogs in the Amazon biome. The grey area is the range of projected sawlog demand in 2060, based on increases in sawnwood consumption in South America estimated with the Global Forest Products Model (see methods).

tential volume recovery of Amazonian production forests that is unlikely be attained in the real world. Climate change is also expected to decrease timber stocks and productivity through drier and hotter climate leading to higher mortality of large trees[48] (Figure 7.4a). Increased frequency and intensity of disturbances are expected to decrease potential timber stocks while timber productivity is enhanced due to the decreased proportion of less productive old-growth stands (Figure 7.4b).

7.4 Future timber production in integrated forest landscapes

Our results show that with current cutting cycles and logging intensities, forest regrowth is too slow to recover timber stocks (Figure 7.2, Figure 7.3), highlighting the need to decrease the pressure on natural production forests by adopting longer cutting cycles, and reducing logging intensities and incidental damage to the stand through reduced-impact techniques[49]. Silvicultural interventions applied to increase the stocking, growth, and commercial yields from merchantable species (e.g., liana cutting, future crop tree liberation, and enrichment planting) could also help to turn

[47] S. PAILLER (2018). « Re-election incentives and deforestation cycles in the Brazilian Amazon ». In : *Journal of Environmental Economics and Management* 88, p. 345–365.

[48] CORLETT (2016). « The Impacts of Droughts in Tropical Forests », cf. note 14, p. 109.

[49] PUTZ et al. (2008). « Reduced-impact logging : Challenges and opportunities », cf. note 105, p. 12.

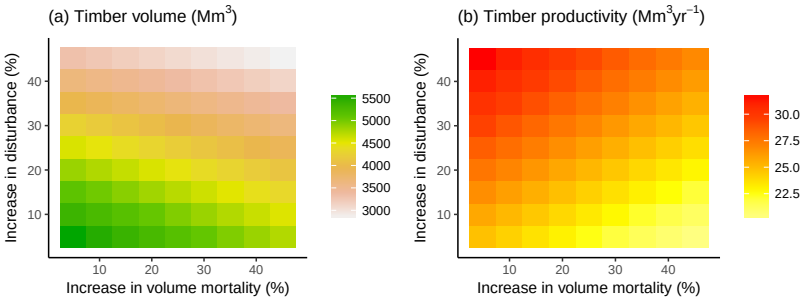

FIGURE 7.4 – Predicted effect of an increase in future disturbance regime (y-axis) and annual mortality (x-axis) on (a) potential timber volume and (b) annual volume productivity in all Amazonian areas available for logging. Increasing the disturbance regime (e.g. more frequent fires) decreases the proportion of old-growth stands and reduces the overall maturity of forests while increasing the annual mortality (e.g. in a drier and hotter climate) decreases the long-term volume potential of forests. The effects of increased disturbance regime and annual mortality are illustrated in Figure 7.13.

the tide of forest depletion, but widespread use of such treatments will require changing the predominant approach of timber mining to forest management[50]. Adoption of more sustainable logging rules will decrease the financial benefits from legal selective logging and potentially lead to an increase in illegal logging and forest conversion[51]. This means that parallel to adopting longer cutting cycles, additional efforts on law enforcement will be needed to avoid promotion of illegal practices. These policies should include regional coordination to avoid illegal trade and displacements effects[52]. The economic viability of tropical forest management will also increase with timber prices, which are currently low compared to production costs[53], and with sawmill efficiency, currently around 35%[54]. Another opportunity to increase financial revenues is to develop economic mechanisms to value other goods and services provided by the forest such as carbon storage (e.g., REDD+), hydrology, biodiversity, ecotourism, and non-timber forest product management[55].

Global demand for timber is expected to increase[56], which will unlikely be met if current unsustainable logging practices continue[57]. Adopting longer cutting cycles will not be enough : the question now is how to produce the additional timber needed to meet rising demands for wood products. Additional sources of timber could come from various restoration systems : plantations of exotic or native species, enriched secondary or degraded forests[58], integrated crop-livestock-forestry systems, and other agroforestry systems[59]. Tree plantations have the potential to produce large quantities of timber on relatively small areas : timber plantations in Brazil, mostly fast-growing eucalyptus and pine, can produce 200-400 $m^3 ha^{-1}$ of roundwood on 10-15-year cycles[60], but technical alternatives with native species are still scarce in Amazonia[61]. The rising interest in tropical forest restoration, initiated by the Bonn challenge in 2011[62], has led Brazil to commit to restoring 12 Mha of forest by 2030[63], and has motivated an unprecedented initiative to restore 30,000 ha of forests in the Brazilian Amazon

[50] F. E. PUTZ (2013). « Complexity confronting tropical silviculturalists ». In : *Managing Forests as Complex Adaptive Systems (C. Messier, K. Puettmann, and D. Coates)*. Routledge. New York, p. 165–186.

[51] POKORNY et PACHECO (2014). « Money from and for forests : A critical reflection on the feasibility of market approaches for the conservation of Amazonian forests », cf. note 139, p. 17.

[52] P. MEYFROIDT et E. F. LAMBIN (2009). « Forest transition in Vietnam and displacement of deforestation abroad ». In : *Proceedings of the National Academy of Sciences* 106.38, p. 16139–16144.

[53] POKORNY et PACHECO (2014). « Money from and for forests : A critical reflection on the feasibility of market approaches for the conservation of Amazonian forests », cf. note 139, p. 17.

[54] R. NASI et al. (2011). « Sustainable forest management and carbon in tropical latin America : The case for REDD+ ». In : *Forests* 2.1, p. 200–217.

[55] J. SALZMAN et al. (2018). « The global status and trends of Payments for Ecosystem Services ». In : *Nature Sustainability* 1.3, p. 136–144.

[56] BUONGIORNO et al. (2012). « Outlook to 2060 for World Forests and Forest Industries : A Technical Document Supporting the Forest Service 2010 RPA Assessment », cf. note 2, p. 107.

[57] SHEARMAN et al. (2012). « Are we approaching 'peak timber' in the tropics ? », cf. note 11, p. 109.

[58] D. LAMB et al. (2005). « Restoration of Degraded Tropical Forest Landscapes ». In : *Science* 310.5754, p. 1628–1632.

by 2023[64]. These initiatives can provide opportunities to combine efforts to restore environmental values (e.g. carbon, biodiversity, and water cycle) including timber production[65], and fund applied research for both ecological restoration and timber production[66].

Promoting restoration will allow a long-term provision of timber, but can have negative effects like additional deforestation due to lower economic value of natural forests[67]. To effectively conserve and restore high environmental value of forests, policies must be thought in an integrated framework at the landscape scale. Jurisdictional approaches are currently emerging from synergies between corporate sector sustainable supply-chain initiatives, government policies, and international programs like REDD+[68]. This convergence of interests has resulted in the creation of pilot "zero-deforestation " jurisdictions[69], with the goal of enhancing social inclusion and rural development while preserving natural resources. Nonetheless, while jurisdictional approaches often focus on avoiding forest conversion, the forest sector has taken little part in these initiatives. The integration of all forest stakeholders in the definition of landscape-level policies and the creation of "zero-degradation-and-restoration" jurisdictions offer a promising way to preserve the remaining tropical forest areas while ensuring the long-term provision of tropical timber worldwide.

7.5 Materials and methods

The data assimilation flowchart is presented in Figure 7.5 : input data are represented as grey boxes on the left and top of the diagram.

7.5.1 Inventory data

On the data assimilation flowchart (Figure 7.5), input data are presented in grey boxes on the left and top of the diagram, with inventory data having clearer boxes with thicker borders. Our study includes data from 15 long-term (8-30 year) experimental forest sites (845 ha total) in the Amazon Basin and on the Guiana Shield (Figure 7.6a) that are part of the TmFO network[70]. All sites are located in *terra firme* forests with mean annual precipitation $\geq$1000 mm, experienced different logging intensities, and have at least one pre-logging census and two post-logging censuses. In each plot, all stems with diameter at breast height (DBH) $\geq$50 cm were measured ; 82% of trees were identified to species and 15% to genus. For sites with plots $\leq$1 ha, data from those with the same treatment were aggregated to mitigate the small plot effect on the variation in density of large trees. Additionally, single measurement plot data from the RadamBrasil project[71] were made available by the Brazilian Institute of Geography and Statistics (IBGE)[72]. We used 2646 1-ha forest inventory plots

[59] M. Yamada et H. L. Gholz (2002). « An evaluation of agroforestry systems as a rural development option for the Brazilian Amazon ». In : *Agroforestry Systems* 55.2, p. 81–87.

[60] D. Tomberlin et al. (2001). « Timber Plantations, Timber Supply and Forest Conservation ». In : p. 85–96.

[61] M. R. Machado et al. (2018). « Silvicultural performance of five forest species in the central Brazilian Amazon ». In : *Acta Amazonica* 48.1, p. 10–17.

[62] J. Aronson et S. Alexander (2013). « Ecosystem restoration is now a global priority : Time to roll up our sleeves ». In : *Restoration Ecology* 21.3, p. 293–296.

[63] Federative Republic of Brazil (2015). « Intended Nationally Determined Contribution Towards ach ». In : *United Nations Framework Convention on Climate Change (UNFCCC)* Sept. P. 6.

[64] The World Bank (2017). *Amazon rainforest to recover 30,000 hectares by 2023*.

[65] Lamb et al. (2005). « Restoration of Degraded Tropical Forest Landscapes », cf. note 58, p. 115.

[66] K. D. Holl (2017). « Research Directions in Tropical Forest Restoration ». In : *Annals of the Missouri Botanical Garden* 102.2, p. 237–250.

[67] R. Pirard et al. (2016). « Do timber plantations contribute to forest conservation ? » In : *Environmental Science and Policy* 57, p. 122–130.

[68] D. Nepstad et al. (2013). « More food, more forests, fewer emissions, better livelihoods : linking REDD+, sustainable supply chains and domestic policy in Brazil, Indonesia and Colombia ». In : *Carbon Management* 4.6, p. 639–658.

[69] Nepstad et al. (2013). Cf. note 68 ; C. Meyer et D. Miller (2015). « Zero Deforestation Zones : The Case for Linking Deforestation-Free Supply Chain Initiatives and Jurisdictional REDD+ ». In : *Journal of Sustainable Forestry* 34.6-7, p. 559–580.

[70] Sist et al. (2015). « The Tropical managed Forests Observatory : A research network addressing the future of tropical logged forests », cf. note 116, p. 12.

[71] Brasil (1973). *Projeto Radambrasil. Levantamento de recursos naturais*, cf. note 14, p. 25.

[72] IBGE (2016). *Data from RadamBrasil project.*

from across the Brazilian Amazon (Figure 7.6b) in which all trees ≥33 cm DBH were measured and identified to species between 1973 and 1982.

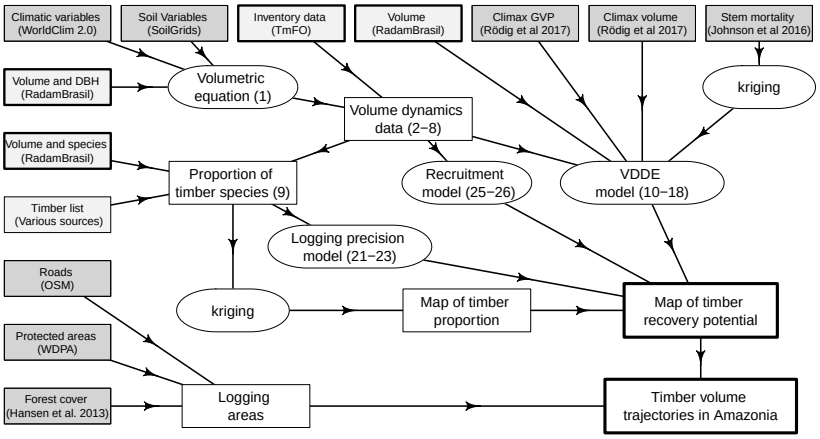

FIGURE 7.5 – Data assimilation diagram. Grey boxes are the input data : spatial data have darker grey boxes and inventory data have thicker borders ; white rectangular boxes are the outputs of the models : intermediate results have thin borders, and final results have thicker borders ; round boxes are the models. Numbers refer to the equations corresponding to each model.

7.5.2 Spatial data

On the data assimilation flowchart (Figure 7.5), spatial data are presented in darker grey boxes. Environmental data were extracted from WorldClim 2.0[73] (precipitation, seasonality of precipitation and solar radiation) and SoilGrids[74] (bulk density, CEC, soil depth, proportion of clay, of sand and of coarse fragment) at 1 km resolution. Annual stem mortality rates (as a proportion of live stems), estimated with the metadata from Johnson and colleagues[75], were extracted from the ForestPlots database[76] and interpolated with the R package *gstat*[77] on a 1° resolution grid. The potential volume, i.e. the volume at climax, and the gross volume productivity at climax were estimated with a recently developed method[78] with the individual-tree-based gap model FORMIND[79]. Potential volume was calculated as the volume of all trees ≥50 cm DBH (per ha) in a mature forest ; climax gross volume productivity (GVP in Figure 7.5) was calculated as the gross volume gain from photosynthesis (before accounting for respiration losses) of trees ≥50 cm DBH in a mature forest. Raster maps of potential volume and climax gross volume productivity were created at 1 km^2 resolution. The map of areas available for logging (Figure 7.9) was constructed as the intersection of 3 maps : a buffer of 25 km around all roads and motorable tracks from the OpenStreetMap database[80] ; the map of areas outside of protected areas from the World Database on Protected Areas[81] (except the category VI of the IUCN classification, *i.e.* areas with sustainable use of natural resources, which we included in the analysis) ; and, pixels with >90% forest cover from the map developed by Hansen and colleagues[82].

[73] FICK et HIJMANS (2017). « WorldClim 2 : new 1-km spatial resolution climate surfaces for global land areas », cf. note 23, p. 29.

[74] T. HENGL et al. (2017). « SoilGrids250m : Global gridded soil information based on machine learning ». In : *PLOS ONE* 12.2. Sous la dir. de B. BOND-LAMBERTY, e0169748.

[75] JOHNSON et al. (2016). « Variation in stem mortality rates determines patterns of above-ground biomass in Amazonian forests : implications for dynamic global vegetation models », cf. note 8, p. 24.

[76] G. LOPEZ-GONZALEZ et al. (2009). *ForestPlots.net Database*.

[77] E. PEBESMA (2004). « Multivariable geostatistics in S : the gstat package. » In : *Computers & Geosciences* 30, p. 683–691.

[78] RÖDIG et al. (2017). « Spatial heterogeneity of biomass and forest structure of the Amazon rain forest : Linking remote sensing, forest modelling and field inventory », cf. note 25, p. 29.

[79] R. FISCHER et al. (2016). « Lessons learned from applying a forest gap model to understand ecosystem and carbon dynamics of complex tropical forests ». In : *Ecological Modelling* 326, p. 124–133.

[80] O. CONTRIBUTORS (2018). *OpenStreetMap*.

[81] UNEP-WCMC et IUCN (2016). *Protected Planet : The World Database on Protected Areas (WDPA)*.

[82] M. C. HANSEN et al. (2013). « High-Resolution Global Maps of 21st-Century Forest Cover Change ». In : *Science* 342.November, p. 850–854. arXiv : 1011.1669v3.

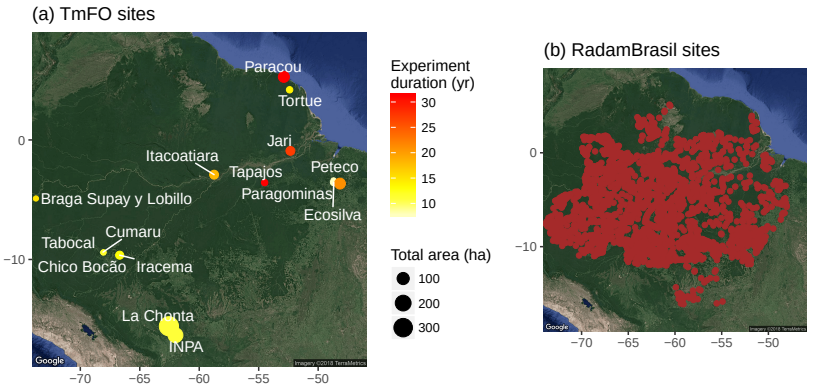

FIGURE 7.6 – Location of inventory sites used in this study. (a) The 15 experimental permanent forest sites : the size of the points represents the total monitored area, and the colour (from yellow to red) represents the total length of the experiment, as the time interval (in years) between the first and the last census. (b) The 2646 1-ha forest inventory plots from the RadamBrasil project.

7.5.3 Volumetric equation.

To convert DBH measurements into volumes we calibrated a volumetric equation with the data (DBH and volume) from the RadamBrasil plots. For each plot p, we calibrated the following equation :

$$log(V_i) = a_p + b \cdot log(DBH_i) \tag{7.1}$$

where V_i (m^3) and DBH_i (cm) are the volume and DBH of a given tree i, a_p is the intercept for plot p, and b is the slope (one for all plots). To predict parameter a for the study area we used a Random Forest model algorithm[83] where predictors are climate variables from WorldClim[84] and soil variables from SoilGrids[85]. The inferred distribution of parameter b was :$b \sim \mathcal{N}(2.174, 0.006^2)$; spatialised parameter a values are shown in Figure 7.14.

7.5.4 Volume dynamics data.

The total volume of plot p in site s at census k is calculated as :

$$V_{k,p} = \sum_{i \in I_{k,p}} V_{i,k} \tag{7.2}$$

where $V_{i,k}$ is the volume of stem i at census k, and $I_{k,p}$ is the set of live stems ≥ 50 cm DBH at census k in plot p.

Due to post-logging silvicultural treatments that induced additional tree mortality for as long as 4 years post-logging[86], , we estimate the minimum volume attained within 4 years after logging and start our recovery study at that time (hereinafter noted census $k = 1$). Post-logging volume loss δV_p from plot p is the difference between the pre-logging volume $V_{0,p}$ and the minimum post-logging volume $V_{1,p}$:

$$\delta V_p = V_{0,p} - V_{1,p} \tag{7.3}$$

[83] L. BREIMAN (2001). « Random forests ». In : *Machine Learning* 45.1, p. 5–32. arXiv : /dx . doi . org / 10 . 1023{\%}2FA{\%}3A1010933404324 [http:].

[84] FICK et HIJMANS (2017). « WorldClim 2 : new 1-km spatial resolution climate surfaces for global land areas », cf. note 23, p. 29.

[85] HENGL et al. (2017). « SoilGrids250m : Global gridded soil information based on machine learning », cf. note 74, p. 117.

[86] RUTISHAUSER et al. (2015). « Rapid tree carbon stock recovery in managed Amazonian forests », cf. note 166, p. 20 ; PIPONIOT et al. (2016b). « Carbon recovery dynamics following disturbance by selective logging in Amazonian forests », cf. note 5, p. 50.

Annual volume gain (from growth of trees $\geq$ 50 cm DBH and recruitment of trees $<$ 50 cm DBH) at census $k \geq 2$ in plot p is calculated as :

$$\Delta V g_{k,p} = \left(\sum_{i \in I_{k,p}} (V_{i,k} - V_{i,k-1}) \right) (t_k - t_{k-1})^{-1} \tag{7.4}$$

where t_k is the number of years between the first post-logging census $k = 1$ and census k (in years).

The contribution of recruitment to annual volume gain is calculated as :

$$pR_{k,p} = \left(\sum_{i \in (I_{k,p} \setminus I_{k-1,p})} V_{i,k} \right) (t_k - t_{k-1})^{-1} (\Delta V g_{k,p})^{-1} \tag{7.5}$$

where $I_{k,p} \setminus I_{k-1,p}$ are all live trees with $DBH < 50$ cm at census $k-1$ and $DBH \geq 50$ cm at census k.

Annual volume loss from mortality is calculated as :

$$\Delta V m_{k,p} = \left(\sum_{i \in (I_{k-1,p} \setminus I_{k,p})} V_{i,k-1} \right) (t_k - t_{k-1})^{-1} \tag{7.6}$$

where $(I_{k-1,p} \setminus I_{k,p})$ are all live trees $\geq$ 50 cm DBH at census k that are dead at census $k-1$.

The VDDE model is calibrated with cumulative volume changes (gain and loss) instead of annual volume changes, because they are less prone to stochastic variations. Cumulative volume gain (cVg) and cumulative volume mortality (cVm) are defined as :

$$cV g_{k,p} = \sum_{1 \leq i \leq k} (\Delta V g_{i,p})(t_k - t_{k-1}) \tag{7.7}$$

$$cV m_{k,p} = \sum_{1 \leq i \leq k} (\Delta V m_{i,p})(t_k - t_{k-1}) \tag{7.8}$$

7.5.5 Proportion of timber species.

Our list of Amazonia-wide timber species is derived from : (i) a working list of commercial timbers[87] ; (ii) commercial species lists provided by national forest services[88] ; and, (iii) timber species identified by TmFO site principal investigators (personal communications). The list of potential timber species found in both forest inventories used in this study and the complete list of commercial

[87] J. Mark et al. (2014). *A Working List of Commercial Timber Tree Species*. Rapp. tech., p. 13–48.

[88] S. N. F. y. d. F. S. Peru (2016). *Lista Oficial de Especies Forestales Maderables Aprovechables con Fines Comerciales* ; S. Guitet et al. (2016). *Sylviculture pour la production de bois d'oeuvre des forêts du Nord de la Guyane*. April. ONF ; S. F. B. Brasil (2016). *Espécies madeireiras de interesse comercial*.

species is provided in the supplementary material (Section 7.7.1). The proportion of potential timber in the total volume was then calculated as :

$$\omega_{k,p} = \frac{\sum_{i \in T_{k,p}} V_{i,k}}{V_{k,p}} \tag{7.9}$$

where $T_{k,p}$ are all individuals from species on the list of timber species, at census k in plot p.

7.5.6 The VDDE model

The Volume Dynamics with Differential equations (VDDE) model that was introduced and described in detail in[89] was calibrated with volume dynamics data (volumes, volume gain, volume mortality, post-logging volume loss) from permanent sample plots. Calibration was carried out using an adapted form of the Hamiltonian Monte Carlo using Stan's programming language[90], and was developed in R[91] (Table 7.1 provides parameters prior and posterior).

The total volume of trees ≥ 50 cm DBH at census k in plot p was modelled as :

$$V_{k,p} \sim log\mathcal{N}(\mu V_{k,p}\ ,\ \sigma_V^2) \tag{7.10}$$

with σ_V the standard deviation, and $\mu V_{k,p}$ the expected volume at census k in plot p defined as[92] :

$$\begin{aligned}\mu V_{k,p} &= Vol(\tau_{1,p} + t_k) \\ &= \frac{\alpha_{G,p}}{\theta}\Big(1 - \frac{\theta \cdot e^{-\beta_G(\tau_{1,p}+t_k)} - \beta_G \cdot e^{-\theta(\tau_{1,p}+t_k)}}{\theta - \beta_G}\Big) \\ &- \left(\frac{\alpha_{G,p}}{\theta} - vmax_p\right)\Big(1 - \frac{\theta \cdot e^{-\beta_M \cdot (\tau_{1,p}+t_k)} - \beta_M \cdot e^{-\theta(\tau_{1,p}+t_k)}}{\theta - \beta_M}\Big)\end{aligned} \tag{7.11}$$

where Vol is the volume prediction as a function of the stand maturity, described in[93] ; $\tau_{1,p}$ is post-logging forest maturity ; t_k is the number of years between the first post-logging census and census k ; $\alpha_{G,p}$ is the climax gross volume productivity ($m^3 ha^{-1} yr^{-1}$) ; $vmax_p$ is the potential volume ($m^3 ha^{-1}$) ; β_G and β_M are the rates at which the climax gross volume productivity and mortality are reached ; θ is the rate of volume loss from respiration. The volume gain, from the growth of trees ≥ 50 cm DBH (including new recruits) was modelled as :

$$cVg_{k,p} \sim log\mathcal{N}(\mu G_{k,p}\ ,\ \sigma_G^2) \tag{7.12}$$

with σ_G the standard deviation, and $\mu G_{k,p}$ the expected volume gain at census k, in plot p defined as[94] :

[89] Piponiot et al. (2018). « Assessing timber volume recovery after disturbance in tropical forests – A new modelling framework », cf. note 15, p. 109.

[90] Carpenter et al. (2017). « Stan : A Probabilistic Programming Language », cf. note 29, p. 30.

[91] R Core Team (2017). *R : A Language and Environment for Statistical Computing*, cf. note 28, p. 30.

[92] Piponiot et al. (2018). « Assessing timber volume recovery after disturbance in tropical forests – A new modelling framework », cf. note 15, p. 109.

[93] Ibid.

[94] Ibid.

$$\mu G_{k,p} = \int_{\tau_{1,p}}^{\tau_{1,p}+t_k} \Big(\alpha_{G,p} \cdot (1 - e^{-\beta_G \cdot t}) - \theta \cdot \mu V_{t,p}\Big) dt \qquad (7.13)$$

Annual volume loss from tree mortality in plot p at census k was modelled as :

$$cVm_{k,p} \sim log\mathcal{N}(\mu M_{k,p}\ ,\ \sigma_M^2) \qquad (7.14)$$

with σ_M the standard deviation, and $\mu M_{k,p}$ the expected volume mortality at census k, in plot p defined according to equation[95] :

[95] Ibid.

$$\mu M_{k,p} = \int_{\tau_{1,p}}^{\tau_{1,p}+t_k} \Big(\alpha_{M,p} \cdot (1 - e^{-\beta_M \cdot t})\Big) dt \qquad (7.15)$$

Volume loss caused by logging in plot p was modelled as[96] :

[96] Ibid.

$$\delta V_{s,p} \sim \mathcal{N}(\mu D_{s,p}\ ,\ \sigma_D^2) \qquad (7.16)$$

with σ_D the standard deviation, and $\mu D_{k,p}$ the expected post-logging volume loss in plot p from site s defined as[97] :

[97] Ibid.

$$\mu D_{s,p} = Vol(\tau_{0,s}) - Vol(\tau_{1,p}) \qquad (7.17)$$

where $\tau_{0,s}$ is pre-logging maturity estimated at site s (see equation 7.20).

We also used 1216 single-measurement plots (RadamBrasil) in minimally disturbed forests[98] as our reference for undisturbed forests. We model their volume as :

[98] A Tyukavina et al. (2016). « Pan-tropical hinterland forests : mapping minimally disturbed forests ». In : *Global Ecology and Biogeography* 25.2, p. 151–163.

$$V_p \sim log\mathcal{N}(Vol(\tau_{0,p})\ ,\ \sigma_{radam}^2) \qquad (7.18)$$

with σ_{radam} the standard deviation ; $Vol(\tau_{0,p})$ the expected volume in plot p according to equation 7.11 ; $\tau_{0,p}$ was estimated with equation 7.20, setting the pre-logging disturbance δi to 0 (plots located in minimally disturbed forests).

7.5.7 Modelling spatial variation in volume dynamics.

Model parameters β_G, β_M and θ were assumed to be constant across Amazonia. 3 parameters of the VDDE model were expressed as a function of spatially-explicit variables : (i) the climax gross volume productivity α_G ; (ii) the potential volume $vmax$, and (iii) the pre-logging forest maturity τ_0. The climax gross volume productivity α_G was extracted from the map obtained with FORMIND[99] (see paragraph "Spatially-explicit variables"). Because the climax volume $vmax$ is expected to vary with soil

[99] Rödig et al. (2017). « Spatial heterogeneity of biomass and forest structure of the Amazon rain forest : Linking remote sensing, forest modelling and field inventory », cf. note 25, p. 29.

and topography, we allowed it to vary between plots among and within site. The climax volume in plot p was modelled as :

$$vmax_p \sim \mathcal{N}(Vclimax_s, \sigma^2_{vmax}) \tag{7.19}$$

where σ_{vmax} is the standard deviation, and $Vclimax_s$ is the climax volume predicted with FORMIND[100] at site s (see paragraph "Spatially-explicit variables").

The pre-logging maturity $\tau_{0,s}$ in site s was modelled as :

$$\tau_{0,s} = \left(\frac{1}{mort_s}\right)^{\lambda} \cdot (1 - \delta i_s) \tag{7.20}$$

where $mort_s$ is the annual stem turnover rate (%)[101], and $\lambda > 0$ is a power parameter to the relationship between the maturity and the stem turnover rate. In our study area, Western Amazonian forests grow on nutrient-rich but unstable soils[102] and are thus more prone to natural disturbances like big blow-downs[103] than northeastern Amazonian forests. Frequent disturbances and high resource availability favour fast-growing species with high turnover rates. For this reason we chose the stem turnover rate as a proxy of the disturbance regime. Because in some sites there were human disturbances prior to the logging experiment, we added a parameter δi_s that represents the gap between the estimated and the expected pre-logging maturity at site s (Table 7.1 provides parameters prior and posterior).

7.5.8 Proportion of potential timber species.

Proportion of potential timber species. Let ω_0 be the proportion of pre-logging total volume composed of potential timber species. We make the conservative assumption that in the absence of logging this proportion is constant. Timber proportions in the 2660 RadamBrasil plots and pre-logging in TmFO plots were interpolated to generate a map of potential timber proportion (Figure 7.8). Because most plots were installed during the 1970s[104], this map does not account for the impact of logging and forest degradation that occurred during the following decades[105]. It represents the maximum timber proportion (in % of the total volume) that can be expected at each location.

7.5.9 Logging precision model.

Because logging targets timber species, each harvest modifies their proportion in the total volume. The relationship between the volume of timber species extracted $Vext$ and the total volume loss δV was modelled as follows[106] :

$$\frac{Vext}{\delta V} = \omega ext \sim \mathcal{B}eta(\alpha, \beta) \tag{7.21}$$

[100] Rödig et al. (2017). « Spatial heterogeneity of biomass and forest structure of the Amazon rain forest : Linking remote sensing, forest modelling and field inventory », cf. note 25, p. 29.

[101] Johnson et al. (2016). « Variation in stem mortality rates determines patterns of above-ground biomass in Amazonian forests : implications for dynamic global vegetation models », cf. note 8, p. 24.

[102] Quesada et al. (2012). « Basin-wide variations in Amazon forest structure and function are mediated by both soils and climate », cf. note 1, p. 23.

[103] Espírito-Santo et al. (2014). « Size and frequency of natural forest disturbances and the Amazon forest carbon balance », cf. note 5, p. 23.

[104] Brasil (1973). *Projeto Radambrasil. Levantamento de recursos naturais*, cf. note 14, p. 25.

[105] Asner et al. (2006). « Condition and fate of logged forests in the Brazilian Amazon. », cf. note 78, p. 9 ; Foley et al. (2007). « Amazonia revealed : forest Degradation and Loss of Ecosystem Goods and Services in the Amazon Basin », cf. note 8, p. 109 ; H. K. Gibbs et al. (2010). « Tropical forests were the primary sources of new agricultural land in the 1980s and 1990s ». In : *Proceedings of the National Academy of Sciences* 107.38, p. 16732–16737.

[106] Piponiot et al. (2018). « Assessing timber volume recovery after disturbance in tropical forests – A new modelling framework », cf. note 15, p. 109.

with $\alpha > 0$, $\beta > 0$ the shape parameters.

$$E\left(\omega ext\right) = \frac{\alpha}{\alpha + \beta} = \omega_0^{1-\psi} \tag{7.22}$$

$$Var\left(\omega ext\right) = e \cdot \left(1 - E\left(\omega ext\right)\right) \cdot E\left(\omega ext\right) \tag{7.23}$$

with $e > 0$ an error parameter and $\psi \in [0, 1]$ the logging precision : when $\psi = 1$ only timber species were killed during logging operations (no incidental damage) ; when $\psi = 0$, logging randomly killed timber and non-timber species. $Var(\omega ext) = 0$ when $\omega_0 = 0$ or when $\omega_0 = 1$: when there are only/no timber trees, only timber/non-timber trees killed. The post-logging proportion of timber volume was calculated as :

$$\omega_1 = \frac{V_0 \cdot \omega_0 - Vext}{V_0 - \delta V} = \omega_0 \frac{V_0 - Vext \cdot \omega_0^{-1}}{V_0 - Vext \cdot \omega_0^{\psi-1}} \tag{7.24}$$

where V_0 and ω_0 are the pre-logging volume and proportion of timber volume respectively (parameters prior and posterior are in Table 7.1, and model predictions are presented in Figure 7.10).

7.5.10 Recruitment model.

After logging, the proportion of timber volume recovers by recruitment into the $\geq$ 50 cm DBH class. We assume that the proportion of timber volume in trees $<$ 50 cm DBH is ω_0, the same as trees $\geq$ 50 cm DBH and is not affected by logging. Let ω_j be the proportion of commercial timber volume j years after logging. In our simulations, we thus update ω_{j+1} according to the following equation :

$$\begin{aligned} Vol(\tau_1 + j + 1) \cdot \omega_{j+1} =& Vol(\tau_1 + j) \cdot \omega_j \\ &+ g(\tau_1 + j) \cdot \left(\underbrace{\omega_0 \cdot pR_j}_{\text{recruitment}} + \underbrace{\omega_j \cdot (1 - pR_j)}_{growth} \right) \\ &- m(\tau_1 + j) \cdot \omega_j \end{aligned} \tag{7.25}$$

with $\tau_1 + j$ the stand maturity and $Vol(\tau_1 + j)$ the corresponding volume j years after logging ; pR_j the proportion of recruitment over the total volume gain $g(\tau_1 + j)$, and $m(\tau_1 + j)$ the volume loss from mortality j years after logging. We model the proportion of recruitment of trees $<$ 50 cm DBH in plot p as :

$$logit(pR_p) \sim \mathcal{N}\Big(\gamma_0 + \gamma_1 \cdot ln(V_p) \ , \ \sigma_R^2\Big) \tag{7.26}$$

where γ_0 and $\gamma_1 > 0$ are respectively the intercept and slope of the relationship, and σ_R the standard deviation. In this model,

the proportion of recruitment is 1 when the total volume is null and decreases thereafter. Because there was strong inter-annual variation in the number of recruited trees, we used the mean value pR_p and the mean volume V_p over all censuses in each plot p (Table 7.1 provides parameters prior and posterior).

7.5.11 Accounting for defective stems

A significant part of large trees in natural forests have hollows or other defects that make them unsuitable for timber uses[107]. The proportion of commercial volume with defects unacceptable for sawmills ranges 20-50% in the Brazilian Amazon[108] ; an extensive data collection in forest concessions in French Guiana reported that on average 20% of harvestable stems had hollows and were not harvested (ONF : personnal communication ;[109]). We thus multiplied all timber volumes in our simulations by a factor (1-$Pdef$), with $Pdef$ the proportion of defective volume modelled as :

$$Pdef \sim \mathcal{B}eta(2, 8) \tag{7.27}$$

The mean value of $Pdef$ is thus a conservative 20% ; to reflect the uncertainty on this value, we chose a distribution with a large 95% credibility interval (3% - 48%).

7.5.12 Simulations of timber recovery.

Simulations were carried for every pixel of a 1° grid. We simulated 5 scenarios : (1) standard logging rules (logging intensity $Vext = 20$ m^{3}ha^{-1}, cutting cycle 30 yrs) ; (2) low logging intensity (10 m^3ha^{-1}) with a median cutting cycle (30 years) ; (3) high logging intensity (30 m^3ha^{-1}) with a median cutting cycle ; (4) short cutting cycle (15 years) with a median logging intensity (20 m^3ha^{-1}) ; (4) long cutting cycle (65 years) with a median logging intensity (20 m^3ha^{-1}).

In each scenario, we consider that each year $\frac{1}{trot}$ of the area available for logging is actually logged (with $trot$ the cutting cycle), so that an area is logged every $trot$ years and the total area logged each year is constant. Due mostly to slope restrictions in Amazonia, the area logged typically represent 60% of the total area allocated for logging[110]. Using data from logging concessions in French Guiana (reported in Figure 7.15), we multiplied the annual harvested area by a coefficient $\pi \sim \mathcal{N}_{t[0,1]}(0.58, 0.13^2)$, where $\mathcal{N}_{t[0,1]}$ is the normal distribution truncated between 0 and 1.

To propagate errors on results, the following steps were repeatedly taken :

1. At each location, model parameters are drawn from their posterior distribution. Timber volumes (per ha) are calcula-

[107] Putz (2013). « Complexity confronting tropical silviculturalists », cf. note 50, p. 115.

[108] T. P. Holmes et al. (2002). « Financial and ecological indicators of reduced-impact logging performance in the eastern Amazon ». In : *Forest Ecology and Management* 163, p. 93–110 ; D. Valle et al. (2006). « Identifying bias in stand-level growth and yield estimations : A case study in eastern Brazilian Amazonia ». In : *Forest Ecology and Management* 236.2-3, p. 127–135 ; E. M. Nogueira et al. (2006). « Volume and biomass of trees in central Amazonia : influence of irregularly shaped and hollow trunks ». In : *Forest Ecology and Management* 227.1-2, p. 14–21.

[109] Guitet et al. (2016). *Sylviculture pour la production de bois d'oeuvre des forêts du Nord de la Guyane*, cf. note 88, p. 119.

[110] T. R. Feldpausch et al. (2006). « Biomass, harvestable area, and forest structure estimated from commercial timber inventories and remotely sensed imagery in southern Amazonia ». In : *Forest Ecology and Management* 233.1, p. 121–132 ; A. Verissimo et al. (2006). *Areas para produção florestal manejada : detalhamento do macrozoneamento ecológico econômico do Estado do Pará*. Rapp. tech., p. 1–81 ; A. A. Silva (2014). *Concessão Florestal no Amazonas : Estudos da viabilidade de implantação na Floresta Estadual Tapauá*. Rapp. tech.

ted as :

$$V_{t,pix,l} = Vol(\tau_{t,pix,l}) \cdot \omega_{t,pix,l} \cdot (1 - Pdef) \quad (7.28)$$

where $V_{t,pix,l}$ is the predicted timber volume t years after the first harvest in pixel pix in scenario l, $\tau_{t,pix,l}$ is the predicted maturity , $Vol(\tau_{t,pix,l})$ is the volume of all trees ≥ 50 cm DBH according to equation 7.11, $\omega_{t,pix,l}$ is the proportion of timber volume and $Pdef$ is the proportion of defective volume ;

2. For each pixel, each time step $t \in [1, 300]$ and each scenario $1 \leq l \leq 5$, the total timber volume is calculated as :

$$Vtot_{t,l} = \sum_{pix} [(V_{t,pix,l}) \cdot area_{pix} \cdot \pi] \quad (7.29)$$

where $V_{t,pix,l}$ is the timber volume (per ha) t years after the first harvest in pixel pix in scenario l ; and $area_{pix} \cdot \pi$ is the area (ha) inside pixel pix that is available for logging.

3. The real extracted volume (per ha) from each pixel pix is calculated as the minimum between the extracted volume in scenario l (*i.e.* the timber volume expected to be harvested) and the timber volume at the time of logging (*i.e.* the timber volume actually available in pixel pix). The total extracted volume at year t is the sum of the actual extracted volume from areas logged at t.
4. Potential timber volume recovery (%) is calculated as the increase in potential timber volume over the first cutting cycle, divided by the total extracted volume (Figure 7.2). The annual timber recovery is calculated as the increase in potential timber volume between two consecutive years (Figure 7.3).

Steps 1-4 were repeated 100 times and summary statistics were calculated. Timber recovery and timber extraction were compared to the current and future demand for sawlogs. Current demand was assessed as the production of sawlogs in the Amazon region in 2004, 31 Mm^3 according to the Imazon[111]. Future increase in demand was assumed to follow the trend of increase in sawnwood consumption in South America as projected with the Global Forest Products Model[112]. We thus computed the proportional increase predicted between 2006 and 2060 for 4 Intergovernmental Panel on Climate Change Scenarios (A1B, A2, B2 and A1B-Low Fuelwood)[113] and multiplied the current demand for sawlogs by this increase to get the future demand for sawlogs (Figure 7.3).

[111] Lentini et al. (2005). *Fatos Florestais da Amazônia 2005 (Amazonian Forest Facts)*, cf. note 1, p. 107.

[112] Buongiorno et al. (2012). « Outlook to 2060 for World Forests and Forest Industries : A Technical Document Supporting the Forest Service 2010 RPA Assessment », cf. note 2, p. 107.

[113] Ibid.

7.6 Data and code availability

The data used in the analyses are available at https ://figshare.com/s/336dcbff400a812a56ea.

Associated computer codes are available at https ://figshare.com/s/9873edea9c1e8fe98993.

Acknowledgements This study was partially funded by the GFclim project (FEDER 20142020, Project GY0006894), an Investissement d'Avenir grant of the ANR (CEBA : ANR-10-LABEX-0025), the Sao Paulo Research Foundation (FAPESP : 2013/16262–4 and 2013/50718–5) and carried out in the framework of the Tropical managed Forests Observatory (TmFO), supported by the Sentinel Landscape program of CGIAR (Consultative Group on International Agricultural Research) – Forest Tree and Agroforestry Research Program. We would also like to thank Marie-Gabrielle Piketty for her valuable comments.

Competing Interests The authors declare that they have no competing financial interests.

Correspondence Correspondence and requests for materials should be addressed to C.P. (camille.piponiot@gmail.com) and B.H. (bruno.herault@cirad.fr).

Authors' contribution Data Acquisition : all authors. Conception and design : CP, BH. Model Development : CP, BH, ERo. Data analysis and interpretation : CP, BH. Writing the manuscript : CP, ERo, FEP, ERu, PS, LB, BH. Manuscript revision : all authors.

TABLE 7.1 – Parameters description. For each model, we describe the parameters used in this study : their name, meaning, prior distribution and the maximum likelihood and 95% credibility interval (between brackets) of the posterior.

Model	Parameter	Description	Prior	Posterior
Volume dynamics	λ	Power on turnover rate	$\mathcal{U}(1.2, 1.5)$	1.4 [1.4, 1.5]
	δi_s	Pre-logging maturity loss	$\mathcal{U}(0, 1)$	0.17 [0.0011, 0.62]
	$t_{1p,s}$	Post-logging maturity	$\mathcal{U}(0, t_{0s})$	64 [44, 370]
	β_G	Volume gain rate	$\mathcal{U}(0, ln(2))$	0.0041 [0.0028, 0.0039]
	β_M	Volume mortality rate	$\mathcal{U}(0, \frac{\alpha_G \beta_G}{\alpha_M})$	0.0024 [0.0014, 0.0022]
	θ	Respiration rate	$\mathcal{U}(0, 0.1)$	0.022 [0.019, 0.022]
	σ_V	Volume stand. dev.	$\mathcal{N}_{[0,+\infty[}(0, 1)$	0.086 [0.082, 0.12]
	σ_G	Vol. gain stand. dev.	$\mathcal{N}_{[0,+\infty[}(0, 1)$	0.39 [0.34, 0.41]
	σ_M	Vol. mort. stand. dev.	$\mathcal{N}_{[0,+\infty[}(0, 1)$	0.33 [0.3, 0.37]
	σ_D	Logging vol. loss stand. dev.	$\mathcal{N}_{[0,+\infty[}(0, 1)$	8.5 [7.6, 9.6]
	σ_{radam}	Vol. stand. dev. (Radam)	$\mathcal{N}_{[0,+\infty[}(0, 1)$	0.75 [0.71, 0.86]
Logging precision	ψ	Logging precision	$\mathcal{U}(0, 1)$	0.56 [0.46, 0.65]
	e	Log. prec. error	$\mathcal{U}(0, 1)$	0.33 [0.22, 0.58]
Proportion of recruitment	γ_0	Intercept	$\mathcal{N}(0, 10^{-3})$	2.7 [2.2, 3.2]
	γ_1	Slope	$\mathcal{N}(0, 10^{-3})$	-0.57 [-0.68, -0.44]
	σ_R	Standard deviation	$\mathcal{N}_{[0,+\infty[}(0, 1)$	0.24 [0.21, 0.31]

7.7 Supplementary materials

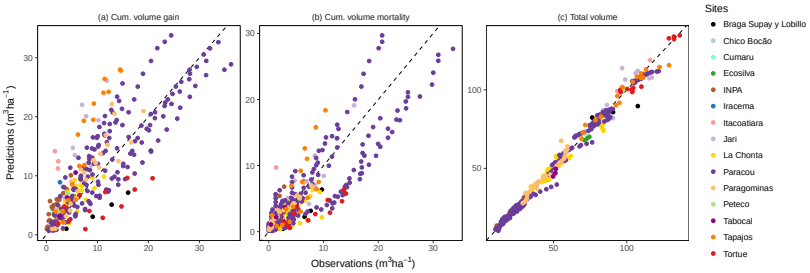

FIGURE 7.7 – Goodness of fit of the model predictions to the dynamic volume data. Observed values of (a) cumulative volume gain, (b) cumulative volume mortality and (c) total volume ($m^3 ha^{-1}$) are on the x-axis, while the corresponding predicted values are on the y-axis. Points of the same colour are from the same site (see legend on the right panel).

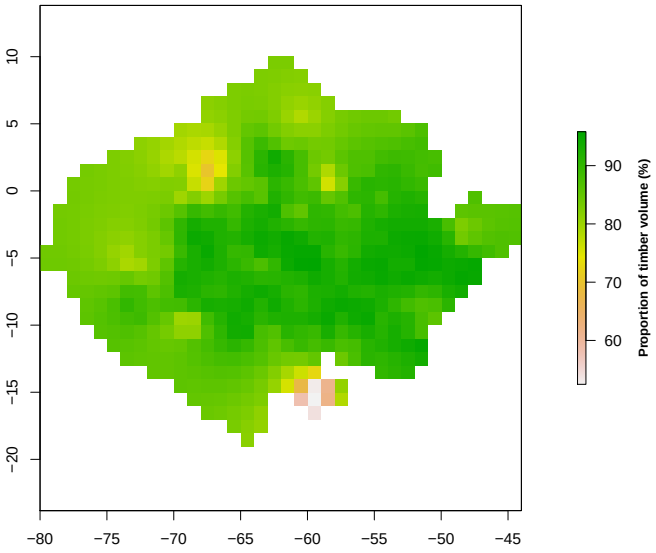

FIGURE 7.8 – Map of timber proportion in Amazonia. This map was built by interpolating the proportion of potential timber volume in 3500 ha of forest inventory plots (prior to logging). The proportion of timber volume is the proportion of the total volume that is found in timber species (the list of timber species is provided at theend of the supplementary material).

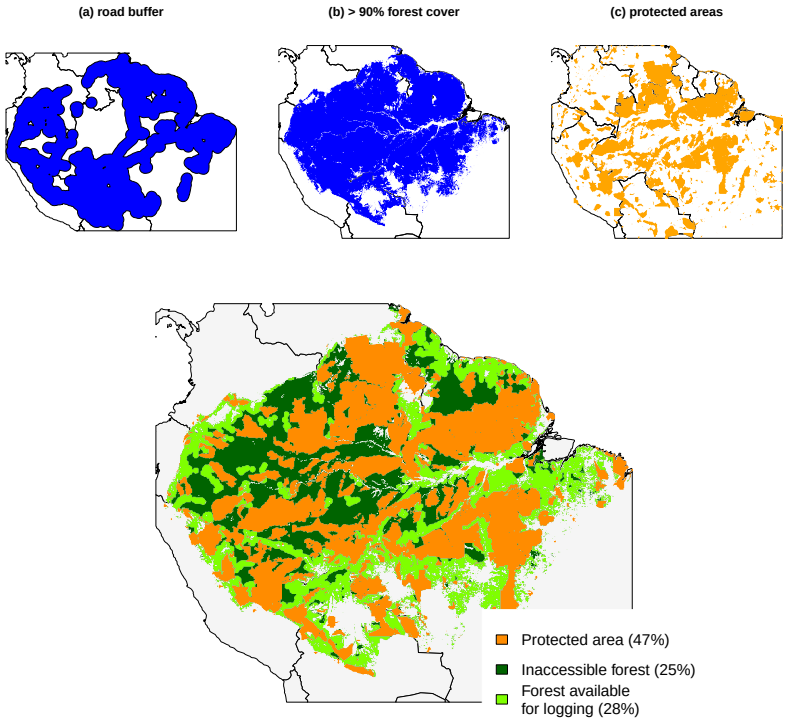

FIGURE 7.9 – Map of areas available for logging. (a) Areas within 25 km of a vehicle way (blue) ; (b) areas with forest cover > 90% (blue) (c) areas inside protected areas (orange). (d) Area considered as available for selective logging in this study, that obtained as the intersection of maps (a) and (b), from which areas in (c) were excluded.

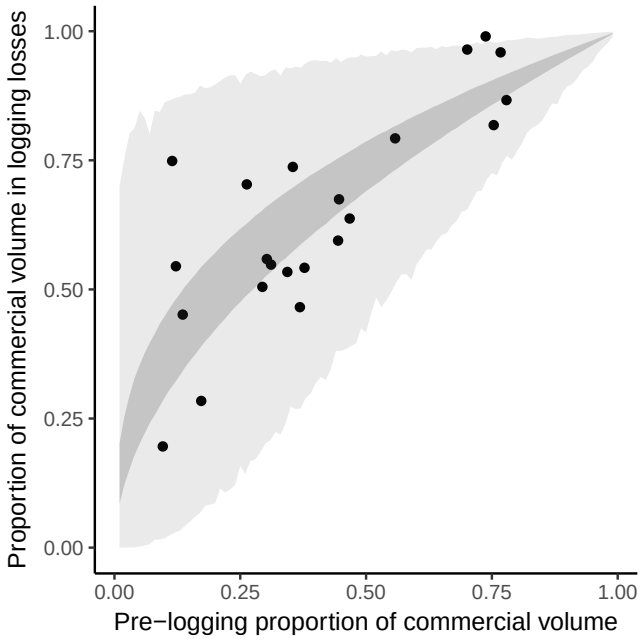

FIGURE 7.10 – Prediction of the logging precision (proportion of timber volume in logging losses), as a function of pre-logging proportion of timber volume. Each point is a logged plot. The shaded area is the 95% credibility interval of predictions, with the darker area being the 95% credibility interval of the expectation.

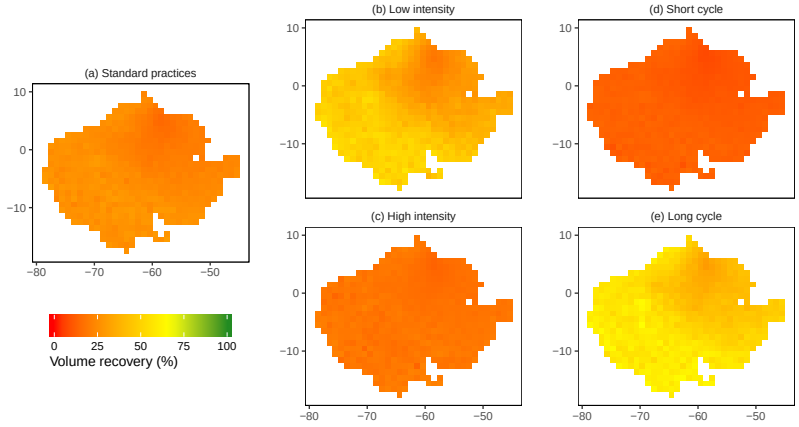

FIGURE 7.11 – Lower bound of the 95% credibility interval on potential timber volume recovery in Amazonia after one selective harvest predicted under 5 scenarios : (a) standard practices : 20 m^3ha^{-1} of timber extracted and a cutting cycle length of 30 years ; (b) low logging intensity : 20 m^3ha^{-1}, 30 years ; (c) high logging intensity : 30 m^3ha^{-1}, 30 years ; (d) short cutting cycle : 15 years, 20 m^3ha^{-1} ; (e) long cutting cycle : 65 years, 20 m^3ha^{-1}. Colours range from red (no recovery) to green (full recovery).

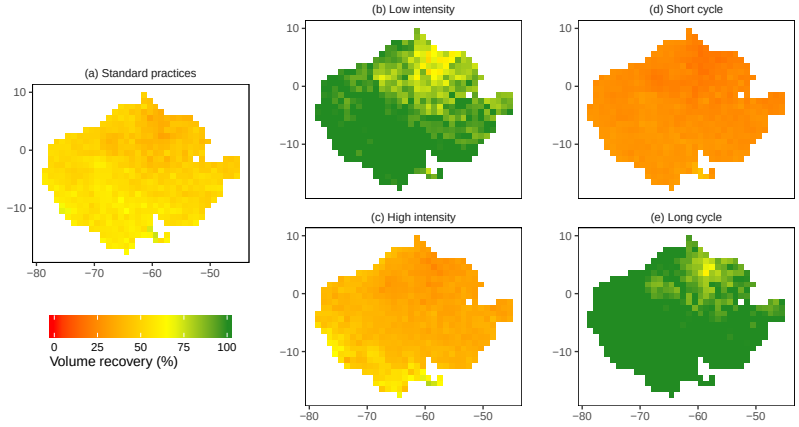

FIGURE 7.12 – Upper bound of the 95% credibility interval on potential timber volume recovery in Amazonia after one selective harvest predicted under 5 scenarios : (a) standard practices : 20 m^3ha^{-1} of timber extracted and a cutting cycle length of 30 years ; (b) low logging intensity : 20 m^3ha^{-1}, 30 years ; (c) high logging intensity : 30 m^3ha^{-1}, 30 years ; (d) short cutting cycle : 15 years, 20 m^3ha^{-1} ; (e) long cutting cycle : 65 years, 20 m^3ha^{-1}. Colours range from red (no recovery) to green (full recovery).

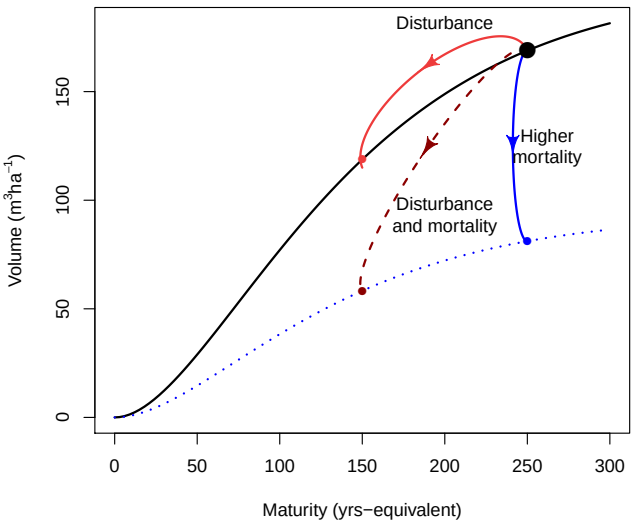

FIGURE 7.13 – Effect of higher mortality rate and disturbance regime on the volume predictions. The black thick curve is the predicted volume (y axis) as a function of the stand maturity (x axis). The black dot is the initial position of the stand. The dark red arrow is the effect of a higher disturbance regime, i.e. decrease in the stand maturity but volume potential is not affected and the stand can recover its initial volume if the disturbances stop. The blue arrow is the effect of a higher annual mortality rate, resulting in a decrease in the potential volume : the blue dotted line is the new volume predictions. The purple arrow is the combined effect of higher disturbance regime and annual mortality.

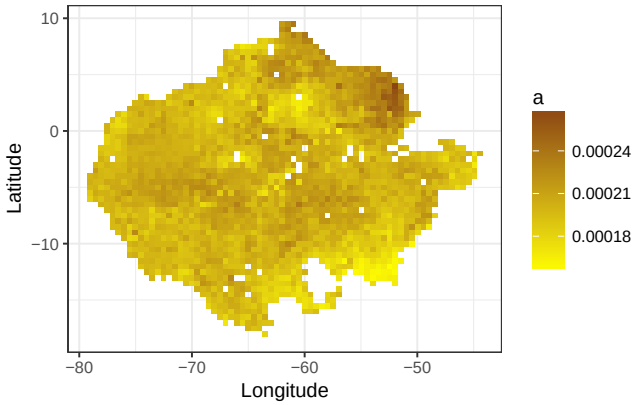

FIGURE 7.14 – Map of predicted values of the intercept a in the volumetric equation 7.1.

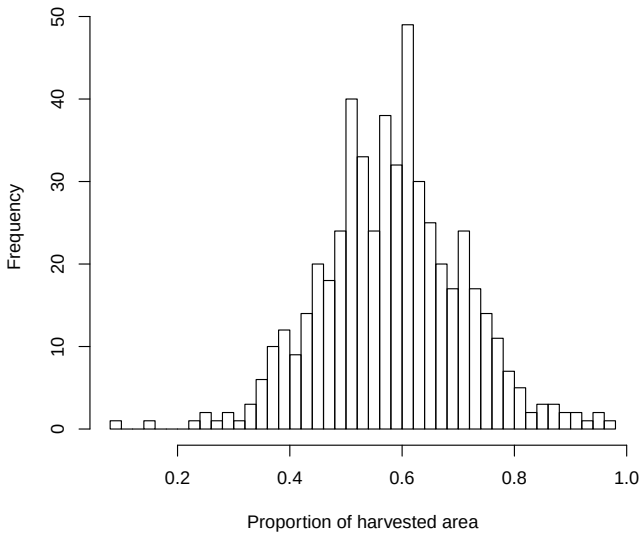

FIGURE 7.15 – Histogram of the proportion of the total area that has actually been harvested in French Guiana logging concessions from 1995 to 2016. The data have been reported by the French national forest service (ONF).

7.7.1 List of potential timber species

Here we provide the complete list of the 943 species recorded in the forest inventories used in this study (from RadamBrasil or TmFO data) that were registered as commercial in either (i) the Timber working List[114], (ii) commercial species lists provided by national forest services[115] or (iii) timber species provided by TmFO sites principal investigators (personal communications).

Abarema jupunba, Abarema mataybifolia, Acacia bonariensis, Acacia huilana, Acacia kuhlmannii, Acosmium cardenasii, Acosmium dasycarpum, Acosmium nitens, Acrodiclidium aureum, Agonandra brasiliensis, Agonandra silvatica, Albizia niopoides, Albizia pedicellaris, Alchornea discolor, Alchornea triplinervia, Alchorneopsis floribunda, Aldina retusa, Alexa grandiflora, Alexa wachenheimii, Allantoma lineata, Amaioua guianensis, Amanoa congesta, Amanoa guianensis, Ambelania acida, Amburana cearensis, Ampelocera ruizii, Amphirrhox longifolia, Anacardium giganteum, Anacardium occidentale, Anacardium spruceanum, Anadenanthera colubrina, Anadenanthera peregrina, Andira coriacea, Andira inermis, Andira parviflora, Aniba burchellii, Aniba canelilla, Aniba citrifolia, Aniba guianensis, Aniba hostmanniana, Aniba panurensis, Aniba rosaeodora, Aniba taubertiana, Aniba williamsii, Annona exsucca, Annona paludosa, Annona prevostiae, Anthodiscus amazonicus, Antonia ovata, Apeiba albiflora, Apeiba aspera, Apeiba echinata, Apeiba glabra, Apeiba membranacea, Apeiba petoumo, Apuleia leiocarpa, Apuleia molaris, Aspidosperma album, Aspidosperma cuspa, Aspidosperma cylindrocarpon, Aspidosperma desmanthum, Aspidosperma discolor, Aspidosperma excelsum, Aspidosperma helstonei, Aspidosperma macrocarpon, Aspidosperma megalocarpon, Aspidosperma multiflorum, Aspidosperma nitidum, Aspidosperma oblongum, Aspidosperma obscurinervium, Aspidosperma polyneuron, Aspidosperma populifolium, Aspidosperma pyrifolium, Aspidosperma rigidum, Aspidosperma sandwithianum, Aspidosperma spruceanum, Aspidosperma tomentosum, Aspidosperma vargasii, Astronium fraxinifolium, Astronium gracile, Astronium graveolens, Astronium lecointei, Astronium urundeuva, Bagassa guianensis, Balfourodendron riedelianum, Balizia pedicellaris, Batesia floribunda, Batocarpus amazonicus, Bertholletia excelsa, Bixa arborea, Bixa orellana, Bocageopsis multiflora, Bocoa prouacensis, Bombacopsis nervosa, Bombax globosum, Bombax munguba, Bowdichia nitida, Bowdichia virgilioides, Brosimum acutifolium, Brosimum alicastrum, Brosimum amplicoma, Brosimum aubletii, Brosimum gaudichaudii, Brosimum guianense, Brosimum lactescens, Brosimum lanciferum, Brosimum paraense, Brosimum parinarioides, Brosimum potabile, Brosimum rubescens, Brosimum uleanum, Brosimum utile, Buchenavia capitata, Buchenavia grandis, Buchenavia guianensis, Buchenavia huberi, Buchenavia nitidissima, Buchenavia parvifolia, Buchenavia punctata, Buchenavia tetraphylla, Buchenavia tomentosa, Byrsonima ae-

[114] Mark et al. (2014). *A Working List of Commercial Timber Tree Species*, cf. note 87, p. 119.

[115] Peru (2016). *Lista Oficial de Especies Forestales Maderables Aprovechables con Fines Comerciales*, cf. note 88, p. 119; Guitet et al. (2016). *Sylviculture pour la production de bois d'oeuvre des forêts du Nord de la Guyane*, cf. note 88, p. 119; Brasil (2016). *Espécies madeireiras de interesse comercial*, cf. note 88, p. 119.

rugo, Byrsonima densa, Byrsonima laevigata, Byrsonima spicata, Cabralea canjerana, Caesalpinia pluviosa, Calatola venezuelana, Callisthene fasciculata, Calophyllum brasiliense, Calycophyllum spruceanum, Campsiandra laurifolia, Candolleodendron brachystachyum, Capirona decorticans, Capirona huberiana, Capparidastrum frondosum, Caraipa densifolia, Caraipa grandifolia, Caraipa punctulata, Caraipa racemosa, Carapa guianensis, Carapa procera, Carapa surinamensis, Cariniana decandra, Cariniana domestica, Cariniana estrellensis, Cariniana ianeirensis, Cariniana micrantha, Cariniana rubra, Caryocar brasiliense, Caryocar glabrum, Caryocar microcarpum, Caryocar villosum, Caryodendron amazonicum, Casearia decandra, Casearia gossypiosperma, Casearia guianensis, Casearia javitensis, Casearia pitumba, Casearia sylvestris, Cassia adiantifolia, Cassia apoucouita, Cassia ferruginea, Cassia leiandra, Cassia spruceana, Cassipourea guianensis, Catostemma commune, Catostemma fragrans, Cecropia sciadophylla, Cedrela fissilis, Cedrela odorata, Cedrelinga cateniformis, Ceiba burchellii, Ceiba pentandra, Ceiba samauma, Centrolobium microchaete, Centrolobium paraense, Chaetocarpus schomburgkianus, Chamaecrista apoucouita, Chaunochiton kappleri, Chaunochiton Kappleri, Cheiloclinium cognatum, Chimarrhis turbinata, Chlorophora tinctoria, Chrysophyllum anomalum, Chrysophyllum argenteum, Chrysophyllum auratum, Chrysophyllum gonocarpum, Chrysophyllum lucentifolium, Chrysophyllum oppositum, Chrysophyllum pomiferum, Chrysophyllum prieurii, Chrysophyllum sanguinolentum, Chrysophyllum venezuelanense, Chytroma basilaris, Clarisia biflora, Clarisia racemosa, Clathrotropis macrocarpa, Coccoloba mollis, Commelina virginica, Conceveiba guianensis, Copaifera duckei, Copaifera glycycarpa, Copaifera guianensis, Copaifera langsdorffii, Copaifera multijuga, Copaifera reticulata, Cordia alliodora, Cordia bicolor, Cordia glabrata, Cordia goeldiana, Cordia nervosa, Cordia sagotii, Cordia trichotoma, Couepia bracteosa, Couepia caryophylloides, Couepia guianensis, Couepia habrantha, Couepia leptostachya, Couepia magnoliifolia, Couepia obovata, Couepia parillo, Couma guianensis, Couma macrocarpa, Couma utilis, Coumarouna ferrea, Coumarouna rosea, Couratari calycina, Couratari gloriosa, Couratari guianensis, Couratari macrosperma, Couratari multiflora, Couratari oblongifolia, Couratari pulchra, Couratari stellata, Couroupita guianensis, Crudia amazonica, Crudia aromatica, Cupania scrobiculata, Curatella americana, Cybianthus guyanensis, Cybianthus microbotrys, Cyclolobium blanchetianum, Dacryodes nitens, Dactyloides nitens, Dalbergia spruceana, Dendrobangia boliviana, Dendropanax arboreus, Dialium guianense, Dialyanthera parvifolia, Diatenopteryx sorbifolia, Dicorynia guianensis, Didymopanax morototoni, Dimorphandra exaltata, Dimorphandra glabrifolia, Dimorphandra mollis, Dimorphandra parviflora, Dimorphandra polyandra, Dinizia excelsa, Diospyros capreifolia, Diospyros carbonaria, Diospyros guianensis, Diospyros vestita, Diploon venezuelana, Diplotropis

martiusii, Diplotropis purpurea, Diplotropis racemosa, Diplotropis triloba, Dipteryx alata, Dipteryx magnifica, Dipteryx odorata, Dipteryx polyphylla, Dipteryx punctata, Discophora guianensis, Drypetes fanshawei, Drypetes variabilis, Duckeodendron cestroides, Duckesia verrucosa, Duguetia cauliflora, Duguetia echinophora, Duroia eriopila, Duroia longiflora, Duroia micrantha, Ecclinusa guianensis, Ecclinusa ramiflora, Eglerodendron pariry, Elizabetha paraensis, Elizabetha princeps, Elvasia elvasioides, Emmotum fagifolium, Emmotum nitens, Endlicheria bracteata, Endlicheria bracteolata, Endlicheria melinonii, Endopleura uchi, Enterolobium contortisiliquum, Enterolobium maximum, Enterolobium oldemanii, Enterolobium schomburgkii, Enterolobium timbouva, Eperua falcata, Eperua grandiflora, Eperua oleifera, Eperua rubiginosa, Eriotheca globosa, Eriotheca longipedicellata, Eriotheca longitubulosa, Erisma calcaratum, Erisma laurifolium, Erisma uncinatum, Erythrina glauca, Eschweilera amara, Eschweilera amazonica, Eschweilera apiculata, Eschweilera blanchetiana, Eschweilera chartaceifolia, Eschweilera collina, Eschweilera congestiflora, Eschweilera coriacea, Eschweilera decolorans, Eschweilera grandiflora, Eschweilera grandifolia, Eschweilera odora, Eschweilera ovata, Eschweilera paniculata, Eschweilera parviflora, Eschweilera pedicellata, Eschweilera sagotiana, Eschweilera simiorum, Eschweilera squamata, Eschweilera wachenheimii, Eugenia anastomosans, Eugenia coffeifolia, Eugenia cupulata, Eugenia lambertiana, Eugenia latifolia, Eugenia patrisii, Eugenia pseudopsidium, Euplassa pinnata, Euterpe oleracea, Euxylophora paraensis, Fagara acreana, Fagara rhoifolia, Ferdinandusa elliptica, Ferdinandusa paraensis, Ficus boliviana, Ficus insipida, Ficus killipii, Ficus maroniensis, Ficus nymphaeifolia, Ficus pertusa, Ficus piresiana, Ficus trigona, Fusaea longifolia, Gallesia integrifolia, Garcinia benthamiana, Garcinia madruno, Gaulettia parillo, Genipa americana, Glycydendron amazonicum, Goupia glabra, Goupia longipendula, Guarea glabra, Guarea guidonia, Guarea kunthiana, Guarea kunthii, Guarea macrophylla, Guarea membranacea, Guatteria citriodora, Guatteria poeppigiana, Guatteria pteropus, Guatteria punctata, Guatteria schomburgkiana, Guazuma ulmifolia, Guibourtia chodatiana, Gustavia hexapetala, Handroanthus serratifolius, Hasseltia floribunda, Hebepetalum humiriifolium, Heisteria densifrons, Heisteria flexuosa, Heisteria ovata, Helicostylis pedunculata, Helicostylis tomentosa, Heliocarpus americanus, Hevea brasiliensis, Hieronyma alchorneoides, Hieronyma oblonga, Hirtella bicornis, Hirtella glandistipula, Hirtella glandulosa, Hirtella hispidula, Hirtella piresii, Hirtella racemosa, Holopyxidium jarana, Huberodendron swietenioides, Humiria balsamifera, Humiriastrum excelsum, Humiriastrum subcrenatum, Hura crepitans, Hymenaea courbaril, Hymenaea intermedia, Hymenaea oblongifolia, Hymenaea parvifolia, Hymenolobium excelsum, Hymenolobium flavum, Hymenolobium modestum, Hymenolobium petraeum, Hymenolobium pulcherrimum, Hymenolobium sericeum, Ilex inundata, Inga

acreana, Inga alba, Inga bourgonii, Inga capitata, Inga cayennensis, Inga cylindrica, Inga gracilifolia, Inga heterophylla, Inga jenmanii, Inga lomatophylla, Inga longipedunculata, Inga marginata, Inga melinonis, Inga nobilis, Inga paraensis, Inga pezizifera, Inga rubiginosa, Inga sarmentosa, Inga splendens, Inga stipularis, Inga thibaudiana, Inga tubiformis, Inga umbellifera, Iryanthera crassifolia, Iryanthera grandis, Iryanthera hostmannii, Iryanthera juruensis, Iryanthera macrophylla, Iryanthera sagotiana, Iryanthera tricornis, Jacaranda copaia, Jacaranda cuspidifolia, Jacaratia spinosa, Joannesia heveoides, Kielmeyera coriacea, Labatia macrocarpa, Lacistema grandifolium, Lacmellea aculeata, Lacunaria crenata, Lacunaria jenmanii, Laetia procera, Lecythis chartacea, Lecythis corrugata, Lecythis holcogyne, Lecythis idatimon, Lecythis lurida, Lecythis paraensis, Lecythis persistens, Lecythis pisonis, Lecythis poiteaui, Lecythis prancei, Lecythis zabucajo, Leonia glycycarpa, Licania alba, Licania apetala, Licania canescens, Licania densiflora, Licania glabriflora, Licania granvillei, Licania heteromorpha, Licania hypoleuca, Licania kunthiana, Licania latifolia, Licania latistipula, Licania laxiflora, Licania licaniiflora, Licania longistyla, Licania macrophylla, Licania majuscula, Licania membranacea, Licania micrantha, Licania ovalifolia, Licania parviflora, Licania parvifructa, Licania polita, Licania pruinosa, Licania robusta, Licania sclerophylla, Licania sprucei, Licaria aritu, Licaria brasiliensis, Licaria cannella, Licaria chrysophylla, Licaria crassifolia, Licaria debilis, Licaria martiniana, Licaria rigida, Licaria triandra, Lindackeria paraensis, Loreya arborescens, Lucuma glabrescens, Luehea divaricata, Luehea grandiflora, Luehea speciosa, Lueheopsis duckeana, Lueheopsis rugosa, Mabea piriri, Machaerium acutifolium, Machaerium inundatum, Machaerium scleroxylon, Machaerium villosum, Maclura tinctoria, Macoubea guianensis, Macrolobium acaciifolium, Macrolobium bifolium, Macrolobium campestre, Macrolobium chrysostachyum, Macrolobium multijugum, Macrolobium unijugum, Mahurea palustris, Manilkara amazonica, Manilkara bidentata, Manilkara cavalcantei, Manilkara huberi, Manilkara paraensis, Manilkara surinamensis, Maquira coriacea, Maquira guianensis, Maquira sclerophylla, Martiodendron elatum, Martiodendron parviflorum, Matisia cordata, Maytenus oblongata, Mezilaurus itauba, Mezilaurus lindaviana, Mezilaurus synandra, Miconia chrysophylla, Miconia minutiflora, Miconia tschudyoides, Micrandropsis scleroxylon, Micropholis cyrtobotrya, Micropholis egensis, Micropholis guyanensis, Micropholis longipedicellata, Micropholis melinoniana, Micropholis mensalis, Micropholis obscura, Micropholis venulosa, Minquartia guianensis, Minquartia punctata, Mora paraensis, Moronobea coccinea, Morus alba, Mouriri brevipes, Mouriri collocarpa, Mouriri crassifolia, Mouriri huberi, Myracrodruon urundeuva, Myrcia decorticans, Myrcia fallax, Myrcia magnoliifolia, Myrciaria floribunda, Myrocarpus fastigiatus, Myrocarpus frondosus, Myroxylon balsamum, Naucleopsis caloneura, Naucleopsis

guianensis, Nectandra cissiflora, Nectandra cuspidata, Nectandra globosa, Nectandra micranthera, Nectandra mollis, Nectandra pichurim, Nectandra purusensis, Nectandra rubra, Neoxythece elegans, Neoxythece robusta, Ochroma lagopus, Ochroma pyramidale, Ocotea aciphylla, Ocotea acutangula, Ocotea amazonica, Ocotea argyrophylla, Ocotea bofo, Ocotea caudata, Ocotea cernua, Ocotea cinerea, Ocotea costulata, Ocotea fragrantissima, Ocotea glomerata, Ocotea guianensis, Ocotea javitensis, Ocotea longifolia, Ocotea neesiana, Ocotea nigra, Ocotea oblonga, Ocotea opifera, Ocotea percurrens, Ocotea petalanthera, Ocotea puberula, Ocotea rubra, Ocotea splendens, Ocotea subterminalis, Ocotea tomentella, Oenocarpus bataua, Olmediophaena maxima, Onychopetalum amazonicum, Ormosia amazonica, Ormosia arborea, Ormosia bolivarensis, Ormosia coccinea, Ormosia coutinhoi, Ormosia fastigiata, Ormosia melanocarpa, Ormosia nobilis, Ormosia paraensis, Ormosiopsis flava, Osteophloeum platyspermum, Otoba parvifolia, Ouratea decagyna, Ouratea guianensis, Oxandra asbeckii, Pachira aquatica, Pachira dolichocalyx, Palicourea guianensis, Panopsis rubescens, Panopsis sessilifolia, Parahancornia amapa, Parahancornia fasciculata, Paramachaerium ormosioides, Parapiptadenia rigida, Paraprotium amazonicum, Parinari campestris, Parinari excelsa, Parinari montana, Parinari rodolphii, Parkia decussata, Parkia gigantocarpa, Parkia multijuga, Parkia nitida, Parkia oppositifolia, Parkia paraensis, Parkia pendula, Parkia platycephala, Parkia ulei, Parkia velutina, Paypayrola guianensis, Peltogyne catingae, Peltogyne confertiflora, Peltogyne lecointei, Peltogyne paniculata, Peltogyne paradoxa, Peltogyne venosa, Pentaclethra macroloba, Pera glabrata, Perebea mollis, Perebea rubra, Phyllocarpus riedelii, Phyllostylon rhamnoides, Piptadenia gonoacantha, Piptadenia rigida, Piptadenia suaveolens, Pithecellobium decandrum, Pithecellobium elegans, Pithecellobium racemosum, Plathymenia reticulata, Platonia insignis, Platymiscium filipes, Platymiscium floribundum, Platymiscium pinnatum, Platymiscium trinitatis, Platymiscium ulei, Platypodium elegans, Pleurothyrium parviflorum, Podocarpus rospigliosii, Poecilanthe effusa, Pogonophora schomburgkiana, Poraqueiba guianensis, Poraqueiba paraensis, Poraqueiba sericea, Posoqueria latifolia, Pourouma melinonii, Pourouma mollis, Pouteria ambelaniifolia, Pouteria anomala, Pouteria bangii, Pouteria bilocularis, Pouteria caimito, Pouteria cicatricata, Pouteria cladantha, Pouteria cuspidata, Pouteria engleri, Pouteria eugeniifolia, Pouteria fimbriata, Pouteria flavilatex, Pouteria glomerata, Pouteria gongrijpii, Pouteria guianensis, Pouteria hispida, Pouteria jariensis, Pouteria laevigata, Pouteria lasiocarpa, Pouteria laurifolia, Pouteria melanopoda, Pouteria nemorosa, Pouteria oblanceolata, Pouteria opposita, Pouteria oppositifolia, Pouteria platyphylla, Pouteria procera, Pouteria reticulata, Pouteria rodriguesiana, Pouteria sagotiana, Pouteria singularis, Pouteria torta, Pouteria venosa, Pouteria virescens, Pradosia cochlearia, Pradosia inophylla, Pradosia ptychandra, Prieurella prieurii, Protium

altsonii, Protium apiculatum, Protium aracouchini, Protium decandrum, Protium giganteum, Protium guianense, Protium heptaphyllum, Protium nodulosum, Protium opacum, Protium pallidum, Protium paniculatum, Protium paraense, Protium pilosissimum, Protium puncticulatum, Protium sagotianum, Protium subserratum, Protium tenuifolium, Protium trifoliolatum, Prunus myrtifolia, Pseudolmedia laevis, Pseudolmedia multinervis, Pseudopiptadenia psilostachya, Pseudopiptadenia suaveolens, Pterocarpus amazonicus, Pterocarpus officinalis, Pterocarpus rohrii, Pterogyne nitens, Qualea albiflora, Qualea cyanea, Qualea dinizii, Qualea paraensis, Qualea parviflora, Qualea psidiifolia, Qualea rosea, Qualea tessmannii, Quiina guianensis, Quiina integrifolia, Quiina obovata, Quiina oiapocensis, Rauvolfia paraensis, Recordoxylon speciosum, Rheedia gardneriana, Rheedia macrophylla, Rhodostemonodaphne grandis, Rhodostemonodaphne morii, Rhodostemonodaphne rufovirgata, Richardella macrophylla, Richardella sericea, Rinorea bahiensis, Rinorea guianensis, Roupala montana, Ruizterania albiflora, Saccoglottis amazonica, Saccoglottis guianensis, Sacoglottis cydonioides, Sacoglottis guianensis, Sagotia racemosa, Sandwithia guyanensis, Sapindus saponaria, Sapium glandulosum, Sapium marmieri, Sarcaulus brasiliensis, Schefflera decaphylla, Schefflera morototoni, Schinopsis brasiliensis, Schizolobium amazonicum, Schizolobium parahyba, Sclerolobium chrysophyllum, Sclerolobium melanocarpum, Sclerolobium paraense, Scleronema micranthum, Scleronema praecox, Sextonia rubra, Sickingia tinctoria, Simaba cedron, Simaba morettii, Simarouba amara, Simira rubescens, Siparuna cuspidata, Siparuna decipiens, Siparuna guianensis, Sloanea brevipes, Sloanea grandiflora, Sloanea guianensis, Sloanea laxiflora, Sorocea guilleminiana, Spondias lutea, Spondias mombin, Sterculia apetala, Sterculia elata, Sterculia excelsa, Sterculia multiovula, Sterculia pruriens, Sterculia speciosa, Stryphnodendron adstringens, Stryphnodendron guianense, Stryphnodendron polystachyum, Stryphnodendron pulcherrimum, Stylogyne ambigua, Swartzia arborescens, Swartzia grandifolia, Swartzia guianensis, Swartzia laevicarpa, Swartzia panacoco, Swartzia polyphylla, Swartzia racemosa, Swartzia recurva, Swartzia viridiflora, Sweetia fruticosa, Swietenia macrophylla, Symphonia globulifera, Symplocos martinicensis, Syzygiopsis oppositifolia, Tabebuia aurea, Tabebuia impetiginosa, Tabebuia insignis, Tabebuia ochracea, Tabebuia serratifolia, Tabernaemontana attenuata, Tabernaemontana undulata, Tachigali glauca, Tachigali goeldiana, Tachigali guianensis, Tachigali melinonii, Tachigali myrmecophila, Tachigali paniculata, Tachigali paraensis, Tachigali richardiana, Tachigalia alba, Tachigalia cavipes, Tachigalia myrmecophila, Talisia furfuracea, Talisia hexaphylla, Talisia microphylla, Talisia praealta, Talisia simaboides, Tapirira bethanniana, Tapirira guianensis, Tapirira obtusa, Tapura capitulifera, Taralea oppositifolia, Terminalia amazonia, Terminalia guyanensis, Terminalia oblonga, Tetragastris altissima, Tetragastris hostmannii, Tetragastris panamensis, Te-

tragastris pilosa, Theobroma grandiflorum, Theobroma microcarpum, Theobroma obovatum, Theobroma subincanum, Thyrsodium guianense, Thyrsodium paraense, Thyrsodium puberulum, Thyrsodium spruceanum, Torresea acreana, Torresia acreana, Touroulia guianensis, Trattinnickia burserifolia, Trattinnickia demerarae, Trattinnickia rhoifolia, Trichilia micrantha, Trichilia pleeana, Trichilia quadrijuga, Trichilia schomburgkii, Trymatococcus amazonicus, Trymatococcus oligandrus, Uncaria guianensis, Unonopsis rufescens, Urbanella excelsa, Vantanea guianensis, Vantanea micrantha, Vantanea parviflora, Vatairea erythrocarpa, Vatairea guianensis, Vatairea macrocarpa, Vatairea paraensis, Vatairea sericea, Vataireopsis speciosa, Vataireopsis surinamensis, Virola carinata, Virola duckei, Virola elongata, Virola kwatae, Virola melinonii, Virola michelii, Virola multicostata, Virola multinervia, Virola pavonis, Virola sebifera, Virola surinamensis, Virola theiodora, Vismia cayennensis, Vitex guianensis, Vitex polygama, Vitex triflora, Vochysia guianensis, Vochysia haenkeana, Vochysia lanceolata, Vochysia maxima, Vochysia neyratii, Vochysia obscura, Vochysia surinamensis, Vochysia tomentosa, Vochysia vismiifolia, Votomita guianensis, Vouacapoua americana, Vouacapoua pallidior, Vouarana guianensis, Xylopia aromatica, Xylopia benthamii, Xylopia nitida, Zanthoxylum acuminatum, Zanthoxylum ekmanii, Zanthoxylum rhoifolium, Zanthoxylum riedelianum, Zeyheria tuberculosa, Zollernia paraensis, Zygia racemosa, Zygia tetragona

Chapitre 8

Compromis entre services écosystémiques dans les forêts de production

Ce chapitre vise à faire une synthèse des méthodes développées au cours de cette thèse afin d'analyser les compromis entre services écosystémiques fournis par les forêts de production (carbone, diversité et bois d'œuvre) à l'échelle de l'Amazonie. Cette étude permet d'étudier ces compromis à large échelle, ce qui a rarement été fait, mais est crucial pour informer les politiques de gestion des forêts qui se font souvent à l'échelle nationale, voire internationale, et non à l'échelle locale.

Les 3 services écosystémiques étudiés sont optimisés grâce à une méthode inspirée du logiciel d'optimisation spatiale *Marxan with Zones*[1]. L'Amazonie est divisée en 556 pixels, chacun pouvant être exploité avec différentes intensités et cycles d'exploitation, ou laissé sans exploitation. Les prédictions des émissions de carbone ont été faites à partir des modèles développés aux chapitres 3 et 4. La récupération du volume a été modélisée à partir des résultats du chapitre 7. L'effet de l'exploitation sur la biodiversité, qui n'a pas fait l'objet d'un chapitre à part entière dans cette thèse, a été ici modélisé à partir de cartes de richesse de mammifères et amphibiens élaborées à partir des données de l'IUCN[2]. Ces vertébrés ont été choisis car ils jouent un rôle clé dans le fonctionnement de l'écosystème. L'effet de l'exploitation a été modélisé comme une fonction linéaire de l'intensité d'exploitation (en $m^3 ha^{-1}$, à partir de données issues d'une métanalyse[3].

Les résultats montrent qu'un compromis majeur existe entre la récupération du volume de bois, et donc l'approvisionnement à long terme en bois d'œuvre, et la conservation de la biodiversité ainsi que le stockage de carbone. Pour optimiser la récupération du bois, la meilleure stratégie est une exploitation extensive, avec de faibles intensités sur l'ensemble des forêts de production ; pour optimiser le carbone et la conservation, la meilleure stratégie est

[1] M. E. Watts et al. (2009). « Marxan with Zones : Software for optimal conservation based land- and sea-use zoning ». In : *Environmental Modelling and Software* 24.12, p. 1513–1521.

[2] Jenkins et al. (2013). « Global patterns of terrestrial vertebrate diversity and conservation », cf. note 25, p. 3.

[3] Burivalova et al. (2014). « Thresholds of Logging Intensity to Maintain Tropical Forest Biodiversity », cf. note 150, p. 18.

d'exploiter à de fortes intensités les zones les plus externes de l'Amazonie.

Ces résultats soulignent l'importance de définir des priorités pour les politiques de gestion des forêts de production. Si les preneurs de décision choisissent de construire de nouvelles routes et d'ouvrir de nouvelles zones pour l'exploitation tout en diminuant l'intensité et le cycle légal d'exploitation, cela permettrait de maintenir plus longtemps l'approvisionnement en bois, mais diminuerait la biodiversité et le stockage de carbone. Si les politiques décident de restreindre la surface des forêts de production pour conserver leur valeur environnementale, il faudra alors se préparer à une disparition rapide de la ressource en bois dans les forêts exploitées.

No win-win strategy for Amazonian production forests : regional trade-offs between land sharing for timber or land sparing for biodiversity and carbon

Camille Piponiot[1,2,3,4], Ervan Rutishauser[5,6], Plinio Sist[4], Nataly Ascarrunz[7], Laurent Descroix[8], Marcelino Carneiro Guedes[9], Euridice Honorio Coronado[10], Milton Kanashiro[11], Juan Carlos Licona[7], Lucas Mazzei[11], Marcus Vinicio Neves d'Oliveira[12], Marielos Peña-Claros[13], Alexander Shenkin[14], Cintia Rodrigues de Souza[15], Edson Vidal[16], Thales West[17] & Bruno Hérault[4,18]

1. Université de Guyane, UMR EcoFoG (Agroparistech, CNRS, Inra, Université des Antilles, Cirad), Kourou, French Guiana.
2. Cirad, UMR EcoFoG (Agroparistech, CNRS, Inra, Université des Antilles, Université de Guyane), Kourou, French Guiana.
3. CNRS, UMR EcoFoG (Agroparistech, Inra, Université des Antilles, Université de Guyane, Cirad), Kourou, French Guiana.
4. Cirad, Univ Montpellier, UR Forests and Societies, Montpellier, France.
5. CarboForExpert, Hermance, Switzerland.
6. Smithsonian Tropical Research Institute, Balboa, Ancón 03092, Panamá.
7. Instituto Boliviano de Investigación Forestal, Santa Cruz, Bolivia
8. ONF-Guyane, Réserve de Montabo, 97307 Cayenne, French Guiana.
9. Embrapa Amapá, Macapá, Brazil.
10. Instituto de Investigaciones de la Amazonía Peruana, Iquitos, Peru.
11. Embrapa Amazônia Oriental, Belém, Brazil
12. Embrapa Acre, Rio Branco, Brazil.
13. Forest Ecology and Forest Management Group, Wageningen University, Wageningen, Netherlands.
14. Environmental Change Institute, University of Oxford, Oxford, United Kingdom.
15. Embrapa Amazônia Ocidental, Manaus, Brazil.
16. Departamento de Ciências Florestais, University of São Paulo, Piracicaba, Brazil.
17. Department of Biology, University of Florida, Gainesville, United States.
18. INP-HB (Institut National Polytechnique Félix Houphouët Boigny), Yamoussoukro, Côte d'Ivoire.

Abstract Tropical forests harbor most terrestrial carbon and diversity on Earth. Despite increased attention in national and international policies, they are still being deforested or degraded at high rates. In Amazonia, the largest tropical forest on Earth, a sixth of the remaining natural forests is dedicated for timber production. Conciliating timber production with the provision of other ecosystem services remains a major challenge for forest managers and policy-makers. This study applies a spatial optimization of logging in Amazonian production forests to analyze potential trade-offs between 3 ecosystem services (namely carbon storage, biodiversity conservation and timber production). Results

show that the main trade-off lies between long-term timber provision through a land-sharing strategy (i.e. extensive logging with low intensities) and carbon and diversity retention through a land-sparing strategy (i.e. intensive logging concentrated in the outer fringes of the Amazon region). Policy-makers may have no choice but to opt for one of these two strategies, depending on management goals and societal demands. These choices may potentially have huge implications for the future of Amazonian forests and our results highlight the need for a regional cooperation among Amazonian countries to enhance coherent and trans-boundary forest management.

8.1 Introduction

Tropical forests are of inestimable value for humanity. In addition to mitigating climate change by storing about 30% of the biosphere carbon[4], tropical forests also harbor half of the world biodiversity[5], have a crucial role in regulating hydrological cycles[6], and furnish a wide range of timber and non-timber goods. Tropical forests are also the first source of new agricultural land, being lost at a higher-than-ever speed (2101 km^2 per year between 2000-2012[7]), and the remaining forests are being increasingly degraded by human activities[8].

To tackle tropical deforestation, governments have long focused on forests conservation, mostly by setting up protected areas with restricted access and usage for human populations. However, this simple dichotomy (protected or not) poorly reflects the wide gradient of forest uses and their effects on tropical forests[9]. Because it is impossible, and unethical, to protect all tropical forests and ban humans, tropical forest management aims at reconciling forest conservation and sustainable production of goods and services.

In the tropics, c. 40% of the sawn wood traded annually arises from natural forests[10]. Brazil is among the largest producers of tropical round wood, with 81 million m^3 (48% of its production) of logs harvested annually (2005-2008) in natural tropical forests[11]. Selective logging is the dominant harvesting system in use, consisting in felling a few commercial trees and leaving the rest of the forest to natural dynamics. To avoid predatory logging practices that have depleted Amazonian forests of their most valuable timbers[12], governments have implemented a set of logging rules, including minimum cutting cycles, i.e. time periods between two logging events (e.g., 20 years in Bolivia and Peru, 35 years in Brazil, and 65 years in French Guiana[13]), and maximum logging intensities ranging 20-30 m^3ha^{-1}, with an estimated mean logging intensity around 20 m^3ha^{-1} in the Brazilian Amazon[14].

Because most of the forest cover remains after logging operations, selectively logged forests still harbor most of their initial carbon stocks, biodiversity, and other environmental goods and

[4] Y. Pan et al. (2013). « The Structure, Distribution, and Biomass of the World's Forests ». In : *Annual Review of Ecology, Evolution, and Systematics* 44.1, p. 593–622.

[5] S. L. Pimm et al. (2014). « The biodiversity of species and their rates of extinction, distribution, and protection ». In : *Science* 344.6187. arXiv : 1132.

[6] Fisher et al. (2009). « The land-atmosphere water flux in the tropics », cf. note 13, p. 2.

[7] Hansen et al. (2013). « High-Resolution Global Maps of 21st-Century Forest Cover Change », cf. note 82, p. 117.

[8] P. Potapov et al. (2017). « The last frontiers of wilderness : Tracking loss of intact forest landscapes from 2000 to 2013 ». In : *Science Advances* 3.1, e1600821.

[9] Gibson et al. (2011). « Primary forests are irreplaceable for sustaining tropical biodiversity », cf. note 155, p. 18 ; R. R. de Castro Solar et al. (2015). « How pervasive is biotic homogenization in human-modified tropical forest landscapes ? » In : *Ecology Letters* 18.10, p. 1108–1118.

[10] T. Payn et al. (2015). « Changes in planted forests and future global implications ». In : *Forest Ecology and Management* 352, p. 57–67.

[11] Blaser et al. (2011). *Status of Tropical Forest Management 2011*, cf. note 1, p. vi.

[12] Richardson et Peres (2016). « Temporal decay in timber species composition and value in amazonian logging concessions », cf. note 62, p. 7.

[13] Blaser et al. (2011). *Status of Tropical Forest Management 2011*, cf. note 1, p. vi.

[14] Asner et al. (2005). « Selective Logging in the Brazilian Amazon », cf. note *a*, p. 7.

services[15]. It has frequently been argued that integrating selectively logged forests into tropical forest conservation schemes is of primary importance[16]. Even though the value of production forests in providing Ecosystem Services (ESs) is increasingly recognized, trade-offs between ESs have rarely been investigated at large scale. Most conservation programs and payments for ESs indeed focus on one particular feature (e.g. carbon in REDD+ programs[17]), which may result in an underestimation of forests multifunctionality and in sub-optimal forest management[18]. The few studies that have tackled the issue of multicriteria decision-making in the context of tropical forests have been conducted at local scale. For instance, a study in a logging concession in Suriname found that trade-offs between carbon stock conservation and timber recovery are mediated by logging intensity[19]. Even though these studies provide a useful insight for forest managers, most conservation-related policies apply at larger scales[20]. There is thus a need to inform policy-making with a regional assessment of ESs and potential trade-offs among them.

Here we aim at optimizing, in a spatially-explicit framework, ESs provision in Amazonian production forests. We analyze the effect of different logging intensities (no logging or 10-20-30 m^3ha^{-1}) and cutting cycle duration (15-30-65 years) on the provision of three ESs : carbon storage, biodiversity, and timber production. Our main research questions are : (i) how to improve the provision of ESs in Amazonian production forests ? (ii) are there trade-offs between ESs ? and (iii) what are the best strategies for providing timber in future production forests, depending on forest management objectives and projected demand for high-quality timber ?

To answer these questions, we first optimize each ES (carbon, timber, and biodiversity) separately with a timber production target of 35 Mm^3yr^{-1} (equivalent to the current timber production in Amazonia[21]). We then combine all three ESs in a single optimization framework and analyze how ES provisions are affected by the relative weight given to each ES. Finally, we quantify ES provision under 7 different management strategies, depending on total timber production (see Table 8.1 for strategy description).

[15] Putz et al. (2012). « Sustaining conservation values in selectively logged tropical forests : the attained and the attainable », cf. note 102, p. 11.

[16] Edwards et al. (2014b). « Maintaining ecosystem function and services in logged tropical forests », cf. note 3, p. vi.

[17] T. Laing et al. (2016). « Understanding the demand for REDD+ credits ». In : *Environmental Conservation* 43.4, p. 389–396.

[18] Van der Plas et al. (2018). « Continental mapping of forest ecosystem functions reveals a high but unrealised potential for forest multifunctionality », cf. note 163, p. 19.

[19] Roopsind et al. (2018). « Trade-offs between carbon stocks and timber recovery in tropical forests are mediated by logging intensity », cf. note 133, p. 16.

[20] L. Hein et al. (2006). « Spatial scales, stakeholders and the valuation of ecosystem services ». In : *Ecological Economics* 57.2, p. 209–228.

[21] Lentini et al. (2005). *Fatos Florestais da Amazônia 2005 (Amazonian Forest Facts)*, cf. note 1, p. 107.

8.2 Materials and methods

8.2.1 Study region

8.2.2 Study region

The study region is the Amazon region, located in tropical South America. Amazonia is the most diverse and carbon-rich tropical biome on Earth[22], and is covered by around 600 Mha of tropical rainforest, of which 400 Mha are intact forests without detectable human footprint[23]. Today 48% of Amazonian forests are under a

[22] Avitabile et al. (2016). « An integrated pan-tropical biomass map using multiple reference datasets », cf. note 5, p. 1 ; Pimm et al. (2014). Cf. note 5.

[23] Potapov et al. (2017). Cf. note 8.

dense network of protection areas[24] (Figure 8.1). However since the 1970' and the opening of the Transamazonian - the first road built deep inside the forest - 13.3% of the original forest extent has been clearcut, mainly for agricultural purposes : cattle ranching and, more recently, soybean production[25].

Even though Amazonia has already been deeply impacted by human activities and road building has continued steadily since the 1970', a great part of the biome is at a great distance from any road and thus inaccessible to most commercial activities (Figure 8.1).

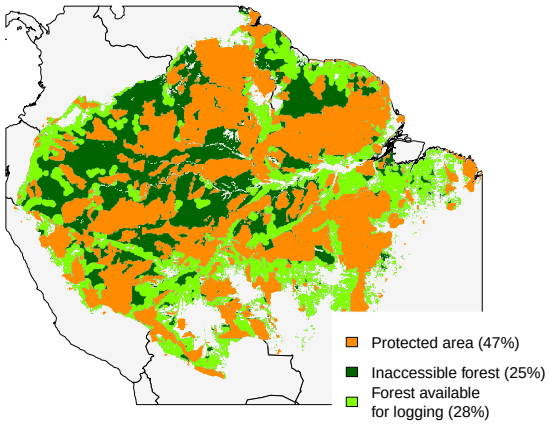

FIGURE 8.1 – Availability of Amazonian forests for logging (forest cover > 90%). Orange areas are protected areas (except category VI of the IUCN), and are not included in our analysis. Dark green areas are forests that are > 25 km away from any road or track ; light green areas are forests that are close (≤ 25 km) to a road or track.

Timber production through selective logging is the dominant forest use in the region, in terms of extent and generated income[26]. About 15% of Amazonian forests are designated for timber production[27]. If selectively logged forests still retain most of their original levels of carbon and diversity[28], forest recovery and resilience post-logging largely depend on implementation of logging in the field, the logging intensity and the cutting cycle length, *i.e.* the time left to the forest to recover[29]. In Amazonia, logging intensities vary between 5-30 m^3 of timber extracted per ha, with an estimated average around 20 $m^3 ha^{-1}$ in the Brazilian Amazon[30]. Official minimum cutting cycle length varies from one country to another, from 20 years (e.g. Peru, Bolivia[31]) to 65 years (French Guiana).

8.2.3 Optimization framework

In this paper we use a methodology adapted from the optimization software *Marxan with Zones*[32], using the package *prioritzr*[33] developed in the statistical programming language R[34]. The goal of this optimization is to find a spatial configuration of different land uses in a landscape divided into *planning units* that minimizes a cost function given pre-defined objectives.

[24] UNEP-WCMC et IUCN (2016). *Protected Planet : The World Database on Protected Areas (WDPA)*, cf. note 81, p. 117.

[25] P. FEARNSIDE (2017). *Deforestation of the Brazilian Amazon*. T. 1. May 2018, p. 1–58.

[26] BLASER et al. (2011). *Status of Tropical Forest Management 2011*, cf. note 1, p. vi.

[27] FAO (2011). *The State of Forests in the Amazon Basin, Congo Basin and Southeast Asia*, cf. note 1, p. 1.

[28] PUTZ et al. (2012). « Sustaining conservation values in selectively logged tropical forests : the attained and the attainable », cf. note 102, p. 11.

[29] RUTISHAUSER et al. (2015). « Rapid tree carbon stock recovery in managed Amazonian forests », cf. note 166, p. 20 ; PIPONIOT et al. (2018). « Assessing timber volume recovery after disturbance in tropical forests – A new modelling framework », cf. note 15, p. 109.

[30] ASNER et al. (2005). « Selective Logging in the Brazilian Amazon », cf. note *a*, p. 7.

[31] FREDERICKSEN et al. (2003). « Sustainable forestry in Bolivia - Beyond planning logging », cf. note 93, p. 10 ; BLASER et al. (2011). *Status of Tropical Forest Management 2011*, cf. note 1, p. vi.

[32] WATTS et al. (2009). « Marxan with Zones : Software for optimal conservation based land- and sea-use zoning », cf. note 1, p. 139.

[33] J. HANSON et al. (2018). *prioritizr : Systematic Conservation Prioritization in R*.

[34] R CORE TEAM (2017). *R : A Language and Environment for Statistical Computing*, cf. note 28, p. 30.

Planning units and logging types

Amazonia was divided into a 1°-grid of 556 planning units. In each pixel, we only considered areas suitable for logging in Amazonia (Figure 8.1), *i.e.* areas that (i) have at least 90% of forest cover according to Hansen et al.[35], (ii) are accessible, i.e. within 25 km of a road or track[36], and (iii) are not under a full protection status[37] (except category VI of the International Union for the Conservation of Nature (IUCN), which corresponds to a "sustainable use" and was considered as being available for logging purposes). Based on data from forest concessions in French Guiana and Brazil, 42% of those areas was considered as unsuitable for logging (slopes, areas around rivers and streams, etc)[38].

Each pixel can be allocated to one of the following logging types : a logging intensity of 10 (Low), 20 (Medium) or 30 m^3ha^{-1} (High) and a cutting cycle length of 15 (Short), 30 (Medium) or 65 years (Long), or No Logging. Medium intensity and cutting cycle length correspond to current median logging practices in Amazonia.

[35] Hansen et al. (2013). « High-Resolution Global Maps of 21st-Century Forest Cover Change », cf. note 82, p. 117.

[36] contributors (2018). *OpenStreetMap*, cf. note 80, p. 117 ; Asner et al. (2006). « Condition and fate of logged forests in the Brazilian Amazon. », cf. note 78, p. 9.

[37] UNEP-WCMC et IUCN (2016). *Protected Planet : The World Database on Protected Areas (WDPA)*, cf. note 81, p. 117.

[38] C. Piponiot et al. « Can timber provision from Amazonian natural forests be sustainable ? » In : *Nature Sustainability*.

Looking for trade-offs between ESs

The first step is to evaluate the effect of the weight given to each ES in the optimization, and to look for potential trade-offs between ESs (Figures 8.2 and 8.3). Targets are constant but costs can vary depending on the weight of each ES.

Targets Selective logging will have to meet the demand for tropical timber in South America. A timber production target of 35 Mm^3yr^{-1}[39] was set, corresponding to the timber production in Amazonian natural forests.

For effective conservation of biological diversity, and especially species that are highly sensitive to forest degradation, managers should seek to protect most of the remaining intact forest landscapes, which is irreplaceable for biodiversity conservation[40]. Because Amazonian forests have high levels of endemism and all regions are not equivalent in terms of species composition, we set a forest conservation target (referred to as 'conservation target') as follows : for each of the 6 ecoregions defined by ter Steege et al.[41] (the Guiana Shield, eastern Amazon, southeastern Amazon, central Amazon, southwestern Amazon, and northwestern Amazon), 80% of the current intact forest landscape (according to Tyukavina et al.[42]) shall remain unlogged. This conservation target can include forests in protected areas, inaccessible forests (> 25 km from a road or track), or forests inside planning units that have been allocated to the "No Logging" type.

[39] Lentini et al. (2005). *Fatos Florestais da Amazônia 2005 (Amazonian Forest Facts)*, cf. note 1, p. 107.

[40] Gibson et al. (2011). « Primary forests are irreplaceable for sustaining tropical biodiversity », cf. note 155, p. 18.

[41] H. Ter Steege et al. (2013). « Hyperdominance in the Amazonian Tree Flora ». In : *Science* 342.6156, p. 1243092–1243092.

[42] Tyukavina et al. (2016). « Pantropical hinterland forests : mapping minimally disturbed forests », cf. note 98, p. 121.

Costs In our optimization framework, the cost of logging in a planning unit is estimated as the loss of ESs (carbon emissions,

biodiversity loss, and timber stocks decrease) caused by logging operations. The biodiversity loss is approximated with the loss of two vertebrate taxa : mammals and amphibians. In the case of carbon and timber, ES losses are partially offset by forest recovery before the next cutting cycle (see section 8.2.4).

The total cost of allocating logging type z to planning unit p is estimated as :

$$Cost_{p,z} = \alpha_C \cdot \frac{Cemi_{p,z}}{\overline{Cemi}} + \alpha_B \cdot \frac{Rloss_{p,z}}{\overline{Rloss}} + \alpha_T \cdot \frac{Prod_{p,z} - Rec_{p,z}}{\overline{Prod - Rec}} - K \tag{8.1}$$

where $Cemi_{p,z}$ and $Rloss_{p,z}$ are carbon emissions and vertebrates species loss at the end of the first cutting cycle in a planning unit p when allocated to logging type z (see equations 8.7 and 8.8). $Prod_{p,z}$ is the timber extracted and $Rec_{p,z}$ the timber recovered at the end of the cutting cycle : $Prod_{p,z} - Rec_{p,z}$ is thus the net timber loss (see equation 8.3). ES losses are standardized by their respective sample mean $\overline{Cemi}$, $\overline{Rloss}$, and $\overline{Prod - Rec}$. α_C, α_B and α_T are the respective weight given to carbon, biodiversity and timber costs in the optimization. They are bounded between 0 and 1 and $\alpha_C + \alpha_B + \alpha_T = 1$. A constant K was added to avoid negative costs (when volume or carbon recovery exceed volume or carbon losses). K is set to the minimum cost value across all planning units and all logging types.

To analyze the effect of the weight given to each ES in the final results we tested different α values. First, we tested 3 scenarios to optimize each ES provision independently : the coefficient of one cost is equal to 1 and the others to 0 (Figure 8.2). Then we ran 66 simulations with all combinations of weights from 0 to 1, with 0.1 steps. Results were then interpolated with the package *ggtern* (Figure 8.3). In balanced costs strategies (Figure 8.4) we set $\alpha_C = \alpha_B = \alpha_T = \frac{1}{3}$.

Evaluating different strategies for future timber provision

In a second step we test 7 different strategies (Table 8.1) : (i) *Timber* : only timber recovery is optimized in order to ensure long-term timber production, (ii) *Carbon* : only carbon is optimized as a climate change mitigation strategy, (iii) *Balanced* : all 3 ES costs are balanced in the optimization, as a multifunctionality strategy, (iv) *Current* : all 3 ES costs are balanced but only medium (30-yr) cutting cycles are allowed, (v) *STY* : sustained timber yields (STY) are required, i.e. timber must be recovered at the end of the first cutting cycle, (vi) *Road building* : all areas, except currently-protected areas, are made available for logging, and (vii)

TABLE 8.1 – All 7 strategies tested in this study. "Currently accessible" are areas that have > 90% forest cover, are not protected and are within 25 km of an existing road or track (Figure 8.1). "All unprotected" are all areas with > 90% forest cover outside protected areas.

	Acronym	Strategy	Planning unit area	ES cost	STY target
(i)	Timber	Long-term timber production	Currently accessible	Timber	No
(ii)	Carbon	Climate change mitigation	Currently accessible	Carbon	No
(iii)	Balanced	Multifunctionality	Currently accessible	Balanced	No
(iv)	Current	Only 30-yr cutting cycles	Currently accessible	Balanced	No
(v)	STY	Sustained timber yields	Currently accessible	Balanced	Yes
(vi)	Road building	Building roads to previously inaccessible areas	All unprotected	Balanced	No
(vii)	STY + Road building	Sustained timber yields with road building	All unprotected	Balanced	Yes

STY - Road building : STY are required and all areas, except currently-protected areas, are made available for logging (STY + land-sharing strategy).

In all scenarios (i-v), the area suitable for logging is the same as defined previously (*Currently accessible* in Table 8.1). In the "Road building" scenarios (v-vi), we hypothesize that additional roads will be built : the new area suitable for logging (*All unprotected* in Table 8.1) corresponds to the total area with forest cover > 90% outside protected areas (independently of their current distance to a road), minus the 42% corresponding to slopes and areas near rivers (see section 8.2.3).

Targets The production target (total timber harvested) varies between 10-80 Mm^3yr^{-1}, with a 10 Mm^3yr^{-1} step (Figure 8.4). The intact-forest target is maintained to 80%. In the STY strategies (see Table 8.1 and section 8.2.3), we add an additional STY target : the total timber recovered in logged areas must be equal or higher than the total timber production.

Costs In the "Carbon" strategy, the total cost is proportional to carbon emissions ($\alpha_C = 1$ and $\alpha_B = \alpha_T = 0$). In the "Timber" strategy, the total cost is proportional to timber stocks loss ($\alpha_T = 1$ and $\alpha_B = \alpha_C = 0$). In all other strategies costs are balanced between all 3 ESs ($\alpha_C = \alpha_B = \alpha_T = \frac{1}{3}$).

8.2.4 Quantifying the effect of logging on ESs

Timber production and recovery

From a previously developed volume recovery model calibrated at the Amazonian scale[43], we extracted : (i) the total volume $vtot_p$ (m^3ha^{-1}) in pixel p, (ii) the proportion of potentially commercial timber $\omega 0_p$ and (iii) the potential timber recovery $vrec_{p,z}$ at the

[43] PIPONIOT et al., « Can timber provision from Amazonian natural forests be sustainable ? », cf. note 38, p. 145.

end of a cutting cycle $trot_z$ and after a logging intensity $vext_z$ (z being the logging type). All parameters were set to their maximum likelihood value.

The mean annual timber production over the first cutting cycle in pixel p in logging type z is equal to :

$$Prod_{p,z} = \frac{min(vext_z, (vtot_p \cdot \omega 0_p)) \cdot area_p}{trot_z} \tag{8.2}$$

where $vext_z$ is the extracted volume in logging type z, $vtot_p \cdot \omega 0_p$ is the potential timber volume (the actual extracted volume cannot exceed the potential timber volume), $area_p$ is the area available for logging and $trot_z$ is the cutting cycle length.

The mean annual timber recovery over the first cutting cycle in pixel p in logging type z is equal to :

$$Rec_{p,z} = \frac{vrec_{p,z} \cdot area_p}{trot_{p,z}} \tag{8.3}$$

Carbon emissions

The effect of logging on carbon emissions is here quantified as the mean difference to the initial carbon stock over the cutting cycle. It was assessed as the difference of two terms : (i) the initial carbon loss caused by logging, (ii) minus the carbon storage from forest regrowth, averaged over the cutting cycle.

The initial carbon loss caused by logging is threefold : (i) from extracted logs ; (ii) from road building (deforestation), (iii) from incidental damage during logging operations[44].

[44] Piponiot et al. (2016a). « A methodological framework to assess the carbon balance of tropical managed forests », cf. note 6, p. 34.

The carbon emissions from extracted logs in pixel p under logging type z was assessed as :

$$Cext_{p,z} = Prod_{p,z} \cdot WDext_p \cdot area_p \tag{8.4}$$

with $Prod_{p,z}$ the actual logging intensity (in $m^3 ha^{-1}$), $area_p$ is the area available for logging (ha) in pixel p and $WDext_p$ is the mean wood density of commercial trees in pixel p (see supplementary material 8.6.2 for wood density estimation).

The carbon emissions from road building were assessed as :

$$Cdefor_{p,z} = Pdefor \cdot acs_p \cdot area_p \tag{8.5}$$

where $Pdefor = 4.7\%$ is the estimated proportion of a logged area that is deforested for infrastructure (roads, logging decks and main skid trails) according to Piponiot et al.[45] and acs_p is the mean aboveground carbon density ($MgC.ha^{-1}$) in planning unit p, extracted from a global carbon map[46].

[45] Ibid.

[46] Avitabile et al. (2016). « An integrated pan-tropical biomass map using multiple reference datasets », cf. note 5, p. 1.

Carbon losses from damaged trees were assessed as follows :

$$Cdam_{p,z} = \frac{acs_p - Prod_{p,z} \cdot WDext_p}{1 + \left(\frac{acs_p}{Prod_{p,z} \cdot WDext_p} - 1\right)^{\theta}} \cdot area_p \quad (8.6)$$

with θ a parameter of the model : the model justification and calibration are presented in the supplementary material 8.6.1.

Post-logging carbon recovery $Crec_{p,z}$ was assessed with the methodology developed by Piponiot et al.[47]. All parameters were set to their maximum likelihood value.

[47] Piponiot et al. (2016b). « Carbon recovery dynamics following disturbance by selective logging in Amazonian forests », cf. note 5, p. 50.

For each pixel p and each logging type z, the mean annual carbon emissions from pixel p under logging type z are thus calculated as :

$$Cemi_{p,z} = Cext_{p,z} + Cdefor_{p,z} + Cdam_{p,z} - \sum_{t=1}^{trot_z} \frac{Crec_{t,p,z}}{trot_z} \quad (8.7)$$

Biodiversity

We chose to model the effect of logging on amphibians and mammals richness because they are key animals in forest ecosystems : amphibians are good indicators of global ecosystem health[48] and mammals ensure many ecosystem functions, among which pollination[49] and seed dispersal[50]. We used global maps of mammals and amphibians richness derived from IUCN species range maps[51], which can fairly represent patterns of conservation priority[52].

[48] H. H. Welsh et L. M. Ollivier (1998). « Stream Amphibians as Indicators of Ecosystem Stress : A Case Study from California's Redwoods ». In : *Ecological Applications* 8.4, p. 1118–1132 ; J. P. Collins et A. Storfer (2003). « Global amphibian declines : sorting the hypotheses ». In : *Diversity and Distributions* 9, p. 89–98.

[49] T. H. Fleming et al. (2009). « The evolution of bat pollination : A phylogenetic perspective ». In : *Annals of Botany* 104.6, p. 1017–1043. arXiv : `arXiv:1011.1669v3`.

[50] S. J. Wright et al. (2000). « Poachers Alter Mammal Abundance, Seed Dispersal, and Seed Predation in a Neotropical Forest ». In : *Conservation Biology* 14.1, p. 227–239 ; R. Muscarella et T. H. Fleming (2007). « The role of frugivorous bats in tropical forest succession ». In : *Biological Reviews* 82.4, p. 573–590.

[51] Jenkins et al. (2013). « Global patterns of terrestrial vertebrate diversity and conservation », cf. note 25, p. 3 ; C. N. Jenkins (2018). *Mapping the World's Biodiversity.*

[52] I. Maréchaux et al. (2017). « The value of coarse species range maps to inform local biodiversity conservation in a global context ». In : *Ecography* 40.10, p. 1166–1176. arXiv : `ecog.02097 [10.1111]`.

The impact of logging on mammals and amphibians was assessed with the equation :

$$Rloss_{p,z} = (Rm_p \cdot \beta m + Ra_p \cdot \beta a) \cdot vext_z \cdot area_p \quad (8.8)$$

where $Rloss_{p,z}$ is the loss of vertebrate richness (mammals and amphibians) in pixel p and logging type z, Rm_p and Ra_p are the pre-logging richness of mammals and amphibians respectively[53], $\beta m = 1.44$ and $\beta a = 1.53$ are the estimated slopes of post-logging species loss in the Neotropics for mammals and amphibians respectively, according to Burivalova et al.[54]. $vext_z$ is the logging intensity in logging type z. We hypothesize that amphibians and mammals richness do not recover after logging (no effect of cutting cycle length).

[53] Jenkins et al. (2013). « Global patterns of terrestrial vertebrate diversity and conservation », cf. note 25, p. 3.

[54] Burivalova et al. (2014). « Thresholds of Logging Intensity to Maintain Tropical Forest Biodiversity », cf. note 150, p. 18.

8.3 Results

8.3.1 Trade-offs between ESs

Location and intensity In the base scenario, maximizing carbon and biodiversity retention results in preserving 80% of available forests, and logging 20% of available forests under the highest

intensity (30 m^3ha^{-1}) and shortest cutting cycle (15 yr) allowed (Figure 8.2d-e). Logged pixels are distributed in the most external areas of Amazonia : in southeastern Amazonia for both carbon and biodiversity, in northern Amazonia for carbon and in the southwestern border of Amazonia for biodiversity (Figure 8.2a-b). By contrast, minimizing timber loss results in a different pattern : only 5% of the available area is not logged, 14% is logged under high-intensity short-cycle logging, and 81% of the available area is logged under low-intensity (10 m^3ha^{-1}) long-cycle (65 yr) logging (Figure 8.2f). Low-intensity logging is distributed in almost every region of Amazonia, except in the northeast where high-intensity logging prevails (Figure 8.2c).

FIGURE 8.2 – Results of spatial optimization with a unique ecosystem cost. Production target is set to 35 Mm^3yr^{-1}. Green areas are not logged. (a) and (d) Minimizing carbon emissions. (b) and (e) Minimizing vertebrates richness loss. (c) and (f) Minimizing timber loss. In maps (a-c) the size of each dot is proportional to the planning unit area (total area available for logging) ; the total area allocated to each logging type is represented in the histograms (d-f). Logging type color (blue - purple - red) represent the logging intensity (Light : 10, Medium : 20 and High : 30 m^3ha^{-1}). The logging type transparency represents the cutting cycle length (Short : 15, Medium : 30, Long : 65 years) : light colors correspond to longer cycles. Only the 6 (out of 10) logging types that were allocated during the optimization appear on the graph.

ES values When optimizing biodiversity (i.e. when biodiversity weight is 100%), carbon emissions are 0% higher than the optimal value (when optimizing only carbon emissions, i.e. when carbon weight is 100% : Figure 8.3b) and timber loss is 34% higher than the optimal value (Figure 8.3c). When optimizing carbon, biodiversity loss is 40% higher than the optimal value (Figure 8.3a) and timber loss is 37% higher than the optimal value (Figure 8.3c). When optimizing timber, carbon emissions are 158% higher than the optimal value (Figure 8.3b) and biodiversity loss is 228% higher than the optimal value (Figure 8.3a). When costs are balanced (carbon weight = biodiversity weight = timber weight), carbon emissions are 17% higher than the optimal value (Figure 8.3b), biodiversity loss is 11% higher than the optimal value (Figure 8.3a) and timber loss is 35% higher than the optimal value (Figure 8.3c).

From this sensitivity analysis, one major trade-off axis emerges between carbon and biodiversity retention vs. timber recovery.

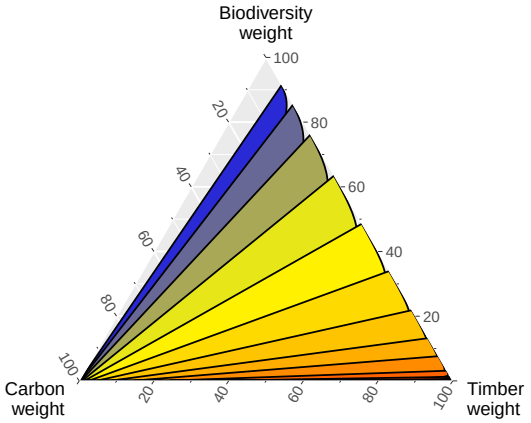

(a) Biodiversity cost.

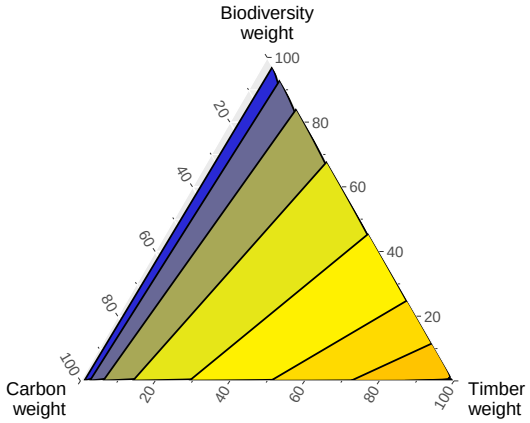

(b) Carbon cost.

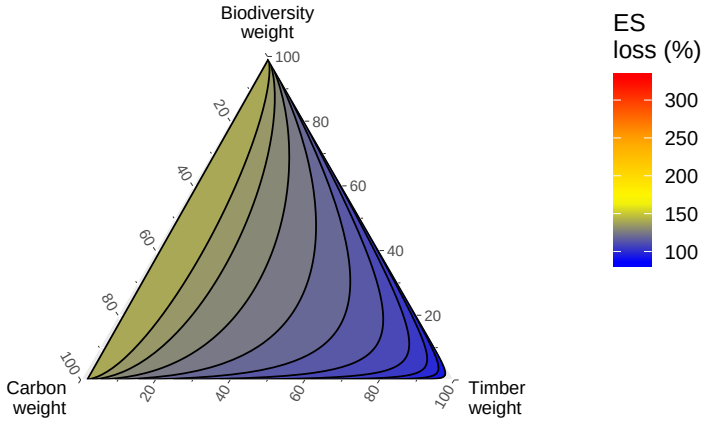

(c) Timber cost.

FIGURE 8.3 – ES costs depending on the weight given to each ES in the optimization process. Each ES loss is expressed as a proportion (%) of the ES loss when only this ES is optimized (weight = 100%). For example a carbon cost of 150% means that carbon emissions are 50% higher than when only carbon emissions are minimized (i.e. "optimal" carbon emissions).

8.3.2 Effect of change in timber production and strategy choice

The effect of changing the timber demand (timber production target from 10 to 80 Mm^3) was tested on 7 different logging strategies (Table 8.1).

For all strategies except one (the *Timber* strategy), the total area harvested increases with the total production target (Figure 8.4a). In the *Timber* strategy however, the total area logged is at its maximum value (around 80 Mha) even for low production targets : the increase in timber production results in an increase in the mean logging intensity and a decrease in the mean cutting cycle length (Figure 8.4b-c). Provision of ESs (carbon, biodiversity, and timber) decreases when production increases (Figure 8.4d-f). Three groups of strategies have consistently different behaviors in this analysis : (i) a group of strategies that optimize non-timber ESs (*Carbon*, *Balanced*, *Current* and *Road building*), (ii) the timber-optimizing strategy (*Timber*), and (iii) the group of sustainable-production strategies (*STY*, *STY + Road building*).

In the first group of strategies, most pixels that are logged have maximum logging intensity (30 m^3ha^{-1}, Figure 8.4b) and minimum cutting cycle (15 yr, Figure 8.4c), except for the *Current* strategy for which, by definition, only 30-yr cutting cycles are allowed (Table 8.1). For low production targets (10-30 Mm^3yr^{-1}) mean logging intensity is between 20-30 m^3ha^{-1} and mean cutting cycle length is between 15-40. When the production target is above 30 Mm^3yr^{-1}, mean logging intensity and mean cutting cycle length reach their maximum (resp. minimum) value, meaning that almost all logged pixels are allocated to the High-intensity Short-cycle logging type : these results are similar to those in Figure 8.2. As a consequence, the total area logged increases linearly with the timber production target (Figure 8.4a) : producing more timber is mostly done by logging additional areas. All 3 ESs decrease almost linearly with production target (Figure 8.4d-f). The *Carbon*, *Balanced* and *Road building* strategies result in similar ES values : the 3 strategies retain $\geq 90\%$ carbon and biodiversity (Figure 8.4e-f), but timber stocks are not recovered (Figure 8.4d). The *Current* strategy has significantly lower ES values for all 3 ES considered (Figure 8.4d-f).

The timber-optimizing strategy has a different behavior when the production target increases. When the production target is low (10 Mm^3yr^{-1}), logging is exclusively done under low intensities (10 m^3ha^{-1}, Figure 8.4b) and long cutting cycles (65 yr, Figure 8.4c). When the timber production increases, the proportion of area logged under high-intensity short-cycle logging increases, especially in the northeastern regions of Amazonia (see Supplementary figure 8.8 for the spatial distribution of logging types), which in turn increases the mean logging intensity (Figure 8.4b)

and decreases the mean cutting cycle length (Figure 8.4c). Almost the entire area available (80 Mha) is logged, independently of the production target (Figure 8.4a). The total timber retained is $> 100\%$ (i.e. timber stocks are recovered) when the production target was under 50 Mm^3ha^{-1}, and $< 100\%$ above 50 Mm^3ha^{-1}. The carbon and diversity retained were the lowest in this strategy (Figure 8.4e-f).

The third group of strategies (sustainable production) retain, by definition, 100% of timber stocks (Figure 8.4d). Producing more than 50 Mm^3yr^{-1} was impossible with the STY strategy. Even when increasing the total area available ("STY + Road building"), the total production could go no further than 70 Mm^3yr^{-1}. The mean logging intensity and cutting cycle length stay constant with these two strategies : 16 m^3ha^{-1} and 50 yr respectively (Figure 8.4b-c). The total area logged increases almost twice faster when the production target increases than for the first group of strategies (Figure 8.4a). As a consequence, the carbon and biodiversity retained also decrease faster (Figure 8.4e-f).

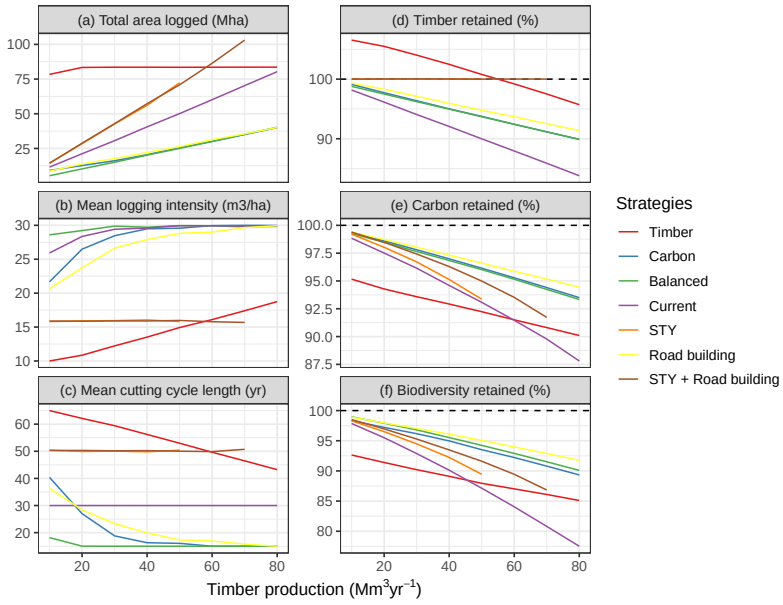

FIGURE 8.4 – Characterization of different strategies for timber production, depending on the value of timber demand. (a) Total area logged (Mkm^2). (b) Mean logging intensity in logged areas (m^3ha^{-1}). (c) Mean cutting cycle length (yr). (d) Proportion of initial timber stocks that remain at the end of the cutting cycle (%). (e) Proportion of initial carbon stocks that remain at the end of the cutting cycle (%). (f) Proportion of initial mammals and amphibians richness that remain at the end of the cutting cycle (%). The 7 strategies' characteristics are summarized in Table 8.1. "STY" and "STY + Road building" strategies could not sustainably provide more than 50 and 70 Mm^3 of annual timber production respectively. In plots (d-f), values are calculated over all areas outside of protected areas. Additional maps with distribution of logging types (intensity, cutting cycle) are provided in the supplementary materials (Figure 8.8).

8.4 Discussion

8.4.1 Importance of regional studies for forest management

The optimization approach applied in this study can have many implications for forest management. Ecosystem services in selectively logged forests have often been studied but usually, they

were analyzed separately[55] : there has been little investigation on the trade-offs that exist between ESs. Among the few studies that exist on the subject, a trade-off between carbon retention and volume recovery has been shown at the local scale, where those trade-offs depend on the logging intensity and silvicultural treatments applied[56]. Trade-offs have also been reported between timber production and species richness[57]. Local studies can inform forest owners, but the latter will base their decisions on a limited set of locally-relevant objectives. Their goal is usually to maximize financial benefits, may it be through timber or non-timber forest products harvesting, eco-tourism or payments for ecosystem services.

Climate change mitigation and nature conservation goals are however more relevant at regional to global scales[58] : e.g. delimitation of protected areas and forest concessions[59], definition of logging rules (maximum logging intensities, minimum cutting cycle length, minimum cutting size, protected tree species)[60], road-building[61]. Informing these policies with large-scale multicriteria analyses will thus be key if we want to develop evidence-based policies. Today few studies have assessed regional-scale ESs tradeoffs in Amazonia (e.g. a recent study analyzes tradeoffs between forest conservation and agriculture at the basin scale[62]) ; to our knowledge, none has focused on forests managed for timber production. Our study is thus an important step in the planning of future logging management in Amazonia, that needs to be informed on where and how logging should be done depending on future demand for timber and other ESs.

One important point to bear in mind is that results presented here only account for the first cutting cycle : this is particularly important in the sustained-timber-yields strategy because even though yields are sustained during the first cutting cycle they could decrease afterward. Today there is almost no data on multi-cycle logging in Amazonia : most monitored plots have been logged only once[63], although actual logging in Amazonia may comprise multiple illegal reentries[64]. Gathering more information on the effect of several logging cycles on forest dynamics will be of utmost importance to understand what future production forests will look like.

Finally, even though our findings provide an interesting insight on potential trade-offs that future forest managers and decision-makers will face, a large part (20-60%) of logging is done illegally in the Amazon[65]. Changing logging rules to maintain the environmental value of production forests can be jeopardized by the lack of control over their application. Improving Amazonian forests' governance will be key to maintain ecosystem services through informed management.

[55] Putz et al. (2012). « Sustaining conservation values in selectively logged tropical forests : the attained and the attainable », cf. note 102, p. 11.

[56] Roopsind et al. (2018). « Trade-offs between carbon stocks and timber recovery in tropical forests are mediated by logging intensity », cf. note 133, p. 16.

[57] Burivalova et al. (2014). « Thresholds of Logging Intensity to Maintain Tropical Forest Biodiversity », cf. note 150, p. 18.

[58] Hein et al. (2006). « Spatial scales, stakeholders and the valuation of ecosystem services », cf. note 20, p. 143.

[59] A. Veríssimo et al. (2002). « National forests in the Amazon ». In : *Science* 298.5586, p. 1478.

[60] Blaser et al. (2011). *Status of Tropical Forest Management 2011*, cf. note 1, p. vi.

[61] W. F. Laurance et al. (2014). « A global strategy for road building ». In : *Nature* 513.7517, p. 229–232.

[62] C. S. O'Connell et al. (2018). « Balancing tradeoffs : Reconciling multiple environmental goals when ecosystem services vary regionally ». In : *Environmental Research Letters* 13.6, p. 064008.

[63] Sist et al. (2015). « The Tropical managed Forests Observatory : A research network addressing the future of tropical logged forests », cf. note 116, p. 12.

[64] I. Tritsch et al. (2016). « Multiple patterns of forest disturbance and logging shape forest landscapes in Paragominas, Brazil ». In : *Forests* 7.12.

[65] Finer et al. (2014). « Logging Concessions Enable Illegal Logging Crisis in the Peruvian Amazon », cf. note 95, p. 10 ; Brancalion et al. (2018). « Fake legal logging in the Brazilian Amazon », cf. note 95, p. 10.

8.4.2 How to improve ES provision in production forests ?

The main strategy for maintaining high ES value in production forests has been so far to implement logging rules that limit the cutting cycle length (20-65 years) and the logging intensity (20-30 m^3ha^{-1})[66]. Those logging rules were thought as a compromise between producing enough timber to make financial benefits, and letting the forest recover long enough to make logging sustainable[67]. Several studies showed however that current logging rules are not enough to recover pre-logging forest characteristics[68]. Moreover, our results show that implementing intermediate logging rules leads to sub-optimal management of production forests : 30-yr cutting cycles and medium intensities (20 m^3ha^{-1}) are virtually never selected in the optimization process (Figure 8.2), and a restriction to 30-yr cutting cycles increases the loss of all ESs (cf. the *Current* strategy in Figure 8.4d-f).

The spatial configuration of optimal logging (Figure 8.2) highlights major regional differences in Amazonian forests. Forests of the Guiana Shield (northeastern Amazonia) are less prone to natural disturbances[69] and have thus adapted to those environmental conditions with low turnover rates and slow-growing species[70]. Because they recover timber slowly, they are not selected for logging when the demand for timber is low (see Supplementary material, Figure 8.8). When the demand for timber is high, however, Guiana shield forests are allocated to high-intensity logging when timber recovery is optimized (Figure 8.2c) because high logging intensities are predicted to decrease the forest maturity, thus making the forest more productive[71].

Nevertheless, Guiana shield forests provide other ESs : they harbor large amounts of carbon[72] and vertebrates diversity[73], and are thus not selected for logging when biodiversity and carbon are optimized (Figure 8.2a-b). Additionally, other studies found that forests of the Guiana Shield also play a crucial role in the Amazonian hydrological cycle[74], enhancing the importance of their conservation in future management strategies. As for the Guiana Shield, northern and central Amazonian forests harbor high levels of vertebrates diversity[75] and carbon[76] and are thus rarely selected for logging in this study when biodiversity conservation and carbon storage are prioritized (Figure 8.2a-b). If conservation is the main objective of Amazonian forest management, the consolidation of the protected area network in central and northeastern Amazonian forests will provide high benefits for conservation and climate change mitigation, especially if this promotes a higher connectivity between existing protected areas[77].

Southeastern forests, in turn, have lower levels of diversity and carbon. They are thus often allocated to high-intensity short-cycle logging when carbon and biodiversity are optimized (Figure 8.2a-

[66] Blaser et al. (2011). *Status of Tropical Forest Management 2011*, cf. note 1, p. vi.

[67] A. H. W. Seydack (2012). « Regulation of Timber Yield Sustainability for Tropical and Subtropical Moist Forests : Ecosilvicultural Paradigms and Economic Constraints ». In : *Continuous Cover Forestry*, p. 129–165.

[68] Zimmerman et Kormos (2012). « Prospects for Sustainable Logging in Tropical Forests », cf. note 102, p. 11.

[69] Espírito-Santo et al. (2014). « Size and frequency of natural forest disturbances and the Amazon forest carbon balance », cf. note 5, p. 23.

[70] Johnson et al. (2016). « Variation in stem mortality rates determines patterns of above-ground biomass in Amazonian forests : implications for dynamic global vegetation models », cf. note 8, p. 24 ; Quesada et al. (2012). « Basin-wide variations in Amazon forest structure and function are mediated by both soils and climate », cf. note 1, p. 23.

[71] Piponiot et al. (2018). « Assessing timber volume recovery after disturbance in tropical forests – A new modelling framework », cf. note 15, p. 109 ; E. Rödig et al. (2018). « The importance of forest structure for carbon fluxes of the Amazon rainforest ». In : *Environmental Research Letters* 13.5, p. 054013 ; H. Pérez-España et F. Arreguín-Sánchez (1999). « A measure of ecosystem maturity ». In : *Ecological Modelling* 119.1, p. 79–85.

[72] Avitabile et al. (2016). « An integrated pan-tropical biomass map using multiple reference datasets », cf. note 5, p. 1.

[73] Jenkins et al. (2013). « Global patterns of terrestrial vertebrate diversity and conservation », cf. note 25, p. 3.

[74] Staal et al. (2018). « Forest-rainfall cascades buffer against drought across the Amazon », cf. note 14, p. 2 ; C. I. Bovolo et al. (2018). « The Guiana Shield rainforests—overlooked guardians of South American climate ». In : *Environmental Research Letters* 13.7, p. 074029.

[75] Jenkins et al. (2013). « Global patterns of terrestrial vertebrate diversity and conservation », cf. note 25, p. 3.

[76] Avitabile et al. (2016). « An integrated pan-tropical biomass map using multiple reference datasets », cf. note 5, p. 1.

[77] A. J. Hansen et R. DeFries (2007). « Ecological mechanisms linking protected areas to surrounding lands ». In : *Ecological Applications* 17.4, p. 974–988.

b). However, because of previous forest degradation in the region through fire events, logging and forest fragmentation[78], that affect particularly large trees[79], the timber productivity may have been overestimated, even with closed canopies[80]. Restoring degraded forests through silvicultural interventions may be an opportunity to increase timber yields[81], but such interventions are costly and will require to adopt policies and financial incentives, e.g. through payments for ecosystem services[82].

8.4.3 Land-use strategies, trade-offs and implications for policy-making

Our results reveal that the main trade-off is between a long-term provision of timber and forest conservation for carbon (climate change mitigation) and biodiversity (Figure 8.3). These results fit into the "land sharing vs land sparing" debate : with a given timber demand, should logging focus on intensely-logged areas and conserve the rest as intact forest, or should it use the entire landscape under low-intensity logging ? Edwards and colleagues[83] showed that land-sparing logging retained higher levels of biodiversity in a Bornean forest concession. Because land-sparing logging creates heterogeneous landscapes and maintains higher levels of β-diversity, it has a higher potential for maintaining biodiversity at the landscape scale[84]. Our findings also show that land-sparing logging (e.g. the *Balanced* strategy) not only minimizes biodiversity loss (Figure 8.2b, Figure 8.4f), but it can also reduce carbon emissions (Figure 8.2a, Figure 8.4e). However the land-sparing strategy performs rather poorly in terms of timber recovery (Figure 8.3d), compared to a land-sharing strategy (e.g. the *Timber* strategy, Figure 8.4d).

There seems to be little place for a win-win strategy between timber production and forest conservation : the current strategy of intermediate logging rules leads to increased ES loss (Figure 8.4d-f). The fate of Amazonian production forests should thus depend on political choices and on future societal demand for ESs. If maintaining long-term timber supply from natural forests is thought to be the goal[85], then low-intensity logging should be widely applied in the Amazon, especially in the western part of the basin (Figure 8.2c). However, if the societal demand to preserve carbon and biodiversity continues to increase (e.g. carbon-based policies like REDD+[86], or the 1992 Rio convention on biodiversity[87]), then policies should focus on conserving intact inland forests while allowing high-intensity logging in the skirts of the Amazon basin. This type of policy will result in a fast depletion of timber stocks in those over-harvested forests. Alternative ways of producing timber, such as active forest restoration with intensive silviculture and mixed-species timber plantations[88], should then be implemented in the meantime, in order to have new productive forests once the over-harvested forests are depleted.

[78] Foley et al. (2007). « Amazonia revealed : forest Degradation and Loss of Ecosystem Goods and Services in the Amazon Basin », cf. note 8, p. 109 ; Davidson et al. (2012). « The Amazon basin in transition », cf. note *a*, p. 8.

[79] Laurance (2000). « Conservation : Rainforest fragmentation kills big trees », cf. note 55, p. 6 ; J. J. Gerwing (2002). « Degradation of forests through logging and fire in the eastern Brazilian Amazon ». In : *Forest Ecology and Management* 157.1-3, p. 131–141.

[80] Asner et al. (2004). « Spatial and temporal dynamics of forest canopy gaps following selective logging in the eastern Amazon », cf. note 63, p. 7.

[81] Lamb et al. (2005). « Restoration of Degraded Tropical Forest Landscapes », cf. note 58, p. 115.

[82] Salzman et al. (2018). « The global status and trends of Payments for Ecosystem Services », cf. note 55, p. 115.

[83] Edwards et al. (2014a). « Land-sharing versus land-sparing logging : reconciling timber extraction with biodiversity conservation », cf. note 152, p. 18.

[84] de Castro Solar et al. (2015). « How pervasive is biotic homogenization in human-modified tropical forest landscapes ? », cf. note 9, p. 142.

[85] D. J. Zarin et al. (2007). « Beyond reaping the first harvest : Management objectives for timber production in the Brazilian Amazon ». In : *Conservation Biology* 21.4, p. 916–925.

[86] C. M. Stickler et al. (2009). « The potential ecological costs and cobenefits of REDD : A critical review and case study from the Amazon region ». In : *Global Change Biology* 15.12, p. 2803–2824.

[87] J. H. Barton (1992). « Biodiversity at Rio ». In : *BioScience* 42.10, p. 773–776.

[88] Lamb et al. (2005). « Restoration of Degraded Tropical Forest Landscapes », cf. note 58, p. 115.

Interestingly, the "Road building" and the "Balanced" strategies, which only differ in terms of area accessible for logging (Table 8.1), give similar results. Building new roads (i.e., in the "Road building" strategy) does not increase the total area logged (Figure 8.4a) ; it gives more options for the choice of logged pixels, and thus increases ES provision (Figure 8.4d-f), but the difference with the "Balanced" strategy is small. Yet, logging roads open the forest to other uses, like hunting, wood-fuel harvesting and deforestation, which can increase carbon and biodiversity costs[89]. Depending on the level of governance, forests can undergo long-lasting additional degradation that was not accounted for in this study but could increase the environmental cost of road-building strategies. Overall, building new roads to increase the area of production forests in Amazonia may not be a good strategy for future ESs provision.

[89] Laurance et al. (2009). « Impacts of roads and linear clearings on tropical forests », cf. note 40, p. 4.

8.5 Conclusion

This study shows that large-scale trade-offs exist between maintaining timber stocks and maximizing biodiversity and climate change mitigation in Amazonian production forests. Land-sharing strategies that promote low-intensity logging in entire regions of the Amazon basin will result in sub-optimal biodiversity and high carbon emissions at the regional level, but land-sparing strategies that maximize global forest conservation will result in timber depletion of highly logged areas, and will thus require finding alternative timber sources in the future. Our results stress the importance of management choices for future production forests depending on societal demand for ecosystem services.

8.6 Supplementary material

8.6.1 Carbon damage model

To estimate carbon emissions from logging damage we calibrated a model with data from 115 plots (129.25 ha total) in 11 experimentally logged sites spread in Amazonia[90]. In all plots the identity of harvested trees was recorded, and at least one pre-logging and 2 post-logging forest inventories were carried out. In each forest inventory the diameter at breast height (DBH) of all stems > 20 cm DBH were measured, and trees were identified to the lowest taxonomic level (83% species, 16% genus, 2% not identified). From forest inventories the above ground carbon and wood density of all trees > 20 cm DBH were estimated with the R package BIOMASS[91].

[90] Sist et al. (2015). « The Tropical managed Forests Observatory : A research network addressing the future of tropical logged forests », cf. note 116, p. 12.

[91] Réjou-Méchain et al. (2017). « BIOMASS : An R Package for estimating above-ground biomass and its uncertainty in tropical forests », cf. note 18, p. 27.

The carbon extracted from plot j was estimated as :

$$Cext_j = \sum_i \underbrace{a_j \cdot DBH_i^b}_{\text{volume of tree } i} \cdot WD_i \tag{8.9}$$

with DBH_i is the DBH of the logged tree i, WD_i is its wood density and a_j, b are the two parameters of a volumetric equation calibrated at the Amazonian scale[92].

[92] Piponiot et al., « Can timber provision from Amazonian natural forests be sustainable ? », cf. note 38, p. 145.

The carbon of damage was estimated as :

$$Cdam_j = C0_j - Cext_j - Cmin_j \tag{8.10}$$

where $C0_j$ is the pre-logging above ground carbon of all trees > 20 cm DBH in plot j, and $Cmin_j$ is the minimum above ground carbon during the 4 years following logging operations (Figure 8.5).

We define the following variables :

- $RatioExt_j = \frac{Cext_j}{C0_j}$ is the proportion of the initial above-ground carbon $C0_j$ that is extracted of the plot j ;
- $RatioDam_j = \frac{Cdam_j}{C0_j - Cext_j}$ is the proportion of damage in the carbon left in plot j after logging operations.

We calibrated the following model (see Figure 8.6) :

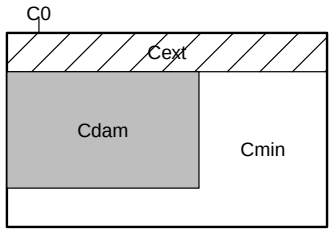

Figure 8.5 – Diagram of carbon pools in the damage model.

$$logit(RatioDam_j) \sim \mathcal{N}(\theta \cdot logit(RatioExt_j), \sigma_D^2) \tag{8.11}$$

with θ the slope of the relationship, and σ_D the standard deviation.

8.6.2 Wood density estimation

We used 2646 1-ha forest inventory plots spanned over the Brazilian Amazon from the RadamBrasil project[93], in which all trees

[93] IBGE (2016). *Data from RadamBrasil project*, cf. note 72, p. 116.

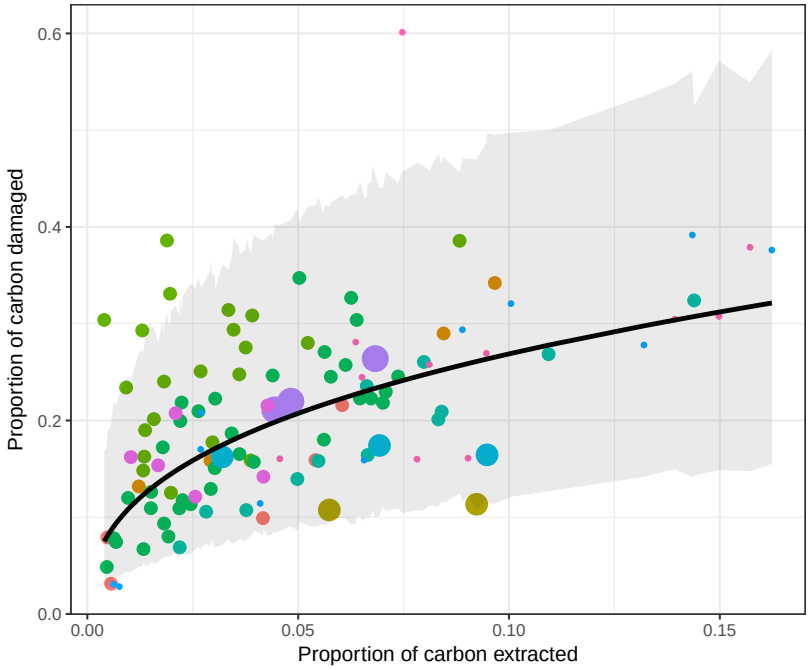

FIGURE 8.6 – Carbon damage model. Coloured dots are data from one plot, with each colour representing one site and the size of the dot being proportional to the plot's size. The black line is the maximum likelihood prediction, and the shaded area is the 95% confidence interval.

≥33 cm diameter at breast height (DBH) were measured, identified to the species level and had their volume estimated.

In every plot we estimated the mean wood density of all commercial stems (as defined in a previous study[94]) with the R package BIOMASS[95]. Values were then interpolated with the R package *automap*[96] on a 1° resolution grid (Supplementary figure 8.7).

[94] PIPONIOT et al., « Can timber provision from Amazonian natural forests be sustainable? », cf. note 38, p. 145.

[95] RÉJOU-MÉCHAIN et al. (2017). « BIOMASS : An R Package for estimating above-ground biomass and its uncertainty in tropical forests », cf. note 18, p. 27.

[96] PEBESMA (2004). « Multivariable geostatistics in S : the gstat package. », cf. note 77, p. 117.

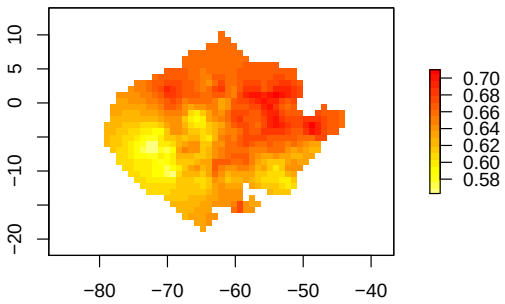

FIGURE 8.7 – Map of predicted wood density from interpolation of RadamBrasil data

8.6.3 Increasing timber demand - maps

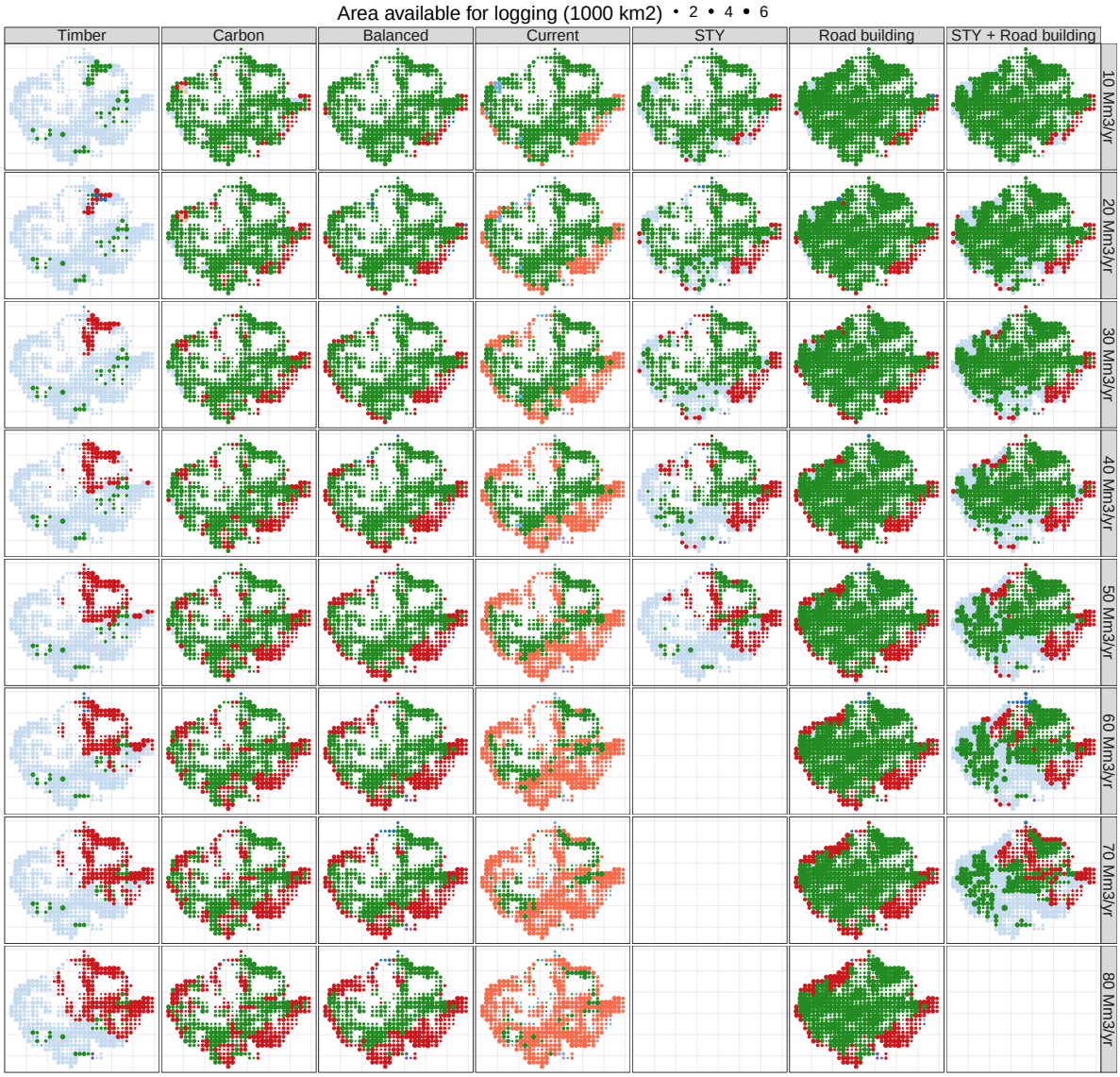

(a)

FIGURE 8.8 – Results of spatial optimization with varying demand for timber (from 10 to 50 Mm^3/yr), and under different scenarios.

Chapitre 9

Discussion générale

Nous avons vu dans les chapitres précédents comment l'exploitation sélective du bois modifiait l'approvisionnement de services écosystémiques dans les forêts de production à l'échelle du bassin amazonien. La plupart des études précédentes traitant des compromis entre services écosystémiques ont été menés à des échelles locales, de la parcelle à la concession forestière. Or, l'échelle déterminante pour la prise de décision en matière de politique forestière et de conservation est l'échelle régionale. La thèse présentée ici permet donc d'apporter des éléments de réflexion essentiels pour la gestion future des forêts de production en Amazonie.

L'une des originalités de cette étude est le fait d'avoir une quantification et un historique précis des perturbations dans les parcelles d'études, ce qui est rarement le cas dans les forêts perturbées d'Amazonie (voir par exemple le travail de Poorter et al. sur les forêts secondaires[1]). Cela a permis de faire le lien entre les dynamiques des forêts étudiées et l'intensité des perturbations récentes (ici l'exploitation). Alors que l'intensité et la fréquence des perturbations est prévue d'augmenter dans le futur proche en Amazonie, ce type d'étude permet de mieux comprendre ce que seront les forêts amazoniennes de demain.

[1] L. Poorter et al. (2016). « Biomass resilience of Neotropical secondary forests ». In : *Nature* 530.7589, p. 211–214.

Dans les deux premiers chapitres les émissions de carbone et l'évolution post-exploitation de la biomasse en Amazonie ont été quantifiées, et des différences régionales ont été décrites. Les régions au nord-est de l'Amazonie, en particulier le plateau des Guyanes, sont des forêts historiquement peu perturbées : cela se reflète dans la plus longue durée nécessaire pour retrouver la structure initiale de la forêt après l'exploitation, et notamment le volume des plus gros arbres[2]. Les forêts au sud de l'Amazonie sont des forêts contraintes par de hauts niveaux de stress hydrique (faibles précipitations, saison sèche plus longue), qui explique un potentiel de stockage de carbone après l'exploitation plus faible[3]. Au contraire les forêts du nord-ouest amazonien, qui sont aussi les plus riches en espèces animales et végétales[4], ont un régime de perturbations historique beaucoup plus élevé et semblent plus

[2] cf. Chapitre 7

[3] cf. Chapitre 4

[4] Bass et al. (2010). « Global conservation significance of Ecuador's Yasuní National Park », cf. note 85, p. 9.

résilientes à ce nouveau type de perturbation qu'est l'exploitation.

Du point de vue de la gestion forestière, l'une des conclusions principales de cette étude est que l'exploitation du bois en forêt naturelle amazonienne telle qu'elle est pratiquée aujourd'hui ne sera pas suffisante pour répondre sur le long terme à une demande croissante en bois. De plus, de nombreuses hypothèses plutôt optimistes ont été faites. En particulier, plusieurs modifications à long terme des forêts de production n'ont pas été prises en compte : des conséquences de l'exploitation, directes et indirectes (risques de feux et un accès facilité pour d'autres usagers) ainsi que les effets des changements climatiques. Les effets potentiels de ces modifications sont discutés ici, ainsi que les possibilités d'adaptation de la gestion forestière face à ces risques.

En termes de conservation de la biodiversité et de mitigation des changements climatiques par le stockage de carbone, les résultats présentés dans cette thèse indiquent que la meilleure stratégie reste de préserver l'intégrité des zones intactes de cœur de l'Amazonie, tout en intensifiant l'exploitation dans les zones externes pour approvisionner la demande en bois. Cette stratégie demande d'anticiper la perte rapide de la ressource en bois d'œuvre par la surexploitation, en lançant une transition vers d'autres systèmes de production de bois d'œuvre. Les opportunités et défis d'une telle transition forestière sont donc discutés dans ce chapitre.

Ces constats amènent à poser la question de la durabilité : puisque les pratiques actuelles ne sont pas durables au sens où elles entraînent une perte progressive de la ressource exploitée, peut-on modifier les pratiques pour les rendre durables ? Faut-il redéfinir la notion de durabilité, et sur quoi baser ce nouveau concept ?

Enfin, le rôle de la recherche dans la gestion des écosystèmes, point de départ de cette thèse, sera discuté selon deux problématiques majeurs : (i) comment donner des informations concrètes et utiles quand les objets d'étude sont hautement incertains, et (ii) l'importance des interactions, mais aussi leurs difficultés, au sein de la recherche et entre la recherche et la société.

9.1 Futurs défis pour la production de bois en Amazonie

9.1.1 Une production de bois limitée

Une récupération du bois d'œuvre trop lente

Les valeurs de récupération des stocks de bois d'œuvre (toutes espèces commerciales confondues) estimées dans cette thèse sont relativement faibles : entre 0.1 et 0.4 m^3 par ha et par an. Certaines régions semblent avoir un plus grand potentiel de récupération, notamment au nord et à l'ouest de l'Amazonie, mais même dans ces

régions l'exploitation ne peut être durable (en termes de récupération de la ressource en bois) qu'avec des cycles d'exploitation longs (> 60 ans) et des prélèvements faibles (de l'ordre de 10 $m^3 ha^{-1}$)[5].

[5] cf. Chapitre 7

Les cycles de rotation tels que définis aujourd'hui en Amazonie sont souvent trop courts pour permettre de récupérer la ressource (par exemple, 20 ans en Bolivie et au Pérou, 35 ans au Brésil[6]). Ces résultats ne sont pas propres à cette thèse : les études concordantes abondent, et même lorsque des techniques de réduction des dégâts sont appliquées, il est rare de retrouver le stock initial de bois à la fin du cycle[7].

[6] Blaser et al. (2011). *Status of Tropical Forest Management 2011*, cf. note 1, p. vi.

[7] Zimmerman et Kormos (2012). « Prospects for Sustainable Logging in Tropical Forests », cf. note 102, p. 11.

Les recommandation pour assurer la durabilité de la ressource sont souvent de minimiser les impacts tout en augmentant la durée des cycles de rotations[8]. Dans les résultats apportés par cette thèse, il semblerait effectivement qu'en allongeant les cycles de rotation (> 60 ans), en prélevant une grande diversité d'essences, et en limitant l'intensité d'exploitation, l'exploitation puisse être durable, au moins du point de vue de la production de bois. Cependant, deux facteurs au moins restent à prendre en compte : (i) à l'échelle de la concession, exploiter à de faibles intensités et attendre aussi longtemps entre 2 cycles peut ne pas être économiquement viable, car le coût d'ouverture des pistes d'exploitation est élevé par rapport aux bénéfices engendrés, et (ii) à l'échelle régionale, la production doit approvisionner le marché local de bois d'œuvre : la surface des forêts disponibles pour la production en Amazonie n'est aujourd'hui pas suffisante pour atteindre la demande actuelle en exploitation à de faibles intensités avec de longs cycles d'exploitation[9].

[8] A. Huth et T. Ditzer (2001). « Long-term impacts of logging in a tropical rain forest — a simulation study ». In : *Forest Ecology and Management* 142.1-3, p. 33–51.

[9] cf. chapitre 7

Effets de l'abattage sélectif de quelques individus

Les effets à court terme Les estimations de récupération du bois d'œuvre ont été faites sous des hypothèses relativement optimistes, et en particulier le fait qu'un grand nombre d'espèces aient été considérées comme potentiellement commerciales [10]. Dans la réalité, la liste des espèces commercialisées pour le bois d'œuvre est beaucoup plus restreinte, et quelques espèces ayant une forte valeur sur le marché sont surexploitées et dans certaines régions d'Amazonie leur densité a fortement diminué. C'est le cas par exemple de l'acajou d'Amérique (*Swietenia macrophylla*)[11], une espèce dont le bois a fait l'objet d'une surexploitation opportuniste depuis des décennies en Amazonie[12]. A court terme, cette quasi-disparition des espèces les plus précieuses peut diminuer les profits de l'exploitation au point de la rendre non viable d'un point de vue économique[13].

[10] cf. chapitre 7

[11] J. Grogan et al. (2010). « Overharvesting driven by consumer demand leads to population decline : Big-leaf mahogany in South America ». In : *Conservation Letters* 3.1, p. 12–20.

[12] R. E. Rice et al. (1997). « Can Sustainable Management Save Tropical Forests ? » In : *Scientific American* 276.4, p. 44–49 ; T. A. Branch et al. (2013). « Opportunistic exploitation : An overlooked pathway to extinction ». In : *Trends in Ecology and Evolution* 28.7, p. 409–413.

[13] Rice et al. (1997). Cf. note 12.

Les effets à long terme L'abattage sélectif des individus adultes des essences exploitées pose un problème pour la régénération de ces mêmes espèces. La population de semenciers entraîne

une diminution de la proportion de graines des espèces exploitées dans le sol forestier. Déterminer les impacts sur la génération suivante est difficile avec le peu de recul actuel sur la question, mais il est probable que sur de longues périodes les populations des espèces exploitées diminuent progressivement. Si certaines de ces espèces ont un rôle crucial dans le fonctionnement de la forêt, ce rôle sera alors perdu et la forêt durablement modifiée. Par exemple, les espèces exploitées sont souvent en Amazonie de grands arbres de canopée à croissance relativement lente et à longue durée de vie. Une perte de ces espèces, si elles n'ont pas d'équivalent fonctionnel dans la communauté locale, pourrait amener à une diminution de la hauteur de canopée et une augmentation du taux de mortalité.

Dans le biais créé par la sélection des arbres exploités, il y a aussi ceux laissés sur pied par les exploitants. Souvent, ce sont des individus sondés creux, qui risquent d'être refusés en scierie car trop défectueux. Ainsi, les semenciers des espèces exploitées laissés sur pied sont souvent des arbres défectueux. Si les défauts (formation de creux, déformations du tronc) s'avèrent être héréditaires, ces pratiques pourraient provoquer la sélection progressive de jeunes arbres défectueux après plusieurs cycles d'exploitation.

Adaptation de la gestion De nombreuses méthodes de sylviculture visant à augmenter la productivité des forêts et éviter la disparition des essences commerciales ont été proposées et testées sur des parcelles expérimentales[14]. Certaines de ces techniques pourraient permettre de réduire les risque de disparition des espèces exploitées. Ces techniques agissent de deux façons : soit en diminuant la compétition des autres espèces par l'élimination des grands individus des espèces non-commerciales (on parle alors d'éclaircissement) ; soit en augmentant la régénération des essences exploitées, par exemple en replantant dans les trouées d'exploitation des plantules de ces mêmes essences.

Bien que les expériences de sylviculture aient donné des résultats plutôt encourageants[15], ces techniques ne sont quasiment jamais utilisées dans les forêts tropicales. Ce décalage peut s'expliquer par un manque de communication entre le monde de la recherche et les exploitants forestiers : certains exploitants n'ont pas connaissance de ces techniques ni de leurs effets potentiels sur la productivité. Il est possible aussi que les industriels craignent la mauvaise presse que pourraient avoir des pratiques de modification intensive de la forêt, alors qu'aujourd'hui, l'image que cherchent à donner les organes de certification est celle de forêts quasi-naturelles (voir Figure 9.1). Un autre frein pour les exploitants peut être le besoin d'investir juste après l'exploitation pour appliquer les traitements sylvicoles, pour des gains de productivité qui n'arrivent qu'après plusieurs décennies et qui sont soumis à de nombreux risques (pillage par de l'exploitation illégale, feux,

[14] Peña-Claros et al. (2008). « Regeneration of commercial tree species following silvicultural treatments in a moist tropical forest », cf. note 107, p. 12 ; De Avila et al. (2015). « Medium-term dynamics of tree species composition in response to silvicultural intervention intensities in a tropical rain forest », cf. note 65, p. 7 ; L. Kammesheidt et al. (2001). « History of logging and silvicultural treatments in the western Venezuelan plain forests and the prospect for sustainable forest management ». In : *Forest Ecology and Management* 148.1-3, p. 1–20.

[15] Putz et Romero (2014). « Futures of tropical forests (sensu lato) », cf. note 110, p. 12.

tempête, etc.). La dissuasion est d'autant plus forte si le régime foncier est incertain, ou dans le cas de contrats de concession à court terme (< 30 ans). La faible gouvernance des forêts de production pousse au gain rapide, et non au maintien à long terme de leur productivité.

Alors que, dans les régions tempérées, les forêts de production ont été profondément modifiées et sont aujourd'hui le produit de traitements sylvicoles intenses pour favoriser les espèces les plus productives[16], sous les tropiques ces interventions humaines sont presque inexistantes. Cette différence peut s'expliquer par l'histoire et la quantité de ressource disponible. En Europe par exemple, la surface forestière a progressivement diminué sous l'action de l'homme au cours du Moyen-âge et jusqu'à la fin du XVIII^{e} siècle, jusqu'à poser des problèmes d'approvisionnement en bois, ce qui a motivé la gestion et la plantation de nouvelles forêts[17]. En Amazonie, les forêts naturelles intactes couvrent encore 4 millions de km^2 et la limite des ressources forestières est encore loin d'être atteinte[18]. L'investissement dans la plantation et la gestion des forêts n'a donc pas encore eu beaucoup de succès, car il suffit pour extraire du bois d'aller chercher un peu plus loin dans des forêts n'ayant pas encore de régime foncier bien déterminé. Cela pourra changer dans un futur proche avec la part croissante de forêts fortement dégradées par des feux, des sécheresses et de l'exploitation illégale[19]. Les forêts dégradées, qui sont plus accessibles, car majoritairement à proximité des routes et des foyers d'occupation humaine, constituent un énorme potentiel pour la production de bois. Aujourd'hui peu productives, ces forêts peuvent être activement restaurées pour produire du bois ou d'autres produits non-ligneux. D'autres pays tropicaux tels que le Viêtnam, dont les ressources forestières avaient atteint des niveaux critiques, ont déjà entamé ce processus de transition forestière[20].

Figure 9.1 – Publicité du Forest Stewardship Council dans le métro de São Paulo, Brésil. «Choisissez des produits avec le label FSC et aidez à conserver les forêts». Source : www.marketingtoolkitfsc.org

[16] H. Spiecker (2003). « Silvicultural management in maintaining biodiversity and resistance of forests in Europe—temperate zone ». In : *Journal of Environmental Management* 67.1, p. 55–65.

[17] E. P. Farrell et al. (2000). « European forest ecosystems : building the future on the legacy of the past ». In : *Forest Ecology and Management* 132, p. 5–20.

[18] Tyukavina et al. (2016). « Pantropical hinterland forests : mapping minimally disturbed forests », cf. note 98, p. 121.

[19] Potapov et al. (2017). « The last frontiers of wilderness : Tracking loss of intact forest landscapes from 2000 to 2013 », cf. note 8, p. 142.

[20] P. Meyfroidt et E. F. Lambin (2008). « Forest transition in Vietnam and its environmental impacts ». In : *Global Change Biology* 14.6, p. 1319–1336.

Effets potentiels de l'extraction de biomasse

Les effets potentiels Les forêts situées à l'est de l'Amazonie, loin de l'apport de sédiments par la cordillère des Andes, poussent sur des sols anciens et lessivés, donc pauvres en nutriments[21]. Dans ces forêts, la majeur part du stock de nutriments ne se trouve pas dans le sol, mais dans la biomasse elle-même. Cette biomasse est principalement stockée dans les plus gros arbres, qui sont donc les réservoirs de nutriments de ces forêts. Quand ces gros arbres meurent, les nutriments fertilisent le sol et sont recyclés par les arbres vivants[22]. Par contre, si les gros arbres sont extraits de la forêt, comme pendant l'exploitation, les nutriments présents dans leur tronc ne retournent pas dans la litière et c'est donc une perte nette pour l'écosystème. Cette perte, dans des forêts où les nutriments (phosphore, azote, potassium) sont limitants pour la croissance des arbres, pourrait entraîner une diminution de la

[21] Quesada et al. (2011). « Soils of Amazonia with particular reference to the RAINFOR sites », cf. note 3, p. 1.

[22] Grau et al. (2017). « Nutrient-cycling mechanisms other than the direct absorption from soil may control forest structure and dynamics in poor Amazonian soils », cf. note 7, p. 24.

biomasse. Ce ne sont aujourd'hui que des hypothèses mais, si elles sont avérées, les conséquences pourraient être amplifiées lorsque la biomasse des dégâts liés à l'exploitation est aussi extraite de la forêt, pour en faire par exemple du bois de chauffe ou être utilisée dans des centrales électriques.

Adaptation de la gestion Face à ce type de risque, une possibilité serait de compenser la perte de nutriments après l'exploitation. Cela demande d'identifier quels sont les nutriments limitants pour la croissance des individus dans ces écosystèmes, et de quantifier les pertes dues à l'exploitation. Une autre possibilité est d'éviter l'exploitation dans les régions orientales de l'Amazonie où les sols sont les plus pauvres, mais cette solution pourrait être difficile à accepter pour l'industrie forestière historiquement implantée dans ces régions.

9.1.2 Conséquences d'une faible gouvernance

La faible application des lois diminue leur efficacité

En Amazonie l'exploitation du bois est principalement illégale : il est estimé qu'entre 20 et 60% du bois extrait des forêts naturelles en Amazonie brésilienne n'est pas conforme aux législations en place[23], et dans les pays frontaliers la situation n'est pas toujours meilleure[24]. Une pratique courante est d'utiliser des permis d'exploitation, dans lesquels le stock d'essences de haute valeur commerciale a été surestimé, pour «légaliser »du bois extrait de zones adjacentes[25].

Tant que de telles pratiques continueront de prévaloir, les bénéfices liés à l'adoption de nouvelles législations resteront limités : dans l'exemple de la surexploitation de l'acajou mentionné ci-dessus (section 9.1.1), l'adoption de nouvelles réglementations n'a pas empêché le commerce illégal et sa dispartion rapide dans certaines régions d'Amazonie[26]. Le manque de gouvernance dans les forêts tropicales en général, et dans les forêts amazoniennes en particulier, est donc un frein majeur à l'adoption de nouvelles pratiques. Cela est d'autant plus vrai que les législations sont contraignantes (temps de rotation rallongés, intensités réduites, contrôle des dégâts), car l'exploitation illégale devient alors encore plus avantageuse. De manière générale, la littérature scientifique abonde sur les techniques pour diminuer l'impact de l'exploitation sélective, mais le manque de d'études sur l'applicabilité de ces méthodes et leur intérêt pour les populations et gestionnaires explique leur faible adoption et la prévalence de l'exploitation illégale aujourd'hui[27].

[23] Lawson et al. (2010). « Illegal Logging and Related Trade. Indicators of the Global Response », cf. note 5, p. 34.

[24] Finer et al. (2014). « Logging Concessions Enable Illegal Logging Crisis in the Peruvian Amazon », cf. note 95, p. 10 ; P. Pacheco (2004). « Law compliance : Bolivia case study ». In : *FAO, Rome. Meilleures pratiques pour l application des lois dans le secteur forestier* 102, p. 1–25.

[25] Brancalion et al. (2018). « Fake legal logging in the Brazilian Amazon », cf. note 95, p. 10.

[26] A. G. Blundell et R. E. Gullison (2003). « Poor regulatory capacity limits the ability of science to influence the management of mahogany ». In : *Forest Policy and Economics* 5.4, p. 395–405.

[27] B. Hari Poudyal et al. (2018). « Evolutionary dynamics of selective logging in the tropics : A systematic review of impact studies and their effectiveness in sustainable forest management ». In : *Forest Ecology and Management* 430.August, p. 166–175.

L'exploitation ouvre les forêts

À l'échelle d'un massif forestier, l'une des conséquences les plus importantes de l'exploitation est que cette dernière requiert la construction de routes qui ouvrent la forêt de manière quasi-irréversible[28]. Une fois les routes construites, celles-ci facilitent l'accès aux forêts pour d'autres usagers[29], rendant difficile et coûteux le contrôle des activités humaines dans le massif forestier. Cette facilité d'accès provoque une dégradation progressive des forêts :

- par la chasse[30], qui diminue le nombre de disperseurs et réduit ainsi la biomasse des forêts affectées[31] ;
- par l'exploitation illégale[32] ;
- par la déforestation[33] ;
- par des feux non contrôlés[34].

Cette dégradation réduit significativement la valeur environnementale des forêts exploitées. L'absence de prise en compte de ces effets indirects de l'exploitation est d'ailleurs l'une des limites majeures de l'étude présentées au Chapitre 8.

Adaptation de la gestion

Aujourd'hui de nombreux facteurs expliquent la faible gouvernance des forêts de production en Amazonie, pami lesquelles (i) les faibles moyens alloués au contrôle des forêts par les gouvernements[35], (ii) la corruption très répandue, qui fragilise l'action publique, (iii) le régime foncier incertain sur les fronts pionniers[36], (iv) de régulières «amnisties environnementales»[37] qui encouragent l'illégalité. La gestion durable des forêts ne sera pas efficace tant que ces forêts n'auront pas de régime de gouvernance stable et solide. Il est indispensable de renforcer le contrôle des forêts.

Ces questions de gouvernance sont fondamentales mais complexes, et il est difficile de les traiter rapidement. Parmi les pistes d'amélioration qui émergent aujourd'hui, des approches hybrides de gestion entre l'Etat et les communautés locales et petits exploitants ont montré des succès locaux, par exemple dans la région de l'Acre en Amazonie brésilienne[38], mais ces exemples sont encore limités. L'avènement des technologies de télédétection au cours des dernières décennies a permis une plus grande transparence dans l'usage des forêts[39]. L'automatisation de la détection de la déforestation développé par l'Agence des Etudes spatiales brésilienne[40] a été un outil de lutte efficace contre la déforestation[41]. Des outils similaires pour la détection de l'exploitation forestière sont en cours de développement[42].

[28] S. G. Perz et al. (2007). « Unofficial road building in the Brazilian Amazon : Dilemmas and models for road governance ». In : *Environmental Conservation* 34.2, p. 112–121.

[29] Laurance et al. (2009). « Impacts of roads and linear clearings on tropical forests », cf. note 40, p. 4.

[30] Peres et Lake (2003). « Extent of Nontimber Resource Extraction in Tropical Forests : Accessibility to Game Vertebrates by Hunters in the Amazon Basin », cf. note 164, p. 20.

[31] Peres et al. (2016). « Dispersal limitation induces long-term biomass collapse in overhunted Amazonian forests », cf. note 67, p. 7.

[32] Tritsch et al. (2016). « Multiple patterns of forest disturbance and logging shape forest landscapes in Paragominas, Brazil », cf. note 64, p. 154.

[33] Asner et al. (2006). « Condition and fate of logged forests in the Brazilian Amazon. », cf. note 78, p. 9.

[34] C. A. Peres et al. (2006). « Detecting anthropogenic disturbance in tropical forests ». In : *Trends in Ecology & Evolution* 21.5, p. 227–229.

[35] Rice et al. (1997). « Can Sustainable Management Save Tropical Forests ? », cf. note 12, p. 163 ; A. Agrawal et al. (2008). « Changing Governance of the World's Forests ». In : *Science* 320.5882, p. 1460–1462.

[36] Simmons (2004). « The Political Economy of Land Conflict in the Eastern Brazilian Amazon », cf. note 45, p. 5.

[37] Soares-Filho et al. (2014). « Cracking Brazil ' s Forest Code », cf. note 94, p. 10.

[38] S. Perz et al. (2008). « Road building, land use and climate change : Prospects for environmental governance in the Amazon ». In : *Philosophical Transactions of the Royal Society B : Biological Sciences* 363.1498, p. 1889–1895. arXiv : `arXiv:1011.1669v3`.

[39] D. O. Fuller (2006). « Tropical forest monitoring and remote sensing : A new era of transparency in forest governance ? » In : *Singapore Journal of Tropical Geography* 27.1, p. 15–29.

[40] *Instituto Nacional de Pesquisas Espaciais* ou INPE

[41] Nepstad et al. (2014). « Slowing Amazon deforestation through public policy and interventions in beef and soy supply chains. », cf. note 50, p. 5.

[42] INPE (2010). *INPE e Serviço Florestal firmam parceria para monitorar concessões.*

9.1.3 Les changements climatiques

Modifications de la structure et de la composition

Les changements climatiques récents d'origine anthropique ont comme principal impact en Amazonie une augmentation de la saisonnalité des précipitations : augmentation de la durée de la saison sèche dans les zones les plus australes du bassin, et augmentation de la fréquence des épisodes de sécheresse et de pluies intenses[43]. Ces changements ont plusieurs conséquences sur les caractéristiques des forêts : l'un des principaux effets est l'augmentation du taux de mortalité[44], et donc un turnover plus rapide[45]. Cette surmortalité provoque une modification de la structure, notamment par la perte de gros arbres plus vulnérables aux sécheresses[46] et moins stables en cas de sol engorgé[47] : la structure se rapproche donc de forêts plus jeunes. Toutes les espèces n'étant pas égales face au stress hydrique, une augmentation de la fréquence des sécheresses provoquera aussi une modification de la composition[48]. Il est prévu que les espèces à faible surface foliaire (SLA : specific leaf area) et à forte densité de bois, qui sont des traits favorisant la résistance à la sécheresse, survivent mieux aux nouvelles conditions climatiques[49]. Il existe cependant un compromis entre résistance à la sécheresse (fort investissement dans la structure, bois dense) et croissance rapide (faible investissement dans la structure hydraulique, bois léger). On peut donc imaginer que, tant que les épisodes de sécheresse restent suffisamment espacés, les trouées laissées par les arbres de canopée morts durant les épisodes de sécheresse soient colonisées par des arbres à croissance rapide et à faible densité de bois, qui mourront lors du prochain épisode de sécheresse. Si la fréquence des sécheresses augmente, ces espèces vulnérables risquent de disparaître au profit d'arbres à croissance lente mais plus résistants à ces conditions extrêmes. En termes de structure, on peut s'attendre dans le futur à avoir des forêts plus basses et plus riches en petites tiges, avec des taux de mortalité plus élevés et des taux de croissance plus faibles. L'abondance des lianes pourrait aussi augmenter sous l'effet des changements climatiques, ce qui limiterait davantage la croissance des arbres par la compétition accrue pour la lumière et pour l'eau[50].

Ces modifications peuvent entraîner une diminution de certains services rendus par les forêts de production : diminution du stockage de carbone[51] et du stock de volume commercial[52], disparition potentielle de certaines espèces non-adaptées aux nouvelles conditions climatiques[53]. Dans le cas extrême où les nouvelles conditions compromettraient la résilience des forêts naturelles, les changements climatiques pourraient alors provoquer une transition vers d'autres types d'écosystèmes comme les savanes[54].

L'effet conjoint des changements climatiques et de la gestion pour la production de bois est encore difficile à évaluer, mais

[43] Kitoh et al. (2011). « Climate change projections over South America in the late 21st century with the 20 and 60 km mesh Meteorological Research Institute atmospheric general circulation model (MRI-AGCM) », cf. note 16, p. 2.

[44] C. D. Allen et al. (2010). « A global overview of drought and heat-induced tree mortality reveals emerging climate change risks for forests ». In : *Forest Ecology and Management* 259.4, p. 660–684. arXiv : arXiv:1011.1669v3.

[45] V. Leitold et al. (2018). « El Niño drought increased canopy turnover in Amazon forests ». In : *New Phytologist* 219.3, p. 959–971.

[46] Bennett et al. (2015). « Larger trees suffer most during drought in forests worldwide », cf. note 69, p. 7.

[47] M. Aubry-Kientz et al. (2013). « Toward Trait-Based Mortality Models for Tropical Forests ». In : *PLoS ONE* 8.5, e63678.

[48] K. J. Feeley et al. (2012). « The relative importance of deforestation, precipitation change, and temperature sensitivity in determining the future distributions and diversity of Amazonian plant species ». In : *Global Change Biology* 18.8, p. 2636–2647.

[49] M. Uriarte et al. (2016). « A trait-mediated, neighbourhood approach to quantify climate impacts on successional dynamics of tropical rainforests ». In : *Functional Ecology* 30.2, p. 157–167.

[50] S. A. Schnitzer et F. Bongers (2011). « Increasing liana abundance and biomass in tropical forests : Emerging patterns and putative mechanisms ». In : *Ecology Letters* 14.4, p. 397–406.

[51] T. R. Feldpausch et al. (2016). « Amazon forest response to repeated droughts ». In : *Global Biogeochemical Cycles* 30.7, p. 964–982.

[52] cf. Chapitre 6

[53] K. J. Feeley et al. (2016). « Disappearing climates will limit the efficacy of Amazonian protected areas ». In : *Diversity and Distributions* 22.11, p. 1081–1084.

[54] cf. Section 9.3.2

certaines études montrent un effet d'atténuation de la surmortalité liée aux sécheresses dans les forêts exploitées à l'ouest de l'Amazonie, l'une des régions où les épisodes de sécheresses de 2005 et 2010 ont été les plus intenses[55]. Ceci peut être dû à l'éclaircissement du peuplement par l'exploitation, et donc à une diminution de la compétition lors des années où la ressource en eau est particulièrement limitante. Parallèlement, l'exploitation peut augmenter la probabilité de départs de feux les années de sécheresses, dans le cas où il y a beaucoup de dégâts d'exploitation inflammables[56].

[55] M. V. N. D'Oliveira et al. (2017). « Twenty years monitoring growth dynamics of a logged tropical forest in Western Amazon ». In : *Pesquisa Florestal Brasileira* 37.92, p. 493–502.

[56] A. R. Holdsworth et C. Uhl (1997). « Fire in Amazonian Selectively Logged Rain Forest and the Potential for Fire Reduction ». In : *Ecological Applications* 7.2, p. 713.

Adaptation de la gestion

Les modifications probables des caractéristiques des forêts dans le contexte de changements climatiques demanderont une adaptation de la gestion. De nombreuses espèces aujourd'hui exploitées sont vulnérables aux sécheresses qui diminue leur croissance et leur taux de survie[57]. Pour continuer à produire du bois dans le futur, il faudra donc s'adapter à ces changements en élargissant la liste d'espèces commerciales et en exploitant des espèces plus adaptées aux sécheresses, qui deviendront plus abondantes. La résistance des espèces aux évènements climatiques extrêmes doit aussi être prise en compte dans le cas d'enrichissements des trouées d'exploitation ou de la restauration de forêts dégradées.

[57] Fargeon et al. (2016). « Vulnerability of Commercial Tree Species to Water Stress in Logged Forests of the Guiana Shield », cf. note 12, p. 109.

L'augmentation des conditions favorables aux feux de forêts[58] demandera aussi une gestion adaptée à ce type de risque. Les risques de feu dans les forêts exploitées sont surtout liés au bois mort des dégâts d'exploitation, plus inflammable, et à l'entrée de lumière dans les trouées d'exploitation qui diminue l'humidité de l'air et augmente la température, créant un microclimat propice au départ de feu. Les techniques d'exploitation à faible impact visant à réduire les dégâts grâce à l'abattage directionnel et la planification des pistes pourraient permettre de limiter ces risques[59]. Dans le cas où des interventions sylvicoles permettraient d'augmenter la croissance et la régénération de certaines espèces commerciales, il serait alors judicieux de favoriser des espèces résistantes aux feux. Cependant, il existe aujourd'hui encore peu d'information sur la résistance au feu des espèces. Leur résistance au feu est souvent approximée par des mesures de traits tels que l'épaisseur de l'écorce, mais le rôle de ces caractéristiques dans les mécanismes de défense au feu est encore ambigu dans les forêts tropicales[60].

[58] Jolly et al. (2015). « Climate-induced variations in global wildfire danger from 1979 to 2013 », cf. note 73, p. 8.

[59] F. E. Putz et M. A. Pinard (1993). « Reduced-impact logging as a carbon-offset method ». In : *Conservation Biology*, p. 755–757.

[60] C. E. T. Paine et al. (2010). « Functional explanations for variation in bark thickness in tropical rain forest trees ». In : *Functional Ecology* 24.6, p. 1202–1210.

Les épisodes de fortes précipitations devraient aussi augmenter, ce qui risque d'augmenter l'érosion des sols. L'exploitation met momentanément les sols à nu sur les pistes et les trouées d'exploitation et augmente ainsi l'érosion[61], mais cet effet peut aussi être atténué dans le cas d'exploitation à faible impact où les dégâts sont contrôlés et les pistes d'exploitation réduites au

[61] N. A. Chappell et al. (2004). « Sources of suspended sediment within a tropical catchment recovering from selective logging ». In : *Hydrological Processes* 18.4, p. 685–701.

minimum.

9.2 Opportunités pour une transition forestière en Amazonie

9.2.1 Implications d'une stratégie de préservation

Intensifier pour préserver

Le développement d'une stratégie de gestion des forêts amazoniennes devra répondre aux attentes de la société en termes de services écosystémiques. Bien que la demande locale en bois d'œuvre reste forte, la valeur attribuée à d'autres services est de plus en plus grande. La prise de conscience des changements climatiques récents, et de leurs conséquences pour le fonctionnement des écosystèmes dont dépendent les sociétés humaines, a été un moteur récent pour des politiques de mitigation de ces changements climatiques. Le stockage du carbone atmosphérique par la végétation vivante connaît donc aujourd'hui un vif intérêt des politiques internationales[62]. De la même façon, la crise actuelle de la biodiversité et ses conséquences a entraîné un intérêt de l'opinion et des politiques publiques pour ces questions, bien que la biodiversité soit un terme qui reste aujourd'hui vague et regroupe un grand nombre d'interprétations[63]. Il est probable que les questions autour du carbone, de la biodiversité et des autres services rendus par les forêts amazoniennes auront une importance grandissante dans la définition de leur gestion. Or les résultats présentés dans cette thèse, et en particulier dans le chapitre 8, mènent à la conclusion suivante : développer une exploitation extensive en exploitant l'intégralité des forêts disponibles aujourd'hui permettrait de produire du bois sur le long terme, mais entraînerait une forte diminution de la diversité et du stock de carbone de ces forêts.

Dans une optique de préservation de la diversité et de la biomasse des forêts amazoniennes, la meilleure stratégie serait de limiter l'exploitation aux zones les plus externes de l'Amazonie. À ces résultats s'ajoutent les conséquences de l'ouverture de routes dans la forêt dans un contexte de faible gouvernance[64], discuté en section 9.1.2 : exploiter de nouvelles zones jusqu'alors inaccessibles au cœur de l'Amazonie risquerait d'accélérer la dégradation de ces forêts.

Épuisement rapide des stocks de bois

Pour pouvoir subvenir à la demande en bois tout en limitant la surface des forêts exploitées, il faudrait alors favoriser de fortes intensités d'exploitation. Dans ces conditions, il est très probable qu'après un ou deux cycles d'exploitation les stocks de bois ne soient pas récupérer dans les zones exploitées. Le modèle présenté

[62] T. Stocker (2014). *Climate Change 2013 - The Physical Science Basis*. Sous la dir. d'Intergovernmental Panel on Climate Change. Cambridge : Cambridge University Press. arXiv : arXiv:1011.1669v3.

[63] E. Masood (2018). « The battle for the soul of biodiversity ». In : *Nature* 560.7719, p. 423–425.

[64] Perz et al. (2007). « Unofficial road building in the Brazilian Amazon : Dilemmas and models for road governance », cf. note 28, p. 167 ; Laurance et al. (2009). « Impacts of roads and linear clearings on tropical forests », cf. note 40, p. 4.

au chapitre 6 prédit qu'avec une exploitation intense (30 m^3) à cycle de rotation court (15 ans), seul 10-30% du stock exploité serait récupéré après la première rotation, voire moins si seules quelques espèces sont exploitées. Avec des niveaux si faibles, il est probable que l'exploitation ne soit plus économiquement viable. Mettre en place une telle stratégie demande donc d'anticiper ce manque à venir pour la production de bois. Aujourd'hui, peu de sources alternatives de bois existent dans la région : il n'existe quasiment aucune expérience de plantations de bois d'œuvre à une échelle opérationnelle[65], et les politiques publiques ainsi que les projets de recherche se concentrent aujourd'hui sur l'exploitation sélective, sans envisager d'autres options de production. Pour pouvoir maintenir à la fois l'intégrité des forêts amazoniennes encore intactes et une production de bois à long terme, la mise en place d'alternatives viables doit être faite dès maintenant. Ainsi, le bois produit pourra être récolté dans quelques décennies, quand les forêts de production ne sera plus à même de fournir la demande.

[65] C. Sabogal et al. (2006). *Silvicultura na Amazonônia brasileira : avaliação de experiências e recomendações para implementação e melhoria dos sistemas* ; J. R. Costa et al. (2013). « Cultivo e Manejo do Mogno (Swietenia macrophylla King) ». In : *Embrapa Amazônia Ocidental* 1.1517- 3135, p. 36.

9.2.2 Comment produire du bois à long terme

Potentiel des forêts secondaires et dégradées

En Amazonie, environ 13% de la surface totale des forêts a été déforestée, principalement dans l' «arc de déforestation »au sud-est du Brésil. En parallèle de cette déforestation, 23% des zones déforestées sont aujourd'hui abandonnées et couvertes d'une végétation secondaire[66]. La surface des forêts dégradées par des feux, l'exploitation ou la fragmentation atteint aussi des valeurs similaires[67]. Il existe donc aujourd'hui en Amazonie des dizaines de millions d'hectares de forêts fortement dégradées ou secondaires.

Les forêts secondaires et dégradées présentent un potentiel intéressant pour la production de bois : il existe en Amérique centrale de nombreux exemples de forêts secondaires qui sont aujourd'hui utilisées pour produire du bois[68]. En Amazonie, les forêts dégradées et secondaires sont sujettes à de nombreuses perturbations humaines (nouveau cycle de déforestation ou d'exploitation, feux[69]). Ces forêts ont donc une structure très différente des forêts anciennes : elles ne possèdent notamment plus les gros arbres qui sont l'intérêt principal de l'exploitation sélective[70]. Pour pouvoir avoir des forêts secondaires productives l'une des premières choses à faire serait donc de diminuer ce régime de perturbations auxquelles elles sont aujourd'hui soumises.

Les résultats encourageants d'Amérique centrale ne sont cependant pas directement transposables partout en Amazonie : les taux d'accumulation de biomasse mesurés dans les forêts secondaires d'Amérique centrale sont souvent élevés, mais certaines régions d'Amazonie ont des taux de récupération plus lents[71] [72]. Une raison peut être la faible fertilité des sols dans certaines régions d'Amazonie. L'historique de la zone avant la reforestation

[66] A. P. D. Aguiar et al. (2016). « Land use change emission scenarios : Anticipating a forest transition process in the Brazilian Amazon ». In : *Global Change Biology* 22.5, p. 1821–1840.

[67] Tyukavina et al. (2017). « Types and rates of forest disturbance in Brazilian Legal Amazon, 2000–2013 », cf. note 26, p. 112.

[68] D. Piotto (2007). « Growth of native tree species planted in open pasture, young secondary forest and mature forest in humid tropical costa rica ». In : *Journal of Tropical Forest Science* 19.2, p. 92–102.

[69] Aguiar et al. (2016). Cf. note 66 ; Tritsch et al. (2016). « Multiple patterns of forest disturbance and logging shape forest landscapes in Paragominas, Brazil », cf. note 64, p. 154.

[70] D. Rappaport et al. (2018a). « Quantifying long-term changes in carbon stocks and forest structure from Amazon forest degradation ». In : *Environmental Research Letters*.

[71] Poorter et al. (2016). « Biomass resilience of Neotropical secondary forests », cf. note 1, p. 161.

[72] cf. article en annexe : «Slow rate of secondary forest carbon accumulation in the Guianas compared with the rest of the Neotropics»

a aussi un impact significatif sur le taux de récupération[73]. Dans de nombreux cas une restauration active peut être nécessaire[74], au moins dans la première décennie de reforestation, afin d'assurer le retour à un écosystème forestier.

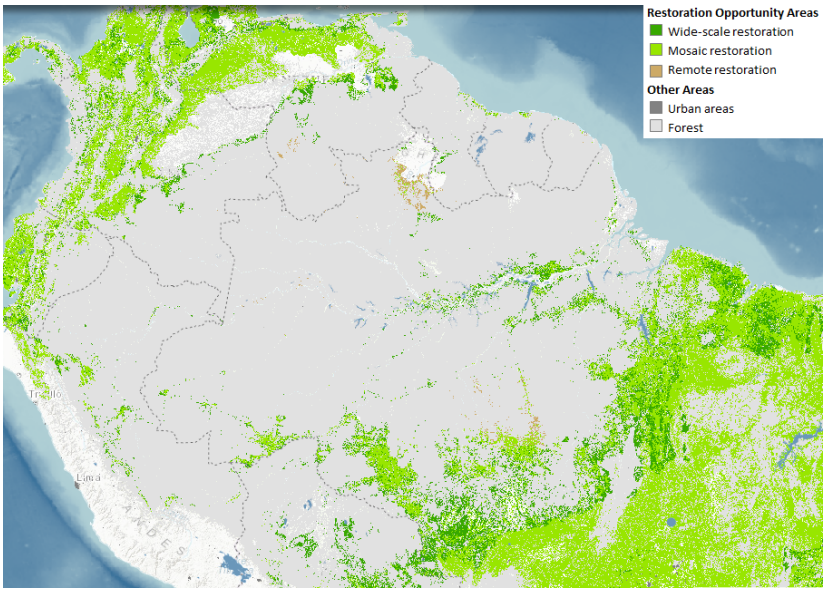

FIGURE 9.2 – Zones avec un fort potentiel pour la restauration. In World Resources Institute, 2018[a].

[a]WRI (2018). *Atlas of Forest Landscape Restoration Opportunities.*

Opportunités pour la restauration

Face à la perte continue de forêts, principalement sous les tropiques[75], l'intérêt de la communauté internationale pour la restauration de zones déforestées ou dégradées a connu un succès grandissant, qui s'est concrétisé en 2011 par le challenge de Bonn lancé par l'IUCN et l'engagement de 47 pays à restaurer 150 millions d'hectares de forêts d'ici 2020 et 350 millions d'hectares d'ici 2030[76] (Figure 9.3). Par exemple, le Brésil s'est engagé à restaurer 12 millions d'hectares d'ici 2030 et le Pérou 3,2 millions d'hectares d'ici 2020[77] . Ces initiatives peuvent être un moyen d'apporter un soutien technique et financier pour la restauration de forêts secondaires et dégradées en Amazonie.

Dans de nombreux cas, la restauration nécessite des investissements financiers importants : pour compenser les coûts d'opportunité dans les zones productives, protéger la zone et éviter les feux, ou planter des arbres et éviter la compétition avec les graminées[78]. Or les objectifs des engagments du Bonn Challenge sont ambitieux, et les fonds alloués limités : des aires prioritaires devront donc être définies[79]. La production de bois, ainsi que d'autres produits non-ligneux, peut aussi être une source de revenus et permettre de financer la restauration des forêts[80]. Par exemple, la production de bois en marge des forêts replantées a permis de financer la restauration de grandes surfaces déforestées à Bahia, au Brésil[81]. Allier restauration et production de bois pourrait donc être une

[73]R. L. CHAZDON et al. (2003). « Community and phylogenetic structure of reproductive traits of woody species in wet tropical forests ». In : *Ecological Monographs* 73.3, p. 331–348.

[74]P. MELI et al. (2017). « A global review of past land use, climate, and active vs. passive restoration effects on forest recovery ». In : *PLoS ONE* 12.2, p. 1–17.

[75]X.-P. SONG et al. (2018b). « Global land change from 1982 to 2016 ». In : *Nature* 560.7720, p. 639–643.

[76]B. CHALLENGE (2011). *The Challenge : a global effort.*

[77]Ibid.

[78]R. BENINI et al. (2016). *Manual De Restauração Da Vegetação Nativa.* Rapp. tech. The Nature Conservancy.

[79]M. VERDONE et A. SEIDL (2017). « Time, space, place, and the Bonn Challenge global forest restoration target ». In : *Restoration Ecology* 25.6, p. 903–911.

[80]LAMB et al. (2005). « Restoration of Degraded Tropical Forest Landscapes », cf. note 58, p. 115.

[81]C. C. SILVA (2018). « Impacto ecológico e silvicultural do uso e colheita de eucalipto consorciado com espécies arbóreas nativas para a restauração da Mata Atlântica ». Thèse de doct. Piracicaba : Universidade de São Paulo.

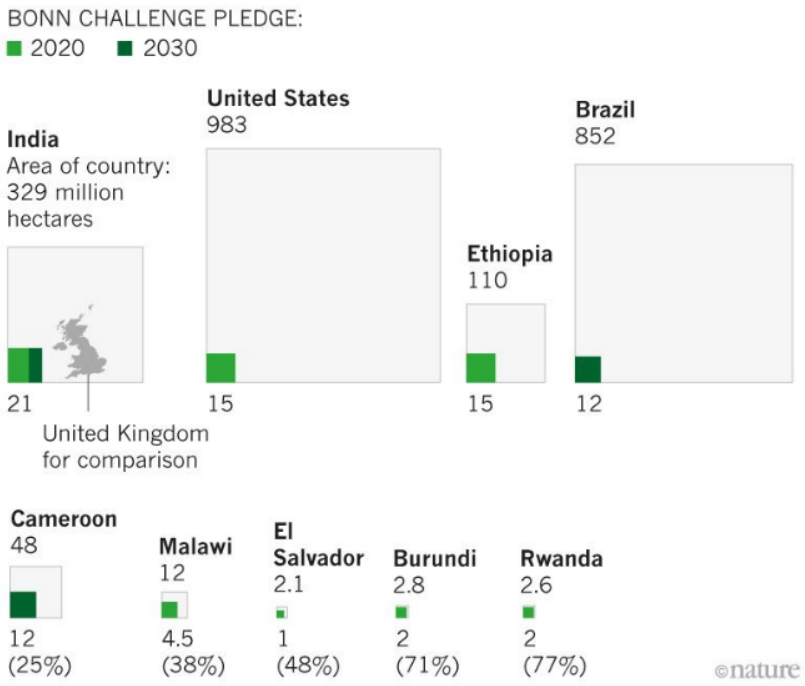

FIGURE 9.3 – Principaux engagements nationaux pour la restauration après le Bonn challenge. In Cernansky, 2018[a].

[a]R. CERNANSKY (2018). « How to plant a trillion trees ». In : *Nature* 560.7720, p. 542–544.

stratégie intéressante pour fournir la demande en bois et financer la restauration.

Cette alliance entre production de bois et restauration reste sujette à des débats sur la définition même de la restauration. Si l'un des principaux buts de la restauration est la production de bois, des espèces commercialisables seront plantées et leur croissance pourra être assistée, par exemple par des éclaircies. Des arbres seront ensuite extraits régulièrement de la forêt pour la production de bois. Les forêts ainsi restaurées ne ressembleront probablement pas aux forêts originellement présentes. Ce type de restauration est compatible avec la définition proposée par le manuel de restauration de l'IUCN (*Forest Lanscape Restoration handbook*)[82] : «un processus visant à retrouver une intégrité écologique et améliorer le bien-être humain dans des zones déforestées ou dégradées ». Cette définition, plutôt pragmatique et anthropo-centrée, insiste plus sur la notion de bien-être (donc de service écosystémique) mais reste très vague quant aux caractéristiques finales de l'écosystème restauré. À l'inverse, dans la littérature scientifique on retrouve plus souvent une vision plus stricte de la restauration, telle que définie par la *Society for Ecological Restoration* : «Le processus d'assistance à la récupération d'un écosystème qui a été dégradé, endommagé ou détruit ». Dans ce cas, la restauration vise à retrouver des écosystèmes aussi proches que possible des écosystèmes d'origine.

[82]I. ITTO (2007). *The Forest Landscape Restoration Handbook*.

Perspectives pour le futur

Les défis sont aujourd'hui nombreux pour atteindre les objectifs de restauration fixés pour les pays du bassin amazonien :

- former et développer sur place les compétences nécessaires à la mise en place des projets de restauration[83],
- développer des pépinières et rendre les plantules facilement accessibles[84],
- développer des connaissances techniques (itinéraires techniques, associations d'espèces adaptées aux conditions environnementales) spécifiques à la région amazonienne.

Le manque d'études et de cas concrets de plantations ou forêts secondaires restaurées en Amazonie rend difficile l'évaluation du potentiel de production de bois hors forêts naturelles[85]. Alors que les monocultures d'espèces exotiques (eucalyptus, pin), principalement pour la pâte à papier, sont bien développées dans le sud du Brésil, les études sur des espèces natives en plantations mixtes pour du bois d'œuvre sont quasiment inexistantes dans la région. Ce type de plantation a pourtant un grand potentiel pour la restauration comme pour la production de bois. En effet, de nombreuses d'espèces locales, naturellement présentes dans les forêts amazoniennes, ont un bois prisé et un taux de croissance rapide. C'est le cas par exemple de l'acajou (*Swietenia macrophylla*) déjà mentionné, ou de *Jacaranda copaia*. Pourtant, les rares tentatives de monoculture ont été un échec, car elles ont été les proies d'herbivores tels que *Hypsipyla grandella* qui ont décimé les jeunes arbres plantés[86]. Développer des plantations mixtes, outre les bénéfices en terme de productivité déjà observés dans les plantations multispécifiques[87], pourrait aider à combattre l'effet des prédateurs par effet de dilution (diminution de la densité de chaque espèce), et répartir les risques liés aux changements climatiques[88]. Il est donc urgent de développer ce type de recherche afin d'accompagner les projets de restauration avec un bagage technique et scientifique suffisant.

Pour pouvoir développer une politique cohérente, tant en termes de gestion forestière que de restauration, il est nécessaire de coordonner les actions à l'échelle la plus pertinente, celle du biome amazonien. En effet, même si des mesures ambitieuses sont prises dans l'un des pays concernés, elles pourront entraîner des mécanismes de fuite qui diminueraient leur efficacité, tels que ceux observés au Viêtnam après sa transition forestière[89]. Or, peu d'accords transnationaux existent aujourd'hui autour de la gestion des forêts amazoniennes : la transition forestière en Amazonie, si elle a lieu, devra se faire avec le développement d'une politique transamazonienne.

[83] Sabogal et al. (2006). *Silvicultura na Amazonônia brasileira : avaliação de experiências e recomendações para implementação e melhoria dos sistemas*, cf. note 65, p. 171.

[84] D. L. Haase et A. S. Davis (2017). « Developing and supporting quality nursery facilities and staff are necessary to meet global forest and landscape restoration needs ». In : *Reforesta* 2017.4, p. 69–93.

[85] Sabogal et al. (2006). *Silvicultura na Amazonônia brasileira : avaliação de experiências e recomendações para implementação e melhoria dos sistemas*, cf. note 65, p. 171.

[86] Costa et al. (2013). « Cultivo e Manejo do Mogno (Swietenia macrophylla King) », cf. note 65, p. 171.

[87] D. Piotto (2008). « A meta-analysis comparing tree growth in monocultures and mixed plantations ». In : *Forest Ecology and Management* 255.3-4, p. 781–786.

[88] M. R. Guariguata et al. (2008). « Mitigation needs adaptation : Tropical forestry and climate change ». In : *Mitigation and Adaptation Strategies for Global Change* 13.8, p. 793–808.

[89] Meyfroidt et Lambin (2009). « Forest transition in Vietnam and displacement of deforestation abroad », cf. note 52, p. 115.

9.3 Qu'entend-on par exploitation durable ?

9.3.1 Maintenir les services écosystémiques...

Des modifications profondes dans les forêts exploitées

Le paradigme de l'exploitation durable (*Sustainable Forest Management* en anglais), promue par des organismes tels que l'Organisation Internationale des Bois Tropicaux (OIBT ou ITTO en anglais), voudrait que la gestion des forêts tropicales permette d'éviter «la réduction de leur valeur intrinsèque et productivité future»[90]. Or, de nombreuses études montrent que ces objectifs sont hautement optimistes et rarement atteints[91]. Nos résultats convergent avec les conclusions de ces articles : bien que les stocks de carbone puissent être récupérés à la fin d'un cycle d'exploitation moyen de 30 ans[92], la structure et la composition des forêts exploitées mettent quant à elles beaucoup plus de temps à retrouver des valeurs similaires à l'état pré-exploitation[93]. Cela explique pourquoi les volumes de bois, même sous des hypothèses plutôt optimistes, ne sont pas récupérés au bout de 30 ans[94].

L'exploitation sélective, bien qu'elle n'entraîne qu'une perte partielle et transitoire du couvert forestier, modifie cependant le régime de perturbations en imposant des perturbations plus intenses et plus fréquentes que les perturbations naturelles par chablis. Comparées à d'autres biomes tropicaux, les forêts amazoniennes semblent peu résilientes aux perturbations : les taux historiques de récupération sont relativement faibles[95]. Il semble donc difficile de maintenir les caractéristiques des forêts anciennes, qui ont évolué pendant des centaines d'années, en laissant une régénération passive entre des cycles d'exploitation de quelques dizaines d'années seulement.

Exploiter la forêt tout en récupérant les caractéristiques pré-exploitation à la fin de chaque rotation est donc irréaliste, et ressemble plus au mythe de Sisyphe : à peine a-t-on atteint le but désiré que la forêt est à nouveau exploitée. Peut-être faut-il abandonner l'idée de maintenir les forêts exploitées dans un état proche des forêts naturelles. Cette idée semble encore aujourd'hui difficile à accepter par tous[96]. En effet, les organismes de certification jouent aujourd'hui sur l'image d'une exploitation alliant production et conservation (exemple en Figure 9.1).

Assurer le maintien d'un niveau de base

Le premier critère à remplir pour pouvoir parler d'exploitation durable est d'assurer une provision de bois sur le long terme. Pour cela, il faut que la quantité de bois récupérée soit au moins égale à la quantité perdue lors de l'exploitation ; il en va de même pour les stocks de carbone. Si cet équilibre des flux entrants et

[90] ITTO (1992). *Criteria for the measurement of sustainable forest management*, cf. note 90, p. 10.

[91] Zimmerman et Kormos (2012). « Prospects for Sustainable Logging in Tropical Forests », cf. note 102, p. 11 ; Putz et al. (2012). « Sustaining conservation values in selectively logged tropical forests : the attained and the attainable », cf. note 102, p. 11.

[92] Rutishauser et al. (2015). « Rapid tree carbon stock recovery in managed Amazonian forests », cf. note 166, p. 20 ; Piponiot et al. (2016b). « Carbon recovery dynamics following disturbance by selective logging in Amazonian forests », cf. note 5, p. 50.

[93] P. A. Martin et al. (2013). « Carbon pools recover more quickly than plant biodiversity in tropical secondary forests ». In : *Proceedings of the Royal Society B : Biological Sciences* 280.1773, p. 20132236–20132236 ; D. Rappaport et al. (2018b). « Quantifying long-term changes in carbon stocks and forest structure from Amazon forest degradation ». In : *Environmental Research Letters*.

[94] Piponiot et al. (2018). « Assessing timber volume recovery after disturbance in tropical forests – A new modelling framework », cf. note 15, p. 109.

[95] L. E. S. Cole et al. (2014). « Recovery and resilience of tropical forests after disturbance ». In : *Nature Communications* 5.May, p. 1–7.

[96] Putz et Romero (2014). « Futures of tropical forests (sensu lato) », cf. note 110, p. 12.

sortants n'est jamais atteint, la ressource en bois va progressivement diminuer jusqu'à disparaître. Cet équilibre peut être atteint après quelques cycles d'exploitation, pour des stocks de volume inférieurs aux stocks initiaux. En effet, parce que l'exploitation modifie la structure des forêts en éliminant les plus gros individus, elle les rapproche des forêts plus jeunes et plus dynamiques[97]. De telles forêts, très anthropisées, peuvent être productives et avoir des caractéristiques (structure, stock de carbone) qui restent stables au fil des cycles d'exploitation : c'est déjà le cas dans certaines forêts exploitées d'Asie[98]. Ces prédictions restent à vérifier en Amazonie, car il existe peu d'expériences de multiples cycles d'exploitations dans la région. De plus, au cours de cette thèse ont été principalement abordés les stocks de carbone et de bois, mais le maintien d'autres services, tels que la diversité (spécifique ou fonctionnelle), sont plus complexes à évaluer et méritent d'être plus profondément étudiés.

[97] cf. Chapitre 6

[98] P. Sist et al. (2003). « Sustainable cutting cycle and yields in a lowland mixed dipterocarp forest of Borneo ». In : *Annals of Forest Science* 60.8, p. 803–814. arXiv : 0503174 [physics] ; T. C. Khai et al. (2016). « Stand structure, composition and illegal logging in selectively logged production forests of Myanmar : Comparison of two compartments subject to different cutting frequency ». In : *Global Ecology and Conservation* 7, p. 132–140.

D'un point de vue pratique, une possibilité pour assurer le maintien d'un niveau stable de services écosystémiques serait de définir un niveau minimum de récupération (en termes de volume de bois, carbone, diversité) à partir duquel un massif forestier peut être réexploité. Dans ce cas, les cycles d'exploitation n'auraient pas une durée constante, mais dépendraient directement de la résilience des forêts exploitées. Des inventaires forestiers sont donc nécessaires pour suivre l'évolution du volume commercial, et déterminer le moment du deuxième cycle d'exploitation. Avec l'augmentation de la précision des données de télédétection, il est aujourd'hui de plus en plus facile et de moins en moins coûteux de mesurer d'autres caractéristiques (stocks de carbone[99], diversité des arbres de canopée[100]) sur de grandes surfaces.

[99] Avitabile et al. (2016). « An integrated pan-tropical biomass map using multiple reference datasets », cf. note 5, p. 1.

[100] G. P. Asner et al. (2017). « Airborne laser-guided imaging spectroscopy to map forest trait diversity and guide conservation ». In : *Science (New York, N.Y.)* 355.6323, p. 385–389.

9.3.2 Ou maintenir les écosystèmes qui les fournissent ?

Variabilité temporelle de la valeur accordée aux écosystèmes

Définir la gestion des forêts à long terme pour le maintien de certains services écosystémiques est cependant risqué. En effet, des avancées technologiques majeures pourront peut-être un jour permettre de trouver une alternative au bois d'œuvre de haute qualité issu des forêts naturelles[101], ou bien du bois d'œuvre sera produit à coût réduit en plantation. À l'inverse, d'autres besoins pourraient apparaître qui sont aujourd'hui difficile à prédire. Gérer les forêts pour optimiser le maintien à long terme de services qui aujourd'hui trouvent un intérêt pourrait ne pas être optimal du point de vue des gestionnaires de demain.

[101] J. Song et al. (2018a). « Processing bulk natural wood into a high-performance structural material ». In : *Nature* 554.7691, p. 224–228.

La priorité n'est donc pas la durabilité des services écosystémiques *per se*, mais le maintien du fonctionnement des écosystèmes qui les assurent. Mais le problème n'est pas résolu pour autant :

encore faut-il savoir comment définir si un écosystème a changé d'état ou non, et dans quelles limites les écosystèmes peuvent se maintenir malgré les perturbations.

Perte de résilience et points de basculement

Pour maintenir les écosystèmes et les fonctions clé dont ils dépendent, il faut déjà pouvoir définir à partir de quand on considère que l'écosystème a changé. Pour cela, la notion de résilience définie dans le chapitre 1, est centrale. En effet, tant que l'écosystème est capable de revenir à l'état de référence (par exemple une forêt ancienne), on peut encore considérer que l'on est face au même type d'écosystème. Par contre, lorsque les mécanismes permettant la résilience sont compromis, l'écosystème peut basculer dans un autre état stable aux propriétés complètement différentes, et ne plus pouvoir revenir à son état précédent.

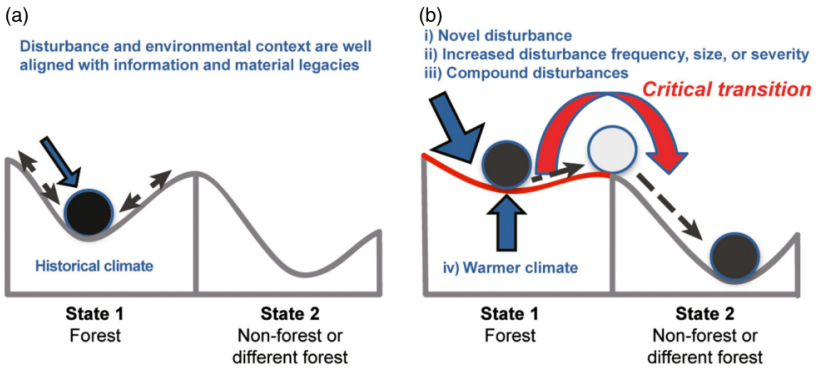

FIGURE 9.4 – Schéma de la perte progressive de résilience d'un système (boule) après modification du régime de perturbations. In Johnstone *et al.*, 2016[a].

[a] J. F. JOHNSTONE et al. (2016). « Changing disturbance regimes, ecological memory, and forest resilience ». In : *Frontiers in Ecology and the Environment* 14.7, p. 369–378. arXiv : arXiv:1011.1669v3.

Ce basculement a souvent été représenté par l'analogie avec une boule (l'écosystème) sur un plan présentant plusieurs creux (Figure 9.4), chaque creux correspondant à un état stable du système agissant comme un point d'attraction. Dans cette représentation, la résilience du système dans un état donné dépend de la profondeur du creux. Les modifications des conditions environnementales (climat, érosion du sol) peuvent diminuer cette résilience (Figure 9.4). Un nouveau régime de perturbation, s'il est suffisamment intense, peut amener le système à passer dans un autre état stable, qui ne lui permet plus de revenir seul à l'état de départ. Cela peut être le cas de l'exploitation sélective lorsque les cycles de rotation sont trop rapprochés ou l'intensité d'exploitation trop forte pour permettre la récupération de la forêt. Lorsque les mécanismes de résilience sont ainsi enrayés, on parle de forêt dégradée[102].

Les forêts amazoniennes sont de plus en plus dégradées sous l'effet des perturbations humaines[103]. En effet, bien que les forêts aient la capacité de se régénérer après des perturbations, la modification de la fréquence et de l'ampleur des perturbations anthropiques ne connaît pas de précédent historique et risque de compromettre leur résilience. La crise actuelle de la biodiversité

[102] J. GHAZOUL et al. (2015). « Conceptualizing Forest Degradation ». In : *Trends in Ecology and Evolution* 30.10, p. 622–632.

[103] FOLEY et al. (2007). « Amazonia revealed : forest Degradation and Loss of Ecosystem Goods and Services in the Amazon Basin », cf. note 8, p. 109.

présente aussi un risque[104]. En forêt amazonienne, cette érosion de la diversité est liée en particulier à la perte des habitats naturels et leur fragmentation par la déforestation[105], et des effets additionnels de sur-exploitation des ressources : sur-exploitation de certaines essences commerciales, chasse, etc. Dans le cas de la chasse, l'apparition de forêts vides (*empty forests* en anglais) à proximité des activités humaines a significativement diminué la dispersion des espèces végétales, et par conséquent leur diversité[106] et leur biomasse[107]. Un autre effet particulièrement redouté des activités humaines est la modification du régime de précipitations, dû à la fois à la déforestation qui réduit l'évapotranspiration et aux changements climatiques globaux. Ce changement des précipitations risque de faire passer une partie des forêts amazoniennes vers des états proches des savanes[108].

[104] T. H. Oliver et al. (2015a). « Declining resilience of ecosystem functions under biodiversity loss ». In : *Nature Communications* 6, p. 10122.

[105] Haddad et al. (2015). « Habitat fragmentation and its lasting impact on Earth's ecosystems », cf. note 54, p. 6.

[106] R. Bagchi et al. (2018). « Defaunation increases the spatial clustering of lowland Western Amazonian tree communities ». In : *Journal of Ecology* 106.4, p. 1470–1482. arXiv : 0608246v3 [arXiv:physics].

[107] Peres et al. (2016). « Dispersal limitation induces long-term biomass collapse in overhunted Amazonian forests », cf. note 67, p. 7.

[108] G. F. Pires et M. H. Costa (2013). « Deforestation causes different subregional effects on the Amazon bioclimatic equilibrium ». In : *Geophysical Research Letters* 40.14, p. 3618–3623.

Définir un espace de fonctionnement sécurisé

Cette dégradation progressive de la résilience des écosystèmes, et leur possible basculement vers d'autres états, pose la question des limites critiques du maintien des écosystèmes. Cette notion d'«espace de fonctionnement sécurisé»(*safe operating space*[109] en anglais) a de nombreuses implications pratiques pour la gestion des écosystèmes. Elle permet de définir des limites d'utilisation des écosystèmes, mais aussi les efforts à apporter pour rétablir les conditions nécessaires à leur maintien.

Dans le cas de l'exploitation forestière, il serait intéressant d'étudier quelles limites de prélèvement mettent en péril la stabilité de l'écosystème forestier, afin de définir un espace de prélèvement sécurisé de l'exploitation. Une possibilité serait de l'étudier avec un modèle dynamique défini à l'échelle du paysage, similaire à celui développé par Staver et al.[110]. Le but est de décrire les phases de transitions entre les écosystèmes forêt, savane et sans arbres (herbes), qui ont été décrits comme trois équilibres stables sous les tropiques[111], et estimer à partir de quelle intensité de prélèvement l'exploitation peut faire passer d'un écosystème forêt à savane (ou sans arbre).

La proposition est la suivante : dans un espace fini (nombre total d'unités du paysage N fixe), on définit 4 classes de végétation qui occupent l'intégralité de l'espace (bien que le modèle ne soit pas spatialement explicite). Les quatre classes sont : l'herbe (la végétation par défaut), la forêt mature, la forêt secondarisée[112], et la savane. D'un pas de temps à l'autre une partie des unités du paysage peuvent passer d'une classe de végétation à l'autre (Figuire 9.5). Les paramètres gouvernant la proportion de transitions d'une classe à l'autre dépendent du climat et des activités humaines (intensité de la déforestation et de l'exploitation).

Le modèle tel que pensé par Staver et al. est déterministe, mais il est aussi possible de décrire la distribution des classes de

[109] J. Rockström et al. (2009). « A safe operating space for humanity ». In : *Nature* 461.7263, p. 472–475. arXiv : 461472a [10.1038].

[110] A. C. Staver et al. (2011). « Tree cover in sub-Saharan Africa : Rainfall and fire constrain forest and savanna as alternative stable states ». In : *Ecology* 92.5, p. 1063–1072.

[111] Hirota et al. (2011). « Global Resilience of Tropical Forest and Savanna to Critical Transitions », cf. note 132, p. 16.

[112] ici cela comprend les forêts dégradées et les forêts secondaires

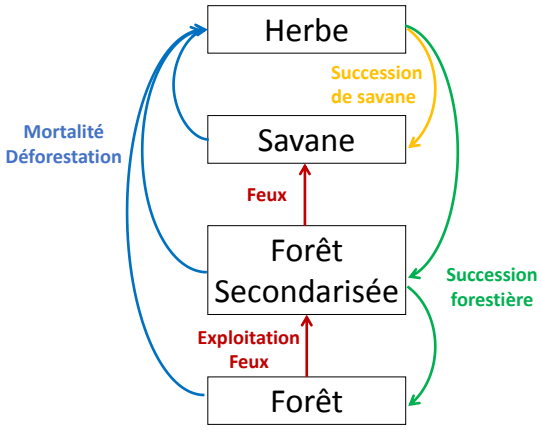

FIGURE 9.5 – Illustration de la transition entre différents types de végétation.

végétation à chaque moment t selon une loi multinomiale dont le vecteur de probabilité dépend de la distribution à $t-1$ et des paramètres de transition.

On peut aussi imaginer des interactions entre les différentes classes de végétation, agissant sur la transition d'une classe à l'autre :

- une plus grande proportion de savane et d'herbe pourrait favoriser les feux et donc le passage des forêts primaires vers des forêts secondaires et des savanes ;
- une grande proportion de forêt accélérerait la succession forestière (herbe vers forêt secondaire vers forêt) grâce par exemple à des mécanismes de dispersion de graines.
- une grande proportion d'herbe et de savane faciliterait l'accès aux forêts et donc augmenterait les taux de déforestation et d'exploitation.

Une fois la structure du modèle décrite, les paramètres de transition pourraient être calibrés grâce à des séries d'images satellite où la végétation a été classifiée.

La deuxième étape serait la simulation de différents scénarios d'exploitation pour voir jusqu'où le couvert forestier peut être maintenu, et quand apparaissent des transitions vers d'autres classes de végétation (exemple en Figure 9.6). Pour cela, l'Amazonie peut être divisée en un nombre raisonnable de pixels (selon la capacité de calcul) au sein desquels les conditions climatiques peuvent être considérées homogènes à un instant donné. Pour chaque pixel l'évolution de la proportion des classes de végétation est simulée en fonction des modalités d'exploitation, qui influent sur la valeur de la transition forêt vers forêt secondarisée. On s'attend à un basculement vers une végétation dominée par la savane, qui signalerait alors les limites de la résilience des forêts à l'exploitation. L'effet des futurs scénarios climatiques pourrait être pris en compte si les paramètres de transition sont écrits en fonction des conditions climatiques.

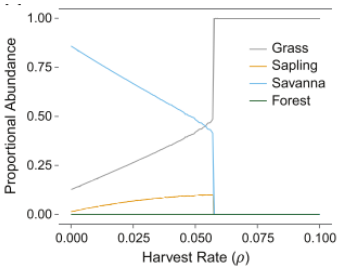

FIGURE 9.6 – Illustration du basculement d'une végétation dominante à l'autre en fonction de l'intensité de l'exploitation. In Tredennick et al., 2015.

9.4 Que peut apporter la recherche à la gestion des écosystèmes ?

Depuis l'ère industrielle, l'humanité a modifié la biosphère et l'ensemble des écosystèmes dont elle dépend avec une ampleur qui ne connaît pas de précédent : c'est la raison pour laquelle cette nouvelle ère est aujourd'hui appelée l'Anthropocène[113]. La perte continue des écosystèmes et de la diversité qu'ils abritent est l'un des principaux problèmes auquel doivent faire face les sociétés humaines actuelles, et ce problème ne deviendra que plus prégnant dans les décennies à venir. La gestion des écosystèmes est donc devenue un enjeu majeur, pour lequel les décisions devraient être informées par l'ensemble des connaissances existantes. Or les gestionnaires et décideurs politiques ont en général un agenda bien rempli et de nombreux dossiers à traiter simultanément : leur temps passé à analyser l'information disponible avant de prendre une décision est limité. Le rôle du chercheur est donc de trouver l'information existante ou de créer les données nécessaires (par du travail de terrain, des expérimentations) afin de retransmettre une vision aussi complète que possible du problème et permettre une prise de décision informée. Ce rôle à l'interface entre l'information et la décision est complexe, car il demande un certain degré d'implication dans la vie politique qui ne fait pas partie de la vision classique de la recherche.

[113] P. J. Crutzen (2002). « Geology of mankind ». In : *Nature* 415.6867, p. 23.

9.4.1 Avoir un message clair dans un monde incertain

L'une des difficultés majeures pour travailler à l'interface entre le réel et les prises de décisions est le décalage entre le grand niveau d'incertitude des informations obtenues lors du processus de recherche, et le besoin de conclusions claires et concises pour prendre des décisions.

Des données limitées

La recherche en générale, et l'écologie en particulier, sont confrontées à la contradiction suivante : elles visent à étudier des systèmes réels, infiniment complexes, à partir de données par nature limitées.

L'une des principales limites pour la gestion des écosystèmes est la très faible quantité de données disponibles par rapport à l'étendue des écosystèmes à étudier, et les périodes de temps sur lesquelles ces écosystèmes évoluent. Par exemple, en Amazonie, la représentativité des données d'inventaires forestiers est extrêmement faible, et il y a des régions entières pour lesquelles il n'existe quasiment aucune donnée d'inventaire[114]. La vision actuelle des forêts naturelles en Amazonie se base donc sur une infime fraction de ces forêts. De plus, une bonne moitié des parcelles d'inventaire

[114] K. Feeley (2015). « Are we filling the data void ? An assessment of the amount and extent of plant collection records and census data available for tropical South America ». In : *PLoS ONE* 10.4.

n'a été mesurée qu'une seule fois[115] et les suivis de dynamiques forestières se basent sur une part plus petite encore de ces forêts.

Bien sûr les moyens, financiers et humains, sont souvent limitant pour l'acquisition de données. Un autre problème, qui est particulièrement limitant pour l'acquisition de données sur le long terme, est le besoin de la recherche de s'adapter aux fluctuations de l'agenda politique pour obtenir des financements. Une conséquence est qu'il est souvent plus facile de trouver des financements pour l'acquisition de données totalement nouvelles que pour la consolidation de suivis déjà en place[116]. C'est par exemple le cas d'une des institutions du réseau TmFO, l'IBIF [117] en Bolivie, qui a des parcelles exploitées suivies pendant plus de 10 ans, mais qui depuis 6 ans ne peut plus trouver de financement pour refaire des campagnes de terrain.

En plus de l'investissement pour acquérir les données, il faut ensuite les conserver et les valoriser afin qu'elles puissent être utilisées. Beaucoup de données ainsi acquises sont perdues, inutilisables ou inaccessibles. Ainsi les services forestiers brésiliens et boliviens, qui demandent aux concessionnaires une grande quantité de données (inventaires, plan détaillé de l'exploitation), possèdent une mine d'informations, mais celles-ci sont dans la plupart des cas soit quasi inaccessibles à cause de la difficulté pour les obtenir auprès de l'administration, soit illisibles car les bases de données n'ont jamais été nettoyées[118].

La difficulté d'accès à certains types de données peut aussi créer des biais dans l'échantillonnage. Par exemple, la distribution des parcelles de suivi forestier en Amazonie s'est faite dans les zones les plus accessibles, notamment par les fleuves, pour des raisons logistiques évidentes. Cela a pu créer un biais en sélectionnant principalement des parcelles d'ancienne occupation amérindienne. De même, les parcelles de suivi de forêts exploitées, comme dans le cas de TmFO, ont été faites dans la plupart des cas en partenariat avec des entreprises d'exploitation. Elles sont donc représentatives de l'exploitation industrielle, suivant le cadre légal et souvent avec des techniques d'exploitation à faible impact, et ne permettent pas d'étudier l'impact de l'exploitation illégale non contrôlée.

De la transparence dans les étapes de modélisation

La prise de décisions se base sur des prédictions faites à partir des données limitées. Ces prédictions sont donc dans la grande majorité faites en dehors de l'intervalle de calibration (dans le temps et dans l'espace). Cette extrapolation demande donc de faire des hypothèses simplificatrices lourdes et souvent difficiles à vérifier : la linéarité de la relation entre deux variables ou l'indépendance de deux variables entre elles[119]. De plus, lorsqu'on travaille sur des échelles de temps de plusieurs décennies, ce qui est souvent le cas pour la gestion des écosystèmes, les conditions

[115] Lopez-Gonzalez et al. (2009). *ForestPlots.net Database*, cf. note 76, p. 117.

[116] D. Lamb (2017). « Long-term ecological monitoring and institutional memories ». In : *Ecological Management and Restoration* 18.3, p. 200–204.

[117] Instituto Boliviano de Investigación Forestal

[118] Fredericksen et al. (2003). « Sustainable forestry in Bolivia - Beyond planning logging », cf. note 93, p. 10.

[119] J. R. Miller et al. (2004). « Spatial Extrapolation : The Science of Predicting Ecological Patterns and Processes ». In : *BioScience* 54.4, p. 310.

environnementales peuvent changer, ce qui rend les prédictions encore plus incertaines. La construction des modèles doit donc favoriser la robustesse des prédictions (*i.e.* leur validité en dehors de l'intervalle de calibration) quitte à sacrifier leur précision, qui serait de toutes façons illusoire vu le décalage entre l'incertitude liée aux données et la précision des résultats affichés. Le plus difficile est de trouver un équilibre entre un modèle trop simpliste et qui ne permettrait donc pas d'apporter beaucoup d'information pertinente sur le phénomène étudié, et un modèle trop complexe qui serait à la fois opaque (modèle «black box») et dépendant des particularités des données utilisées[120].

[120] V. Grimm (2005). « Pattern-Oriented Modeling of Agent-Based Complex Systems : Lessons from Ecology ». In : *Science* 310.5750, p. 987–991. arXiv : arXiv:1011.1669v3.

Les hypothèses faites sont des choix subjectifs, et donc par conséquent tout résultat de recherche est subjectif, conditionnel à des hypothèses sous-jacentes et plus ou moins explicites. Pour que les résultats soient interprétés correctement, il est donc indispensable d'être entièrement transparent sur les hypothèses faites lors des étapes de modélisation, car les résultats ne peuvent être interprétés que sous la lumière de ces hypothèses. Enfin, les niveaux d'incertitudes sur les prédictions faites doivent être rapportés, après avoir intégré l'ensemble des sources d'incertitudes des données.

La transparence par rapport aux incertitudes des résultats est sûrement l'une des étapes les plus complexes. En effet, un message simple et claire facilite la compréhension et a donc plus de chances d'être entendu. Mais pour pouvoir être compris dans son intégralité et avec exactitude, le message scientifique doit être aussi complet que possible, en particulier sur les zones de doutes qu'il comporte. Il serait dangereux pour les décideurs de construire la gestion des écosystèmes en fonction d'un unique résultat, sans capacité d'adaptation à des comportements différents de l'écosystème. Par exemple, l'application de temps de rotation fixes pour l'exploitation sélective s'est basée sur des résultats établis localement, sans prendre en compte l'incertitude sur ces résultats ni leur variabilité spatiale. Bien qu'aujourd'hui, de nombreuses études montrent que ces cycles ne sont pas suffisants pour récupérer la ressource en bois, les législations manquent de flexibilité et ne permettent pas l'adaptation de la gestion à ce nouveau type d'information.

Une façon de transmettre l'idée de l'incertitude sur les prédictions de la recherche est la construction de plusieurs scénarios possibles pour le futur[121]. Ces scénarios peuvent dans l'idéal être construits avec l'ensemble des acteurs impliqués dans la gestion des écosystèmes. Ainsi, la gamme de prédictions peut donner une idée de la sensibilité des résultats aux hypothèses faites dans le modèle.

[121] G. D. Peterson et al. (2003). « Scenario Planning : a Tool for Conservation in an Uncertain World ». In : *Conservation Biology* 17.2, p. 358–366. arXiv : arXiv:1011.1669v3.

Quelle gestion dans un monde incertain ?

Les changements qui affecteront les écosystèmes dans le futur proche sont hautement incertains, et en termes de prédictions la recherche peut au mieux donner des tendances globales. Comment la gestion, qui a besoin de prendre des décisions concrètes, peut-elle s'adapter à ce manque de certitude ?

Parce que les connaissances sont incertaines et susceptibles de changer, la gestion doit être flexible : en apportant des changements progressifs et, dans la mesure du possible, réversibles, et en évaluant en continu l'impact de ces changements. Cela demande une recherche qui soit, comme vu précédemment, en interaction continuelle avec les acteurs de la gestion. En termes de modélisation, une telle recherche requiert des modèles capables d'intégrer de nouvelles données et à s'adapter aux connaissances nouvellement acquises. En fonction de ces nouvelles informations, la gestion pourra être réévaluée et modifiée si besoin.

Face changements majeurs qui sont prévus dans le futur (et en particulier les changements climatiques), plusieurs stratégies peuvent être développées. Les stratégies à court terme, majoritaires aujourd'hui dans la gestion forestière, favorisent la résistance des écosystèmes à ces changements : par exemple le contrôle des feux de forêt. Ces stratégies ne sont pas viables sur le long terme, car les changements sont inévitables. Il faut donc penser des stratégies complémentaires qui permettront aux écosystèmes de s'adapter aux nouvelles conditions : dans l'exemple des feux de forêt cela peut se traduire par la plantation d'espèces plus résistantes au feu[122]. Jouer sur plusieurs stratégies à la fois, et favoriser la diversité (par exemple en plantant un grand nombre d'espèces), permet de réduire les risques.

Longtemps, la gestion des écosystèmes a cherché à réduire la variabilité de leur fonctionnement pour faciliter leur gestion et assurer une provision continue de services écosystémiques[123]. Le paradigme a aujourd'hui changé et l'importance de cette variabilité dans les mécanismes de résilience et d'adaptation des écosystèmes est de plus en plus reconnue. Alors que les trajectoires possibles des écosystèmes dans le futur sont innombrables, il est important de maintenir les capacités d'adaptation à l'ensemble de ces changements. Cette capacité d'adaptation passe par la diversité des organismes vivants (notamment les diversités génétiques et fonctionnelles), mais aussi la diversité des milieux et des conditions environnementales pour maintenir cette diversité d'organismes[124]. Des stratégies de gestion maintenant une hétérogénéité des paysages et une diversité des organismes, et encourageant des prélèvements des ressources variables dans le temps et l'espace, permettraient d'augmenter la résilience des écosystèmes[125].

[122] C. I. Millar et al. (2007). « Climate change and forest of the future : Managing in the face of uncertanity ». In : *Ecological Applications* 17.8, p. 2145–2151.

[123] S. R. Carpenter et al. (2015). « Allowing variance may enlarge the safe operating space for exploited ecosystems ». In : *Proceedings of the National Academy of Sciences* 112.46, p. 14384–14389.

[124] T. H. Oliver et al. (2015b). « Biodiversity and Resilience of Ecosystem Functions ». In : *Trends in ecology & evolution* 30.11, p. 673–684.

[125] Carpenter et al. (2015). Cf. note 123.

9.4.2 Développer une approche intégrative

Une multiplicité de points de vue

Une limite des prises de décision est qu'elles sont faites par un nombre restreint d'acteurs, qui ont donc une vision du problème très marquée par leur propre expérience et intérêts (cf. par exemple les travaux de Hukkinen[126]). Ils vont ainsi avoir tendance à prendre la décision qui leur semble optimale par rapport à un point de vue très particulier ou à des intérêts dominants à un instant donné. Par exemple, une vision courante dans les cercles politiques de pays amazoniens est l'importance du développement du territoire par la construction de routes, alors que les bénéfices pour les populations locales sont ambigus[127]. En Bolivie par exemple, la construction d'une route dans le parc national d'Isiboro-Sécure a été décidée en 2017 malgré les protestations des populations locales, car la construction de la route risque d'augmenter la déforestation liée à la culture de coca, et donc augmenter les conflits fonciers et la violence dans la région[128]. Un autre exemple amazonien concerne l'usage et le contrôle des feux : selon le type de connaissances mobilisé et le niveau dans la hiérarchie politique, les conclusions diffèrent quant aux risques que représente le feu et à sa réglementation[129]. Le rôle de la recherche dans ce type de situation est d'intégrer l'ensemble des perceptions du problème, et les conséquences que pourrait avoir le projet pour chacun des intérêts en jeu. Ce rôle est d'autant plus difficile que le chercheur est lui-même influencé par son point de vue et ses convictions.

[126] J. Hukkinen (1995). « Corporatism as an impediment to ecological sustenance : the case of Finnish waste management ». In : *Ecological Economics* 15.1, p. 59–75.

[127] S. Wunder (2001). « Poverty alleviation and tropical forests-what scope for synergies ? » In : *World Development* 29.11, p. 1817–1833. arXiv : S0305-750X(01)00070-5 ; Simmons (2004). « The Political Economy of Land Conflict in the Eastern Brazilian Amazon », cf. note 45, p. 5.

[128] Á. Fernández-Llamazares et al. (2018). « New law puts Bolivian biodiversity hotspot on road to deforestation ». In : *Current Biology* 28.1, R15–R16.

[129] T. Devisscher et al. (2018). « Deliberation for wildfire risk management : Addressing conflicting views in the Chiquitania, Bolivia ». In : *The Geographical Journal* April, p. 1–17.

Une multiplicité d'approches

Les approches multi-, inter- et trans-disciplinaires connaissent un succès grandissant[130] et sont jugées indispensables pour pouvoir résoudre les défis de la gestion des ecosystèmes[131] De plus, la diversité des approches favorise l'association d'idées et donc la créativité, et pourrait permettre de trouver des solutions originales pour les problèmes environnementaux de demain. Pourtant, elles sont encore difficiles à mettre en place. Plusieurs raisons peuvent expliquer cela, parmi lesquelles les difficultés de compréhension entre différentes approches. Pour pouvoir travailler à l'interface entre plusieurs disciplines, il faut d'abord une traduction entre elles, car chaque discipline utilise un système de pensée particulier avec sa propre terminologie et ses concepts clé. Cela demande un investissement en temps qui est difficile à avoir aujourd'hui alors qu'on demande de plus en plus d'efficacité de la part des chercheurs (notamment en termes de publication, etc.). Ensuite, les recherches interdisciplinaires connaissent moins de succès dans le domaine de la recherche : les articles publiés sont moins cités par d'autres autres articles scientifiques, bien qu'ils soient plus cités dans des rapports et articles non scientifiques[132]. De plus, il est plus difficile d'avoir des financements pour des projets de

[130] M. MacLeod et M. Nagatsu (2016). « Model Coupling in Resource Economics : Conditions for Effective Interdisciplinary Collaboration ». In : *Philosophy of Science* 83.3, p. 412–433.

[131] H. Ledford (2015). « How to solve the world's biggest problems ». In : *Nature* 525.7569, p. 308–311 ; C. C. Hicks et al. (2016). « Engage key social concepts for sustainability ». In : *Science* 352.6281, p. 38–40. arXiv : arXiv : 1011 . 1669v3 ; D. Bertuol-Garcia et al. (2018). « A conceptual framework for understanding the perspectives on the causes of the science–practice gap in ecology and conservation ». In : *Biological Reviews* 93.2, p. 1032–1055.

[132] R. Barthel et R. Seidl (2017). « Interdisciplinary collaboration between natural and social sciences - Status and trends exemplified in groundwater research ». In : *PLoS ONE* 12.1, p. 1–27.

recherche interdisciplinaires souvent jugés trop risqués, et pour lesquels il n'existe pas de jury à même de juger la pertinence[133]. Une possibilité pour diminuer le biais négatif envers les projets interdisciplinaires est de les identifier lors de l'évaluation des projets, pour ensuite leur assigner un jury avec une expérience dans plusieurs des domaines abordés.

[133] L. Bromham et al. (2016). « Interdisciplinary research has consistently lower funding success ». In : *Nature* 534.7609, p. 684–687. arXiv : NIHMS150003.

Créer des interactions

Construire la recherche en interaction avec le reste de la société, et ce, dès la conception des sujets de recherche, permet d'augmenter son impact sur la prise de décision[134]. En identifiant tous les acteurs concernés par un projet de recherche, et en construisant les problématiques avec des interlocuteurs clé, les résultats auront plus de chance d'être ensuite utiles et d'avoir un impact réel sur les prises de décision. Cette co-construction ne s'arrête pas à la définition du projet : les objectifs peuvent être redéfinis au fur et à mesure de l'élaboration de nouveaux résultats, par des allers-retours entre la recherche et les acteurs concernés[135]. Par exemple, dans la thèse présentée ici, la facilité de communication et les relations historiques avec l'Office National des Forêts en Guyane française ont permis leur participation dès le départ du projet. Le Service Forestier brésilien a aussi été impliqué dans le projet, notamment autour des questions d'émissions carbone des concessions forestières. Enfin, une étape importante est l'évaluation des impacts du projet de recherche sur la gestion effective des écosystèmes, une fois le projet fini. Cette étape de validation *ex post* permet de tirer des leçons des réussites et des failles du projet, afin d'améliorer la mise en place des projets suivants.

[134] C. Cvitanovic et al. (2016). « From science to action : Principles for undertaking environmental research that enables knowledge exchange and evidence-based decision-making ». In : *Journal of Environmental Management* 183, p. 864–874.

[135] C. Cvitanovic et al. (2015). « Improving knowledge exchange among scientists and decision-makers to facilitate the adaptive governance of marine resources : A review of knowledge and research needs ». In : *Ocean and Coastal Management* 112, p. 25–35.

De manière générale les interactions entre recherche et décideurs sont difficiles et rarement mises en place. La première raison est le besoin de trouver des interlocuteurs intéressés et prêts à prendre le temps pour participer à l'élaboration de la recherche. Cela nécessite une prise de conscience des questions de conservation, et une relation de confiance des décideurs envers le monde scientifique. Cette confiance n'est pas toujours au rendez-vous, et en particulier sur les questions de conservation. Par exemple, au Brésil, les décideurs sont souvent sceptiques par rapport au rôle de l'Amazonie dans le cycle du carbone et accusent régulièrement les scientifiques d'être biaisés par leurs liens avec des institutions étrangères qui leur font négliger les intérêts nationaux[136]. Ce type de situation souligne encore l'importance de la construction d'une relation forte entre le monde de la recherche et l'ensemble de la société, et en particulier les preneurs de décision.

[136] M. Lahsen (2009). « A science–policy interface in the global south : the politics of carbon sinks and science in Brazil ». In : *Climatic Change* 97.3-4, p. 339–372.

Cela peut résulter en des décisions qui peuvent ne pas sembler optimales par rapport aux connaissances du problème acquises au cours du processus de recherche. Cela peut être dû à plusieurs raisons :

- un seul axe, jugé primordial (souvent, le retour économique), est optimisé ;
- les décisions sont biaisées, car les décideurs favorisent, consciemment ou non, des intérêts personnels au détriment des intérêts de l'ensemble de la société ; cela peut être exacerbé par des mécanismes de corruption[137] ou de corporatisme[138] ;
- il existe un décalage temporel entre les bénéfices à long terme et la durée de vie des projets et de l'agenda politique ;
- la complexité du message du chercheur et le besoin de prendre des décisions rapide, qui ne permet pas au décideur de s'attarder pour considérer l'intégralité des options et de leurs conséquences ;
- un manque de confiance des décideurs politiques envers le monde de la recherche et leurs conclusions[139].

Dans la plupart des cas cités ci-dessus, la distance entre les résultats de la recherche et la prise de décision effective vient d'un manque de communication entre chercheurs et preneurs de décision, soit que le message n'ai pas été reçu correctement (déformation, compréhension partielle), soit qu'il existe une forme de méfiance envers la sphère de la recherche. Dans tous les cas, ces limites peuvent être dépassées en entretenant un lien proche entre la recherche et la sphère politique. Cela peut passer par la participation à des meetings et des conférences organisés par et pour les preneurs de décision, ou en les contactant directement, en écrivant des lettres pour informer de certains résultats. Plutôt que de fournir des recommandations, trop liées à un système de valeurs personnel, définir un ensemble des possibles avec les acteurs concernés, et exposer les conséquences attendues, offre la possibilité d'une prise de décision informée par l'ensemble des enjeux.

[137] Pailler (2018). « Re-election incentives and deforestation cycles in the Brazilian Amazon », cf. note 47, p. 114.

[138] Hukkinen (1995). « Corporatism as an impediment to ecological sustenance : the case of Finnish waste management », cf. note 126, p. 184.

[139] Lahsen (2009). « A science–policy interface in the global south : the politics of carbon sinks and science in Brazil », cf. note 136, p. 185.

Chapitre 10

Annexes

Methods in Ecology and Evolution

BRITISH ECOLOGICAL SOCIETY

Methods in Ecology and Evolution 2017, **8**, 1163–1167 doi: 10.1111/2041-210X.12753

APPLICATION

BIOMASS: an R package for estimating above-ground biomass and its uncertainty in tropical forests

Maxime Réjou-Méchain*[,1,2], Ariane Tanguy[1], Camille Piponiot[3], Jérôme Chave[4] and Bruno Hérault[5]

[1]*French Institute of Pondicherry, UMIFRE 21/USR 3330 CNRS-MAEE, Pondicherry, India;* [2]*UMR AMAP, IRD, F-34000 Montpellier, France;* [3]*Université de la Guyane, UMR 'Ecologie des Forêts de Guyane' (AgroparisTech, Cirad, CNRS, Inra, Université des Antilles), Kourou Cedex F-97379, French Guiana;* [4]*Laboratoire Evolution et Diversité Biologique UMR 5174, CNRS, Université Paul Sabatier, 118 route de Narbonne, 31062 Toulouse, France; and* [5]*Cirad, UMR 'Ecologie des Forêts de Guyane' (AgroparisTech, CNRS, Inra, Université de Guyane, Université des Antilles), Kourou Cedex F-97379, French Guiana*

Summary

1. Estimating forest above-ground biomass (AGB), or carbon (AGC), in tropical forests has become a major concern for scientists and stakeholders. However, AGB assessment procedures are not fully standardized and even more importantly, the uncertainty associated with AGB estimates is seldom assessed.

2. Here, we present an R package designed to compute both AGB/AGC estimate and its associated uncertainty from forest plot datasets, using a Bayesian inference procedure. The package builds upon previous work on pantropical and regional biomass allometric equations and published datasets by default, but it can also integrate unpublished or complementary datasets in many steps.

3. BIOMASS performs a number of standard tasks on input forest tree inventories: (i) tree species identification, if available, is automatically corrected; (ii) wood density is estimated from tree species identity; (iii) if height data are available, a local height–diameter allometry may be built; else height is inferred from pantropical or regional models; (iv) finally, AGB/AGC are estimated by propagating the errors associated with all the calculation steps up to the final estimate. R code is given in the paper and in the appendix for the purpose of illustration.

4. The BIOMASS package should contribute to improved standards for AGB calculation for tropical forest stands, and will encourage users to report the uncertainties associated with stand-level AGB/AGC estimates in future studies.

Key-words: allometry, error propagation, forest carbon, height–diameter relationship

Introduction

The increase in carbon dioxide in the atmosphere and its effect on climate has brought forest carbon accounting to the forefront of the research and political agenda. Much attention is currently being given to tropical forests as they contain c. 55% of the carbon stored in the terrestrial vegetation, and tropical deforestation and degradation account for more than 10% of global anthropogenic greenhouse gas emissions (Le Quere *et al.* 2013). However, large uncertainties are still associated with these carbon stock estimates.

Forest carbon stocks, whether estimated through remote sensing or pure field-based approaches, are most often derived from forest inventories at least at one step. However, the way these forest inventories are converted into carbon stock estimates currently varies among studies. This results in variation among estimates that are not attributable solely to natural variability, but also to methodological considerations, the focus of the present contribution.

Estimating above-ground biomass (AGB) accurately includes several steps, such as the assignment of a wood density value to a tree, the choice of a biomass allometric model or the choice of a height–diameter (H–D) model when tree height data are incomplete or absent. Errors associated with all these steps are rarely accounted for in the final AGB estimate (see however Chave *et al.* 2004; Molto, Rossi & Blanc 2013; Chen, Laurin & Valentini 2015; Mermoz *et al.* 2015). For instance, a major source of error comes from the uncertainty in inferring height when it has not been measured directly and accurately. Different generic models have been proposed that depend either on regional variation (Feldpausch *et al.* 2012) or on bioclimatic constraints (Chave *et al.* 2014), although it is advisable to develop local H–D allometries because local abiotic or biotic (e.g. competition) conditions may significantly impact H–D relationships.

In this paper, we present an open source R package (R Core Team 2016) dedicated to the estimation of AGB and its

*Correspondence author. E-mail: maxime.rejou@gmail.com

uncertainty from tropical forest inventories. The goal of the BIOMASS package is to streamline many of the steps that are now being conducted by operators as illustrated in Fig. 1).

Test datasets

1 KarnatakaForest, which contains tree inventory data from 96 forest plots (1 ha) established in the central Western Ghats of India (Ramesh *et al.* 2010).
2 NouraguesHD, which contains tree inventory data, including height measurements, from two 1-ha plots established in the Nouragues Ecological Research Station, in French Guiana (see Réjou-Méchain *et al.* 2015 for methods).

```
install.packages("BIOMASS", dependencies = TRUE)
library(BIOMASS)
data(NouraguesHD)
```

Accounting for diameter

Tree diameter is a compulsory entry in our package. Note that diameter measurements are prone to errors and that a careful check prior to the analyses may correct some obvious errors.

Accounting for wood density

Wood density, the oven dry weight divided by green volume of wood, displays a 10-fold variation among tree species (Chave *et al.* 2009) and thus constitutes an important determinant of tree biomass. Because wood density is almost never measured for individual trees in forest inventories, a wood density value is often assigned to each tree from an independent database based on taxonomic identity (Flores & Coomes 2011). The getWoodDensity function from the BIOMASS package assigns a wood density value to each taxon using the global wood density (GWD) database as a reference (Chave *et al.* 2009; Zanne *et al.* 2009). Additional wood density values can be added using the addWoodDensityData argument. By default, getWoodDensity assigns to each taxon a species- or genus-level average if at least one wood density value in the same genus as the focal taxon is available in the reference database. For unidentified trees or if the genus is missing in the reference database, the stand-level mean wood density is assigned to the tree (based on trees for which a value was attributed). In the inputs of the function, each tree may be assigned to a stand through the stand argument, i.e. a vector of factors, such as plots, habitats or successional status. The family option also assigns to the trees a family-level wood density average, but it should be borne in mind that the taxon-average approach gives relatively poor estimates above the genus level (Flores & Coomes 2011). The region option allows the user to only consider wood density values from a specific region in the GWD database. However, Flores & Coomes (2011) showed that more accurate wood density averages are obtained with the global GWD database (without subsetting GWD by region).

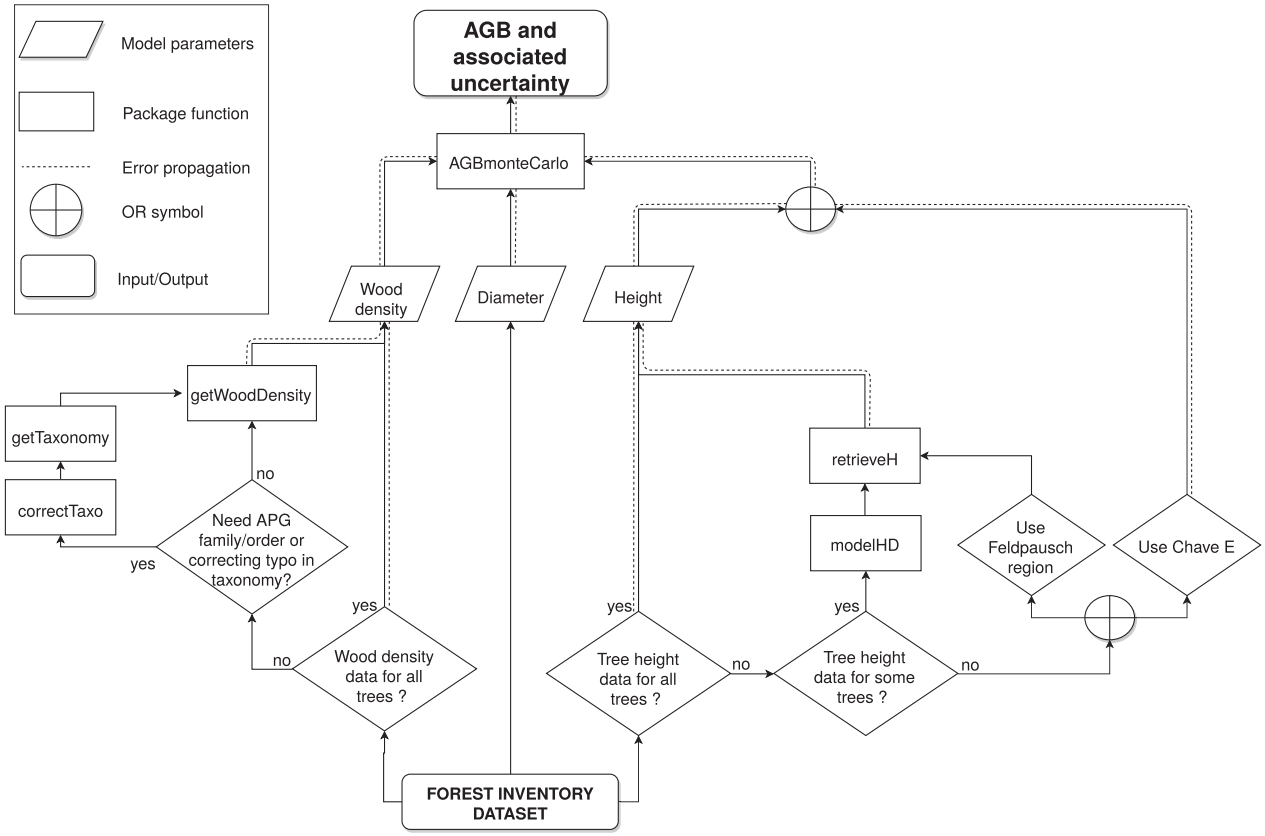

Fig. 1. Workflow of the BIOMASS package.

In our experience, taxonomic names in forest inventories are prone to typos. We implemented the function `correctTaxo` to correct typos in scientific names using the Taxonomic Name Resolution Service (TNRS; Boyle *et al.* 2013) via the Taxosaurus interface (http://taxosaurus.org/). This function has been adapted from the *tnrs* function of the `taxize` R package (Chamberlain & Szöcs 2013). Note that the taxonomy of the GWD database has been also submitted to TNRS to match the outputs from `correctTaxo`. The `getTaxonomy` function provides the APG III order and family names with genus names as entry.

```
Taxo <- correctTaxo(genus = NouraguesHD$genus,
species = NouraguesHD$species)
WDdata <- getWoodDensity(genus = Taxo
$genusCorrected, species = Taxo$speciesCorrected,
  stand = NouraguesHD$plotId)
```

Accounting for tree height

Tree height plays a key role in AGB calculation. Using tree height measurements for all trees is thus by far the most accurate method to infer AGB (Chave *et al.* 2014). However, accurate tree height measurements are rare, or rarely exhaustive, in closed-canopy tropical forests. Hence, a recommended strategy is to construct a stand-specific H–D allometry using a subset of well-measured trees (Réjou-Méchain *et al.* 2015). Trees selected for height measurement should be ideally sampled equally across size classes. Several H–D models have been proposed in the literature [see for instance the `lmfor` R package (Mehtatalo 2017)]. In the `BIOMASS` package the `modelHD` function contains five models to fit height H–D relationships in the tropics: three log–log polynomial models with order varying from 1 to 3, a three-parameter Weibull model (Feldpausch *et al.* 2012) and a two-parameter Michaelis–Menten model (Molto *et al.* 2014). By default, `modelHD` fits all the models and outputs the associated statistics (RSE and bias) for model assessment.

```
Hmodel <- modelHD(D = NouraguesHD$D, H = NouraguesHD
$H, method = "log2", useWeight = TRUE)
Hlocal <- retrieveH(D = NouraguesHD$D, model =
Hmodel)
```

If the study site misses tree height measurements, two alternatives may be used in the `retrieveH` function. First, the continent- or region-specific H–D models proposed by Feldpausch *et al.* (2012) may be used through the `region` argument. Second, a generic H–D model based on a single bioclimatic predictor E (eqn 6a in Chave *et al.* 2014) may be used through the `coord` argument.

```
Hfeld <- retrieveH(D = NouraguesHD$D, region =
"GuianaShield")
HchaveE <- retrieveH(D = NouraguesHD$D, coord = cbind
(NouraguesHD$long, NouraguesHD$lat))
```

AGB calculation

Once tree diameter, wood density and tree height have been retrieved for each tree, the generalized allometric model eqn 4 of Chave *et al.* (2014) can be used with the `computeAGB` function where AGB values are reported in Mg instead of in kg (Mg is the conventional unit for AGB values).

```
AGBtree <- computeAGB(D = NouraguesHD$D, WD = WDdata
$meanWD, H = Hlocal$H)
```

In the course of our package development, we identified an inaccurate statement in Chave *et al.* (2014). Contrary to a statement made in the paper, eqn 7 of that paper was not fitted directly with the data but was obtained by combining eqns 4 and 6. The directly fitted equation, including Baskerville (1972) correction, has the following expression:

$$\mathrm{AGB} = \exp(-2{\cdot}024 - 0{\cdot}896 \cdot E + 0{\cdot}920 \cdot \ln(\mathrm{WD}) + 2{\cdot}795 \cdot \ln(\mathrm{D}) - 0{\cdot}0461 \cdot [\ln(\mathrm{D})^2])$$

where the bioclimatic compound parameter E is the same as the one given in Chave *et al.* (2014). This is the equation implemented in the current version of `computeAGB` function when the site coordinates are given.

```
AGBtree <- computeAGB(D = NouraguesHD$D, WD = WDdata
$meanWD, coord = cbind(NouraguesHD$long,
  NouraguesHD$lat))
```

Propagating errors

In the `BIOMASS` package, the `AGBmonteCarlo` function allows the user to propagate different sources of error up to the final AGB estimate, as explained below.

DIAMETER MEASUREMENT ERROR

In the `Dpropag` argument of the `AGBmonteCarlo` function, the user can set diameter measurement errors by providing either a residual standard error (RSE) or a vector of errors (SD values) associated with diameters. Random and independent errors are assigned to diameters at each iteration in the `AGBmonteCarlo` function using a truncated normal distribution with a range of diameter values of (0·1, 500) cm. By default, the error propagation assumes that no errors were made on diameter measurements. An example of diameter measurement error is given in the `Dpropag` argument, taken from the Barro Colorado Island permanent plot where two types of errors were identified: large and small errors on 5 and 95% of the trees respectively (Chave *et al.* 2004).

WOOD DENSITY ERROR

To account for uncertainty in wood density values, the user can provide either a RSE or a vector of errors (SD values) associated with wood density values through the `errWD` argument of the `AGBmonteCarlo` function. At each iteration, errors

are assigned randomly and independently to wood density values using a truncated normal distribution with a range of (0·08, 1·39) g cm^{-3}, the minimum and maximum wood density values observed in the GWD database respectively. As a possibility, the `getWoodDensity` function outputs prior values on the uncertainty on wood density values using the mean SD at the species, genus and family levels calculated on taxa having at least 10 wood density values in the GWD database.

TREE HEIGHT ERROR

Here again, the user can provide either a RSE or a vector of errors (SD values) associated with tree height values through the `errH` argument of the `AGBmonteCarlo` function. Random errors are assigned independently to tree height values using a truncated normal distribution with a range of (1·3, maxH + 15) m, where maxH is the maximum tree height of the dataset. The RSE for the generic H–D models, or the RSE resulting from the local H–D models, are stored in the outputs of the `retrieveH` and `modelHD` function respectively. If real tree height measurements are available for all trees, the user should decide whether a height-related random error should be added in the error propagation.

ALLOMETRIC MODEL ERROR

To account for uncertainty in Chave *et al.* (2014) model parameters, eqns 4 and 7 have been inferred using a Markov chain Monte Carlo algorithm (code in Appendix S1, Supporting Information) in a Bayesian framework with uninformative priors. Chains of posterior vector, i.e. the model coefficients and RSE (RSEp), were stored to be used in the final error propagation step in the *AGBmonteCarlo* function (see below). To infer the models, we used the tree destructive dataset of Chave *et al.* (2014) available at http://chave.ups-tlse.fr/pantropical_allometry.htm.

FINAL PROPAGATION

Errors are propagated through a Monte Carlo scheme in the `AGBmonteCarlo` function, where the following steps are repeated *n* times:

1 When appropriate, diameter, wood density and height values are simulated adding a random error for each tree as described above.

2 Allometric model parameters are set up randomly picking up a single vector of posterior parameters applied simultaneously to all the trees of a stand (i.e. corresponding to a systematic error).

3 Tree AGB is computed using (1) and (2).

4 A single error term is added for all trees independently from the distribution $N(0, RSEp)$.

The procedure yields a distribution of *n* tree AGB values (*n*, the number of iterations, is an argument of the `AGBmonteCarlo` function), which are then summed by stand to provide *n* stand AGB values from which summary statistics are reported (mean, median and 95% credibility interval).

```
AGBmc <- AGBmonteCarlo(D = NouraguesHD$D, WD = WDdata
$meanWD, H = Hlocal$H,
  errWD = WDdata$sdWD, errH = Hlocal$RSE, Dpropag =
  "chave2004")
```

As an option in the `AGBmonteCarlo` function, the results can be provided in carbon instead of biomass (`Carbon` argument) using a mean biomass to carbon ratio of 0·471 and a standard deviation of 0·206 (calculated from carbon content of tropical angiosperms stems compiled by Thomas & Martin 2012a, b).

Figure 2 illustrates the outputs from the `AGBmonteCarlo` function for the two Nouragues plots using three different approaches. It shows that for those two plots, the mean AGB and its uncertainty were highly consistent between methods, indicating that both Chave' eqn 7 and Feldpaush regional H–D model perform well in that study area.

Focusing on a single plot from Nouragues, Fig. 3 shows how the different sources of errors contribute to the global error and how these relative contributions depend on the number of sampled trees. It confirms that the allometric error is the most important (Chave *et al.* 2004; Molto, Rossi & Blanc 2013), followed by the H–D model error. It also shows that the global error decreases rapidly with sampling size, because random errors are averaged. Note that this averaging effect depends on the tree size distribution of the stand and is thus site-specific.

Availability

The current stable version of the package requires R 3.3.0 and can be downloaded from CRAN (https://cran.r-project.org/web/packages/BIOMASS/) or installed directly in R with

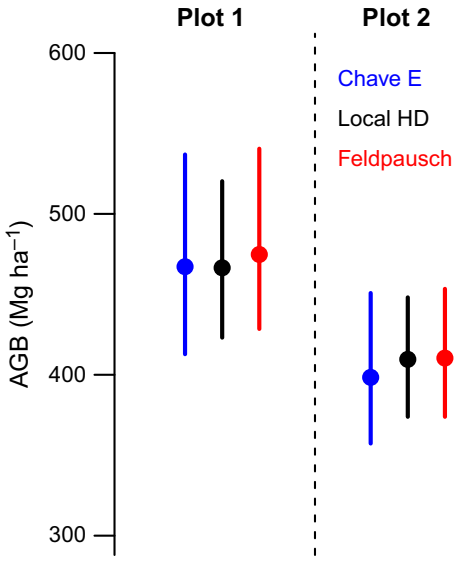

Fig. 2. Comparison of above-ground biomass estimation and uncertainty from three different methods in two 1-ha plots from French Guiana (Nouragues). Chave E: Chave *et al.* 2014 eqn 7 model; Local H–D: use of a mix of directly measured tree height (H) and of estimated ones by a local height–diameter (H–D) model; Feldpausch: use of the regional Guiana Shield Feldpausch H–D model. The R code used for generating this figure is available in Appendix S2.

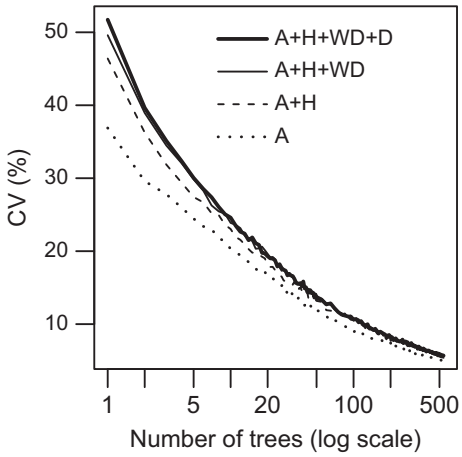

Fig. 3. Above-ground biomass uncertainty (coefficient of variation, CV) as a function of the number of sampled trees and using different sources of errors for a 1-ha plot from French Guiana (Nouragues). A, allometric error; H, height–diameter error (from the Guiana Shield Feldpausch model); WD, wood density error; D, diameter error (Chave et al. 2004). The R code used for generating this figure is available in Appendix S2.

`install.package("BIOMASS")`. A vignette (i.e. a tutorial) is available for this package (https://cran.r-project.org/web/packages/BIOMASS/vignettes/VignetteBiomass.html). `BIOMASS` depends on five existing `R` packages: (i) `raster` (Hijmans 2016); (ii) `msm` (Jackson 2011); (iii) `minpack.lm` (Elzhov *et al*. 2016); (iv) `httr` (Wickham 2016); and (v) `jsonlite` (Ooms 2014).

Authors' contributions

M.R.M. and A.T. conceived and designed the package; B.H. and C.P. developed the Metropolis algorithm for the allometric models; all authors contributed to developing R functions; M.R.M. wrote the paper with inputs from the other authors.

Acknowledgements

We thank two anonymous reviewers for their valuable insights as well as some users for their feedbacks on the first version of the package. We acknowledge financial support from Investissement d'Avenir grants managed by Agence Nationale de la Recherche (CEBA, ref. ANR-10-LABX-25-01; TULIP: ANR-10-LABX-0041). Salaries of M.R.M. and A.T. were supported by the French Ministry of Foreign affairs. The authors have no conflicts of interest to declare.

Data accessibility

The wood carbon content data from which the mean and standard deviation is used in the package are available from https://doi.org/10.5061/dryad.69sg2 (Thomas & Martin 2012b). The GWD dataset is available from http://datadryad.org/handle/10255/dryad.235 (Zanne *et al.* 2009) and the KarnatakaForest dataset is available from https://doi.org/10.6084/m9.figshare.c.3303531.v1, both of which are included in the BIOMASS package as well.

References

Baskerville, G.L. (1972) Use of logarithmic regression in the estimation of plant biomass. *Canadian Journal of Forest Research*, **2**, 49–53.

Boyle, B., Hopkins, N., Lu, Z. *et al*. (2013) The taxonomic name resolution service: an online tool for automated standardization of plant names. *BMC Bioinformatics*, **14**, 1.

Chamberlain, S.A. & Szöcs, E. (2013) Taxize: taxonomic search and retrieval in R. *F1000Research*, **2**, 191. doi: 10.12688/f1000research.2-191.v1.

Chave, J., Condit, R., Aguilar, S., Hernandez, A., Lao, S. & Perez, R. (2004) Error propagation and scaling for tropical forest biomass estimates. *Philosophical Transactions of the Royal Society of London Series B-Biological Sciences*, **359**, 409–420.

Chave, J., Coomes, D., Jansen, S., Lewis, S.L., Swenson, N.G. & Zanne, A.E. (2009) Towards a worldwide wood economics spectrum. *Ecology Letters*, **12**, 351–366.

Chave, J., Réjou-Méchain, M., Búrquez, A. *et al*. (2014) Improved allometric models to estimate the aboveground biomass of tropical trees. *Global Change Biology*, **20**, 3177–3190.

Chen, Q., Laurin, G.V. & Valentini, R. (2015) Uncertainty of remotely sensed aboveground biomass over an African tropical forest: propagating errors from trees to plots to pixels. *Remote Sensing of Environment*, **160**, 134–143.

Elzhov, T.V., Mullen, K.M., Spiess, A.-N. & Bolker, B. (2016) *Minpack.lm: R interface to the Levenberg–Marquardt nonlinear least-squares algorithm found in minpack, plus support for bounds*. Available at: https://CRAN.R-project.org/package = minpack.lm (accessed 22 September 2016).

Feldpausch, T.R., Lloyd, J., Lewis, S.L. *et al*. (2012) Tree height integrated into pantropical forest biomass estimates. *Biogeosciences*, **9**, 3381–3403.

Flores, O. & Coomes, D.A. (2011) Estimating the wood density of species for carbon stock assessments. *Methods in Ecology and Evolution*, **2**, 214–220.

Hijmans, R.J. (2016) *Raster: Geographic data analysis and modeling*. Available at: https://CRAN.R-project.org/package = raster (accessed 22 September 2016).

Jackson, C.H. (2011) Multi-state models for panel data: the msm package for R. *Journal of Statistical Software*, **38**, 1–29.

Le Quere, C., Andres, R.J., Boden, T. *et al*. (2013) The global carbon budget 1959–2011. *Earth System Science Data Discussions*, **5**, 165–185.

Mehtatalo, L. (2017) *Lmfor: Functions for forest biometrics*. Available at: https://CRAN.R-project.org/package = lmfor (accessed 22 September 2016).

Mermoz, S., Réjou-Méchain, M., Villard, L., Le Toan, T., Rossi, V. & Gourlet-Fleury, S. (2015) Decrease of L-band SAR backscatter with biomass of dense forests. *Remote Sensing of Environment*, **15**, 307–317.

Molto, Q., Rossi, V. & Blanc, L. (2013) Error propagation in biomass estimation in tropical forests. *Methods in Ecology and Evolution*, **4**, 175–183.

Molto, Q., Hérault, B., Boreux, J.-J., Daullet, M., Rousteau, A. & Rossi, V. (2014) Predicting tree heights for biomass estimates in tropical forests–a test from French Guiana. *Biogeosciences*, **11**, 3121–3130.

Ooms, J. (2014) *The jsonlite package: A practical and consistent mapping between json data and r objects*. arXiv:1403.2805 [stat.CO]. Available at: http://arxiv.org/abs/1403.2805 (accessed 22 September 2016).

R Core Team. (2016) *R: A Language and Environment for Statistical Computing*. R Foundation for Statistical Computing, Vienna, Austria. Available at: https://www.R-project.org/ (accessed 22 September 2016).

Ramesh, B.R., Swaminath, M.H., Patil, S.V., Pélissier, R., Venugopal, P.D., Aravajy, S., Elouard, C. & Ramalingam, S. (2010) Forest stand structure and composition in 96 sites along environmental gradients in the central Western Ghats of India. *Ecology*, **91**, 3118.

Réjou-Méchain, M., Tymen, B., Blanc, L., Fauset, S., Feldpausch, T.R., Monteagudo, A., Phillips, O.L., Richard, H. & Chave, J. (2015) Using repeated small-footprint LiDAR maps to infer spatial variation and dynamics of a high-biomass neotropical forest. *Remote Sensing of Environment*, **169**, 93–101.

Thomas, S. & Martin, A. (2012a) Carbon content of tree tissues: a synthesis. *Forests*, **3**, 332–352.

Thomas, S. & Martin, A. (2012b) Dryad wood carbon content database. *Dryad Digital Repository*, https://dx.doi.org/10.5061/dryad.69sg2

Wickham, H. (2016) *Httr: Tools for working with urls and http*. https://CRAN.R-project.org/package = httr.

Zanne, A.E., Lopez-Gonzalez, G., Coomes, D.A. *et al*. (2009) Global wood density database. *Dryad Digital Repository*, http://datadryad.org/handle/10255/dryad.235.

Received 4 January 2017; accepted 26 January 2017
Handling Editor: Sarah Goslee

Supporting Information

Details of electronic Supporting Information are provided below.

Appendix S1. Metropolis algorithm used to generate the posterior distribution of Chave *et al*. (2014)'s model parameters.

Appendix S2. R codes used to produce Figs 2 and 3.

Running head. Secondary succession in a forest of the Guianas

Title. Slow rate of secondary forest carbon accumulation in the Guianas compared with the rest of the Neotropics.

Jérôme Chave*[1], Camille Piponiot[2], Isabelle Maréchaux[1,3,4], Hubert de Foresta[4], Denis Larpin[5], Fabian Jörg Fischer[1], Géraldine Derroire[2], Grégoire Vincent[4], Bruno Hérault[6,7]

1. Laboratoire Evolution et Diversité Biologique, UMR5174, CNRS–Université Paul Sabatier–IRD, Bâtiment 4R1, 118 route de Narbonne F-31062 Toulouse cedex 9, France.
2. Université de la Guyane, UMR 'Ecologie des Forêts de Guyane' (AgroparisTech, Cirad, CNRS, Inra, Université des Antilles), F-97379 Kourou cedex, French Guiana
3. AgroParisTech-ENGREF, 19 avenue du Maine, F-75015 Paris, France.
4. AMAP, Univ Montpellier, IRD, CIRAD, CNRS, INRA, F-34000 Montpellier, France
5. Direction Générale Déléguée aux Musées, Jardins et Zoos, Muséum National d'Histoire Naturelle, 57 rue Cuvier, F-75005 Paris, France
6. Cirad, Univ Montpellier, UR Forests & Societies, F-34000 Montpellier, France.
7. INPHB, Institut National Polytechnique Félix Houphouët-Boigny, Yamoussoukro, Ivory Coast.

*Corresponding author: Jerome Chave, Laboratoire Evolution et Diversité Biologique, UMR5174, CNRS–Université Paul Sabatier–IRD, Bâtiment 4R1, 118 route de Narbonne F-31062 Toulouse cedex 9, France; email: jerome.chave@univ-tlse3.fr

To be submitted to: *Ecological Applications*
Abstract: 308 words, full text wo refs: 5194 words

Abstract

Secondary forests are a prominent component of tropical landscapes, and they constitute a significant atmospheric carbon sink. Rates of carbon accumulation are usually inferred from chronosequence studies, which present limitations. Direct estimates of carbon accumulation based on long-term monitoring of stands are rarely reported. Recent compilations on secondary forest carbon accumulation in the Neotropics are heavily biased geographically as they do not include estimates from the Guiana Shield.

We analysed the temporal trajectory of aboveground carbon accumulation and floristic composition at one 25-ha secondary forest site in French Guiana. This site was clearcut in 1976, abandoned thereafter, and one large plot (6.25 ha) was monitored continuously since. We compared its dynamics with that of a the surrounding old-growth forest. We used Bayesian modelling to assimilate inventory data and simulate the long-term carbon accumulation trajectory at this site. We also assessed the capacity of aerial lidar to monitor forest succession. Canopy change was monitored using two aerial lidar surveys conducted in 2009 and 2017 at the site. Finally, we compared our results with that from secondary forest in Costa Rica, which is one of the rare long-term monitoring programs reaching a duration comparable to our study.

Twenty years after abandonment, aboveground carbon stock was 64.2 [95% credibility interval: 46.4; 89.0] MgC/ha, and this stock increased to 101.3 [78.7; 128.5] MgC/ha twenty years later. The time to accumulate half of the mean aboveground carbon stored in the nearby old-growth forest (185.6 [155.9; 200.2] MgC/ha) was estimated at 35.0 [20.9; 55.9] years. During the first 40 years, the contribution of long-live pioneer species *Xylopia nitida*, *Goupia glabra* and *Laetia procera* to the aboveground carbon stock increased continuously.

Secondary forest structure measured by lidar differed from the nearby old-growth forests and mean-canopy height increased by 1.14 m in eight years, a canopy-height increase consistent with an aboveground carbon accumulation of 7.1 MgC/ha during this period. Long-term AGC accumulation

rate in Costa Rica was almost twice faster than at our site in French Guiana. This may reflect higher fertility of Central American forest communities or a better adaptation of the forest tree community to intense and frequent disturbances. This finding may have important consequences for scaling-up carbon uptake estimates at continental scale.

Keywords: biomass, carbon, forest, French Guiana, regeneration, secondary forests, tropics

Introduction

Tropical forests have undergone massive rates of deforestation and degradation (Hansen et al. 2013) contributing to over 70% of the global terrestrial gross land-use change carbon emissions into the atmosphere (Houghton et al. 2012), which amounts to about 1 PgC/yr for the period 2006-2015 (Le Quéré et al. 2016). Conversely, tropical emissions have been offset by the regrowth of tropical secondary forests, which have contributed an estimated atmospheric carbon sink of 1.6 PgC/yr (Pan et al. 2011). Even though estimates remain debated (Liu et al. 2015), regrowing tropical forests have an enormous potential to reduce atmospheric CO_2 concentrations in the next decades (Houghton et al. 2015, Chazdon et al. 2016). Here, we present results from a new long-term study on tropical forest carbon accumulation in French Guiana.

The vast majority of available information on secondary forest succession is based on chronosequence data, where stands of various successional ages are inventoried once, and forest stand properties are plotted against age. A pitfall of this approach is the difficulty to trace back past land uses and initial conditions of the sites, which can influence successional trajectories (Martin et al. 2013, Chazdon 2014, Arroyo-Rodriguez et al. 2017). In a compilation of chronosequence studies at 43 sites in the Neotropics, Poorter et al. (2016) found an average of 3 MgC/ha/yr aboveground carbon (AGC) accumulation rate in the first 20 years of regrowth, a figure slightly larger than the one assumed in carbon book-keeping methods (Pan et al. 2011, Houghton et al. 2015). The rate of carbon accumulation varied more than tenfold across sites, suggesting that there is a large variation in regrowth pathways. This may be explained by the idiosyncrasies of secondary regrowth, by methodological differences across studies, but also possibly by regional differences.

The key assumption of chronosequence studies is that time can be substituted for space (Johnson and Miyanishi 2008). This approach requires large sample sizes to accurately predict the regrowth trajectory in a given forest landscape, since there is a large variation in the explanatory power of fallow age for carbon accumulation inference (Mora et al. 2015, Becknell et al. 2018a). A preferable alternative relies on the long-term monitoring of permanent forest plots, and such studies are currently rare, and seldom extend beyond two decades of monitoring (Feldpausch et al. 2007, Rozendaal and Chazdon 2015).

Regional modeling of tropical forest regeneration is still impeded by the scarcity of data (Norden et al. 2015). This is particularly critical in the Guiana Shield where few studies on forest secondary succession are available, although this region covers a third of Amazonia. The forests of the Guianas grow on poor soils (Quesada et al. 2011), and old-growth forests in this region store more carbon than the rest of Amazonia (Saatchi et al. 2011), so we would expect that the time needed to reach mature forest biomass would be longer in the Guianas than elsewhere in the Neotropics.

Another limitation of chronosequence studies is that they are based on a sample of small forest plots (typically ranging from 0.01 to 1 ha; Poorter et al. 2016, Becknell et al. 2018), which prevents a robust assessment of regeneration dynamics at the landscape scale (Estes et al. 2018). Remote sensing technology offers the opportunity to scale up plot-based carbon accumulation estimates across entire landscapes. Of the remote-sensing methods, aerial laser scanning offers great potential to monitoring the successional status of forests (Mascaro et al. 2012, Meyer et al. 2013, Englhart et al. 2013, Ene et al. 2016, Becknell et al. 2018b). ALS provides rapid access to forest structure variables, such as canopy height and structure, both of which vary rapidly as forest succession advances (Peña-Claros 2003, Mora et al. 2015, Rozendaal and Chazdon 2015). Mascaro et al. (2012) used aerial lidar to infer the carbon accumulation of a forest landscape in Panama, and more recently Becknell et al. (2018b)

published similar results for a Brazilian Atlantic landscape of Southern Bahia. However, lidar methods of carbon accounting crucially depend on the assumptions of the chronosequence approach, and it would be important to test them. However, aerial lidar has seldom been used to detect changes in canopy height and in canopy structure through time, primarily because the technology has only emerged recently in tropical forest monitoring.

The present study builds on a long-term ecological project at a 25-ha secondary forest stand located within an old-growth forest matrix in French Guiana. This stand has been experimentally clearcut in 1976, and it has been repeatedly monitored thereafter with no human intervention over the past forty years. It thus provides a rare example of a secondary forest, in the Guiana Shield and across the Tropics, that has been monitored continuously for decades. We document the carbon accumulation dynamics during the first forty years of secondary succession.

Based on forest inventories, we first modelled the carbon accumulation trajectory. We hypothesized that carbon accumulation rates would be lower at our site than the mean values reported for the Neotropics (Poorter et al. 2016). Second, we explored the contribution of common species to carbon accumulation, and changes in community-mean wood density through time in the stand. Third, we used two aerial lidar surveys to compare the structure of the forest in 2009 and 2017. We hypothesized that forest height increases through ecological succession, but also that canopy structure changes. We finally compared our results with those obtained at a wet forest site in Costa Rica using the data published by Rozendaal and Chazdon (2015). To our knowledge, this study is the only other published case of a long-term monitoring of secondary forests in the Neotropics, and for this reason it is the only other study directly comparable to ours. We conclude by discussing the role of the geological substrate and soil chemistry on the carbon accumulation rates in the Neotropics.

Methods

Study site and sampling

The study site is located 15 km southwest of the village of Sinnamary, French Guiana (5.30N, 53.05W). It receives around 3000 mm/yr mean annual precipitation and has a two-month dry season (months with < 100 mm rainfall) in September and October. The area is covered by moist tropical forest, with a lidar-derived mean canopy height of about 28 m (Vincent et al. 2012). These forests have relatively infertile soils (Grau et al. 2017), tall canopy, and high biomass (Saatchi et al. 2011).

In July-August 1976, a 10-ha area was logged over as part of a pulp production project that was abandoned soon thereafter. Not all the stems were removed from the site, and an average of 74 stems/ha were left onsite (stems with lower timber value, such as Chrysobalanaceae). In August-September 1976, all remaining trees were cut down and the felled area was extended to 500x500 m (25 ha). Logs were only partly removed and the logging remains (crowns and roots) were left onsite. About 10% of the soil surface was extensively disturbed by logging activities during the time of operation, and about 15% of the clearing was severely burnt by an accidental fire in October 1976 (Sarrailh 1980, Maury-Lechon 1982).

Starting in 1989, a 6.25 ha (250x250 m) plot was monitored for all stems ≥ 10 cm dbh. Stems were mapped, tagged, and their stem diameter measured using a standard protocol. Tree-by-tree reinventory of the plot was conducted every year from 1989 to 1992 and from 1994 to 1996, and approximately every two years from 2003 to 2014. Botanical identifications were initially based on vernacular names, but starting in 2007 a detailed botanical census was conducted. Several of the unidentified trees had died before they could be identified, still resulting in an overall identification rate of over 80% for all the trees dead or alive in the database. In the census conducted in 2014, 87% of the trees were identified. Some genera were common at the onset of the forest regrowth process, and we explored their long-term contribution to the carbon accumulation process. These included the following genera: *Cecropia* (Urticaceae), *Vismia* (Hypericaceae), *Xylopia* (Annonaceae), *Goupia*, (Goupiaceae), *Laetia* (Salicaceae), *Tachigali*, *Albizia*, and *Inga* (Fabaceae), *Miconia* (Melastomataceae), *Jacaranda* (Bignoniaceae), and *Byrsonima* (Malpighiaceae).

Three and a half years after land conversion (1980), de Foresta (1983, 1984) sampled two

transects of 460x2 m (transect 1), and of 532x2 m (transect 2). All stems ≥ 1 cm dbh were measured, mapped, and identified to the species. In the first half of 1988, Larpin (1989) recensused part of transect 1 (404x2 m), again recording all stems ≥ 1 cm dbh. In 2005, transect 1 was extended to an area of 425x4 m, and transect 2 to an area of 530x4 m. Finally, in 2016, we inventoried all stems ≥ 1 cm dbh in nine 0.01-ha square quadrats, evenly located across the permanent tree plot.

For each of the censuses described above, we computed stand-level metrics of the ecological succession, including tree density (trees per ha), basal area (BA, the cumulative cross-sectional area of trunks, in m^2/ha), and live aboveground carbon (AGC; carbon weight, in MgC/ha). To estimate AGC, we used the allometric model developed in Chave et al. (2014), and propagated wood density, trunk measurement and allometric uncertainties on every live tree of the census to the plot-level estimates using the 'biomass' R package (Réjou-Méchain et al. 2017). Wood density estimates were inferred from species-mean values as reported in the global wood density database (Chave et al. 2009). AGC was obtained by converting aboveground oven-dry live biomass into AGC assuming 48% of carbon in oven-dry live matter (Martin and Thomas 2011). We used stem-by-stem inventory data to estimate AGC for stems < 10 cm dbh (1980, 1988, 2005 and 2016), and the 6.25-ha plot to estimate the AGC held in stems ≥ 10 cm dbh (from 1989 to 2015).

We used stem-by-stem inventory data from the transects and 0.01 ha quadrats for stems < 10 cm dbh (1980, 1988, 2005 and 2016), and from the 6.25-ha plot for stems ≥ 10 cm dbh (from 1989 to 2015) in the model inference of carbon accumulation (see below). In addition, we included published aggregated stand basal area records: Prévost (1983) documented the forest regrowth dynamics in two 100x10 m plots three to nine years after stand abandonment, recording all stems ≥ 1 cm dbh from which stand basal area was computed (Sarrailh et al. 1990). In 1995, 52 10x10 m plots (0.52 ha) were inventoried for all trees ≥ 1 cm dbh, and the basal area was reported (Toriola, 1997). All additional inventories are summarized in Table S1.

Carbon accumulation inference

Our dataset included a range of data sources, some highly precise (tree-by-tree inventories), others with some imprecision (published basal area estimates). We thus needed a modelling approach that could accommodate data of varying origins and quality, and predict the most likely trajectory of AGC, and its uncertainty, during forest recovery. To this end, we chose a Monte Carlo inference scheme under a Bayesian framework. Since basal area was available more frequently than AGC, we first modelled basal area increase through time. In accordance with the underlying structure of our data and standard practices in forestry, we decided to separately model the basal area dynamics at sapling (<10 cm dbh) and tree (≥10 cm dbh) stages. From this model, we then inferred the temporal trajectory of AGC, and propagated uncertainties from the data sources to our results.

Mean basal area accumulation through time was modelled in the two compartments as follows:

$$\widehat{BA_{sapling}}(t) = \theta_1 \times (1 - \exp(-\theta_{2a} t)) + \theta_3 \times \exp\left(-\left[\ln\left({}^{t}/_{\theta_4}\right)/\theta_5\right]^2\right) \quad (1)$$

$$\widehat{BA_{tree}}(t) = \theta_6 \times (1 - \exp(-\theta_{2b} t)) \quad (2)$$

In (1), the first term describes the accumulation of sapling basal area through time, $\theta_1$being the asymptotic sapling basal area, and θ_{2a} the rate at which this asymptote is reached. The second term of Eq (1) represents 'boom-and-bust' dynamics, with $\theta_3$the maximum excess sapling basal area, θ_4 (in yr) the time at which this maximum is reached, and θ_5 a kurtosis parameter. Equation (2) models the tree basal area accumulation, where θ_6 is the asymptotic tree basal area, and the rate at which the asymptote is reached, θ_2, differs in the two compartments, hence the subscripts a and b. Aboveground carbon was linked to basal area through a power-law function:

$$\widehat{AGC_{sapling}} = \exp(\theta_9) \times \left(BA_{sapling}\right)^{\theta_{10}} \times \left[\widehat{AGC_{tree}}\right]^{\theta_{11}} \quad (3)$$

$$\widehat{AGC_{tree}} = \exp(\theta_7) \times (BA_{tree})^{\theta_8} \quad (4)$$

In equation (3), the term in $\widehat{AGC_{tree}}$ models a coupling between the sapling and the tree stages effect, since sampling density is expected to correlate with large tree density through a self-thinning effect. Inference of the model parameters was performed using a Hamiltonian Monte-Carlo algorithm (see Appendix). The maximal (asymptotic) value of $\widehat{AGC} = \widehat{AGC_{sapling}} + \widehat{AGC_{tree}}$, AGC_{max}, was inferred from model (3,4) using as a prior a normal distribution with mean 185 MgC/ha and a standard deviation of 12 MgC/ha, which reflects the inter-plot variability. Both estimates were taken from data from the nearby Paracou long-term experimental plots (Rutishauser et al. 2011).

Carbon balance in trees

Next, we explored how AGC dynamics in the tree compartment ≥ 10 cm dbh were affected by AGC accumulation through recruits and tree growth, and AGC loss due to stem mortality. We expected that AGC ingrowth exceeded loss. We conducted this analysis from 1989 to 2014. Carbon balance can be measured using the following equation

$$\Delta AGC_t = NPP_{w,t} + Recruit_t - Loss_t \quad (6)$$

where ΔAGC is the change in AGC, NPP_w is the carbon uptake due to woody growth, $Recruit$ is the carbon uptake due to tree recruitment (individual trees crossing the dbh threshold of 10 cm), and $Loss$ is the carbon loss due to tree mortality. These terms are defined by:

$$NPP_{w,t} = \sum_i \frac{AGC_{i,t+1} - AGC_{i,t}}{\Delta t}, Recruit_t = \sum_{i'} \frac{AGC_{i',t+1}}{\Delta t}, Loss_t = \sum_{i''} \frac{AGC_{i'',t}}{\Delta t} \quad (7)$$

where the first summation runs over all trees alive in both censuses, the second summation runs over saplings at census t that had become trees at census t+1, and the third summation runs over trees that died between the censuses. Some of the consecutive inventories displayed large variation in mortality, and the reported stand fluxes were smoothed using a moving average of the form $\bar{x_i} = 0.25x_{i-1} + 0.5x_i + 0.25x_{i+1}$.

Aerial laser scanning of the study site

We conducted two overflights of the study site using small-footprint aerial lidar sensors. Our first campaign was conducted in April 2009 with a Riegl LMS-280i single return storage capacity operating in last return mode. The second campaign was conducted in September 2017 with a Riegl LMSQ560 full waveform with multiple-return storage capacity. The area overlapping the two surveys was of 400 ha. The lidar point cloud was analysed by first extracting the ground points, to generate a digital terrain model at 1-m spatial resolution.

We next extracted top-of-canopy points to generate a canopy height model also at 1-m spatial resolution. The 500x500 m regrowing forest had a road cutting through the East part of the plot, and we masked this area with a 10-m buffer. Since the two surveys used different sensors and point densities – which could bias the estimated changes in canopy structure between the two surveys –, we determined a reference region of the same size as the regrowth plot taken at random in the undisturbed forest a few hundred meters away. We compared the canopy height changes between the two surveys in the 25-ha regrowth plot and in the nearby old-growth forest control plot.

We finally compared normalized vegetation profiles between these two plots. Normalization uses the ray tracing of laser shots in a 3D mesh to compute local transmittance, which is then inverted to estimate local vegetation density (Tymen et al. 2017, Vincent et al. 2017). This procedure resulted in the estimation of the area of scatterers (both leaves and woody components) within each 1-m^3 voxel of the canopy. This index is called the Plant Area Density (PAD) and is measured in m^2 of scatterers per unit volume (m^2/m^3). We averaged this PAD for each 1-m canopy height layer and compared these PAD profiles computed for 25 50x50m subplots in the secondary forest plot and an equivalent number in the old-growth forest plot. Finally, we summed the PAD vertically, to compute the Plant Area Index (PAI), which is the cumulative area of scatterers per area of ground (in m^2/m^2). This PAI is similar to the commonly measured Leaf Area Index, but also includes woody components.

Comparison of AGC recovery with other Neotropical secondary forest sites

Finally, we used carbon accumulation at 20 years reported by Poorter et al. (2016) for compairson. We selected thirteen lowland Amazonian sites, that receive at least 1500 mm rainfall annually, have a weak seasonality, as characterized by a climatic water deficit ≥ -400 mm/yr (Aragão et al., 2007), and are located < 400 m in elevation: three were in Bolivia (El Tigre, El Turi, Bolpebra), seven in Brazil (three in Eastern Para, two around Manaus and two around the Rio Madeira), two in Colombia (Araracuara and near San Carlos de Rio Negro) and one in Peru (Pucallpa). The only other site in a white-sand forest of the Guiana is that of San Carlos de Rio Negro (Saldarriaga et al. 1988).

Zwetsloot (1981) described a further site in Suriname (Blakawatra) where a 120x80 m experimental plot was set up in 1967 after clear cutting an old-growth forest on well-drained sandy soil to sticky loam soil. Basal area increased to 15.2 m^2/ha within the first 11 years of abandonment (Fig. 8 in Zwetsloot 1981). However, it was not possible to infer carbon accumulation based on basal area increment and we excluded this study from the comparison.

We also took advantage of the recent publication by Rozendaal and Chazdon (2015) who reported on a long-term monitoring in six 1-ha secondary forest plots in Costa Rica. We used their census data to recalculate tree AGC at the three sites that were totally clear-cut prior to abandonment, specifically Juan Enriquez (JE, Chilamate), Lindero Sur (LSUR, La Selva), and Lindero El Peje (LEP, La Selva). To this end, we used the same methods as implemented for the French Guiana plot. The model in Equations (1)-(4) cannot be used for comparison between French Guiana and Costa Rica sites. Thus, we also constructed a simpler model, as follows:

$$\widehat{AGC} = \widehat{AGC_{sapling}} + \widehat{AGC_{tree}} = \theta_{12} + (AGC_{max} - \theta_{12}) \times (1 - \exp(-\theta_{13} t)) \quad (5)$$

This model is such that as time *t* tends to infinity, the expectation on AGC tends to AGC_{max}. We fit Equation (5) separately on the three Costa Rica datasets, using a slightly lower prior on AGC_{max} (normal prior, mean=170 MgC/ha, standard deviation=12 MgC/ha; based on old-growth sites in Rozendaal and Chazdon 2015). For French Guiana, we also assumed a normal prior for AGC_{max} but with different values (mean=185 MgC/ha, standard deviation=12 MgC/ha).

Results

Using model (1)-(4), we found that AGC stocks rose quickly from zero to 37.8 [95% credibility interval: 21.7; 60.1] MgC/ha within the first 10 years, the time at which the transient boom-and-bust dynamics of saplings reached its maximum (Fig. 1). Saplings contributed 61% of the AGC stock 10 yr after stand abandonment. Twenty years after stand abandonment, AGC stock was 64.2 [46.4; 89.0] MgC/ha, and saplings contributed 33.8% of the stocks. After 40 years of regrowth, total AGC stock was estimated at 101.3 [78.7; 128.5] MgC/ha, and sapling AGC at 13.4 [3.7; 26.3] MgC/ha. The maximal AGC, AGC_{max}, was inferred at 185.6 [155.9; 200.2] MgC/ha. Using the simplified exponential model (equation 5), we inferred the time needed to accumulate half of the maximal AGC at 35.0 [20.9; 55.9] years.

Aerial laser scanning revealed that after 40 years (in 2017), median canopy height was 19.5 m in the regrowing plot, compared with 28.7 m in the old-growth forest control site. Comparing the 2017 survey to the 2009 survey (Δt = 8 years), we found that the regrowing forest gained 1.14 m in mean canopy height relative to the control plot, and top-canopy height (95% percentile) gained 1.99 m (Table 1). Thus, ALS-derived mean canopy height increment was in average 0.14 m/yr and top-canopy height increment was 0.25 m/yr. The standard deviation in canopy height growth rates across 1-m^2 subplots was smaller in the regrowing plot (3.1 m) than in the control plot (5.8 m). The secondary forest plot had a significantly lower plant area index (PAI, 10.4 vs 13.8 m^2/m^2). However, the plant area density (PAD) peaked at higher levels in the secondary forest, suggesting that the top canopy is denser in the secondary forest than in the old-growth forest (Fig. 2).

Changes in AGC through time were quantified for eleven taxa (Fig. 3a). *Cecropia spp* and

Vismia spp quickly declined in dominance in the first 20 years, while *Xylopia nitida* Dunal, *Laetia procera* (Poepp.) Eichler, and *Goupia glabra* Aubl. increased in dominance throughout the study period.

Community-wide properties of the forest stand changed significantly during the first 40 years of regrowth. Basal-area weighted wood density across trees ≥ 10 cm dbh increased from 0.48 g/cm^3 12 years after stand abandonment to 0.60 g/cm^3 after 38 years (Fig. 3b), still far from the old-growth estimate of 0.68 g/cm^3 in these forests (Chave et al. 2008).

After 15 years of regrowth, woody NPP in trees ≥ 10 cm dbh varied between 1.7 and 2.2 MgC/ha/yr depending on years (Fig. 4), except for a spike at 2.5 MgC/ha/yr at 18 years. Carbon accumulation due to recruitment was fairly stable throughout the survey period, around 0.5-1 MgC/ha/yr. Stem mortality was variable across years, with a spike of mortality 19 years after stand abandonment, largely explaining the interannual variation in net carbon accumulation (which varied from 0.6 to over 2.2 Mg/ha/yr).

We also compared our results with those obtained elsewhere in the Neotropics. Across the 13 sites retained from Poorter et al. (2016), AGC values 20 years after abandonment ranged between 40.6 MgC/ha and 107.8 MgC/ha, with a mean of 74.7±17.9 MgC/ha (mean±standard error across sites). Thus, our value of 64.2 MgC/ha after 20 years is in the lower end, though not exceptionally low, of the range reported for Amazonian rainforests.

Finally, fitting equation (5) at the three Costa Rica plots, we found that maximal AGC was 176 [152; 184] MgC/ha at Juan Enriquez, 157 [147; 177] MgC/ha at Lindero El Peje, and 162 [150; 182] MgC/ha at Lindero Sur. Given these inferred estimates, the time to reach half of the maximum AGC was almost twice shorter than at our site, at 24 [21; 28.5] yr at Juan Enriquez, 16 [14; 19] yr at Lindero El Peje, and 20 [17.5; 23.5] yr at Lindero Sur.

Discussion

Long-term trends in carbon accumulation at a French Guiana site

We here report results on the long-term aboveground carbon accumulation dynamics in a secondary forest of French Guiana. Initially, AGC accumulation peaked three years after abandonment. AGC accumulation rate remained high after ten years and declined slowly thereafter. For instance, between 32 and 40 years after abandonment, the inferred AGC accumulation rate was 1.73 MgC/ha/yr on average, almost half of the mean of the first 20 years (3.2 MgC/ha/yr). Thus, the potential of secondary forests for carbon emission mitigation is limited beyond the twenty-year horizon of forest regrowth.

After ten years, sapling AGC stock declined, while tree AGC continued to increase, a consequence of increasing size-biased competition in regrowing mixed-species forests (Farrior et al. 2016). However, after 40 years of regrowth, sapling AGC still represented 13.2% of total AGC, a proportion that was twice larger than our estimate after 100 years of regrowth. By comparison, sapling AGC was estimated at 4 MgC/ha in a nearby old-growth forest i.e. about 2% of the total stock (Baraloto et al. 2011). Thus, the decline in sapling AGC stock was extremely slow, and saplings remained a significant component of the carbon stock during a long period during forest regrowth. Similar to our study, Hughes et al. (1999) found that sapling AGC was over twice larger in 50-year old secondary forests than in nearby primary forests of Los Tuxtlas, Mexico (see their Table 4). Thus, saplings account for a significant part of the biomass dynamics in secondary forests and studying sapling dynamics offers insights on the pace of forest recovery.

Remote sensing and carbon accumulation monitoring

Remote sensing technology is able to detect variation in forest carbon stocks from variation in forest canopy height and this is an opportunity for carbon mapping (Mascaro et al. 2012). For instance, the space GEDI mission by NASA will use full waveform lidar to infer forest canopy structure and height

in forests worldwide (Dubayah et al. 2010, Saatchi et al. 2012, Qi and Dubayah 2016). Another mission, BIOMASS (P-band Synthetic Aperture Radar, SAR) funded by the European Space Agency will give similar information but over a 5-year period. Importantly, these approaches are calibrated using forest plots of different AGC stocks, and thus substitute space for time as in the chronosequence approach.

In our study, canopy height, as measured by lidar, changed distinctively in eight years of succession (2009 to 2017), as shown in Table 1. Comparing canopy-height metrics in 2009 and 2017 revealed that the canopy height increment was larger for the 95% top-canopy height metric (+1.99 m during the period) than for mean-canopy height (+1.14 m). The faster increase of top-canopy height than mean-canopy height is explained by significant structural changes in canopy structure. The 41-yr secondary forest was still very different from the neighboring old-growth forest, being much shorter and with a plant area density more densely packed towards the top of the canopy (Fig 2b). However, the plant area index (PAI) was lower in the secondary forest than in the neighboring old-growth forest. Thus, even if the canopy of secondary forests is more densely packed towards the top, the lower PAI of the secondary forest stand implies that that ground retrieval is not an issue in secondary forest stands, because the laser beam transmission through the canopy directly depends on PAI, according to the Beer-Lambert law.

In the space-for-time approach we could have used information from the literature to predict the rate of carbon accumulation in the forest. For instance, using aerial lidar data and forest inventories from French Guiana and Gabon, Labrière et al. (in press) showed that AGC was related to mean-canopy height linearly and consistently across continents, with a slope of 6.2 MgC/ha/m. Using our mean-canopy height increment of 1.14 m during the study period, we would have inferred a carbon accumulation of +7.1 MgC/ha. Because we have a direct measurement of carbon accumulation at this site, we can use it to assess this estimate provided by a generic model. In 2009, the total forest AGC was estimated at 57.1 MgC/ha, and in 2017 at 64.2 MgC/ha, thus taking the difference of the values, we obtain +7.1 MgC/ha, which is precisely the model estimate.

We conclude that at our site, both the space-for-time substitution and the simple assumption that AGC increases linearly with mean-canopy height yield excellent predictions. It would be important to further examine how forest structure varies along other successional pathways, and at other sites.

Influence of floristic turnover on carbon accumulation

The burst-and-boom dynamics we described in the early stages of forest regrowth was primarily driven by a drastic floristic turnover, as has been documented elsewhere in the tropics (Gómez-Pompa and Vázquez-Yanes 1981, Peña-Claros 2003). After ten years, short-lived pioneers at our site, e.g. *Vismia spp*, and *Cecropia obtusa*, were almost fully replaced by a cohort of species referred to as long-lived pioneers (Finegan 1996). The most typical long-live pioneer taxa, *Xylopia nitida*, *Goupia glabra*, and *Laetia procera*, are present early on during the successional process, but they are also frequently found as emergents in primary forests. At our site, they were still increasing in dominance after 40 years, which may result from their remarkable physiology suited to thrive in the high evaporative demand conditions of both early successional stages and high canopy position. For example, photosynthetic uptake of *Goupia glabra* appears to be maintained during the dry season (Silva et al. 2011), owing to its relatively low leaf water potential at turgor loss point (Maréchaux et al. 2016). The patterns of change in dominance of *Vismia* were intermediate between short-lived and long-lived pioneers. This pattern may be linked to the partial burning of the site (Norden et al. 2011), and is also consistent with the light-demanding physiology of this genus (Silva et al. 2011).

The long-term tree inventory within our study plot allowed us to explore the interannual patterns of woody NPP and carbon loss in trees. This analysis confirmed that the plot acts as a significant carbon sink throughout the monitoring period, but also evidenced strong patterns of temporal variation (Fig. 4). For instance, carbon loss through mortality varied twofold with a peak at almost 1.5 MgC/ha/yr after twenty years of regeneration, followed by a low at around 0.6 MgC/ha/yr after year 30. These patterns are at least in part due to the species turnover at the site, especially the

rapid decline in species with low wood density, such as *Vismia* and *Cecropia*, which were replaced by species with intermediate wood density during the same period. Importantly, we assumed that wood density was constant among trees within a species. While this assumption appears reasonable at community scale, evidence suggests that at least some species shift in wood density along succession (Plourde et al. 2015). If verify that would imply that more research is necessary to clarify the demographic drivers of the carbon cycle in secondary forests (Muscarella et al. 2017).

Regional variation in carbon accumulation

Across the Neotropics, regrowing forests have different disturbance histories, soil fertility, proximities to seed sources, climate conditions, and all these factors may alter the successional trajectory of the forest (Chazdon 2003, Chazdon et al. 2007, Arroyo-Rodríguez et al. 2017). Our study site is a special case as it gathers favorable conditions for enhanced recovery: it was abandoned directly after clearcut, part of the biomass was left onsite, and it is surrounded by old-growth forest. While we should therefore have expected a relatively rapid recovery, we found that recovery rates were relatively slow compared to other rainforest sites. Even though methodological differences across studies may contribute to the observed variability, we hypothesize that the slow recovery is due to the floristic composition and the relatively poor soils in the Guiana Shield. To our knowledge, only study on secondary forest carbon accumulation in the Guiana Shield previous to ours was that of Saldarriaga et al. (1988), at the Venezuela-Colombia border and on sandy-soil forest (San Carlos de Rio Negro). AGC accumulation at San Carlos was exceptionally low, at 40.6 MgC/ha after twenty years of regeneration, much lower than at our site (64 MgC/ha). This slow forest growth could be explained by constraints due to low-fertility white sand soil. However, our study demonstrates that even on clayey soil, forest regrowth appears to be slower in the Guianas than in the rest of the lowland Amazon (74.7 MgC/ha after 20 years, range [40.6; 107.8]; n=13; Poorter et al. 2016) perhaps due to a combination of low fertility (Grau et al. 2017) and high AGC stocks (Saatchi et al. 2011).

Cole et al. (2014), studying changes in floristic composition from pollen cores at many tropical sites, found that Central American forests tended to recover from disturbances twice faster than South American forests. We found that regrowth dynamics was about twice faster in sites in Costa Rica than at our site, confirming Cole et al. (2014)'s argument. This finding is of relevance in the mapping of the carbon sequestration potential in secondary Neotropical forests, as done by Chazdon et al. (2016). The carbon accumulation curve used by Chazdon et al. (2016) was of the Michaelis-Menten form $AGC = AGC_{max} \times Age/(a_{50} + Age)$, where a_{50} is the time to reach half of the maximum stock of carbon. They modelled a_{50} as a function of bioclimatic variables, and found that the rate of carbon accumulation varied little and was primarily controlled by climate. Our analysis suggests that Equation (5) reflects the dynamics of carbon accumulation better than Chazdon et al. (2016)'s model both in French Guiana and Costa Rica. Indeed, we did attempt to fit our French Guiana data with a Michaelis-Menten equation but this model was a poorer fit than model (5). It would be important to reassess this problem with more long-term datasets.

An interpretation of the difference in the recovery from disturbances between our site in French Guiana and the sites in Costa Rica is that many Central American forests grow on fertile soil derived from volcanic substrates and should receover faster than in French Guiana. Also, these forests have long been exposed to major disturbances, such as hurricanes or volcanoes, and their flora may recover faster from disturbances. Focusing on difference in the physiological ecology of pioneer species between Costa Rica and French Guiana could help unravel whether the fast recovery of these forests is related to an adaptation to disturbance, or to higher soil fertility.

Conclusion

We found that, at our site in French Guiana, the carbon accumulation rate was at the low end of chronosequence data for Latin America and for Amazonia. This could be because the vast forested area underlain by the Guiana Shield displays a low carbon accumulation potential. Also, the first 20 years of carbon accumulation dynamics are a poor predictor of the next 20 years. This result is

important for carbon mitigation strategies (Chazdon et al. 2016) and confirms that more long-term studies should be documented across the Neotropics. One opportunity to better assimilate field data, remote sensing information, and ecological hypothesis into predictive frameworks is offered by individual-based forest growth models (Shugart et al. 2015; Maréchaux and Chave 2017; Rödig et al. 2017). We hope that carefully documented studies such as the one provided here will accelerate the development and intercomparison of such models.

Acknowledgements

We gratefully acknowledge funding by "Investissement d'Avenir" programs managed by Agence Nationale de la Recherche (CEBA, ref. ANR-10-LABX-25-01; TULIP, ref. ANR-10-LABX-0041; ANAEE-France: ANR-11-INBS-0001), from CNES (BIOMASS pluriannual project), and from ESA (as part of the BIOMASS mission program).

Authors' contributions

JC conceived the idea conducted the analyses and led the writing of the manuscript; IM, HdF, DL, FJF, and GV collected the data; CP, BH, JC and GV analysed the data. All authors contributed critically to the drafts and gave final approval for publication.

Literature cited

Aragão, L. E. O., Y. Malhi, R. M. Roman- Cuesta, S. Saatchi, L. O. Anderson, and Y. E. Shimabukuro. 2007. Spatial patterns and fire response of recent Amazonian droughts. Geophysical Research Letters **34**.

Arroyo- Rodríguez, V., F. P. Melo, M. Martínez- Ramos, F. Bongers, F., R. L. Chazdon, J. A. Meave, N. Norden, B. A. Santos, I. R. Leal, and M. Tabarelli. 2017. Multiple successional pathways in human- modified tropical landscapes: new insights from forest succession, forest fragmentation and landscape ecology research. Biological Reviews **92**:326–340.

Baraloto, C., S. Rabaud, Q. Molto, B. Hérault, L. Blanc, C. Fortunel, N. Davila, I. Mesones, M. Rios, E. Valderrama, and P. V. A. Fine. 2011. Disentangling stand and environmental correlates of aboveground biomass in Amazonian forests. Global Change Biology 17:2677–2688.

Becknell, J. M., S. Porder, S., Hancock, R. L. Chazdon, M. A. Hofton, J. B. Blair, and J. R. Kellner. 2018a. Chronosequence predictions are robust in a Neotropical secondary forest, but plots miss the mark. Global Change Biology 24:933–943.

Becknell, J. M., M. Keller, D. Piotto, M. Longo, M. N. dos Santos, M. A. Scaranello, R. B. de Oliveira Cavalcante, and S. Porder. 2018b. Landscape-scale lidar analysis of aboveground biomass distribution in secondary Brazilian Atlantic forest. Biotropica 50:520-530.

Blanc, L., M. Echard, B. Hérault, D. Bonal, E. Marcon, J. Chave, and C. Baraloto. 2009. Dynamics of aboveground carbon stocks in a selectively logged tropical forest. Ecological Applications 19:1397–1404.

Brown, S., and A. E. Lugo. 1990. Tropical secondary forests. Journal of Tropical Ecology, 6, 1–32.

Chave, J., J. Olivier, F. Bongers, P. Châtelet, P.-M. Forget, P. van der Meer, and P. Charles-Dominique. 2008. Above-ground biomass and productivity in a rain forest of eastern South America. Journal of Tropical Ecology 24:355–366.

Chave, J., D. Coomes, S. Jansen, S. L. Lewis, N. G. Swenson, and A. E. Zanne. 2009. Towards a worldwide wood economics spectrum. Ecology Letters 12:351–366.

Chazdon, R. L. 2003. Tropical forest recovery: legacies of human impact and natural disturbances. Perspectives in Plant Ecology, Evolution and Systematics 6:51–71.

Chazdon, R.L., S. G. Letcher, M. van Breugel, M. Martínez-Ramos, F. Bongers, and B. Finegan. 2007. Rates of change in tree communities of secondary Neotropical forests following major disturbances. Philosophical Transactions of the Royal Society of London B 362:273–289.

Chazdon, R. L. 2014. Second growth: the promise of tropical forest regeneration in an age of deforestation. University of Chicago Press.

Chazdon, R. L. et al. 2016. Carbon sequestration potential of second-growth forest regeneration in the Latin American tropics. Science Advances 2:e1501639.

Cole, L. E. S., S. A. Bhagwat, and K. J. Willis. 2014. Recovery and resilience of tropical forests after disturbance. Nature Communications 5:3096.

de Foresta, H. 1983. Hétérogeneité de la vegetation pionnière en forêt tropicale humide: exemple d'une coupe papetière en forêt guyanaise. Acta Oecologica 4:221–235.

de Foresta, H. 1984. Heterogeneity in early tropical forest regeneration after cutting and burning: Arbocel, French Guiana. in A. C. Chadwick and S. L. Sutton (eds.) "Tropical Rain Forest, The Leeds Symposium", Leeds, England, Leeds Philosophical & Litterary Society Ltd.: 242–253.

Dubayah, R. O., S. L. Sheldon, D. B. Clark, M. A. Hofton, J. B. Blair, G. C. Hurtt, and R. L. Chazdon. 2010. Estimation of tropical forest height and biomass dynamics using lidar remote sensing at La Selva, Costa Rica. Journal of Geophysical Research: Biogeosciences 115(G2).

Ene, L.T. et al. 2016. Large-scale estimation of aboveground biomass in miombo woodlands using airborne laser scanning and national forest inventory data. Remote Sensing of Environment 186:626-636.

Englhart, S., J. Jubanski, and F. Siegert. 2013. Quantifying dynamics in tropical peat swamp forest biomass with multi-temporal LiDAR datasets. Remote Sensing 5:2368-2388.

Estes, L., P. R. Elsen, T. Treuer, L. Ahmed, K. Caylor, J. Chang, J. J. Choi and E. C. Ellis. 2018. The spatial and temporal domains of modern ecology. Nature Ecology & Evolution, 2, 819.

Farrior, C. E., S. A. Bohlman, S. Hubbell, and S. W. Pacala. 2016. Dominance of the suppressed: Power-law size structure in tropical forests. Science 351:155–157.

Feldpausch, T. R., C. D. C. Prates-Clark, E. Fernandes and S. J. Riha. 2007. Secondary forest growth deviation from chronosequence predictions in central Amazonia. Global Change Biology 13:967–979.

Finegan, B. 1996. Pattern and process in neotropical secondary rain forests: the first 100 years of succession. Trends in Ecology and Evolution 11:119–124.

Gómez-Pompa, A. and C. Vázquez-Yanes. 1981. Successional studies of a rain forest in Mexico. In Forest Succession (pp. 246-266). Springer New York.

Grau, O. et al. 2017. Nutrient-cycling mechanisms other than the direct absorption from soil may control forest structure and dynamics in poor Amazonian soils. Scientific Reports 7:45017.

Hansen, M.C. et al. 2013. High-resolution global maps of 21st-century forest cover change. Science 342:850–853.

Houghton, R.A., J. L. House, J. Pongratz, G. R. van der Werf, R. S. DeFries, M. C. Hansen, C. Le Quéré, and N. Ramakutty. 2012. Carbon emissions from land use and land-cover change. Biogeosciences 9:5125–5142.

Houghton, R.A., B. Byers, and A.A. Nassikas. 2015. A role for tropical forests in stabilizing atmospheric CO2. Nature Climate Change 5:1022–1023.

Hughes, R. F., J. B. Kauffman, and V. J. Jaramillo. 1999. Biomass, carbon, and nutrient dynamics of secondary forests in a humid tropical region of Mexico. Ecology 80:1892–1907.

Johnson, E.A., and K. Miyanishi. 2008. Testing the assumptions of chronosequences in succession. Ecology Letters 11:419–431.

Labrière, N. et al. 2018. In situ data from the TropiSAR and AfriSAR campaigns as a support to upcoming spaceborne biomass missions. IEEE JSTARS. In press.

Larpin, D. 1989. Floristic composition and structure of a 11.5 year old secondary forest in French Guiana. Revue d'Ecologie (Terre et Vie) 44:209–224.

Le Quéré, C. et al. 2016. Global carbon budget 2016. Earth System Science Data 8:605–649.

Liu, Y. Y., A. I. van Dijk, R. A. De Jeu, J. G. Canadell, M. F. McCabe, J. P. Evans, and G. Wang. 2015. Recent reversal in loss of global terrestrial biomass. Nature Climate Change 5:470–474.

Maréchaux, I., M. K. Bartlett, P. Gaucher, L. Sack, and J. Chave. 2016. Causes of variation in leaf-level drought tolerance within an Amazonian forest. Journal of Plant Hydraulics 3:004.

Maréchaux, I., and J. Chave. 2017. An individual- based forest model to jointly simulate carbon and tree diversity in Amazonia: description and applications. Ecological Monographs 87:632–664.

Martin, A. R., and S. C. Thomas. 2011. A reassessment of carbon content in tropical trees. PloS One 6:e23533.

Martin, P. A., A. C. Newton, and J. M. Bullock. 2013. Carbon pools recover more quickly than plant biodiversity in tropical secondary forests. Proceedings of the Royal Society B 280:20132236.

Mascaro, J., G. P. Asner, D. H. Dent, S. J. DeWalt, and J. S. Denslow. 2012. Scale-dependence of aboveground carbon accumulation in secondary forests of Panama: a test of the intermediate peak hypothesis. Forest Ecology and Management 276:62–70.

Maury-Lechon, G. 1982. Régénération forestière en Guyane française: recrû sur 25 ha de coupe papetière en forêt dense humide (Arbocel). Bois et Forêts des Tropiques 197:3–21.

Meyer, V., S. S. Saatchi, J. Chave, J. W. Dalling, S. Bohlman, G. A. Fricker, C. Robinson, M. Neumann, and S. Hubbell. 2013. Detecting tropical forest biomass dynamics from repeated airborne lidar measurements. Biogeosciences 10:5421–5438.

Mora, F., M. Martínez- Ramos, G. Ibarra- Manríquez, A. Pérez- Jiménez, J. Trilleras, and P. Balvanera. 2015. Testing chronosequences through dynamic approaches: time and site effects on tropical dry forest succession. Biotropica 47:38–48.

Muscarella, R., M. Lohbeck, M. Martínez- Ramos, L. Poorter, J. E. Rodríguez- Velázquez, M. van Breugel, and F. Bongers. 2017. Demographic drivers of functional composition dynamics. Ecology 98:2743-2750.

Norden, N., R. C. Mesquita, T. V. Bentos, R. L. Chazdon, and G. B. Williamson. 2011. Contrasting community compensatory trends in alternative successional pathways in central Amazonia. Oikos 120:143–151.

Pan, Y. et al. 2011. A large and persistent carbon sink in the world's forests. Science 333:988–993.

Peña-Claros, M. 2003. Changes in forest structure and species composition during secondary forest succession in the Bolivian Amazon. Biotropica 35:450–461.

Plourde, B. T., V. K. Boukili, and R. L. Chazdon. 2015. Radial changes in wood specific gravity of tropical trees: inter- and intraspecific variation during secondary succession. Functional Ecology 29:111–120.

Pons, T. L., and G. Helle. 2011. Identification of anatomically non-distinct annual rings in tropical trees using stable isotopes. Trees 25:83–93.

Poorter, L. et al. 2016. Biomass resilience of Neotropical secondary forests. Nature 530:211–214.

Prévost, M.-F. 1983. Etude de la régénération: la végétation secondaire, piste de Saint-Elie en Guyane. In Le Projet ECEREX (Guyane) : analyse de l'écosystème forestier tropical humide et des modifications apportées par l'homme. ORSTOM, 195–213.

Qi, W., and R. O. Dubayah. 2016. Combining Tandem-X InSAR and simulated GEDI lidar

observations for forest structure mapping. Remote Sensing of Environment 187:253-266.

Réjou-Méchain, M., A. Tanguy, C. Piponiot, J. Chave, B. Hérault. 2017. BIOMASS: An R Package for estimating aboveground biomass and its uncertainty in tropical forests. Methods in Ecology and Evolution 8:1163–1167.

Rödig, E., M. Cuntz, J. Heinke, A. Rammig, and A. Huth. 2017. Spatial heterogeneity of biomass and forest structure of the Amazon rain forest: Linking remote sensing, forest modelling and field inventory. Global Ecology and Biogeography 26:1292–1302.

Rozendaal, D., and R.L. Chazdon. 2015. Demographic drivers of tree biomass change during secondary succession in northeastern Costa Rica. Ecological Applications 25:506–516.

Rutishauser, E., F. Wagner, B. Hérault, E. A. Nicolini, and L. Blanc. 2010. Contrasting above- ground biomass balance in a Neotropical rain forest. Journal of Vegetation Science 21:672-682.

Saatchi, S. S., et al. 2011. Benchmark map of forest carbon stocks in tropical regions across three continents. Proceedings of the National Academy of Sciences, 108:9899–9904.

Saatchi, S., L. Ulander, M. Williams, S. Quegan, T. LeToan, H. Shugart, and J. Chave. 2012. Forest biomass and the science of inventory from space. Nature Climate Change 2:826–827.

Saldarriaga, J. G., D.C. West M. L. Tharp, and C. Uhl. 1988. Long-term chronosequence of forest succession in the upper Rio Negro of Colombia and Venezuela. Journal of Ecology 76:938–958.

Sarrailh, J.-M. 1980. L'écosystème forestier guyanais. Etude écologique de son évolution sous l'effet des transformations en vue de sa mise en valeur. Bois et Forêts des Tropiques 189:31–36.

Sarrailh, J.-M. 1989. L'opération ECEREX. Etudes sur la mise en valeur de l'écosystème forestier guyanais après déboisement. Le point sur les recherches en cours. Bois et Forêts des Tropiques 219:79–97.

Sarrailh, J.-M., H. de Foresta, G. Maury-Lechon, and M.-F. Prévost. 1990. La régénération après coupe papetière: Parcelle Arbocel. In J. M. Sarrailh (Ed.), Mise en valeur de l'écosystème forestier guyanais (pp. 187–208). INRA-CTFT.

Shugart, H. H., G. P. Asner, R. Fischer, A. Huth, N. Knapp, T. Le Toan, and J. K. Shuman. 2015. Computer and remote- sensing infrastructure to enhance large- scale testing of individual- based forest models. Frontiers in Ecology and the Environment 13:503-511.

Silva, C. E. M., J. F. C. Gonçalves, and E. C. Alves. 2011. Photosynthetic traits and water use of tree species growing on abandoned pasture in different periods of precipitation in Amazonia. Photosynthetica 49:246-252.

Solberg, S., B. Gizachew, E. Næsset, T. Gobakken, O. M. Bollandsås, E. W. Mauya, H. Olsson, R. Malinbwi, and E. Zahabu. 2015. Monitoring forest carbon in a Tanzanian woodland using interferometric SAR: a novel methodology for REDD+. Carbon Balance and Management 10:14.

Toriola Lafuente, D. 1997. Régénération naturelle en Guyane Française: ARBOCEL, une jeune forêt secondaire de 19 ans. Unpublished doctoral dissertation, Paris University.

Tymen, B., G. Vincent, E. A. Courtois, J. Heurtebize, J. Dauzat, I. Maréchaux, and J. Chave. 2017. Quantifying micro-environmental variation in tropical rainforest understory at landscape scale by combining airborne LiDAR scanning and a sensor network. Annals of Forest Science 74:32.

Vincent, G., D. Sabatier, L. Blanc, J. Chave, E. Weissenbacher, R. Pélissier, E. Fonty, J.-F. Molino, and P. Couteron. 2012. Accuracy of small footprint airborne LiDAR in its predictions of tropical moist forest stand structure. Remote Sensing of Environment 125:23–33.

Vincent, G., C. Antin, M. Laurans, J. Heurtebize, S. Durrieu, C. Lavalley, and J. Dauzat. 2017. Mapping plant area index of tropical evergreen forest by airborne laser scanning. A cross-validation study using LAI2200 optical sensor. Remote Sensing of Environment 198:254–266.

Zwetsloot, H. 1981. Forest succession on a deforested area in Suriname. Turrialba 31:369–379.

Tables

Table 1. Canopy height in the regrowing plot compared to the control plot in 2009 and in 2017. All values are expressed in m. Canopy height was measured from the canopy height model at 1-m resolution using four possible metrics: mean, median, top 90% and top 95%. Canopy height increase was named Δ in the regrowing plot and Δ_C in the control plot.

	Regrowing plot			Control plot			
	2009	2017	Δ	2009	2017	Δ_C	Δ- Δ_C
Mean	17.81	19.42	**1.61**	27.53	28	0.47	**1.14**
Median	18.04	19.43	**1.39**	28.27	28.56	0.29	**1.10**
90%	23.01	24.86	**1.85**	36.00	36.06	0.06	**1.79**
95%	24.43	26.48	**2.05**	38.00	38.06	0.06	**1.99**

Figure legends

Figure 1. Changes in forest structure during a 40-yr secondary regrowth in a forest of French Guiana. (a) Basal area (m^2/ha), and (b) aboveground carbon (AGC, in MgC/ha). In both panels, white circles represent sapling measurements (< 10 cm dbh), white squares represent tree measurements (≥ 10 dbh cm), and black circles represent total measurements (saplings plus trees). Lines represent the best fits of Equations (1)-(4), with light-shaded areas showing the 95% credibility intervals of the sapling and tree models. Dark-shaded areas represent the 95% credibility intervals of the curves for saplings plus trees.

Figure 2. Remote sensing of the study area using a small-footprint aerial lidar scanning technique (in 2017). (a) Canopy height model at 1 m resolution, where the secondary forest site is clearly visible at the Northeast of the scene (a small fraction of the stand is crossed by a paved road). (b) Plant area index (in m^2 of matter per m^2 of ground) as inferred from a ray-tracing algorithm (see methods). In both panels, the regrowing forest plot is illustrated in red, and the control plot in black.

Figure 3. Community-wide changes in trees (≥ 10 dbh cm). Panel (a) describes changes in aboveground carbon (AGC, in MgC/ha) for the 11 dominant tree genera of trees in the permanent inventory plot. Panel (b) describes changes in stand-averaged wood density (weighted by basal area). The tree census started 12 years after plot abandonment.

Figure 4. Carbon fluxes in the tree plot (in MgC/ha/yr). Grey circles represent woody NPP, grey triangles represent ingrowth into the ≥10 cm dbh tree category, grey crosses represent carbon loss due to mortality, and black circles represent the balance of these components (woody NPP plus ingrowth minus loss).

Figure 5. Comparison of the AGC accumulation curve in French Guiana (black solid line) and that of three sites in Costa Rica (data from Rozendaal and Chazdon 2015). Lines and 95% credibility intervals were obtained from fitting the model of Equation (5).

Figure 1.

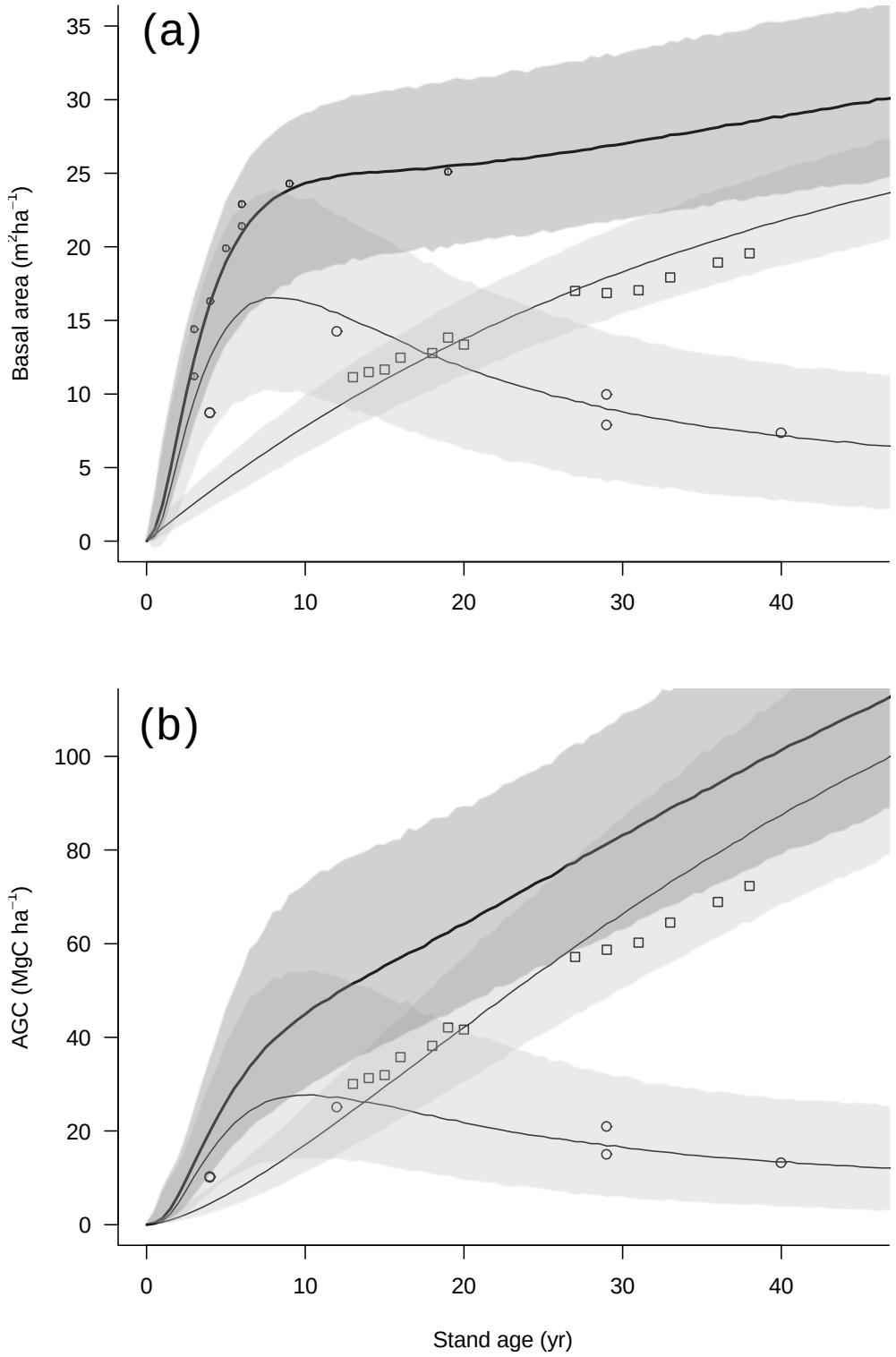
(a)
Basal area (m²ha⁻¹)
0
5
10
15
20
25
30
35
0
10
20
30
40
(b)
AGC (MgC ha⁻¹)
0
20
40
60
80
100
0
10
20
30
40
Stand age (yr)

Figure 2

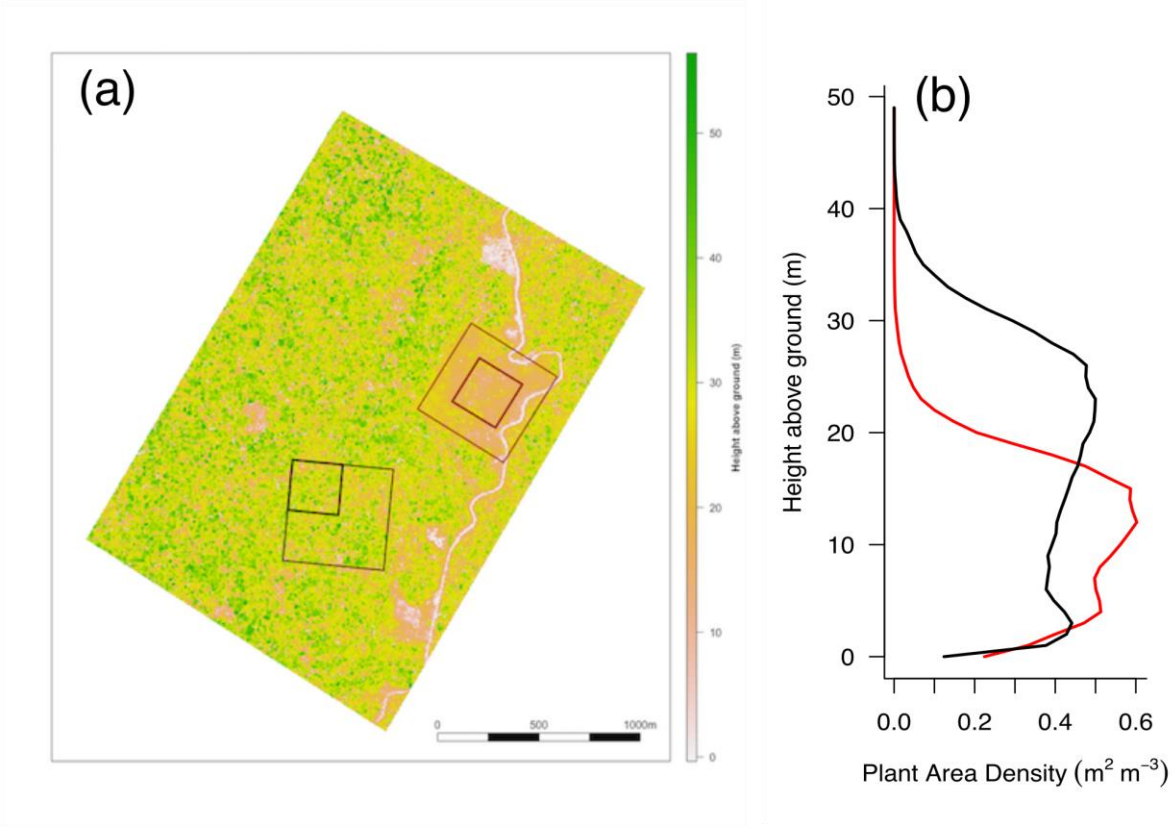
(a)
0
500
1000m
Height above ground (m)
0
10
20
30
40
50
(b)
Height above ground (m)
0
10
20
30
40
50
0.0
0.2
0.4
0.6
Plant Area Density (m^2 m^{-3})

Figure 3.

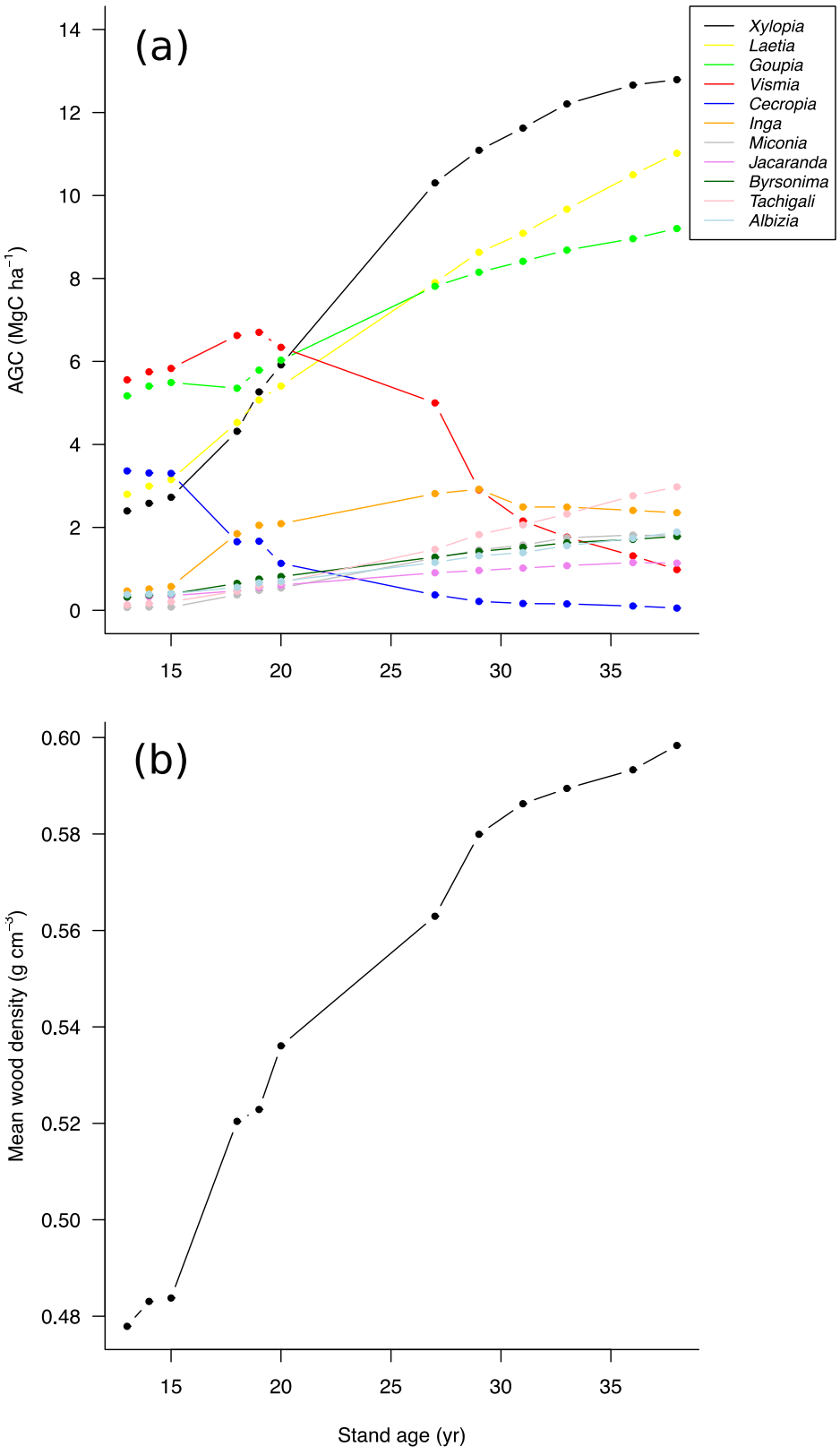
(a)
AGC (MgC ha^{-1})
0
2
4
6
8
10
12
14
15
20
25
30
35
Xylopia
Laetia
Goupia
Vismia
Cecropia
Inga
Miconia
Jacaranda
Byrsonima
Tachigali
Albizia
(b)
Mean wood density (g cm^{-3})
0.48
0.50
0.52
0.54
0.56
0.58
0.60
15
20
25
30
35
Stand age (yr)

Figure 4.

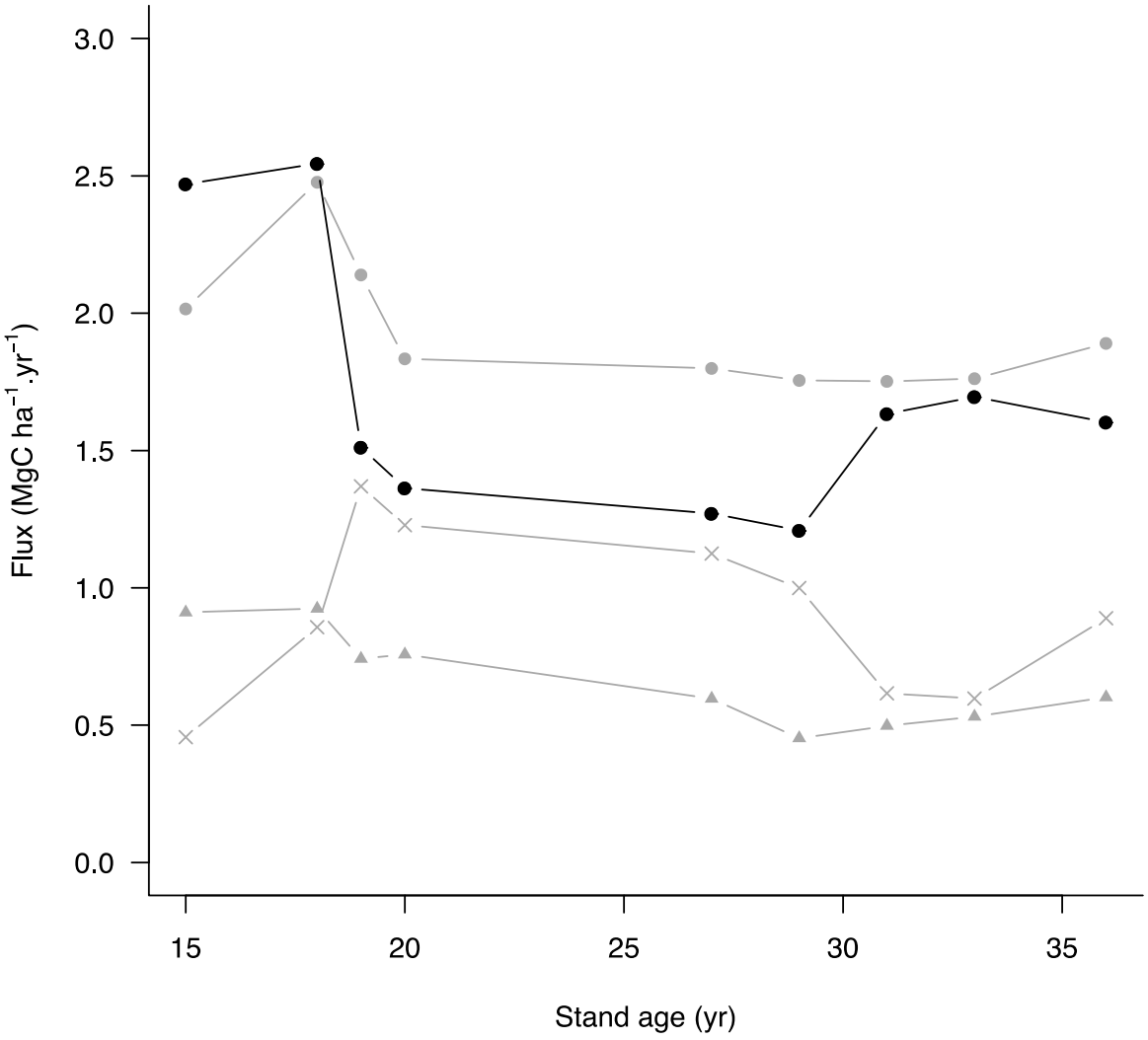

Figure 5

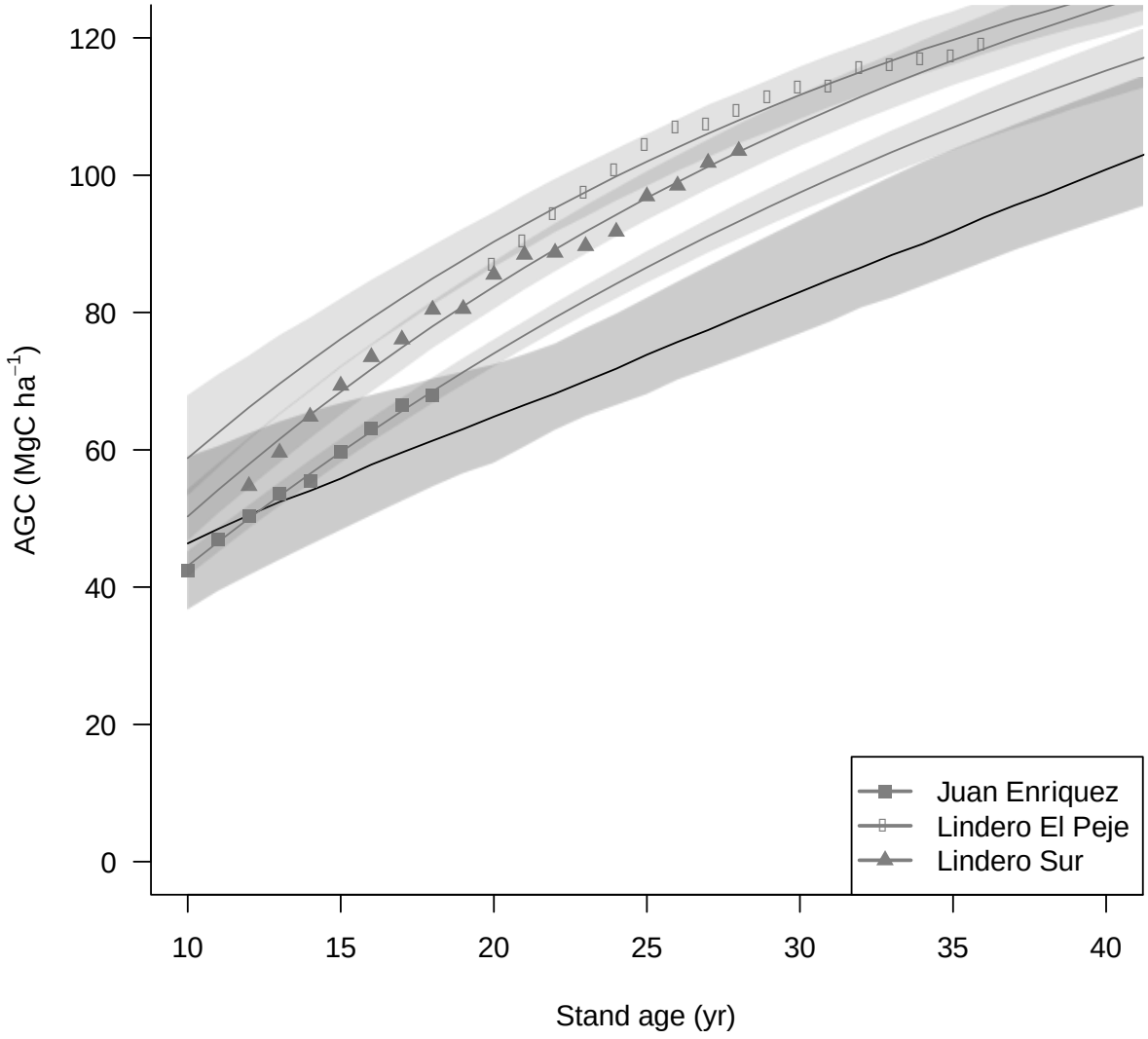
120
100
80
60
40
20
0
AGC (MgC ha^{-1})
10
15
20
25
30
35
40
Stand age (yr)
Juan Enriquez
Lindero El Peje
Lindero Sur

SI-1. Bayesian inference of the model parameters.

We built a hierarchical framework to infer the parameters in the model (1-4). All parameters are reported in Table S1. We modelled $BA_{sapling}$ and BA_{tree} using the functions described in the main text:

$$G(\theta_{1\ldots5},t) = \theta_1 \times \left(1 - e^{-\theta_{2a}t}\right) + \theta_3 \times e^{-\left(\frac{log\left(t/\theta_4\right)}{\theta_5}\right)^2}$$

$$H\left(\theta_{2,6},t\right) = \theta_6 \times \left(1 - e^{-\theta_{2b}t}\right)$$

More precisely, $BA_{sapling}$ and BA_{tree} were taken to be random variables with the following kernels:

$$BAsapling_t \sim N\left(G(\theta_{1\ldots5},t); \sigma_1 \times \sqrt{G(\theta_{1\ldots5},t)}\right)$$

$$BAtree_t \sim N\left(H\left(\theta_{2,6},t\right); \sigma_2 \times \sqrt{H\left(\theta_{2,6},t\right)}\right)$$

where $\sigma_1$and σ_2 are error terms. The second step was to relate *AGC* and *BA*. As described in the main text, we assumed:

$$I\left(\theta_{7,8},t\right) = \theta_7 + \theta_8 \times log(BAtree)$$

The Bayesian model was chosen as follows:

$$AGCtree_t \sim logN\left(I\left(\theta_{7,8},t\right);\ \sigma_4\ \right)$$

$$AGCsapling_t \sim logN\left(\theta_9 + \theta_{10} \times log(BAsapling) + \theta_{11} \times I\left(\theta_{7,8},t\right);\ \sigma_5\ \right)$$

Models were inferred in a Bayesian framework using the joint model likelihood in a HMC scheme under Stan (https://www.jstatsoft.org/article/view/v076i01). A list of priors is given in table S1.

Table S1. List of model parameters, prior and posterior distributions (median values, [95% credibility intervals]). BAall, basal area of all trees ≥ 1 cm dbh from the literature; BAinf, basal area of all trees ranging from 1 to 10 cm dbh from original surveys; BAsup, basal area of all trees ≥ 1 cm dbh from original surveys; AGCsup, aboveground carbon content (uncertainties propagated) of all trees ≥ 10 cm dbh estimated from original surveys; AGCinf, aboveground carbon content (uncertainties propagated) of all trees < 10 cm dbh estimated from original surveys.

Model	**Parameter**		**Prior**	**Posterior**
BAinf	σ_1	Error term	U [0.01 ;1]	0.799 [0.41;0.97]
	θ_1	Asymptotic value	U[0 ;8]	6.811 [0.155;7.735]
	θ_{2a}	Return rate	U[θ_{2b} ;0.05]	0.046 [0.026;0.049]
	θ_3	Max value of the transient boom-and-bust	U[0 ;20]	15.131 [12.396;17.678]
	θ_4	Time (yr) at which θ_3 is obtained	U[0 ;30]	6.514 [6.501;10.046]
	θ_5	shape parameter	U[0 ; 5]	1.191 [1.089;1.994]
BAsup	σ_2	Error term	U[0.01 ;1]	0.31 [0.231;0.489]
	θ_6	Asymptotic value	U[25 ;35]	32.73 [30.52;34.93]
	θ_{2b}	Return rate	U[0 ;0.05]	0.028 [0.024;0.03]
BAall	σ_3	Error term	U[0.01 ;1]	0.301 [0.229;0.927]

AGCsup	σ_4	Error term	U[0.01 ;0.5]	0.025 [0.034;0.29]	
	θ_7	Intercept	U[-5 ;5]	-0.721 [-1.77;0.656]	
	θ_8	Slope	U[1 ;3]	1.269 [0.678;1.736]	
AGCinf	σ_5	Error term	U[0.01 ;0.5]	0.022 [0.015;0.041]	
	θ_9	Intercept	U[-5 ; 5]	-0.721 [-1.77;0.656]	
	θ_{10}	Slope	U[0 ;2]	1.269 [0.678;1.736]	
	θ_{11}	control for the competition from trees ≥ 10 cm dbh	U[0 ;2]	0.187 [0.098;0.261]	θ_{11}
AGC	σ_6	Error term	U[0 ;10]	2.44 [0.545;4.003]	
	θ_{12}	intercept	U[0 ;40]	17.259 [0.10;39.80]	
	θ_{13}	Return rate	U[0 ;1]	0.02 [0.013;0.03]	

SI-2. Published Arbocel plot data

Table S2. Inventories of the stand where all trees ≥ 1 cm dbh have been measured and identified to species. Area is the total area covered by the census. Basal area is in m^2/ha. In inventories > 10 years after forest abandonment, BA contributed by trees ≥ 10 cm dbh was corrected using the 4-ha census plot results. Studies with available tree-by-tree inventories are noted 'a', while those where tree-by-tree inventories were unavailable are noted 'b'.

Stand age	Area (ha)	Basal area	Group	Source
3	0.1	14.4	b	Prévost (1981)
3	0.1	11.2	b	Sarrailh et al. (1990)
4	0.1	16.3	b	Sarrailh et al. (1990)
4	0.092	11.2	a	De Foresta (1983)
4	0.106	11.2	a	De Foresta (1983)
5	0.1	19.9	b	Sarrailh et al. (1990)
6	0.1	21.4	b	Prévost (1981)
6	0.1	22.9	b	Sarrailh et al. (1990)
9	0.1	24.3	b	Sarrailh et al. (1990)
12	0.0808	25.4	a	Larpin (1989)
19	0.52	25.1	b	Toriola (1997)
29	0.1696	24.8	a	De Foresta (unpublished)
29	0.182	26.8	a	De Foresta (unpublished)
40	0.09	27.6	a	this study

Mapping carbon recovery hotspots in Amazonia

Janet Pelley

Scientists have raised alarms over the massive scale of selective logging in the Amazon rainforest, which is home to 30% of the world's forest carbon. But a growing body of research shows that degraded forests recovering from harvesting can soak up tons of atmospheric carbon, helping to keep global warming below 2°C. Now, a new study has created the first map of carbon recovery in Amazonia, revealing the best and worst places for recovery (*eLife* 2016; doi:10.7554/eLife.21394).

Amazonian deforestation brings to mind images of smoldering treeless plots. But government policies to discourage clearcutting have now made way for selective logging, which targets only the removal of merchantable species so that forest cover is left in place. Yet the practice is extensive: loggers selectively harvest about 2 million hectares of the Brazilian Amazon per year, roughly equal to the area deforested, according to Camille Piponiot, a tropical ecologist with the Université de Guyane (Kourou, French Guiana).

G Padié

Naturally regenerated forests can store lots of carbon.

In 2015, using data from the Tropical managed Forests Observatory (TmFO), investigators determined that selectively logged Amazon forests could recover their carbon stocks in just 7 to 21 years after cutting. "However, we were surprised that the [2015] study didn't find differences in carbon dynamics across the Amazonian region", Piponiot says. So she and her team decided to mine the trove of data collected by the TmFO on 133 disturbed plots across Amazonia. The data helped the scientists create a model that links measures of climate, soil quality, logging intensity, and number of surviving trees to the recovery of aboveground carbon stocks. The researchers ran the model to predict carbon recovery 10 years after a hypothetical case of selectively logging the entire Amazon rainforest.

The resulting map shows that the drier south would recover only about half the aboveground carbon regained by wetter northern regions. "Those differences are mostly explained by higher carbon storage by the growth of trees that survived logging in northern Amazonia", she continues. Survivors are bigger and can store more carbon than newly recruited saplings. "This study demonstrates that less harmful logging techniques that protect survivors should improve carbon storage during forest regrowth."

"The results support recommendations that governments modify forest plans to put logging in the high-recovery areas while protecting the less-resilient areas as parkland", says Greg Asner, an ecologist at Stanford University (Stanford, CA). Piponiot's study corroborates earlier findings that degraded forests are highly valuable for carbon uptake, he concludes. ■

Climate engineering less feasible but still needed?

Heidi Swanson

When first devised, plans to capture CO_2 on a colossal scale via climate engineering (CE) seemed like the stuff of the future. Yet ocean fertilization and atmospheric aerosol injection will theoretically make it possible to remove large amounts of CO_2 from the atmosphere and to divert the Sun's warming rays away from the Earth's surface.

On January 24, a new CE report was published, wrapping up the first phase of two 3-year periods of funding from the German Research Foundation (*Earth's Future* 2017; doi:10.1002/2016EF000446). The report summarizes the key findings of studies supported under a Priority Program (SPP 1689) to investigate the effectiveness of solar radiation management and CO_2 removal using CE technologies.

The new results are not promising. Virtually all of the CE strategies tackled by researchers' modeling studies were estimated to be less effective and less affordable than a 2009 paper published by the Royal Society (http://bit.ly/1PFp7nY) had anticipated. Andreas Oschlies, a theoretical marine biogeochemist and report coauthor (GEOMAR Helmholtz Centre for Ocean Research, Kiel, Germany), says that even supposedly "green" CE methods, such as afforestation, "are all nice if applied at a small scale in your garden, but if you want to make a dent in our CO_2 record, you have to apply them at an industrial scale. And then they don't look so nice and 'green' anymore."

It is not news that an industrial-scale implementation of CE would be challenging. Before the Priority Program was funded, German stakeholders' take on CE could be described as a sense of collective skepticism. "Overcoming our own moral dilemma that we have to study something we don't really want to make happen has been and still is challenging", says Oschlies.

But the 2015 Paris Agreement to limit global long-term temperature increases to 1.5°C may require a renewed interest in CE technologies, despite these new findings highlighting their drawbacks. "CE might be the only option – with many different flavors – that could allow us to reach [the goals of the Paris Agreement]", Oschlies admits. "Whether we like it or not, we have to think about CE." ■